

Development of LRFD Procedures for Bridge Pile Foundations in Iowa

Volume III: Recommended Resistance Factors with Consideration of Construction Control and Setup



**Final Report
February 2012**



IOWA STATE UNIVERSITY
Institute for Transportation

Sponsored by
Iowa Highway Research Board
(IHRB Project TR-584)
Iowa Department of Transportation
(InTrans Project 08-313)

About the Bridge Engineering Center

The mission of the Bridge Engineering Center (BEC) is to conduct research on bridge technologies to help bridge designers/owners design, build, and maintain long-lasting bridges.

About the Institute for Transportation

The mission of the Institute for Transportation (InTrans) at Iowa State University is to develop and implement innovative methods, materials, and technologies for improving transportation efficiency, safety, reliability, and sustainability while improving the learning environment of students, faculty, and staff in transportation-related fields.

Disclaimer Notice

The contents of this report reflect the views of the authors, who are responsible for the facts and the accuracy of the information presented herein. The opinions, findings and conclusions expressed in this publication are those of the authors and not necessarily those of the sponsors.

The sponsors assume no liability for the contents or use of the information contained in this document. This report does not constitute a standard, specification, or regulation.

The sponsors do not endorse products or manufacturers. Trademarks or manufacturers' names appear in this report only because they are considered essential to the objective of the document.

Non-Discrimination Statement

Iowa State University does not discriminate on the basis of race, color, age, religion, national origin, sexual orientation, gender identity, genetic information, sex, marital status, disability, or status as a U.S. veteran. Inquiries can be directed to the Director of Equal Opportunity and Compliance, 3280 Beardshear Hall, (515) 294-7612.

Iowa Department of Transportation Statements

Federal and state laws prohibit employment and/or public accommodation discrimination on the basis of age, color, creed, disability, gender identity, national origin, pregnancy, race, religion, sex, sexual orientation or veteran's status. If you believe you have been discriminated against, please contact the Iowa Civil Rights Commission at 800-457-4416 or Iowa Department of Transportation's affirmative action officer. If you need accommodations because of a disability to access the Iowa Department of Transportation's services, contact the agency's affirmative action officer at 800-262-0003.

The preparation of this (report, document, etc.) was financed in part through funds provided by the Iowa Department of Transportation through its "Agreement for the Management of Research Conducted by Iowa State University for the Iowa Department of Transportation," and its amendments.

The opinions, findings, and conclusions expressed in this publication are those of the authors and not necessarily those of the Iowa Department of Transportation.

Technical Report Documentation Page

1. Report No. IHRB Projects TR-584	2. Government Accession No.	3. Recipient's Catalog No.	
4. Title and Subtitle Development of LRFD Procedures for Bridge Pile Foundations in Iowa — Volume III: Recommended Resistance Factors with Consideration of Construction Control and Setup		5. Report Date February 2012	
		6. Performing Organization Code	
7. Author(s) S. S. AbdelSalam, K. W. Ng, S. Sritharan, M. T. Suleiman, and M. Roling		8. Performing Organization Report No. InTrans Project 08-313	
9. Performing Organization Name and Address Institute for Transportation Iowa State University 2711 South Loop Drive, Suite 4700 Ames, IA 50010-8664		10. Work Unit No. (TRAIS)	
		11. Contract or Grant No.	
12. Sponsoring Organization Name and Address Iowa Highway Research Board Iowa Department of Transportation 800 Lincoln Way Ames, IA 50010		13. Type of Report and Period Covered Final Report	
		14. Sponsoring Agency Code	
15. Supplementary Notes Visit www.intrans.iastate.edu for color PDFs of this and other research reports.			
16. Abstract <p>The Federal Highway Administration (FHWA) mandated utilizing the Load and Resistance Factor Design (LRFD) approach for all new bridges initiated in the United States after October 1, 2007. As a result, there has been a progressive move among state Departments of Transportation (DOTs) toward an increased use of the LRFD in geotechnical design practices. For the above reasons, the Iowa Highway Research Board (IHRB) sponsored three research projects: TR-573, TR-583 and TR-584. The research information is summarized in the project web site (http://srg.cce.iastate.edu/lrfd/). Two reports of total four volumes have been published. Report volume I by Roling et al. (2010) described the development of a user-friendly and electronic database (PILOT). Report volume II by Ng et al. (2011) summarized the 10 full-scale field tests conducted throughout Iowa and data analyses. This report presents the development of regionally calibrated LRFD resistance factors for bridge pile foundations in Iowa based on reliability theory, focusing on the strength limit states and incorporating the construction control aspects and soil setup into the design process. The calibration framework was selected to follow the guidelines provided by the American Association of State Highway and Transportation Officials (AASHTO), taking into consideration the current local practices. The resistance factors were developed for general and in-house static analysis methods used for the design of pile foundations as well as for dynamic analysis methods and dynamic formulas used for construction control. The following notable benefits to the bridge foundation design were attained in this project: 1) comprehensive design tables and charts were developed to facilitate the implementation of the LRFD approach, ensuring uniform reliability and consistency in the design and construction processes of bridge pile foundations; 2) the results showed a substantial gain in the factored capacity compared to the 2008 AASHTO-LRFD recommendations; and 3) contribution to the existing knowledge, thereby advancing the foundation design and construction practices in Iowa and the nation.</p>			
17. Key Words LRFD — bridge pile foundations — resistance factors — static analysis — dynamic analysis — dynamic formulas — design — construction — setup		18. Distribution Statement No restrictions.	
19. Security Classification (of this report) Unclassified.	20. Security Classification (of this page) Unclassified.	21. No. of Pages 312	22. Price NA

DEVELOPMENT OF LRFD PROCEDURES FOR BRIDGE PILE FOUNDATIONS IN IOWA VOLUME III: RECOMMENDED RESISTANCE FACTORS WITH CONSIDERATION OF CONSTRUCTION CONTROL AND SETUP

**Final Report
February 2012**

Principal Investigator

Sri Sritharan
Professor

Department of Civil, Construction, and Environmental Engineering, Iowa State University

Co-Principal Investigator

Muhannad T. Suleiman
Assistant Professor

Department of Civil and Environmental Engineering, Lehigh University

Graduate Research Assistants

Sherif S. AbdelSalam; Kam W. Ng, and Matthew Roling

Authors

Sherif S. AbdelSalam, Kam W. Ng, Sri Sritharan, Muhannad T. Suleiman, and Matthew Roling

Sponsored by
The Iowa Highway Research Board
(IHRB Projects TR-584)

Preparation of this report was financed in part
through funds provided by the Iowa Department of Transportation
through its research management agreement with the
Institute for Transportation
(InTrans Projects 08-313)

A report from
Institute for Transportation
Iowa State University
2711 South Loop Drive, Suite 4700
Ames, IA 50010-8664
Phone: 515-294-8103
Fax: 515-294-0467
www.intrans.iastate.edu

TABLE OF CONTENTS

ACKNOWLEDGMENTS	XXV
CHAPTER 1: OVERVIEW	1
1.1. Introduction to LRFD	1
1.2. Scope of Research.....	2
1.3. Research Plan.....	2
1.4. Benefits of the Research	3
1.5. Report Outline.....	3
CHAPTER 2: DESIGN OF PILE FOUNDATIONS.....	5
2.1. Allowable Stress Design	5
2.2. Load and Resistance Factor Design	5
2.2.1. Basic Principles	5
2.2.2. Implementation.....	6
2.2.3. Calibration by Fitting to ASD	7
2.2.4. Calibration using Reliability Theory.....	9
2.2.5. Target Reliability Index	13
2.3. Framework of Calibration.....	13
2.4. Current AASHTO-LRFD Specifications.....	16
2.4.1. Static Methods.....	16
2.4.2. Dynamic Methods	18
2.5. Regionally Calibrated Resistance Factors	20
2.5.1. Background	21
2.5.2. State DOTs Implementation.....	23
2.6. Construction Control of Deep Foundations	24
2.6.1. Design Versus Construction Stages	24
2.6.2. Definition of Quality Control.....	26
2.6.3. Combining Static and Dynamic Methods	26
CHAPTER 3: DIFFERENT PILE ANALYSIS PROCEDURES	28
3.1. Static Analysis Methods	28
3.1.1. Determination of Soil Properties.....	28
3.1.2. Pile Capacity in Cohesive Soils	30
3.1.3. Pile Capacity in Cohesionless Soils	40
3.1.4. Iowa Blue Book Method	47
3.1.5. The DRIVEN Computer Program.....	47
3.1.6. SPT-97.....	47
3.1.7. Comparison of Different Static Methods	48
3.2. Dynamic Analysis Methods.....	48
3.2.1. Pile Driving Analyzer.....	48
3.2.2. Case Pile Wave Analysis Program.....	51
3.2.3. Wave Equation Analysis Program	52
3.2.4. Comparison of Different Dynamic Methods.....	53
3.3. Dynamic Formulas.....	54

3.3.1.	General	54
3.3.2.	Commonly used Formulas	56
3.3.3.	Comparison of Different Formulas	63
3.4.	Pile Static Load Test	67
3.4.1.	Overview	67
3.4.2.	Acceptance Criteria	68
CHAPTER 4:	COLLECTION OF DATA	74
4.1.	Nationwide Survey of State DOTs	74
4.1.1.	Previous Surveys	74
4.1.2.	Goals and Topic Areas of the Survey	75
4.1.3.	Major Findings	76
4.1.4.	Reported LRFD Resistance Factors	84
4.1.5.	Summary and Conclusions	88
4.2.	Survey of Iowa County Engineering Offices	89
4.2.1.	Foundation Practice	90
4.2.2.	Timber Pile Usage	92
4.2.3.	Pile Analysis and Design	93
4.2.4.	Pile Drivability/Quality Control	96
4.2.5.	Contribution from Engineering Firms	97
4.1.	Historical Database Overview	99
4.3.1.	General Description and Overview	99
4.3.2.	Usable Load Tests in PILOT	99
4.2.	An Overview of Field Tests	100
CHAPTER 5:	SELECTED CALIBRATION FRAMEWORK	101
5.1.	Summary	101
5.2.	Soil Profile Categorization	101
5.3.	Criterion of Sorting the Database	102
5.4.	Determination of Soil Parameters	102
5.5.	Selected Pile Analysis Procedures	104
5.5.1.	Static Methods	104
5.5.2.	Dynamic Methods	105
5.5.3.	Dynamic Formulas	105
5.6.	Determination of Pile Nominal Capacity	106
5.7.	Selected Reliability Approach and Parameters	107
5.7.1.	First Order Second Moment	107
5.7.2.	Distribution Quality Tests	108
5.7.3.	Target Reliability Index	108
5.7.4.	Dead Load to Live Load Ratio	109
CHAPTER 6:	PRELIMINARY RESISTANCE FACTORS	110
6.1.	Static Analysis Methods	110
6.1.1.	Pile Capacity	110
6.1.2.	Goodness of Fit Test	114
6.1.3.	Histograms and Frequency Distribution	116
6.1.4.	LRFD Resistance Factors	120

6.1.5.	Sensitivity to Reliability Index	122
6.1.6.	Efficiency of Different Methods	124
6.1.7.	Equivalent Factor of Safety	126
6.1.8.	Regional Factors vs. Design Specifications	127
6.1.9.	Examination of the Resistance Factors	127
6.1.10.	Construction Control Aspects	131
6.2.	Dynamic Analysis Methods	132
6.2.1.	Capacity from WEAP	132
6.2.2.	Goodness of Fit Test	134
6.2.3.	Histograms and Frequency Distribution	136
6.2.4.	LRFD Resistance Factors	140
6.2.5.	Sensitivity to Reliability Index	142
6.2.6.	Efficiency of Different Methods	143
6.2.7.	Equivalent Factor of Safety	145
6.2.8.	Regional Factors vs. Design Specifications	146
6.2.9.	Examination of the Resistance Factors	147
6.2.10.	Soil Setup	150
6.2.11.	LRFD Considering Soil Setup	152
6.2.12.	Construction Control	155
6.3.	Dynamic Formulas	166
6.3.1.	Pile Capacity	166
6.3.2.	Goodness of Fit Test	168
6.3.3.	Histograms and Frequency Distribution	168
6.3.4.	LRFD Resistance Factors	173
6.3.5.	Sensitivity to Reliability Index	175
6.3.6.	Efficiency of Different Methods	177
6.3.7.	Equivalent Factor of Safety	179
6.3.8.	Regional Factors vs. Design Specifications	179
6.3.9.	Examination of the Resistance Factors	180
6.3.10.	Construction Control	184
CHAPTER 7: RECOMMENDATIONS FOR DESIGN AND CONSTRUCTION		189
7.1.	Static Methods	189
7.1.1.	Design Tables	189
7.1.2.	Design Charts	190
7.1.3.	Improved Resistance Factors for Iowa Blue Book Method	192
7.2.	Dynamic Analysis	193
7.2.1.	Design Tables	193
7.2.2.	Design Charts	195
7.3.	Dynamic Formulas for Steel H-Piles	197
7.3.1.	Design Tables	197
7.3.2.	Design Charts	199
7.4.	Dynamic Formulas for Timber Piles	201
7.4.1.	Design Tables	201
7.4.2.	Design Charts	202
7.5.	Summary of Resistance Factors	203
7.6.	Pile Resistance and Target Driving Resistance	210

CHAPTER 8: SUMMARY AND CONCLUSIONS	214
8.1. Summary of Research	214
8.2. Major Outcomes and Conclusions	214
8.2.1. Static Analysis Methods	215
8.2.2. Dynamic Analysis Methods	216
8.2.3. Dynamic Formulas	217
8.2.4. Recommendations	218
8.3. Future Research	218
REFERENCES	219
APPENDIX A: FLOWCHARTS SUMMARIZING TWO LRFD SURVEYS	227
APPENDIX B: SUPPLEMENTAL GRAPHS SUMMARIZING ADDITIONAL LRFD CALIBRATION	238

LIST OF FIGURES

Figure 2.1: LRFD failure criterion between the PDFs of load and resistance	6
Figure 2.2: Probability of failure and reliability index (after Withiam et al. 1998)	9
Figure 2.3: Framework of the LRFD resistance factors calibration for design and construction methods of analysis.....	15
Figure 2.4: Typical design and construction cycle	25
Figure 2.5: Current design and construction practice in the state of Iowa	25
Figure 3.1: Measured values of α as back calculated from static load tests compared with several proposed functions for α (from Coduto, 2001)	32
Figure 3.2: Adhesion values for piles in cohesive soils (after Tomlinson, 1979)	34
Figure 3.3: Adhesion factors for driven piles in clay soils (after Tomlinson, 1980).....	35
Figure 3.4: The β coefficient versus soil type using ϕ' angle (after from Fellenius, 1991)	36
Figure 3.5: The N_t coefficient versus soil type using ϕ' angle (after Fellenius, 1991)	36
Figure 3.6: Chart for λ factor using pile penetration length (after Vijayvergiya and Focht, 1972).....	37
Figure 3.7: Penetrometer design curve for pile side friction in sand (after FHWA, 2007)	39
Figure 3.8: Design curve for skin-friction in clays recommended by Schmertmann (1978)	39
Figure 3.9: Procedure suggested for estimating the pile end bearing capacity by Nottingham and Schmertman, 1975).....	40
Figure 3.10: Correction factor C_F for K_δ when $\delta \neq \phi$ (after Nordlund, 1979)	45
Figure 3.11: Chart for estimating the α_f coefficient from ϕ (after Nordlund, 1979).....	45
Figure 3.12: Chart for estimating the N'_q coefficient from ϕ (after Bowles, 1977).....	46
Figure 3.13: Relationship between the toe resistance and ϕ in sand (after Meyerhof, 1976).....	46
Figure 3.14: Relationship between resistance and penetration under a single hammer blow (after Cummings 1940).....	55
Figure 3.15: Example of determining the pile capacity using Davisson's method	69
Figure 3.16: Example of determining the pile capacity using the shape of curvature method	69
Figure 3.17: Example of determining the pile capacity using the limited total settlement method	70
Figure 3.18: An Example of determining the pile capacity using De Beer's method	71
Figure 3.19: Determining the capacity using Chin's method (after Parakash et al., 1990)	71
Figure 4.1: U.S. Map summarizing the typical soil formations, average depth to bedrock, commonly used deep foundation categories, types and sizes, and static analysis methods used in different states.....	77
Figure 4.2: Distribution of the most commonly used driven pile types for bridge foundations	78
Figure 4.3: Distribution of the most commonly used drilled shaft types for bridge foundations	78
Figure 4.4: The usage of different methods for the design of bridge foundations.....	79

Figure 4.5: Extent of LRFD implementation for bridge foundations from survey in 2008.....	80
Figure 4.6: Most commonly used static analysis methods for the design of deep foundations	81
Figure 4.7: Most commonly used dynamic analysis methods for the design of deep foundations	82
Figure 4.8: Most commonly used dynamic formulas for deep foundations	82
Figure 4.9: Methodologies used for readjusting the pile penetration length	83
Figure 4.10: Expected effect of soil relaxation on the pile capacity at the EOD.....	83
Figure 4.11: Effect of soil setup on the pile capacity at the EOD	83
Figure 4.12: Histograms, frequency and 95% CI of the reported regional LRFD resistance factors for steel H-pile in different soil types	87
Figure 4.13: Summary of Responses from Iowa County Engineers to the Local Survey on Pile Design and Construction Practices	91
Figure 4.14: Main criteria of selecting the appropriate type of deep bridge foundation	92
Figure 4.15: Distribution of the most commonly used types of driven piles for bridges	92
Figure 4.16: Distribution of bridge types recommended for timber piles	93
Figure 4.17: Distribution of soil types recommended for use with timber piles	94
Figure 4.18: Personnel conducting the analysis and design of deep foundations in Iowa.....	95
Figure 4.19: Most commonly used design specifications by Iowa County engineers.....	95
Figure 4.20: Engineering private consulting firms that conduct bridge designs in Iowa	95
Figure 4.21: Most commonly used methods of analysis for the design of driven piles	96
Figure 4.22: Criteria determining pile driving termination	97
Figure 4.23: Frequency of performing quality control tests on driven piles	97
Figure 5.1: A flowchart describing the framework of developing the LRFD resistance factors for Iowa soils	103
Figure 5.2: Summary of the usable data available from PILOT in different soil types.....	104
Figure 5.3: Cumulative capacity for different piles from PILOT using different approaches of determining pile nominal capacity from SLT	106
Figure 5.4: A sample analysis of resistance factors for static methods was conducted using a wide range of β starting from 1.5 to 4.0 for steel driven piles in clay	109
Figure 6.1: Comparison between the accumulative actual PILOT pile capacities using Davisson and the predicted pile capacities using different static analysis methods.....	114
Figure 6.2: Goodness of fit test for the Blue Book method in sand.....	115
Figure 6.3: Goodness of fit test for the Blue Book method in clay	115
Figure 6.4: Goodness of fit test for the Blue Book method in mixed soil	115
Figure 6.5: Summary of the normal distributed PDFs of the K_{sx} for the 34 cases of steel H-piles designed in sand using different static analysis methods.....	117
Figure 6.6: Summary of the normal distributed PDFs of the K_{sx} for the 20 cases of steel H-piles designed in clay using different static analysis methods	117

Figure 6.7: Summary of the normal distributed PDFs of the K_{sx} for the 26 cases of steel H-piles designed in mixed soil using different static analysis methods	118
Figure 6.8: Summary of the lognormal distributed PDFs of the K_{sx} for the 34 cases of steel H-piles designed in sand using different static analysis methods	118
Figure 6.9: Summary of the lognormal distributed PDFs of the K_{sx} for the 20 cases of steel H-piles designed in clay using different static analysis methods	118
Figure 6.10: Summary of the lognormal distributed PDFs of the K_{sx} for the 26 cases of steel H-piles designed in mixed soil using different static analysis methods	119
Figure 6.11: Histogram and frequency distribution of K_{sx} for 34 cases of steel H-piles designed in sand using the Blue Book method	119
Figure 6.12: Histogram and frequency distribution of K_{sx} for 20 cases of steel H-piles designed in clay using the Blue Book method	119
Figure 6.13: Histogram and frequency distribution of K_{sx} for 26 cases of steel H-piles designed in mixed soil using the Blue Book method	120
Figure 6.14: Summary of the preliminary LRFD resistance factors for static methods and the corresponding efficiency factors based on a target reliability of 2.33 for sand soil	121
Figure 6.15: Summary of the preliminary LRFD resistance factors for static methods and the corresponding efficiency factors based on a target reliability of 2.33 for clay soil	122
Figure 6.16: Summary of the preliminary LRFD resistance factors for static methods and the corresponding efficiency factors based on a target reliability of 2.33 for mixed soil	122
Figure 6.17: Preliminary LRFD resistance factors for different static methods corresponding to a wide range of reliability indices in sand soils	123
Figure 6.18: Preliminary LRFD resistance factors for different static methods corresponding to a wide range of reliability indices in clay soils	123
Figure 6.19: Preliminary LRFD resistance factors for different static methods corresponding to a wide range of reliability indices in mixed soils	124
Figure 6.20: Efficiency factors for static methods corresponding to different β in sand	125
Figure 6.21: Efficiency factors for static methods corresponding to different β in clay	125
Figure 6.22: Efficiency factors for static methods corresponding to different β in mixed soil	126
Figure 6.23: Nominal and Factored pile design capacities using different static methods and compared to SLT results for Clarke – Clay soil	129
Figure 6.24: Nominal and Factored pile design capacities using different static methods and compared to SLT results for Cedar – Sand soil	129
Figure 6.25: Nominal and Factored pile design capacities using different static methods and compared to SLT results for Poweshiek – Mixed soil	130
Figure 6.26: Nominal measured and calculated capacities for the 10 field tested piles using Davisson's criterion versus static analysis methods	131
Figure 6.27: Factored measured and calculated capacities for the 10 field tested piles	

using Davisson's criterion versus static analysis methods	131
Figure 6.28: Accumulative actual PILOT pile capacities using Davisson and the predicted pile capacities using WEAP based on different soil input methods	134
Figure 6.29: Goodness of fit test for the WEAP based on Iowa DOT in sand	135
Figure 6.30: Goodness of fit test for the WEAP based on Iowa DOT in clay	135
Figure 6.31: Goodness of fit test for the WEAP based on Iowa DOT in mixed soil.....	136
Figure 6.32: Summary of the normal distributed PDFs of the K_{sx} for the 11 cases of steel H-piles designed using WEAP in sand using different input approaches	137
Figure 6.33: Summary of the normal distributed PDFs of the K_{sx} for the 12 cases of steel H-piles designed using WEAP in clay using different input approaches	137
Figure 6.34: Summary of the normal distributed PDFs of the K_{sx} for the nine cases of steel H-piles designed using WEAP in mixed soil using different input approaches	137
Figure 6.35: Summary of the lognormal distributed PDFs of the K_{sx} for the 11 cases of steel H-piles designed using WEAP in sand based on different input approaches	138
Figure 6.36: Summary of the lognormal distributed PDFs of the K_{sx} for the 12 cases of steel H-piles designed using WEAP in clay based on different input approaches	138
Figure 6.37: Summary of the lognormal distributed PDFs of the K_{sx} for the nine cases of steel H-piles designed using WEAP in mixed soil based on different input approaches	138
Figure 6.38: Histogram and frequency distribution of K_{sx} for 11 cases of steel H-piles designed using WEAP in sand based on the Iowa DOT method	139
Figure 6.39: Histogram and frequency distribution of K_{sx} for 12 cases of steel H-piles designed using WEAP in clay based on the Iowa DOT method	139
Figure 6.40: Histogram and frequency distribution of K_{sx} for nine cases of steel H-piles designed using WEAP in mixed soil based on the Iowa DOT method	139
Figure 6.41: Summary of the preliminary LRFD resistance factors of WEAP and the corresponding efficiency factors based on a target reliability of 2.33 for sand soil.....	141
Figure 6.42: Summary of the preliminary LRFD resistance factors for WEAP and the corresponding efficiency factors based on a target reliability of 2.33 for clay soil.....	141
Figure 6.43: Summary of the preliminary LRFD resistance factors for WEAP and the corresponding efficiency factors based on a target reliability of 2.33 for mixed soil.....	142
Figure 6.44: Preliminary LRFD resistance factors for WEAP corresponding to a wide range of reliability indices in sand soils	142
Figure 6.45: Preliminary LRFD resistance factors for WEAP corresponding to a wide range of reliability indices in clay soils	143
Figure 6.46: Preliminary LRFD resistance factors for WEAP corresponding to a wide	

range of reliability indices in mixed soils.....	143
Figure 6.47: Efficiency factors for WEAP corresponding to different β in sand	144
Figure 6.48: Efficiency factors for WEAP corresponding to different β in clay	145
Figure 6.49: Efficiency factors for WEAP corresponding to different β in mixed soil.....	145
Figure 6.50: Nominal and Factored pile design capacities using WEAP different soil input methods and compared to SLT results for Clarke – Clay soil.....	148
Figure 6.51: Nominal and Factored pile design capacities using WEAP different soil input methods and compared to SLT results for Cedar – Sand soil	148
Figure 6.52: Nominal and Factored pile design capacities using WEAP different soil input methods and compared to SLT results for Poweshiek – Mixed soil	148
Figure 6.53: Nominal measured and calculated capacities for the 10 field tested piles using Davisson’s criterion versus WEAP	150
Figure 6.54: Factored measured and calculated capacities for the 10 field tested piles using Davisson’s criterion versus WEAP	150
Figure 6.55: Soil setup design charts for WEAP and CAPWAP.....	154
Figure 6.56: Cumulative distribution of the ratio of WEAP to Iowa Blue Book	156
Figure 6.57: Normal distribution comparison for clay before and after considering construction control at EOD condition	157
Figure 6.58: Normal distribution comparison for mixed soil before and after considering construction control at EOD condition	158
Figure 6.59: Normal distribution comparison for sand soil before and after considering construction control at EOD condition	158
Figure 6.60: Normal distribution comparison for clay soil before and after considering additional construction control factor for soil setup	160
Figure 6.61: The maximum limit of the construction control factor at EOD for clay	162
Figure 6.62: The maximum limit of the construction control factor for the EOD plus setup condition for clay	163
Figure 6.63: The maximum limit of the construction control factor for the EOD condition for mixed soil.....	164
Figure 6.64: The maximum limit of the construction control factor for the EOD condition for sand soil.....	165
Figure 6.65: Accumulative actual PILOT pile capacities using Davisson and the predicted pile capacities using different dynamic formulas	168
Figure 6.66: Goodness of fit test for the Iowa DOT ENR formula in sand.....	169
Figure 6.67: Goodness of fit test for the Iowa DOT ENR formula in clay.....	169
Figure 6.68: Goodness of fit test for the Iowa DOT ENR formula in mixed soils.....	170
Figure 6.69: Summary of the normal distributed PDFs of the K_{sx} for the 13 cases of steel H-piles designed using different dynamic formulas in sand	170
Figure 6.70: Summary of the normal distributed PDFs of the K_{sx} for the eight cases of steel H-piles designed using different dynamic formulas in clay	170
Figure 6.71: Summary of the normal distributed PDFs of the K_{sx} for the 13 cases of steel	

H-piles designed using different dynamic formulas in mixed soils	171
Figure 6.72: Summary of the lognormal distributed PDFs of the K_{sx} for the 13 cases of steel H-piles designed using different dynamic formulas in sand	171
Figure 6.73: Summary of the lognormal distributed PDFs of the K_{sx} for the eight cases of steel H-piles designed using different dynamic formulas in clay	171
Figure 6.74: Summary of the lognormal distributed PDFs of the K_{sx} for the 13 cases of steel H-piles designed using different dynamic formulas in mixed soils	172
Figure 6.75: Histogram and frequency distribution of K_{sx} for 11 cases of steel H-piles designed using Iowa DOT ENR formula in sand	172
Figure 6.76: Histogram and frequency distribution of K_{sx} for 12 cases of steel H-piles designed using Iowa DOT ENR formula in clay	172
Figure 6.77: Histogram and frequency distribution of K_{sx} for nine cases of steel H-piles designed using Iowa DOT ENR formula in mixed soils	173
Figure 6.78: Summary of the preliminary LRFD resistance factors of dynamic formulas and the corresponding efficiency factors based on a target reliability of 2.33 for sand soil.....	174
Figure 6.79: Summary of the preliminary LRFD resistance factors for dynamic formulas and the corresponding efficiency factors based on a target reliability of 2.33 for clay soil	175
Figure 6.80: Summary of the preliminary LRFD resistance factors for dynamic formulas and the corresponding efficiency factors based on a target reliability of 2.33 for mixed soil.....	175
Figure 6.81: Preliminary LRFD resistance factors for different dynamic formulas corresponding to a wide range of reliability indices in sand soils.....	176
Figure 6.82: Preliminary LRFD resistance factors for different dynamic formulas corresponding to a wide range of reliability indices in clay soils.....	176
Figure 6.83: Preliminary LRFD resistance factors for different dynamic formulas corresponding to a wide range of reliability indices in mixed soils	177
Figure 6.84: Efficiency factors for dynamic formulas corresponding to different β in sand.....	178
Figure 6.85: Efficiency factors for dynamic formulas corresponding to different β in clay	178
Figure 6.86: Efficiency factors for dynamic formulas corresponding to different β in mixed soil.....	179
Figure 6.87: Nominal and Factored pile design capacities using different dynamic formulas and compared to SLT results for Clarke – Clay soil	182
Figure 6.88: Nominal and Factored pile design capacities using different dynamic formulas and compared to SLT results for Cedar – Sand soil	182
Figure 6.89: Nominal and Factored pile design capacities using different dynamic formulas and compared to SLT results for Poweshiek – Mixed soil.....	182
Figure 6.90: Nominal measured and calculated capacities for the 10 field tested piles using Davisson’s criterion versus dynamic formulas	183
Figure 6.91: Factored measured and calculated capacities for the 10 field tested piles using Davisson’s criterion versus dynamic formulas	184

Figure 6.92: AD test for the Iowa DOT Modified ENR to Iowa Blue Book ratio in sand soil for the usable steel piles for dynamic formulas	185
Figure 6.93: AD test for the Iowa DOT Modified ENR to Iowa Blue Book ratio in clay soil for the usable steel piles for dynamic formulas	185
Figure 6.94: AD test for the Iowa DOT Modified ENR to Iowa Blue Book ratio in mixed soil for the usable steel piles for dynamic formulas	185
Figure 6.95: Original and corrected lognormal probability distributions in sand soil.....	186
Figure 6.96: Original and corrected lognormal probability distributions in clay soil	186
Figure 6.97: Original and corrected lognormal probability distributions in mixed soil	187
Figure 7.1: Resistance factors for static methods corresponding to different β in sand soil	191
Figure 7.2: Resistance factors for static methods corresponding to different β in clay soil	191
Figure 7.3: Resistance factors for static methods corresponding to different β in mixed soil.....	192
Figure 7.4: Resistance factors for WEAP corresponding to different β in sand.....	195
Figure 7.5: Resistance factors for WEAP corresponding to different β in clay for EOD.....	196
Figure 7.6: Resistance factors for WEAP corresponding to different β in clay for setup	196
Figure 7.7: Resistance factors for WEAP corresponding to different β in clay for BOR.....	197
Figure 7.8: Resistance factors for WEAP corresponding to different β in mixed soil	197
Figure 7.9: Resistance factors for dynamic formulas and steel H-piles corresponding to different β in sand	199
Figure 7.10: Resistance factors for dynamic formulas and steel H-piles corresponding to different β in clay.....	200
Figure 7.11: Resistance factors for dynamic formulas and steel H-piles correspond to different β in mixed soil.....	200
Figure 7.12: Resistance factors for dynamic formulas and timber piles correspond to different β	202
Figure 7.13: Ratio of pile driving resistance at 24-hour retap to target driving resistance at EOD plotted in respect to N_a	213
Figure A.1. Flowchart representing questions of the first section of the nationwide survey	227
Figure A.2. Flowchart representing questions of the second section of the nationwide survey.....	228
Figure A.3. Continue questions of the second section of the nationwide survey	229
Figure A.4. Continue questions of the second section of the nationwide survey	230
Figure A.5. Continue questions of the second section of the nationwide survey	231
Figure A.6. Flowchart representing questions of the third section of the nationwide survey.....	232
Figure A.7. Flowchart representing questions of the fourth section of the nationwide survey.....	233
Figure A.8. Flowchart representing questions of the first section of the local survey	234
Figure A.9. Flowchart representing questions of the second section of the local survey	234

Figure A.10. Flowchart representing questions of the third section of the local survey	235
Figure A.11. Flowchart representing questions of the third/fourth sections of the local survey.....	236
Figure A.12. Flowchart representing questions of the fourth section of the local survey	237
Figure B.1. Goodness of fit test for the SPT-Meyerhof method in sand	238
Figure B.2. Goodness of fit test for the α -API method in sand	238
Figure B.3. Goodness of fit test for the β -Method in sand	239
Figure B.4. Goodness of fit test for the Nordlund method in sand	239
Figure B.5. Goodness of fit test for the Blue Book method in sand	239
Figure B.6. Goodness of fit test for the SPT-Meyerhof method in clay	240
Figure B.7. Goodness of fit test for the α -API method in clay	240
Figure B.8. Goodness of fit test for the β -Method in clay	240
Figure B.9. Goodness of fit test for the Nordlund method in clay.....	241
Figure B.10. Goodness of fit test for the Blue Book method in clay.....	241
Figure B.11. Goodness of fit test for the SPT-Meyerhof method in mixed soil.....	241
Figure B.12. Goodness of fit test for the α -API method in mixed soil.....	242
Figure B.13. Goodness of fit test for the β -Method in mixed soil	242
Figure B.14. Goodness of fit test for the Nordlund method in mixed soil	242
Figure B.15. Goodness of fit test for the Blue Book method in mixed soil.....	243
Figure B.16. Histogram and frequency distribution of K_{sx} for 35 cases of steel H-piles designed in sand using the SPT-Meyerhof method	243
Figure B.17. Histogram and frequency distribution of K_{sx} for 35 cases of steel H-piles designed in sand using the α -API method	243
Figure B.18. Histogram and frequency distribution of K_{sx} for 35 cases of steel H-piles designed in sand using the β -method.....	244
Figure B.19. Histogram and frequency distribution of K_{sx} for 35 cases of steel H-piles designed in sand using the Nordlund method.....	244
Figure B.20. Histogram and frequency distribution of K_{sx} for 15 cases of steel H-piles designed in clay using the SPT-Meyerhof method.....	244
Figure B.21. Histogram and frequency distribution of K_{sx} for 15 cases of steel H-piles designed in clay using the α -API method	245
Figure B.22. Histogram and frequency distribution of K_{sx} for 15 cases of steel H-piles designed in clay using the β -method	245
Figure B.23. Histogram and frequency distribution of K_{sx} for 15 cases of steel H-piles designed in clay using the Nordlund method	245
Figure B.24. Histogram and frequency distribution of K_{sx} for 32 cases of steel H-piles designed in mixed soil using the SPT-Meyerhof method.....	246
Figure B.25. Histogram and frequency distribution of K_{sx} for 32 cases of steel H-piles designed in mixed soil using the α -API method.....	246

Figure B.26. Histogram and frequency distribution of K_{sx} for 32 cases of steel H-piles designed in mixed soil using the β -method	246
Figure B.27. Histogram and frequency distribution of K_{sx} for 32 cases of steel H-piles designed in mixed soil using the Nordlund method	247
Figure B.28. Nominal and Factored pile design capacities using different static methods and compared to SLT results for Mahaska – Mixed soil	247
Figure B.29. Nominal and Factored pile design capacities using different static methods and compared to SLT results for Mills – Clay soil	247
Figure B.30. Nominal and Factored pile design capacities using different static methods and compared to SLT results for Polk – Clay soil	248
Figure B.31. Nominal and Factored pile design capacities using different static methods and compared to SLT results for Jasper – Clay soil	248
Figure B.32. Nominal and Factored pile design capacities using different static methods and compared to SLT results for Clarke – Clay soil	248
Figure B.33. Nominal and Factored pile design capacities using different static methods and compared to SLT results for Buchanan (long) – Clay soil	249
Figure B.34. Nominal and Factored pile design capacities using different static methods and compared to SLT results for Buchanan (short) – Mixed soil	249
Figure B.35. Nominal and Factored pile design capacities using different static methods and compared to SLT results for Poweshiek – Mixed soil	249
Figure B.36. Nominal and Factored pile design capacities using different static methods and compared to SLT results for Des Moines – Sand soil	250
Figure B.37. Nominal and Factored pile design capacities using different static methods and compared to SLT results for Cedar – Sand soil	250
Figure B.38. Goodness of fit test for the WEAP based on ST method in sand	251
Figure B.39. Goodness of fit test for the WEAP based on SA method in sand	251
Figure B.40. Goodness of fit test for the WEAP based on Blue Book method in sand	251
Figure B.41. Goodness of fit test for the WEAP based on Iowa DOT in sand	252
Figure B.42. Goodness of fit test for the WEAP based on Driven method in sand	252
Figure B.43. Goodness of fit test for the WEAP based on ST method in clay	252
Figure B.44. Goodness of fit test for the WEAP based on SA method in clay	253
Figure B.45. Goodness of fit test for the WEAP based on Blue Book method in clay	253
Figure B.46. Goodness of fit test for the WEAP based on Iowa DOT in clay	253
Figure B.47. Goodness of fit test for the WEAP based on Driven method in clay	254
Figure B.48. Goodness of fit test for the WEAP based on ST method in mixed soil	254
Figure B.49. Goodness of fit test for the WEAP based on SA method in mixed soil	254
Figure B.50. Goodness of fit test for the WEAP based on Blue Book method in mixed soil	255
Figure B.51. Goodness of fit test for the WEAP based on Iowa DOT in mixed soil	255
Figure B.52. Goodness of fit test for the WEAP based on Driven method in mixed soil	255
Figure B.53. Histogram and frequency distribution of K_{sx} for 13 cases of steel H-piles	

designed using WEAP in sand based on the ST method	256
Figure B.54. Histogram and frequency distribution of K_{sx} for 13 cases of steel H-piles designed using WEAP in sand based on the SA method.....	256
Figure B.55. Histogram and frequency distribution of K_{sx} for 13 cases of steel H-piles designed using WEAP in sand based on the Blue Book method	256
Figure B.56. Histogram and frequency distribution of K_{sx} for 13 cases of steel H-piles designed using WEAP in sand based on the Iowa DOT method	257
Figure B.57. Histogram and frequency distribution of K_{sx} for 13 cases of steel H-piles designed using WEAP in sand based on the Driven method.....	257
Figure B.58. Histogram and frequency distribution of K_{sx} for 8 cases of steel H-piles designed using WEAP in clay based on the ST method.....	257
Figure B.59. Histogram and frequency distribution of K_{sx} for 8 cases of steel H-piles designed using WEAP in clay based on the SA method	258
Figure B.60. Histogram and frequency distribution of K_{sx} for 8 cases of steel H-piles designed using WEAP in clay based on the Blue Book method	258
Figure B.61. Histogram and frequency distribution of K_{sx} for 8 cases of steel H-piles designed using WEAP in clay based on the Iowa DOT method	258
Figure B.62. Histogram and frequency distribution of K_{sx} for 8 cases of steel H-piles designed using WEAP in clay based on the Driven method	259
Figure B.63. Histogram and frequency distribution of K_{sx} for 12 cases of steel H-piles designed using WEAP in mixed soil based on the ST method.....	259
Figure B.64. Histogram and frequency distribution of K_{sx} for 12 cases of steel H-piles designed using WEAP in mixed soil based on the SA method	259
Figure B.65. Histogram and frequency distribution of K_{sx} for 12 cases of steel H-piles designed using WEAP in mixed soil based on the Blue Book method	260
Figure B.66. Histogram and frequency distribution of K_{sx} for 12 cases of steel H-piles designed using WEAP in mixed soil based on the Iowa DOT method	260
Figure B.67. Histogram and frequency distribution of K_{sx} for 12 cases of steel H-piles designed using WEAP in mixed soil based on the Driven method	260
Figure B.68. Summary of the lognormal distributed PDFs of the K_{sx} for the 13 cases of steel H-piles designed using WEAP in sand based on different input approaches	261
Figure B.69. Summary of the normal distributed PDFs of the K_{sx} for the 13 cases of steel H-piles designed using WEAP in sand using different input approaches	261
Figure B.70. Summary of the lognormal distributed PDFs of the K_{sx} for the 8 cases of steel H-piles designed using WEAP in clay based on different input approaches	261
Figure B.71. Summary of the normal distributed PDFs of the K_{sx} for the 8 cases of steel H-piles designed using WEAP in clay using different input approaches	262
Figure B.72. Summary of the lognormal distributed PDFs of the K_{sx} for the 12 cases of steel H-piles designed using WEAP in mixed soil based on different input approaches	262

Figure B.73. Summary of the normal distributed PDFs of the K_{sx} for the 12 cases of steel H-piles designed using WEAP in mixed soil using different input approaches.....	262
Figure B.74. Nominal and Factored pile design capacities using WEAP different soil input methods and compared to SLT results for Mahaska – Mixed soil	263
Figure B.75. Nominal and Factored pile design capacities using WEAP different soil input methods and compared to SLT results for Mills – Clay soil	263
Figure B.76. Nominal and Factored pile design capacities using WEAP different soil input methods and compared to SLT results for Polk – Clay soil	263
Figure B.77. Nominal and Factored pile design capacities using WEAP different soil input methods and compared to SLT results for Jasper – Clay soil	264
Figure B.78. Nominal and Factored pile design capacities using WEAP different soil input methods and compared to SLT results for Clarke – Clay soil.....	264
Figure B.79. Nominal and Factored pile design capacities using WEAP different soil input methods and compared to SLT results for Buchanan (long) – Mixed soil.....	264
Figure B.80. Nominal and Factored pile design capacities using WEAP different soil input methods and compared to SLT results for Buchanan (short) – Mixed soil.....	265
Figure B.81. Nominal and Factored pile design capacities using WEAP different soil input methods and compared to SLT results for Poweshiek – Mixed soil	265
Figure B.82. Nominal and Factored pile design capacities using WEAP different soil input methods and compared to SLT results for Des Moines – Sand soil.....	265
Figure B.83. Nominal and Factored pile design capacities using WEAP different soil input methods and compared to SLT results for Cedar– Sand soil	266
Figure B.84. Goodness of fit test for the Gates formula in sand	267
Figure B.85. Goodness of fit test for the FHWA formula in sand.....	267
Figure B.86. Goodness of fit test for the ENR formula in sand.....	267
Figure B.87. Goodness of fit test for the Iowa DOT ENR formula in sand	268
Figure B.88. Goodness of fit test for the Janbu formula in sand	268
Figure B.89. Goodness of fit test for the PCUBC formula in sand	268
Figure B.90. Goodness of fit test for the WSDOT formula in sand	269
Figure B.91. Goodness of fit test for the Gates formula in clay	269
Figure B.92. Goodness of fit test for the FHWA formula in clay	269
Figure B.93. Goodness of fit test for the ENR formula in clay	270
Figure B.94. Goodness of fit test for the Iowa DOT ENR formula in clay	270
Figure B.95. Goodness of fit test for the Janbu formula in clay	270
Figure B.96. Goodness of fit test for the PCUBC formula in clay	271
Figure B.97. Goodness of fit test for the WSDOT formula in clay	271
Figure B.98. Goodness of fit test for the Gates formula in mixed soils	271
Figure B.99. Goodness of fit test for the FHWA formula in mixed soils.....	272
Figure B.100. Goodness of fit test for the ENR formula in mixed soils.....	272

Figure B.101. Goodness of fit test for the Iowa DOT ENR formula in mixed soils	272
Figure B.102. Goodness of fit test for the Janbu formula in mixed soils	273
Figure B.103. Goodness of fit test for the PCUBC formula in mixed soils	273
Figure B.104. Goodness of fit test for the WSDOT formula in mixed soils	273
Figure B.105. Histogram and frequency distribution of K_{sx} for 11 cases of steel H-piles designed using Gates formula in sand	274
Figure B.106. Histogram and frequency distribution of K_{sx} for 11 cases of steel H-piles designed using FHWA formula in sand.....	274
Figure B.107. Histogram and frequency distribution of K_{sx} for 11 cases of steel H-piles designed using ENR formula in sand	274
Figure B.108. Histogram and frequency distribution of K_{sx} for 11 cases of steel H-piles designed using Iowa DOT ENR formula in sand	275
Figure B.109. Histogram and frequency distribution of K_{sx} for 11 cases of steel H-piles designed using Janbu formula in sand	275
Figure B.110. Histogram and frequency distribution of K_{sx} for 11 cases of steel H-piles designed using PCUBC formula in sand	275
Figure B.111. Histogram and frequency distribution of K_{sx} for 11 cases of steel H-piles designed using WSDOT formula in sand	276
Figure B.112. Histogram and frequency distribution of K_{sx} for 12 cases of steel H-piles designed using Gates formula in clay	276
Figure B.113. Histogram and frequency distribution of K_{sx} for 12 cases of steel H-piles designed using FHWA formula in clay	276
Figure B.114. Histogram and frequency distribution of K_{sx} for 12 cases of steel H-piles designed using ENR formula in clay	277
Figure B.115. Histogram and frequency distribution of K_{sx} for 12 cases of steel H-piles designed using Iowa DOT ENR formula in clay	277
Figure B.116. Histogram and frequency distribution of K_{sx} for 12 cases of steel H-piles designed using Janbu formula in clay	277
Figure B.117. Histogram and frequency distribution of K_{sx} for 12 cases of steel H-piles designed using PCUBC formula in clay	278
Figure B.118. Histogram and frequency distribution of K_{sx} for 12 cases of steel H-piles designed using WSDOT formula in clay	278
Figure B.119. Histogram and frequency distribution of K_{sx} for 9 cases of steel H-piles designed using Gates formula in mixed soils	278
Figure B.120. Histogram and frequency distribution of K_{sx} for 9 cases of steel H-piles designed using FHWA formula in mixed soils.....	279
Figure B.121. Histogram and frequency distribution of K_{sx} for 9 cases of steel H-piles designed using ENR formula in mixed soils	279
Figure B.122. Histogram and frequency distribution of K_{sx} for 9 cases of steel H-piles designed using Iowa DOT ENR formula in mixed soils	279
Figure B.123. Histogram and frequency distribution of K_{sx} for 9 cases of steel H-piles designed using Janbu formula in mixed soils	280

Figure B.124. Histogram and frequency distribution of K_{sx} for 9 cases of steel H-piles designed using PCUBC formula in mixed soils	280
Figure B.125. Histogram and frequency distribution of K_{sx} for 9 cases of steel H-piles designed using WSDOT formula in mixed soils	280
Figure B.126. Summary of the lognormal distributed PDFs of the K_{sx} for the 11 cases of steel H-piles designed using different dynamic formulas in sand	281
Figure B.127. Summary of the normal distributed PDFs of the K_{sx} for the 11 cases of steel H-piles designed using different dynamic formulas in sand	281
Figure B.128. Summary of the lognormal distributed PDFs of the K_{sx} for the 12 cases of steel H-piles designed using different dynamic formulas in clay	281
Figure B.129. Summary of the normal distributed PDFs of the K_{sx} for the 12 cases of steel H-piles designed using different dynamic formulas in clay	282
Figure B.130. Summary of the lognormal distributed PDFs of the K_{sx} for the 9 cases of steel H-piles designed using different dynamic formulas in mixed soils	282
Figure B.131. Summary of the normal distributed PDFs of the K_{sx} for the 9 cases of steel H-piles designed using different dynamic formulas in mixed soils	282
Figure B.132. Nominal and Factored pile design capacities using dynamic formulas and compared to SLT results for Mahaska – Mixed soil.....	283
Figure B.133. Nominal and Factored pile design capacities using dynamic formulas and compared to SLT results for Mills – Clay soil	283
Figure B.134. Nominal and Factored pile design capacities using dynamic formulas and compared to SLT results for Polk – Clay soil.....	283
Figure B.135. Nominal and Factored pile design capacities using dynamic formulas and compared to SLT results for Jasper – Clay soil	284
Figure B.136. Nominal and Factored pile design capacities using dynamic formulas and compared to SLT results for Clarke – Clay soil	284
Figure B.137. Nominal and Factored pile design capacities using dynamic formulas and compared to SLT results for Buchanan (long) – Clay soil	284
Figure B.138. Nominal and Factored pile design capacities using dynamic formulas and compared to SLT results for Buchanan (short) – Mixed soil	285
Figure B.139. Nominal and Factored pile design capacities using dynamic formulas and compared to SLT results for Poweshiek – Mixed soil.....	285
Figure B.140. Nominal and Factored pile design capacities using dynamic formulas and compared to SLT results for Des Moines – Sand soil	285
Figure B.141. Nominal and Factored pile design capacities using dynamic formulas and compared to SLT results for Cedar – Sand soil	286

LIST OF TABLES

Table 2.1: Load factors used for LRFD resistance factors calibration by fitting to ASD	8
Table 2.2: Resistance factors and corresponding FS using calibration done by fitting to ASD with a DL/LL=3.0 (after Allen et al., 2005)	8
Table 2.3: AASHTO recommended random variables for loads (after Nowak, 1999)	12
Table 2.4: LRFD resistance factors for static analysis methods (after 2007 AASHTO).....	17
Table 2.5: LRFD resistance factors for dynamic analysis (after 2007 AASHTO).....	19
Table 2.6: The ϕ for number of static load tests conducted per site (after 2007 AASHTO).....	19
Table 2.7: Number of dynamic tests with signal matching analysis per site to be conducted during production pile driving (after 2007 AASHTO)	19
Table 2.8: LRFD resistance factors for dynamic analysis methods and dynamic formulas (after 2010 AASHTO)	20
Table 3.1: Different correlations between SPT N-values and different soil parameters	29
Table 3.2: D_r , ϕ , and γ corresponding to corrected SPT N-values (after Bowles, 1977)*	30
Table 3.3: Ranges of q_u and γ with respect to un-corrected SPT (after Bowles, 1977)*.....	30
Table 3.4: Different correlations between CPT and different soil parameters	30
Table 3.5: Approximate range of β and N_t coefficients (after Fellenius, 1991)	36
Table 3.6: Represents CPT C_f values (after the FHWA, 2007)	39
Table 3.7: Side resistance correlations for the SPT-Schmertmann method.....	42
Table 3.8: Tip resistance correlations for the SPT-Schmertmann method	42
Table 3.9: Critical bearing depth ratio for the SPT-Schmertmann method	43
Table 3.10: Evaluating K_δ for piles when $\omega = 0^\circ$ and $V = 0.0093$ to $0.093 \text{ m}^3/\text{m}$	44
Table 3.11: Evaluating K_δ for piles when $\omega = 0^\circ$ and $V = 0.093$ to $0.93 \text{ m}^3/\text{m}$	44
Table 3.12: Comparison of the commonly used static analysis methods for calculating pile capacity	49
Table 3.13: Summary of the equations required for different static methods	50
Table 3.14: Represents a comparison between the three dynamic analysis methods	53
Table 3.15: Representative values of hammer efficiency for use in dynamic pile driving formulas (after Bowles 1996)	58
Table 3.16: Recommended values for C_1 (inches/blow) - temporary elastic compression of the pile head and driving cap (after Chellis 1961)	59
Table 3.17: Recommended values for C_3 (inches/blow) - temporary elastic compression of the soil surrounding the pile (after Chellis 1961).....	59
Table 3.18: Summary of results from Chellis (1949)	63
Table 3.19: Summary of results from Spangler and Mumma (1958).....	64
Table 3.20: Summary of statistical parameters from Olson and Flaate (1967)	66
Table 3.21: Comparison between pile ultimate capacity determination methods including the appropriate pile types for each method, the recommended static load test type, advantages, limitations, and applicability for each method.....	73

Table 4.1: Summary of the reported LRFD resistance factors, sorted according to different pile types, static analysis methods, and soil types	86
Table 4.2: Mean values and standard deviations of the reported regional resistance factors according to different pile and soil types.....	88
Table 4.3: Mean values and standard deviations of the reported regional resistance factors according to different static analysis methods and soil types.....	88
Table 4.4: Comparison between the reported resistance factors and the recommended factors in NCHRP 507 and 2007 AASHTO-LRFD Specifications.....	88
Table 4.5: PILOT database summary	100
Table 5.1: Selected correlations used to determine soil parameters based on SPT N-values.....	104
Table 6.1: Nominal Davisson's capacity of the piles from PILOT, as well as those obtained for static analysis methods in clay	111
Table 6.2: Nominal Davisson's capacity of the piles from PILOT, as well as those obtained for static analysis methods in sand.....	112
Table 6.3: Nominal Davisson's capacity of the piles from PILOT, as well as those obtained for static analysis methods in mixed soil	113
Table 6.4: Summary of the normality checks using AD test as well as the 95% CI probability test for all the 15 subsets	116
Table 6.5: Summary of the preliminary regionally calibrated LRFD resistance factors for different static analysis methods in different soil types.....	121
Table 6.6: Different values of the LRFD resistance factors provided for static methods in design specifications versus the Iowa preliminary regionally calibrated factors	127
Table 6.7: Summary of the 10 field tests' ID, location, average soil formation, measured nominal capacities, and predicted nominal capacities using different static methods.....	130
Table 6.8: Nominal Davisson's capacity of the piles from PILOT as well as using WEAP analysis based on different soil input methods in clay	133
Table 6.9: Nominal Davisson's capacity of the piles from PILOT as well as using WEAP analysis based on different soil input methods in sand.....	133
Table 6.10: Nominal Davisson's capacity of the piles from PILOT as well as using WEAP analysis based on different soil input methods in mixed soil.....	134
Table 6.11: Summary of the preliminary regionally calibrated LRFD resistance factors for WEAP using different soil input methods in different soil types	140
Table 6.12: Different values of the LRFD resistance factors provided for WEAP in design specifications versus the Iowa preliminary regionally calibrated factors.....	146
Table 6.13: Summary of the 10 field tests' ID, location, average soil formation, measured nominal capacities, and predicted nominal capacities using WEAP.....	149
Table 6.14: Method dependent scale factors and concave factors for Eq. 6.2.....	151
Table 6.15: LRFD parameters for WEAP and CAPWAP at EOD, normal, BOR, and EOD plus setup	153
Table 6.16: The original resistance factors used in calculating the designed pile capacities	157

Table 6.17: Summary of recommended parameters for considering construction control.....	161
Table 6.18: Nominal Davisson's capacity of the piles from PILOT as well as using different dynamic formulas in clay.....	166
Table 6.19: Nominal Davisson's capacity of the piles from PILOT as well as using different dynamic formulas in mixed soil.....	167
Table 6.20: Nominal Davisson's capacity of the piles from PILOT as well as using different dynamic formulas in sand soil	167
Table 6.21: Summary of the preliminary regionally calibrated LRFD resistance factors for dynamic formulas in different soil types.....	174
Table 6.22: Different values of the LRFD resistance factors provided for dynamic formulas in design specifications versus the Iowa preliminary regionally calibrated factors.....	180
Table 6.23: Summary of the 10 field tests ID, location, average soil formation, measured nominal capacities, and the predicted nominal capacities using different dynamic formulas	183
Table 7.1: Recommended LRFD resistance factors for static methods.....	190
Table 7.2: Highest efficiency static methods and corresponding resistance factors.....	190
Table 7.3: Improved resistance factors for Iowa Blue Book method	193
Table 7.4: Recommended LRFD resistance factors for WEAP	194
Table 7.5: Highest efficiency WEAP methods and corresponding resistance factors.....	194
Table 7.6: Recommended LRFD resistance factors for dynamic formulas and steel H- piles.....	198
Table 7.7: Highest efficiency dynamic formulas and corresponding resistance factors for steel H-piles	199
Table 7.8: Recommended LRFD resistance factors for dynamic formulas and timber piles	201
Table 7.9: Highest efficiency dynamic formulas and corresponding resistance factors for timber piles	202
Table 7.10: Summary of recommended resistance factors for design	206
Table 7.11: Summary of recommended resistance factors for construction control	207
Table 7.12: Recommended resistance factors for design rounded to nearest 0.05	208
Table 7.13: Recommended resistance factors for construction control rounded to nearest 0.05	209
Table 7.14: Summary of 26 production steel H-piles that were retapped at 24 hours.....	212

ACKNOWLEDGMENTS

The authors would like to thank the Iowa Highway Research Board (IHRB) for sponsoring this research project. Special recognition to the following individuals who served on the technical advisory committee of this research project for their guidance and advice: Ahmad Abu-Hawash, Dean Bierwagen, Lyle Brehm, Ken Dunker, Kyle Frame, Steve Megivern, Curtis Monk, Michael Nop, Gary Novey, John Rasmussen, and Bob Stanley. The members of this committee represent Office of Bridges and Structures, Soils, Design Section, and Office of Construction of the Iowa Department of Transportation (DOT), the Federal Highway Administration (FHWA) Iowa Division, and the Iowa County Engineers. Finally, the authors express their gratitude to all respondents of the surveys conducted nationwide and locally, as well as Sandra Larson, Mark Dunn, and Norm McDonald.

CHAPTER 1: OVERVIEW

1.1. Introduction to LRFD

Various sources of uncertainties are inherent in the design loads and capacity calculations of driven piles commonly used for bridge foundations. Accordingly, engineers ensure safe designs of foundation by assuming a factor of safety based on their experience and subjective judgment. This methodology is historically known as the Allowable Stress Design (ASD) method or the Working Stress Design (WSD) method. On the other hand, these uncertainties can be quantified using probability-based theories and be accounted for in design, thereby achieving bridge foundations engineered with consistent levels of reliability. The above reasons motivate the development of the Load and Resistance Factor Design (LRFD) method.

One of the many benefits of developing the LRFD approach for design of bridge pile foundations is handling the uncertainties associated with different design parameters by utilizing a rational framework of probability theory, thereby leading to a constant degree of reliability. Moreover, the LRFD provides a consistent design approach for the entire bridge (i.e., superstructure and substructure) and ensures an overall uniformity in design and construction. According to Paikowsky et al. (2004), the LRFD-based designs are intended to yield efficient foundation designs with reliabilities equal to or greater than those resulting from the ASD method.

Over the past few decades, significant efforts have been directed towards the application and development of the LRFD resistance factors for deep bridge foundations. Nevertheless, the application of LRFD to bridge substructures has been relatively slow (DiMaggio, 1999), due to the various deficiencies embedded in the early LRFD codes and design specifications, accounting for large uncertainties in soil properties, thus resulting in conservative resistance factors. Consequently, the Federal Highway Administration (FHWA) allowed the development of regionally calibrated LRFD resistance factors for bridge substructures, utilizing existing databases. This calibration requires the existence of adequate local databases that provide comprehensive information about previous deep foundation practices, including pile load tests and quality soil data. According to the recommendations by the American Association of State Highway and Transportation Officials (AASHTO 2008 interims), developing regionally calibrated resistance factors that depends on the local soil conditions and practices could even lead to a more cost effective design.

In 2000, the FHWA mandated that all new bridges initiated in the United States after October 1, 2007 must follow the LRFD approach. Since then, there has been a progressive move toward the increased use of the LRFD in geotechnical design practices among the State Departments of Transportation (DOTs). Accordingly, several State DOTs started developing their own regionally calibrated resistance factors to reduce the conservatism associated with the design specifications, as well as to build on the long-gained local experience and available pile load test databases.

1.2. Scope of Research

The overall scope of this research was to develop regionally calibrated LRFD resistance factors for bridge pile foundations in Iowa based on reliability theory, focusing on the strength limit states, along with incorporating the construction control aspects and soil setup into the design process. This was attained after examining the current pile design and construction procedures used by Iowa DOT and developing the appropriate LRFD recommendations that are consistent with the available local database and bridge design practices. This scope was achieved based on two parts: a) the recently developed local database of Pile Load Tests (PILOT), and b) ten full-scale instrumented pile Static Load Tests (SLTs) at bridge sites located in different geological conditions in the State of Iowa. The volume I report of this project (Roling et al., 2010) provided a detailed description of the PILOT database, while the volume II report (Ng et al., 2010) presented the results of the full-scale pile tests and associated geotechnical investigations. This report in the third volume of this series focuses on the calibration of the LRFD resistance factors for static and dynamic pile analysis methods as well as for dynamic formulas. Using the outcomes of this research, a design guide to be used by the Iowa DOT and county engineering offices is currently under development, which will be presented in the next and final volume.

1.3. Research Plan

In this report, three major tasks were planned and executed to successfully achieve the scope of research. The following information briefly describes the three tasks and the main components involved in each.

Task A: Literature Review and Collection of Important Historical Information

The first task involved a comprehensive literature review of different design approaches used for bridge pile foundations including ASD and LRFD methods. This review detailed the basic principles of the LRFD along with the typical calibration framework according to the AASHTO guidelines and other design specifications. An inclusive collection of the work previously conducted by different State DOTs regarding the development of LRFD resistance factors is provided in addition to the recent applicatory research. The first task also incorporated a review of different pile analysis methods, including static and dynamic methods, as well as dynamic formulas. In order to develop the LRFD resistance factors, backgrounds on each of the local “In-house” methods used by Iowa DOT were presented. The last component of the first task was the conducting of both a nationwide and a local survey to State DOTs and Iowa County engineers, respectively, to better understand the current/prospective design and construction practices.

Task B: Analysis of Data and Preliminary Recommendations

In this task, preliminary regionally calibrated LRFD resistance factors for bridge pile foundations were developed based on the local database (PILOT). The database was sorted into several categories based on different pile and soil types. The resistance factors were developed for each category using the First Order Second Moment (FOSM) reliability method and compared to the previously used ASD factor of safety. This analysis was conducted for the most commonly used static and dynamic methods and formulas, as well as for the Iowa DOT in-house methods. Aside from the resistance factors, other parameters were developed to provide a measure of the relative

efficiency and economy between the different methods. One main component of this task was the consideration of the construction control aspects in the design, which was attained by combining the static and dynamic methods during the design stage. Moreover, the amount of gain in the pile capacity due to soil setup with respect to time was studied herein and the corresponding resistance factors were calculated. The last component of this task was to provide a reliable, simple, and cost-effective design and construction procedure based on the preliminary LRFD resistance factors developed for bridge pile foundations in Iowa.

Task C: Verification and Final Recommendations

The main purpose of this task was to examine the performance of the developed preliminary LRFD resistance factors by means of the recently conducted 10 full-scale pile load tests covering most soil formations in Iowa. In this task, the preliminary resistance factors were statistically tested and compared to field measured capacities to ensure the LRFD-based pile designs are safe, reliable, consistent, and economic. A comparison was performed between the regionally calibrated factors and the AASHTO recommendations. After verification and presentation of the preliminary results to the advisory panel, the research was focused on developing the final LRFD recommendations, which are then integrated into the design guide.

1.4. Benefits of the Research

This research has numerous direct benefits to the bridge infrastructure in Iowa. First, the development and implementation of the LRFD approach will ensure uniform reliability and consistency in the design and construction processes of bridge pile foundations. Second, the research outcomes will enable the Iowa DOT to fulfill the FHWA requirements that have mandated the use of the LRFD since October 2007. One indirect benefit of this research is the development of a permanent LRFD calibration framework, which will add to the existing knowledge and database, thus providing an opportunity to advance future foundation design and practice.

1.5. Report Outline

This report consists of eight chapters describing the literature, development, verification, and recommendations of the regionally calibrated LRFD resistance factors for Iowa DOT. A brief summary of the content in each chapter is presented below:

- **Chapter 1 – Overview:** A brief introduction to the LRFD advantages compared to the ASD method, as well as the overall scope and benefits of the research.
- **Chapter 2 – Design of Pile Foundations:** A literature review and background information on the principles and development of the LRFD resistance factors for geotechnical uses; a discussion of the typical calibration framework as well as the associated construction control aspects; and an evaluation of similar studies performed by other State DOTs, as well as the related research work conducted on the topic.
- **Chapter 3 – Different Pile Analysis Procedures:** Introduction to the basic principles of static and dynamic analysis methods as well as dynamic formulas used in the design and construction of pile foundations; and the basic correlations required for determining various soil properties from laboratory and field tests.

- **Chapter 4 – *Collection of Data*:** Major findings of two recently developed nationwide and local surveys issued to State DOTs and Iowa County engineers, respectively, concerning the current LRFD design and construction practices of deep bridge foundations; and an overview on the locally developed database (PILOT) and the full-scale pile and soil testing plan.
- **Chapter 5 – *Selected Calibration Method*:** Summary of the calibration framework selected for developing the regionally calibrated LRFD resistance factors with consideration to the local design and practice conditions.
- **Chapter 6 – *Preliminary Resistance Factors Calculation*:** Preliminary LRFD resistance factors for static and dynamic analysis methods as well as dynamic formulas; correlations between different methods to account for the construction control aspects in the design stage; the effect of soil setup on the pile capacity and the corresponding resistance factors; and verification and tests of the performance of the preliminary LRFD resistance factors; and assessments to the current codes and design specifications to show possible cost savings associated with the regionally calibrated resistance factors.
- **Chapter 7 – *Design and Construction Recommendations*:** Final recommendations for direct use of the LRFD resistance factors in the design and construction processes of bridge pile foundations in Iowa. The final LRFD resistance factors were calculated based on adjustments to PILOT database to include the recently conducted pile static load tests.
- **Chapter 8 – *Summary and Conclusions*:** Summary of the work completed as well as the major outcomes and conclusions of the study; and necessary future research direction.

CHAPTER 2: DESIGN OF PILE FOUNDATIONS

This chapter provides a detailed review and background information on the principles and development of the Load and Resistance Factor Design (LRFD) approach for geotechnical uses. In addition, the chapter summarizes the typical resistance factor calibration framework and the associated construction control aspects.

2.1. Allowable Stress Design

From the early 1800s until the mid-1950s, the ASD approach has been used in the design of superstructures and substructures, in which the actual loads to act on the structures were compared to the capacity (or resistance) and an adequate Factor of Safety (FS) was ensured. According to Paikowsky et al. (2004), a pile design based on the ASD approach cannot ensure consistent and reliable performance of the foundations. This major drawback of the ASD is due to the ignoring of various sources and levels of uncertainty associated with loads and capacities of deep foundations. Consequently, the selected FS for deep foundations is highly conservative. However, the FS can be typically reduced when extreme loads, such as collision and seismic loads, are used in the design (Allen, 2005). Engineers generally assumed the FS based on different levels of confidence in the design and construction control. Particularly in the design of deep foundations, selection of the appropriate FS was greatly dependent on the experience and subjective judgment of the engineer (Paikowsky et al., 2004). According to Becker and Devata (2005), loads and capacities are probabilistic, not deterministic in nature, and thus the artificial FS must be replaced by a probability-based design approach that better deals with rational geotechnical properties.

2.2. Load and Resistance Factor Design

Since the mid-1950s, the LRFD approach has been developed for structural design with the objective of ensuring a uniform degree of reliability throughout the structure. The basic hypothesis of the LRFD is quantifying the uncertainties based on probabilistic approaches, which aims to achieve engineered designs with consistent levels of reliability (or probability of failure). In the LRFD approach, different load types and combinations are multiplied by load factors while resistances are multiplied by resistance factors, and the factored loads should not exceed the factored resistances by any amount. There are several advantages to using the LRFD approach instead of the ASD approach for designing deep foundations. The most important advantage of the LRFD approach is handling the uncertainties associated with design parameters by utilizing a rational framework of probability theory, leading to a constant degree of reliability. Consequently, the LRFD provides a consistent design approach for the entire structure (i.e., superstructure and substructure), which improves the overall design and construction perspective. Furthermore, in the design process, the LRFD approach does not require the same amount of experience and engineering judgment as the ASD approach.

2.2.1. Basic Principles

In the LRFD approach, loads are multiplied by load factors that are usually greater than one, while capacities are multiplied by resistance factors less than one. A simple definition of failure is the instance, in which the factored loads exceed the factored capacities. The basic equation of

the LRFD-based design can be expressed as follows:

$$\phi_i R_i \geq \sum \gamma_i Q_i \quad [2.1]$$

where R_i is the resistance, ϕ_i is the resistance factor, Q_i is structural load, and γ_i is the load factor. The uncertainties associated with resistances and loads can be defined through the distribution of their Probability Density Functions (PDFs). As can be seen in Figure 2.1, the probabilistic approach used for the LRFD development allows for determination of the overlap area between the PDFs of loads and resistances. This overlap area is statistically restricted to a certain acceptable level, which defines the acceptable risk of failure. According to Kyung (2002), the overlap area depends on: 1) the relative position of the PDFs, which is determined by μ_Q and μ_R (i.e., the mean bias for loads and resistances, respectively); 2) the dispersion of the PDFs, determined by σ_Q and σ_R (i.e., the standard deviation for loads and resistances, respectively); and 3) the shape of the PDFs.

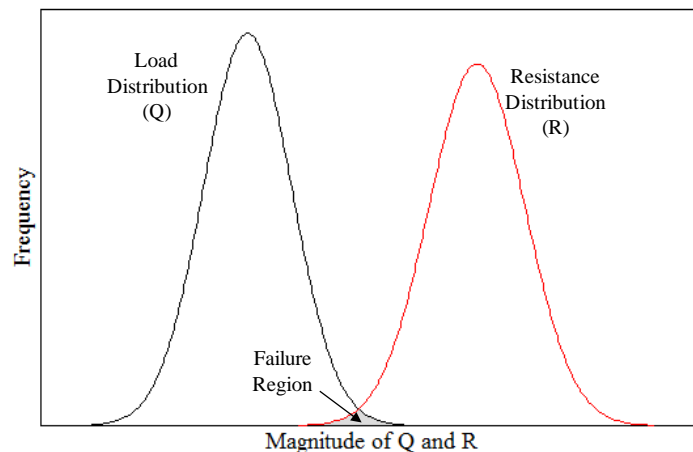


Figure 2.1: LRFD failure criterion between the PDFs of load and resistance

2.2.2. Implementation

Over the past two decades, significant efforts have been directed towards development and application of the LRFD approach in geotechnical engineering. In 1989, the American Association of State Highway and Transportation Officials (AASHTO) developed their first geotechnical LRFD specifications. In the early 1990's, the FHWA Manual for the Design of Bridge Foundations was released, followed by the National Corporate Highway Research Program (NCHRP) Report 343 by Barker et al. (1991). The NCHRP Report 343 later became the basis for the foundation section of the 1994 AASHTO Bridge Design Specifications (AASHTO, 1994). The AASHTO specifications were used in the foundations of offshore structures (Hamilton and Murff, 1992; Tang, 1993) as well as general foundation design (Kulhawy et al., 1996). The 1994 AASHTO Specifications mainly focused on load uncertainties rather than resistance uncertainties and did not include many subjective factors in geotechnical practice.

The 2004 AASHTO-LRFD Design Specifications (AASHTO, 2004) were also developed based on the report by Barker et al. (1991); however, the LRFD resistance factors were based on reliability theory along with fitting to the FS of the ASD approach. It was found that the LRFD

resistance factors calibrated by fitting to the ASD did not provide the desired level of reliability (Withiam et al., 1998). To overcome this problem, the NCHRP and FHWA funded research in developing LRFD recommendations, resulting in two major reports by Paikowsky, et al. (2004), and Allen et al. (2005). The 2007 AASHTO-LRFD bridge design specifications (2008 revised interims) include the outcomes of the study by Allen et al. (2005) in addition to the details provided by Barker et al. (1991) and Paikowsky et al. (2004).

Although the LRFD approach for designing structural elements has been well established and implemented in design codes around the world, its application to geotechnical design has been relatively slow (DiMaggio, 1999). This motivated the FHWA to mandate the application of the LRFD in bridges initiated after October 1, 2007 in the United States. Despite the FHWA mandated deadline, not all State Departments of Transportation (DOTs) have adopted the LRFD in their foundation designs. This was suspected to be due to the increased cost of foundations as a result of the conservatism in the LRFD bridge design specifications, which accounts for the large variation in soil parameters, as well as the different levels of uncertainty associated with determining the capacity of deep foundations (Paikowsky et al., 2004). Consequently, regionally calibrated resistance factors are permitted in LRFD to minimize the unnecessary conservatism built into the design if these factors are developed in a consistent manner with the approach suggested in the 2007 AASHTO-LRFD specifications. Two different calibration techniques were used to develop the LRFD geotechnical resistance factors. The first was proposed by Barker et al. (1991) using the fitting to the ASD method, and the second is the reliability theory used by Paikowsky et al. (2004). The following sections provide a brief discussion on both techniques.

2.2.3. Calibration by Fitting to ASD

According to Allen (2005), fitting a new design approach to an old one is initially valid when beginning to mandate a new design specification that depends on a different design philosophy. In the case of LRFD, calibration by fitting to ASD is used if the data required for the statistical analysis is not available. In this case, the LRFD resistance factors obtained by fitting to the ASD method should be only used as a benchmark to provide the same degree of safety that was provided by the ASD. However, this does not satisfy the LRFD reliability based requirements. Calibration by fitting can be performed using the following equation:

$$\phi = \frac{\gamma_{DL}(\frac{DL}{LL}) + \gamma_{LL}}{(\frac{DL}{LL} + 1)FS} \quad [2.2]$$

where

ϕ = Resistance factor

γ_{DL} = Load factor for Dead Loads (DL) assumed in according to Table 2.1

γ_{LL} = Load factor for Live Loads (LL) assumed in according to Table 2.1

DL/LL = Dead load to live load ratio

From Eq. [2.2], it can be observed that the resistance factor mainly depends on the DL to LL ratio. The DL/LL ratio could range between 1.0 and 4.0 for bridge structures depending on the bridge span and other factors. Barker et al., (1991), recommended a DL/LL ratio of 3.0 for bridge structures. On the other hand, Paikowsky et al., (2004), suggested that the ratio should be within the range of 2.0 to 2.5, noting that this range is reasonable and applicable for long span

bridges. According to Allen (2005) and Paikowsky et al. (2004), the DL/LL ratio has a small influence on the LRFD resistance factors when calibrated based on the reliability theory, which will be discussed later in this chapter. Allen (2005) considered a DL/LL ratio of 3.0 to be consistent with the previous work done by Barker (1991), and thus it can directly compare with the developed resistance factors (see Table 2.2). In the State of Iowa, the DOT is using a DL/LL ratio of 1.5. However, as previously mentioned, the differences in DL/LL ratio do not greatly influence the values of the calibrated resistance factors. In case of DL/LL = 3.0, a more simplified correlation between the LRFD resistance factor and the ASD factor of safety can be found, where Eq. [2.2] can be rewritten as:

$$FS = \frac{\gamma_{DL} \frac{DL}{LL} + \gamma_{LL}}{\phi \left(\frac{DL}{LL} + 1 \right)} \quad [2.3]$$

This means that in case of DL/LL = 3.0 and using the 2004 AASHTO load factors:

$$\phi = \frac{1.25(3.0) + 1.75}{(3.0 + 1)FS} = \frac{1.375}{FS} \quad [2.4a]$$

In addition, in case of DL/LL = 3.0 and using the load factors from Barker et al., (1991):

$$\phi = \frac{1.30(3.0) + 2.17}{(3.0 + 1)FS} = \frac{1.518}{FS} \quad [2.4b]$$

Table 2.1: Load factors used for LRFD resistance factors calibration by fitting to ASD

Load Type	Recommended LFD Load Factors (after Barker et al., 1991)	Recommended LRFD Load Factors (after 2004 AASHTO specifications)
Dead Load	1.30	1.25
Live Load	2.17	1.75

Table 2.2: Resistance factors and corresponding FS using calibration done by fitting to ASD with a DL/LL=3.0 (after Allen et al., 2005)

Factor of Safety	Resistance Factor	
	Recommended LRFD Factors (after Barker et al., 1991)	Recommended LRFD Factors (after 2004 AASHTO specifications)
1.5	1.00	0.92
1.8	0.84	0.76
1.9	0.80	0.72
2.0	0.76	0.69
2.25	0.67	0.61
2.5	0.61	0.55
2.75	0.55	0.50
3.0	0.51	0.46
3.5	0.43	0.39
4.0	0.38	0.34

2.2.4. Calibration using Reliability Theory

The objective of the reliability theory is to limit the probability of failure (P_f) of structures, i.e., probability of loads exceeding the resistances to a certain acceptable extent. As shown in Figure 2.1, Q and R are two PDFs representing the loads and resistances, respectively. As previously discussed, the area of overlap between the two PDFs is considered as failure. By subtracting the two PDFs (i.e., $R - Q$), the area to the left of the zero axis is considered to be the failure region (see Figure 2.2). In this case, the probability of failure can be replaced by the reliability index (β). The reliability index stands for the number of standard deviations (σ) representing the distance between the zero axis and the mean of $R - Q$. The general process used by Barker, et al. (1991) and Paikowsky, et al. (2004) to develop the regionally calibrated LRFD resistance factors based on the reliability theory is as follows:

- Gather the data required for statistical analysis
- Calculate parameters such as the mean, standard deviation, and Coefficient of Variation (COV) for load and resistance PDFs
- Determine the best-fit of each PDF (e.g., normal, lognormal)
- Select the appropriate statistical method for calibration
- Select a target β based on the margin of safety required in design specifications, and by considering the recommended levels of reliability used for geotechnical designs
- Use the recommended load factors provided in the design code
- Calculate the regionally calibrated LRFD resistance factors

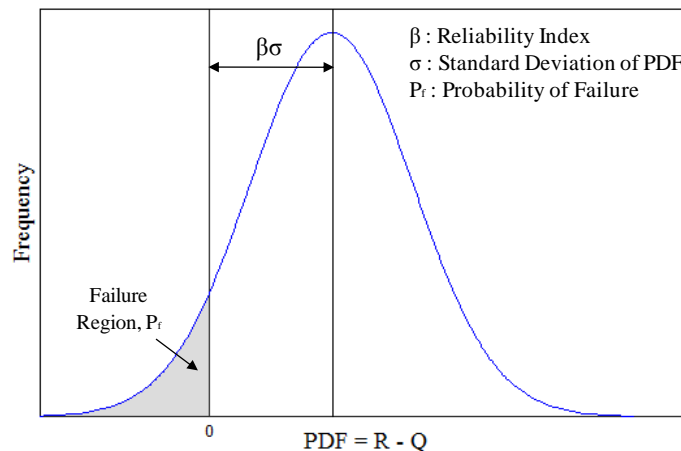


Figure 2.2: Probability of failure and reliability index (after Withiam et al. 1998)

Several statistical methods with different degrees of sophistication have been used for the LRFD resistance factors calibration. According to Kyung (2002), the most commonly used methods are the First Order Second Moment (FOSM) and First Order Reliability Methods (FORM). As noted by Allen et al. (2005), the FOSM is a straightforward technique, in which the random variables are represented by their first two moments, i.e., the mean (μ) and standard deviation (σ), while the Coefficient of Variation (COV) can be calculated by dividing the standard deviation by the mean. Paikowsky et al. (2004) performed the analysis using both methods (FOSM and FORM) and concluded that the difference between the two is relatively small (did not exceed 10% on average), and the FOSM provides the slightly conservative resistance factors. This difference is

linked to the estimation of the coefficient of variation for loads, which can be improved using a modified FOSM method described in Section 2.2.4.2. Moreover, the existing 2008 AASHTO-LRFD specifications are based on the FOSM assuming a lognormal distribution of the load and resistance PDFs. According to Allen et al. (2005), an advanced method known as the Monte Carlo simulation has been used for performing the reliability analyses. Allen et al. (2005) as well as Nowak and Collins (2000) have shown that all of these advanced methods should produce similar results to one another, which may indicate that a less sophisticated approach such as the FOSM would also provide similar results to other more sophisticated approaches. The following section provides a mathematical derivation of the basic equations of the FOSM method.

2.2.4.1 First Order Second Moment (FOSM)

Scott and Salgado (2003) indicated that the lognormal distribution, which better represents and models the transient loads, fully characterizes the loads by its first two moments. These authors added that the magnitude of the transient loads and resistances found in geotechnical problems cannot take negative values and the lognormal distribution can better represent their product even if the variables themselves are not lognormally distributed. Therefore, in accordance with the 2008 AASHTO-LRFD specifications, the load and resistance PDFs are assumed to follow lognormal distribution. The derivation of the FOSM basic Eq. [2.25] necessary to calculate the LRFD resistance factors is illustrated as follows:

According to Figure 2.2, failure occurs when the loads exceed the resistance. Since the PDFs are assumed to follow the lognormal distribution, the probability of failure will be:

$$P = P[(\ln Q_R - \ln Q_L) < 0] \quad [2.5]$$

The mean bias for the loads and resistances is defined as a ratio of the nominal (actual) and the mean predicted values as follows:

$$\lambda_L = \frac{Q_{Ln}}{\bar{Q}_L} \quad [2.6]$$

$$\lambda_R = \frac{Q_{Rn}}{\bar{Q}_R} \quad [2.7]$$

Assuming that both load and resistance follow a lognormal distribution and are statistically separate and independent variables, the mean difference will be:

$$\bar{U} = \ln \bar{Q}_R - \ln \bar{Q}_L \quad [2.8]$$

On the other hand, for the lognormal distributed PDFs, the standard deviation for the difference between loads and resistances will be:

$$\sigma_U = \sqrt{\sigma_{\ln Q_L}^2 + \sigma_{\ln Q_R}^2} \quad [2.9]$$

By considering the relationship between the standard deviation and the COV for a lognormal distribution:

$$\sigma_{\ln Q_L}^2 = \ln(1 + \text{COV}_{Q_L}^2) \quad [2.10]$$

$$\sigma_{\ln Q_R}^2 = \ln(1 + \text{COV}_{Q_R}^2) \quad [2.11]$$

According to Macgregor (1976), in case the $\text{COV} < 0.6$, the previous expressions can be approximated as follows:

$$\sigma_{\ln Q_L}^2 = \text{COV}_{Q_L}^2 \quad [2.12]$$

$$\sigma_{\ln Q_R}^2 = \text{COV}_{Q_R}^2 \quad [2.13]$$

From Figure 2.2, the reliability index, β , is simply the ratio of the mean and standard deviation (Allen, 1975; Macgregor, 1976; Becker, 1996) as follows:

$$\beta = \frac{\ln \bar{Q}_R - \ln \bar{Q}_L}{\sqrt{\sigma_{\ln Q_L}^2 + \sigma_{\ln Q_R}^2}} \quad [2.14]$$

Substituting Eqs. [2.12] and [2.13] into Eq. [2.14],

$$\beta = \frac{\ln \bar{Q}_R - \ln \bar{Q}_L}{\sqrt{\text{COV}_{Q_L}^2 + \text{COV}_{Q_R}^2}} \quad [2.15]$$

$$\ln \bar{Q}_R - \ln \bar{Q}_L \geq \beta \sqrt{\text{COV}_{Q_L}^2 + \text{COV}_{Q_R}^2} \quad [2.16]$$

Lind (1971) has shown that:

$$\sqrt{\text{COV}_{Q_L}^2 + \text{COV}_{Q_R}^2} = \alpha \text{COV}_{Q_L} + \alpha \text{COV}_{Q_R} \quad [2.17]$$

where α is a separation coefficient having a value between 0.707 and 1.0, depending on the ratio $\text{COV}_{Q_R}/\text{COV}_{Q_L}$ (after Lind, 1971). By adapting the equation below:

$$\ln \bar{Q}_R - \ln \bar{Q}_L = \ln \left(\frac{\bar{Q}_R}{\bar{Q}_L} \right) \quad [2.18]$$

Substituting Eqs. [2.17] and [2.18] into Eq. [2.16],

$$\ln \left(\frac{\bar{Q}_R}{\bar{Q}_L} \right) \geq \beta \alpha \text{COV}_{Q_L} + \beta \alpha \text{COV}_{Q_R} \quad [2.19]$$

$$\therefore \frac{\bar{Q}_R}{\bar{Q}_L} \geq e^{(\beta \alpha \text{COV}_{Q_L} + \beta \alpha \text{COV}_{Q_R})} \quad [2.20]$$

Eq. [2.20] may be rearranged as follows:

$$\bar{Q}_R (e^{-\beta \alpha \text{COV}_{Q_R}}) \geq \bar{Q}_L (e^{\beta \alpha \text{COV}_{Q_L}}) \quad [2.21]$$

From Eqs. [2.6] and [2.7], Eq. [2.21] will be:

$$Q_{Rn} \lambda_R (e^{-\beta \alpha \text{COV}_{Q_R}}) \geq Q_{Ln} \lambda_L (e^{\beta \alpha \text{COV}_{Q_L}}) \quad [2.22]$$

Based on Eqs. [2.21] and [2.22], one can assume that the LRFD factors for load and resistance are ϕ_L and ϕ_R , respectively, as follows:

$$\phi_R = \lambda_R (e^{-\beta \alpha \text{COV}_{Q_R}}) \quad [2.23]$$

$$\phi_L = \lambda_L (e^{\beta \alpha \text{COV}_{Q_L}}) \quad [2.24]$$

By separating the loads into dead loads (DL) and live loads (LL), and by rearranging the formula according to the recommended AASHTO-LRFD Probabilistic characteristics of random variables for loads (after Nowak, 1999; Paikowsky et al., 2004), Eqs. [2.22, 2.23, and 2.24] can be rewritten as follows:

$$\phi_R = \frac{\lambda_R \left(\frac{\gamma_{DL} Q_{DL}}{Q_{LL}} + \gamma_{LL} \right) \sqrt{\frac{(1 + \text{COV}^2_{Q_{DL}} + \text{COV}^2_{Q_{LL}})}{(1 + \text{COV}^2_{Q_R})}}}{\left(\frac{\lambda_{Q_{DL}} Q_{DL}}{Q_{LL}} + \lambda_{Q_{LL}} \right) \exp \left\{ \beta_T \sqrt{\ln \left[(1 + \text{COV}^2_{Q_R}) (1 + \text{COV}^2_{Q_{DL}} + \text{COV}^2_{Q_{LL}}) \right]} \right\}} \quad [2.25]$$

where

γ_{DL} = Load factor for dead loads (see Table 2.3)

γ_{LL} = Load factor for live loads (see Table 2.3)

$\lambda_{Q_{DL}}$ = Bias for dead loads (see Table 2.3)

$\lambda_{Q_{LL}}$ = Bias for live loads (see Table 2.3)

$\frac{Q_{DL}}{Q_{LL}}$ = Dead load to live load ratio (usually ranging from 1.5 to 3.5 for bridge structures)

Table 2.3: AASHTO recommended random variables for loads (after Nowak, 1999)

Load Type	Load Factor (γ_D, γ_L)	Load Bias ($\lambda_{QD}, \lambda_{QL}$)	Load COV ($\text{COV}_{QD}, \text{COV}_{QL}$)
Dead Load (D.L.)	1.25	1.05	0.1
Live Load (L.L.)	1.75	1.15	0.2

From Eq. [2.25], it can be observed that the mean bias (or the mean), the standard deviation, and the COV are all utilized in the FOSM equation. Therefore, a higher COV would probably yield a higher LRFD resistance factor, which may not be obvious. Actually, it is important to highlight the fact that: a higher resistance factor does not necessarily reflect a higher efficiency of the design capacity of a pile foundation. According to McVay et al. (2000), the efficiency of the different design methods cannot be reflected from the value of the resistance factor.

Consequently, McVay et al. demonstrated an efficiency factor, which is the ratio of the resistance factor to the bias of the method (ϕ/λ). This factor indicates the efficiency and economy of each design method in different soil and pile types. By this efficiency factor, McVay avoided the misconception between the economy of the different design methods and the high values of LRFD resistance factors.

2.2.4.2 Modified First Order Second Moment (FOSM)

To reduce the difference in resistance factors calibrated using the FOSM method and the FORM, Bloomquist et al. (2007) proposed a modified FOSM method where the coefficient of variation for loads was replaced with Eq. [2.26].

$$COV_{Q_{DL}}^2 + COV_{Q_{LL}}^2 = \frac{\frac{Q_{DL}^2}{Q_{LL}^2} \lambda_{Q_{DL}}^2 COV_{Q_{DL}}^2 + \lambda_{Q_{LL}}^2 COV_{Q_{LL}}^2}{\frac{Q_{DL}^2}{Q_{LL}^2} \lambda_{Q_{DL}}^2 + 2 \frac{Q_{DL}}{Q_{LL}} \lambda_{Q_{DL}} \lambda_{Q_{LL}} + \lambda_{Q_{DL}}^2} \quad [2.26]$$

Substituting Eq. [2.26] into the resistance factor Eq. [2.25], the modified FOSM equation yielded as such

$$\phi_R = \frac{\lambda_R \left(\frac{\gamma_{DL} Q_{DL}}{Q_{LL}} + \gamma_{LL} \right) \sqrt{\frac{\left(\frac{\frac{Q_{DL}^2}{Q_{LL}^2} \lambda_{Q_{DL}}^2 COV_{Q_{DL}}^2 + \lambda_{Q_{LL}}^2 COV_{Q_{LL}}^2}{1 + \frac{\frac{Q_{DL}^2}{Q_{LL}^2} \lambda_{Q_{DL}}^2 + 2 \frac{Q_{DL}}{Q_{LL}} \lambda_{Q_{DL}} \lambda_{Q_{LL}} + \lambda_{Q_{DL}}^2} \right)}}{(1 + COV_{Q_R}^2)}}}{\left(\frac{\lambda_{Q_{DL}} Q_{DL}}{Q_{LL}} + \lambda_{Q_{LL}} \right) \exp \left\{ \beta_T \ln \left[\left(1 + COV_{Q_R}^2 \right) \left(1 + \frac{\frac{Q_{DL}^2}{Q_{LL}^2} \lambda_{Q_{DL}}^2 COV_{Q_{DL}}^2 + \lambda_{Q_{LL}}^2 COV_{Q_{LL}}^2}{\frac{Q_{DL}^2}{Q_{LL}^2} \lambda_{Q_{DL}}^2 + 2 \frac{Q_{DL}}{Q_{LL}} \lambda_{Q_{DL}} \lambda_{Q_{LL}} + \lambda_{Q_{DL}}^2} \right) \right] \right\}} \quad [2.27]$$

2.2.5. Target Reliability Index

In LRFD specifications, the targeted reliability index (β) is defined as the measure of safety associated with a probability of failure (P_f). The probability of failure represents the probability of the condition, at which the resistance multiplied by the resistance factors will be less than the load multiplied by the load factors (Paikowsky et al., 2004). Rosenbleuth et al. (1972) presented an approximate relation between the probability of failure and the reliability index as follows:

$$P_f = 460e^{-4.3\beta} \quad [2.28]$$

According to Meyerhof (1970), β is in a limited range of 3 to 3.6 for foundations, which was reduced to a range from 2.0 to 2.5 (Barker et al., 1991) for driven piles, depending on its redundancy. This is because failure of one pile does not necessarily imply that the pile group will fail. In NCHRP report 507 (by Paikowsky et al., 2004), the following recommendations were provided for reliability indices and the associated P_f for LRFD resistance factors calibration:

- For redundant piles, defined as five or more piles per pile cap, the recommended probability of failure is $P_f = 1\%$, corresponding to a target reliability index of $\beta = 2.33$.
- For non-redundant piles, defined as four or fewer piles per pile cap, the recommended probability of failure is $P_f = 0.1\%$, corresponding to a reliability index of $\beta = 3.00$.

2.3. Framework of Calibration

First, the development of the LRFD resistance factors requires an adequate pile load test database. This database should include reliable data conducted in the same region (State) of the

desired LRFD calibration to account for the different, unique levels of variation in soil and geology, as well as the design and construction practices. However, if the anticipated regional database is not available, it would be acceptable for another database with similar conditions to be used if it can effectively represent the local conditions. Following the procedures provided in the NCHRP-507 report by Paikowsky et al. (2004) and the FHWA-NHI report by Allen (2005), the framework for developing the LRFD geotechnical resistance factors can be essentially summarized as follows:

- 1) Develop a comprehensive and reliable pile static load test database, including: a) sufficient soil parameters and profiles; b) pile properties and geometry; c) pile driving information (or drilled shaft information) such as hammer properties and dates of driving (dates of EOD and BOR); d) acceptable static load test data, i.e., the accepted load-displacement relationship at the pile head indicating the pile failure load or the pile ultimate capacity in the field. The database should include a large number of data points so that it can be successfully used for the reliability-based LRFD calibration.
- 2) Sort the database into different groups, where each group represents a specific soil and pile type. For example, an appropriate group would represent load tests conducted on driven steel H-piles in sand. The precision and efficiency of the expected LRFD resistance factors is higher whenever the number of variables among each group is limited. As previously indicated, the number of data points within each group must be sufficient for the analysis.
- 3) Calculate the actual capacity of piles for all groups using the load-displacement relationship obtained from the load test results. Consistency of the selected criterion of calculating the pile ultimate capacity is required for all data points, i.e., when selecting Davisson's criterion it should be used for all piles within all groups.
- 4) Calculate the nominal capacity of piles for all groups using any desired static or dynamic analysis methods or dynamic formulas. Also in-house methods can be used to calculate the nominal capacity and therefore LRFD resistance factors of a specific in-house method can be considered in the calibration.
- 5) Determine the bias of the methods used, or the actual to nominal pile capacity ratios, for all groups.
- 6) Determine the distribution of the Probability Density Functions (PDFs) within each group in the database, i.e., normal or lognormal distributed. Also determine the best-fit for each dataset using any of the statistical distribution identification tests available such as Anderson Darling test (discussed in Chapter 5).
- 7) Select the appropriate reliability approach that will be used for the LRFD resistance factors calibration such as the FOSM or the FORM. This selection depends on the degree of sophistication anticipated in the analysis.
- 8) Calculate the statistical parameters required in the desired reliability approach. For example, the mean, standard deviation, the target reliability index, DL/LL ratio, and the dead and live load factors based on the AASHTO recommendations.
- 9) Calculate the regional LRFD resistance factors, compare the results within the resistance factors calibrated by fitting to the ASD factor of safety and then determine the efficiency factors of each group.

- 10) Check the reliability and consistency of the calibrated resistance factors by conducting full-scale pile load tests in different soil types and then develop recommendations for the LRFD-based design for bridge pile foundations.

Figure 2.3 represents a flowchart that shows the previous steps of the LRFD resistance factors calibration.

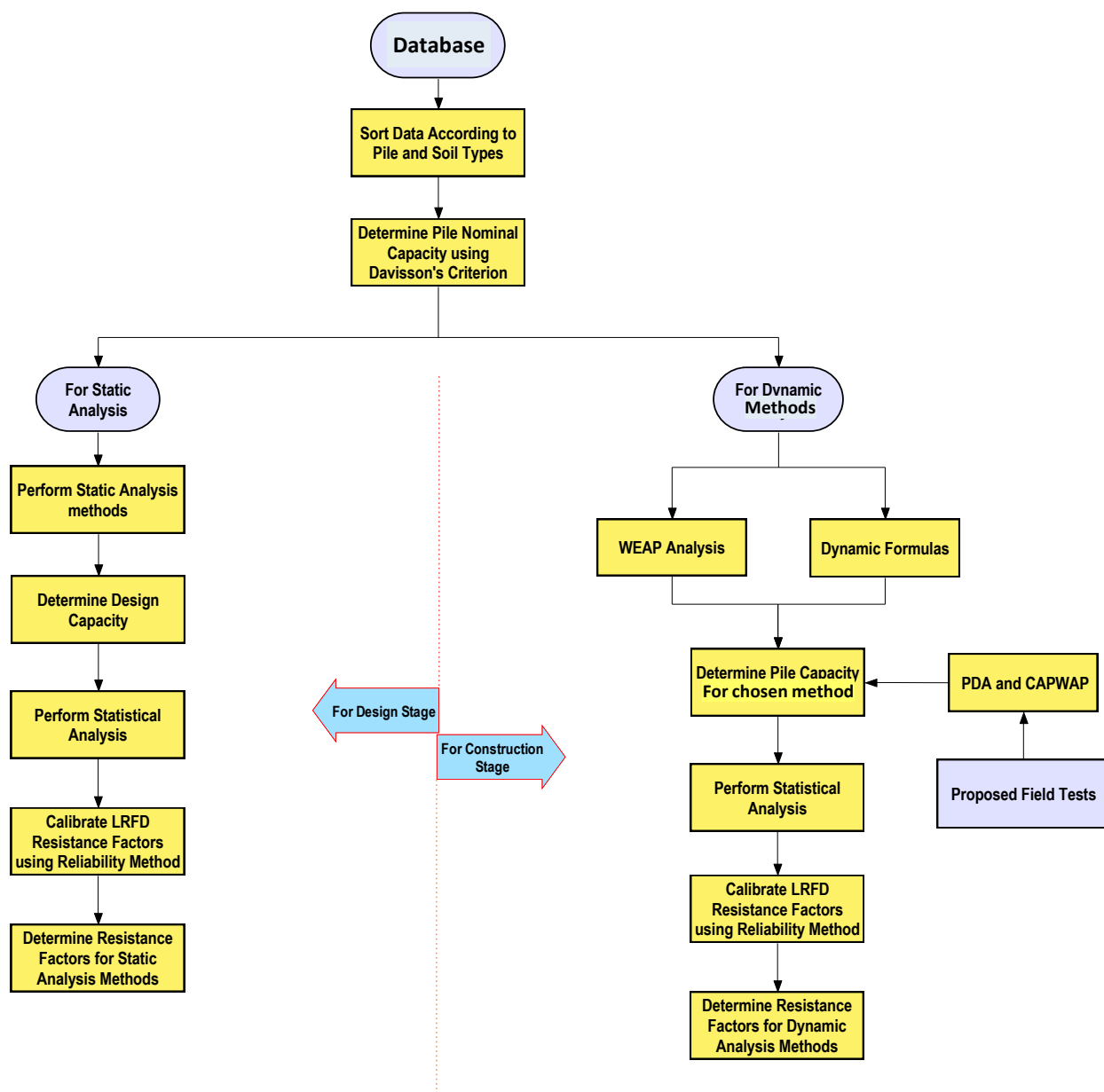


Figure 2.3: Framework of the LRFD resistance factors calibration for design and construction methods of analysis

As can be seen in the figure, the static analysis methods are used during the design stage of the project while the dynamic analysis and dynamic formulas take place during the construction stage of the project. A discussion on the main difference between the two stages and the construction control aspects are provided later in this chapter.

2.4. Current AASHTO-LRFD Specifications

The source of the initial resistance factors provided by the AASHTO-LRFD Specifications (2004) was the NCHRP Report 343 by Barker et al. (1991). Resistance factors were calibrated using a combination of reliability theory and by fitting to ASD, which according to Allen (2005) did not meet the objective of providing a consistent level of safety in design. The AASHTO-LRFD Bridge Design Specifications (2007) were revised based on the NCHRP Report 507 by Paikowsky et al. (2004) and the FHWA-NHI report by Allen (2005). As previously indicated, the calibration framework used to develop the geotechnical resistance factors in the NCHRP as well as the FHWA reports was mainly based on the reliability theory. Subsequently, the AASHTO-LRFD Bridge Design Specifications (2010) were revised to minimize the conservatism presented in the AASHTO-LRFD Bridge Design Specifications (2007) as well as simplify the application of the recommended resistance factors.

As is discussed in the next chapter of this report, there are three different methods of analysis that can be used to estimate the pile nominal capacity, which are: 1) Static analysis methods; 2) Dynamic analysis methods; and 3) Dynamic formulas. From a geotechnical aspect, the nominal pile design capacity can be defined as the maximum calculated axial compressive load that the soil-pile system can handle without excessive settlement. This capacity is calculated during the design or construction stages of the foundation depending on the soil and pile properties as well as the pile driving conditions. The AASHTO-LRFD Specifications (2007) provided resistance factors for the three pile analysis methods in different soil types with due consideration to different levels of site variability and construction control.

2.4.1. Static Methods

Different static analysis methods are used to estimate the number and length of piles required to release the bidding and contracting documents during the initial design stage. Selecting the appropriate static method requires sufficient knowledge of the site subsurface conditions and different deep foundation types. As can be seen in Table 2.4, the current AASHTO specifications provide the LRFD resistance factors for a single axially loaded pile using six different static analysis methods in sand, clay and mixed soils. These static analysis methods were also used to estimate the geotechnical LRFD resistance factors for uplift capacity of a single pile. The AASHTO resistance factors were mainly developed from load test results obtained on piles with diameters of 600 mm (23.6 inches) or less. The pile nominal capacity calculated using different static analysis methods should be multiplied by the appropriate resistance factors that are presented in Table 2.4 (adapted from the AASHTO-LRFD Specifications (2007)). The recommended AASHTO factors are based on redundant pile groups. As described in the AASHTO (2007) Section 10.5.5.2.3 for driven piles, if the pile group is less than five piles, the resistance factors should be reduced by 20% to reflect a higher target reliability index of $\beta_T = 3.0$ or more. The current AASHTO Specifications (2010) maintain the resistance factors as shown in Table 2.4 except for a resistance factor of 0.50, which was added for the uplift resistance of a single pile in the instance in which a dynamic test with signal matching is used.

Table 2.4: LRFD resistance factors for static analysis methods (after 2007 AASHTO)

Condition/Resistance Determination Method		ϕ
Nominal Resistance of Single Pile in Axial Compression – Static Analysis Methods, ϕ_{stat}	Skin Friction and End Bearing: Clay and Mixed Soils: α -method (<i>Tomlinson, 1987; Skempton, 1951</i>)	0.35
	β -method (<i>Esrig & Kirby, 1979; Skempton, 1951</i>)	0.25
	λ -method (<i>Vijayvergiya & Focht, 1972; Skempton, 1951</i>)	0.40
	Skin Friction and End Bearing: Sand Nordlund/Thurman Method (<i>Hannigan et al., 2005</i>)	0.45
	SPT-method (<i>Meyerhof</i>)	0.30
	CPT-method (<i>Schmertmann</i>) End Bearing in rock (<i>Canadian Geotech. Society, 1985</i>)	0.50 0.45
Block Failure, ϕ_{bl}	Clay	0.60
Uplift Resistance of Single Pile, ϕ_{up}	Nordlund Method	0.35
	α -method	0.25
	β -method	0.20
	λ -method	0.30
	SPT-method	0.25
	CPT-method	0.40
	Load test	0.60
Group Uplift Resistance, ϕ_{ug}	Sand and clay	0.50
Horizontal Geotechnical Resistance of Single Pile or Pile Group	All soils and rock	1.0
Structural Limit State	Steel piles	See the provisions of Article 6.5.4.2 in 2007 AASHTO-LRFD specifications
	Concrete piles	See the provisions of Article 5.5.4.2.1.1 in 2007 AASHTO-LRFD specifications
	Timber piles	See the provisions of Article 8.5.2.2 and 8.5.2.3 in 2007 AASHTO specifications
Pile Drivability Analysis, ϕ_{da}	Steel piles	See the provisions of Article 6.5.4.2 in 2007 AASHTO-LRFD specifications
	Concrete piles	See the provisions of Article 5.5.4.2.1 in 2007 AASHTO-LRFD specifications
	Timber piles	See the provisions of Article 8.5.2.2 in 2007 AASHTO-LRFD specifications
	In all three Articles identified above, use ϕ identified as “resistance during pile driving”	

2.4.2. Dynamic Methods

Tables 2.5, 2.6, and 2.7 are adopted from the AASHTO-LRFD Bridge Design Specifications (2007) for dynamic analysis methods. Referring to Tables 2.5, 2.6, and 2.7, the application of various resistance factors were depending on the means of pile capacity verification (i.e., pile static load tests (SLTs) and either dynamic tests or wave equation analyses (WEAP)) as well as depending on the site variability and the number of static and dynamic tests conducted at the site. Generally, the resistance factors increase as the reliability of the field verification methods increase (Allen, 2005). As described in AASHTO (2007) Section 10.7.3.8.2, the SLT is the best way to determine the actual (nominal) pile capacity, which shall not be performed sooner than five days after driving. The SLT shall follow the procedures specified in ASTM D 1143 (ASTM, 2007) Quick Load Test Method. The Davisson's failure criterion is recommended for piles with diameters smaller than 600mm (23.6 inches). A resistance factor of 0.65 should be used if the pile design verification method uses dynamic tests with signal matching (CAPWAP) at the Beginning of Restrike (BOR). AASHTO (2007) recommended that the CAPWAP technique should be performed evenly within a pier and across the entire structure in order to justify the use of the specified resistance factors. On the other hand, a resistance factor of 0.40 should be used if the design capacity is verified by means of WEAP at the End of Driving (EOD) conditions.

The AASHTO-LRFD Bridge Design Specifications (2010) removed the complexity by selecting the resistance factor based on site variability and number of test piles, and simplified the resistance factors for dynamic analysis methods as shown in Table 2.8. As similarly described in the AASHTO (2007) for driven piles, if the resistance factors are to be applied to non-redundant pile groups, the factors should be reduced by 20 % to reflect a higher target reliability index (β_T) of 3.0 or more. Furthermore, the resistance factors were determined mainly from load test results obtained from piles with diameters of 610 mm (2 ft) or less. A static or dynamic load test should be considered to verify the pile performance if a pile diameter larger than 610 mm (2 ft) is used during design. The combination of static and/or dynamic tests should be established based on the degree of site variability, which is characterized using field and laboratory exploration and pile load test program. Note that the resistance factors (0.65 and 0.75) for dynamic testing without static load testing were developed for the beginning of restrike (BOR) conditions. The application of resistance factors calibrated for the end of driving (EOD) conditions may yield conservative results because of soil setup. The 0.50 resistance factor for wave equation analysis is established based on calibration by fitting to past ASD practice. Local experience or test results should be used in wave equation analysis to enhance the confidence of pile resistance estimation, and field verification of hammer performance should be conducted.

Table 2.5: LRFD resistance factors for dynamic analysis (after 2007 AASHTO)

Condition/Resistance Determination Method		Resistance Factor
Nominal Resistance of Single Pile in Axial Compression - Dynamic Analysis and Static Load Test Methods, ϕ_{dyn}	Driving criteria established by static load test(s) in combination with dynamic testing or wave equation analyses	Values in Table 2.6*
	Driving criteria established by dynamic test with signal matching at beginning of re-drive (BOR) conditions of only at least one production pile per pier, but no less than the number of tests per site provided in Table 2-16	0.65*
	Wave equation analysis, without pile dynamic measurements or load test, at end of drive conditions only	0.40*

*Reduces 20 percent for non-redundant pile groups

Table 2.6: The ϕ for number of static load tests conducted per site (after 2007 AASHTO)

Number of Static Load Tests per Site	Resistance Factor, ϕ		
	Site Variability		
	Low	Medium	High
1	0.80	0.70	0.55
2	0.90	0.75	0.65
3	0.90	0.85	0.75
More than or equal 4	0.90	0.90	0.80

Table 2.7: Number of dynamic tests with signal matching analysis per site to be conducted during production pile driving (after 2007 AASHTO)

Site Variability	Low	Medium	High
Number of Piles Located Within Site	Number of Piles with Dynamic Tests and Signal Matching Analysis Required (BOR)		
Less than or equal 15	3	4	6
16-25	3	5	8
26-50	4	6	9
51-100	4	7	10
101-500	4	7	12
More than 500	4	7	12

Table 2.8: LRFD resistance factors for dynamic analysis methods and dynamic formulas (after 2010 AASHTO)

Condition/Resistance Determination Method		Resistance Factor
Nominal Resistance of Single Pile in Axial Compression - Dynamic Analysis and Static Load Test Methods, Φ_{dyn}	Driving criteria established by successful static load test of at least one pile per site condition and dynamic testing ^(a) of at least two piles per site condition, but no less than 2% of the production piles	0.80 ^(b)
	Driving criteria established by successful static load test of at least one pile per site condition without dynamic testing	0.75 ^(b)
	Driving criteria established by dynamic testing ^(a) conducted on 100% of production piles	0.75 ^(b)
	Driving criteria established by dynamic test ^(a) , quality control by dynamic testing ^(a) of at least two piles per site condition, but no less than 2% of the production piles	0.65 ^(b)
	Wave equation analysis, without pile dynamic measurements or load test but with field confirmation of hammer performance	0.50 ^(b)
	FHWA-modified Gates dynamic pile formula (End of drive condition only)	0.40 ^(b)
	Engineering News (as defined in Article 10.7.3.8.5 of AASHTO Specifications (2010)) dynamic pile formula (End of Drive condition only)	0.10 ^(b)

^(a) Dynamic testing requires signal matching, and best estimates of nominal resistance are made from a restrike.

Dynamic tests are calibrated to the static load test, when available.

^(b) Reduces 20 percent for non-redundant pile groups.

2.5. Regionally Calibrated Resistance Factors

Several code users indicated that the recommended LRFD resistance factors led to inappropriate design, which conflicted with their experiences (Goble, 1999). Moreover, the current version of the AASHTO-LRFD specifications has other shortcomings. For example, they do not provide resistance factors for all static analysis methods for pile design, including obviously the “in-house” methods developed by different DOTs (Kyung 2002). Since the design specifications were developed for general use, the AASHTO-LRFD bridge design specifications account for large uncertainties in soil properties, resulting in conservative resistance factors (Paikowsky et al., 2004). In addition, AbdelSalam et al. (2008) revealed that: a) the 2007 AASHTO-LRFD design specifications do not distinguish between different pile types used in practice; and b) as permitted by AASHTO, development of regionally calibrated LRFD resistance factors, for specific soil conditions, pile types, and construction practices would help overcome the aforementioned limitations, resulting in more cost-effective pile foundations.

The regionally calibrated LRFD resistance factors can be aimed for a specific geographical region with unique soil conditions and construction practices. The development of such resistance factors for a given pile type and geological region requires the existence of adequate

static load test data as well as quality soil parameters from in-situ testing. With the existence of such data, regionally calibrated resistance factors can be developed following the approach suggested in the AASHTO LRFD Specifications (2007). As a part of this study, a nationwide survey was conducted in 2008, which indicated that at least five state DOTs had already developed their own regionally calibrated resistance factors based on the reliability theory to improve the cost-effectiveness of deep foundations. The survey also indicated that about 13 state DOTs were in a transition stage from ASD to LRFD, and they were using preliminary regionally calibrated resistance factors by fitting to the ASD. Complete details of the survey outcome are presented in Chapter 4 of this report.

2.5.1. Background

In 2000, Liang and Nawari investigated the AASHTO-LRFD resistance factors for driven piles using a pile static load test database, which covered a spectrum of variation in soil formations, as well as different pile types and geometry. Liang and Nawari (2000) studied the LRFD resistance factors for 11 different static analysis methods suitable for determining the pile design capacity. The results were compared to ASD factor of safety and indicated that the resistance factors ranged between 0.69 and 0.55 at $\beta=2.0$ for most of the static methods that they used. They have also provided design tables indicating the resistance factors at different β values. This study proved that utilizing regionally calibrated LRFD resistance factors could lead to a significant gain in the pile design capacity.

Other studies were conducted to evaluate the assumptions considered in the AASHTO-LRFD code to develop the resistance factors, such as using the same load factors developed for structural members to maintain design consistency (Withiam et al., 1997). In assessing the usage of the typical load factors in the calibration of the LRFD for substructures, Scott et al. (2003) employed the First Order Second Moment (FOSM) reliability based analysis to calculate the load factors. They then compared the results to different load factors presented in various design codes. Different load combinations were applied in the strength limit state and the average values calculated showed a comparable agreement with the AASHTO and U.S. codes. As a conclusion, the FOSM reliability approach based on the statistical approach for calculating the load and resistance factors for the LRFD was found to be a good. Scott et al. (2003) assumed a lognormal Probability Density Function (PDF) in the FOSM analysis, and according to Ellingwood et al. (1980), the lognormal distribution is a more precise model for transient loads than normal distribution. Moreover, the lognormal distribution represents the product of several positive random variables, even if these variables do not individually follow the lognormal assumption.

As a part of the previous work done to evaluate the performance of the AASHTO-LRFD resistance factors in unique soil types, Thibodeau and Paikowsky (2005) conducted a large load test program including 23 statically, load tested piles in distinctive subsurface conditions containing glacio-delatic silt and sand deposits. The main concern of the study was the difficult subsurface conditions, which led to higher pile static capacity predictions than expected. Thibodeau and Paikowsky (2005) found that the over-prediction of static methods was due to the overestimation of soil properties for the glacio-delatic deposits. Accordingly, in order to achieve better efficiency, a local calibration for the LRFD resistance factors was recommended for this specific soil type. However, despite the over-prediction of typical static analysis methods, they acknowledged that the recommended resistance factors in the NCHRP 507 performed better than

the ASD specifications at that time, where in some cases the ASD factor of safety was less than unity.

Abu-Hejleh et al. (2009) demonstrated that the LRFD design procedures for driven H-piles and cast-in-place pipe piles and assisted with the interpretation of AASHTO-LRFD design specifications for driven piles in design and construction practice. The study mainly focused on the geotechnical strength limit state for a single pile. Abu-Hejleh et al. (2009) highlighted the importance of performing field verification tests (i.e., dynamic tests), which can account for pile setup, relaxation, and soil plugging for steel H-piles. In their study, setup was reported in sand and for steel H-piles; however, as discussed in detail in Ng et al. (2011), setup normally occurs in cohesive soils. Moreover, according to Abu-Hejleh et al. (2009), static analysis methods were considered more accurate, and therefore they were recommended for soft silty/clays and hard rocks, and it was conservatively assumed that static analysis predictions are corresponding to the BOR conditions. As for the pile structural limit state, Abu-Hejleh et al. (2009) assumed a resistance factor of 0.5 and 0.6 at hard driving conditions for steel H-piles and cast-in-drilled-holes piles, respectively. These resistance factors were slightly increased in case of easy driving. The study illustrated significant cost savings when using LRFD instead of ASD in the design of pile foundations, especially when incorporating locally calibrated LRFD resistance factors. Finally, Abu-Hejleh et al. (2009) were concerned about evaluating the serviceability limit in the LRFD design of foundations, especially when large loads were permitted in the strength limit states.

Many calibration frameworks have been conducted based on the reliability analysis using large databases. However, Foye et al. (2009) indicated that reliability analyses based on databases do not necessarily account for uncertainties caused by soil variation, soil testing techniques, and the analysis model used to calculate the foundation capacity. Foye et al. (2009) developed the LRFD resistance factors for driven pipe piles in sand by isolating various sources of uncertainties using two design approaches. The first was using the direct design method, and the second was using the property-based design method. Direct methods are those that depend on a direct correlation with soil in-situ tests, while the property-based design methods depend on laboratory and field test results. In their study, the LRFD resistance factors were separated for skin- friction and end bearing components. Foye et al. (2009) indicated that the direct method is more accurate than the property-based method and resulting with higher LRFD resistance factors, as the property-based method requires several soil property assumptions. Foye et al. (2009) claimed that the calibration technique used in the NCHRP-507 (Paikowsky et al., 2004) is based on a lumped database, as it did not discriminate between the various sources of uncertainty that contributed to the observed scatter between prediction and measurements. Recently, McVay et al. (2010) indicated that the current design specifications depend on constant resistance factors that ignore the effect of soil variation along the shaft. For that reason, they developed design charts for both single and groups of pile layouts, considering the effect of soil variability for the shaft and tip resistance components.

Separating the skin-friction and end bearing components of the pile resistance and development of corresponding resistance factors are crucial topics that were ignored in many codes. In 2002, Kuo et al. developed the resistance factors by only considering the skin friction for a database consisting of 185 drilled shafts, and then compared the difference by considering the total resistance. They concluded that the difference depends largely on the pile type, installation

technique, and soil profile. Lai et al. (2008) separated the resistance components using conventional static analysis methods and developed the resistance factors based on a database containing 13 load tested steel piles. However, only a few studies have addressed this issue, as separating shaft and tip resistances requires either the conducting of SLTs on instrumented piles or using Osterburg cells, which are expensive and time consuming.

In addition, the disadvantage of the current geotechnical LRFD practice is recognized, as it only accounts for the strength limit states. Starting in 1994, Green (1994) observed various technical problems that arose while using the Ontario LRFD code, and recommended an improved communication between the structural and geotechnical engineers to ensure that the serviceability and strength limits were properly identified. Goble (1996) indicated the need for additional research that included the serviceability limit states into the LRFD code. Scott and Salgado (2003) also identified the importance of this issue, especially for cohesive soils, where the settlement is not immediate and the use of the unity as a resistance factor recommended by the AASHTO for serviceability checks may not be appropriate. Consequently, several studies were conducted on this topic during the last few years. Some studies were based on the prediction of the pile load-displacement relationship as well as the selection of the design capacity and corresponding settlement in a reliability-based manner. The load-transfer method (t-z method) has been extensively used to model the load-displacement curves and to perform the reliability analysis of deep foundations (Misra and Roberts 2006, Misra et al. 2007). Robert et al. (2008) developed a practical LRFD method for the simultaneous design of deep foundations at both the strength and service limit states using the t-z method. Recently, Abu-Hejleh et al. (2009) developed the LRFD design of drilled shafts based on the Cone Penetration Test (CPT) data for serviceability limits, indicating that settlement can control the design in particular soil types, especially when large loads are permitted.

2.5.2. State DOTs Implementation

The FHWA mandated that after October 1, 2007, all new bridges initiated in the United States must follow the LRFD approach, and since then, a general move toward the increased use of the LRFD among state DOTs for structural and geotechnical design practices. In 1997, the Florida Department of Transportation (FDOT) developed a LRFD Code for their bridge design (Passe, 1997). Although no probabilistic analysis was performed in the calibration process, the FDOT was a pioneer among other state DOTs in implementing the LRFD for geotechnical applications. In 2002, North Carolina Department of Transportation (NCDOT) developed the resistance factors in a framework of reliability theory for axially loaded driven piles. After that, many State DOTs had calculated their own LRFD resistance factors. According to a recent survey by AbdelSalam et al. (2008), responses obtained from more than 30 DOTs revealed that over 50% of the state DOTs are currently using the LRFD method for pile design, while only 30% of the DOTs are still in the transition phase from the ASD method to the LRFD. The study also revealed that about 30% of the DOTs employing the LRFD for piles have utilized their regionally calibrated resistance factors to improve the cost-effectiveness of pile foundations. At least five state DOTs have adopted regionally calibrated resistance factors based on reliability theory, and 13 state DOTs, among those that are still in a transition stage to the LRFD, have adopted preliminary and regionally calibrated resistance factors by fitting to the ASD.

2.6. Construction Control of Deep Foundations

In this section, the difference between the pile design and construction stages is presented. This is followed by a simplified definition for the construction control of deep bridge foundations. Finally, the possibility of considering the construction control aspects during the design stage is discussed.

2.6.1. Design Versus Construction Stages

Site investigation and soil parameters determination are the first step in the design stage of any bridge project. Soil parameters are commonly evaluated by performing laboratory and/or field tests such as Standard Penetration Test (SPT) and cone Penetration Test (CPT), depending on the soil type and desired accuracy of determining a soil profile. The second step in the design stage is identifying the possible foundation schemes based on the results of the investigation, load requirements, importance of the structure, and local experience. Calculating the capacity of the selected foundation type and determining the length and number of the necessary piles is the third step of the design stage. In order to perform this step, static analyses must take place. In the case of driven piles, a dynamic analysis (WEAP) can be considered for hammer evaluation, feasibility of installation, and structural adequacy of the pile. The main purpose of the design stage is to perform structural and geotechnical analyses in order to provide a reasonable estimate for the required foundation type, length, number, and size. Hence, this process will serve in assembling the bidding documents concerning the bridge substructure.

In the construction stage, design verification and construction control should be carried out by means of SLT and/or dynamic analysis. The assigned capacity and the final specifications should be determined from the construction stage. There should not be a large difference between the pile-designed capacity and the measured capacity in the field, and it should maintain the same degree of reliability. In some important projects, the design stage relies on pile SLT and/or dynamic analysis rather than performing static analysis (Paikowsky et al., 2004). Figure 2.4 provides a flowchart briefly describing the typical design and construction cycle. As shown in Figure 2.4, after determining the preliminary pile design capacity by performing the static analysis, a pile deformation analysis takes place to ensure that the design capacity does not lead to excessive settlement or deformations to the structure. As previously mentioned, the construction stage takes place after releasing the bidding (contracting) documents, during which design verification is performed by means of SLT, or using the PDA and CAPWAP. A full pile length is required by Iowa DOT when regarding the construction practice of deep foundations. The main difference arises in the construction stage, as the majority of contractors depend on WEAP analysis for design verification and construction control. Some other contractors keep driving the pile until refusal, which in some cases, could damage the steel pile and in other cases may lead to unnecessarily high resistance. Figure 2.5 summarizes the pile design and construction practice in the State of Iowa.

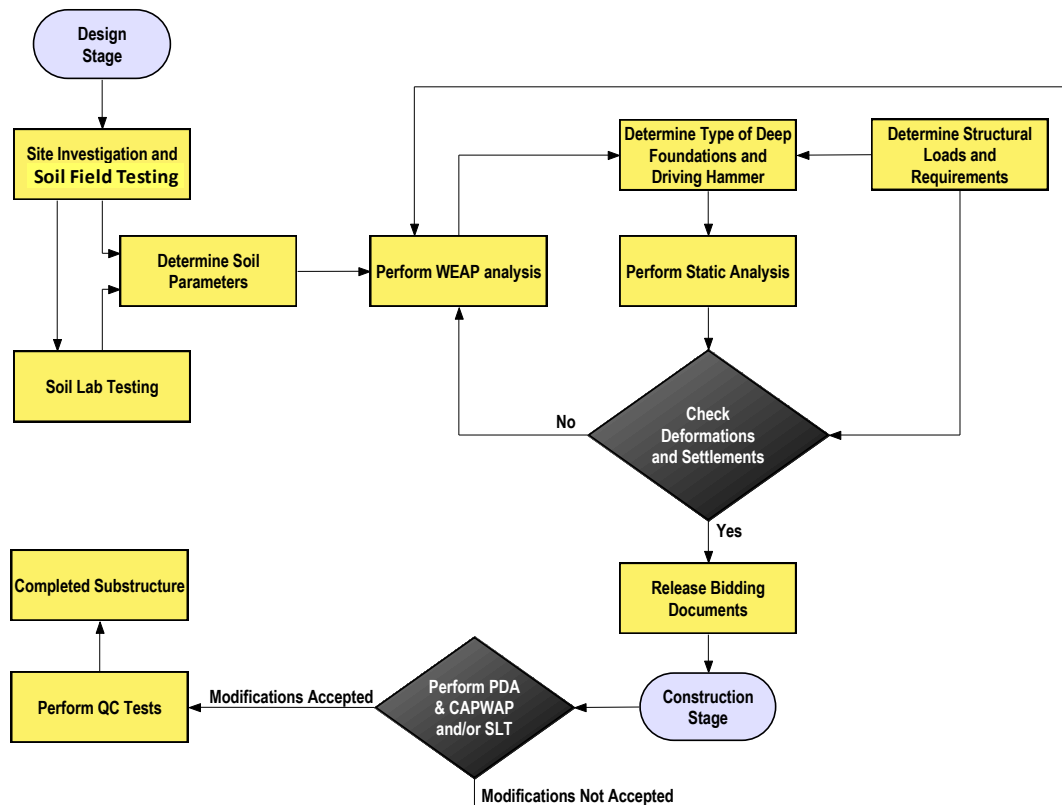


Figure 2.4: Typical design and construction cycle

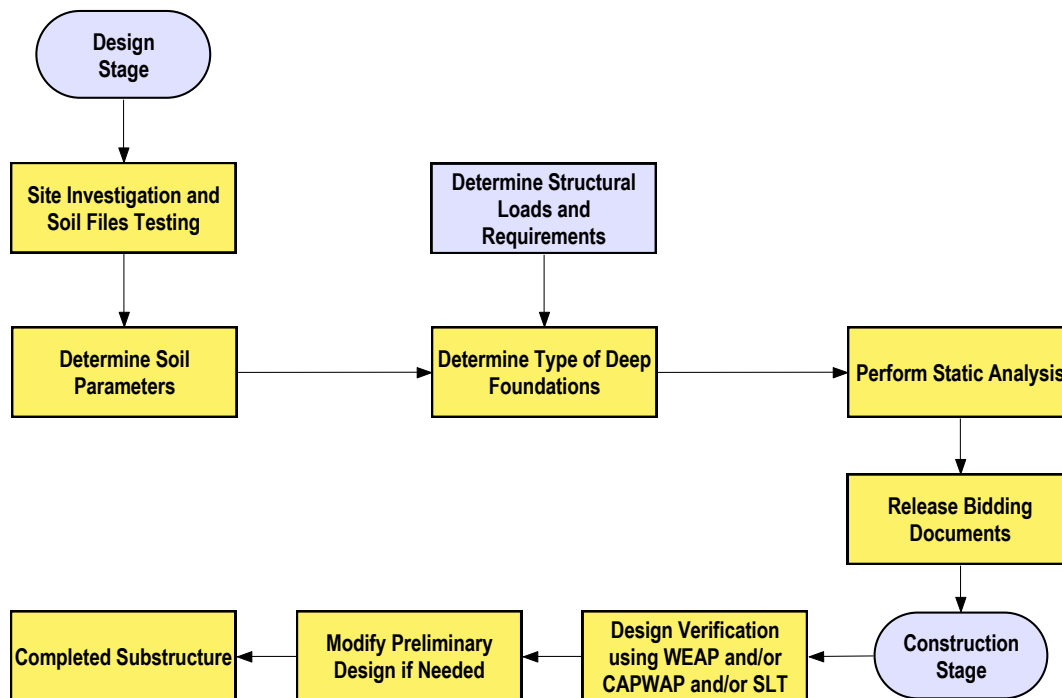


Figure 2.5: Current design and construction practice in the state of Iowa

2.6.2. Definition of Quality Control

Construction control of pile foundations, including Quality Control (Q.C.), is a general term that accounts for several field-conducted procedures and can be separated into parts; the first to check/verify the pile design capacity and integrity, and the second to utilize quality assurance (after Paikowsky et al., 2004). According to the previous definition, one can suppose that construction control mainly consists of pile design verification and quality assurance.

Design verification is typically carried out through means of SLTs, dynamic analysis (e.g., WEAP, PDA, etc.), or dynamic formulas (e.g., ENR, FHWA Gates, etc.). It accounts for soil variability, driving conditions, and any other conditions that could affect the pile capacity. In some cases, design verification is replaced by engineering judgment and experience. An example of this would be the driving of the pile into a hard bedrock layer or driving until pile refusal. Although, the previous judgmental methodologies are practiced in various regions, design verification cannot guarantee an acceptable pile final capacity and may lead to unnecessary conservatism. Therefore, it is very important to conduct dynamic analysis or pile SLTs during the construction stage to ensure safe and cost-efficient foundations.

Quality assurance is to guarantee a quality soil investigation and parameters determination during the design stage and to ensure pile competence during and after driving. Pile competence can be carried out by means of pile verticality tests, dynamic tests using PDA, and other pile quality tests. The LRFD resistance factors for deep foundations are based on a convenient degree of quality. Therefore, geotechnical engineers should at least assure and maintain the same degree of quality to fully exploit the benefits of the LRFD methodology for geotechnical purposes. Hence, it is important to perform such quality assurance tests while providing a guideline for the required quality assurance limits. Paikowsky et al. (2004) proposed a framework for the establishment of knowledge-based factors for both the design and construction control methods. These factors can be accounted for by means of modifying a constant (ξ) to be multiplied by the LRFD resistance factors. However, this exercise would require statistical analysis of additional data.

2.6.3. Combining Static and Dynamic Methods

As previously mentioned, the design stage depends on a static analysis method. Several static analysis methods could be used for calculating the pile capacity, where each static method has its own LRFD resistance factors, depending on different soil and pile types. On the other hand, the construction control tests have their own LRFD resistance factors that are used for design verification purposes. A method to combine static analysis with dynamic analysis is proposed in this report to minimize the discrepancy in pile capacities estimated during the design stage and verified during the construction stage. Paikowsky et al. (2004) reported that the AASHTO-LRFD Bridge Design Specifications (2001) were not clear for geotechnical practice due to the existence of a modifier factor (λ_v), which was multiplied with the LRFD resistance factors to integrate the construction control methods into the design stage. Recently, some State DOTs have adopted a correction factor for static methods. For example, Long et al. (2009) studied the agreement between static methods and dynamic formulas for the Illinois DOT (IDOT). The focus of this study was to determine the average difference between static methods and dynamic formulas, as some static methods were considered inaccurate. The correction factor developed by IDOT is

somewhat different from the previously mentioned modifier factor (λ_v), as it is supposed to be applied to static methods before performing the calibration for the LRFD resistance factors. Therefore, it modifies the nominal design capacity attained from different static methods. Based on these modified capacities, the LRFD resistance factors are calibrated. In summary, the IDOT combined Dynamic and Static analyses in order to determine the most useful method for the pile design in their region.

CHAPTER 3: DIFFERENT PILE ANALYSIS PROCEDURES

This chapter provides a detailed review as well as background information on the principles of different analysis methods used for the design of deep bridge foundations. A review on the different criteria used to determine the pile nominal capacity from the load-displacement response is also presented.

3.1. Static Analysis Methods

Several methods are available to predict the nominal axial capacity of driven piles. They include the static analysis methods, which have been developed empirically or semi-empirically using field test data. Static analysis methods are fairly straightforward and typically utilized during the design stage. There are numerous limitations for each static method and selecting the most appropriate method for a specific design problem will depend on the site geology, pile type, extent of available soil parameters, and local practice. Static methods only estimate the pile nominal capacity without determining the corresponding movements, i.e., they only determine the strength limit state of a pile foundation and not the vertical settlement. Many soil strength parameters are required for different static analysis methods, and are directly measured or calculated based on correlations to in-situ and/or laboratory soil tests. The following sections provide a summary on the most common correlations used to calculate different soil strength parameters, followed by an overview on the most frequently used static analysis methods for determining the nominal capacity of pile foundations.

3.1.1. Determination of Soil Properties

Most of the static methods directly or indirectly utilize the soil shear strength parameters when calculating the capacity of pile foundations. These parameters could be determined using laboratory tests or correlations to field tests such as the SPT or CPT. There are several errors that should be considered and corrected while using SPT N-values, where the N-value is the number of blows required to drive a standard split spoon sampler to a distance of 1.0 ft (30 cm). Cheney and Chassie (1993) have studied the common SPT errors and found the effects of the soil overburden pressure being one of these errors, as well as the variation in the free fall of the drive weight, which affects the driving efficiency. The efficiency of the system can be determined by comparing the Kinetic Energy (KE) with the Potential Energy (PE), meaning that the Energy Ratio (ER) is equal to KE/PE. Despite its disadvantages, the SPT is considered as one of the most commonly used soil field tests, and many soil strength correlations were developed based on this test. According to the AASHTO LRFD Bridge Design Specifications (2007), the ER is equal to 60% for routine engineering practice in the United States. The N-value corresponding to 60% is termed N_{60} , which can be calculated if the field efficiency is different from 60% by using the following equation:

$$N_{60} = (ER/60\%) \times N \quad [3.1]$$

Peck et al. (1974) have presented a normalization parameter (C_n) that should be multiplied by the N_{60} in order to correct the N-values for the effect of overburden pressure in non-cohesive soils. The corrected SPT N-value is:

$$N_{160} = C_n \times N_{60} \quad [3.2]$$

$$C_n = 0.77 \log_{10} \left(\frac{1.92}{\sigma'_v} \right), \quad C_n < 2.0 \quad (S.I. units) \quad [3.3]$$

$$C_n = 0.77 \log_{10} \left(\frac{40}{\sigma'_v} \right), \quad C_n < 2.0 \quad (English units) \quad [3.4]$$

where

σ'_v = Effective vertical stress

The SPT has been used in correlations for soil unit weight (γ), relative density (D_r), angle of internal friction (ϕ), and unconfined compressive strength (S_u). There are several correlations between the SPT N-values and different soil parameters. These different correlations are presented in Table 3.1. According to Paikowsky et al. (2004), the best correlation for determining ϕ in cohesionless soils is provided by Peck Hanson and Thornburn (1974), and it is recommended to limit ϕ below 36° . The most common correlation used to estimate the S_u from SPT is also the one provided by Terzaghi and Peck (1967) using the uncorrected N-values. Tables 3.2 and 3.3 after Bowles (1977) summarize different ranges of D_r , ϕ , and γ with respect to corrected and uncorrected N-values, respectively. On the other hand, there are many empirical correlations to estimate the soil shear strength parameters from the CPT test. As shown in Table 3.4, the S_u and ϕ were mainly calculated based on the CPT cone tip resistance (q_c), as well as the soil effective overburden pressure (σ'_v). According to Paikowsky et al. (2004), the best correlation for determining S_u is by Hara (1974), while the correlation used by Robertson and Campanella (1983) was most commonly used for calculating the soil internal friction angle. There are many empirical correlations to calculate other soil parameters from the CPT, which are summarized in Kulhawy and Mayne (1990).

After this preview of different correlations used to determine soil parameters from SPT and CPT, it is appropriate to indicate that not all of these correlations were used in this study. Only some of the correlations have been chosen, as is presented later in Chapter 5.

Table 3.1: Different correlations between SPT N-values and different soil parameters

Soil Properties	SPT Correlation	Reference
ϕ (deg.)	$54 - 27.6 \exp(-0.014N_{160})$	Peck, Hanson and Thornburn (1974)
	$\tan^{-1}[N/(12.2 + 20.3\sigma')^{0.34}]$	Schmertmann (1975)
S_u (bar) (1 bar = 14.5 psi)	$0.06 N$	Terzaghi and Peck (1967)
	$0.29 N^{0.72}$	Hara (1974)
D_r	after Gibbs and Holtz	Kulhawy and Mayne, 1990

Table 3.2: D_r , ϕ , and γ corresponding to corrected SPT N-values (after Bowles, 1977)*

Description	Very Loose	Loose	Medium	Dense	Very Dense
Relative density, D_r	0 – 0.15	0.15 – 0.35	0.35 – 0.65	0.65 – 0.85	0.85 – 1.00
Corrected SPT N-value	0 to 4	4 to 10	10 to 30	30 to 50	50+
Internal friction Angle, ϕ	25 – 30°	27 – 32°	30 – 35°	35 – 40°	38 – 43°
Unit weight, γ (kN/m ³) (1 kN/m ³ = 6.24 pcf)	11.0 – 15.7	14.1 – 18.1	17.3 – 20.4	17.3 – 22.0	20.4 – 23.6

*Use 5% larger values for granular material.

Table 3.3: Ranges of q_u and γ with respect to un-corrected SPT (after Bowles, 1977)*

Description	Very soft	Soft	Medium	Stiff	Very Stiff	Hard
S_u (kPa) (1 kPa = 0.145 psi)	0 – 24	24 – 48	48 – 96	96 – 192	192 – 384	384+
Un-corrected SPT N-value	0 to 2	2 to 4	4 to 8	8 to 16	16 – 32	32+
γ (kN/m ³) (1 kN/m ³ = 6.24 pcf)	15.8 – 18.8	15.8 – 18.8	17.3 – 20.4	18.8 – 22.0	18.8 – 22.0	18.8 – 22.0

*Correlations should be used for preliminary estimates only

Table 3.4: Different correlations between CPT and different soil parameters

Soil Properties	CPT Correlation	Reference
ϕ (deg.)	$[0.1 + 0.38 * \log(q_c/\sigma'_v)]$	Robertson and Campanella (1983)
S_u (bars) (1 bar = 14.5 psi)	$(q_c - \sigma_o)/N_k$	Hara (1974)

3.1.2. Pile Capacity in Cohesive Soils

Static analysis methods model the complex soil-structure-interaction problem in a simplified form to determine the pile capacity. Static analysis methods are used for the design of pile foundations, which are necessary in releasing the bidding documents. Therefore, the main purpose of using static analysis methods in the project design stage is to perform a structural and geotechnical analysis in order to provide a reasonable estimate for the required foundation type, capacity, number, length, and size. Hence, this process will help assemble the construction bidding documents that concern the bridge substructure. Different static methods have been designed empirically or semi-empirically based on a reasonable agreement with pile load tests. Some of these methods were based on field tests conducted in cohesive soils (i.e., clayey soils), which restrict their usage in designs for similar soil types. These methods, include the Alpha (α) method, Beta (β) method, Lambda (λ) method, and CPT-method. On the other hand, there are static methods that have been developed based on field tests performed in cohesionless soils (i.e., sandy soils). Among these methods are the SPT-method and Nordlund's method. All the available static methods in literature are presented in this report, along with the methods that

have been recommended for the design of pile foundations by the 2008 AASHTO-LRFD specifications, the FHWA-LRFD highway bridge substructures reference manual (2007) and the NCHRP 507 LRFD report by Paikowsky et al. (2004).

Prior to using the static analysis methods, designers should be familiar with the limitations of each method and be able to choose the appropriate method that better represents the specific soil-pile conditions. Moreover, static methods should not be the only approach used for designing deep foundations, and several verification techniques should be performed regularly to check the design. Many state DOTs have developed their own static analysis methods that better represent their unique soil conditions and construction practices. These locally developed methods are generally referred to as the “In-house” methods. In 1989, the Iowa DOT developed their foundation soil information charts to perform pile foundation design (Dirks and Kam 1989), which were revised in 1994. The Iowa design charts were given the name “*Blue Book*” (sometimes referred to as “*BB*”). In summary, the BB is an in-house static analysis approach that was specially developed for Iowa soils, by combining different static analysis methods to enhance the pile capacity predictions (AbdelSalam et al. 2011). The different static analysis methods, as well as the BB method, are briefly described in the next sections.

3.1.2.1 The α -API Method

The α -method (API-1974) is a semi-empirical, total stress approach for calculating the pile skin friction using the soil undrained shear strength (S_u). This method was mainly developed for cohesive or clayey soils. It has been used for many years and has proven to provide reasonable design capacities for displacement and non-displacement piles. The method depends on the alpha factor (α), which is indirectly related to the S_u . The factor was back calculated from several pile load tests. The main equation used for calculating the pile unit shaft resistance is:

$$f_s = \alpha \cdot S_u \quad [3.5]$$

where

f_s = Unit side-friction resistance

α = Adhesion factor

S_u = Undrained shear strength in soil adjacent to the foundation

Numerous functions have been developed for correlating the α -value to different soil properties and pile types. Among the most commonly used functions are those developed by Tomlinson (1957), Peck (1958), the American Petroleum Institute (API-1974), and Tomlinson (1980). Figure 3.1 presents some of the different correlations used to calculate α after Vesic (1977). It is clear from the figure that there is a large scatter among the α -values, which requires local experience while selecting the suitable function used in the design of piles. According to Coduto (2001), although the API (1974) function was mainly developed for the design of offshore piles, it is probably most suitable for the design of driven piles. The equations used to determine α -values based on the API are:

For; $S_u < 25$ kPa (500 psf):

$$\alpha = 1 \quad [3.6]$$

For; 25 kPa (500 psf) < S_u < 75 kPa (1500 psf):

$$\alpha = 1.0 - 0.5 \left(\frac{S_u - 25 \text{ kPa}}{50 \text{ kPa}} \right) \quad (\text{S.I. units}) \quad [3.7]$$

$$\alpha = 1.0 - 0.5 \left(\frac{S_u - 500 \text{ lb/ft}^2}{1000 \text{ lb/ft}^2} \right) \quad (\text{English units}) \quad [3.8]$$

For; $S_u > 75 \text{ kPa (1500 psf)}$:

$$\alpha = 0.5 \quad [3.9]$$

On the other hand, O'Neill and Reese (1999) have developed a bearing capacity factor (N_c) to calculate the end bearing resistance of deep foundations in cohesive soil based on the soil total undrained shear strength as follows:

$$q'_t = N_c^* \times S_u \quad [3.10]$$

where

q'_t = Net unit end bearing resistance

S_u = Undrained shear strength of the soil between pile tip and 2B below the tip

B = Pile diameter

N_c^* = Bearing capacity factor (after O'Neill and Reese, 1999)

$N_c^* = 6.5$ if $S_u \leq 25 \text{ kPa (500 psf)}$ [3.11]

$N_c^* = 8.0$ at $S_u = 50 \text{ kPa (1000 psf)}$ [3.12]

$N_c^* = 9.0$ at $S_u \geq 100 \text{ kPa (2000 psf)}$ [3.13]

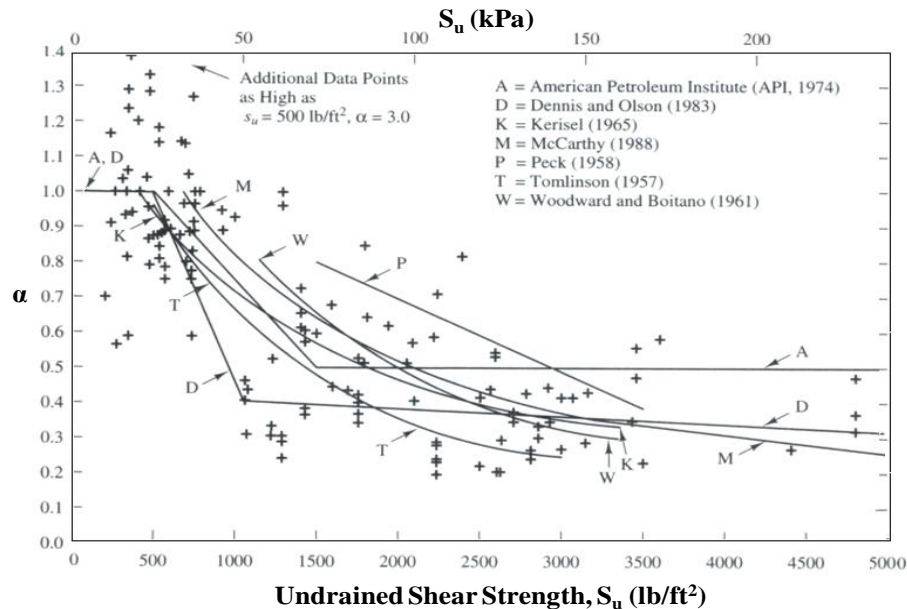


Figure 3.1: Measured values of α as back calculated from static load tests compared with several proposed functions for α (from Coduto, 2001)

As previously indicated, the S_u was calculated based on the correlation to the uncorrected SPT N-values provided by Terzaghi and Peck (1967). This raised many arguments against the

reliability of the α -method, even though the S_u was determined based on laboratory testing because the soil sampling method can cause significant disturbance to the soil properties (Jardine et al., 2005). They added that in case of driven piles, the driving process itself could lead to significant changes in soil properties, such as the soil remolding next to the pile. This may directly affect the calculated pile skin-friction based on the α -method. However, the method has been widely used as it still provides relatively reasonable pile capacities in cohesive soils (Coduto, 2001).

3.1.2.2 The α -Tomlinson Method

Among the common functions that have been developed to correlate the α -value to the soil undrained shear strength is the function developed by Tomlinson (1980). The α -Tomlinson has been widely used especially in stiff clays. This method accounts for different pile materials (i.e., concrete, timber, or steel piles) and provides reasonable capacity estimates for large displacement piles. Hence, it may not be the most suitable method for driven piles. The method relies on the α -values, which in turn depend on the bearing embedment in stiff clay and the width of the pile. The equation used for calculating skin friction using α -Tomlinson is similar to α -API, with the value of α being the only difference. The corresponding equation is as follows:

$$f_s = \alpha \cdot S_u \quad [3.14]$$

where

f_s = Unit side-friction resistance

α = Adhesion factor (from Figures 3.2 and 3.3 after Tomlinson 1979 and 1980, respectively)

S_u = Undrained shear strength in soil adjacent to the foundation

The same Eq. [3.10] based on the α -API method is used to calculate the end bearing resistance of the pile.

3.1.2.3 The β -Method

The β -method (Burland, 1973) is a semi-empirical approach based on effective stresses calculated from the vertical effective overburden stress. The method was developed to model the long-term drained shear strength. It can be used for different soil types such as clay, silt, sand, or gravel, and can even be used for layered soil profiles. According to Fellenius (1991), the beta factor (β) is affected by the soil type, mineralogy, density, strength, pile insulation technique, and other factors. The values of β range between 0.23 and 0.8, but cannot exceed 2 for over-consolidated soils as suggested by Esrig and Kirby (1979). The β -method has been found to work best for piles in normally consolidated and lightly over-consolidated soils. However, the method tends to overestimate the pile capacity for heavily over-consolidated soils (AASHTO-interim 2006). The β -method equation for calculating the unit skin friction is as follows:

$$f_s = \beta \cdot \bar{P}_0 \quad [3.15]$$

where

f_s = Unit side-friction resistance

B = Bjerrum-Burland β coefficient = $K_s \tan \delta$ (or use Table 3.5 and Figure 3.4)

\bar{P}_0 = Average effective overburden pressure along the pile shaft (kPa)

K_s = Earth pressure coefficient
 Δ = Friction angle between pile and soil

In order to calculate the end bearing resistance of the pile, Eq. [3.16] is used:

$$q_t = N_t \cdot P_t \quad [3.16]$$

where

N_t = End bearing capacity coefficient (can be found from Table 3.5 and Figure 3.5, after Fellenius, 1991)

P_t = Effective overburden pressure at pile toe (kPa)

Note that N_t and P_t are functions of soil internal friction angle (ϕ') which, in turn, can be calculated using empirical correlations to SPT N-values or from laboratory testing.

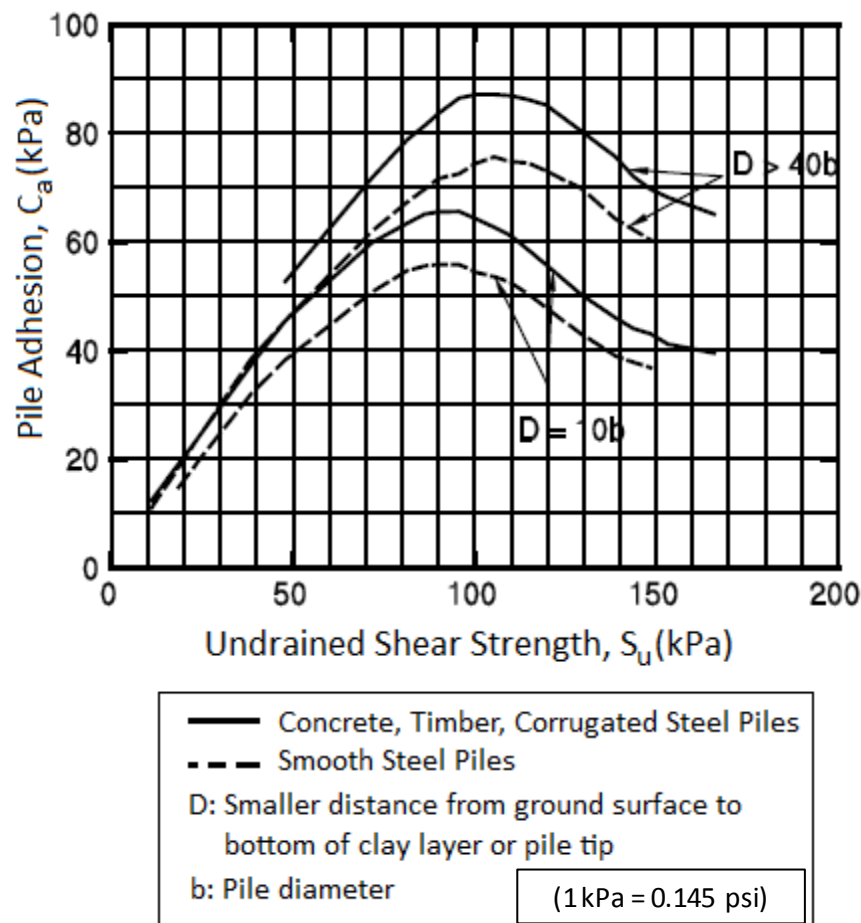


Figure 3.2: Adhesion values for piles in cohesive soils (after Tomlinson, 1979)

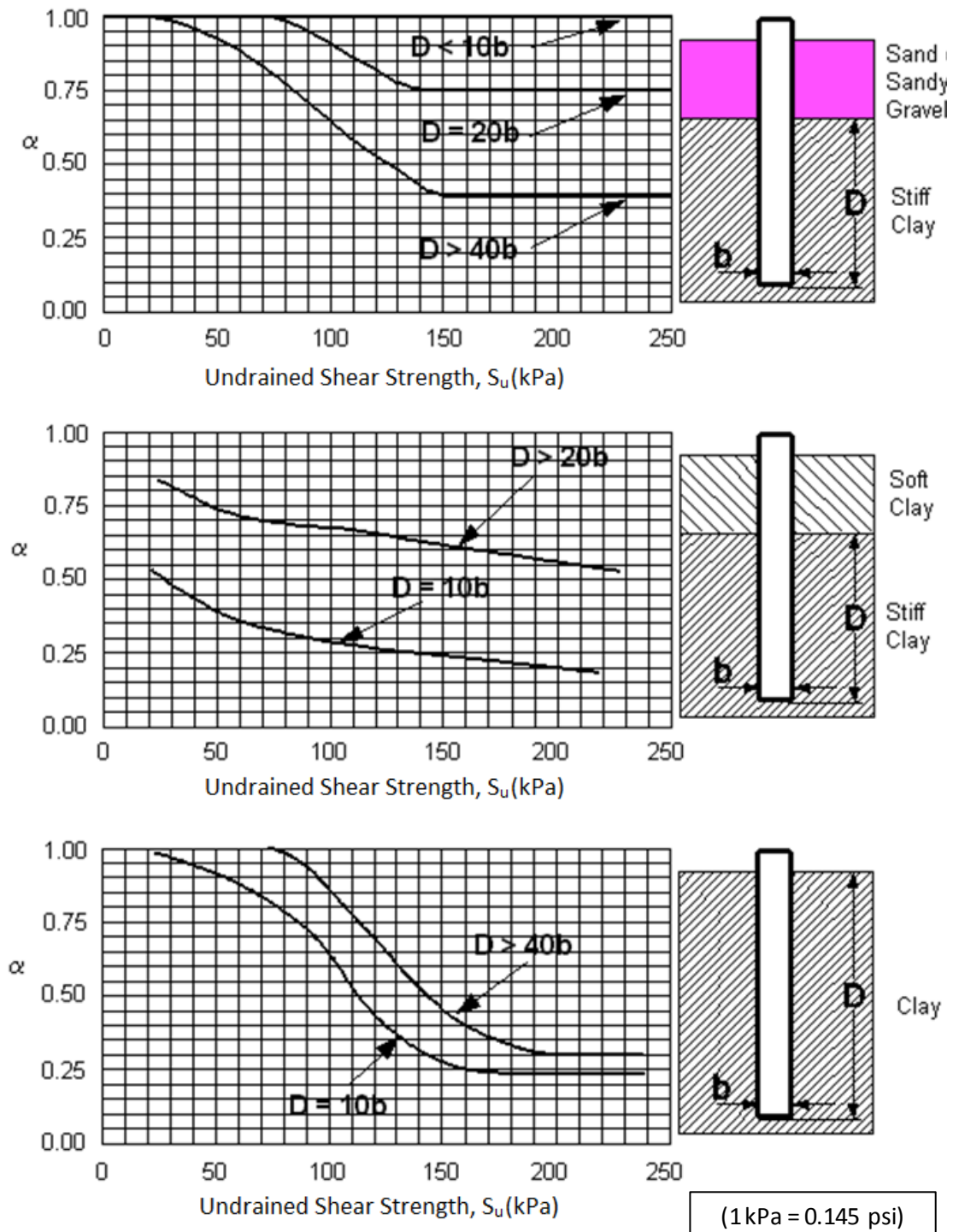


Figure 3.3: Adhesion factors for driven piles in clay soils (after Tomlinson, 1980)

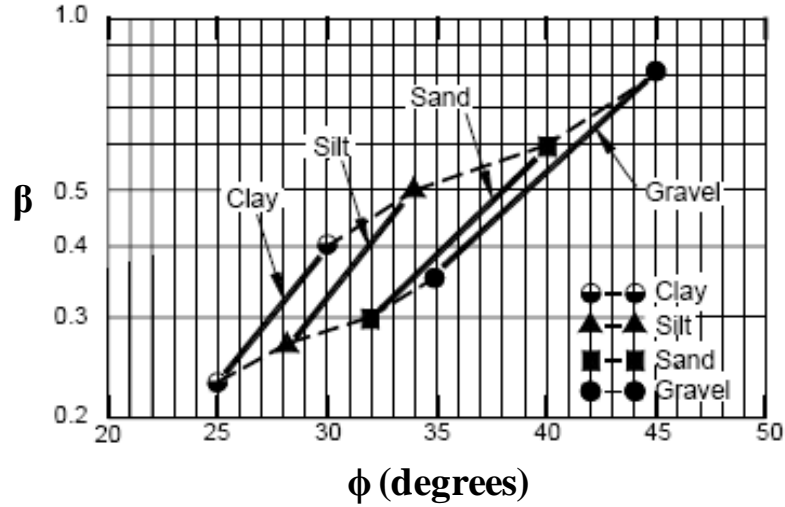


Figure 3.4: The β coefficient versus soil type using ϕ' angle (after from Fellenius, 1991)

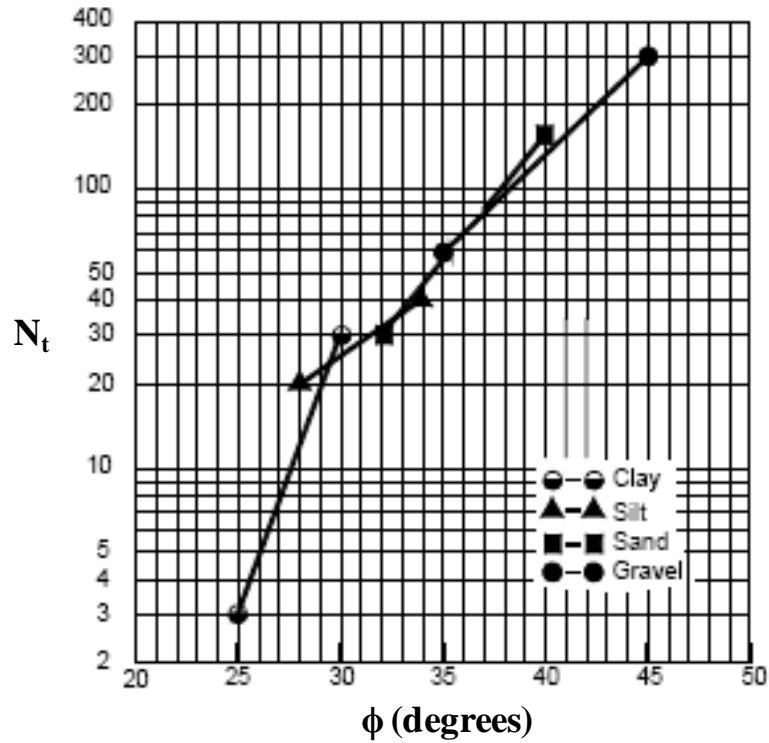


Figure 3.5: The N_t coefficient versus soil type using ϕ' angle (after Fellenius, 1991)

Table 3.5: Approximate range of β and N_t coefficients (after Fellenius, 1991)

Soil type	ϕ' (deg.)	β	N_t
Clay	25 – 30	0.23 – 0.40	3 – 30
Silt	28 – 34	0.27 – 0.50	20 – 40
Sand	32 – 40	0.30 – 0.60	30 – 150
Gravel	35 – 45	0.35 – 0.80	60 – 300

3.1.2.4 The λ -Method

The λ -method (Corps of Engineers, 1992) is an empirical approach based on effective stresses induced in the soil (calculated from the vertical effective overburden stress) and the total soil stress (calculated from undrained shear strength). This method may be used to relate the unit skin friction to the passive earth pressure (AASHTO-interim 2006). The value of λ was empirically determined by examining the results attained from various load tests that were conducted on steel pipe piles in cohesive soils, and thus, this method is more accurate if used for same soil and pile conditions. Eq. [3.17] is used to calculate the skin friction:

$$q_s = \lambda(\sigma'_v + 2S_u) \quad [3.17]$$

where

- $\sigma'_v + 2S_u$ = Passive lateral earth pressure (ksf)
- σ'_v = Effective vertical stress at midpoint of soil layer under consideration (ksf)
- S_u = Undrained shear strength of soil (ksf)
- λ = Empirical coefficient (see Figure 3.6; after Vijayvergiya and Focht, 1972)

In order to calculate the end bearing resistance of the pile in cohesive soil, use the same equations of the α -method, mentioned previously (based on O'Neill and Reese, 1999).

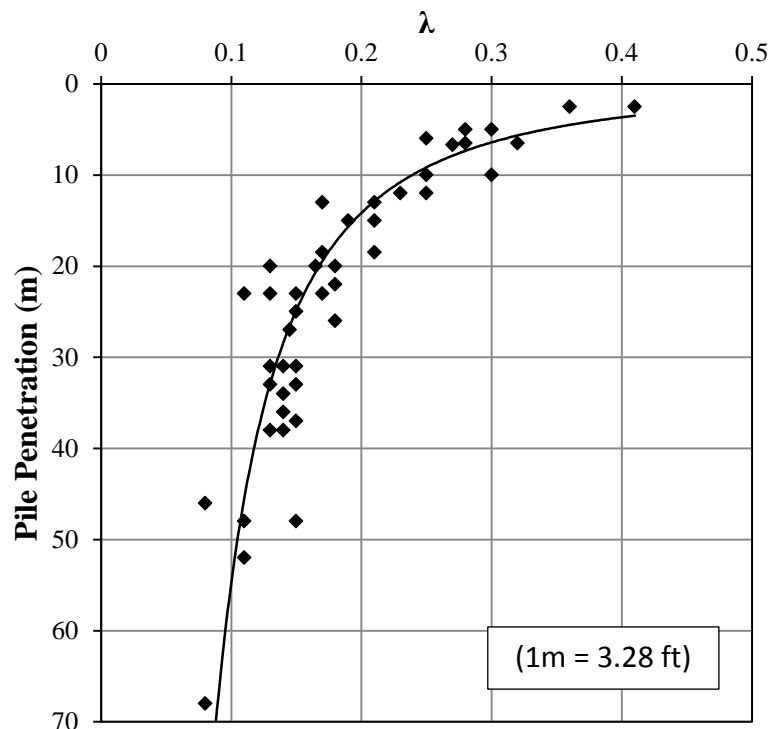


Figure 3.6: Chart for λ factor using pile penetration length (after Vijayvergiya and Focht, 1972)

3.1.2.5 The CPT-Method

Nottingham and Schmertmann (1975) developed an empirical approach for calculating the pile capacity based on the CPT, which is applied to cohesive and cohesionless soils. Correlations to CPT provide accurate pile design capacities, especially with driven piles. Moreover, it provides continuous readings for the soil profile and can take the effect of different soil layers into consideration. The cone tip resistance (q_c) is used to determine the end bearing resistance of piles, while the sleeve friction (f_s) is used to determine the skin friction resistance along the shaft. The ultimate shaft resistance in cohesionless soils can be calculated as follows:

$$R_s = K \left[\frac{1}{2} (\bar{f}_s A_s)_{0 \text{ to } 8b} + (\bar{f}_s A_s)_{8b \text{ to } D} \right] \quad [3.18]$$

If \bar{f}_s is not available, the shaft resistance in cohesionless soils could be determined from the cone tip resistance as follows:

$$R_s = C_f \sum q_c \cdot A_s \quad [3.19]$$

In the case of cohesive soils, the shaft resistance could be determined using the following expression:

$$R_s = \alpha' \cdot \bar{f}_s \cdot A_s \quad [3.20]$$

where

- K = Ratio of unit pile shaft resistance to unit cone sleeve friction in sands (use Figure 3.7)
- D = Embedded pile length
- b = Pile width or diameter
- \bar{f}_s = Average unit sleeve friction from CPT at the point considered
- A_s = Pile-soil surface area over at the point considered
- C_f = Factor obtained from Table 3.6 (after the FHWA-LRFD reference manual, 2007)
- q_c = Average cone tip resistance along the pile length
- α' = Ratio of pile shaft to sleeve friction (use Figure 3.8, after Schmertmann, 1978)

The ultimate tip resistance (or the pile end bearing) shall be determined as follows:

$$q_t = \frac{q_{c1} + q_{c2}}{2} \quad [3.21]$$

where

- q_{c1} = Average of cone tip resistance over distance xb following the path 1-2-3 using the minimum path rule in the upward direction (Figure 3.9 after Nottingham and Schmertman, 1975)
- b = Pile diameter
- x = Value from 0.7 to 4.0 below pile tip as shown in Figure 3.9
- q_{c2} = Average of cone tip resistance over distance $8b$ following the path 3-4 using the minimum path rule as shown on Figure 3.9.

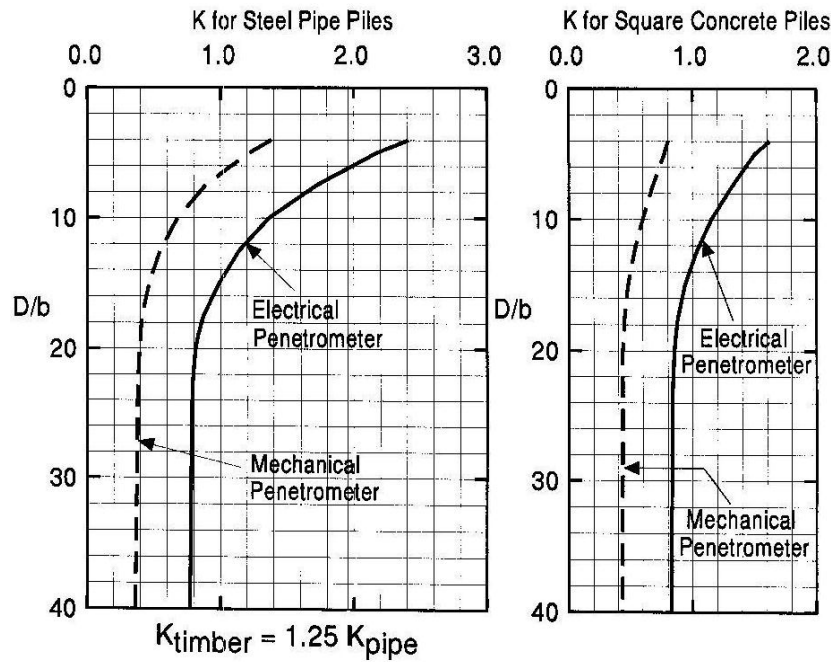


Figure 3.7: Penetrometer design curve for pile side friction in sand (after FHWA, 2007)

Table 3.6: Represents CPT C_f values (after the FHWA, 2007)

Type of piles	C_f
Precast concrete	0.012
Timber	0.018
Steel displacement	0.012
Open end steel pipe	0.008

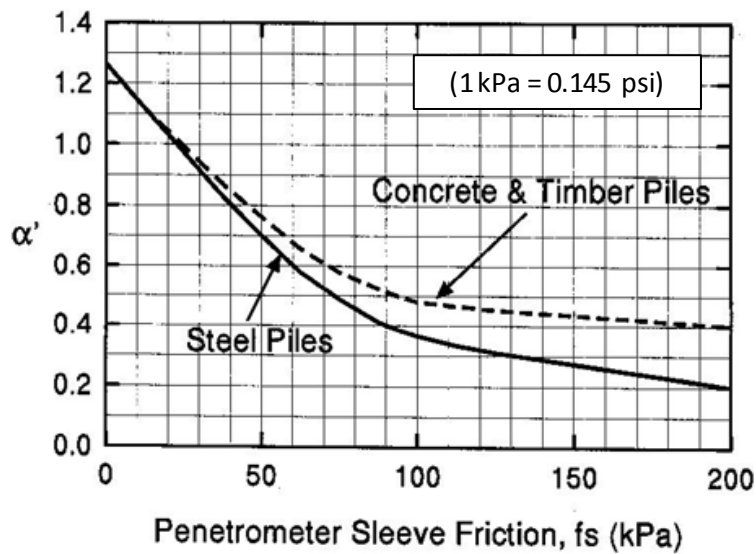


Figure 3.8: Design curve for skin-friction in clays recommended by Schmertmann (1978)

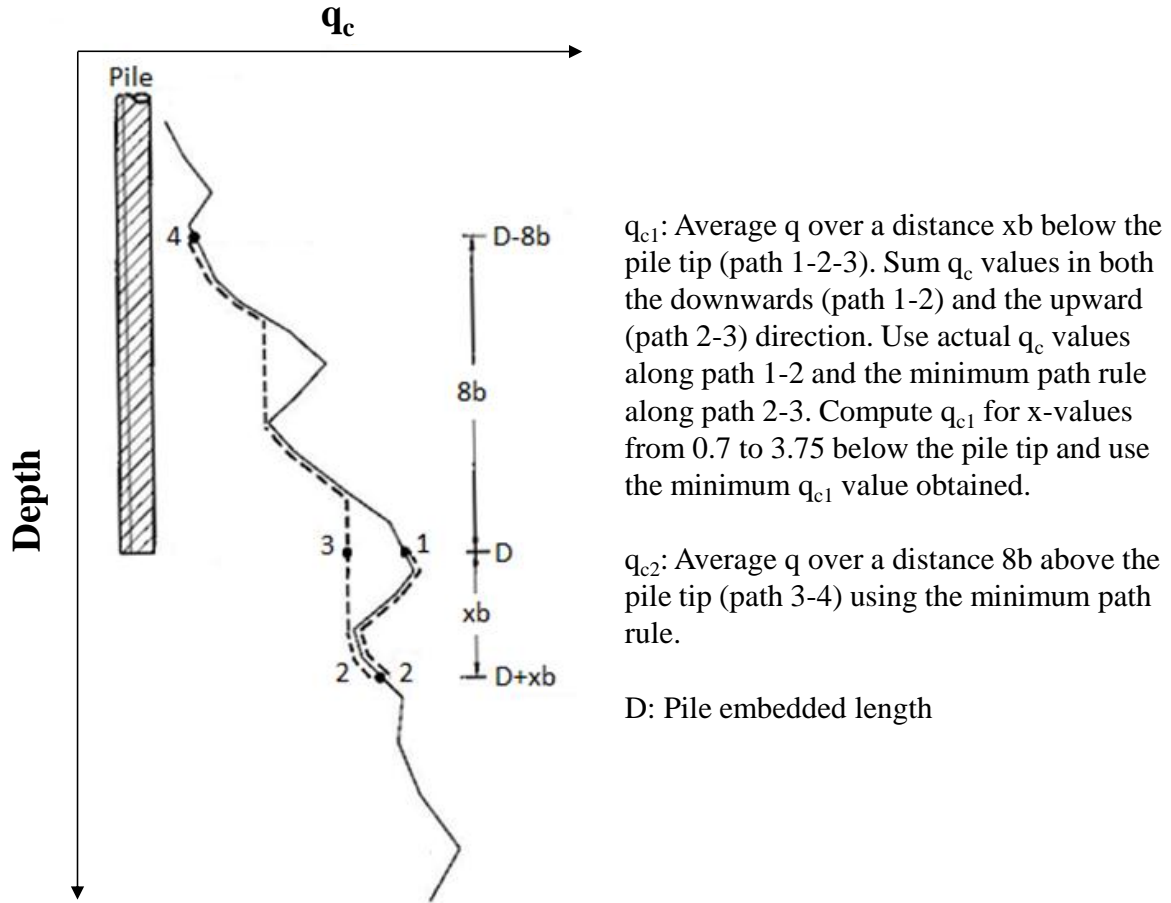


Figure 3.9: Procedure suggested for estimating the pile end bearing capacity by Nottingham and Schmertman, 1975)

3.1.3. Pile Capacity in Cohesionless Soils

3.1.3.1 The SPT-Meyerhof Method

The SPT-Meyerhof method (Meyerhof, 1976/1981) is an empirical approach for calculating the pile capacity based on SPT tests conducted in cohesionless soils such as sands and non-plastic silts. According to the FHWA-LRFD reference manual (2007), the SPT method should be only used for preliminary estimates of the pile capacity, not for final design recommendations. This is due to the non-reproducibility of SPT N -values and simplified assumptions contained in the method. Meyerhof (1976) reported different correlations and provided some limitations on shaft and tip resistance according to the pile type (displacement or non-displacement pile). Based on the SPT-Meyerhof method for piles driven to a depth D_b in cohesionless soil, the end bearing capacity is calculated using the following:

$$q_t = \frac{40 \bar{N}'_b D_b}{b} \leq 400 \bar{N}'_b \quad \text{kPa} \quad (\text{SI Units}) \quad [3.22]$$

$$q_t = \frac{0.8 \bar{N}'_b D_b}{b} \leq \bar{N}'_b \quad \text{ksf} \quad (\text{English Units}) \quad [3.23]$$

where

\bar{N}'_b = Average SPT blow counts (blows/1ft) of the bearing stratum extended to 3b below pile tip and corrected for overburden pressure

b = Pile diameter

D_b = Pile embedment depth in the bearing stratum

The skin friction for displacement piles (e.g., closed end pipe piles) in cohesionless soils for the SPT-Meyerhof method is calculated using the following equations:

$$f_s = 2\bar{N}' \quad \text{kPa} \quad (\text{SI Units}) \quad [3.24]$$

$$f_s = \frac{\bar{N}'}{25} \quad \text{ksf} \quad (\text{English Units}) \quad [3.25]$$

The skin friction for non-displacement piles (e.g., Steel H-piles) in cohesionless soils for the SPT-Meyerhof method is calculated using following equations:

$$f_s = \bar{N}' \quad \text{kPa} \quad (\text{SI Units}) \quad [3.26]$$

$$f_s = \frac{\bar{N}'}{50} \quad \text{ksf} \quad (\text{English Units}) \quad [3.27]$$

where

f_s = Unit skin friction (shaft resistance) for driven pile

\bar{N}' = Average SPT blow counts along the pile and corrected for overburden pressure

3.1.3.2 The SPT-Schmertmann Method

The SPT-Schmertmann method (Lai and Graham, 1995) is an empirical approach based on SPT N-values, which is applicable in sand, clay, and mixed soils. This method is conservative, as it ignores the shaft resistance when the N-value is less than five blows/ft, and also limits the N-value to 60 blows/ft. The correlations used for calculating the skin friction for different piles and soil types are presented in Table 3.7. It is clear from Table 3.7 that all the correlations depend on the uncorrected SPT N-values. On the other hand, in order to calculate unit end bearing, the following equation is used:

$$q_p = \frac{(\text{average } q_p)_{8B \text{ above desired point}} + (\text{average } q_p)_{3.5B \text{ below desired point}}}{2} \quad [3.28]$$

where

q_p = Weighted average tip resistance from Table 3.8

B = Pile diameter

The ultimate tip resistance is fully mobilized if the actual bearing embedment length (D_A) is equal to the critical bearing embedment length (D_C). D_C is determined using Table 3.9. In case of $D_A < D_C$, the mobilized tip resistance for H-piles is reduced. In order to calculate the exact reduction in tip resistance, the following equations are used:

If $D_A < D_C$ and the bearing layer is stronger than the overlying layer:

$$q_p = q_{LC} + \frac{D_A}{D_C} (q_T - q_{LC}) \quad [3.29]$$

$$CSFBL = \frac{SFBL}{q_T} \left[q_{LC} + \frac{D_A}{2D_C} (q_T - q_{LC}) \right] \quad [3.30]$$

where

q_p = Reduced tip resistance

q_T = Unit tip resistance at layer change

q_{LC} = Uncorrected unit tip resistance at pile tip

CSFBL = Reduced side resistance in bearing layer

SFBL = Uncorrected side resistance in bearing layer

If $D_A > D_C$ and the bearing layer stronger than the overlying layer, then:

$$CSFACD = \frac{USFACD}{q_{CD}} [q_{LC} + 0.5(q_{CD} - q_{LC})] \quad [3.31]$$

where

CSFACD = Corrected side resistance between the top of the layer and the critical depth

USFACD = Uncorrected side resistance from the top of the bearing layer to critical depth

q_{CD} = Unit tip resistance at critical depth

Table 3.7: Side resistance correlations for the SPT-Schmertmann method

Type	Soil Description	Ultimate unit shaft resistance q_p (tsf)		
		Concrete piles	Steel H-piles	Pipe piles
1	Clay	$2.0N(110-N)/4006.6$	$2N(110-N)/5335.94$	$0.949+0.238\ln N$
2	Mixed soil	$2.0N(100-N)/4583.3$	$-0.0227+0.033N-(4.57610^{-1})^* N^2 + 2.465(E-6*N^3)$	$0.243+0.147\ln N$
3	Sands	0.019N	0.0116N	$0.058+0.152\ln N$
4	Limestone	0.01N	0.0076N	$0.018+0.134\ln N$

Table 3.8: Tip resistance correlations for the SPT-Schmertmann method

Type	Soil Description	Ultimate unit tip resistance q_p (tsf)	
		Concrete and Steel H-piles	Pipe piles
1	Clay	0.7N	0.48N
2	Mixed soil	1.6N	0.96N
3	Sands	3.2N	1.312N
4	Limestone	3.6N	1.92N

Table 3.9: Critical bearing depth ratio for the SPT-Schmertmann method

Type	Soil Description	Critical depth ratio (D_c/B)
1	Clay	2
2	Mixed soil	4
3	Sands ($N \leq 12$)	6
	Sands ($N \leq 30$)	9
	Sands ($N > 30$)	12
4	Limestone	6

3.1.3.3 The Nordlund Method

The SPT-Nordlund method (Nordlund and Thurman, 1963) is a semi-empirical approach based on field observations from pile static load tests. It accounts for different pile shapes (i.e., constant diameter or tapered piles), as well as pile materials and types, including steel H-piles, closed and open-ended pipe piles, and timber piles. According to Hannigan et al. (2005), this method is preferred in cohesionless soils, such as sandy and gravelly soils, as the pile load tests used to develop the Nordlunds' design curves were conducted in sandy soils. Moreover, the load tests were conducted for piles with diameters (widths) less than 500mm (19.6 inches), which meant that the method over predicted the capacity for piles with widths larger than 500mm (19.6 inches). A detailed pile design procedure using the Nordlund method is provided in the FHWA Design and Construction of Driven Pile Foundations, Workshop manual, Volumes I (1997). For tapered piles, the total ultimate pile capacity (shaft resistance and end bearing) for Nordlund method is calculated using the following equation:

$$Q_u = \sum_{d=0}^{d=D} K_\delta \times C_f \times P_d \times \frac{\sin(\delta+\omega)}{\cos \omega} C_d \times \Delta d + \alpha_t \times N'_q \times A_t \times P_t \quad [3.32]$$

In case of piles with uniform cross sections, the capacity is calculated using the equation:

$$Q_u = K_\delta \times C_f \times P_d \times \sin \delta \times C_d \times D + \alpha_t \times N'_q \times A_t \times P_t \quad [3.33]$$

$$\text{or, it can be written as: } Q_u = K_\delta \times C_f \times P_d \times \sin \delta \times C_d \times D + q_L \times A_t \quad [3.34]$$

where

d = Depth

D = Embedded pile length

K_δ = Coefficient of lateral earth pressure at depth d (Tables 3.10 and 3.11)

C_f = Correction factor for K_δ when $\delta \neq \phi$ (use Figure 3.10)

P_d = Effective overburden pressure at the center of depth increment d

δ = Friction angle between soil and pile

ω = Angle of pile taper from vertical

C_d = Pile perimeter at depth d

Δd = Length of pile segment

α_t = Factor depending on pile depth-width relationship (use Figure 3.11)

N'_q = Bearing capacity factor (use Figure 3.12)

A_t = Pile toe area

P_t = Effective overburden pressure at pile toe $\leq 150 \text{ kPa} \leq 3.2 \text{ ksf}$

q_L = Limiting unit tip resistance (use Figure 3.13)

Table 3.10: Evaluating K_δ for piles when $\omega = 0^\circ$ and $V = 0.0093$ to $0.093 \text{ m}^3/\text{m}$

ϕ	Displaced Volume (V), m^3/m									
	0.01	0.02	0.03	0.04	0.05	0.06	0.07	0.07	0.08	0.09
25	0.70	0.75	0.77	0.79	0.80	0.82	0.83	0.84	0.84	0.85
26	0.73	0.78	0.82	0.84	0.86	0.87	0.88	0.89	0.90	0.91
27	0.76	0.82	0.86	0.89	0.91	0.92	0.94	0.95	0.96	0.97
28	0.79	0.86	0.90	0.93	0.96	0.98	0.99	1.01	1.02	1.03
29	0.82	0.90	0.95	0.98	1.01	1.03	1.05	1.06	1.08	1.09
30	0.85	0.94	0.99	1.03	1.06	1.08	1.10	1.12	1.14	1.15
31	0.91	1.02	1.08	1.13	1.16	1.19	1.21	1.24	1.25	1.27
32	0.97	1.10	1.17	1.22	1.26	1.30	1.32	1.35	1.37	1.39
33	1.03	1.17	1.26	1.32	1.37	1.40	1.44	1.46	1.49	1.51
34	1.09	1.25	1.35	1.42	1.47	1.51	1.55	1.58	1.61	1.63
35	1.15	1.33	1.44	1.51	1.57	1.62	1.66	1.69	1.72	1.75
36	1.26	1.48	1.61	1.71	1.78	1.84	1.89	1.93	1.97	2.00
37	1.37	1.63	1.79	1.90	1.99	2.05	2.11	2.16	2.21	2.25
38	1.48	1.79	1.97	2.09	2.19	2.27	2.34	2.40	2.45	2.50
39	1.59	1.94	2.14	2.29	2.40	2.49	2.57	2.64	2.70	2.75
40	1.70	2.09	2.32	2.48	2.61	2.71	2.80	2.87	2.94	3.00

Table 3.11: Evaluating K_δ for piles when $\omega = 0^\circ$ and $V = 0.093$ to $0.93 \text{ m}^3/\text{m}$

ϕ	Displaced Volume (V), m^3/m									
	0.093	0.186	0.279	0.372	0.465	0.558	0.651	0.744	0.837	0.93
25	0.85	0.9	0.92	0.94	0.95	0.97	0.98	0.99	0.99	1
26	0.91	0.96	1	1.02	1.04	1.05	1.06	1.07	1.08	1.09
27	0.97	1.03	1.07	1.1	1.12	1.13	1.15	1.16	1.17	1.18
28	1.03	1.1	1.14	1.17	1.2	1.22	1.23	1.25	1.26	1.27
29	1.09	1.17	1.22	1.25	1.28	1.3	1.32	1.33	1.35	1.36
30	1.15	1.24	1.29	1.33	1.36	1.38	1.4	1.42	1.44	1.45
31	1.27	1.38	1.44	1.49	1.52	1.55	1.57	1.6	1.61	1.63
32	1.39	1.52	1.59	1.64	1.68	1.72	1.74	1.77	1.79	1.81
33	1.51	1.65	1.74	1.8	1.85	1.88	1.92	1.94	1.97	1.99
34	1.63	1.79	1.89	1.96	2.01	2.05	2.09	2.12	2.15	2.17
35	1.75	1.93	2.04	2.11	2.17	2.22	2.26	2.29	2.32	2.35
36	2	2.22	2.35	2.45	2.52	2.58	2.63	2.67	2.71	2.74
37	2.25	2.51	2.67	2.78	2.87	2.93	2.99	3.04	3.09	3.13
38	2.5	2.81	2.99	3.11	3.11	3.29	3.36	3.42	3.47	3.52
39	2.75	3.1	3.3	3.45	3.45	3.65	3.73	2.8	3.86	3.91
40	3	3.39	3.62	3.78	3.78	4.01	4.1	4.17	4.24	4.3

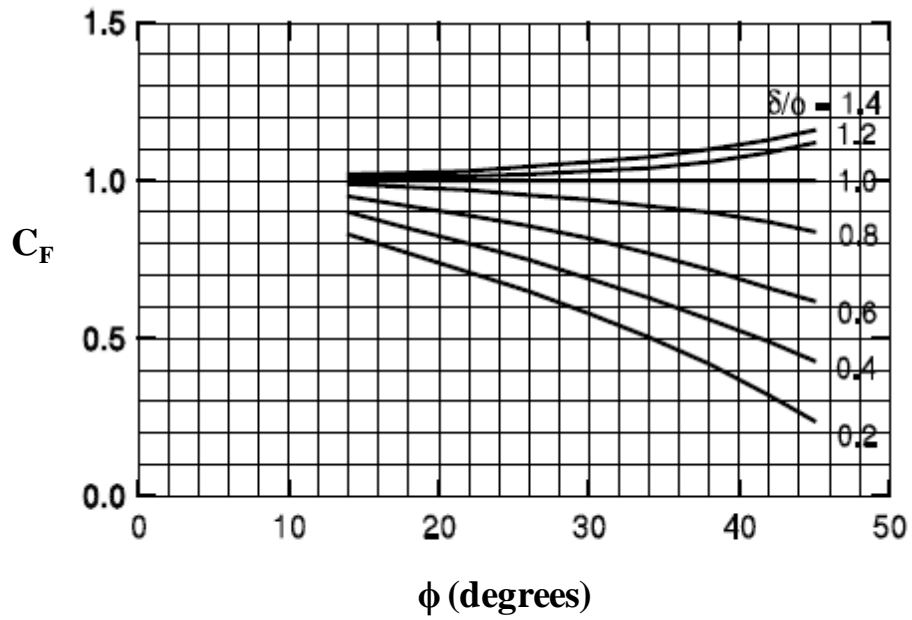


Figure 3.10: Correction factor C_F for K_δ when $\delta \neq \phi$ (after Nordlund, 1979)

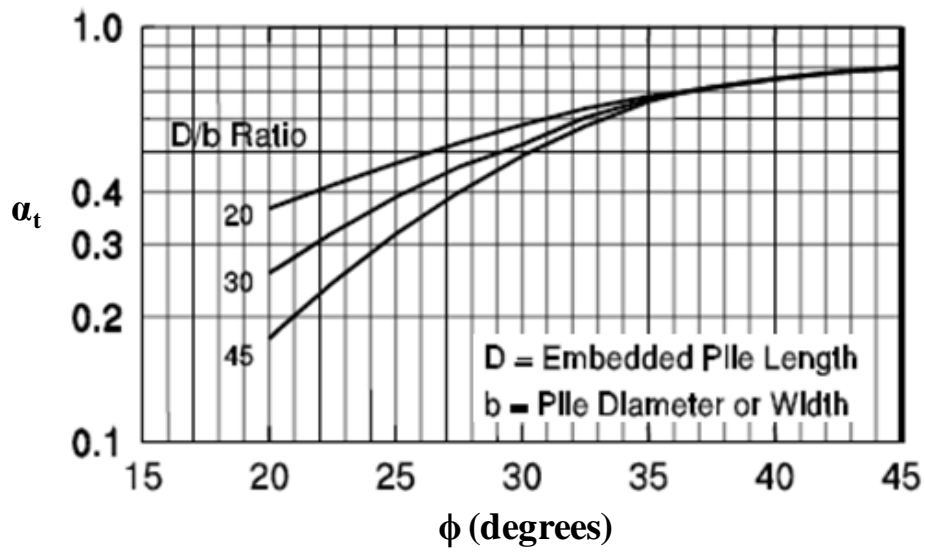


Figure 3.11: Chart for estimating the α_t coefficient from ϕ (after Nordlund, 1979)

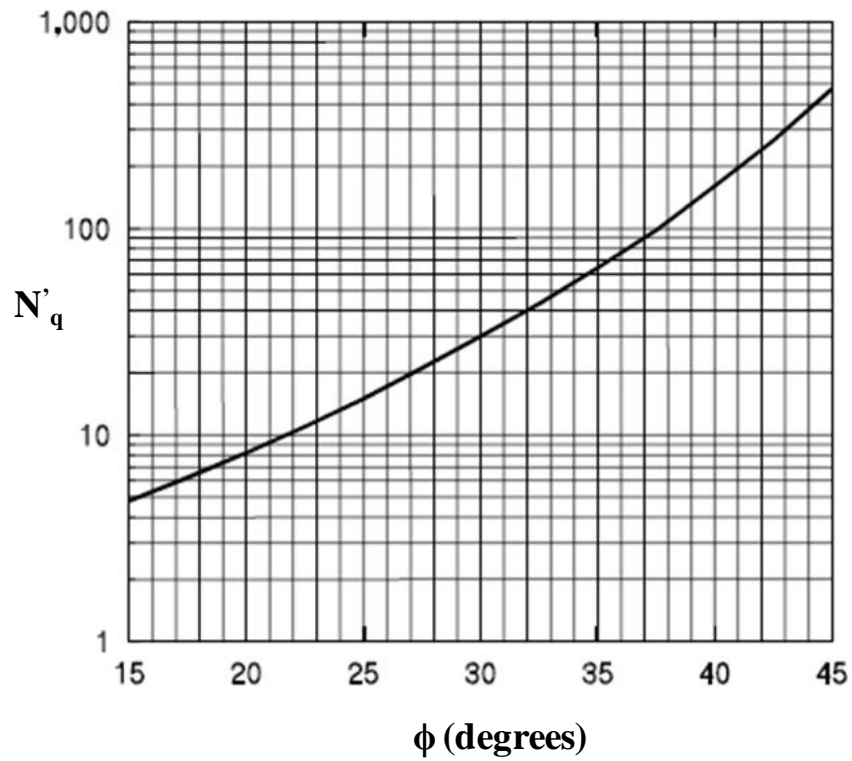


Figure 3.12: Chart for estimating the N'_q coefficient from ϕ (after Bowles, 1977)

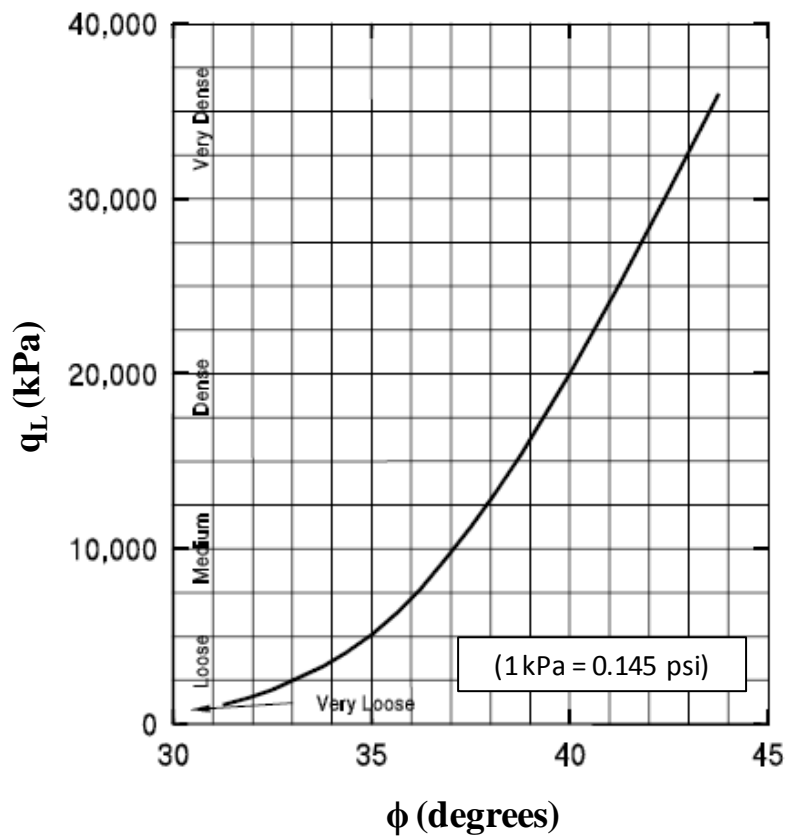


Figure 3.13: Relationship between the toe resistance and ϕ in sand (after Meyerhof, 1976)

3.1.4. Iowa Blue Book Method

The Iowa Foundation soils information chart for pile design (or Iowa Blue Book) was developed in 1989 by Dirks and Kam and was revised by the Iowa DOT in 1994. The Blue Book (BB) enables the design engineer to calculate the pile skin friction, as well as the end bearing separately. A combination of the SPT-Meyerhof method (Meyerhof, 1976/1981) and α -Tomlinson method (Tomlinson 1980) was used to develop the pile skin friction design charts for different soil types. On the other hand, the wave equation concepts were used to develop the end bearing charts. The BB was calibrated to more than 280 pile load tests, which have been performed in the State of Iowa since 1968. The BB design chart accounted for different pile materials and geometry. Practically the only soil parameter required during the pile design using the BB is the SPT corrected N-values, and hence, it is considered a simple method. The BB has proven to provide a relatively consistent pile design compared to other complex static analysis methods. The major limitation of the BB is including an embedded factor of safety equal to 2.0, making it relatively conservative compared to other design methods and also violates the basic principles of the LRFD approach.

3.1.5. The DRIVEN Computer Program

The DRIVEN computer program was developed for calculating the pile capacity by the FHWA in 1998. This program calculates the capacity of open and closed end pipe piles, steel H-piles, concrete piles, and other pile types. From the DRIVEN user manual by Mathias and Cribbs (1998), the user inputs the soil layers, unit weights, and strength parameters, including the percentage of strength loss during driving. After selecting the pile type, the program calculates the pile capacity versus depth. It can be used for cohesive and cohesionless soils. Nordlund method and the α -method (previously described in this chapter) are used for calculating pile capacity in the DRIVEN program for cohesionless and cohesive layers, respectively. Several analysis options are available, in which unsuitable soil layers and the scourable soils can be excluded in the ultimate pile capacity estimation. Using DRIVEN, the pile capacity can be calculated at the EOD, as well as BOR. There are options that account for pile plugging also. The program provides a compatible output data file with the GRLWEAP wave equation program to facilitate the running of a drivability study with a higher level of accuracy. This program is available online for geotechnical engineers at the FHWA official website.

3.1.6. SPT-97

SPT-97 is a WindowsTM-based computer program developed by the Florida DOT (FDOT) and the University of Florida. It calculates the pile capacity based on the SPT-Schmertmann method (Lai and Graham. 1995), which was mentioned earlier in this chapter. This method was used in NCHRP Report 507 (Paikowsky, et al., 2004) for calibrating the LRFD resistance factors. According to the Paikowsky, et al., 2004, this computer program proved to work normally with the exception of two cases: 1) there is a problem in correcting the pile resistance when $D_c < D_a$ (critical bearing depth is smaller than actual), in which this problem might occur for Iowa soils due to relatively low D_c ; and 2) the capacity is incorrectly computed for pipe piles. This program is available online for geotechnical engineers at the FDOT official website.

3.1.7. Comparison of Different Static Methods

It is important to compare and select the appropriate static analysis method for a specific design problem. This should be based on the soil and pile types, the extent of available soil parameters, as well as the degree of accuracy needed from the design analysis. Table 3.12 summarizes the most commonly used static analysis methods and provides a brief description of the approach used to drive each method, the recommended soil type, design parameters and in-situ tests needed, as well as the advantages and limitations corresponding to different methods. On the other hand, Table 3.13 summarizes the required equations for calculating the shaft and tip resistances using different static analysis methods, and clearly indicates the appropriate soil type recommended for each method along with the required soil parameters or in-situ tests required for the analysis.

3.2. Dynamic Analysis Methods

The dynamic analysis methods have unique advantages over the static analysis methods when estimating the pile capacity, as they can be used to control pile construction, detect pile damage, evaluate driving hammer performance, assess soil resistance distribution, determine dynamic soil parameters and evaluate time dependent pile capacity. Based on the wave propagation theory, the dynamic analysis was first proposed by St. Venant almost a century ago and has been progressively developed in the United States since then. Different dynamic methods are now being routinely used and have been incorporated into a standard specification for deep pile foundations by the American Society for Testing and Materials (ASTM D4945-2008). The dynamic analysis methods used in this project were Pile Driving Analyzer (PDA), Case Pile Wave Analysis Program (CAPWAP), and Wave Equation Analysis Program (WEAP), which will be briefly introduced in the following sections. Detailed descriptions and analyses of these three dynamic methods are provided in the Volume II report of this project by Ng, et al. (2010).

3.2.1. Pile Driving Analyzer

Pile Driving Analyzer (PDA) is a data acquisition system that was developed in the 1960s by Goble and his students at the Case Western Reserve University. PDA uses the Case method, which requires the measurements of pile strains and accelerations to 1) estimate pile capacity, 2) investigate the development of soil resistances as a function of time, 3) evaluate pile data quality, 4) assess the soil resistance distribution, 5) determine the pile integrity, and 6) evaluate the driving system performance. The pile strains and accelerations are measured near the pile top using a pair of transducers and accelerometers. The strain and acceleration signals, which were measured at every hammer impact on the test pile during pile driving and the re-strike, were converted by PDA to force and velocity records respectively, as a function of time. The PDA records of the field tests were given in the Volume II report of this project by Ng, et al. (2010).

Table 3.12: Comparison of the commonly used static analysis methods for calculating pile capacity

Method	Approach	Recommended soil type	Design Parameters needed	Advantages	Limitations
SPT	Empirical	Non-cohesive soils	Results from SPT test. (i.e., N-value blow counts)	Commonly used SPT test, and availability of N-values for most construction projects, also it is a simple and easy method to use	The SPT test is not a reliable test compared to other lab and/or in-site tests.
Nordlund	Semi-empirical	Non-cohesive soils	Charts provided by Nordlund and Thurman (see Hannigan et al., 2005)	It accounts for pile shape (i.e. tapered piles), as well as pile material and type (i.e. Steel H-piles, closed and open-end piles, timber piles).	The angle of soil internal friction is calculated using the SPT test N-values. The method over predicts the capacity for piles with widths larger than 600 mm.
α-method	Semi-empirical	Cohesive soils	Total stress soil parameters are needed (i.e., undrained shear strength soil parameter)	This method has been used widely especially in cohesive soils .It has been used for many years and it proved to give reasonable results for displacement and non-displacement piles.	There are several types of relations for α factor that give a large scatter and require engineering judgment and local experience when choosing the suitable relation.
β-method	Semi-empirical	Cohesive and Non-cohesive soils	Effective stresses calculated from the vertical effective overburden stress	The method was developed to model the long-term drainage shear strength. β -method can be used for different soil types and it can be used for layered soil profiles	The method tends to overestimate the pile capacity for heavily over consolidated soils.
CPT	Empirical	Cohesive and Non-cohesive soils	Results of CPT test. (Sleeve friction and cone tip resistance)	CPT is an accurately performed test, and the CPT method is very satisfactory especially for driven piles. It could be used in layered soils.	The CPT test is considered an expensive test.

Table 3.13: Summary of the equations required for different static methods

Soil Type	Method	Shaft Resistance	Tip Resistance	Required Soil Parameters
Cohesive	α-API (API-1974)	$f_s = \alpha \times S_u$	If: $S_u \leq 25$ kPa $q_t = 6.5 S_u$	S_u (undrained shear)
	α-Tomlinson (Tomlinson, 1980)		If: $S_u = 50$ kPa $q_t = 8.0 S_u$	S_u ; D_b (pile embedment)
	λ- Method (US Army Corps of Engineers, 1992)	$f_s = \lambda(\sigma'_v + 2S_u)$	If: $S_u \geq 100$ kPa $q_t = 9.0 S_u$	S_u ; γ (soil unit weight)
Cohesive/ Cohesionless	β-Method (Burland, 1973)	$f_s = \beta \times \bar{P}_o$	$q_t = N_t \times P_t$	ϕ ; γ
	CPT-Method (Nottingham and Schmertmann, 1975)	$f_s = K \left[\frac{1}{2} (\bar{f}_s A_s)_{0 \text{ to } 8b} + (\bar{f}_s A_s)_{8b \text{ to } D} \right]$	$q_t = \frac{q_{c1} + q_{c2}}{2}$	CPT; D_b
Cohesionless	SPT-Meyerhof Method (Meyerhof, 1976/1981)	$f_s = \frac{\bar{N}'}{25}$ (ksf)	$q_t = \frac{0.8 \bar{N}'_b \cdot D_b}{b}$ $\leq \bar{N}'_b$ (ksf)	SPT; D_b
	SPT-Schmertmann Method (Lai and Graham, 1995)	$f_s = f(N)$ (see Section 3.1.3.2)	$q_t = f(N)$ (see Section 3.1.3.2)	SPT
	Nordlund Method (Nordlund and Thurman, 1963)	$q_{total} = K_\delta \times C_f \times P_d \times \sin \delta \times C_d \times D + \alpha_t \times N'_q \times A_t \times P_t$		ϕ ; γ ; D_b
In-house for cohesive/ cohesionless	Iowa Blue Book Method (Dirks and Kam, 1989)	Use the revised design charts for different soil and pile types		SPT

The Case method assumes the dynamic soil resistance as a linear function of a viscous damping coefficient and a pile toe velocity. Based on this assumption, PDA estimates the pile capacity by using the maximum static resistance (RMX) and by searching for time t_1 in the force and velocity records that gives the largest value of static soil resistance (RSP). PDA estimates the shaft resistance (SFR) and subtracts the SFR from the RMX to determine the end bearing. As a result, the soil resistance distribution along the embedded pile length is estimated. PDA evaluates the driving system performance by computing the maximum hammer energy (EMX), which was used in calculating the energy transferred ratio (ETR), and by estimating the stroke (STK) of the open-ended diesel hammers used in the field tests. Besides evaluating the hammer performance, PDA monitors the pile integrity during driving by calculating and comparing the maximum compressive and tensile stresses with the allowable stresses given by the users. The AASHTO LRFD Bridge Design Specifications (2007) were used by limiting the allowable driving stress of the Grade 50 HP 10 x 42 steel piles that were used in the field tests to 45 ksi. In addition, pile quality was assessed by PDA using the term BTA, derived by Rausche and Goble (1979), to describe the severity of pile damage. One of the main purposes of using PDA in this project was for evaluating time-dependent pile capacity. The soil setup noticeably increased the capacities of the test piles embedded in the clay profile. To measure the gain in the pile capacity, the pile was tested using PDA at the beginning of several re-strikes (BOR) over the specified duration after the end of driving (EOD).

Subsequently, the PDA force and velocity records were input to the Case Pile Wave Analysis Program (CAPWAP) to accurately estimate the static shaft resistance and the end bearing capacity, predict the load settlement curve, as well as determine the dynamic soil parameters (i.e., quakes and damping factors). The detailed descriptions of PDA and its analyses may be found in the Volume II report of this project by Ng, et al. (2010).

3.2.2. Case Pile Wave Analysis Program

Using PDA records as input data, Goble and his students developed a rigorous, numerical modeling technique in the 1970s, which is now known as CAPWAP (Pile Dynamics, Inc. 2000), for more accurate estimations of pile capacity, soil resistance distribution, and dynamic soil properties. CAPWAP adopted the Smith (1962) soil-pile model using the wave equation algorithm in the analysis to perform a signals-matching process with the combination of several analytical techniques, as described by Pile Dynamics, Inc. (2000) and Ng (2011). CAPWAP divides the pile into a series of lumped masses connected with linear elastic springs and linear viscous dampers. The pile lumped masses are linked to a series of soil models described with elastic-plastic springs and linear viscous dampers. The soil static resistances (R_s) and soil quakes (q) are used to define the soil elastic-plastic springs, and damping factors are used to characterize the viscous dampers of the soil models. The soil static resistance at each soil segment, soil quake, the Smith's damping factor (J_s) and the Case damping factor (J_c) are adjusted until the best signal matching the measured and the computed signal are achieved. The summation of all adjusted soil resistances along the pile shaft provides the soil shaft resistance, and the total pile capacity is determined by adding the shaft resistance with the soil resistance, adjusted at the pile toe. The soil quakes and soil damping factors for the soil segments, along the shaft and the soil segment at the toe, are determined from the best signal matching. CAPWAP analyses for both EOD and re-strikes were performed, and the results were summarized in Volume II report of this project by Ng, et al. (2010).

3.2.3. Wave Equation Analysis Program

The wave equation analysis method was first introduced by Smith (1962), and was adopted and upgraded by Goble and Rausche (1976) into a commercial Wave Equation Analysis Program (WEAP). WEAP performs a one-dimensional wave equation analysis, and simulates the motion and force of a pile when driven by a hammer. It is commonly used to assess a pile's behavior before the pile is actually driven in the field. WEAP requires the modeling of the hammer driving system, pile, and surrounding soil as the input, computing the hammer blow count, the axial driven pile stresses, hammer performance, and pile bearing capacity. Unlike CAPWAP, which uses PDA records, WEAP models the different hammer driving system with entirely different combinations of masses, springs, and/or dampers. The latest WindowsTM operating the WEAP program (GRLWEAP) has a database of various hammer types that allows a more accurate and convenient hammer modeling.

WEAP analyses were performed at EOD as well as several re-strikes that were based on five options of inputting the soil information and properties. The five soil input options were 1) GRLWEAP soil type based method (ST); 2) GRLWEAP SPT N-value based method (SA); 3) the Federal Highway Administration (FHWA) DRIVEN program; 4) Iowa Blue Book (Iowa DOT steel pile Design Chart); and 5) Iowa DOT approach in practice. The GRLWEAP ST method provided the easiest procedure for inputting the soil information, as it required only the identification of soil types. The GRLWEAP SA method required the input of uncorrected SPT N-values, soil types, and soil unit weights, which were obtained from the in-situ SPT tests and laboratory soil tests. The DRIVEN program provided a more detailed method for describing the soil profile, and created an input file for WEAP analysis. Basically, it uses the SPT N-value and undrained shear strength (S_u) to characterize the granular and cohesive soil strength, respectively. The Iowa Blue Book method provided a direct input of the unit shaft and unit toe resistances into the WEAP's variable resistance distribution table for pile analyses. The Iowa DOT method uses the SPT N-values as the only soil parameter and inputs them into the WEAP's variable resistance distribution table, with respect to the depth at which the SPT N-values were measured. In this project, the following assumptions were considered along with the five options for characterizing the soil information in the WEAP analyses:

- 1) Water table remained constant at EOD and at re-strikes.
- 2) The shaft resistance percentage used in the bearing graph analysis was determined and similarly assumed from the static geotechnical analysis.
- 3) No residual stress analysis was considered.
- 4) The soil geostatic stress within the pre-drilling depth was treated as an overburden pressure, and the pile embedded length did not include the pre-drilling depth.
- 5) A bearing graph analysis with proportioning the shaft and toe resistances was selected.

The soil quake (q) and damping coefficient (C_s) are the two important dynamic soil parameters that describe the soil model. Smith's quake values were used in the WEAP analyses for all five options. The recommended Smith's damping factors (J_s) for shaft and toe soil segments were used in the WEAP analyses for all the options except the Iowa DOT method. The Iowa DOT has developed a range of damping factors based on a more detailed description of soil types, which are presented in Volume II report of this project (Ng et al. 2011). Furthermore, the Smith's damping factors were applied constantly to all soil segments in ST, SA, DRIVEN and Iowa Blue

Book methods. Unlike those methods, various damping factors used in the Iowa DOT method were based on the detailed soil description at the depth of consideration. Pile capacities at EOD and at several re-strikes were estimated using the measured hammer blow from the bearing graph analysis. Furthermore, the bearing graph analysis estimated the hammer stroke as well as the pile compressive and tensile stresses as a function of blow counts. In summary, WEAP estimated capacity, evaluated hammer performance, and ensured pile integrity.

3.2.4. Comparison of Different Dynamic Methods

Although dynamic analysis methods have been recognized in pile industries as one of the routine methods in design and evaluating driven piles, it is important to highlight the comparisons between PDA, CAPWAP, and WEAP. Table 3.14 briefly describes the approaches, assumptions, advantages, and limitations associated with each of the three dynamic analysis methods.

Table 3.14: Represents a comparison between the three dynamic analysis methods

Method	Approaches	Assumptions	Advantages	Limitations
PDA	<ul style="list-style-type: none"> • Measure pile top strain and acceleration • Case Method based on theory of wave propagation 	<ul style="list-style-type: none"> • Uniform and linear elastic piles • Rigid plastic soils. • Soil damping resistance at pile toe 	<ul style="list-style-type: none"> • Quick and less expensive • Checks pile and hammer performances • Evaluates pile capacity over time • Non-destructive 	<ul style="list-style-type: none"> • No account for soil damping along pile shaft • Less accurate in pile capacity estimation • Case damping is not well quantified
CAPWAP	<ul style="list-style-type: none"> • PDA records as input • Perform signal matching • Use wave equation algorithm • Smith's soil-pile model 	<ul style="list-style-type: none"> • Linear elastic pile • Elastic-plastic soil • Lumped masses • Linear viscous pile and soil damping 	<ul style="list-style-type: none"> • Accurate • Estimates soil resistance distribution • Evaluates pile capacity over time • Estimates dynamic soil properties 	<ul style="list-style-type: none"> • Requires operational and interpretational skills • Non-unique results • Variable dynamic soil properties with time
WEAP	<ul style="list-style-type: none"> • One-dimensional wave equation analysis • Requires soil-pile-hammer information • Input soil profile • Smith's soil-pile model 	<ul style="list-style-type: none"> • Linear elastic pile • Elastic-plastic soil • Lumped masses • Linear viscous pile and soil damping • Constant dynamic soil properties 	<ul style="list-style-type: none"> • Less expensive • Driving analysis • Evaluates pile and hammer performance and ensures pile integrity before driving • Pile construction control 	<ul style="list-style-type: none"> • Requires hammer information • Dynamic soil properties are not well quantified • Requires hammer blow count measurement for pile setup estimation

3.3. Dynamic Formulas

3.3.1. General

Dynamic pile driving formulas have been used for the prediction of the static bearing capacity of pile foundations for well over 180 years (Fragaszy et al., 1985). As a consequence of the immense effort and ingenuity put forth by engineers in their development, a multitude of different formulas have been amassed. In fact, Smith (1962) reported that in the early 1960s the editors of *Engineering News Record* had 450 of such formulas on file. Even though a multitude of different dynamic pile driving formulas are in existence, all are based on the assumption that the ultimate capacity of the pile under static loading can be directly related to the driving resistance of the pile during its last stages of embedment (Fragaszy, Higgins, and Lawton 1985). With this in mind, it can also be shown that while a small percentage of the available dynamic pile driving formulas are empirical in nature, the majority are based on Newton's law of impact and conservation of energy principles. In the crudest of fashions, the hammer energy is equated to the work done on the soil by the following equation:

$$W_R \times h = R \times S \quad [3.35]$$

where

W_R = Weight of the pile driving ram,

h = Drop height (stroke) of the ram,

R = Resistance to pile penetration, and

S = Pile penetration distance under one hammer blow, i.e., pile set.

As was acknowledged by Cummings (1940), these definitions of R and S contain certain implied assumptions to the nature of their quantities. To begin with, the definition of S does not explicitly state whether permanent pile penetration or the maximum pile penetration is to be used. The maximum pile penetration, includes the temporary elastic compression of the pile and the soil and can only be measured with the aid of special instrumentation. The permanent pile penetration is significantly easier to obtain and is almost always the chosen form of pile penetration measured and recorded on a pile driving project. Furthermore, the definition of R implies that either R is constant throughout the full depth of penetration, or that R is the average value of a variable resistance to penetration.

To further elaborate on the issues of pile penetration and resistance to pile penetration, Cummings (1940) suggested the three diagrams reproduced in Figure 3.14. Figure 3.14a were intended to be a graphic representation of Eq. [3.35], where the pile penetration is assumed to be a definite quantity ($0-S$), and the resistance is assumed to be uniform over the full depth of the pile penetration. In other words, the work done in moving the pile a distance S against a resistance R , represented by the shaded area of Figure 3.14a, is equivalent to the available work in the hammer at the bottom of its stroke, assuming there were no losses in energy ($W_R h$).

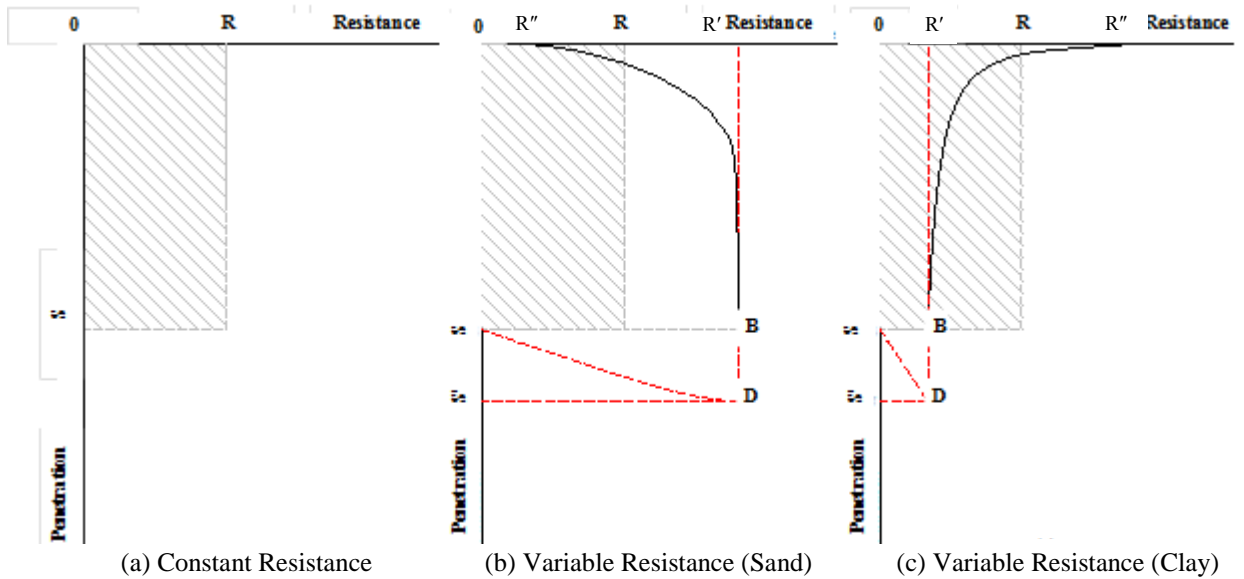


Figure 3.14: Relationship between resistance and penetration under a single hammer blow (after Cummings 1940)

Conversely, in actual pile driving, the resistance versus penetration diagram would not resemble that of Figure 3.14a on account of the presence of some temporary elastic compression of the pile and surrounding soil. Although very little information is available on the concept of resistance to pile penetration, Cummings (1940) suggests that the probability of a variable resistance is much greater than that of a constant resistance. In addition to showing the temporary elastic compression of the pile and the surrounding soil, Figure 3.14b and Figure 3.14c offer two possibilities of variable resistance to pile penetration. In an effort to show how actual pile driving differs from the assumptions on which Eq. [3.35] and Figure 3.14a are based, the shaded area of Figure 3.14a has been superimposed on Figure 3.14b and 3.14c.

Commencing with the problem of resistance to pile penetration, Figure 3.14b assumes that the initial resistance, R'' , is very small and that with an increasing depth of pile penetration the resistance increases to an asymptotic value of R' . This phenomenon is characteristic of a pile driven into a sand soil where the resistance to pile penetration increases as the moving pile compacts the sand. On the other hand, Figure 3.14c assumes a high initial resistance, R'' , which with an increasing depth of pile penetration, decreases to an asymptotic value of R' . This phenomenon is characteristic of a pile driven into a clay soil where the high initial resistance to pile penetration would be explained by the circumstance of soil “set-up” experienced by such soils during a temporary interruption in driving. In either case, the resistance at the end of pile penetration, R' , is not the same as the uniform resistance to pile penetration, R , as is assumed in Figure 3.14a. However, Cummings (1940) proposed that the aforementioned quantities are related by the following equation:

$$R' = C \times R \quad [3.36]$$

where

C = Proportionality coefficient, assumes values more or less than one, depending on whether the resistance versus penetration diagram more closely resembles that of Figure 3.14c or Figure 3.14b.

Advancing to the question of pile penetration, Figure 3.14b and Figure 3.14c depict the permanent pile penetration, S , and the maximum pile penetration, S' . The distance defined by $S-S'$ on the penetration axis represents the temporary elastic compression of the pile that occurs during impact. As expected, this temporary elastic pile compression produces an energy loss that can be quantified by the triangular area $S-B-D$, which is evidenced in both diagrams. Taking into account the aforementioned items, Eq. [3.35] can be modified to more closely represent the actual dynamics of pile driving. The revised equation, as suggested by Cummings (1940) is as follows:

$$W_R \times h = C \times R \times s + Q \quad [3.37]$$

where

Q = All energy losses that occur during impact

In spite of the fact that work diagrams (such as those provided in Figure 3.14 and the field measurements required to produce such diagrams) represent the most rational approach to the dynamics of pile driving as stated by Cummings (1940), relatively few engineers have used such methods to develop dynamic pile driving formulas. Practically all of the dynamic pile driving formulas that are to be found in literature have been derived by means of mathematics and theoretical mechanics with the exception of the Engineering News Record (ENR) Formula, which was derived by A. M. Wellington on the basis of his experience and a work diagram similar to that found in Figure 3.14c. In such cases, Eq. [3.35] is used as a starting point and the ensuing dynamic pile driving formula is derived based upon assumptions concerning the energy losses that occur during impact. Consequently, the great number of dynamic pile driving formulas that can be found in literature is an indication of the wide variety of assumptions that have been made concerning such energy losses.

3.3.2. Commonly used Formulas

As was indicated in the previous section, the vast majority of dynamic pile driving formulas found in literature were derived from Eq. [3.35] by means of varying assumptions concerning the energy losses that occur during the impact from a single hammer blow upon the head of an embedded pile. The three most common types of energy loss deductions, as suggested by Cummings (1940), are as follows:

- a) The energy losses associated with only the temporary elastic compressions of the cap, pile, and/or soil;
- b) The energy losses associated with only the Newtonian theory of impact, as described by the coefficient of restitution; and
- c) The energy losses associated with both the temporary elastic compressions of the cap, pile, and/or soil as well as the Newtonian theory of impact.

In the following subsections, seven different dynamic pile driving formulas will be introduced according to the energy loss deduction assumptions made in their respective derivations. The reader is encouraged to refer to Roling (2010) for a more comprehensive review of some of the most common dynamic pile driving formulas in existence.

3.3.2.1 *Engineering News Record*

The Engineering News Record (ENR) formula, which was first published in 1888 by A. M. Wellington, accounts for energy losses resulting from the temporary elastic compression of the pile, pile cap, and soil. The formula does this through means of a constant term of value: 1.0 inch per blow. Wellington derived this dynamic pile driving formula by equating the applied energy (i.e., the driving energy) to the energy obtained by graphically integrating the area under typical load-settlement curves for timber piles driven by gravity hammers (Chellis 1961). The original form of the ENR formula has been provided in Eq. [3.38], with the recommended application of a factor of safety of six, as suggested by Wellington himself.

$$R_u = \frac{W_R \times h}{s + 1.0} \quad [3.38]$$

where

s = Pile penetration distance under one hammer blow, i.e., pile set, expressed in inches per blow.

Seeing as the original ENR formula of Eq. [3.38] was developed during a time where all piles were made of timber and were driven with gravity hammers. Wellington proposed modifications when the single-acting steam hammer was introduced, and again when the double-acting steam hammer was introduced. These modifications were empirical in nature and were meant to compensate for the lubricant action of the soil that occurred as a result of the more rapid strokes of the new hammers (Argo 1987). That being said, the two modified forms of the ENR formula, which were again, developed for use with timber piles driven by either single-acting or double-acting steam hammers, are provided in Eqs [3.39] and [3.40], respectively, with the retained recommendation for the application of a factor of safety of six in both instances.

$$R_u = \frac{W_R \times h}{s + 0.1} \quad [3.39]$$

$$R_u = \frac{E_h}{s + 0.1} \quad [3.40]$$

where

E_h = Rated hammer energy per blow, and

s = Pile penetration distance under one hammer blow, i.e., pile set, expressed in inches per blow.

3.3.2.2 *Pacific Coast Uniform Building Code*

Derived under the assumption that the energy losses associated with both the temporary elastic compressions of the cap, pile, and/or soil as well as the Newtonian theory of impact are significant, the background associated with the Pacific Coast Uniform Building Code (PCUBC) formula begins with J. F. Redtenbacher. In the year 1859, Redtenbacher put forward the expression that is revealed in Eq. [3.41], and has often been referred to as the “complete” dynamic pile driving formula due to the fact that it incorporates deductions for all of the aforementioned sources of energy losses (Jumikis 1971).

$$W_R \times h = R \times s + \left[W_R \times h \times \left(\frac{W_p \times (1 - e^2)}{W_R + W_p} \right) \right] + \left\{ \frac{R \times C_1}{2} + \frac{R \times C_2}{2} + \frac{R \times C_3}{2} \right\} \quad [3.41]$$

where $C_1 = \frac{R \times L'}{A' \times E'} = \text{temporary elastic compression of the driving cap}, \quad [3.42]$

$$C_2 = \frac{R \times L}{A \times E} = \text{temporary elastic compression of the pile}, \quad [3.43]$$

C_3 = Temporary elastic compression of the soil surrounding the pile,

L' = Length of the driving cap,

A' = Cross-sectional area of the driving cap, and

E' = Young's modulus for the driving cap material.

In fact, it is from this expression shown in Eq. [3.41] that Hiley derived his renowned dynamic pile driving formula. Used extensively in the United Kingdom of Great Britain, Northern Ireland, and also in Europe, the Hiley formula of Eq. [3.44] was developed in an attempt to eliminate some of the errors associated with the theoretical evaluation of energy absorption by a pile-soil system during driving (Olson and Flaate 1967).

$$R_u = \frac{e_h \times W_R \times h}{s + \frac{1}{2}(C_1 + C_2 + C_3)} \cdot \left(\frac{W_R + (e^2)W_p}{W_R + W_p} \right) \quad [3.44]$$

where

e_h = Efficiency of striking hammer; Table 3.15 presents representative values of this variable for hammers in reasonably good operating condition.

Table 3.15: Representative values of hammer efficiency for use in dynamic pile driving formulas (after Bowles 1996)

Type	Hammer Efficiency, e_h
Drop Hammers	0.75-1.00
Single-Acting Steam Hammers	0.75-0.85
Double-Acting Steam Hammers	0.85
Diesel Hammers	0.85-1.00

Recognizing the complexity associated with determining the temporary elastic compressions of the cap and soil (i.e., C_1 and C_3), Hiley established recommended values for these variables as shown in Tables 3.16 and 3.17, respectively. The application of a factor of safety of three is recommended for use with the Hiley dynamic pile driving formula (Fragaszy et al., 1985).

Table 3.16: Recommended values for C_1 (inches/blow) - temporary elastic compression of the pile head and driving cap (after Chellis 1961)

Material to which Hammer Blow is Applied	Driving Stresses on Pile Head or Driving Cap (ksi)			
	0.50	1.00	1.50	2.00
Head of steel H-shaped or pipe piling	0	0	0	0
Head of timber pile	0.05	0.10	0.15	0.20
Precast concrete pile with 3.0 – 4.0 inches of packing inside driving cap	0.12	0.25	0.37	0.50
Precast concrete pile with only 0.5 – 1.0 inch mat pad on head	0.025	0.05	0.075	0.10
Steel-covered cap containing wood packing for steel H-shaped or pipe piling	0.04	0.05	0.12	0.16
3/16 inch fiber disk between two 3/8 inch steel plates for use with Monotube piles subjected to severe driving conditions	0.02	0.04	0.06	0.08

Note: For driving stresses larger than 2.00 ksi, use the value of C_1 provided in the last column.

Table 3.17: Recommended values for C_3 (inches/blow) - temporary elastic compression of the soil surrounding the pile (after Chellis 1961)

Type of Pile	Driving Stresses on Horizontal Projection of Pile Toe (ksi)			
	0.50	1.00	1.50	2.00
Piles of Constant Cross Section	0 – 0.10	0.10	0.10	0.10

In an effort to further alleviate the difficulty associated with the determination of Hiley's rebound coefficients, (i.e., C_1 , C_2 , and C_3) the Pacific Coast Building Officials, later referred to as the International Conference of Building Officials, adopted a modified version of the Hiley dynamic pile driving formula for the construction control of driven pile foundations in their first edition of the Uniform Building Code (UBC), published in 1927. This formula (most commonly referred to as the Pacific Coast Uniform Building Code (PCUBC) formula) attempts to account for the energy losses associated with the temporary elastic compressions of the driving cap and soil by using twice the average energy loss associated with the temporary elastic compression of the pile (Chellis 1961). Although the PCUBC dynamic pile driving formula was removed from the UBC in 1976, its use is still permitted, provided that a factor of safety of four is applied to obtain an allowable resistance to pile penetration (Bowles 1996).

$$R_u = \frac{W_R \times h \left(\frac{W_R + k \times W_p}{W_R + W_p} \right)}{s + \frac{R_u \times L}{A \times E}} \quad [3.45]$$

where

k = 0.25 for steel piles and 0.10 for all other piles.

3.3.2.3 Janbu Formula

The Janbu formula, proposed by Janbu in 1953 (Gulhati and Datta 2005), is based upon the assumption that energy losses resulting from the temporary elastic compressions of the driving cap and soil can be neglected. Although this formula does not directly involve the Newtonian theory of impact, Janbu attempted to account for it by factoring out a series of variables from the general conservation of energy equation, i.e., Eq. [3.37], which proved to be difficult to evaluate. Janbu then combined the variables to form what he has termed as the driving coefficient, C_d . More specifically, this driving coefficient includes terms representing the difference between static and dynamic capacity, the ratio associated with the transfer of load into the soil as a function of depth, and hammer efficiency (Fragaszy, Higgins, and Lawton 1985). Furthermore, the driving coefficient is correlated with the ratio of the pile weight to the weight of the pile driving hammer in an effort to account for the variability in the energy available at the close of the period of restitution. As a result, the Janbu formula in its simplest form, may be expressed as shown in Eq. [3.46], with the recommended application of a factor of safety of three, as reported by Gulhati and Datta (2005).

$$R_u = \left(\frac{e_h \times W_R \times h}{s} \right) \left(\frac{1}{K_u} \right) \quad [3.46]$$

$$\text{where } K_u = C_d \left[1 + \left(1 + \frac{\lambda_e}{C_d} \right)^{1/2} \right], \quad [3.47]$$

$$C_d = 0.75 + 0.15 \left(\frac{W_p}{W_R} \right), \text{ and} \quad [3.48]$$

$$\lambda_e = \frac{e_h \times W_R \times h \times L}{A \times E \times s^2}. \quad [3.49]$$

3.3.2.4 Iowa DOT Modified ENR

Several modifications to Wellington's ENR formula have been made over the years in an attempt to improve the pile bearing capacity prediction capabilities of the original formula, while maintaining its desirable quality of simplicity. Proposed in 1965 by the Michigan State Highway Commission (MSHC) as the product of an extensive study focused on comparing the efficacy of several dynamic pile driving formulas, the MSHC Modified ENR formula, which is presented in Eq. [3.50], modifies the original ENR formula through the multiplication of an additional factor to account for the available kinetic energy after the impact from a single hammer blow upon the head of an embedded pile (Fragaszy, Higgins, and Lawton 1985). As with Wellington's original ENR formula, it is recommended that a factor of safety of six should be applied to the value for the ultimate resistance to pile penetration produced by the MSHC Modified ENR formula.

$$R_u = \left[\frac{W_R \times h}{s + 0.1} \right] \cdot \left[\frac{W_R + (e^2)W_p}{W_R + W_p} \right] \quad [3.50]$$

where

s = Pile penetration distance under 1 hammer blow, i.e., pile set (inches per blow).

Assuming a perfectly inelastic impact between the pile driving hammer and embedded pile (i.e., $e = 0$), and a constant term in the denominator of the MSHC Modified ENR formula, then the Iowa DOT Modified ENR formula, which is presented in Eq. [3.51], is attained. The constant denominator term accounts for all energy losses experienced as a result of temporary elastic compressions in the cap, pile, and soil. Incorporated into the Iowa DOT's *Standard Specifications for Highway and Bridge Construction* manual, the Iowa DOT Modified ENR formula is to be used only in situations where there is no excessive bounce exhibited by the pile driving hammer subsequent to the impartation of the driving blow (Iowa DOT 2008). When a gravity hammer or diesel hammer is used to drive timber, steel H-shaped, or steel shell type piles or when a steam hammer is used to drive any pile type, a factor of safety of four is recommended to be applied to the value produced by Eq. [3.51] for the ultimate resistance to pile penetration. However, factors of safety of $2\frac{2}{3}$ and $1\frac{5}{7}$ are recommended when either a gravity hammer or diesel hammer is used to drive a concrete pile, respectively.

$$R_u = \left[\frac{W_R \times h}{s + z} \right] \left[\frac{W_R}{W_R + W_p} \right] \quad [3.51]$$

where

z = 0.35 inches per blow for timber, steel H-shaped, or steel shell piles driven by a gravity hammer; 0.20 inches per blow for concrete piles driven by a gravity hammer; and 0.10 inches per blow for all piles driven by either a diesel hammer or a steam hammer.

3.3.2.5 Gates Formula

Although some of the dynamic pile driving formulas presented in the preceding subsections were obtained through empirical modifications to establish relationships derived based on assumptions concerning the energy losses that occurred during impact of a single hammer blow upon an embedded pile head, a strictly empirical dynamic formula had yet to be introduced. The Gates formula, proposed by Marvin Gates in 1957, is a strictly empirical relationship between hammer energy, the final pile set, and the measured static pile load test results (Jumikis 1971). The general structure of the formula was developed based on two relationships established by Gates: the resistance to pile penetration directly proportional to the square root of the net hammer energy, as well as the logarithm of the final pile set. Through the application of statistical methods and curve-fitting practice, the final form of the Gates formula was established as revealed in Eq. [3.52] (Gates 1957). Although it is known that the statistical adjustments employed in the development of this formula were based on the results from approximately one hundred static pile load tests, Gates (1957) failed to report the amount of scatter exhibited by this data, in addition to whether or not this data encompassed all soil types. Nonetheless, Gates (1957) recommended that a factor of safety of four be applied to the value for the ultimate resistance to pile penetration obtained from his formula.

$$R_u = \left(\frac{6}{7} \right) \sqrt{e_h \times E_h} \log \left(\frac{10}{s} \right) \quad [3.52]$$

where

R_u = Ultimate resistance to pile penetration expressed in tons,

E_h = Rated hammer energy per blow expressed in foot-pounds per blow, and

s = Pile penetration distance under 1 hammer blow, i.e., pile set (inches per blow).

3.3.2.6 FHWA Modified Gates

The Gates formula of Eq. [3.52] was further enhanced based on statistical correlations with data from additional static pile load tests by Richard Cheney of the FHWA (Paikowsky et al. 2004), as a means to help offset the original formula's tendency to over-predict pile penetration resistance at low driving resistances and under-predict pile penetration resistance at high driving resistances. Generally referred to as the FHWA Modified Gates formula, it is recommended in the 2007 edition of the *AASHTO-LRFD Bridge Design Specifications* (AASHTO, 2007) that this dynamic pile driving formula be used before all other dynamic pile driving formulas in the construction control of driven pile foundations. The exact form of the FHWA Modified Gates formula, as it appears in the 2007 edition of the *AASHTO-LRFD Bridge Design Specifications* (AASHTO, 2007), is provided in Eq. [3.53].

$$R_u = 1.75\sqrt{W_R \cdot h} \log(10 \times N_b) - 100 \quad [3.53]$$

where

- R_u = Ultimate resistance to pile penetration expressed in kips,
- W_R = Weight of the pile driving ram expressed in pounds,
- h = Drop height (stroke) of the ram expressed in feet, and
- N_b = Number of hammer blows for one inch of pile permanent set.

3.3.2.7 WSDOT Formula

In a similar manner to Richard Cheney of the FHWA, the Washington State Department of Transportation (WSDOT) used an expanded database, established by Paikowsky et al. (2004), that was comprised of data from numerous static pile load tests conducted throughout the US to statistically enhance the original Gates dynamic pile driving formula. As with the FHWA Modified Gates formula, the WSDOT dynamic pile driving formula was developed to maintain the low prediction variability of the original Gates formula, while minimizing its tendency to under or over-predict the ultimate pile penetration resistance (Allen 2005). As presented by Allen (2007), the WSDOT formula takes the following form:

$$R_u = 6.6 \times F_{eff} \times W_R \times h \times \ln(10 \times N_b) \quad [3.54]$$

where

- R_u = Ultimate resistance to pile penetration expressed in kips,
- F_{eff} = Equal to 0.55 for air/steam hammers with all pile types, 0.37 for open-ended diesel hammers with concrete or timber piles, 0.47 for open-ended diesel hammers with steel piles, 0.35 for closed-ended diesel hammers with all pile types, 0.58 for hydraulic hammers with all pile types, and 0.28 for gravity hammers with all pile types,
- W_R = Weight of the pile driving ram expressed in kips,
- h = Drop height (stroke) of the ram expressed in feet, and
- N_b = Number of hammer blows for one inch of pile permanent set, averaged over the last four inches of driving.

3.3.3. Comparison of Different Formulas

It is a particularly difficult task to determine which, out of the many dynamic pile driving formulas existing for the construction control of driven pile foundations is best suited, or most accurate for a given situation. Nonetheless, it can be assumed that if one were to exist, the ideal dynamic pile driving formula would be accurate enough to provide a safe, yet economical design, in addition to being suitable for the varying soil conditions and pile sections. With this in mind, numerous studies have been conducted over the past sixty years in an effort to determine the correlation between the bearing capacity of a statically load tested pile and the estimated pile bearing capacity as obtained via dynamic pile driving formulas. In the following subsections, a review of some of the more prominent studies will be presented in a chronological fashion. The reader is referred to Roling (2010) for a more comprehensive review of the numerous comparative studies carried out on dynamic pile driving formulas over the last sixty years.

3.3.3.1 Chellis, 1949

Chellis (1949) is one of the oldest references to have cited comparisons between the predicted pile bearing capacity obtained via dynamic pile driving formulas and the corresponding measured bearing capacity attained from static pile load test results. Using the results from 45 static pile load tests conducted in predominately cohesionless soils and encompassing several different pile types (i.e., mandrel-driven corrugated shell, fluted steel shell, precast concrete, timber, and steel H-shaped piles) and pile driving hammers (i.e., double-acting, differential-acting, and gravity hammers), Chellis (1949) compared the measured ultimate pile capacity against that predicted by the ENR, Hiley, MSHC Modified ENR, Eytelwein, Modified Eytelwein, Navy-McKay, Canadian National Building Code (CNBC), and PCUBC dynamic pile driving formulas. The measured ultimate pile capacity was defined as the load on the net settlement versus load curve where the rate of movement begins to increase sharply in proportion to the increase in load. Based on the results of this comparison, which have been reproduced in Table 3.18, Chellis (1949) concluded that the Hiley, PCUBC, and CNBC dynamic pile driving formulas performed sufficiently well, given the fact that they demonstrated the provision of a safe, yet economical design through application of the recommended factors of safety.

Table 3.18: Summary of results from Chellis (1949)

Dynamic Pile Driving Formula	Ratio of Predicted Load to Measured Ultimate Load (%)	
	Average	Range
Hiley	92	55-125
PCUBC	112	55-220
CNBC	80	55-140
ENR	289	100-700
MSHC Modified ENR	182	98-430
Eytelwein	292	90-1800
Modified Eytelwein	202	98-508
Navy-McKay	-	99-∞

3.3.3.2 Spangler and Mumma, 1958

Spangler and Mumma (1958) compared the allowable bearing capacities predicted by the ENR, PCUBC, Eytelwein, and Rabe dynamic pile driving formulas with the corresponding measured

bearing capacities attained from the results of 58 static pile load tests conducted in locales spanning the entire United States. In other words, this comparative study covered a wide variety of soil conditions and pile types (i.e., steel H-shaped, concrete, timber, Raymond step-tapered, and pipe piles). For each of the aforementioned static pile load tests, the measured ultimate pile capacity was defined by Spangler and Mumma (1958) to be the average value resulting from the application of the following four procedures upon the obtained load versus displacement results:

- a) the load at which net settlement equals 0.25 inches is defined as the failure load,
- b) the load at which the incremental gross settlement divided by the incremental load exceeds 0.03 inches per ton is defined as the failure load,
- c) the load at which the gross settlement curve breaks and passes into a deep straight tangent is defined as the failure load, and
- d) the load at which the tangents to the early flat portion and the steep portion of the load-settlement curve intersect is defined as the failure load.

With this information at hand, an actual factor of safety was determined by dividing the measured ultimate pile capacity by the allowable bearing capacity predicted by the four dynamic pile driving formulas considered in this study. The results of this comparison have been reproduced in Table 3.19.

Table 3.19: Summary of results from Spangler and Mumma (1958)

Factor of Safety	Number of Cases			
	ENR	Eytelwein	PCUBC	Rabe
<1.0	4	6	0	0
1.0-1.5	10	7	1	1
1.5-2.0	10	7	2	13
2.0-3.0	21	21	12	30
3.0-4.0	7	7	5	13
4.0-5.0	5	7	11	1
5.0-8.0	1	3	20	0
>8.0	0	0	7	0
Average Range	0.83-5.38	0.72-5.49	1.22-9.27	1.30-4.00

Defining an unsafe or uneconomical prediction in pile bearing capacity by the event in which the actual factor of safety assumed a value that was less than 1.5 or greater than 4.0, respectively, Spangler and Mumma (1958) arrived at the following general conclusions:

- 1) The ENR dynamic pile driving formula is often “unsafe” for piles with small sets, i.e., pile sets of 0.10 inches per blow or less.
- 2) The actual factor of safety for the ENR formula is usually between 1.5 and 3.0, when used in conjunction with combination end bearing and friction pile foundations, as opposed to the recommended value of 6.0.
- 3) For friction piles, the ENR formula generally provided an actual factor of safety that was greater than 3.0.
- 4) The Eytelwein dynamic pile driving formula produced larger scatter for the actual factor of safety values than the ENR formula and was considered to be unreliable for use with heavy piles driven by light hammers.

- 5) Although the PCUBC dynamic pile driving formula produced the largest scatter for the actual factor of safety values, it generated safe results and was more conservative than both the ENR and Eytelwein formulas.
- 6) The PCUBC formula was considered to be most reliable for long piles driven by heavy hammers.
- 7) Although very difficult to use, the Rabe dynamic pile driving formula produced the best results of the four formulas examined.

3.3.3.3 *Olson and Flaate, 1967*

Olson and Flaate (1967) used the results from 93 static pile load tests conducted on piles driven into sandy soils to evaluate the performance of the ENR, Gow, Hiley, PCUBC, Janbu, Danish, and Gates dynamic pile driving formulas. Although several different criteria were used to determine the measured ultimate pile capacities of the 93 tested piles, Olson and Flaate (1967) only state that this produces a scatter in the results of about 15% instead of providing specific information regarding the static pile load test results themselves. Nevertheless, the measured versus predicted ultimate pile capacities were plotted on an x-y graph and a linear least squares fit was used to find the slope (A) and y-intercept (B) of the best fit line through the data points, as well as the associated correlation coefficient (r). A summary of this statistical data, as compiled by Olson and Flaate (1967), has been provided in Table 3.20. It is important to note that in an ideal situation, the slope (A) would be equal to one, the y-intercept (B) would be equal to zero, and the correlation coefficient (r) would be equal to one.

In all cases presented in Table 3.20, Olson and Flaate (1967) found that the ENR and Gow formulas were clearly inferior to the other five formulas based solely on their remarkably low correlation coefficients. Although no formula was deemed best for use with concrete piles due to the small number of such piles analyzed, the Janbu formula was found to be the most accurate when used with timber and steel piles. Furthermore, the Janbu, Danish, and Gates formulas produced the highest average correlation coefficients under the consideration of all pile types, although those associated with the PCUBC and Hiley formulas were only slightly lower.

3.3.3.4 *Fragaszy, Argo, and Higgins, 1989*

In an effort to determine whether the WSDOT should replace the ENR formula with another dynamic pile driving formula for the estimation of ultimate pile capacity, Fragaszy, Argo, and Higgins (1989) studied the relative performance of the following ten formulas: ENR, MSHC Modified ENR, Hiley, Gates, Janbu, Danish, PCUBC, Eytelwein, Weisbach, and Navy-McKay. Using the data collected from 63 static pile load tests conducted in western Washington and northwest Oregon on open and close-ended steel pipe, steel H-shaped, timber, concrete, hollow concrete, and Raymond step-tapered piles, the ratio of the predicted to measured ultimate pile capacity was determined for each test pile using each of the aforementioned dynamic pile driving formulas. In all cases, the measured ultimate pile capacity was defined as the interception of the line generated by offsetting the pile elastic compression line by a distance equal to the pile diameter divided by 30 with the overall load-settlement curve.

Table 3.20: Summary of statistical parameters from Olson and Flaate (1967)

Pile Type	Dynamic Pile Driving Formula	N	A	B (tons)	r
Timber	ENR	37	0.45	16	0.28
	Gow	37	0.37	18	0.43
	Hiley	37	0.64	19	0.77
	PCUBC	37	0.80	14	0.74
	Janbu ($C_d = 1$)	37	0.98	9	0.86
	Danish	37	0.71	9	0.86
	Gates	37	1.30	-17	0.86
Concrete	ENR	15	0.20	72	0.11
	Gow	15	0.32	69	0.12
	Hiley	15	1.08	24	0.43
	PCUBC	15	1.57	-19	0.75
	Janbu ($C_d = 1$)	15	0.66	23	0.64
	Danish	15	0.60	11	0.69
	Gates	15	1.62	-27	0.65
Steel	ENR	41	0.28	43	0.37
	Gow	41	0.28	42	0.38
	Hiley	41	1.14	-10	0.76
	PCUBC	41	1.07	0	0.79
	Janbu ($C_d = 1$)	41	0.91	7	0.83
	Danish	41	0.89	-16	0.82
	Gates	41	2.34	-83	0.84
All	ENR	93	0.33	37	0.29
	Gow	93	0.32	37	0.36
	Hiley	93	0.92	7	0.72
	PCUBC	93	1.04	2	0.76
	Janbu ($C_d = 1$)	93	0.87	10	0.81
	Danish	93	0.77	-2	0.81
	Gates	93	1.81	-48	0.81

Based upon analyses of the coefficient of variation of the aforementioned ratio for each of the ten investigated dynamic pile driving formulas, Frigaszy, Argo, and Higgins (1989) found the Gates formula to be the most accurate, and the ENR formula to be among the least accurate method. In fact, the coefficient of variation of the ratio of the predicted to measured ultimate pile capacity for the ENR formula was approximately two to three times higher than that for the Gates formula. As an alternative comparison, for each formula, a measure of safety was determined to be the percentage of piles for which the measured ultimate pile capacity was expected to be lower than the predicted ultimate pile capacity. From this information, the Gates formula was again found to be the best, and the ENR formula ranking near the bottom. Finally, Fragaszy, Argo, and Higgins (1989) conducted economic analyses which showed that for the same level of safety, the Gates formula resulted in higher allowable capacities and consequentially lower foundation costs on average.

3.3.3.5 Summary

In short, the various comparative studies presented in the preceding subsections clearly indicate that no one dynamic pile driving formula is consistently better than all of the others. Even when specific combinations of pile, hammer, and/or soil type are considered, it is nearly impossible to predict which formula is best suited for the given situation. Nonetheless, it does appear as though the Hiley, Janbu, PCUBC, and Gates dynamic pile driving formulas are better on average than the remaining multitude of formulas in existence. Likewise, the ENR formula was shown to be among the worst dynamic pile driving formulas in all comparative studies presented, except for the investigation carried out by Ramey and Hudgins (1975). In summary, the methods used for determining the measured ultimate pile capacity from the results of the static load tests varied from study to study, as the accuracy of comparisons drawn between such studies is significantly difficult to assess.

3.4. Pile Static Load Test

3.4.1. Overview

Static Load Tests (SLTs) accurately measure the actual pile behavior under axial vertical compressive loading and characterize the load-settlement relationship at the pile head. Load testing is the most definitive method for determining the nominal capacity of a pile. Testing a pile to failure provides valuable information to the design engineer and is recommended for design verification purposes. SLTs can also assist in calibrating sophisticated design models such as finite element models, making sure that they provide safe results and eliminate excess conservatism. In difficult soil and bedrock conditions, the SLT results are the only means of identifying the actual pile capacity. SLT also helps in generating databases for advanced research.

There are several SLT methods, procedures, and equipment used for purposes of pile routine testing and proof testing, which are all described in the ASTM D-1143 standards (ASTM, 2007). Among the different methods are the Slow Maintained Testing Method (SM) and the Quick Maintained Testing Method (QM). According to the Canadian Foundation Engineering Manual (1985), the SM method is time consuming and can lead to complex SLT data evaluation and interpretation. It was also mentioned that the SM test could affect the pile true load movement behavior during testing. Conversely, the QM test is faster and more efficient when determining the pile capacity and is therefore more preferable than the SM method.

Acceptance of the pile SLT is generally governed by the building codes reviewed by the structural and geotechnical engineers. The structural engineer determines the maximum deflection that a structure can sustain without losing function, while the geotechnical engineer determines the pile bearing capacity and limits the soil-pile resistance to a certain extent at which the deformations do not exceed the plastic behavior. There are several methods for determining the ultimate pile capacity from a SLT, which can be called the SLT acceptance criterion. The commonly used acceptance criteria are briefly described in the following sections.

3.4.2. Acceptance Criteria

As previously described, the static load test is the most accurate test representing the actual response of the piles, and hence it was vital to select a suitable method of determining the pile nominal (maximum, non-factored) capacity from the load-displacement curve. There are several methods for determining the nominal pile capacity from a SLT. These methods have advantages, limitations, and applications that should be addressed. Some of these methods are represented in this report because they are the most commonly used according to design codes.

3.4.2.1 Davisson's Method

The Davisson's criterion (Davisson, 1972) is one of the most popular methods and seems to work best with data from QM tests (Coduto, 2001). The criterion is started simply by drawing a parallel line to the elastic compression line (base line), which is offset by a specified amount of displacement depending on the pile size. This parallel line is called the Davisson line. As can be seen on Figure 3.15, the point of intersection between the Davisson line and the load displacement curve is considered to be the pile nominal capacity. Eq. [3.55] is used to plot the base line on the load-displacement curve:

$$\Delta = \frac{Q_{va} \times L}{AE} \quad [3.55]$$

where

- Δ = Elastic movement of base line
- Q_{va} = Applied load
- A = Cross sectional area of pile
- E = Modulus of elasticity of pile material
- L = Embedded length of pile

In order to draw the Davisson line parallel to the base line, the following expression is used:

$$X = 0.15 + \frac{D}{120} \quad [3.56]$$

where

- X = Offset displacement from the base line (inch)
- D = Pile diameter (inch)

This method was originally recommended for different types of driven piles (Parakash et al., 1990). Davisson's criterion was also used in the NCHRP report-507 by Paikowsky et al. (2004), and was found to perform best overall and was therefore chosen as the only method of determining the pile nominal capacity from the load-displacement curve in this study. One of the main advantages of this method is that it is an objective method. It can be used as an acceptance criterion for the static load test, as the parallel line can be predicted before starting the test. However, Hannigan et al. (2005) supposed some limitations of this method, as it under-predicts the pile capacity for piles with diameters larger than 24 inches. Table 3.21 provides a comparison between Davisson's method and other determination methods and provides the appropriate pile types for each method, the recommended static load test type, advantages, limitations, and applicability.

3.4.2.2 Shape of Curvature Method

As shown in Figure 3.16, the nominal pile capacity in the shape of curvature method (Butler and Hoy's Method, 1977) can be defined as the point of intersection between the elastic compression line and the line tangent to the plastic portion of the load-displacement curve. According to Parakash et al. (1990), this method is applicable for QM tests. The disadvantage of this method is that it penalizes long piles because they will have larger elastic movements, thus underestimating the capacity of longer piles. Table 3.21 provides a comparison between the shape of curvature method and other determination methods.

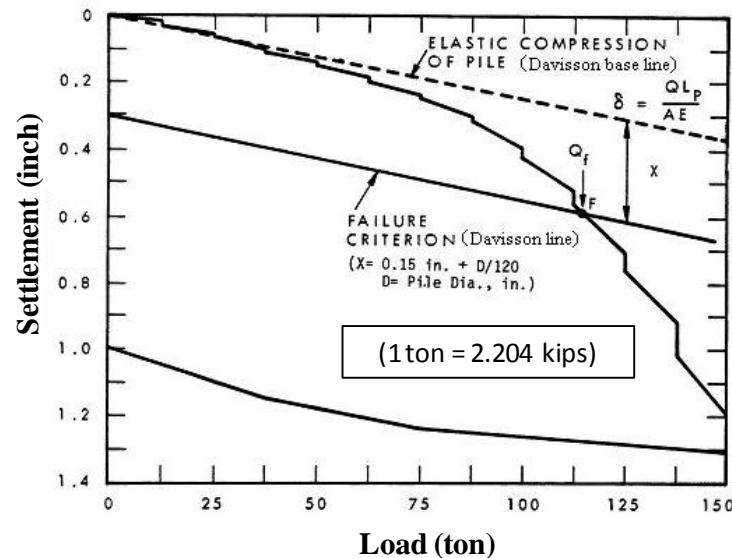


Figure 3.15: Example of determining the pile capacity using Davisson's method

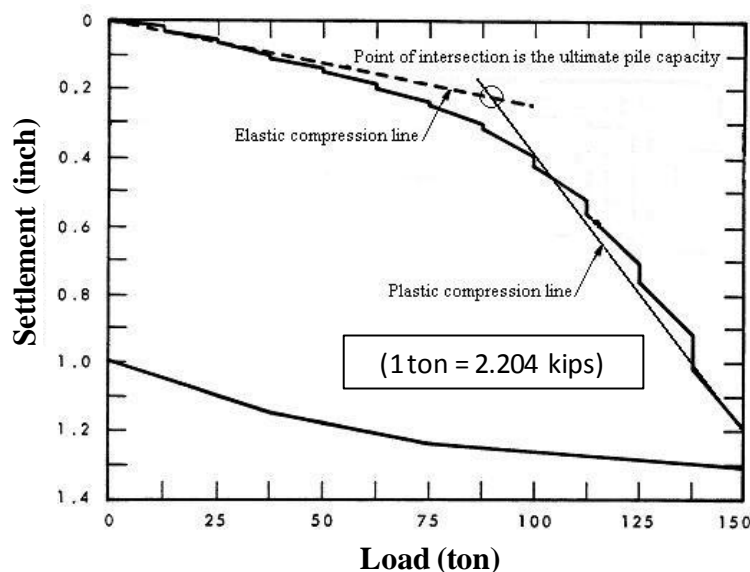


Figure 3.16: Example of determining the pile capacity using the shape of curvature method

3.4.2.3 Limited Total Settlement Method

The pile capacity can be limited at a point where the settlement of the pile is the smallest of 0.1 times the pile diameter or 1 inch. This method is an objective method. It could be used as an acceptance criterion for the static load test, as the limited total settlement line can be predicted even before starting the test. The method is simple and does not require any sophisticated equations, however, the method is not suitable for long piles, as elastic settlement exceeds the limit without inducing plastic deformations. The pile may also fail before reaching the settlement limit of the method. Figure 3.17 provides an example of using the limited total settlement method. Table 3.21 provides a comparison between the limited settlement method and other methods.

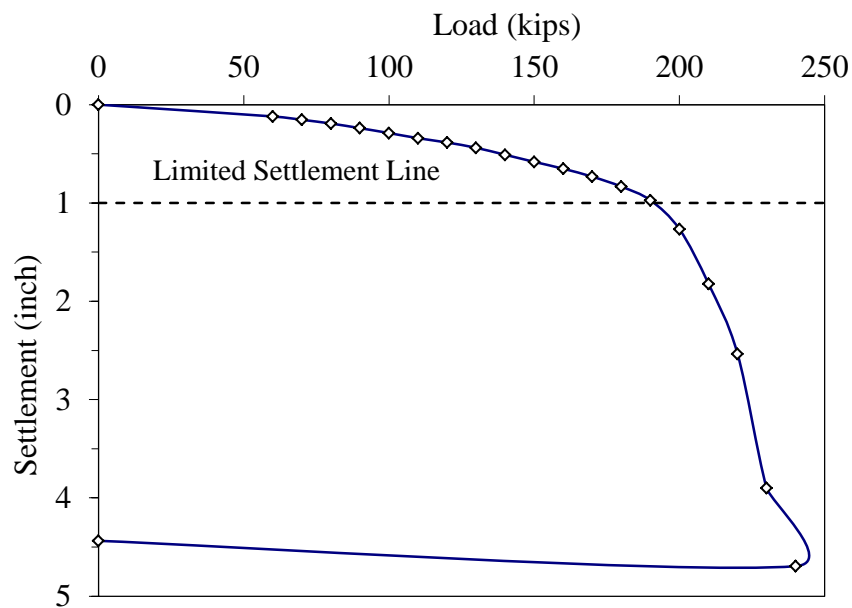


Figure 3.17: Example of determining the pile capacity using the limited total settlement method

3.4.2.4 De Beer's Method

In the De Beer's Method (adapted from Bowles, 1996), the load test data is plotted on a log-log scale, at which the intersection between the two straight portions of the graph will be equal to De Beer's capacity as shown in Figure 3.18. This method was originally proposed for SM tests (Parakash et al., 1990). One of the most common problems with this method is that the two straight portions in the graph cannot be clearly determined. Table 3.21 provides a comparison between the De Beer's method and other determination methods.

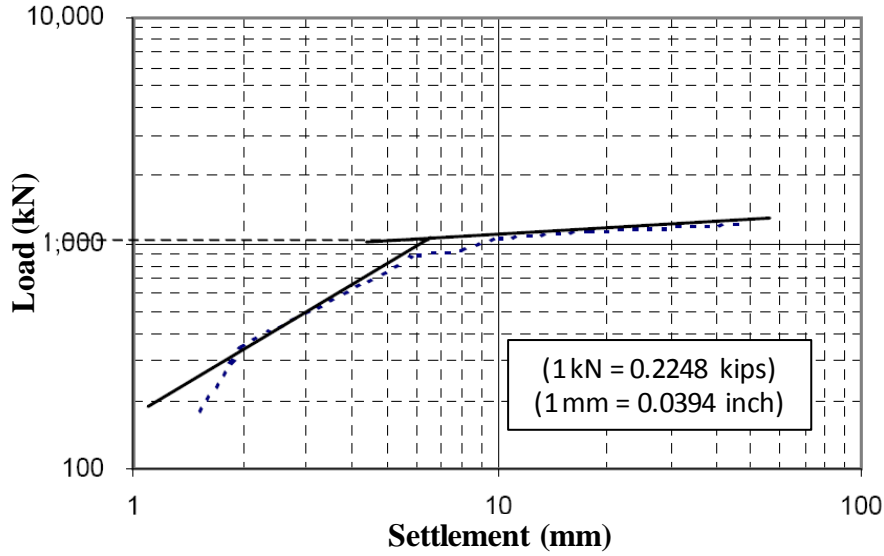


Figure 3.18: An Example of determining the pile capacity using De Beer's method

3.4.2.5 Chin's Method

In Chin's method (Chin 1970/1971), a straight line between Δ/Q_{va} and Δ is plotted where Δ is the displacement and Q_{va} is the corresponding load. Then, the Q_{ult} is equal to $1/C_1$, where C_1 is explained in Figure 3.19. Chin's method was developed for both QM and SM tests. However, it has several disadvantages including the fact that it assumes the load-moment curve is approximately hyperbolic, as well as requiring constant time increments used when conducting the SLT. Moreover, a problem could occur while selecting the straight line passing through the points shown in the figure because sometimes the points do not appear to fall on a straight line. This issue could easily occur unless the test has passed Davisson's failure criterion. According to Parakash et al. (1990), this method may not provide good results for static load tests that are performed according to the ASTM standards, as the tests may not have time load increments that are exactly constant.

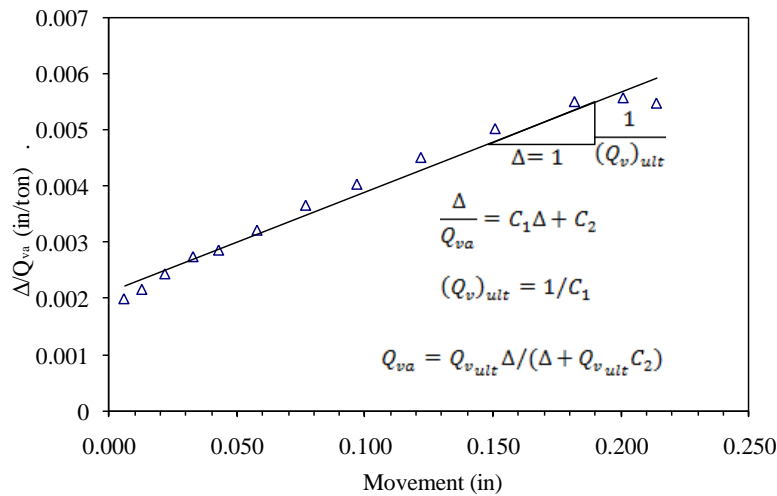


Figure 3.19: Determining the capacity using Chin's method (after Parakash et al., 1990)

3.4.2.6 Iowa DOT Method

The Iowa Foundation Pile Design Chart (Dirks and Kam, 1989) was developed based on the determination of the actual pile failure load using the Louisiana method. The Louisiana method is defined as the intersection between the linear portion tangent of the load-displacement curve and a line with a slope of 0.05 inches per ton at the yield point. The yield point is defined as the intersection between the load-displacement curve and a parallel line to the recovery line at 0.25 inches settlement. This method was essentially adapted for Louisiana soils and is not frequently used in general geotechnical practices. Moreover, the method is relatively sophisticated and was not recommended by any design codes for the LRFD calibration. On the other hand, the Davisson's criterion is an uncomplicated method that has proven to perform better in the case of driven steel H-piles and was recommended for a consistent LRFD calibration framework by the AASHTO and the NCHRP (see Sections 3.4.2.1 and 5.6.).

Table 3.21: Comparison between pile ultimate capacity determination methods including the appropriate pile types for each method, the recommended static load test type, advantages, limitations, and applicability for each method

Method	Year	Recommended pile types	SLT* type	Advantages	Limitations	Comments	Application
Shape of Curvature Method (Fuller and Hoy)	1977	Bored, belled, and small diameter driven concrete piles as well as Franki piles	QM** test	Its yield failure loads are near to actual test failure loads	It is a subjective method, hence, results could greatly vary from one to other	It is a conservative method which is not suitable for long piles	Easy
Davisson's Method	1972	Driven piles as well as Franki piles	QM test	It is an objective method which can be used as a SLT acceptance criterion	For piles with cross-sectional area more than 24 inches, the method under predicts the pile capacity	It is a conservative method (recommended by specifications)	Easy
Chin's Method	1970-1971	N/A	QM and SM*** tests	N/A	Constant time load increments required for accuracy. Also assumes hyperbolic load-settlement relation. Always it gives failure loads higher than that of actual test failure loads	Loads must be higher than that of Davisson's acceptance load	Easy
De Beer's Method	1967-1972	N/A	SM tests	N/A	Subjective method	Drawn on log scale	Moderate
Hansen's 90	1963	Small diameter driven concrete piles	CRP**** tests	N/A	Trial and error	N/A	Moderate
Hansen's 80	1963	N/A	QM and SM tests	Criteria agrees well with plunging failure	Not suitable for tests that include unloading cycles or unachieved plunging	Assumes that the load-displacement curve is parabolic	Moderate
Limited Total Settlement Method	N/A	N/A	N/A	Objective method	Not suitable for long piles, as elastic settlement exceeds limit without inducing plastic deformations	Pile may fail before reaching the settlement limit of the method	Easy
Vander Veen's Method	1953	Small diameter concrete driven piles	N/A	N/A	Time consuming	N/A	Difficult

*Static load test type; **QM: Quick Maintained test2; ***SM: Slow Maintained test; ****CRP: Constant Rate of Penetration Test

CHAPTER 4: COLLECTION OF DATA

4.1. Nationwide Survey of State DOTs

A study was conducted through a web-based survey to determine the current design and construction practices of deep foundations nationwide as part of this research project for the Iowa Highway Research Board (IHRB). In addition to the basic questions relevant to the implementation of the LRFD methods in bridge foundation design practice, information on design and construction practices of deep bridge foundations was gathered and analyzed for the following topic areas: pile analysis and design, pile drivability, pile design verification methods, and quality control.

Two features of this survey are that: 1) this was the first survey to be conducted after the October 1, 2007 deadline imposed by the FHWA, and 2) it focused on collecting detailed information on the design and construction practices of deep bridge foundations. The outcomes of this survey, presented in this chapter, encourage bridge designers to adopt the LRFD method for pile foundation design and highlight the benefits of utilizing the regionally calibrated resistance factors of this method.

4.1.1. Previous Surveys

With an anticipation of implementing the LRFD methodology to new bridge foundations in the United States, several questionnaires and surveys have been conducted over the past decade to monitor the degree of LRFD implementation. In 1999, the FHWA conducted a questionnaire concerning the design and construction practices for deep foundations, which was distributed to State Highway officials, Transportation Research Board (TRB) representatives, and FHWA geotechnical engineers (Paikowsky et al., 2004). Out of a total of 45 responses received, 90% of the respondents used the ASD method for foundation design with a factor of safety ranging from 2.0 to 3.0. Among the respondents, 35% used the AASHTO Load Factor Design (LFD) method, and only 28% used the AASHTO-LRFD method. The survey also collected useful information about the design and construction considerations for both driven piles and drilled shafts.

In 2004, the AASHTO-LRFD Oversight Committee (OC) conducted a survey among the State Departments of Transportation (DOTs) to monitor the degree of implementation of the LRFD approach for bridge substructure design (Moore, 2004), with a follow-up survey in 2005. The committee found that 12 states had fully implemented the LRFD method for foundation design in 2004 and increased to 16 in 2005. In 2006, researchers at the University of Colorado sent a questionnaire to all state DOTs as part of the development of the LRFD strategic plan for foundation design practice in Colorado (Chang, 2006). Only 28 DOTs responded to the questionnaire, and revealed that less than 22% of the respondents had either implemented or began implementation of LRFD for bridge foundations, while the remaining 78% had not even attempted the LRFD implementation. In 2007, the AASHTO-LRFD OC updated the LRFD implementation survey in their progress report (Moore, 2007), which indicated that 44 states would have fully implemented the LRFD approach for all new bridges by the FHWA mandated deadline of October 1, 2007.

Based on the outcomes of the aforementioned questionnaires and surveys, all of which were

conducted before the October 1, 2007 deadline, it was observed that the focus of the past surveys was to examine the degree of LRFD implementation for foundation design. The construction issues and/or details of the design procedures adopted for the bridge foundations were not examined. Consequently, the previous surveys did not provide any information on the use of regionally calibrated resistance factors, nor did they address the design verification and quality control practices adopted for the pile foundations.

4.1.2. Goals and Topic Areas of the Survey

The data for the study reported herein was collected through a web-based survey developed in January 2008 and then distributed to the DOT officials from different states, as well as FHWA engineers. A total of 33 fully completed responses were received in the first quarter of 2008, including one response received from FHWA-Eastern Federal Lands Highway Division (EFLHD), one from Alberta Infrastructure & Transportation, Canada, and the remaining from 31 different state DOTs. With input from the Iowa DOT officials, the survey was designed to be user-friendly and aimed toward gathering information on the current design and construction practices of pile foundations, while emphasizing LRFD and ASD approaches. Although nearly 100 questions were included, the survey utilized several logical branches to minimize the time required to complete the survey; i.e., respondents were not exposed to questions unrelated to their design and construction practice.

The goal of the survey was to determine the current design and construction practices of deep foundations nationwide with focus on the LRFD implementation for bridge substructure design and the current usage of regionally calibrated LRFD geotechnical resistance factors. The survey had the following four topic areas: 1) foundation practice; 2) pile analysis and design; 3) pile drivability; and 4) design verification and quality control.

The foundation practice section contained general questions acquiring information about typical soil formations, average depths to bedrock, routine in-situ and laboratory tests performed on soil, frequency of using deep foundations for bridges, as well as the types and sizes of frequently used piles. The pile analysis and design section was next, which included questions about the use of various design methods, the extent of implementation of the LRFD method, load and geotechnical resistance factors used in accordance with LRFD, factors of safety used with the ASD method, and load factors used with the LRFD method. Information about the different analysis methods used to calculate pile capacity (i.e., static methods, dynamic methods, and dynamic formulas) was also collected.

The third section on pile drivability focused on questions related to soil setup and relaxation, and their effect on the pile capacity in different soil types. Furthermore, this section gathered information on determining the required pile penetration length during driving and the definition of pile refusal. The final section on design verification and quality control obtained information on the pile design verification tests conducted during the construction stage, the frequency of performing the Static Load Test (SLT) on pile foundations, and different methods used for determining the pile nominal capacity based on SLT. At the end of the survey, respondents were asked to share information about the available SLT databases, provide general comments on the survey, as well as their contact details. In the Appendix-A, there are different flowcharts provided for each of the survey sections to show the sequence and logic branching of the

different questions.

4.1.3. Major Findings

A summary of analysis results over the responses received from the 31 state DOTs in the four main topic areas of the survey is presented in this section. In addition, the responses received from FHWA-EFLHD and Alberta Infrastructure & Transportation are highlighted in the presentation of results as necessary.

4.1.3.1. Foundation Practice

Figure 4.1 presents a summary of results obtained for the common foundation practices in different states. Included in this figure are the most common soil formations; average depth to bedrock; the most commonly used category of deep foundations, pile types and sizes; and the static analysis methods used in pile design. Respondents were allowed to identify up to three different soil formations for each state. Consequently, the soil formations shown for each state in Figure 4.1 were based on the survey responses. For the few respondents who opted not to answer this question as well as the state DOTs who did not respond to the survey, the soil formation shown was based on geological maps of Belcher and Flint (1946).

The respondents were allowed to identify an unlimited number of tests in this category. For questions regarding the in-situ and laboratory tests commonly used to define soil parameters, 94% of the respondents claimed to be using the Standard Penetration Test (SPT), 52% use the Cone Penetration Test (CPT), 16% follow the Vane Shear Test (VST), and around 20% perform other uncommon tests. Furthermore, all of the respondents reported to be performing basic laboratory soil tests such as Atterberg limits and soil classification, while 42% claimed that they perform triaxial tests, 35% reported to be performing the unconfined compression test, 29% perform the direct shear test, and 16% perform other uncommon laboratory tests. Despite the subjective nature of the test, the survey confirmed that the majority of respondents depend on SPT tests to determine the basic soil parameters.

The next set of questions gathered information about: the use of different foundation types associated with bridges, the most commonly used categories of deep foundations, along with details about the commonly used types of driven piles and drilled shafts. It was found that about 91% of the respondents use deep foundations more frequently in different soil types, while only 9% depend on shallow foundations to support low volume bridges in shallow bedrock or gravel. Among the deep foundation users, 76% reported the use of driven piles, where 18% use drilled shafts, and 6% use a combination of both. Figures 4.2 and 4.3 highlight the percentage of use of different driven pile types and drilled shafts, respectively. Among the driven pile users, all respondents indicated the use of steel H-piles, while 80% use closed-end pipe piles, 40% use open-end pipe piles, 32% use precast/prestressed concrete piles, 8% use precast concrete piles, 4% use timber piles, and about 12% of the respondents reported using other pile types (e.g., monotube piles, tapered tube piles, and a combination of prestressed concrete and steel H-piles). Among the drilled shaft users, it was found that 83% use cast-in-drilled-hole shafts (CIDH), 50% use soldier piles, 33% use continuous flight auger (CFA), and 33% use micropiles.

Furthermore, the respondents were asked to identify the most common pile size(s) that they use. This information is included in Figure 4.1, which reveals that steel H-piles and

precast/prestressed concrete piles are more commonly used on the East Coast of the United States where the soil formation is mainly composed of a coastal plain and glacial tills. On the West Coast, the soil profile is mainly composed of alluvium soil and therefore open-end pipe piles are more commonly used. Most of the states in the Midwest use steel H-piles due to the main soil profile being composed of glacial tills. In specific areas of the West, the CIDH shafts are also widely used, presumably due to the seismic requirements and the possibility of forming dependable plastic hinges in this foundation shaft.

The bridge foundation practice reported by FHWA-EFLHD was similar to that of the state DOTs. The FHWA indicated that they depend on SPT and CPT when determining the in-situ soil parameters and they mainly perform Atterberg limits and the unconfined compression test as the basic laboratory soil tests. They also indicated that they frequently use deep foundations for bridge construction, especially driven steel H-piles and precast concrete piles.

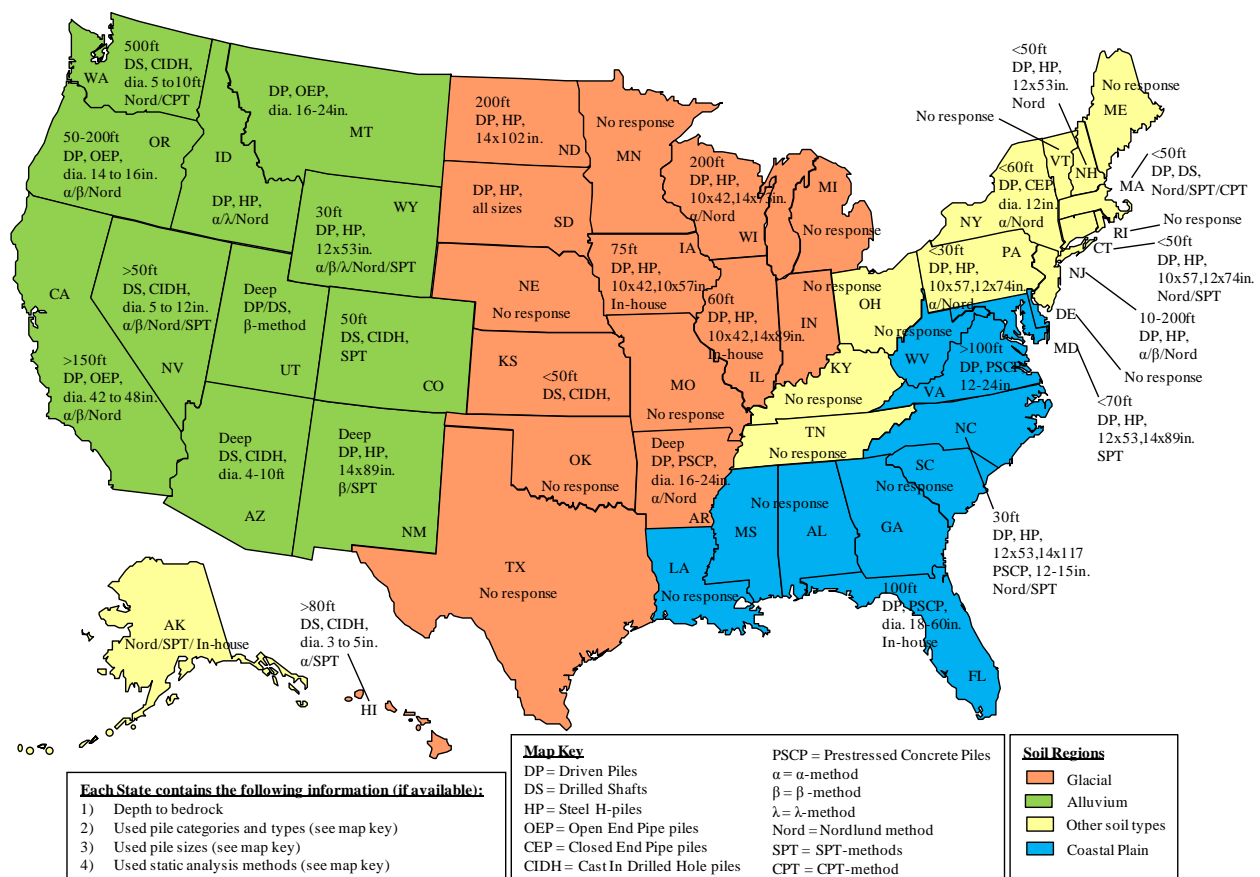


Figure 4.1: U.S. Map summarizing the typical soil formations, average depth to bedrock, commonly used deep foundation categories, types and sizes, and static analysis methods used in different states

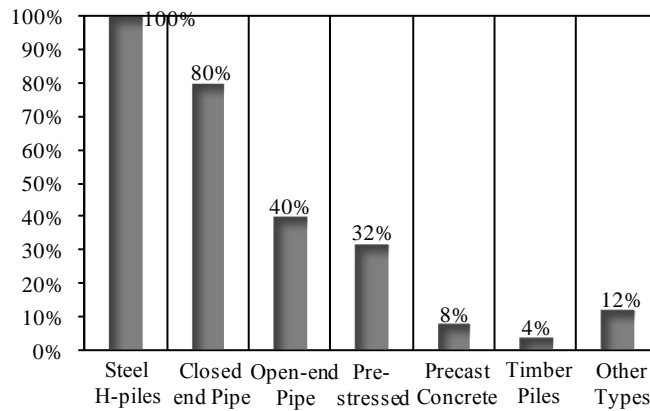


Figure 4.2: Distribution of the most commonly used driven pile types for bridge foundations

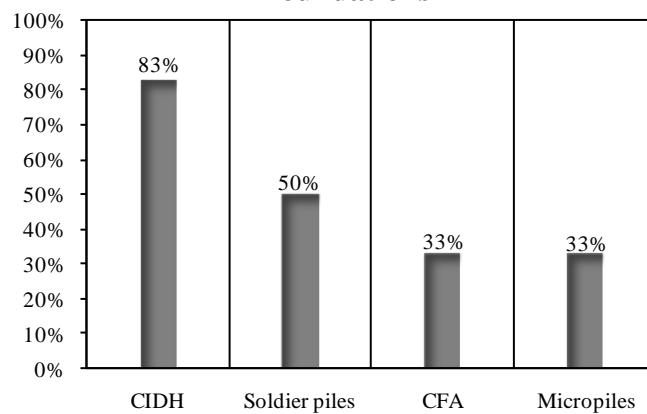


Figure 4.3: Distribution of the most commonly used drilled shaft types for bridge foundations

4.1.3.2. Pile Analysis and Design

The questions for this section were aimed at understanding the deep foundation design and analysis processes practiced by different state agencies. This section began with questions directed at determining the pile resistance criterion in cohesive and cohesionless soils. In cohesive soils, it was found that 88% of the respondents depend on both skin friction and end bearing, 6% of the respondents depend only on skin friction, and 6% indicated that they ignore end bearing only when the average SPT N-value is less than 12 blows per foot. In cohesionless soils, it was found that 87% of the respondents depend on combining the resistances obtained through skin friction and end bearing, 9% depend only on skin friction, and 4% only include the resistance from end bearing when the average SPT N-value is greater than 25 blows per foot.

Additionally, the most preferred method for designing deep foundations was found to be the ASD method, which was confirmed by 45% of the respondents. The primary reason for this choice was due to the respondents' familiarity with the ASD method, as well as the built-in conservatism associated with the AASHTO-LRFD specifications, which increases the cost of bridge foundations. However, the LRFD approach was reported to be the most commonly used method (see Figure 4.4) due to the imposed FHWA mandating deadline. About 52% of respondents are currently using LRFD, while 30% are in a transition stage from ASD to LRFD, and 3% of the respondents are transitioning from LFD to LRFD. As can be seen in Figure 4.4,

about 15% of respondents are still using ASD with a factor of safety ranging from 2 to 2.5.

Figure 4.5 shows the current extent of LRFD implementation in the design of bridge foundations in the United States. This figure was created by combining the 31 responses collected from the state DOTs along with the results of the AASHTO-LRFD OC survey (Moore, 2007) for those 19 DOTs who did not respond to the recent survey. Even though the FHWA mandate was implemented in October 2007, the 15 state DOTs who responded to the survey and the 11 of which who only responded to the AASHTO-OC survey are believed to be either still using the ASD method or in a transition stage to the LRFD approach for designing bridge foundations. Among the DOTs who responded as using the LRFD method for foundation design, 46% are using regionally calibrated resistance factors based on SLT database and reliability theory, 23% are using regionally calibrated factors by fitting to ASD, while 31% are using the geotechnical resistance factors as specified in the current AASHTO Specifications (2007). Information on the assumed risk or probability of failure (P_f) for the LRFD approach to pile foundations was also requested. Since they were not using LRFD or in transition to LRFD, 15 of the respondents did not answer this question. Another nine respondents claimed that they were unaware of the assumed probability of failure. However, four respondents indicated that they rely on a P_f less than 1/100 for the piles, while three of them reported to be using a P_f in the range of 1/5000 to 1/1000. According to Withiam et al. (1998), the measure of safety associated with the probability of failure is defined as the target reliability index (β), which depends on the pile redundancy. On the other hand, Paikowsky et al. (2004) indicated that the reliability indices of 2.33 (corresponding to a $P_f = 1\%$) and 3.00 (corresponding to $P_f = 0.1\%$) are assumed for redundant and non-redundant pile groups, respectively. Therefore, this variation in responses is believed to be a result of the assumed pile redundancy.

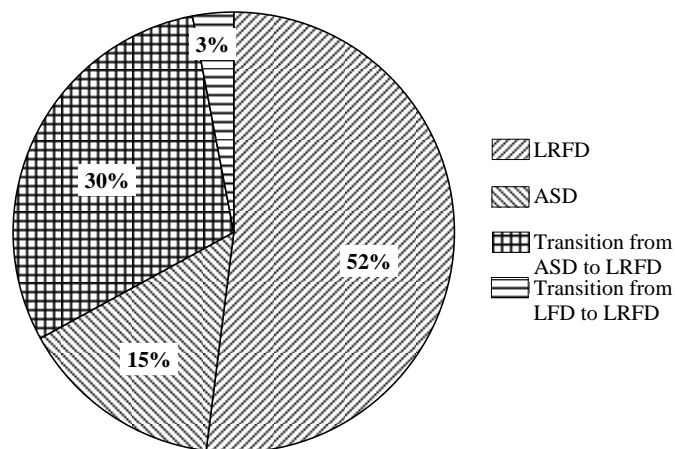


Figure 4.4: The usage of different methods for the design of bridge foundations

The next set of questions gathered information about the different static analysis methods, dynamic analysis methods, and dynamic formulas that are implemented for determining pile capacity. It was found that about 2/3 of the respondents employ a combination of static and dynamic methods. Respondents who claimed using this combination essentially use the static analysis methods for estimating the number of piles and dynamic analysis methods or dynamic formulas for determining the pile penetration length.

As shown in Figure 4.6, the most common static analysis method used for piles in cohesive soils

is the α -method at 42% (Tomlinson, 1957; API, 1974). About 32% respondents claim to be using the β -method (Esrig and Kirby, 1979), 11% use the CPT method (Nottingham and Schmertmann, 1988), and 9% follow the λ -method (US Army Corps of Engineers, 1992). Figure 4.6 also reveals that the most popular static analysis method for piles in cohesionless soils is the Nordlund's method at 63% (Nordlund and Thurman, 1963). About 40% of the respondents use the SPT method (Meyerhof, 1976/1981) while 6% use in-house methods for piles in cohesionless soils. Most of the respondents chose the Nordlund's method as the most accurate static method for sandy soils, and the α -method as the most accurate static method for clayey soils. Note that the survey permitted multiple answers for this particular set of questions. Complete descriptions of the different static analysis methods identified above may be found in Hannigan et al. (1998).

Figure 4.5: Extent of LRFD implementation for bridge foundations from survey in 2008

determining the capacity of deep foundations than either the static analysis methods or dynamic formulas.

In this part of the survey, the different extreme load types used in the design of bridge foundations along with the different methods used for estimating the lateral displacement demand of piles were also inquired. For the extreme load consideration, it was found that 37% of the respondents account for scour load in their design, 25% include earthquake load, 20% account for loads due to collision, and 18% use a combination of extreme loads. All respondents reported lateral displacement as a design consideration for piles. However, the method used for determining the pile displacement varied, as 72% of the respondents use the p-y curves, 14% use the Broms method (Broms, 1964), and 14% use other methods such as the FB-Pier strain wedge theory, point of fixity method, and empirical methods. Different systems have been used to reduce the effect of lateral loads on the bridge pile foundations, and integral abutments are one of the most commonly used systems by many DOTs. Integral abutment bridges are designed without any expansion joints, and hence the lateral loads are directly transferred from the superstructure to the foundations. Therefore, longitudinal and transverse loads acting upon the superstructure may be distributed over a larger number of supports. According to the AASHTO-LRFD bridge design specifications (2008 interim), no skew effects need to be considered when using integrated abutments for bridge skews of 25 degrees or less. Moreover, integral abutments provide added redundancy and capacity for catastrophic events such as seismic events according to Mistry (2005).

In general, the FHWA-EFLHD pile design practice was found to be similar to that of the State DOTs. The FHWA-EFLHD indicated that they were still in a transition stage from ASD to LRFD and were using the resistance factors from the 2007 AASHTO-LRFD Specifications for the LRFD approach. For the design of bridge pile foundations, they indicated the use of static analysis methods such as α -, β -, and Nordlund. As for the pile design verification, the FHWA-EFLHD response noted that they used the SLT less frequently and preferred employing the dynamic analysis methods (i.e., PDA and CAPWAP) and dynamic formulas (i.e., ENR, Gates, and FHWA-modified Gates). A point of contrast between the FHWA-EFLHD and state DOTs' bridge foundation design practice is that FHWA-EFLHD considers the static analysis methods to be more accurate than the dynamic methods as long as the soil strength parameters are adequately obtained.

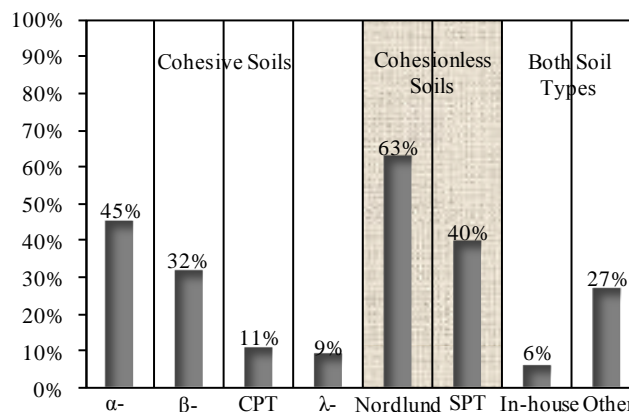


Figure 4.6: Most commonly used static analysis methods for the design of deep foundations

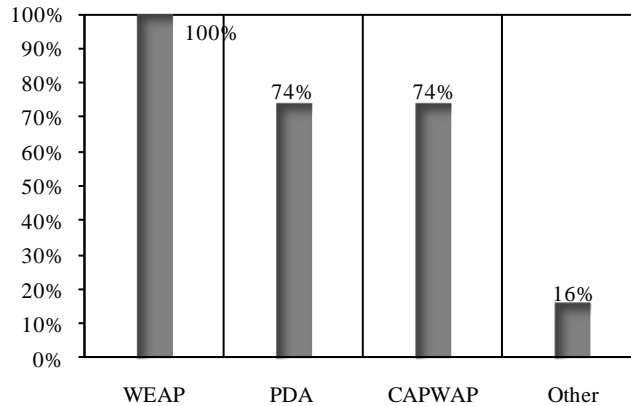


Figure 4.7: Most commonly used dynamic analysis methods for the design of deep foundations

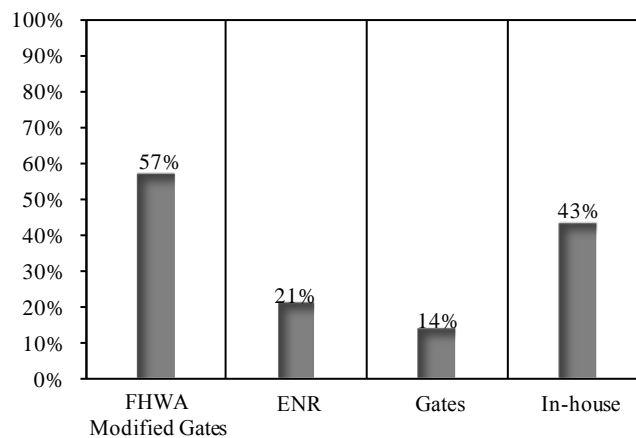


Figure 4.8: Most commonly used dynamic formulas for deep foundations

4.1.3.3. Pile Drivability

In the design stage, the pile penetration length required in the field is estimated using the chosen static analysis method. However, the penetration length may be readjusted during the construction. It was found that 31% of the respondents depend on a WEAP analysis as well as field observations to readjust the pile penetration length, while 20% employ dynamic formulas to make the adjustments, and 15% rely on the initial static analysis results, making no adjustments to pile length in the field (see Figure 4.9). Interestingly enough, 6% of the respondents noted that they drive the pile until refusal, while 4% prefer driving the piles until the bedrock is reached. The remaining 24% of respondents indicated that they use a combination of the aforementioned methods depending on the site conditions and design requirements.

Effects of soil relaxation and setup on the pile capacity were also addressed in this section of the survey, and the results are summarized in Figures 4.10 and 4.11, respectively. More than 50% of the respondents believe that the pile capacity is unaffected by relaxation in cohesive soils. The responses of those indicating that the pile capacity is affected by relaxation were grouped based on the most predominant soil formation that they indicated for their region. Accordingly, 40% of respondents noted that the change in pile capacity would not exceed 5% of the value expected at

End of Driving (EOD) in silty sands, 6% indicated that the effect varies from 5 to 10% in sandy soils, and only 2% assumed that the effect exceeds by 20% of the pile capacity in silts. Similarly, for the influence of soil setup on the pile capacity, 34% of the respondents indicated that the pile capacity increases the value at EOD above 20% in clays and silty clays, 25% indicated that the effect varies from 5 to 10% in glacial tills and clays, 25% indicated that the effect varies from 11 to 20% in clayey silts, 6% indicated that the soil setup effect does not exceed 5% on the pile capacity, and 10% of the respondents assume that the pile capacity is unaffected by soil setup in cohesionless soils.

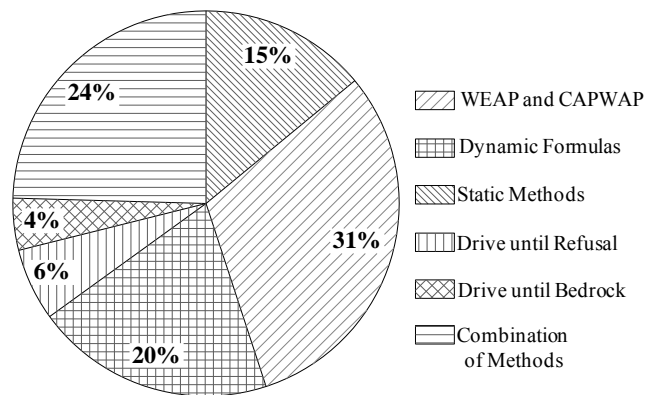


Figure 4.9: Methodologies used for readjusting the pile penetration length

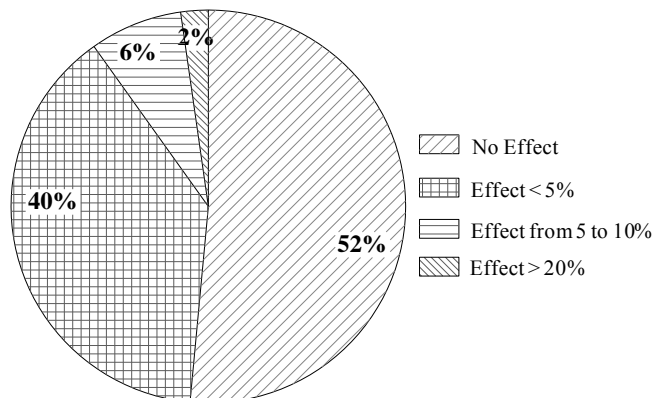


Figure 4.10: Expected effect of soil relaxation on the pile capacity at the EOD

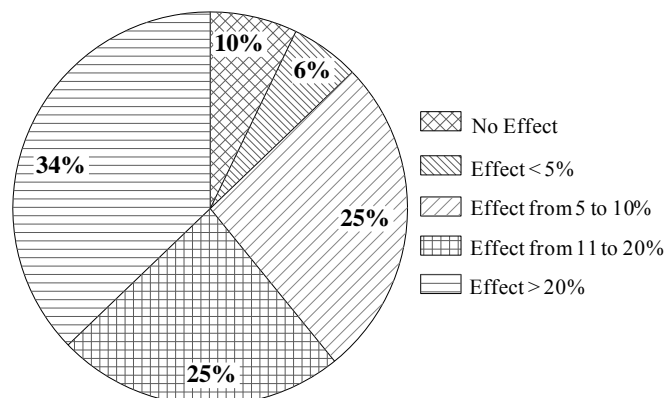


Figure 4.11: Effect of soil setup on the pile capacity at the EOD

4.1.3.4. Design Verification and Quality Control

This final section of the survey focused on design verification and quality control issues. All but one respondent indicated that they perform field tests on 5 to 10% of the installed piles to verify the design capacity. Among several different techniques, about 45% of respondents have used the SLT for design verification, while others predominantly use the dynamic monitoring approach, especially for friction piles (i.e., use of WEAP, PDA and CAPWAP). The WEAP analysis is usually considered as an adequate pile design verification technique for small projects, but for large-scale projects the PDA and CAPWAP are preferred. Among those who use SLT, 73% responded that they use the Davisson's criterion (Davisson, 1972) to define the pile nominal capacity, 26% use the limited total settlement method, 7% use the shape of curvature method, and 13% follow other unspecified methods.

4.1.4. Reported LRFD Resistance Factors

As previously indicated, among those who have already implemented the LRFD approach to their design of bridge foundations, 12 state DOTs use regionally calibrated resistance factors that are more suitable for the local soil types. These resistance factors were calibrated based on local SLT data and by using different reliability theory statistical approaches. Respondents did not indicate which reliability approaches that they used in the LRFD calibration, however, a brief description of the most commonly used approaches is provided in the following paragraph. Of those DOTs who are still in transition to the LRFD, six have adopted preliminary, regionally calibrated resistance factors. These factors were established using their local design and construction experience, as well as the recommended load factors to retain the factor of safety used for the ASD method (calibration by fitting to ASD). This information, which includes details about soil formation, deep foundation practice, and design methodology, is summarized in Table 4.1. Of the respondents, 11 indicated having a collection of SLT data for their state and they are identified in the table.

There are different statistical approaches that can be used for LRFD resistance factors calibration based on reliability theory, such as the First Order Second Moment (FOSM) or the First Order Reliability Method (FORM). According to Allen et al. (2005), the FOSM is a straightforward technique. In the FOSM, the random variables are represented by their first two moments, i.e., the mean (μ) and standard deviation (σ), while the Coefficient of Variation (COV) can be calculated by dividing the standard deviation by the mean. Paikowsky et al., (2004) performed the analysis using both methods (the FOSM and the FORM) and concluded that the difference between them is around 10%, where the FOSM provides slightly conservative resistance factors. Moreover, the 2007 AASHTO-LRFD specifications are based on the FOSM, assuming a lognormal distribution of the loads and resistances' density functions. Another advanced method is the Monte Carlo simulation method, which has been used for performing the reliability analyses. Nowak and Collins (2000) and Allen et al. (2005) have shown that these advanced methods should produce similar results to each other, which may indicate that using a less sophisticated approach like FOSM would be acceptable.

All the regionally calibrated resistance factors reported for different soil and pile types were examined using statistical means in order to determine a representative mean and standard

deviation of the resistance factors and compare with other design specifications. The minimum sample size (N) used in the comparable statistical analyses was equal to or exceeded three. For all datasets, the mean and standard deviation were determined as a function of soil type, pile type and static analysis method. For those datasets with $N < 3$, only the average resistance factors were determined. All of these results are summarized in Tables 4.2 and 4.3. Figure 4.12 represents the histograms and frequency distributions, as well as the confidence intervals for the Probability Density Functions (PDFs) of the reported resistance factors for steel H-pile in different soil types. As shown in Figure 4.12, the PDFs of different datasets were following a normal distribution, as the probability of the upper and lower limits of the true mean of each dataset was found to be within 95% confidence intervals. As indicated by the standard deviations in Table 4.2, it appears that the mean of the reported regionally calibrated resistance factors for a given soil type is somewhat consistent, especially for the steel H-piles. Also note in this table that the mean resistance factor of the open-end pipe piles is greater than that established for the steel H-piles and CIDH shafts. However, it is noted that the resistance factor of the pipe piles is based only on two data points. For resistance factors reported for different static analysis methods in Table 4.3, smaller standard deviations are observed again, indicating less variations in the reported resistance factors for a given method and soil type. Furthermore, it is noted that the in-house methods lead to higher resistance factors than those determined for routinely used static analysis methods.

Table 4.4 compares the mean values of the regionally calibrated resistance factors from Tables 4.2 and 4.3 with those reported in the National Corporate Highway Research Project (NCHRP) report number 507 by Paikowsky et al. (2004) and the 2007 AASHTO-LRFD Specifications. In most cases, it is observed that the AASHTO recommendations are more conservative than those proposed by Paikowsky et al. (2004). Moreover, the mean of the regionally calibrated resistance factors reported by different DOTs in all cases is equal to or greater than the recommended values in NCHRP 507 and the AASHTO Guidelines. In some cases, the regionally calibrated factors are twice as high as those recommended for design practice by AASHTO. Therefore, it is clear that the LRFD regional calibration could result in higher resistance factors as previously shown, which will optimize the pile design accordingly.

The benefits of using regionally calibrated resistance factors in pile design can be realized through a simple design example. Consider a bridge pier with a maximum factored axial load of 2000 kips that is designed with a deep foundation consisting of a 60-ft long steel HP 10 x 42 connected with a concrete cap. The soil formation at the site is firm to very firm glacial clay with silt seams and boulders, and medium soil variability. If the α -API (API, 1974; Coduto, 2001) static analysis method is used for the design of the pile foundation, the axial capacity of a single pile is 127.5 kips. Using the LRFD resistance factor of 0.35 provided in the 2007 AASHTO specifications, the design capacity of a single pile is 44.6 kips, requiring a minimum of 45 piles. If the average regionally calibrated resistance factor of 0.47 for the α -API method is used from Table 4.3, the design capacity of each pile is 60 kips, requiring a total of only 34 piles. This 25% reduction in the number of piles will significantly reduce the foundation cost as it reduces construction costs of both the piles and the pile cap.

Table 4.1: Summary of the reported LRFD resistance factors, sorted according to different pile types, static analysis methods, and soil types

State	Pile Type	Static Analysis		Dynamic Analysis	Dynamic Formulas	LRFD Geotechnical Resistance Factors		
		Cohesive	Cohesionless			Sand	Clay	Mixed
AK	CIDH ⁽¹⁾	α -method	SPT-method	Not used	Not used	0.45	N/A	N/A
CA*	Steel H-piles	CPT-method	Nordlund	$P + C + W^{(2)}$	FHWA-G ⁽³⁾	0.45	0.35	N/A
CO	CIDH	SPT-method	SPT-method	$P + C + W$	ENR, G, FHWA-G	0.1	0.9	0.5
CT*	Prestressed	In-house	In-house	$P + C + W$	Not used	0.65	0.65	0.65
FL*	CIDH	CPT-method	Nordlund	$P + C + W$	In-house	0.65	0.65	0.65
HI	Steel H-piles	β -method	β -method	$P + C + W$	Not used	0.65	0.65	0.65
IA*	Steel H-piles	In-house	In-house	Not used	Not used	0.725	0.725	0.725
ID*	Steel H-piles	β -method	SPT-method	$P + C + W$	FHWA-G	0.45	0.45	0.45
IL	Open- pipe	α -method	Nordlund	Not used	Not used	0.7	0.7	0.7
MA*	Open end pipe	In-house	Nordlund	$P + C + W$	Not used	0.65	0.65	0.65
NH*	Closed-pipe	α -method	Nordlund	$P + C + W$	Not used	0.45	0.35	N/A
NJ*	CIDH	α -method	Nordlund	$P + C + W$	Not used	0.45	0.35	0.4
NM*	Steel H-piles	β -method	Nordlund	$P + C + W$	ENR, G, FHWA-G	0.35	0.45	N/A
NV	Steel H-piles	α -method	Nordlund	Not used	Not used	0.35	0.25	N/A
PA*	Steel H-piles	β -method	Nordlund	$P + C + W$	Not used	0.5	0.5	0.5
PA	Steel H-piles	λ -method	SPT-method	$P + C + W$	Not used	0.45	0.55	0.55
UT*	Steel H-piles	α -method	Nordlund	Not used	Not used	0.5	0.7	0.7
WA	Steel H-piles	In-house	In-house	WEAP	FHWA-G	0.5	0.5	0.5
WY	Steel H-piles	CPT-method	Nordlund	Not used	Not used	0.45	0.35	0.35

*State DOTs having pile static load test database; ⁽¹⁾ CIDH: Cast-In-Drilled-Hole Shafts; ⁽²⁾ $P + C + W$: PDA, CAPWAP, and WEAP; ⁽³⁾ FHWA-G: FHWA-Modified Gates method, where G is Gates method

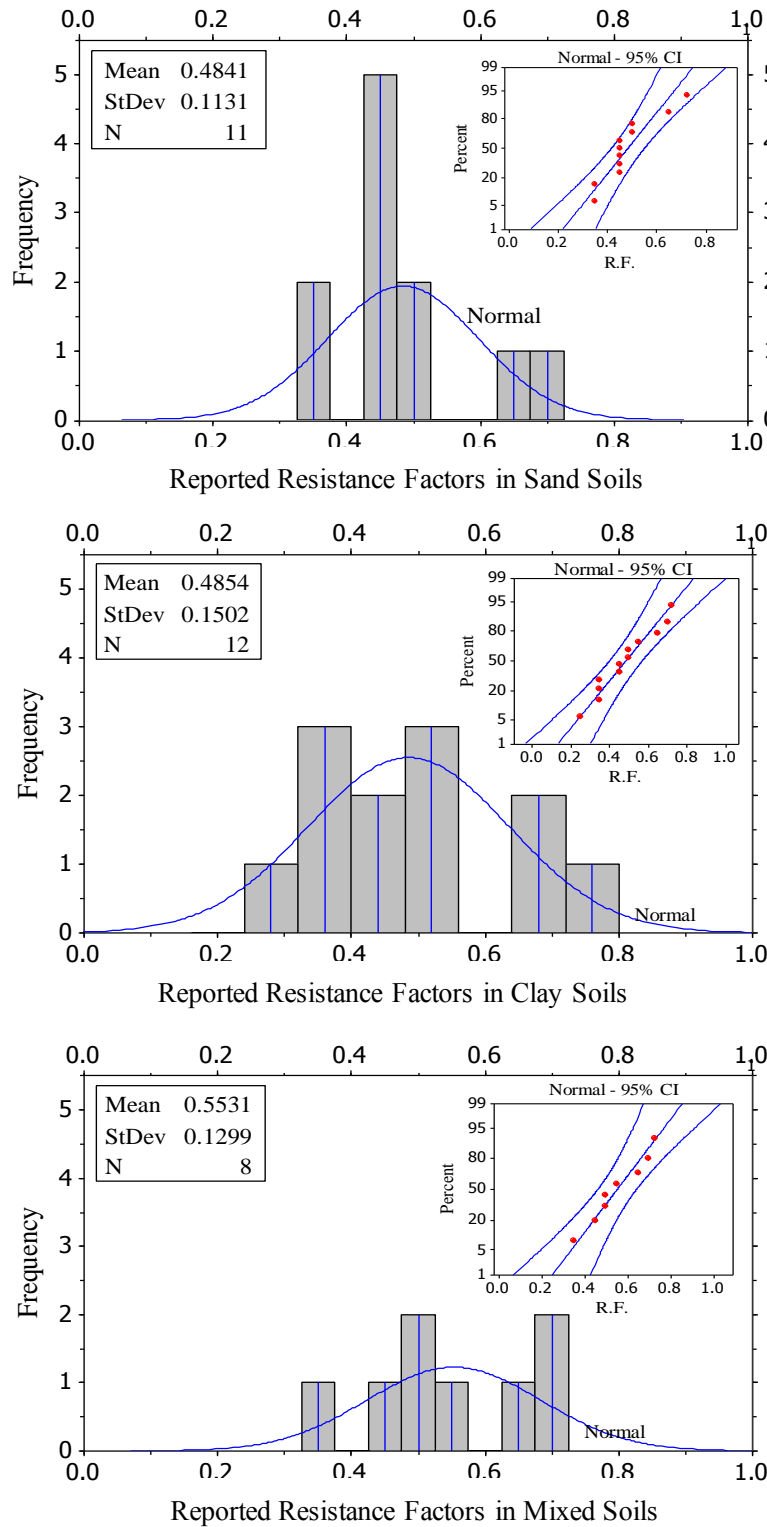


Figure 4.12: Histograms, frequency and 95% CI of the reported regional LRFD resistance factors for steel H-pile in different soil types

Table 4.2: Mean values and standard deviations of the reported regional resistance factors according to different pile and soil types

Pile Type	Reported Factors in Sand			Reported Factors in Clay			Reported Factors in Mixed Soil		
	N ⁽¹⁾	Mean	S.D. ⁽²⁾	N	Mean	S.D.	N	Mean	S.D.
Steel H-pile	11	0.48	0.11	12	0.48	0.15	8	0.55	0.13
CIDH	4	0.4	0.23	3	0.6	0.28	3	0.5	0.13
Open-end Pipe	2	0.65	N/A	2	0.67	N/A	2	0.67	N/A

⁽¹⁾ Sample Size

⁽²⁾ Standard Deviation

Table 4.3: Mean values and standard deviations of the reported regional resistance factors according to different static analysis methods and soil types

Static Analysis Method	Reported Factors in Sand			Reported Factors in Clay			Reported Factors in Mixed Soil		
	N	Mean	S.D.	N	Mean	S.D.	N	Mean	S.D.
Nordlund	11	0.5	0.12	N/A			4	0.53	0.17
SPT method	3	0.45	0.25	N/A			3	0.53	0.11
α-method	N/A			6	0.47	0.19	N/A		
β-method	N/A			4	0.49	0.13	N/A		
CPT method	N/A			3	0.45	0.17	N/A		
In-house	3	0.62	0.11	4	0.63	0.10	3	0.62	0.11

Table 4.4: Comparison between the reported resistance factors and the recommended factors in NCHRP 507 and 2007 AASHTO-LRFD Specifications

Soil Type	Static Analysis Method	NCHRP	AASHTO-Specifications	Mean of Reported Resistance Factors
Sand	SPT- method	0.45	0.3	0.45
	β -method	0.3	N/A	0.65
	Nordlund	0.45	0.45	0.5
	In-house	N/A	N/A	0.62
Clay	α -method	0.45	0.35	0.47
	β -method	0.2	0.25	0.49
	In-house	N/A	N/A	0.63

4.1.5. Summary and Conclusions

This report has presented results from an important survey on the current design and construction practices of deep foundations for bridges. This survey is one of the first to be completed following the FHWA mandate on the use of the LRFD approach in the U.S. for all new bridges, which was initiated after October 1, 2007. The outcomes of the survey are significant in that they give an overview of the current bridge foundation practices and highlight how frequently the state DOTs take advantage of the provision in the AASHTO-LRFD Specification to improve the deep foundation design by employing regionally calibrated geotechnical resistance factors and

the associated benefits. Based on the responses received, the conclusions drawn from the study are as follows:

1. As of June 2008, 52% of the DOTs who responded to the survey have adopted the LRFD approach for the design of deep bridge foundations, while 33% were in a transition phase from ASD to LRFD, and the remaining 15% still followed the ASD approach with a factor of safety ranging from 2 to 2.5. Of those using the LRFD method, six DOTs use geotechnical resistance factors by fitting to ASD, eight are following the 2007 AASHTO-LRFD recommended values, while 12 DOTs have adapted their own regionally calibrated factors based on reliability theory.
2. The mean of the reported regionally calibrated geotechnical LRFD resistance factors were statistically analyzed and presented in Tables 4.1 through 4.4. The LRFD regionally calibrated resistance factors reported for sands and clays are either equal to or greater than the AASHTO recommended values. In sand, the resistance factors are as much as 50% above those recommended by AASHTO, while values of 100% above the recommended values are used for clay. Such large increases in resistance factors will likely reduce the overall cost of deep bridge foundations.
3. In the design stage, state DOTs are using static analysis methods for determining the pile capacity. The most commonly used methods in cohesive soils are the α - and β -methods. On the other hand, the most commonly used static methods in cohesionless soils are the Nordlund and SPT methods. Most of the respondents chose the α -method and the Nordlund method as the most accurate method for determining the pile capacity in cohesive and non-cohesive soils, respectively.
4. During the construction of deep foundations, the DOTs employ either dynamic analysis methods or dynamic formulas to verify the pile capacity estimated by a static analysis method. Although all of the respondents noted that they use WEAP as a dynamic analysis method, 75% indicated that they use a combination of PDA and CAPWAP in addition to WEAP. Of those who use dynamic formulas for pile capacity verification, the majority of respondents use either the FHWA-modified Gates formula or a locally developed formula.

4.2. Survey of Iowa County Engineering Offices

A web-based survey was sent to Iowa County engineers and consulting firms in order to study the current design and construction practices of deep bridge foundations at the local county level. This survey collected information regarding the different types of deep foundations, static and dynamic analysis methods, dynamic pile driving formulas, and construction control procedures used. More specifically, this survey acquired the aforementioned general information via an organizational structure defined by the following four focal areas: (1) foundation practice, (2) timber pile usage, (3) pile analysis and design, and (4) pile drivability/quality control. The findings of the survey are presented there, including the following four main topic areas: 1) foundation practice; 2) timber pile usage; 3) pile analysis and design; and 4) drivability, testing, and quality control. The foundation practice section contained general questions acquiring information about typical soil formations, average depths to bedrock, routine soil in-situ and

laboratory tests, and the frequently used pile types and sizes. Next was the timber pile usage section, which included questions regarding the recommended soil, bridge types to be used in conjunction with timber piles, as well as the likelihood of using timber type piles for future bridge projects.

The third section on pile analysis and design focused on questions concerning who actually performs the design, the adopted design specifications, the extent of implementation of the LRFD method, the use of various static and dynamic analysis methods, and the dynamic formulas used for pile capacity calculation. This section also collected information regarding the calculation of vertical and lateral pile displacements, in addition to the extent to which serviceability checks are conducted during the design process. The fourth section of the survey focused on drivability, testing, and quality control aspects. This section contained questions that acquired information about the methods used to terminate pile driving as well as the effect of soil setup and relaxation on pile capacity. Information on pile design verification tests conducted during the construction stage, the frequency of performing Static Load Tests (SLTs) on pile foundations, and the different methods used for determining the pile nominal capacity from load-displacement results were obtained in this section. At the end of the survey, respondents were asked to share information about available SLT databases and also to provide general comments on the survey and their contact details. Furthermore, an enhanced version of this survey was sent to representatives of different civil engineering consulting firms located in the State of Iowa seeing that a significant portion of the responding counties identified the use of consulting firms for the design and verification of piles. The last subsection in the Major Findings section of this report summarizes the responses collected from these consulting firms. Flowcharts are provided in Appendix-A, which shows the questions included in each section of the local survey.

The major results of this survey received complete responses from engineers located in 44 different counties within the State of Iowa (as seen in Figure 4.13) and will be presented in the following subsections according to the four focal areas previously delineated. Figure 4.13 also presents a summary of results obtained for the common foundation practices in different Iowa counties. Included in this figure are the typical soil formations, the average depth to bedrock, and the most frequently used pile types and sizes.

4.2.1. Foundation Practice

The questions within this first section of the survey focused on obtaining information regarding the main criteria for selecting the appropriate type of deep bridge foundation, the selection potential of drilled shafts over driven piles for present and future bridge projects, as well as the most commonly used types of driven piles. Based on the responses received, it was found that 54.5% of Iowa County engineers rely on past design experience for selection of a given type of driven pile, whereas 18.2% cited economy as the main criteria, 15.9% stated that selection criteria differs between projects, 13.6% reported using the same type of driven pile foundation for all bridge projects, 9.1% cited available construction equipment as the main criteria, and the remaining 11.4% stated the used of another particular selection criterion other than those previously defined (see Figure 4.14).

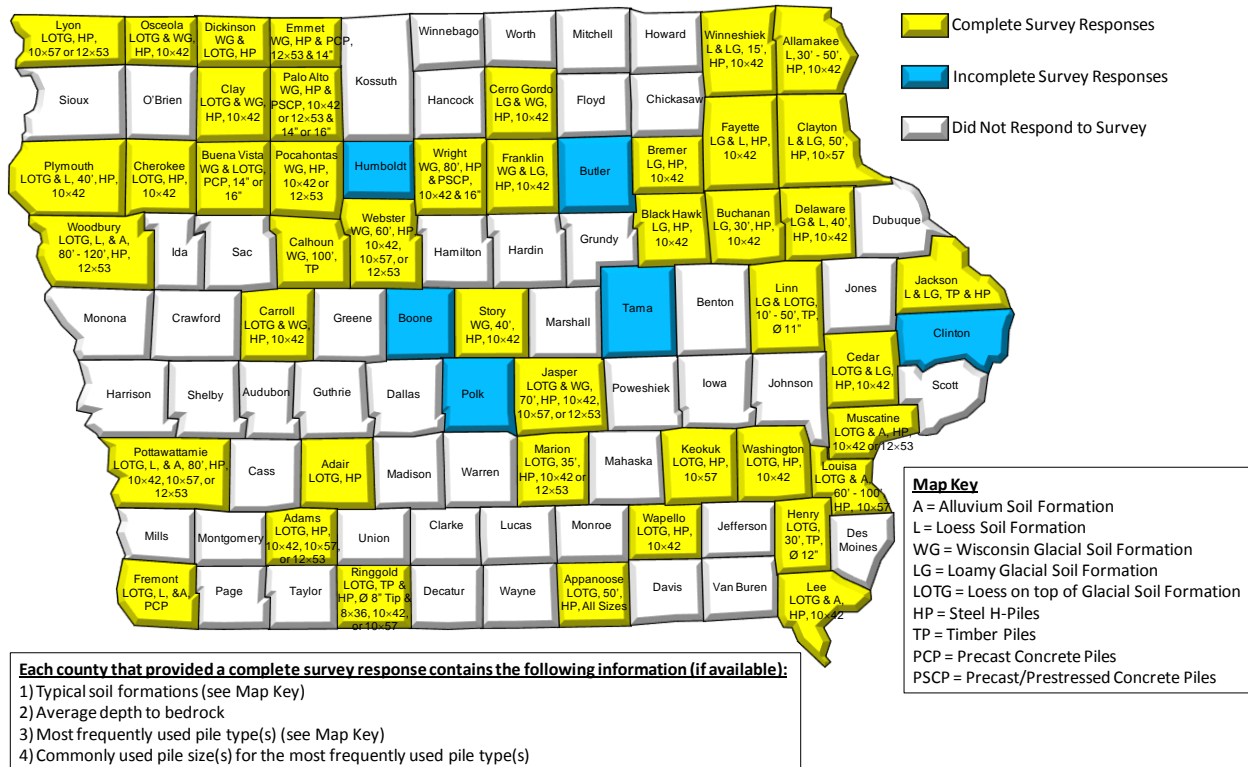


Figure 4.13: Summary of Responses from Iowa County Engineers to the Local Survey on Pile Design and Construction Practices

The survey respondents indicated their use of driven piles over drilled shafts for the contemporary bridge projects. Moreover, they did not indicate any potential increase in their dependency on drilled shafts in the future. Therefore, no further information was obtained regarding the percentage of usage of different types of drilled shafts. However, a distribution of the most commonly used type of driven pile foundations for bridge structures was attained and is presented in Figure 4.15. Explicitly put, all respondents indicated the use of steel H-shaped piles, while 43.2% indicated the use of timber piles, 22.7% cited the use of precast concrete piles, 20.5% reported the use of prestressed concrete piles, 2.3% indicated the use of close-ended steel pipe piles, with the remaining 2.3% reporting the use of other driven pile types.

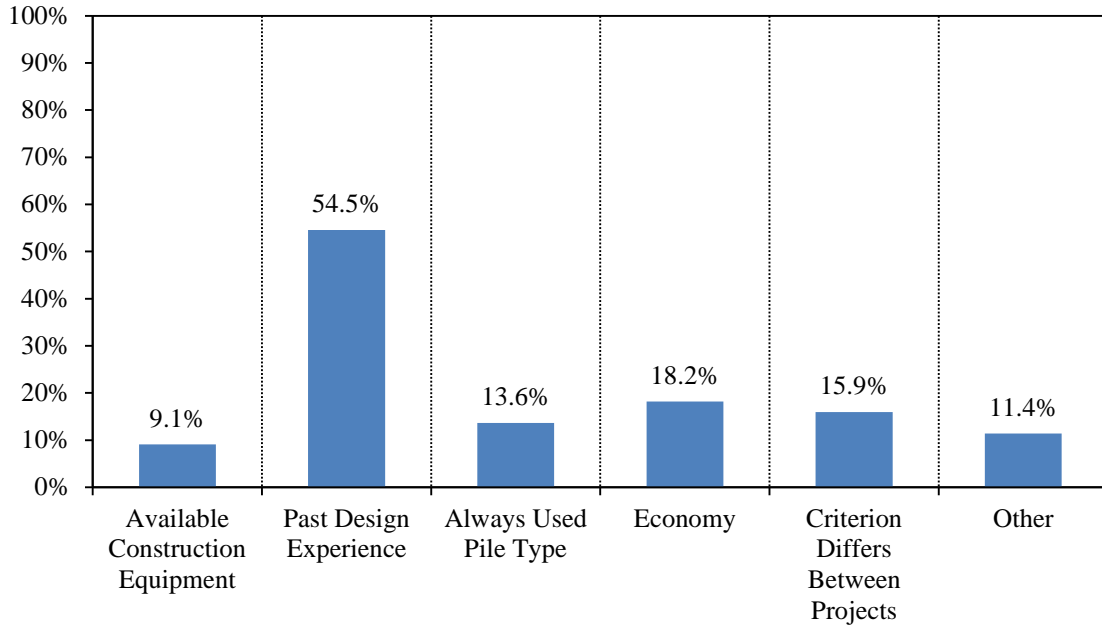


Figure 4.14: Main criteria of selecting the appropriate type of deep bridge foundation

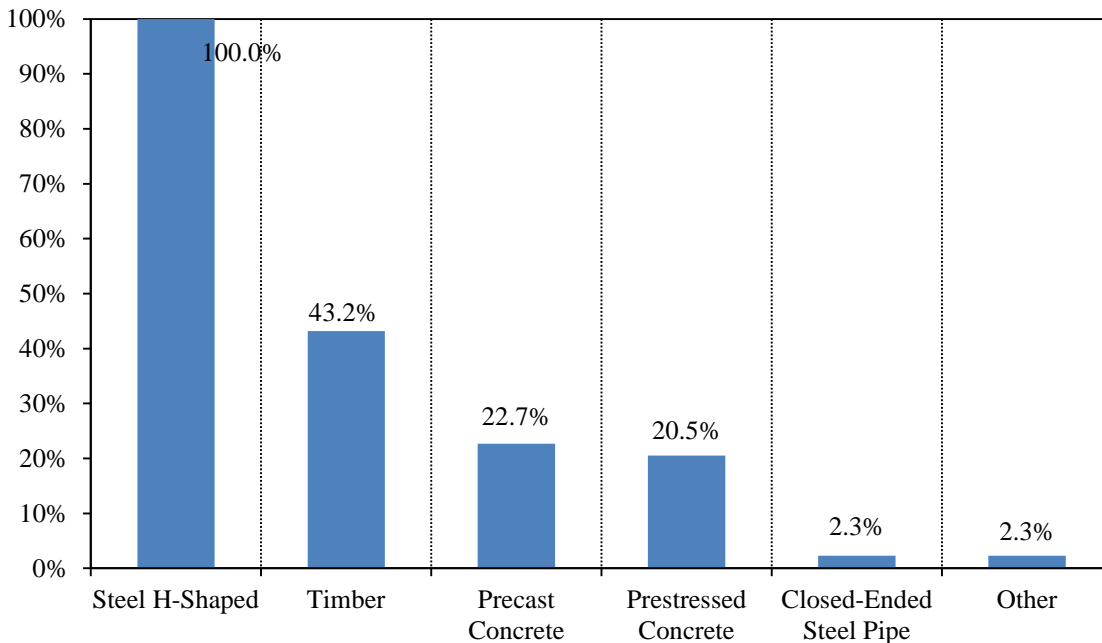


Figure 4.15: Distribution of the most commonly used types of driven piles for bridges

4.2.2. Timber Pile Usage

Questions in the second section of the survey asked the respondents who reported the use of timber piles about the different soil and bridge types recommended for such piles. Based on responses received from Iowa County engineers, it was found that 72.2% use a deep foundation system comprised of timber piles to support low-volume bridges, 55.6% use such pile type for short span bridges, 16.7% do not recommend the use of deep foundation systems comprised of

timber piles for bridge type structures, and 5.6% use such pile type for pedestrian bridges. These aforementioned results have also been provided in graphical form in Figure 4.16. As for the results associated with the soil types recommended for use with driven timber piles, Figure 4.17 clearly shows that clay soils are recommended the most for timber piles. This indicates that the timber piles are most likely used as friction piles with no significant end bearing component.

4.2.3. Pile Analysis and Design

For the pile analysis and design section of the survey, questions were asked to obtain information regarding the personnel conducting the analysis and delivering the design drawings of bridge pile foundations, the specifications used for their design, and the method of analysis most commonly used for driven pile foundation design. From the responses received, it was found that 59% of Iowa County engineers actually perform the design of driven pile foundations for bridge type structures themselves, whereas 39% enlist the services of private engineering consulting firms, with the remaining 2% seeking the aid of the Iowa DOT or other outside agency for their design (see Figure 4.18).

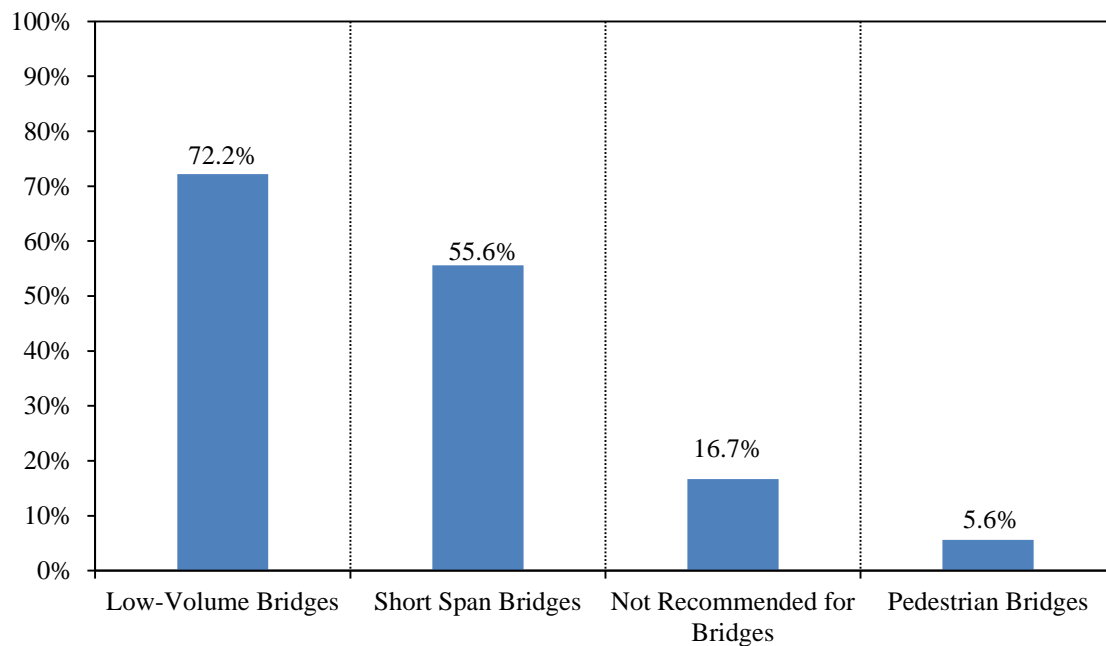


Figure 4.16: Distribution of bridge types recommended for timber piles

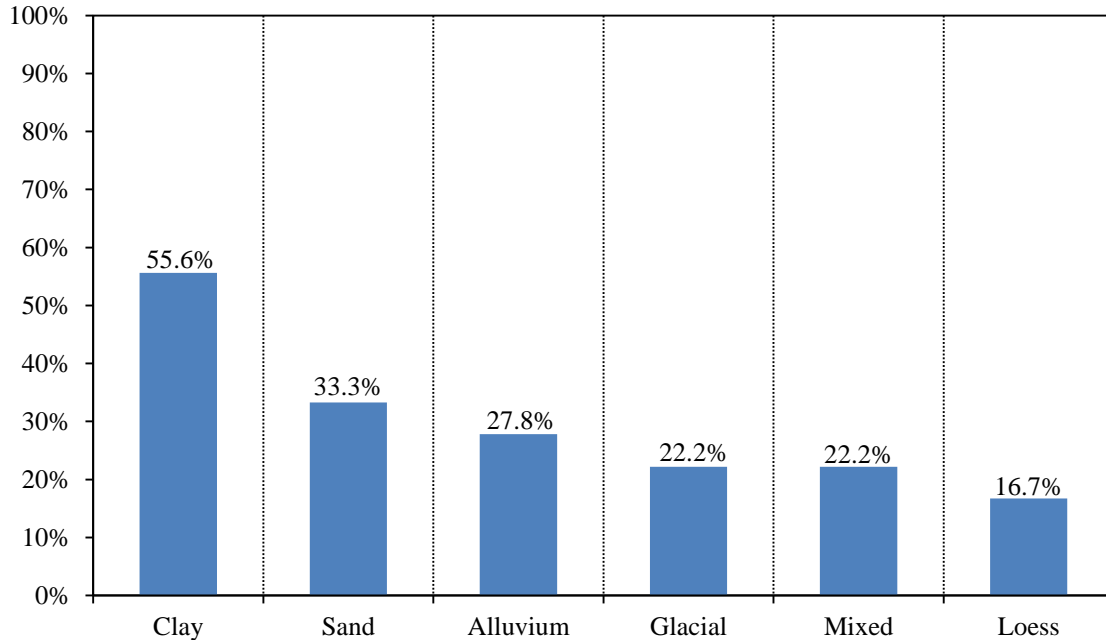


Figure 4.17: Distribution of soil types recommended for use with timber piles

For Iowa County engineers who performed the design of driven pile foundations for bridge structures, 73% cited the Iowa County Bridge Standards (Iowa DOT 2009) as their primary driven pile design specification, 15% acknowledged use of the Iowa ASD/LFD Bridge Design Manual (Iowa DOT 2010), 4% made use of the AASHTO-LRFD Bridge Design Specifications (2007), and the remaining 8% cited other pile design specifications other than those formerly defined (see Figure 4.19). It is important to point out that the aforementioned list of primary driven pile design specifications utilized by Iowa County engineers does not include the Iowa LRFD Bridge Design Manual (Iowa DOT 2010).

On the other hand, it was essential to inquire information about the main engineering private consulting firms conducting almost 40% of the bridge designs for different counties in the State of Iowa. As shown in Figure 4.20, it was found that Calhoun Burns and Associates (CB&A Inc.) are employed around 45% of the designs, and HGM are employed 14% of them, while Shuck-Britson, Kirkham Michael, and IIW Engineers are employed 9%, each. The contribution from consulting firms is summarized in the following subsection (4.2.4.1).

Finally, the method of analysis most commonly used for the design of driven pile foundations is presented in Figure 4.21. The results of the survey showed that 86% of respondents cited the use of dynamic pile driving formulas (i.e., ENR, Gates, etc.) for this particular task, with the remaining 14% reporting the use of static analysis methods (i.e., SPT-Meyerhof, Blue Book methods, etc.). Among different methods, the α -method and the ENR formula are the Iowa County engineers' choice for the design and construction control of driven pile foundations, respectively.

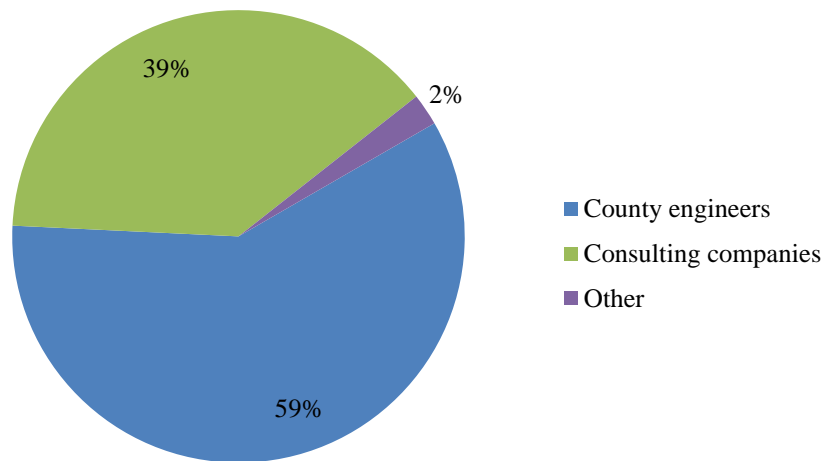


Figure 4.18: Personnel conducting the analysis and design of deep foundations in Iowa

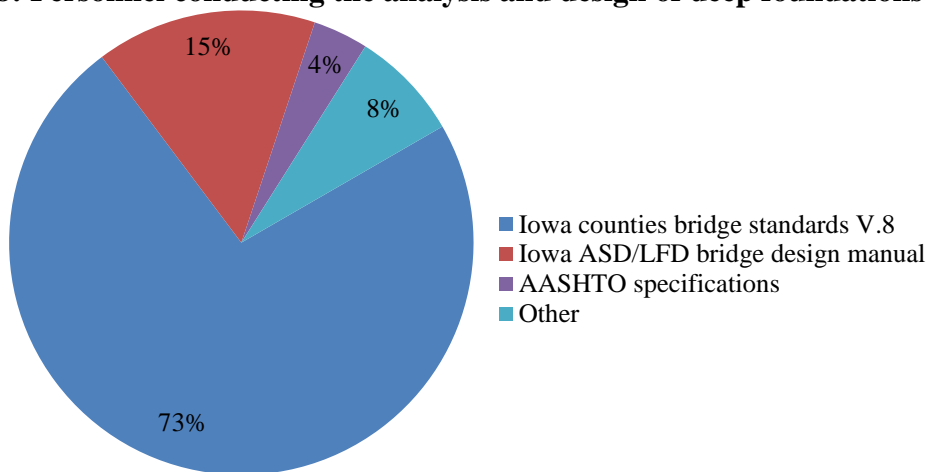


Figure 4.19: Most commonly used design specifications by Iowa County engineers

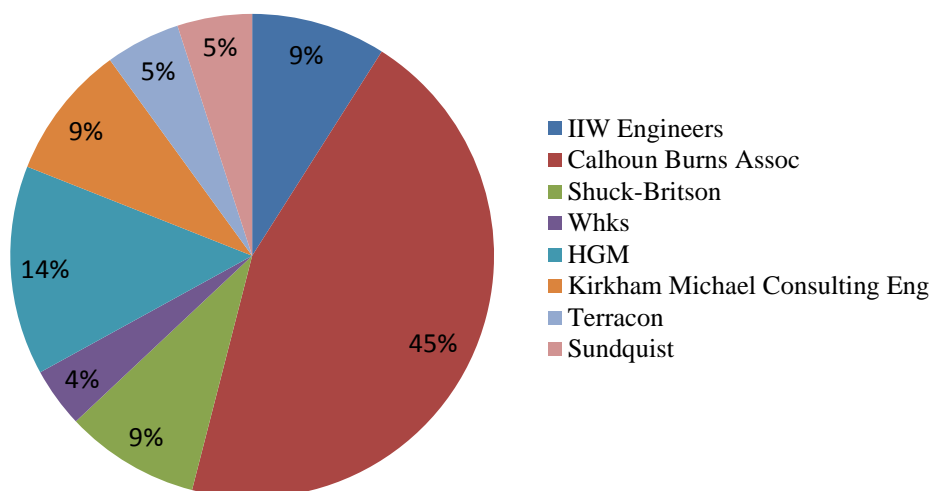


Figure 4.20: Engineering private consulting firms that conduct bridge designs in Iowa

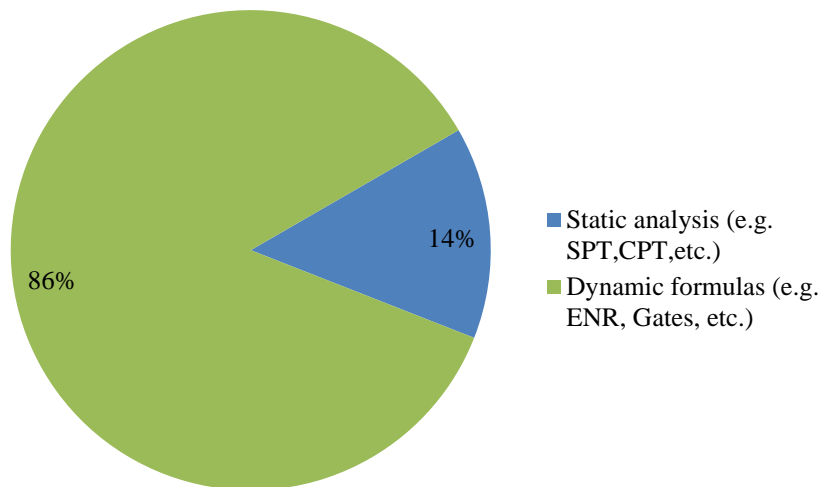


Figure 4.21: Most commonly used methods of analysis for the design of driven piles

4.2.4. Pile Drivability/Quality Control

The questions within this final section of the local survey of Iowa County engineers focused on obtaining information regarding the pile driving termination criterion used in the field, the use of pile Static Load Tests (SLTs) for design verification, and the frequency of conducting different quality control tests. Based upon the responses received, it was found that 61.4% of Iowa County engineers use the Wave Equation Analysis Program (WEAP) and field observations to determine the termination of the pile driving process, 29.5% make use of dynamic pile driving formulas for this same purpose, and 9.1% rely on the initial results produced by static analysis methods in the project's design stages and consequently make no adjustments to the lengths of production piles. These results are presented graphically in Figure 4.22. Regardless of the pile penetration length estimated in the design stages of the project, 15.9% of respondents noted that they drive piles until refusal, where pile refusal is defined by an observed penetration of less than one inch per ten hammer blows. On the other hand, 6.8% indicated that they prefer to drive the piles to end-bear on bedrock. The remaining 4.5% of respondents stated that they use no well-defined method for determining pile-driving termination. Although not nearly as common as the methods presented in Figure 4.22, 9% of respondents did indicate using the pile SLT for pile capacities verification purposes.

Finally, Iowa County engineers were asked to report on the frequency of which quality control tests are performed on piles during driving, such as: Pile Driving Analyzer (PDA), Case Pile Wave Analysis Program (CAPWAP), pile verticality measurements, and inspections of welds used for splicing. As illustrated in Figure 4.23, about 22% of respondents indicated that such quality control tests are always performed on 5% of the installed piles, with 3% of respondents stated that these tests are performed on a more frequent basis (i.e., greater than 5% of the installed piles) and another 19% suggested that these tests are performed on a less frequent basis (i.e., less than 5% of the installed piles). The remaining 56% of respondents indicated that quality control tests foundations are never performed for driven pile.

There are various problems associated with not performing the quality control and pile inspection tests during and after driving. Over-conservatism is among these problems, as most of the county engineers keep driving until pile refusal or end-bear on bedrock, instead of

conducting pile monitoring and quality control tests such as WEAP, PDA or CAPWAP in the field. In some extreme cases, the pile capacity could be less than required in the design, which could occur for various reasons. For example, the pile can be damaged during driving, or unexpected excessive deformation could result from end bearing on shale or weak bedrock. Although quality control tests are relatively expensive and time consuming, there are great benefits associated with them. However, a better way to accurately estimate a pile resistance is to consider these tests even during the design stage. This topic was discussed with more details from the LRFD aspect in Chapter 2, and the LRFD resistance factors accounting for construction control aspects are provided in Chapter 6.

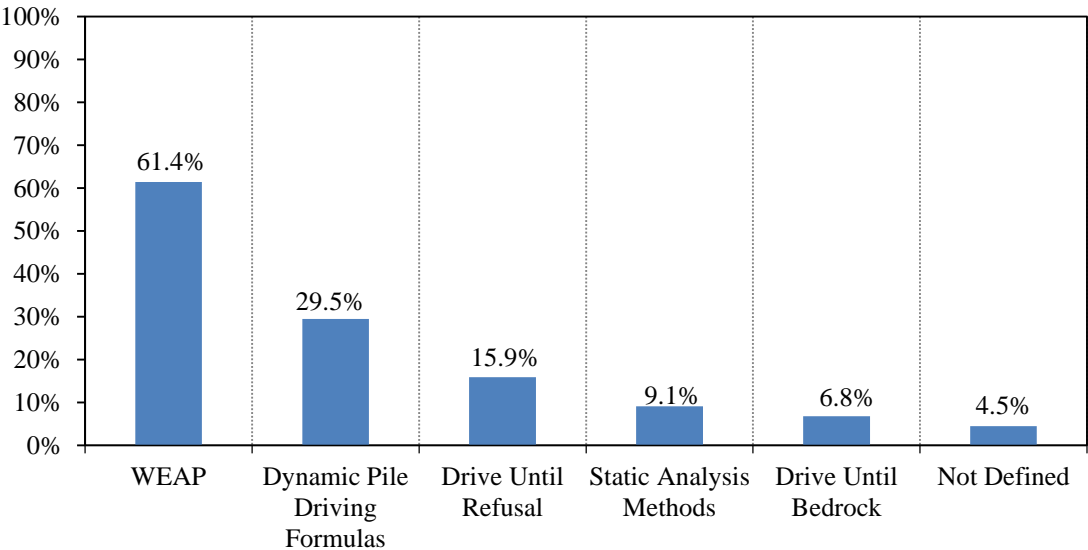


Figure 4.22: Criteria determining pile driving termination

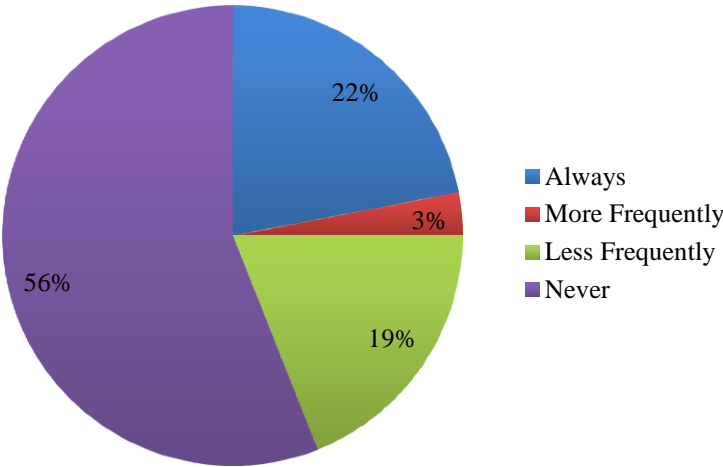


Figure 4.23: Frequency of performing quality control tests on driven piles

4.2.5. Contribution from Engineering Firms

As previously mentioned, 39%, or about 17 different Iowa County engineers, indicated the

employment of private engineering consulting companies/firms for the conducting of deep bridge foundation design procedures, especially for large-scale projects. Consequently, the survey distributed to the Iowa County engineers was modified and forwarded to the most commonly employed consulting firms reported in Figure 4.20. After sending the survey to nine different local and nationwide private engineering consulting firms, eight complete responses were received. Provided in this section of the report is a summary of the received responses concerning the four main topic areas of the survey, including a brief comparison of the main differences between the practices of local county engineers and consulting firms.

For the first section of the survey concerning foundation practice, 50% of the consulting firms indicated that they perform soil in-situ and laboratory tests to establish different soil parameters. SPT was the most commonly used in-situ soil test, with soil classification and Atterberg limits comprising the typical laboratory tests. Interestingly, only one respondent indicated the performance of the one-dimensional consolidation test, with another respondent indicating the use of the triaxial test for large-scale projects. With regards to the main criterion used for the selection of a given type of driven pile foundation, about 44% of the consulting firms indicated a reliance on previous design and construction experience, 28% cited economy as the main criteria, and the remaining 28% stated that the criterion is dictated by either available construction equipment or other alternative means. All respondents indicated that steel H-shaped piles are the most commonly used pile type within their respective regions, followed closely by closed-ended steel pipe piles and precast concrete piles, in that order. Interestingly, only one respondent denoted the use of timber piles. Finally, all respondents expressed their desire to use driven piles over drilled shafts.

In the pile analysis and design section of the survey, 50% of respondents from the consulting firms cited the Iowa LRFD Bridge Design Manual (2009) as their primary driven pile design specification, whereas 37.5% of respondents acknowledged the use of the Iowa County Bridge Standards (11), with the remaining 12.5% make use of the AASHTO-LRFD Bridge Design Specifications (4). Therefore, it is evident that design engineers still prefer local design manuals over the AASHTO specifications, seeing that the latter is characterized by unnecessary conservatism to account for soil variations across the country (6). Furthermore, several questions related to different pile analysis methods were asked to attain a more inclusive image concerning the design and construction practices enacted at the county level. Survey results showed that 60% of the consulting firms rely on dynamic analysis methods to determine design pile capacities, with WEAP analyses based on the SPT N-value soil input method (i.e., SA-method) being the most common, whereas the remaining 40% of respondents indicated the use of conventional static analysis methods based on SPT data. Finally, questions regarding the performance of serviceability limit checks during the design of deep foundations were asked. All responses received from the engineering-consulting firms indicated that the vertical settlement of a single pile or group of piles is not accounted for in design, while half of the respondents indicated that lateral displacements are accounted for in design. This is an important design consideration, which was addressed by only 22% of the county engineers, given the common use of integral abutments in practice.

The last section of the survey acquired information regarding pile drivability and quality control aspects. As expected, more than 75% of respondents indicated that pile design verification is accomplished through WEAP analyses, while the remaining respondents indicated a reliance on

the original design capacity produced by static analysis methods or offered by dynamic formulas. The responses received regarding the effect of soil setup on pile capacity were of particular interest as about 70% of the responding engineering consulting firms indicated that this effect on pile capacity is neglected in design. However, one respondent indicated that soil setup affected pile capacity in a range from 5 to 10%, with another respondent indicating that soil setup can increase pile capacities from anywhere between 11 and 20%, depending on the soil type. Finally, none of the respondents reported the use of pile capacity verification by means of the SLT, as such a test is sophisticated, expensive, and time consuming. Likewise, in regards to the use of other quality control measures, 80% of respondents reported that such tasks are never performed; thus, leading to a hidden increase in the cost of the deep foundation that could have been significantly reduced through the conduction of either simple or sophisticated quality control tests.

4.1. Historical Database Overview

4.3.1. General Description and Overview

Over a twenty-four year period starting from 1966 to 1989, the Iowa DOT collected information concerning 264 pile static load tests conducted in the State of Iowa on steel H-shaped, timber, pipe, monotube, and concrete piles. During this period, all of information collected included details concerning the site location, subsurface conditions, pile type, hammer characteristics, end-of-driving (EOD) blow count, and static load test results. The Iowa DOT stored all of this information in hardcopy format, thus making its usage cumbersome and impractical for the LRFD calibration process. As part of an ongoing research project directed at the development of LRFD procedures for bridge piles in the State of Iowa, the electronic database for Pile Load Tests (PILOT) was developed using Microsoft Office Access™ to allow efficient performance of reference and/or analysis procedures on the amassed dataset.

In addition to the 264 driven piles upon which PILOT was originally formed, data from additional steel H-piles tests conducted as part of this research project has been added to the database. In these tests, piles were instrumented with strain gauges and were dynamically monitored during driving and restrikes, in addition to being statically load-tested to failure. With this additional information, PILOT contained adequate data for the development of regionally calibrated LRFD resistance factors for the following three different sources of pile capacity estimates: static analysis methods (e.g., α -Tomlinson, Nordlund and Thurman, Meyerhof SPT, Schmertmann CPT, etc.), dynamic analysis methods (e.g., WEAP, PDA, CAPWAP), and dynamic pile driving formulas (e.g., Engineering News Record (ENR), Gates, FHWA Modified Gates, Janbu, etc.).

4.3.2. Usable Load Tests in PILOT

A summary of the data currently available in PILOT is presented in Table 4.5. In this table, the total number of pile load tests existing for various pile types is detailed according to the predominant soil type encountered along the embedded pile shaft and the three pile load test dependability classifications (i.e., reliable, usable-static, and usable-dynamic). This classification was explained in the Volume I report of this project by Roling et al. (2010). In Volume I, the importance of PILOT is detailed with a brief description of the structure and key parameters used in the development of the database. A sample application is provided for

confirmation of the economy associated with a regional pile load test database such as PILOT.

Table 4.5: PILOT database summary

Pile Type	Soil Type				Total	Reliable	Usable-Static	Usable-Dynamic
	Sand	Clay	Mixed	Unavailable				
Steel H-Shaped	50	50	60	10	170	147	88	40
Timber	7	43	12	13	75	47	24	9
Pipe	6	3	6	1	16	15	14	2
Monotube	3	0	2	2	7	5	3	3
Concrete	0	0	1	1	2	1	0	0

4.2. An Overview of Field Tests

As part of the project, ten (10) full-scale instrumented piles (HP 42x10) were driven, retapped, and load tested at different locations in the State of Iowa to cover all possible soil regions and geological formations. Five tests were conducted in clayey soil profiles, two in sandy profiles, and three in mixed soil profiles. All the tested piles were monitored during driving using PDA. The instrumented piles were then load tested to failure, and the Davisson capacity was determined for all. The tested piles were loaded using a 400 kips hydraulic jack and the applied load was measured using a 300 kips load cell. In addition to using four 10-in displacement transducers to measure the vertical displacement at the top of the test piles, the piles were instrumented with strain gauges along the shaft and at the pile tip. All the piles were load tested following the Quick Test (QT) procedure of the ASTM D 1143 standards (ASTM, 2007). In all cases, the test pile was loaded in increments of 5% beyond the estimated maximum capacity. The load was kept relatively constant at the end of each load increment for a duration ranging from 5 to 15 minutes, until deflection readings stabilized as required by the standards. After the pile experienced excessive vertical displacement without being able to pick up more load (i.e., pile plunging), the pile was unloaded in five equal load decrements. The soil profiles at the test sites were characterized using in-situ tests such as the CPT, SPT, and Borehole Shear Test (BST), as well as several laboratory tests including basic soil classification, Direct Shear Test (DST) for cohesionless soils, and the 1-D consolidation test for cohesive soils. All the field and laboratory soil and pile testing results were provided in the Volume II report of this project (see Ng et al., 2010). The results from these field tests are used later in this report to verify the values of the developed LRFD resistance factors as presented in Chapters 6 and 7.

CHAPTER 5: SELECTED CALIBRATION FRAMEWORK

This chapter provides a summary on the framework that was selected to develop the LRFD geotechnical resistance factors using the PILOT database as well as a brief discussion of the selecting and sorting criterion adopted for the database. The selected criterion for determining the pile nominal capacity from the static load tests is presented and compared to other methods. The statistical approach used for calibration is clearly specified, in addition to the associated target reliability indices. The dead load to live load ratio (DL/LL) corresponding to the local practice is also determined. At the end of the chapter, the static and dynamic analyses, as well as dynamic formulas that were selected for the LRFD calibration are listed and the reasoning behind selecting these specific static and dynamic methods is clearly indicated.

5.1. Summary

Figure 5.1 presents a flowchart describing the framework of developing the LRFD resistance factors for Iowa soils. In summary, the FOSM reliability theory was selected for the LRFD resistance factors calibration. The PILOT database was grouped according to different pile and soil types. The distribution of different Probability Density Functions (PDFs) for all groups (datasets) was statistically checked to make sure that the PDFs were following the lognormal distribution. The measured pile capacity was determined using Davisson's criterion, while the predicted pile capacity was determined based on different static and dynamic analysis methods. The bias (λ) or the mean ratio of the measured pile capacities was calculated for the FOSM analyses. After the statistical analysis, the regionally developed LRFD resistance factors were compared to different design codes and specifications, as well as to the ASD factor of safety. The developed resistance factors were verified by means of the new pile load tests that were conducted as a part of this study. The developed resistance factors for different static methods were adjusted for consideration of construction control aspects and soil setup. Finally, recommendations for geotechnical LRFD resistance factors were provided for the design and construction of bridge pile foundations in the State of Iowa.

5.2. Soil Profile Categorization

In the 2008 AASHTO-LRFD Specifications, the soil profile was categorized into three main soil types: sand, clay, and mixed soils, which were initially based on Paikowsky et al. (2004) and Allen (2005). The difficulty of determining the average soil profile as sand or clay is the main concern associated with soil categorization, as soil is non-homogenous with large variations along different layers and neither Paikowsky et al. (2004) nor Allen (2005) provide a clear approach for such a determination. In this study, the same soil profile categorization was followed in order to be consistent with the AASHTO and other specifications. In addition, the criterion for categorizing the average soil type was exclusively determined as follows:

- 1) Using laboratory testing to identify the soil type in each layer and classify them according to the Unified Soil Classification System (USCS) following the ASTM D-2487.
- 2) Double-check the soil classification with SPT soil classification correlations.
- 3) Determine the most predominant soil type listed at the end of the USCS classification for all soil layers.
- 4) Categorize the predominant soil types as sand or clay.
- 5) Calculate the percentages of the predominant soil types along the profile.

- 6) Determine the soil category for each site (i.e., sand or clay) based on the predominant soil type that exists along more than 70% of the profile, and consider any site with less than 70% as a mixed site.

5.3. Criterion of Sorting the Database

The Pile LOad Test database (PILOT), produced by Roling et al. (2010), has been used in this study for developing the preliminary LRFD resistance factors. A manual that fully presents and describes the PILOT database is provided in the Volume I report of this project. According to Roling et al. (2010), the Iowa DOT conducted around 264 pile SLTs between the years 1966 and 1989. Among the 264 pile SLTs, only 170 were performed on steel H-piles. In the PILOT database, a total of 147 steel H-pile static load tests were classified as reliable, and 82 of them were classified as usable. The 82 data points representing the driven steel H-piles were sorted and divided into subsets according to different soil types. The main soil types considered in this study were sand, clay and mixed soils. There were 35 available SLTs for the subset in sand, with 15 for the subset in clay, and 32 for mixed soils. Figure 5.2 summarizes the number of usable load tests available from PILOT in different soil types.

5.4. Determination of Soil Parameters

Besides laboratory soil tests, there are many empirical and semi-empirical correlations to estimate the soil shear strength parameters from the SPT in-situ test, most of which were discussed in Chapter 3. There are many other empirical correlations to calculate further soil parameters, which are summarized in Kulhawy and Mayne (1990).

In order to develop the LRFD resistance factors for Iowa, the design capacities of all the piles in the PILOT database were back-calculated using different static and dynamic methods. To back-calculate the pile capacity, different soil shear strength parameters should be determined. Because soil samples are not available for test sites from the database, laboratory tests cannot be conducted. Since the only available information from the database is the SPT blow counts for different soil layers, semi-empirical correlations to the SPT are the only means of determining the soil parameters. Only some of the correlations have been chosen for this project according to the recommendations given by 2008 AASHTO-LRFD specifications, the FHWA LRFD-highway bridge substructures reference manual (2007), as well as the NCHRP 507 LRFD report by Paikowsky et al., 2004. Table 5.1 summarizes the correlations used to determine the soil unit weight (γ), the angle of internal soil friction (ϕ), and the soil undrained shear strength (S_u) based on SPT N-values.

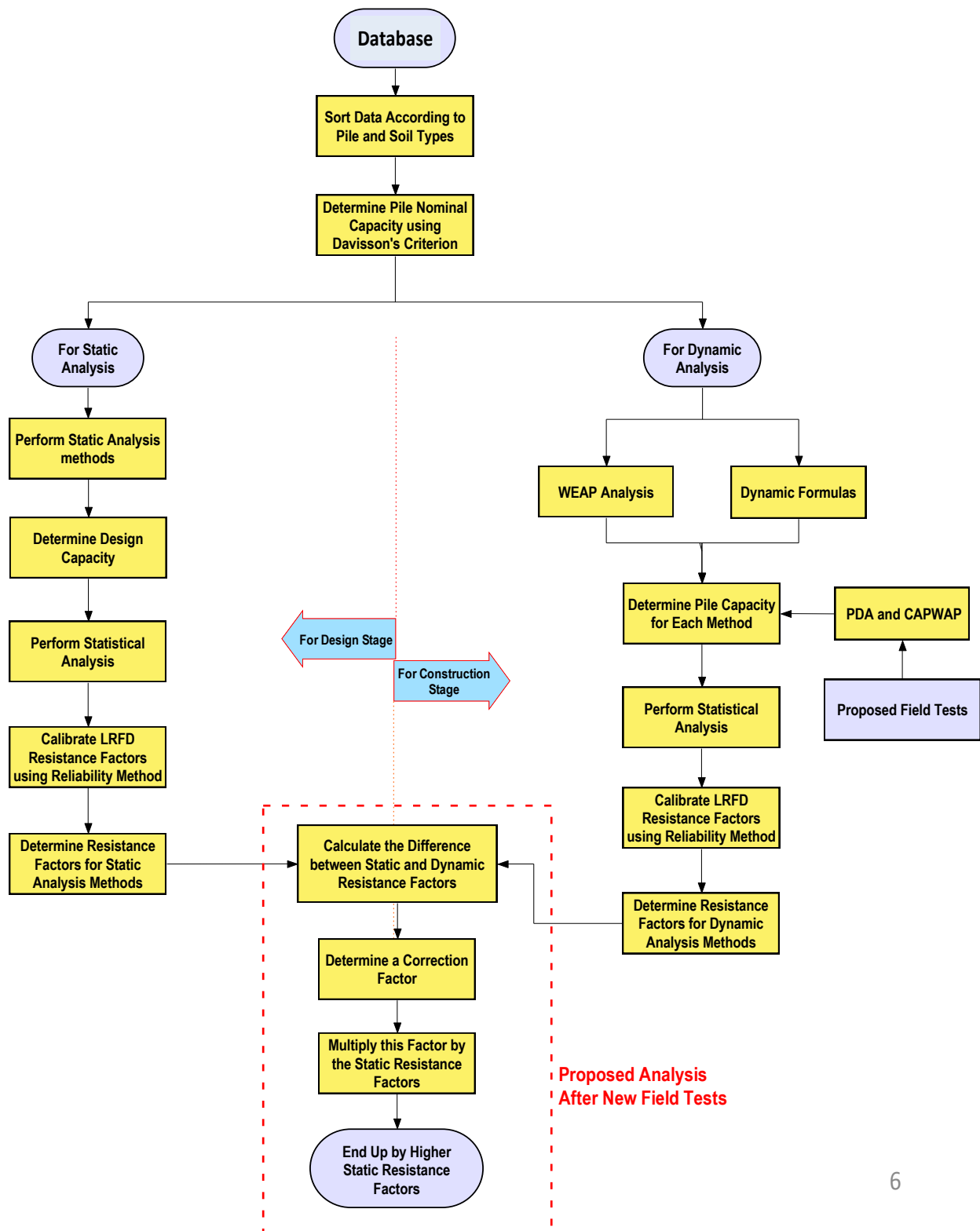


Figure 5.1: A flowchart describing the framework of developing the LRFD resistance factors for Iowa soils

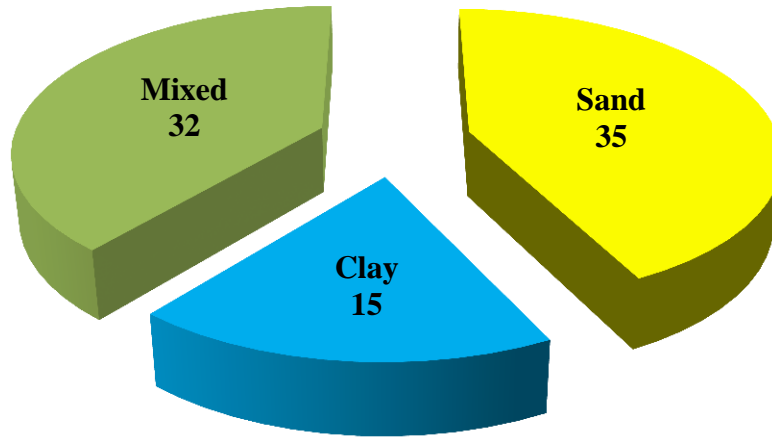


Figure 5.2: Summary of the usable data available from PILOT in different soil types

Table 5.1: Selected correlations used to determine soil parameters based on SPT N-values

Soil Properties	SPT Correlation	Reference
ϕ (deg.)	$54 - 27.6 \exp(-0.014N_{60})$	Peck, Hanson and Thornburn (1974)
S_u (bar) (1 bar = 14.5 psi)	0.06 N	Terzaghi and Peck (1967)
γ (kN/m ³) (1 kN/m ³ = 6.24 pcf)	Based on un-corrected SPT N-values	Bowles (1977)

5.5. Selected Pile Analysis Procedures

The Iowa DOT required the development and calibration of the LRFD resistance factors for static and dynamic methods. Static calibration is represented by static analysis methods, which are mainly used during the design phase, while the dynamic calibration is divided into two parts: dynamic analysis methods, and dynamic formulas, mainly used during construction. There are several static and dynamic methods that can be selected in this study, depending on the most accurate and reliable methods in different soil types, the current local practice and experience in the State of Iowa, and the information available from the PILOT database.

5.5.1. Static Methods

In Chapter 4 of this report, the outcomes of a nationwide survey, as well as a local survey made up of engineers in Iowa counties were presented. As previously mentioned, the two survey outcomes covered specific topics about current foundation practice, pile analysis and design, pile drivability, pile design verification, and quality control. From the national survey, it was found that the α -method and β -method were the most commonly used static analysis methods for piles in cohesive soils. But for static analysis methods in cohesionless soils, Nordlund's method, followed by the SPT-Meyerhof method were most commonly used. Overall, the nationwide survey reflected the reliability of Nordlund's method for sandy soils, and the α -method for clayey soils. All of the above-mentioned static methods have been discussed in Chapter 3, including the advantages and limitations of each method. On the other hand, the local survey of

Iowa counties reflected the dependency that the Iowa DOT and county engineers had on the α -method as the main static analysis method. However, geotechnical engineers in Iowa have been using the Iowa DOT design charts presented in the “Blue Book” (Dirks and Kam, 1989). As discussed in Chapter 3, the Blue Book is an in-house static analysis approach that was especially developed for Iowa soils, and combines some static analysis methods together in order to enhance the pile capacity prediction, as well as to separate the pile skin friction and the end bearing components.

According to literature, national and local practices, as well as availability of data from the PILOT database, five static analysis methods were carefully selected for the LRFD resistance factors calibration in Iowa. In cohesive soils, the α -API method (API-1974), the β -method (Burland, 1973), and the Blue Book method (Dirks and Kam, 1989) were selected for the calibration. In cohesionless soils, the Nordlund (Nordlund and Thurman, 1963), the SPT-Meyerhof (Meyerhof, 1976/1981), as well as the Blue Book method were selected for LRFD resistance factors calibration.

5.5.2. Dynamic Methods

As mentioned earlier in Chapter 3, the WEAP analyses were performed at EOD and at several restrikes based on five options of inputting the soil information and properties. The five options were (1) GRLWEAP Soil Type based method (ST); (2) GRLWEAP SPT N-value based method (SA); (3) the Federal Highway Administration (FHWA) DRIVEN program; (4) the Iowa Blue Book (Iowa DOT pile design chart); and (5) the Iowa DOT approach in practice. The GRLWEAP ST method provided the easiest procedure for inputting the soil information, which only required the identification of soil types. The GRLWEAP SA method required the input of uncorrected SPT N-values, soil types, and soil unit weights, which were obtained from the in-situ SPT tests and laboratory soil tests. The DRIVEN program provided a more detailed method of describing the soil profile and created an input file for WEAP analysis. It used the SPT N-value and undrained shear strength (S_u) to characterize the granular soil strength and cohesive soil strength, respectively. The Iowa Blue Book method directly used and input the unit shaft and unit toe (tip) resistances, given in the Iowa DOT pile design charts, into the WEAP’s variable resistance distribution table for analysis. However, the Iowa DOT method uses the SPT N-value as the only soil parameter, which is input into the WEAP’s variable resistance distribution table with respect to the depth where the SPT N-values were measured. In this project, all of the five above-mentioned soil data input methods were used in the calibration of the LRFD resistance factors for WEAP.

5.5.3. Dynamic Formulas

Many dynamic formulas were developed to predict the static bearing capacity of deep foundations, and the nationwide and local survey results indicated several dynamic formulas were preferred for driven steel H-piles. These dynamic formulas included: the Engineering News Record (ENR) formula, first published in 1888 by A. M. Wellington; the Pacific Coast Uniform Building Code (PCUBC) formula, which began with J. F. Redtenbacher in the year 1859; the Janbu formula, proposed by N. Janbu in 1953; the Iowa DOT Modified ENR “in-house” formula (Iowa DOT 2008); the Gates formula, proposed by Marvin Gates in 1957; FHWA Modified Gates formula, developed by Richard Cheney of the FHWA; and the Washington State

Department of Transportation (WSDOT) formula, after Paikowsky et al. (2004). As described in Chapter 3, the various comparative studies presented in the preceding subsections clearly indicate that there is no specific dynamic pile driving formula that is consistently better than the others. Therefore, in this project, all the above-mentioned (seven) formulas were used for the LRFD calibration in order to accurately determine which formula provided the highest efficiency and economy for Iowa soils.

5.6. Determination of Pile Nominal Capacity

There are several methods for determining the pile nominal capacity (maximum un-factored) from the load-displacement curves, measured at the pile head that were obtained from the SLTs. These methods have several advantages and limitations, which have been already discussed in Chapter 3. In this study, a preliminary analysis was conducted using the Davisson method (Davisson, 1972), Shape of Curvature method (Butler and Hoy's Method, 1977), and the Limited Total Settlement method (after the FHWA design and construction manual, 1997). After analyzing the results of the three methods, Davisson's method was found to be the least conservative method. Figure 5.3 represents a cumulative capacity for 82 different piles from the PILOT database using different approaches for determining the nominal capacity from the SLT results. The figure verifies that Davisson's method is providing a slightly higher pile nominal capacity than the other methods, indicating that Davisson tends to be less conservative for driven steel H-piles. On the other hand, most of the previous LRFD calibrations found in literature were based on the Davisson's method. Paikowsky et al. (2004) found Davisson's method to be the best performing method overall and therefore chose this method as the only method to be used for analyzing load-displacement curves. Moreover, the 2007 AASHTO-LRFD specification was based on Davisson when determining the pile capacity from SLT results. Accordingly, the Davisson's criterion was chosen to represent the pile capacity from the load-displacement curve in PILOT.

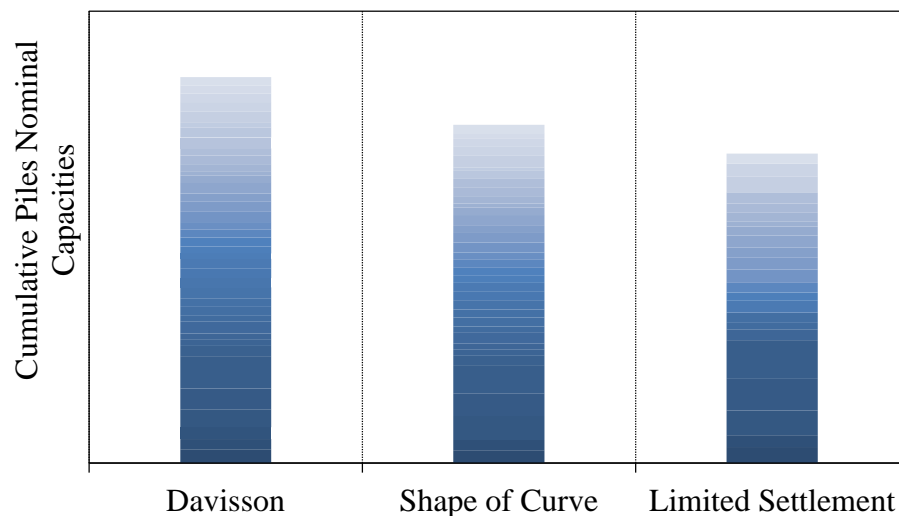


Figure 5.3: Cumulative capacity for different piles from PILOT using different approaches of determining pile nominal capacity from SLT

5.7. Selected Reliability Approach and Parameters

5.7.1. First Order Second Moment

As discussed in Chapter 2, there are several statistical methods with different degrees of sophistication used for the LRFD resistance factor calibration. According to Kyung, (2002), the most commonly used methods are the First Order Second Moment (FOSM) and First Order Reliability Methods (FORM). According to Allen et al. (2005), the FOSM is a straightforward technique. Paikowsky et al., (2004) conducted the analysis using both the FOSM and the FORM methods, and concluded that the difference between the two is relatively small (did not exceed 10% on average) as the FOSM provides slightly conservative resistance factors. Moreover, the existing 2008 AASHTO-LRFD specifications are based on the FOSM, assuming a lognormal distribution of the load and resistance Probability Density Functions (PDFs). According to Allen (2005), other advanced methods, such as the Monte Carlo simulation, have been used for performing the reliability analyses. Nowak and Collins (2000), as well as Allen (2005) have shown that all of these advanced methods should produce similar results to each other, which indicates that using a less sophisticated approach such as the FOSM should still provide satisfactory results when compared to other more sophisticated approaches.

In order to be consistent with the AASHTO specifications, to avoid complexity, and make for easier updates and modifications to the LRFD resistance factors in the future, the FOSM approach was selected for developing the LRFD resistance factors based on PILOT. In Chapter 2, a full derivation for the FOSM basic equation was provided. Given that the PDFs should be following a lognormal distribution, the basic equation of the FOSM is as follows:

$$\varphi_R = \frac{\lambda_R \left(\frac{\gamma_{DL} Q_{DL}}{Q_{LL}} + \gamma_{LL} \right) \sqrt{\frac{(1 + COV_{Q_{DL}}^2 + COV_{Q_{LL}}^2)}{(1 + COV_R^2)}}}{\left(\frac{\lambda_{Q_{DL}} Q_{DL}}{Q_{LL}} + \lambda_{Q_{LL}} \right) \exp \left\{ \beta_T \sqrt{\ln[(1 + COV_R^2)(1 + COV_{Q_{DL}}^2 + COV_{Q_{LL}}^2)]} \right\}}$$

where

- φ_R = Resistance Factor
- γ_{DL} = Load factor for dead loads (equal to 1.25 from AASHTO)
- γ_{LL} = Load factor for live loads (equal to 1.75 from AASHTO)
- $\lambda_{Q_{DL}}$ = Bias for dead loads (equal to 1.05 from AASHTO)
- $\lambda_{Q_{LL}}$ = Bias for live loads (equal to 1.15 from AASHTO)
- $COV_{Q_{DL}}$ = Coefficient of Variation for dead loads (given in AASHTO)
- $COV_{Q_{LL}}$ = Coefficient of Variation for live loads (given in AASHTO)
- λ_R = Bias for resistances (from PDFs)
- COV_R = Coefficient of Variation for resistances (from PDFs)
- β_T = Target Reliability Index (discussed later in this chapter)
- $\frac{Q_{DL}}{Q_{LL}}$ = Dead load to live load ratio (discussed later in this chapter)

5.7.2. Distribution Quality Tests

As indicated in Chapter 2, the lognormal distribution better represents and models the transient load, which is fully characterized by its first two moments. Scott and Salgado (2003) specified that the magnitude of the transient loads and resistances found in geotechnical problems cannot take negative values, and the lognormal distribution can better represent their product even if the variables themselves are not lognormally distributed. According to the 2008 AASHTO-LRFD specifications, the load and resistance PDFs should follow lognormal distribution. On the other hand, the equation used in accordance to the FOSM approach is based on lognormally distributed PDFs.

Many statistical tests can be conducted on the PDFs in order to ensure that they are following a lognormal distribution. Among these tests are: the Anderson Darling test and the Confidence Interval test. In this study, both the Anderson Darling and the Confidence Interval tests were used to check the normality of the random variables. In addition, the best-fit distribution is identified for every PDF. The best-fit determines whether the best distribution for a specific PDF is following either the normal or the lognormal distribution. This normality test can determine whether or not the PDF can be accepted as a lognormally distributed PDF, in order to be eligible for use in the FOSM equation.

5.7.3. Target Reliability Index

The main principle of the LRFD depends on the reliability based statistical approaches in order to determine the probability of failure (P_f) associated with a certain load and resistance. These LRFD principles were extensively discussed in Chapter 2. The FOSM and the FORM are from the reliability-based approaches that have been commonly used for the LRFD calibration. In order to use any of these approaches, a target probability of failure should be selected, which could be represented in the LRFD by means of reliability index (β). According to Barker et al. (1991), different values of the reliability indices ranging from 2.0 to 3.5 (i.e., P_f ranging approximately from 1/100 to 1/1000) can be used in the LRFD calibration for redundant pile groups.

When selecting the appropriate β values in this study, it was understood that the values should be consistent with that which is presented in literature, design codes, and AASHTO-LRFD specifications. As stated in Chapter 2, Paikowsky et al. (2004) used the β values of 2.33 and 3.00 in their calibration for redundant and non-redundant piles, respectively. The current 2008 AASHTO-LRFD specifications were mainly developed based on the recommendations of Paikowsky et al. (2004) and Allen et al. (2005). Consequently, the targeted β values in this study were chosen to be similar to those used in the 2008 AASHTO-LRFD specifications and the NCHRP report 507, i.e., $\beta = 2.33$ ($P_f = 1\%$) for redundant pile groups (consisting of five or more piles/cap), and $\beta = 3.0$ ($P_f = 0.1\%$) for non-redundant pile groups (less than five piles/cap). However, the LRFD resistance factors will be calculated herein for a wider range of β , providing the freedom of selecting any other target reliability and corresponding resistance factors for pile design. A sample analysis was conducted for resistance factors of three different static methods by using a wide range of β starting from 1.5 to 4.0 for steel piles driven in clay soils as shown in Figure 5.4.

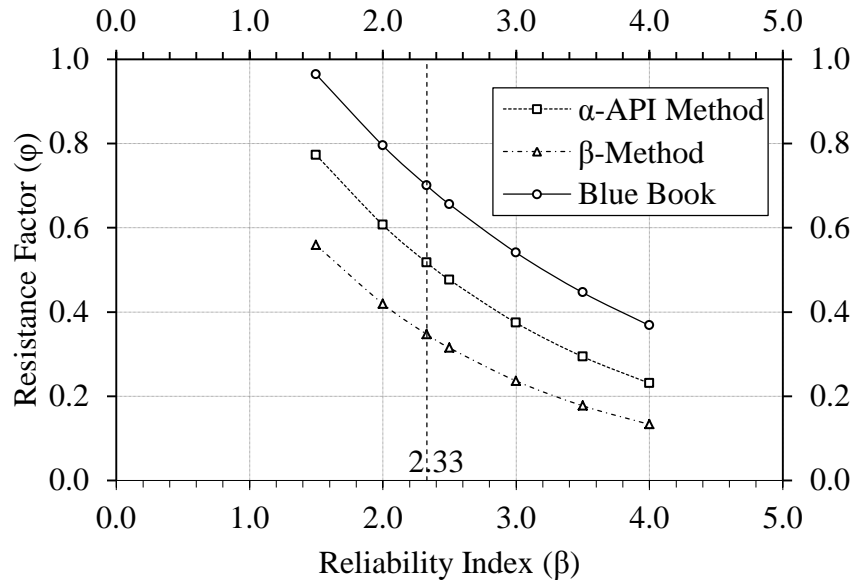


Figure 5.4: A sample analysis of resistance factors for static methods was conducted using a wide range of β starting from 1.5 to 4.0 for steel driven piles in clay

5.7.4. Dead Load to Live Load Ratio

Several load and resistance parameters were used in the FOSM equation required for LRFD calibration. Some of the parameters, such as the load factors, are provided in the AASHTO-LRFD specifications as described in Chapter 2. On the other hand, some other parameters were not defined specifically by the design codes such as the DL/LL ratio used for design of bridges.

As mentioned in Chapter 2, the DL/LL ratios for bridges are defined according to the bridge span, traffic volume, importance of the structure, as well as the conditions associated with the bridge design and construction. Paikowsky et al. (2004) used a DL/LL ratio ranging from 2.0 to 2.5 in the NCHRP 507 report, while Allen (2005) used a relatively conservative DL/LL ratio of 3.0. Iowa DOT uses a DL/LL ratio of 1.5, due to the nature of short span bridges in the state. However, both Nowak (1999) and Paikowsky (2004) indicated that the effect of the DL/LL ratio should have an insignificant influence on the LRFD resistance factors after calibration. This point was clearly discussed and an example was presented in Chapter 2. Consequently, in order to select an appropriate DL/LL ratio to be used without adding excessive conservatism to the design in this study, a DL to LL ratio of 2.0 was decided.

CHAPTER 6: PRELIMINARY RESISTANCE FACTORS

In this chapter, preliminary LRFD geotechnical resistance factors are developed for static and dynamic analysis methods, as well as for dynamic formulas. Calibration of the resistance factors for each analysis method is presented separately and discussed in detail, including histograms and frequency distribution for each subset (group) attained using the PILOT database. The methodology used to determine the best-fit for each Probability Density Function (PDF) of each group is also provided. For the resistance factors corresponding to a wide range of target reliability indices, a sensitivity analysis is considered in order to provide the designer the freedom to select and determine the degree of conservatism in the design. Efficiency factors are also provided to appropriately compare the economy of different methods. Equivalent factors of safety were back calculated from the developed LRFD resistance factors to compare the ASD approach and determine the percentage of gain in the pile capacity when using the LRFD approach. All the regionally developed resistance factors are thus compared with the current design specifications. For verification purposes, the preliminary resistance factors were used to design 10 steel H-piles that were driven and load-tested in different soil regions all over the State of Iowa as part of this study (for more information about field testing, see Vol. II report by Ng et al., 2010). In the next sections, the preliminary LRFD resistance factors are calculated for different static analysis methods, followed by the same for dynamic analysis methods and dynamic formulas. Construction control aspects and soil setup effects are also taken into consideration.

6.1. Static Analysis Methods

As mentioned in Chapter 5, five different pile static analysis methods were used for predicting the design nominal capacity of steel H-piles in this study. These methods included: the Nordlund method, α -API method, β -method, SPT-Meyerhof method, and the Iowa DOT design charts (i.e., the Blue Book or BB method). Spreadsheets were created for each method in order to predict the capacity of the 80 usable piles from PILOT database. In Appendix-B, a sample of the spreadsheets is presented, showing the procedures of calculation and the soil parameters used with each method. The soil parameters were mainly calculated based on the corrected SPT N-values and using the soil correlations previously mentioned in Chapter 5. The Davisson's criterion was the method used for determining the actual pile nominal capacity from static load test results (load-displacement curves).

6.1.1. Pile Capacity

As mentioned in Chapter 5, the average soil profile for each site in the database was classified as sand, clay, or mixed soil. Tables 6.1, 6.2, and 6.3 summarize the nominal capacity of the piles calculated via Davisson's criterion, as well as the predicted capacities using different static analysis methods in clay, sand, and mixed soils, respectively. The identification number and the representative Iowa County for each site are presented in Tables 6.1 to 6.3 and sorted according to different soil types. The tables also show the different sizes of steel H-piles, as well as the time between End of Driving (EOD) and conducting the SLT. As observed in the tables, the number of tests available in clay, sand, and mixed soils are 20, 34, and 26, respectively. It can also be noted that the average time for performing the SLT after EOD is about five (5) days. To roughly compare the actual and predicted capacities, Figure 6.1 presents an accumulative summation for

all predicted capacities using different static analysis methods to the accumulative actual pile capacities that were measured from SLT results using Davisson's criterion. From Figure 6.1, it is clear that some of the static analysis methods overpredict the pile capacity at the EOD such as β and Nordlund methods when compared to Davisson's capacity. This may explain the customary need for relatively high factors of safety for some of the static design methods using the ASD approach, which was taken into consideration during the LRFD resistance factor calibration.

Table 6.1: Nominal Davisson's capacity of the piles from PILOT, as well as those obtained for static analysis methods in clay

ID #	County	L ¹ (ft)	Pile Size (HP)	D ² (kips)	Capacity from Static Methods (kips)					Days SLT ⁸
					BB ³	SPT ⁴	α - ⁵	β - ⁶	Nord ⁷	
6	Decatur	53	10x42	133	125	68	124	222	156	3
11	Hamilton	58	10x42	103	187	114	129	280	229	5
12	Linn	24	10x42	229	170	153	189	111	121	5
15	Cherokee	43	10x42	306	173	115	155	206	135	9
32	Audubon	40	10x42	193	133	106	150	169	131	4
33	Benton	37	10x42	238	176	107	144	160	126	2
42	Linn	24	10x42	92	88	213	320	418	342	5
44	Linn	37	10x42	153	151	98	140	132	123	5
49	Black Hawk	36	10x42	306	182	122	165	141	137	6
51	Johnson	30	10x42	214	191	190	245	146	86	3
57	Hamilton	57	10x42	189	153	72	143	276	185	4
62	Kossuth	45	10x42	112	147	150	204	219	215	5
63	Jasper	63	10x42	74	95	76	154	260	217	2
64	Jasper	71	10x42	137	120	82	172	330	274	1
67	Audubon	32	10x42	157	141	101	132	125	84	4
102	Poweshiek	43	10x42	146	128	115	165	191	148	3
109	Poweshiek	51	12x53	198	192	163	225	314	260	4
130	Pottawattamie	19	12x53	34	26	8	78	21	23	5
145	Pottawattamie	19	10x42	43	19	8	16	21	23	4
147	Woodbury	71	10x42	236	115	68	150	404	373	8

¹ Pile embedded length in soil

² Pile nominal capacity from SLT using Davisson's criterion

³ Pile design capacity using Iowa Blue Book

⁴ Pile design capacity using SPT-Meyerhof method

⁵ Pile design capacity using α -API method

⁶ Pile design capacity using β -method

⁷ Pile design capacity using Nordlund method

⁸ Time between EOD and SLT in days

Table 6.2: Nominal Davisson's capacity of the piles from PILOT, as well as those obtained for static analysis methods in sand

ID #	County	L (ft)	Pile Size (HP)	D (kips)	Capacity from Static Methods (kips)					Days SLT
					BB	SPT-	α -	β -	Nord	
10	Ida	52	10x42	130	133	107	159	194	191	2
13	Delaware	57	10x42	310	232	165	231	285	248	5
17	Fremont	58	10x42	148	142	130	192	257	248	5
19	Marion	22	10x42	110	137	112	127	98	95	5
20	Muscatine	59	10x42	135	162	156	224	289	280	5
24	Harrison	78	10x42	207	173	142	230	384	360	9
34	Dubuque	57	10x42	252	202	113	162	230	222	7
36	Dubuque	59	10x42	247	178	120	176	258	288	8
37	Dubuque	75	10x42	416	257	167	253	406	355	6
40	Linn	72	10x42	281	264	185	283	406	496	7
45	Buchanan	42	10x42	139	167	189	265	244	205	3
48	Black Hawk	42	10x42	162	165	135	183	166	171	5
52	Franklin	32	10x42	70	199	211	231	168	132	8
56	Linn	34	10x42	256	124	123	169	128	89	1
70	Mills	78	10x42	144	191	212	290	337	292	5
74	Benton	55	10x42	169	225	248	228	379	256	33
80	Dubuque	72	12x74	569	414	266	341	635	510	7
81	Black Hawk	40	12x53	101	143	148	165	167	176	3
85	Black Hawk	43	12x53	144	150	102	147	148	177	2
99	Wright	31	10x42	117	147	158	188	106	105	7
133	Pottawattamie	66	10x42	214	134	132	219	272	239	5
138	Pottawattamie	46	10x42	52	97	94	142	157	170	5
139	Pottawattamie	68	12x53	232	168	118	158	387	307	4
140	Pottawattamie	67	10x42	178	140	98	158	265	271	0
141	Pottawattamie	67	10x42	166	214	135	211	315	303	8
143	Pottawattamie	47	10x42	137	93	79	140	151	143	4
148	Linn	65	14x73	301	294	181	255	346	362	3
151	Pottawattamie	78	10x42	225	153	89	184	430	386	4
156	Dubuque	59	14x89	321	327	230	316	393	448	9
157	Dubuque	59	14x89	405	327	230	316	393	448	10
158	Dubuque	74	14x89	654	451	279	401	629	721	4
159	Dubuque	67	14x89	596	404	174	239	329	317	5
160	Dubuque	93	14x89	1000	451	168	263	593	595	4
161	Dubuque	86	14x89	949	465	198	279	531	695	7

Table 6.3: Nominal Davisson's capacity of the piles from PILOT, as well as those obtained for static analysis methods in mixed soil

ID #	County	L (ft)	Pile Size (HP)	D (kips)	Capacity from Static Analysis (kips)					Days SLT
					BB	SPT-	α -	β -	Nord	
3	Fremont	47	10x42	106	138	82	142	189	191	2
4	Jones	51	10x42	88	120	104	164	177	146	2
7	Cherokee	39	10x42	198	156	118	171	195	149	6
8	Linn	54	10x42	191	147	109	186	274	266	8
14	Audubon	30	10x42	126	119	112	148	91	69	6
25	Harrison	58	10x42	252	113	178	268	310	337	4
38	Iowa	43	10x42	110	137	90	150	136	122	2
39	Iowa	55	10x42	182	191	127	218	240	176	4
43	Linn	36	10x42	160	196	193	261	332	273	5
46	Iowa	48	10x42	184	179	116	175	206	187	4
58	Dallas	35	10x42	126	100	89	103	90	61	7
59	Monona	38	10x42	76	89	130	171	158	147	6
66	Black Hawk	43	10x42	202	139	104	152	186	140	5
73	Johnson	47	10x42	261	178	88	104	169	116	6
90	Black Hawk	65	12x53	214	213	194	235	414	381	4
91	Black Hawk	68	12x53	164	218	127	210	393	387	2
96	Story	48	10x42	193	159	111	159	207	158	7
103	Page	34	10x42	205	146	136	185	137	125	7
106	Pottawattamie	36	10x42	166	112	81	118	110	92	6
128	Ringgold	52	10x42	292	159	119	182	224	174	2
134	Pottawattamie	16	10x42	20	20	19	30	18	16	4
135	Pottawattamie	53	12x53	184	115	101	128	199	197	4
136	Pottawattamie	49	10x42	128	84	56	88	148	172	5
137	Pottawattamie	25	10x42	76	84	49	61	70	67	6
146	Shelby	48	10x42	151	147	111	156	217	168	2
155	Boone	46	12x53	70	182	122	155	238	189	9

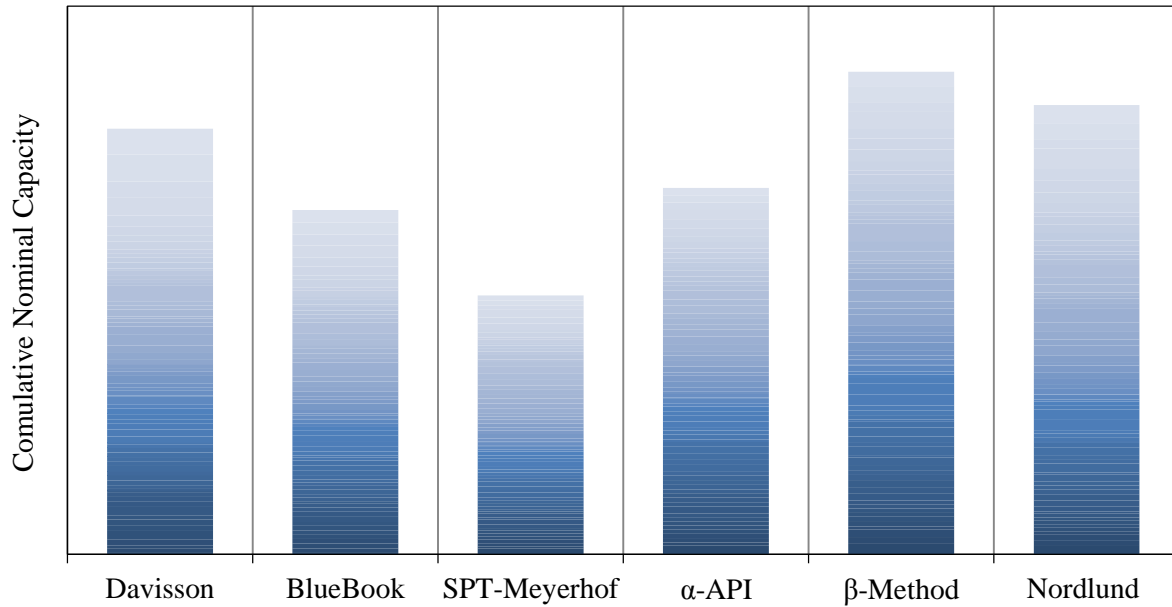


Figure 6.1: Comparison between the accumulative actual PILOT pile capacities using Davisson and the predicted pile capacities using different static analysis methods

6.1.2. Goodness of Fit Test

The first step involved in calculating the LRFD resistance factors using the FOSM approach is to check the normality of all datasets or groups (where each group represents a specific soil type and a certain static analysis method). As discussed in Chapters 2 and 5, the FOSM equation is based on the assumption of lognormally distributed PDFs for all groups. The mean bias (K_{sx}) of each group is the ratio of the nominal measured pile capacity to the predicted pile capacity. For all groups, the K_{sx} was calculated by dividing the Davisson's capacity by the predicted pile capacity using different static analysis methods.

The Anderson Darling (AD) normality test and the 95% Confidence Intervals (95% CI) test were utilized in order to check the normality of each group. According to Chapter 2, these normality tests determine whether the best-fit distribution for a specific PDF follows either a normal or lognormal distribution. For five static analysis methods and three soil types, there were 15 total groups. The PDFs of the 15 groups were tested for normality using AD normality test along with the 95% CI probability test (see Table 6.4). Figures 6.2 to 6.4 provide a plot of the 95% CI for the PDFs representing the K_{sx} between Davisson and the Blue Book method for normal and lognormal distributions in sand, clay, and mixed soils, respectively. The figures also present the AD value (or the Anderson Darling coefficient value). In order to determine which distribution is best fitting the PDFs, the probability of the 95% CI of the best-fit should be greater than 0.05, and the AD value should be less than that of the least-fit distribution. As represented in the figures, the AD value for all subsets is lower and the probability of 95% CI is greater than 0.05 in the case of lognormal. Therefore, all the PDFs are following the lognormal distribution, and the FOSM equation can be used to calculate the LRFD resistance factors. Table 6.4 summarizes the AD values and the best-fit distribution for other PDFs, indicating that the lognormal distribution is accepted for all groups. Other figures representing the 95% CI and the AD values

for the remaining subsets in different soil types are presented in Appendix-B.

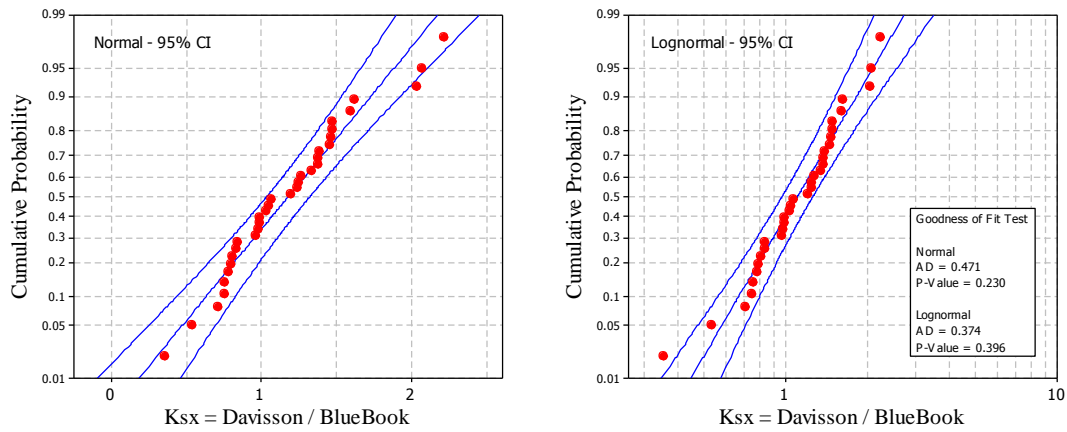


Figure 6.2: Goodness of fit test for the Blue Book method in sand

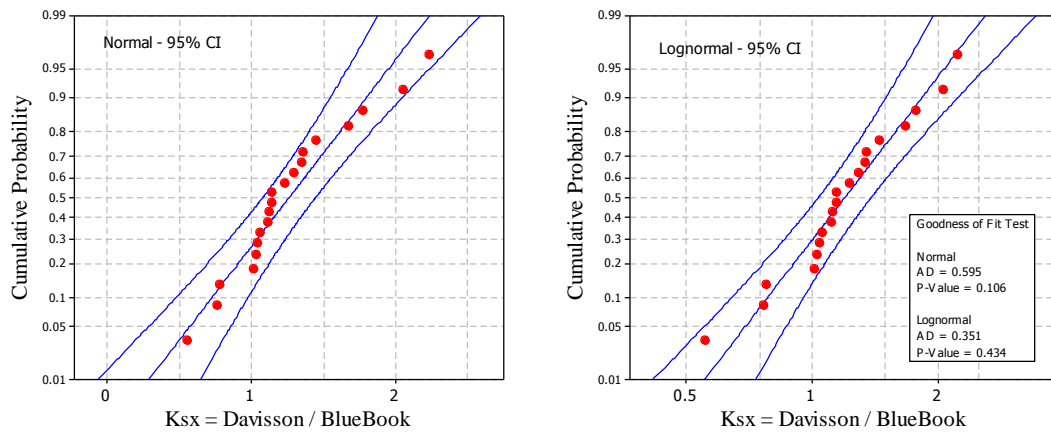


Figure 6.3: Goodness of fit test for the Blue Book method in clay

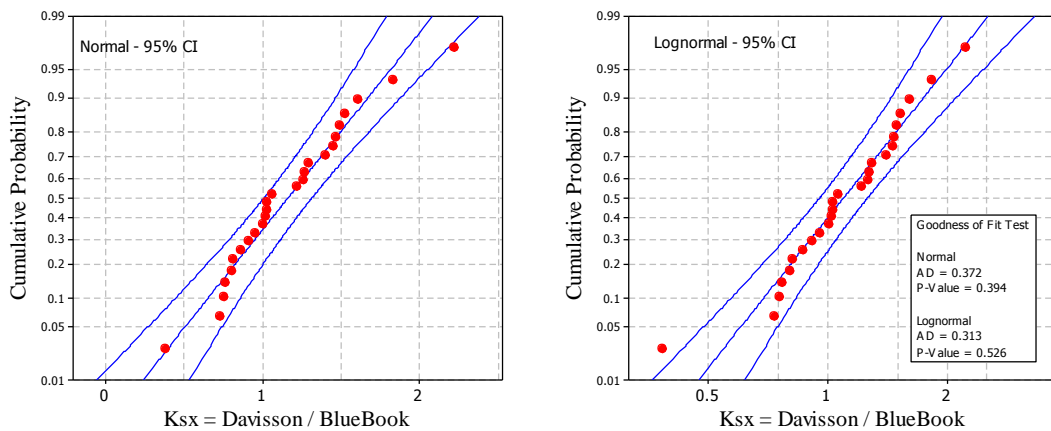


Figure 6.4: Goodness of fit test for the Blue Book method in mixed soil

Table 6.4: Summary of the normality checks using AD test as well as the 95% CI probability test for all the 15 subsets

Soil Type	N ¹	Static Method	Anderson-Darling Normality Test					Best Distribution
			P ² _{Normal}	AD ³ _{Normal}	P _{Lognormal}	AD _{Lognormal}	CV ⁴	
Sand	34	SPT	0.005	1.673	0.435	0.357	0.73	Lognormal
	34	α -API	0.005	1.983	0.621	0.28	0.73	Lognormal
	34	β -	0.005	1.285	0.365	0.39	0.73	Lognormal
	34	Nord	0.005	1.805	0.427	0.361	0.73	Lognormal
	34	BB	0.23	0.471	0.396	0.374	0.73	Lognormal
Clay	20	SPT	0.032	0.797	0.99	0.114	0.72	Lognormal
	20	α -API	0.413	0.36	0.704	0.251	0.72	Lognormal
	20	β -	0.107	0.594	0.31	0.411	0.72	Lognormal
	20	Nord	0.207	0.481	0.222	0.469	0.72	Lognormal
	20	BB	0.106	0.595	0.434	0.351	0.72	Lognormal
Mixed	26	SPT	0.674	0.263	0.422	0.36	0.73	Lognormal
	26	α -API	0.231	0.467	0.89	0.19	0.73	Lognormal
	26	β -	0.389	0.375	0.416	0.363	0.73	Lognormal
	26	Nord	0.136	0.556	0.772	0.234	0.73	Lognormal
	26	BB	0.394	0.372	0.526	0.313	0.73	Lognormal

¹ Sample size within each group

² Probability of following normal distribution

³ Anderson Darling Coefficients

⁴ CV: Critical Value at which the AD cannot exceed, otherwise the distribution is rejected

6.1.3. Histograms and Frequency Distribution

In order to compare different distributions, as well as, determine the differences and scatter among static methods, the normal and the lognormal distributions for all static methods in different soil types were plotted together using the same plotting scale as shown in Figures 6.5 to 6.10. These figures represent the normal and lognormal distributions of PDFs in sand, clay, and mixed soils using same plotting scale for comparison purposes. Among the different methods, it can be observed that the SPT-Meyerhof static method always provides the largest scatter and deviation in sand, and vice versa for the Iowa Blue Book method. The same observation was found in other soil types. This could be an initial indication of the Blue Book method's high efficiency in comparison to other static methods. Another important observation from the figures is that the left tail end of the normal distribution always extended beyond the y axis, causing negative K_{sx} values which is meaningless. This observation strengthens and validates the usage of the lognormal distribution in the analysis.

Presenting a histogram of the K_{sx} ratio with the best-fit distribution (lognormal) is a comprehensive way to show the performance of static methods. Figure 6.11 presents the histogram and frequency distribution of the K_{sx} ratio between Davisson's and Blue Book capacities for 34 cases of driven steel H-piles in sand soils. The parameters of lognormally

distributed PDFs such as N (sample size), Loc (location), and the Scale are presented in the figure. Figures 6.12 and 6.13 represent the histograms and frequency distributions of the K_{sx} ratio for the Blue Book methods in clay and mixed soils, respectively. The histograms and frequency distributions for other static methods in different soil types are provided in Appendix-B.

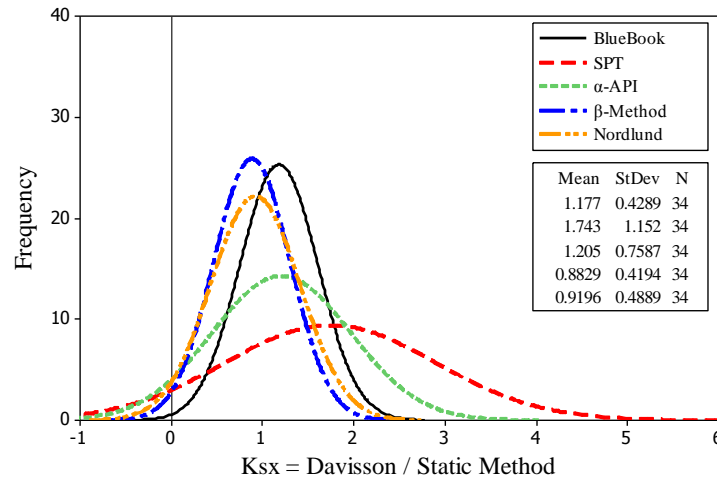


Figure 6.5: Summary of the normal distributed PDFs of the K_{sx} for the 34 cases of steel H-piles designed in sand using different static analysis methods

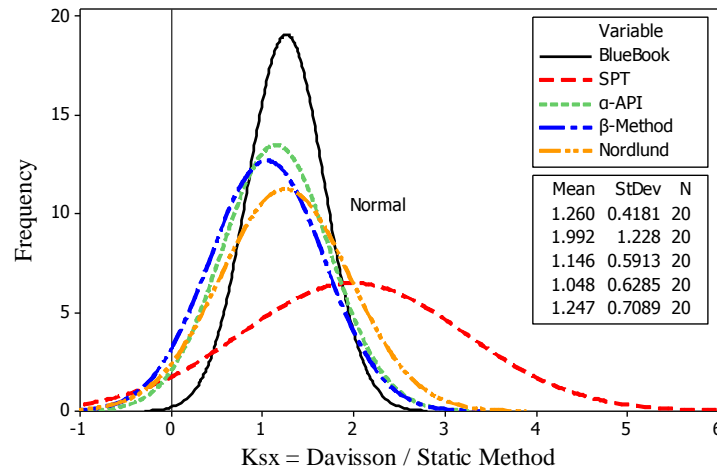


Figure 6.6: Summary of the normal distributed PDFs of the K_{sx} for the 20 cases of steel H-piles designed in clay using different static analysis methods

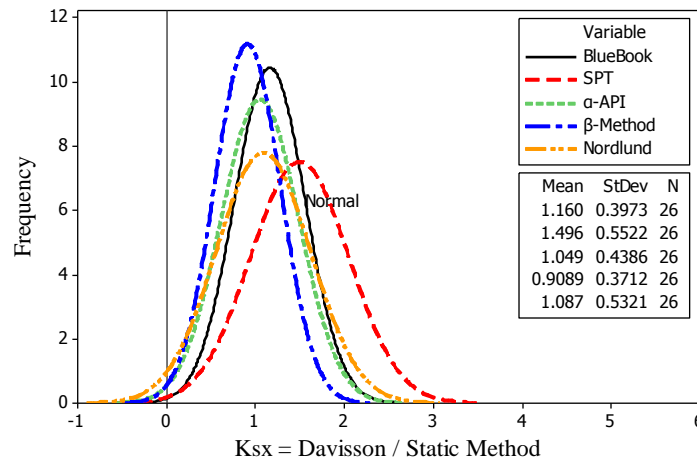


Figure 6.7: Summary of the normal distributed PDFs of the K_{sx} for the 26 cases of steel H-piles designed in mixed soil using different static analysis methods

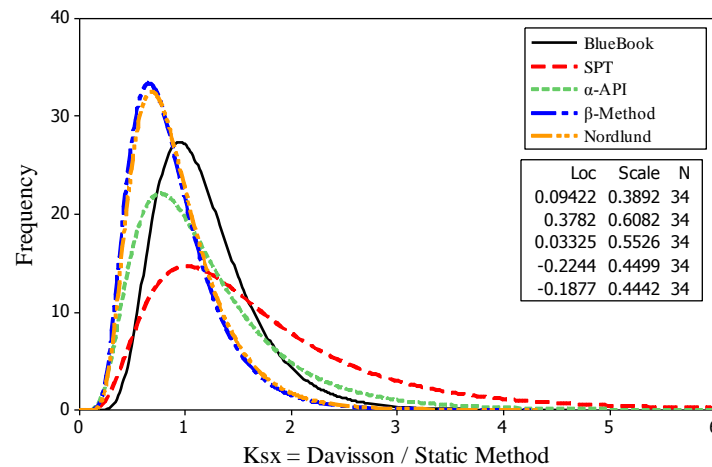


Figure 6.8: Summary of the lognormal distributed PDFs of the K_{sx} for the 34 cases of steel H-piles designed in sand using different static analysis methods

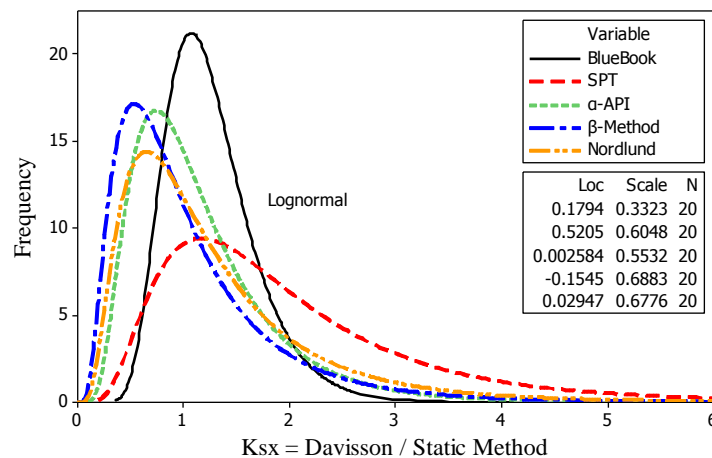


Figure 6.9: Summary of the lognormal distributed PDFs of the K_{sx} for the 20 cases of steel H-piles designed in clay using different static analysis methods

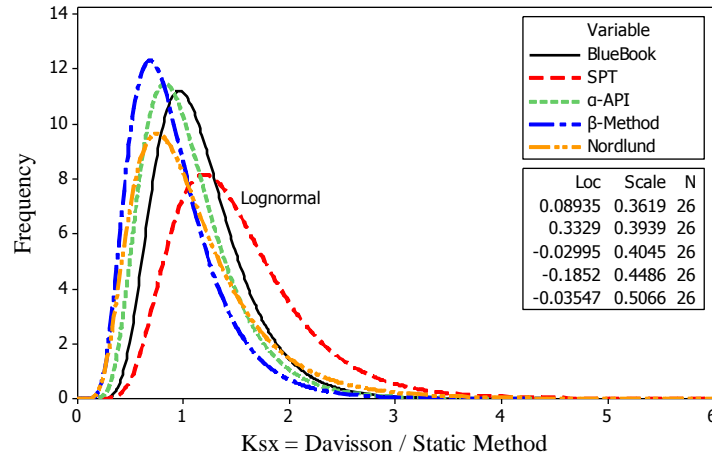


Figure 6.10: Summary of the lognormal distributed PDFs of the K_{sx} for the 26 cases of steel H-piles designed in mixed soil using different static analysis methods

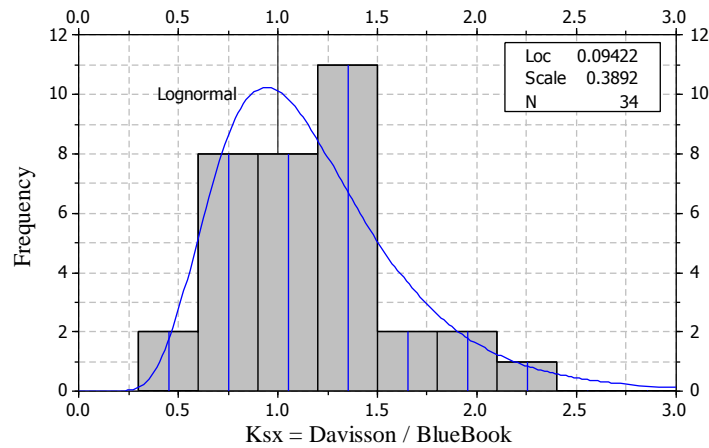


Figure 6.11: Histogram and frequency distribution of K_{sx} for 34 cases of steel H-piles designed in sand using the Blue Book method

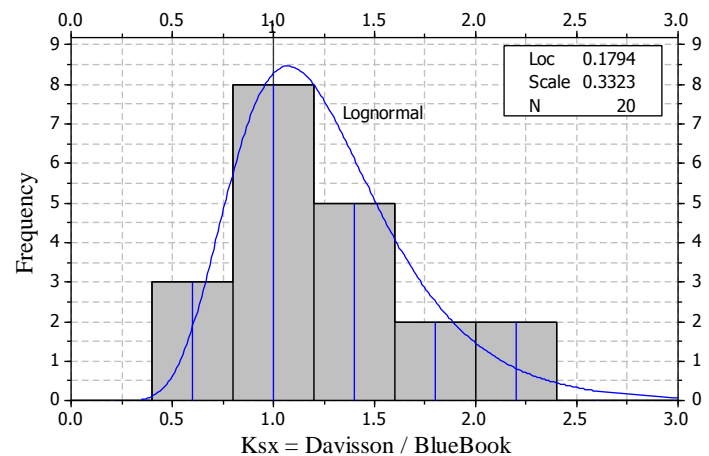


Figure 6.12: Histogram and frequency distribution of K_{sx} for 20 cases of steel H-piles designed in clay using the Blue Book method

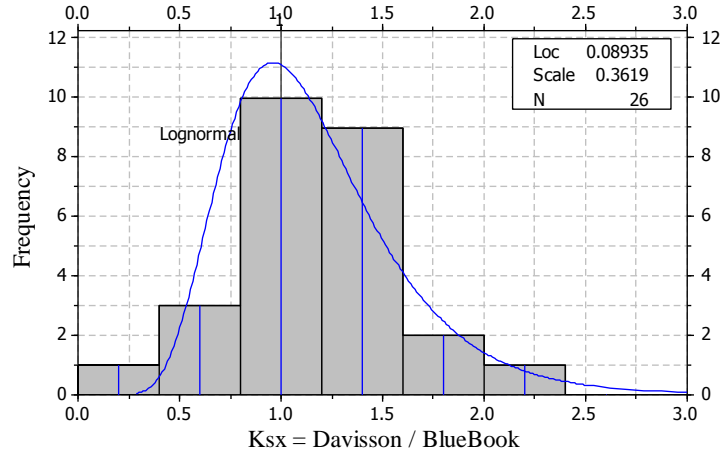


Figure 6.13: Histogram and frequency distribution of K_{sx} for 26 cases of steel H-piles designed in mixed soil using the Blue Book method

6.1.4. LRFD Resistance Factors

The next step in calculating the LRFD resistance factors is to use the PDFs' statistical parameters, the AASHTO (2008 interim) specified load factors, and an adequate target reliability index (β) and DL/LL ratio, as discussed in Chapters 2 and 5. The main statistical parameters required for the reliability analysis include: 1) the relative position of the PDFs, determined by λ_Q and λ_R (i.e., the mean bias for loads and resistances, respectively); 2) the dispersion of the PDFs, determined by σ_Q and σ_R (i.e., the standard deviation for loads and resistances, respectively); and 3) the best-fit of the PDFs (normal or lognormal distribution). Eq. [2.25] of the FOSM approach was used for the calibration. Table 6.5 presents a summary of the preliminary, regionally calibrated LRFD resistance factors for the different static analysis methods used to predict the capacity of driven steel H-piles with respect to three different soil types; sand, clay, and mixed soils. The table includes the required statistical parameters that were used in the FOSM analysis: the sample size (N), mean bias (λ), standard deviation (σ), and the Coefficient of Variation (COV) for each group from PILOT. The resistance factors were calculated for redundant and non-redundant pile groups, and according to Chapters 2 and 5, these were adapted by assuming $\beta=2.33$, and 3.00, respectively. Table 6.5 also includes other essential factors that provide an indication of the economy of each static method, and will be discussed later in this chapter.

For redundant pile groups, the results presented in Table 6.5 indicate that the highest preliminary resistance factor (ϕ) in sand soils is the Blue Book method, followed by SPT-Meyerhof, β -method, α -API, and Nordlund method, in that order, as ϕ values corresponding to 0.56, 0.44, 0.33, 0.32, and 0.31, respectively. The table also shows that the highest ϕ in clay soils is that of the Blue Book method followed by SPT-Meyerhof method, α -API method, Nordlund method, and β -method, in that order, as ϕ values were equal to 0.64, 0.55, 0.39, 0.38, and 0.30, respectively. Table 6.5 also shows that the SPT-Meyerhof method has the highest ϕ in mixed soils, followed by the Blue Book method, the α -API method, Nordlund method, and β -method, in that order, with ϕ values of 0.71, 0.58, 0.45, 0.40, and 0.39, respectively. For non-redundant pile groups, it is observed that the resistance factors are reduced by an average of 30% compared to those of redundant piles. Nevertheless, it is very important to highlight that the efficiency

factors provide a true indication of the efficiency of different methods, rather than the resistance factors which will be explicitly discussed in the following sections. Figures 6.14, 6.15, and 6.16 provide a summary of the LRFD resistance factors and the corresponding efficiency factors based on a target reliability of 2.33 for sand, clay, and mixed soils, respectively.

Table 6.5: Summary of the preliminary regionally calibrated LRFD resistance factors for different static analysis methods in different soil types

Soil Type	N	Static Method	Mean (λ)	St. Dev. (σ)	COV	$\beta=2.33$ (redundant)				$\beta=3.00$ (non-redundant)			
						ϕ^1	ϕ/λ^2	F.S. ³	F.S. _x λ^4	ϕ	ϕ/λ	F.S.	F.S. _x λ
Sand	34	SPT	1.74	1.15	0.66	0.44	0.25	3.24	5.65	0.28	0.16	4.98	8.68
	34	α -API	1.21	0.76	0.63	0.32	0.27	4.38	5.28	0.21	0.18	6.63	7.99
	34	β -	0.88	0.42	0.47	0.33	0.38	4.27	3.77	0.24	0.27	5.98	5.28
	34	Nord	0.92	0.49	0.53	0.31	0.33	4.64	4.27	0.21	0.23	6.69	6.15
	34	BB	1.18	0.43	0.36	0.56	0.48	2.52	2.97	0.42	0.36	3.34	3.93
Clay	20	SPT	1.99	1.23	0.62	0.55	0.28	2.58	5.13	0.37	0.18	3.88	7.72
	20	α -API	1.15	0.59	0.52	0.39	0.34	3.60	4.13	0.28	0.24	5.15	5.90
	20	β -	1.05	0.63	0.60	0.30	0.29	4.72	4.95	0.20	0.19	7.04	7.38
	20	Nord	1.25	0.71	0.57	0.38	0.31	3.71	4.63	0.26	0.21	5.45	6.79
	20	BB	1.26	0.42	0.33	0.64	0.51	2.20	2.77	0.50	0.39	2.86	3.61
Mixed	26	SPT	1.50	0.55	0.37	0.71	0.47	2.01	3.00	0.53	0.36	2.66	3.98
	26	α -API	1.05	0.44	0.42	0.45	0.43	3.17	3.33	0.33	0.31	4.32	4.53
	26	β -	0.91	0.37	0.41	0.39	0.43	3.59	3.26	0.29	0.32	4.86	4.41
	26	Nord	1.09	0.53	0.49	0.40	0.36	3.58	3.89	0.28	0.26	5.05	5.49
	26	BB	1.16	0.40	0.34	0.58	0.50	2.44	2.84	0.44	0.38	3.19	3.71

¹ LRFD geotechnical resistance factor for PILOT

² Efficiency factor

³ Equivalent factor of safety to ASD

⁴ Actual mean factor of safety

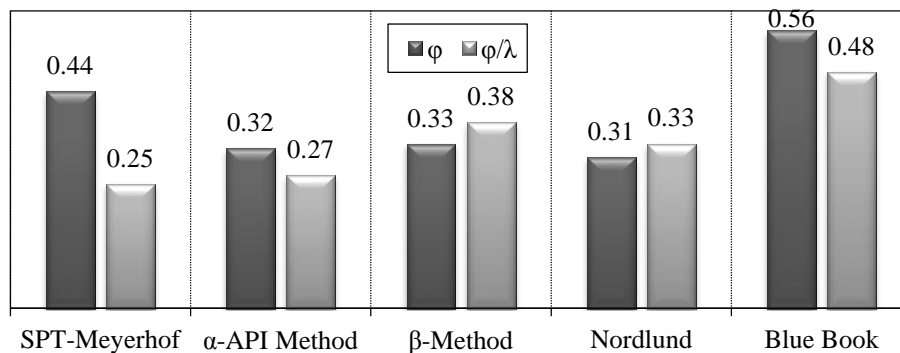


Figure 6.14: Summary of the preliminary LRFD resistance factors for static methods and the corresponding efficiency factors based on a target reliability of 2.33 for sand soil

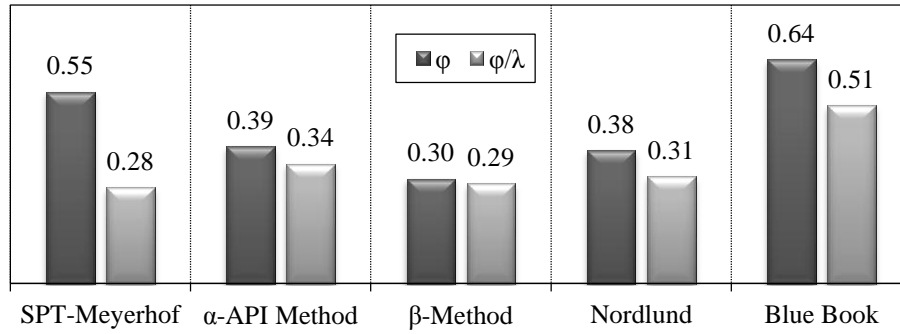


Figure 6.15: Summary of the preliminary LRFD resistance factors for static methods and the corresponding efficiency factors based on a target reliability of 2.33 for clay soil

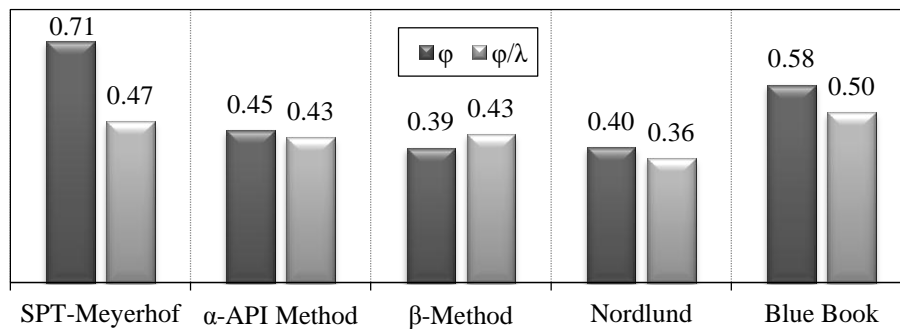


Figure 6.16: Summary of the preliminary LRFD resistance factors for static methods and the corresponding efficiency factors based on a target reliability of 2.33 for mixed soil

6.1.5. Sensitivity to Reliability Index

A sensitivity analysis was conducted to determine the effect on the LRFD resistance factors by changing the target reliability index (β). As shown in Figure 6.17 for sand soils, the resistance factors were found to be very sensitive to any slight change in the reliability index. The analysis was designed to cover a wide range of β starting from 1.5 to 4.0 in order to include all possible variations in the target reliability of bridge pile foundations. The same analysis was conducted for clay and mixed soils as shown in Figures 6.18 and 6.19, respectively. Using Figures 6.17, 6.18, and 6.19, the design engineer can select the appropriate LRFD resistance factors, corresponding to any target reliability index, which depends on the redundancy of the pile groups, importance and life time of the bridge structure, degree of construction control, extent of conservatism in the design, and engineering judgment. However, as previously mentioned, a β of 2.33 for redundant pile groups (five piles or more for each pile cap) is recommended by the 2007 AASHTO and the NCHRP-507 for the design of bridge pile foundations in correspondence to a probability of failure of 1/100.

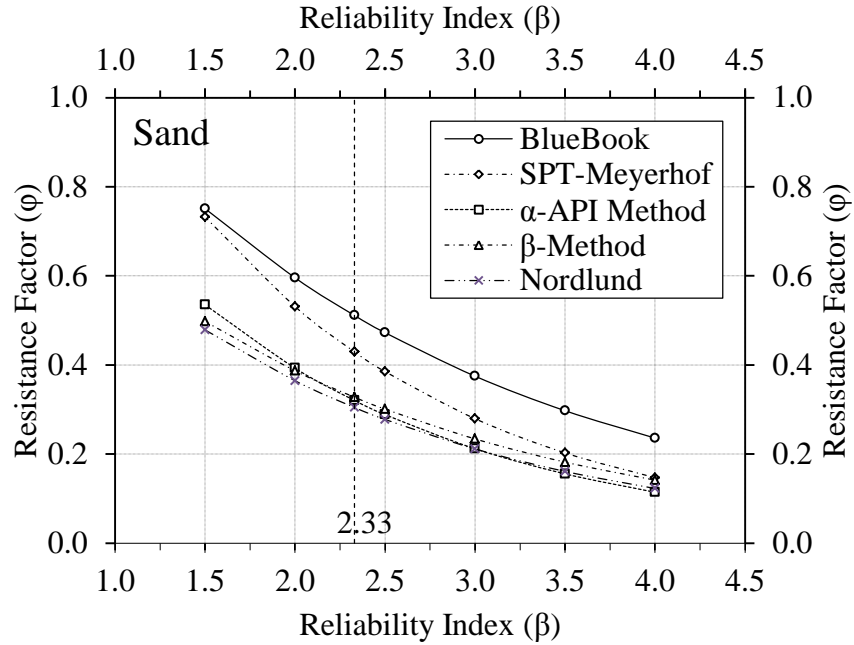


Figure 6.17: Preliminary LRFD resistance factors for different static methods corresponding to a wide range of reliability indices in sand soils

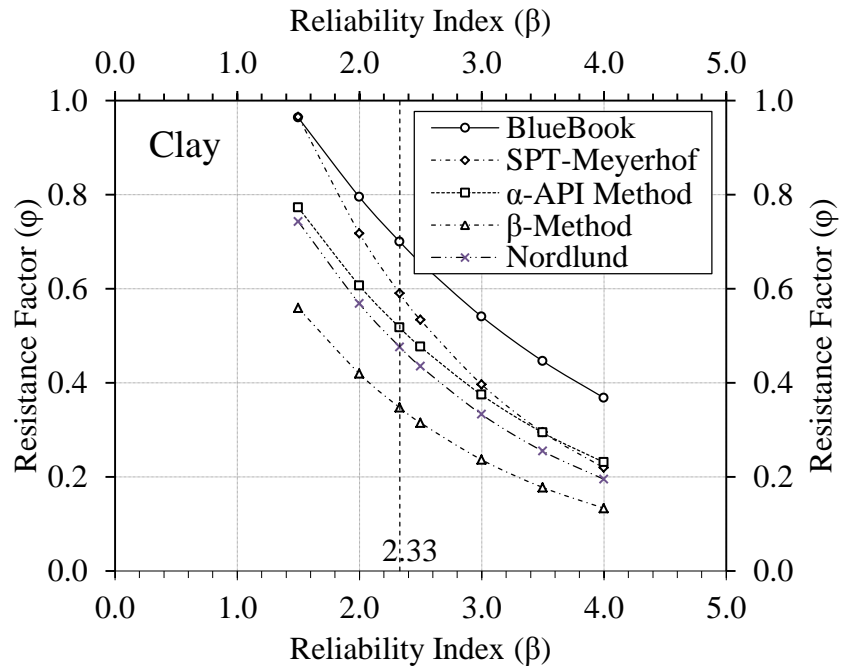


Figure 6.18: Preliminary LRFD resistance factors for different static methods corresponding to a wide range of reliability indices in clay soils

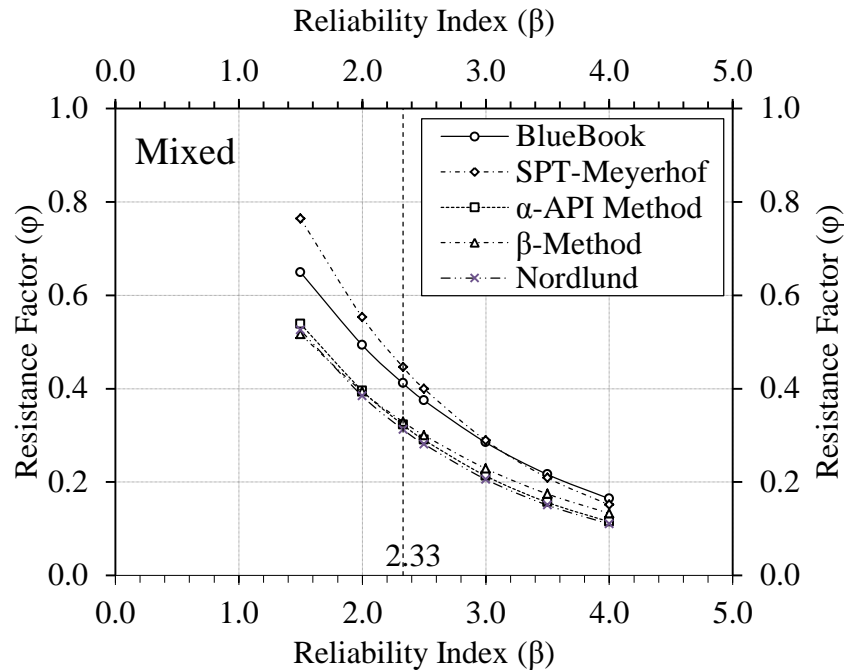


Figure 6.19: Preliminary LRFD resistance factors for different static methods corresponding to a wide range of reliability indices in mixed soils

6.1.6. Efficiency of Different Methods

The efficiency/economy of a static method is not dependent on the corresponding LRFD resistance factor. For example, the factored pile design capacity, calculated using a specific static method, can be lower than that calculated using another static method, although the resistance factor of the first method may be higher than the second. This is essential because the first method might be underestimating the nominal pile capacity, while the second method could be overestimating it. By multiplying both methods with the corresponding LRFD resistance factors, the method with the lower resistance factor could yield a higher pile capacity overall.

In order to determine the efficiency of different static methods that are relative to the actual pile behavior and to each other, an efficiency factor suggested by McVay (2000) was adapted. This efficiency factor (ϕ/λ) is equal to the ratio of the resistance factor to the mean bias of the method. The ϕ/λ factor ranges from 0 to 1.0, in which a higher ϕ/λ is proportional to a higher efficiency. The efficiency factor reflects the economy of the design. In Table 6.5, the ϕ/λ factor was calculated for all groups and it was found that the Blue Book method was the most efficient static method in all soil types, where the ϕ/λ factor values for redundant pile groups were equal to 0.48, 0.51, and 0.50, in sand, clay and mixed soils, respectively. Therefore, the Blue Book method is both efficient and economic in comparison to other static methods in all soil types. Figures 6.20, 6.21, and 6.22 provide the rate of change in the efficiency factors of different static methods corresponding to a wider range of target reliability indices. The design engineer can select the resistance factors as well as the required efficiency/economy in the design.

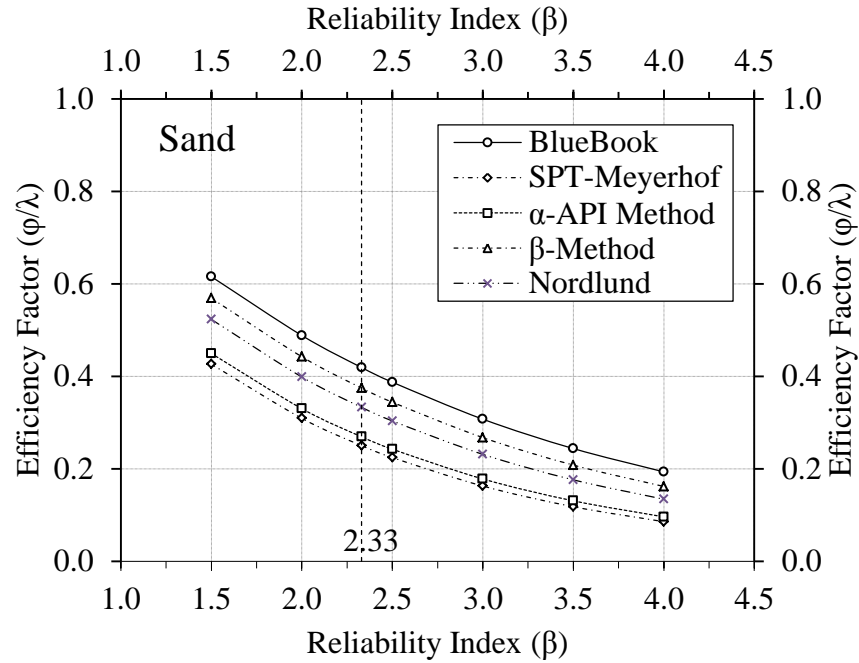


Figure 6.20: Efficiency factors for static methods corresponding to different β in sand

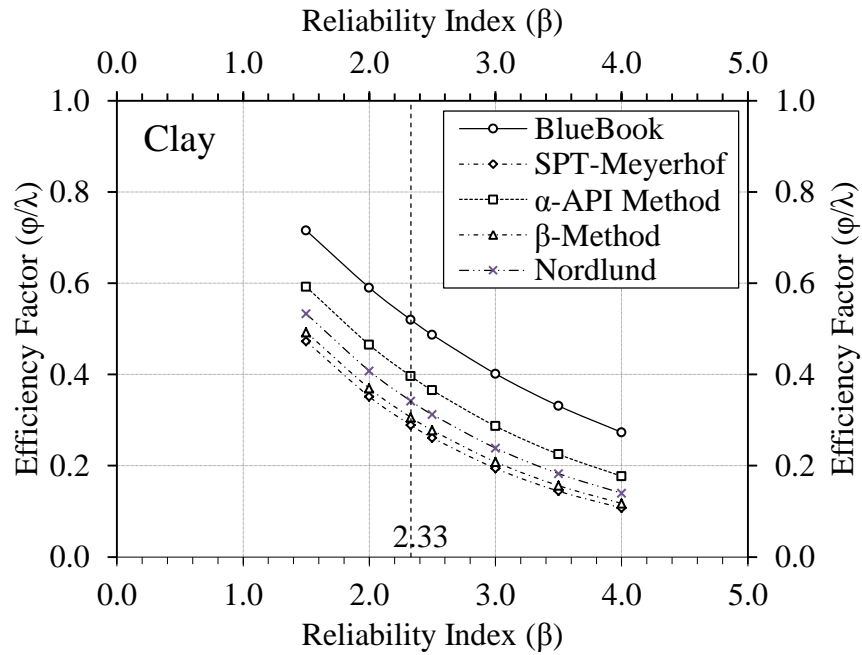


Figure 6.21: Efficiency factors for static methods corresponding to different β in clay

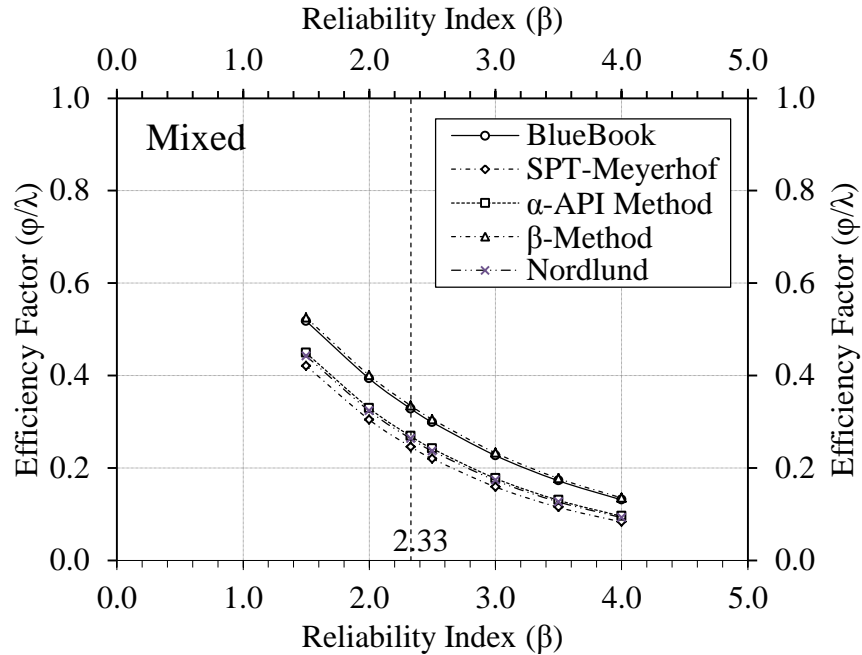


Figure 6.22: Efficiency factors for static methods corresponding to different β in mixed soil

6.1.7. Equivalent Factor of Safety

The economy of the LRFD resistance factors can also be measured by means of the equivalent factor of safety (FS) corresponding to the ASD. This equivalent FS is calculated based on the simplified relation provided by Barker et al. (1991) and is discussed in Chapter 2. As shown in Table 6.5, the equivalent FS is presented for each group based on a $DL/LL = 2$, $\gamma_L = 1.75$, and $\gamma_D = 1.25$, the $FS = 1.4167/\phi$. As can be observed from Table 6.5, the equivalent FS for different static analysis methods ranges from 2.0 to 4.6, with an average of 3.5, without using any construction control methods. This equivalent FS could be reduced by using a construction control technique in accordance to static analysis. However, the equivalent FS is still less conservative than the AASHTO-ASD specifications (1997), which required the conducting of, at minimum, one dynamic test to use a FS of 3.5 for a design based on static methods. On the other hand, the actual FS is calculated by multiplying the mean bias by the equivalent FS. The actual FS represents the overall economy of the method, meaning that whenever the actual FS is lower, the foundation cost is reduced and vice versa. From Table 6.5, it can be observed that the Blue Book method, which is the method with the highest efficiency, is providing the lowest FS among all other static methods, taking into consideration that this actual FS is corresponding to a target reliability of 2.33. The values of the actual FS for the Blue Book method were 2.9, 2.7, and 2.8, in sand, clay, and mixed soils, respectively.

In summary, the back-calculated equivalent FS is within the range of 2.5 and 5.0, as recommended by the ASD specifications (1997). Moreover, the equivalent FS is corresponding to a fixed degree of reliability. Hence, when using the Blue Book method for the design of bridge pile foundations in different soil types, the LRFD approach will be consistently reliable.

6.1.8. Regional Factors vs. Design Specifications

In order to evaluate the difference between the recently developed resistance factors and the existing recommendations, it is essential to compare the preliminary LRFD resistance factors with the current design codes and specifications. Performing such a comparison will help determine whether the regionally calibrated resistance factors are more or less economic than those provided in the design specifications. Provided that these factors are developed in accordance with the AASHTO Specifications (2008), the regionally calibrated LRFD resistance factors are utilized to minimize the unnecessary conservatism built into the AASHTO Specifications and also to improve the cost-effectiveness of deep foundations.

In this study, the 2008 AASHTO-LRFD specifications and the NCHRP-507 (after Paikowsky et al., 2004) were selected for this comparison. Table 6.6 presents the different values of the LRFD resistance factors provided in design specifications versus the Iowa preliminary regionally calibrated LRFD resistance factors. It can be observed in Table 6.6 that the resistance factor for the SPT-Meyerhof method in sand soil is greater than the factor provided in AASHTO specifications by approximately 40%. For β -method in sand, the developed resistance factor is about 3% greater than that recommended by the NCHRP. However, for Nordlund's method in sand, the regionally calibrated resistance factor is 0.31, which is lower than the 0.45 provided in AASHTO. For clay soils, the developed resistance factor for the β -method was 24% and 55% greater than those recommended by NCHRP and AASHTO, respectively. For mixed soils, a significant increase of about 60% in the resistance factors was observed for β -method when compared to AASHTO. Compared to the NCHRP values, there were approximately 20% and 25% increases in the resistance factor were obtained for the α -API and Nordlund methods, respectively.

Table 6.6: Different values of the LRFD resistance factors provided for static methods in design specifications versus the Iowa preliminary regionally calibrated factors

Soil Type	Static Analysis Method	Iowa Preliminary Resistance Factor	AASHTO 2008 Interim	NCHRP 507 Resistance Factors
Sand	SPT-Meyerhof	0.44	0.3	0.45
	β -Method	0.33	N/A	0.3
	Nordlund	0.31	0.45	0.45
Clay	α -API	0.39	N/A	0.45
	β -Method	0.30	0.25	0.2
Mixed	α -API	0.45	N/A	0.35
	β -Method	0.39	0.25	0.2
	Nordlund	0.40	N/A	0.2-0.35

6.1.9. Examination of the Resistance Factors

As a part of this research, 10 full-scale pile load tests were conducted at different locations in the State of Iowa to cover all possible soil regions and geological formations. The instrumented piles

were tested to failure and the Davisson's capacity was determined for all, which represented the actual nominal capacity in the field. Moreover, each test included several in-situ soil tests such as Standard Penetration Test (SPT), Cone Penetration Tests (CPT), and Borehole Shear Tests (BST). Volume II of the project final report (Ng et al., 2010) provides more information regarding the field-testing plan, procedures, and results. The nominal design capacities were back-calculated for all the load-tested piles using different static methods, and the recently developed LRFD resistance factors were applied to these values to determine the factored design capacities. The nominal and factored design capacities, calculated using static methods, were then compared to the measured capacity of the piles in order to monitor the performance as well as validate the preliminary calibrated LRFD resistance factors and to help develop the final design recommendations presented in Chapter 7.

Figure 6.23 presents the calculated nominal and factored capacities of the test pile at Clarke County (clay site) using five different static methods and compared them to the actual nominal and factored capacities from the SLT results using Davisson's criterion. For static methods, the factored capacities were calculated based on the preliminary resistance factors. Assuming low site variability, the AASHTO's recommended factor of 0.8 was used for calculating the actual factored capacity measured from the SLT.

Figure 6.23 indicates that the SPT-Meyerhof method provided a nominal capacity of 88 kips which was unnecessarily over-conservative when compared to the actual nominal capacity of 243 kips from SLT, and the β -method, which provided a very high, overestimated, capacity of 279 kips. Thus, it is clear that there is a large variation in the pile nominal capacities calculated using different static methods. As shown in the same figure, it was noted that this large variation was significantly reduced after applying the preliminary resistance factors. The capacities from static methods were adequately adjusted to a limited value after applying the resistance factors, as all the design capacities did not exceed the actual factored capacity. The Iowa Blue Book method was found to provide a factored capacity of 132 kips which was the least conservative estimate compared to other static methods and to SLT results. As a preface conclusion, it is noted that the preliminary LRFD resistance factors increased the degree of reliability of static analysis methods, providing a consistent range of pile design capacities with no large variation from one method to another. Therefore, static methods are providing a reliable pile capacity in clay soils.

Figures 6.24 and 6.25 represent the same comparison between the predicted nominal and factored pile capacities using different static analysis methods, versus the measured pile capacities from the SLT results at Cedar and Poweshiek Counties (Sand and Mixed soils), respectively. It is clear from the figures that almost the same aforementioned behavior was observed in sand and mixed soils, indicating that the preliminary, regionally developed LRFD resistance factors for Iowa soils appear to be satisfactory. It was also observed that the Blue Book method is economic for all soil types especially in the case of sand and clay soils, while the β -method provided was the most economical method for mixed soils.

Table 6.7 summarizes the 10 field tests' ID numbers, location, average soil formation, measured nominal capacities from SLT results using Davisson's criterion, as well as the predicted nominal capacities using different static methods. After comparing the static pile capacities with the field measured, and after applying the preliminary resistance factors, it was generally found that some

static methods overestimate the capacity, while others are conservative compared to Davisson's method. This conservatism is due to the limited probability of failure associated with the LRFD resistance factors, in addition to the built-in conservatism, which already exists in most of the static analysis methods. It was also found that the Iowa Blue Book method seemed to be less conservative compared to other methods, which agrees with the efficiency of each method. However, this degree of conservatism associated with the LRFD is relatively low, compared to the conventional ASD approach. Consequently, the preliminary regionally calibrated LRFD resistance factors for Iowa provide a reliable and economic design that can certainly be used in the development of final recommendations.

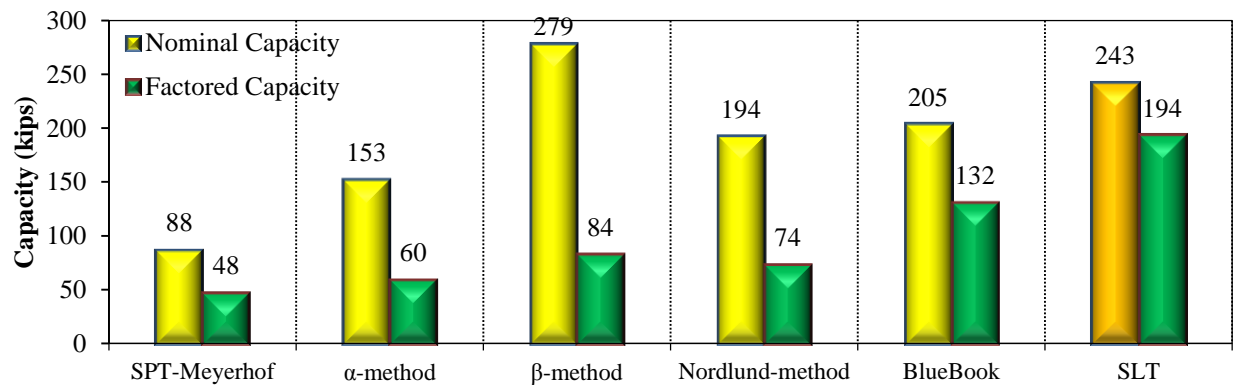


Figure 6.23: Nominal and Factored pile design capacities using different static methods and compared to SLT results for Clarke – Clay soil

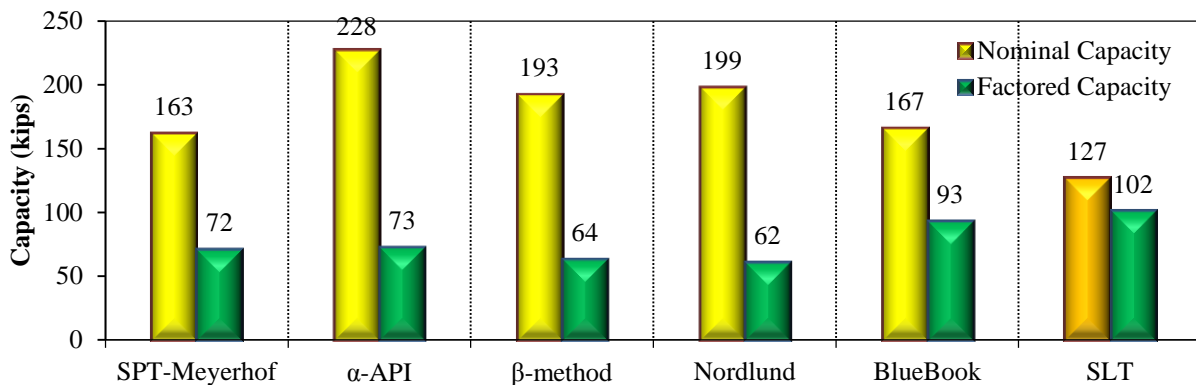


Figure 6.24: Nominal and Factored pile design capacities using different static methods and compared to SLT results for Cedar – Sand soil

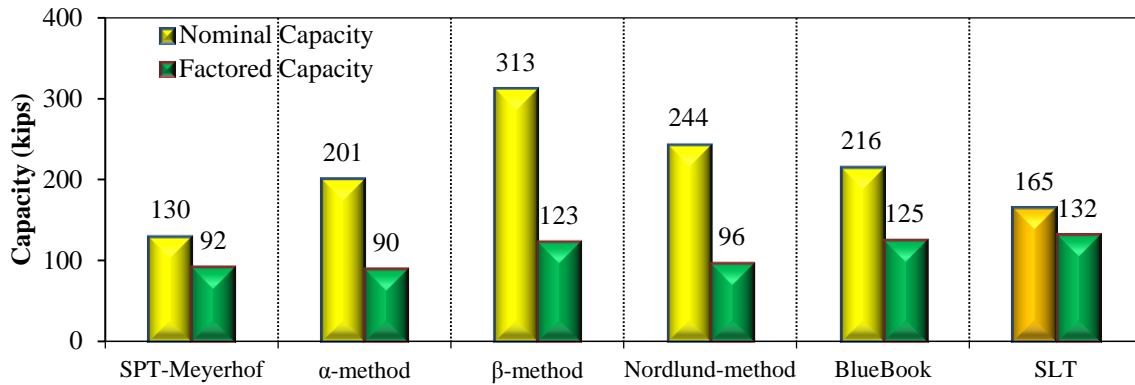


Figure 6.25: Nominal and Factored pile design capacities using different static methods and compared to SLT results for Poweshiek – Mixed soil

Table 6.7: Summary of the 10 field tests' ID, location, average soil formation, measured nominal capacities, and predicted nominal capacities using different static methods

County	ID	Soil Type	Pile Capacity (kips)	Nominal Design Capacity (kips)				
				SPT	Alpha	Beta	Nord	BB
Mahaska	ISU-1	Mix	212	108	168	170	144	127
Mills	ISU-2	Clay	125	104	233	177	81	43
Polk	ISU-3	Clay	150	127	164	145	164	85
Jasper	ISU-4	Clay	154	179	396	271	190	105
Clarke	ISU-5	Clay	243	153	279	194	205	88
Buchanan	ISU-6	Clay	213	151	335	248	188	108
Buchanan	ISU-7	Mix	53	53	68	49	27	34
Poweshiek	ISU-8	Mix	162	201	313	244	216	130
Des Moines	ISU-9	Sand	158	134	198	303	196	178
Cedar	ISU-10	Sand	127	163	228	193	199	167

Figures 6.26 and 6.27 provide a better illustration of the LRFD resistance factors' performance and summarize the previous observations. As shown in Figure 6.26, the x-axis represents the measured pile nominal capacity for the 10 field tests using Davisson's criterion, while the y-axis represents the nominal capacity calculated for the same 10 piles using different static analysis methods. As can be observed from the figure, the points are scattered above and below the neutral line, meaning that in some cases the nominal design capacity is higher than the nominal measured (actual) capacity of the piles, which is unsafe. On the other hand, Figure 6.27 represents the same data, but only after multiplying the nominal capacities by the corresponding LRFD resistance factors. As can be seen from Figure 6.27, the factored design capacities calculated using different static methods did not exceed the actual factored capacities for the load tested piles. This indicates that the LRFD resistance factors succeeded to lower the capacities below the neutral line therefore ensuring reliable designs for the 10 piles.

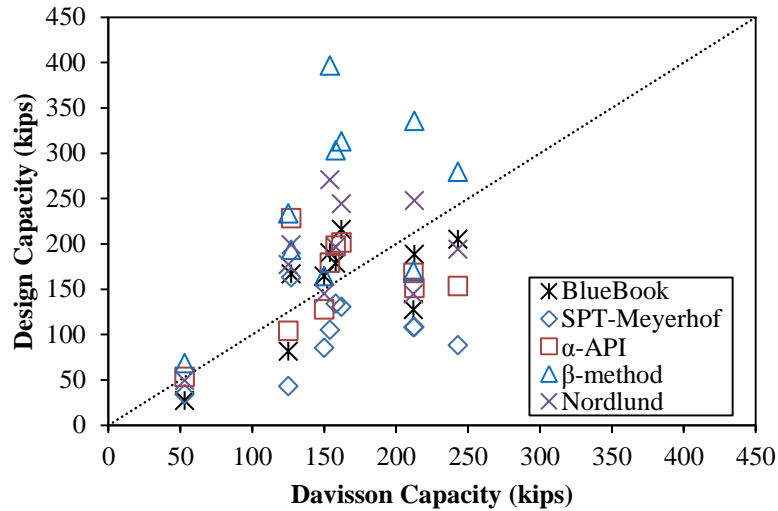


Figure 6.26: Nominal measured and calculated capacities for the 10 field tested piles using Davisson’s criterion versus static analysis methods

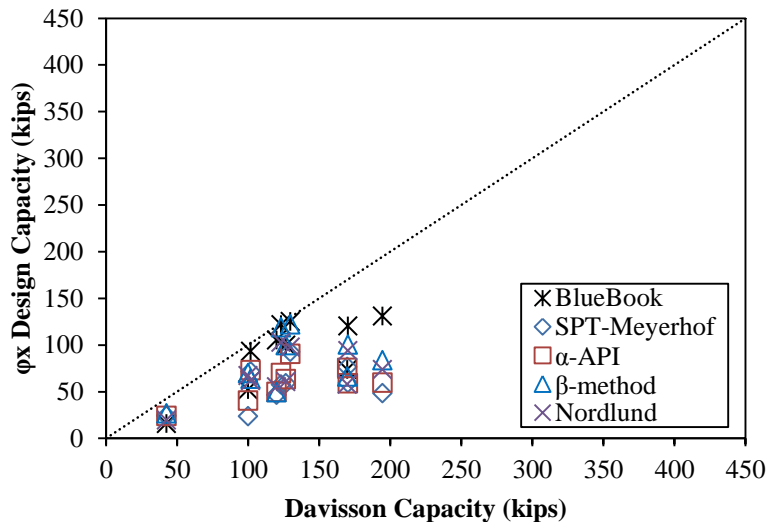


Figure 6.27: Factored measured and calculated capacities for the 10 field tested piles using Davisson’s criterion versus static analysis methods

6.1.10. Construction Control Aspects

As discussed in Chapter 2, the static analysis methods are used in the design stage whereas the dynamic methods and/or SLT are used in the construction stage. Several static analysis methods could be used for predicting the pile capacity, where each static method would have its own LRFD resistance factors, depending on different parameters. The design process is responsible for assembling the construction bidding documents concerning the bridge substructure. After releasing the bidding documents and awarding the contract, the construction stage begins when the design verification is performed. During the construction stage, the pile SLT and/or dynamic monitoring (WEAP or PDA/CAPWAP) have their own LRFD resistance factors that are used for design verification of pile foundations. In this study, additional work was done to consider the construction control aspects in the calibration of the LRFD resistance factors, thus accounting for

the construction aspects even during the design stage (i.e., while using the static analysis methods). To account for construction control, a new resistance factor for a static analysis method was determined by multiplying the mean ratio (or a correction factor) to its originally calibrated resistance factor. This correction factor is the average ratio of factored capacities determined using dynamic methods or dynamic formulas to the factored capacity determined using a static analysis method. The LRFD resistance factors will then be developed for this combination of methods, which reduces the gap between design and construction stages. The correction factor was calculated for the combination of the most efficient static and dynamic methods and is presented later in this chapter (see Section 6.2.12 for WEAP analysis for construction control, and see Section 6.3.10 for dynamic formulas for construction control). For example, the correction factor for the Iowa Blue Book static method was calculated based on the WEAP and the Iowa DOT ENR formula. Moreover, Section 6.2.10 provides details concerning the effect of soil setup on the pile capacity with respect to time. Soil setup was included in the construction control calculations for WEAP.

6.2. Dynamic Analysis Methods

As noted in Chapter 5, dynamic analysis was conducted using wave equation (i.e., WEAP) based on five different soil input methods in this study, these methods included: the ST, SA, Iowa Blue Book, Iowa DOT ENR method, and Driven software. The dynamic capacity was calculated using WEAP for 32 steel piles obtained from PILOT database, which included the hammer and driving information. Davisson's criterion was the method used for determining the actual pile nominal capacity from load test results.

6.2.1. Capacity from WEAP

Tables 6.8, 6.9, and 6.10 represent the nominal capacity of the piles from PILOT in clay, sand, and mixed soils, respectively, that were calculated using Davisson's criterion as well as WEAP based on different soil input methods. As can be seen in the tables, the identification number and the representative Iowa county for each site from the database are presented and sorted according to different soil types. The tables also show the steel H-pile sizes, as well as the time between EOD and the conducting of the SLT. The number of tests available in clay, sand, and mixed soils are 12, 11, and 9, respectively. It can also be seen that the average time of performing the SLT after EOD is about five days. In order to compare the actual and predicted capacity for the available piles from PILOT, an accumulative summation of all capacities calculated using WEAP was presented and compared to the actual capacities determined from the SLT results, as presented in Figure 6.28. From Figure 6.28, it is clear that WEAP under-predicts the pile capacity at the EOD when compared to the actual SLT results.

Table 6.8: Nominal Davisson's capacity of the piles from PILOT as well as using WEAP analysis based on different soil input methods in clay

ID #	County	L (ft)	Pile Size (HP)	D (kips)	Capacity from WEAP (kips)					Days SLT
					ST ¹	SA ²	BB ³	I DOT ⁴	Driven ⁵	
6	Decatur	53	HP 10 x 42	118	71	73	71	82	69	3
12	Linn	23.8	HP 10 x 42	204	154	153	155	170	154	5
42	Linn	23.5	HP 10 x 42	82	81	84	85	92	81	5
44	Linn	37	HP 10 x 42	136	90	92	94	112	90	5
51	Johnson	29.5	HP 10 x 42	190	126	126	128	140	126	3
57	Hamilton	57	HP 10 x 42	168	91	91	94	111	92	4
62	Kossuth	45	HP 10 x 42	100	74	75	76	83	73	5
63	Jasper	63	HP 10 x 42	66	60	60	59	90	60	2
64	Jasper	71	HP 10 x 42	122	72	72	71	89	72	1
67	Audubon	32	HP 10 x 42	140	121	122	121	139	122	4
102	Poweshiek	43	HP 10 x 42	130	117	116	118	130	115	8
109	Poweshiek	51	HP 12 x 53	176	141	141	145	161	142	3

¹ WEAP using ST soil input, ² WEAP using SA soil input, ³ WEAP using BB soil input, ⁴ WEAP using Iowa DOT soil input, ⁵ WEAP using Driven software soil input.

Table 6.9: Nominal Davisson's capacity of the piles from PILOT as well as using WEAP analysis based on different soil input methods in sand

ID #	County	L (ft)	Pile Size (HP)	D (kips)	Capacity from WEAP (kips)					Days SLT
					ST	SA	BB	I DOT	Driven	
10	Ida	52.3	HP 10 x 42	116	61	69	64	53	74	2
17	Fremont	58	HP 10 x 42	132	205	191	219	183	246	5
20	Muscatine	59	HP 10 x 42	120	182	185	173	160	186	5
24	Harrison	78	HP 10 x 42	184	241	238	249	258	324	9
34	Dubuque	57	HP 10 x 42	224	158	160	155	144	159	7
48	Black Hawk	42	HP 10 x 42	144	140	140	130	121	139	5
70	Mills	78	HP 10 x 42	128	138	140	140	128	149	5
74	Benton	55	HP 10 x 42	150	143	135	139	142	177	32
99	Wright	31	HP 10 x 42	104	97	89	93	100	115	7
151	Pottawattamie	77.5	HP 10 x 42	200	133	134	136	113	134	4
158	Dubuque	73.6	HP 14 x 89	582	709	725	666	611	729	4

Table 6.10: Nominal Davisson's capacity of the piles from PILOT as well as using WEAP analysis based on different soil input methods in mixed soil

ID #	County	L (ft)	Pile Size (HP)	D (kips)	Capacity from WEAP (kips)					Days SLT
					ST	SA	BB	I DOT	Driven	
7	Cherokee	39.0	HP 10 x 42	176	88	88	83	106	86	6
8	Linn	54.0	HP 10 x 42	170	142	129	132	144	122	8
25	Harrison	58	HP 10 x 42	224	152	144	147	145	165	4
43	Linn	36.0	HP 10 x 42	142	139	141	141	167	139	5
46	Iowa	48	HP 10 x 42	164	145	148	143	131	97	4
66	Black Hawk	43	HP 10 x 42	180	107	116	107	120	163	5
73	Johnson	46.7	HP 10 x 42	232	165	165	152	129	163	6
90	Black Hawk	65	HP 12 x 53	190	211	196	208	195	213	4
106	Pottawattamie	36.0	HP 10 x 42	148	71	63	61	75	57	6

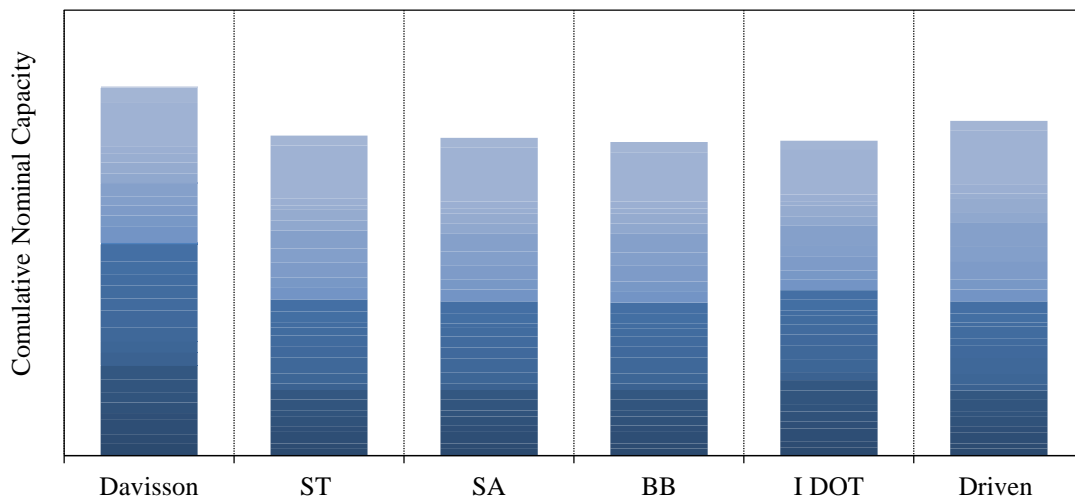


Figure 6.28: Accumulative actual PILOT pile capacities using Davisson and the predicted pile capacities using WEAP based on different soil input methods

6.2.2. Goodness of Fit Test

As discussed in Chapters 2 and 5, the FOSM equation that was used in this study is based on the assumption of lognormally distributed PDFs for all groups. The mean bias (K_{sx}) of each subset is the ratio of the actual nominal pile capacity to the predicted pile capacity. For subsets in different soil types, the K_{sx} was calculated by taking the ratio of the actual pile capacity, which was determined from SLT, to the predicted pile capacity that was determined using WEAP based on five different soil input methods.

Figures 6.29 to 6.31 represent the PDFs and the 95% CI of the K_{sx} ratio for WEAP's Iowa DOT soil input method in sand, clay, and mixed soils, respectively. The figures also present the AD value (or the Anderson Darling coefficient value). In order to determine which distribution is best-fitting to the PDFs, the probability of the 95% CI of the best-fit should be greater than 0.05,

while the AD value should be less than that of the least-fit distribution. As previously mentioned, the figures are comparing normal to lognormal distributions in order to detect which is best fitting for the data subsets. As can be observed from the figures, the AD value for all subsets is lower in the case of lognormal, and the probability of 95% CI is greater in the case of lognormal while still greater than 0.05. Therefore, all the subsets are considered to follow the lognormal distribution, and the FOSM equation is valid for the LRFD calibration. Other figures representing the 95% CI for the rest of the WEAP methods in different soil types are presented in the Appendix-B.

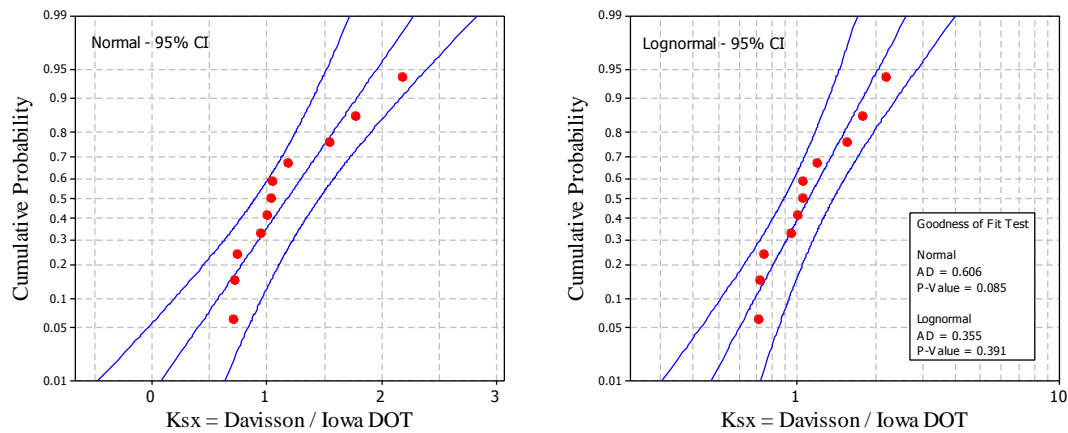


Figure 6.29: Goodness of fit test for the WEAP based on Iowa DOT in sand

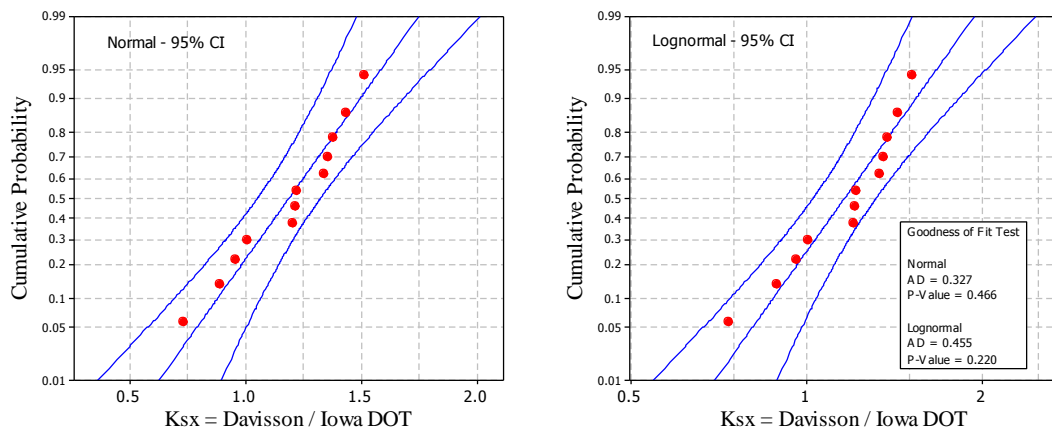


Figure 6.30: Goodness of fit test for the WEAP based on Iowa DOT in clay

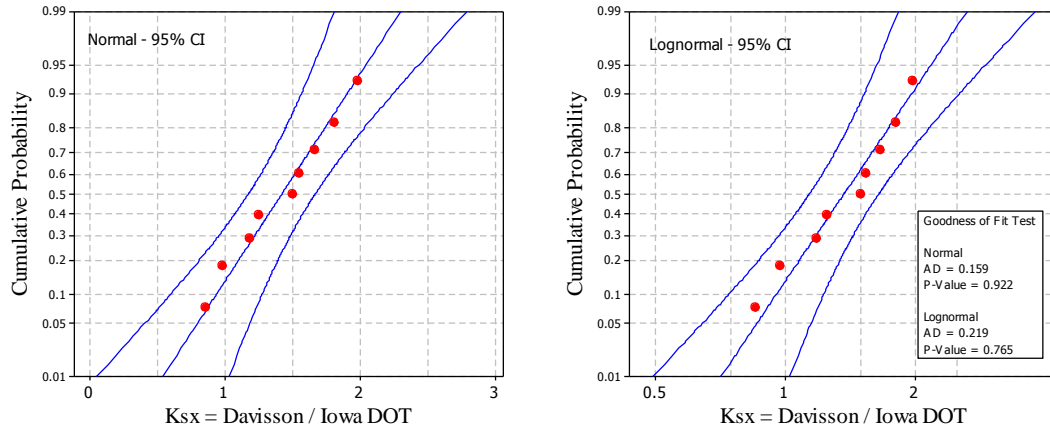


Figure 6.31: Goodness of fit test for the WEAP based on Iowa DOT in mixed soil

6.2.3. Histograms and Frequency Distribution

As shown in Figures 6.32 to 6.37, the normal and the lognormal distributions for different WEAP methods in different soil types were plotted together using the same plotting scale, in order to compare different distribution types, as well as, determine the differences and scatter among different methods. The figures represent the normal and lognormal distributions of PDFs in sand, clay, and mixed soils, respectively, using same plotting scale for comparison purposes. An obvious observation from the figures was observed as the K_{sx} ratio was extended below the zero axis in the case of normal distribution in sand and mixed soils, which is not valid. This again strengthens and validates the usage of lognormal distribution as previously discussed in the preceding sections.

A comprehensive way to show the performance of different WEAP analysis methods can be achieved by presenting the histogram of the K_{sx} , and also by overlaying the best-fit distribution (lognormal) on the histogram. Figure 6.38 presents the histogram and frequency distribution of the K_{sx} ratio between the capacity from Davisson and WEAP based on Iowa DOT ENR soil input methods for 11 cases of driven steel H-piles in sand soils. The parameters of lognormal distributed PDFs such as N (sample size), Loc (location), and the Scale are presented. Figures 6.39 and 6.40 represent the histograms and frequency distributions of the same K_{sx} in clay and mixed soils, respectively. The histograms and frequency distributions for other WEAP methods in different soil types are provided in the Appendix-B.

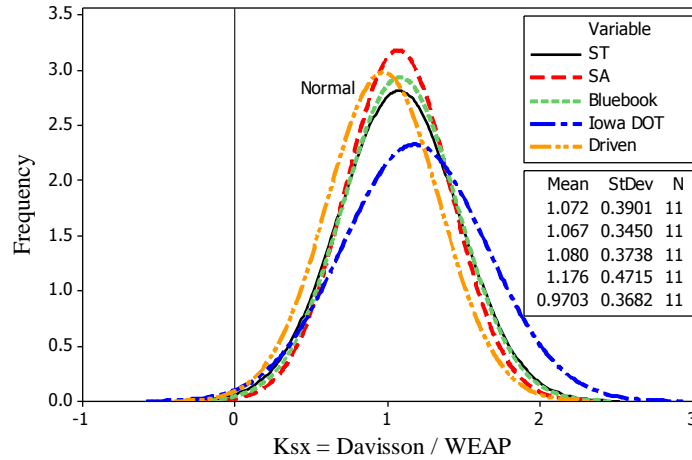


Figure 6.32: Summary of the normal distributed PDFs of the K_{sx} for the 11 cases of steel H-piles designed using WEAP in sand using different input approaches

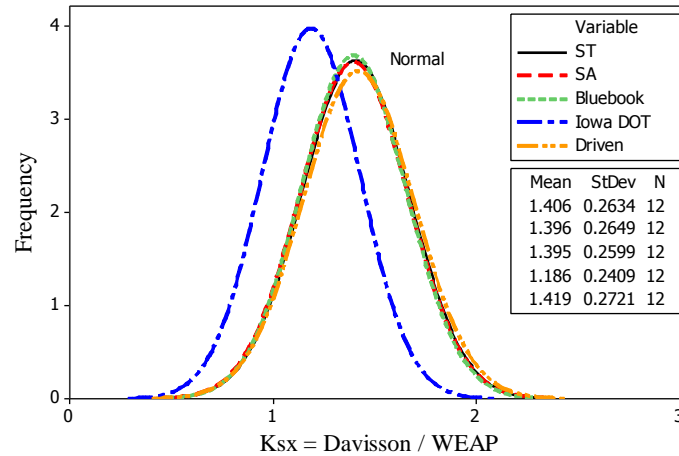


Figure 6.33: Summary of the normal distributed PDFs of the K_{sx} for the 12 cases of steel H-piles designed using WEAP in clay using different input approaches

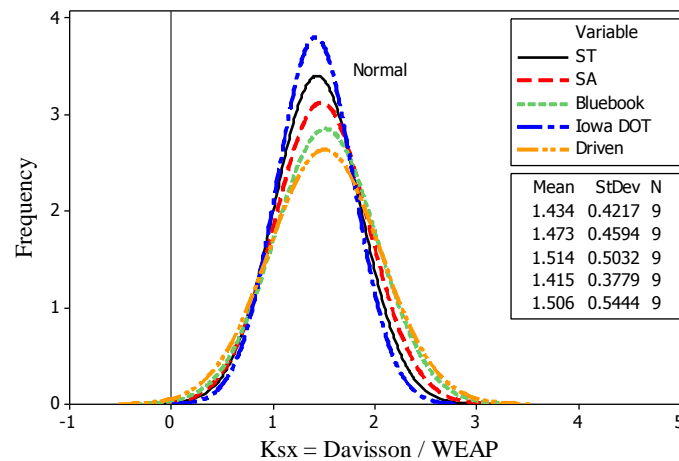


Figure 6.34: Summary of the normal distributed PDFs of the K_{sx} for the nine cases of steel H-piles designed using WEAP in mixed soil using different input approaches

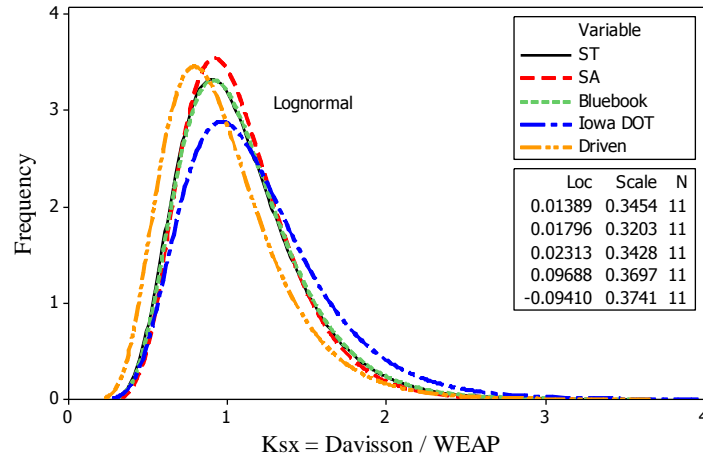


Figure 6.35: Summary of the lognormal distributed PDFs of the K_{sx} for the 11 cases of steel H-piles designed using WEAP in sand based on different input approaches

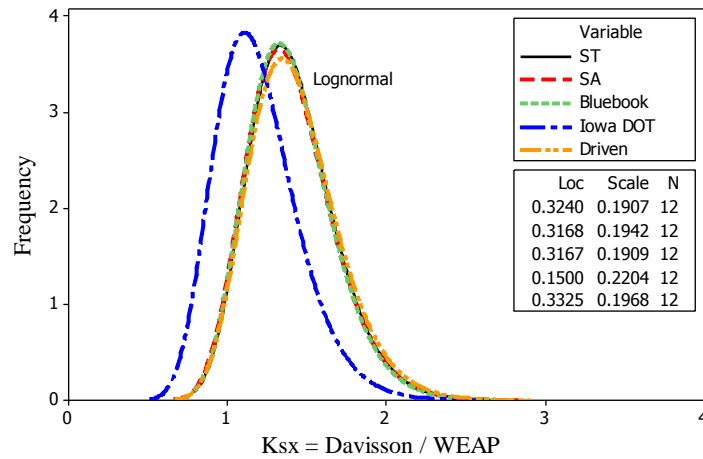


Figure 6.36: Summary of the lognormal distributed PDFs of the K_{sx} for the 12 cases of steel H-piles designed using WEAP in clay based on different input approaches

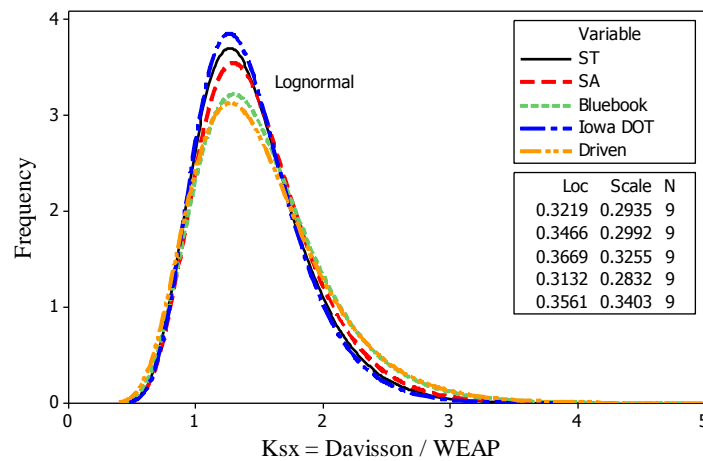


Figure 6.37: Summary of the lognormal distributed PDFs of the K_{sx} for the nine cases of steel H-piles designed using WEAP in mixed soil based on different input approaches

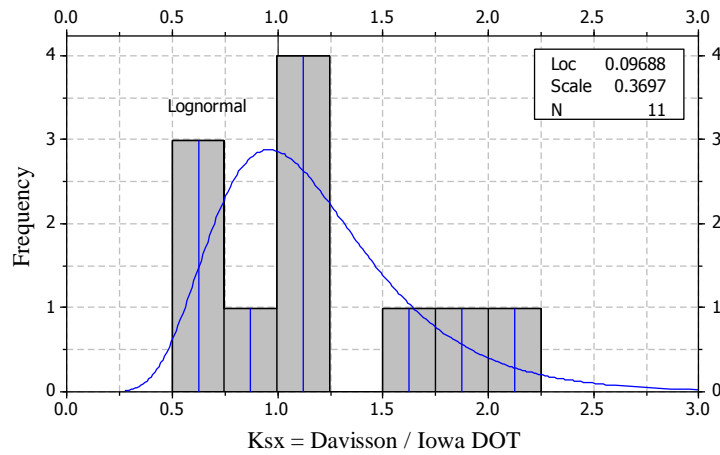


Figure 6.38: Histogram and frequency distribution of K_{sx} for 11 cases of steel H-piles designed using WEAP in sand based on the Iowa DOT method

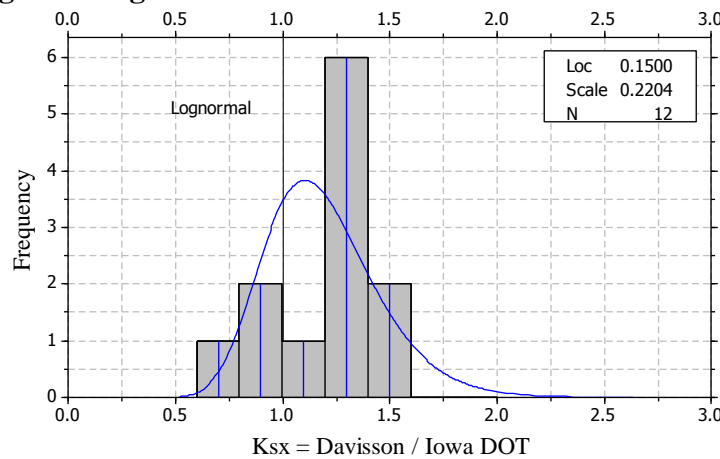


Figure 6.39: Histogram and frequency distribution of K_{sx} for 12 cases of steel H-piles designed using WEAP in clay based on the Iowa DOT method

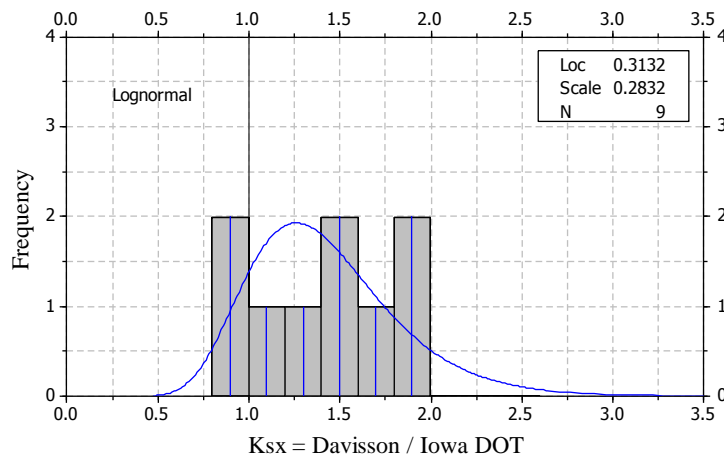


Figure 6.40: Histogram and frequency distribution of K_{sx} for nine cases of steel H-piles designed using WEAP in mixed soil based on the Iowa DOT method

6.2.4. LRFD Resistance Factors

Table 6.11 presents a summary of the preliminary, regionally calibrated LRFD resistance factors for WEAP based on five different soil input methods and also for driven steel H-piles in sand, clay, and mixed soils. The table includes the required statistical parameters that were used in the FOSM analysis: the sample size (N), mean bias (λ), standard deviation (σ), and the Coefficient of Variation (COV) for each group. The LRFD resistance factors were calculated for redundant and non-redundant pile groups, and according to Chapter 2 and 5, this was adapted by assuming $\beta=2.33$, and 3.00, respectively. In the case of clay, the preliminary resistance factors for WEAP were calculated based on SLT results attained five days after End of Driving (EOD). Hence, the values provided in Table 6.11 indirectly account for the soil setup effects on the pile capacity after an average of five days following the EOD. In Sections 6.2.10 and 6.2.11, an extensive explanation is provided for soil setup and the corresponding LRFD resistance factors in clay. Table 6.11 also includes the other essential factors that provide an indication of the accuracy and economy of each dynamic analysis method.

Table 6.11: Summary of the preliminary regionally calibrated LRFD resistance factors for WEAP using different soil input methods in different soil types

Soil Type	N	WEAP Input Method	Mean (λ)	St. Dev. (σ)	COV	$\beta=2.33$ (redundant)				$\beta=3.00$ (non-redundant)			
						ϕ^1	ϕ/λ^2	F.S. ³	F.S. _x λ^4	ϕ	ϕ/λ	F.S.	F.S. _x λ
Sand	11	ST	1.07	0.39	0.36	0.51	0.48	2.77	2.97	0.39	0.36	3.66	3.92
	11	SA	1.07	0.35	0.32	0.55	0.52	2.55	2.73	0.43	0.40	3.31	3.53
	11	BB	1.08	0.37	0.35	0.54	0.50	2.65	2.86	0.41	0.38	3.47	3.74
	11	I DOT	1.18	0.47	0.40	0.52	0.44	2.73	3.21	0.39	0.33	3.68	4.33
	11	Driven	0.97	0.37	0.38	0.45	0.46	3.16	3.07	0.34	0.35	4.21	4.09
Clay	12	ST	1.41	0.26	0.19	0.94	0.67	1.50	2.11	0.78	0.55	1.82	2.56
	12	SA	1.40	0.26	0.19	0.94	0.67	1.52	2.12	0.77	0.55	1.84	2.57
	12	BB	1.40	0.26	0.19	0.94	0.67	1.51	2.10	0.77	0.56	1.83	2.55
	12	I DOT	1.19	0.24	0.20	0.78	0.65	1.82	2.16	0.64	0.54	2.23	2.64
	12	Driven	1.42	0.27	0.19	0.95	0.67	1.50	2.12	0.78	0.55	1.82	2.58
Mixed	9	ST	1.43	0.42	0.29	0.79	0.55	1.79	2.57	0.62	0.43	2.28	3.27
	9	SA	1.47	0.46	0.31	0.78	0.53	1.81	2.66	0.61	0.41	2.32	3.42
	9	BB	1.51	0.50	0.33	0.77	0.51	1.83	2.78	0.59	0.39	2.39	3.61
	9	I DOT	1.42	0.38	0.27	0.82	0.58	1.72	2.43	0.65	0.46	2.16	3.06
	9	Driven	1.51	0.54	0.36	0.72	0.48	1.96	2.95	0.55	0.36	2.59	3.90

¹ LRFD geotechnical resistance factor for PILOT

² Efficiency factor

³ Equivalent factor of safety to ASD

⁴ Actual mean factor of safety

Table 6.11 indicates that for redundant pile groups, WEAP based on the SA method has the highest preliminary LRFD resistance factor (ϕ) in sand soils, followed by Blue Book, Iowa DOT, ST, and Driven based methods, in that order, where the ϕ values were 0.55, 0.54, 0.52, 0.51, and 0.45, respectively. The table shows that WEAP based on Driven and ST methods have the

highest ϕ in clay soils, followed by the Blue Book, SA, and Iowa DOT based methods, in that order, where the ϕ values were 0.95, 0.94, 0.94, 0.94, and 0.78, respectively. Table 6.11 also points out that the Iowa DOT and ST methods provide the highest preliminary ϕ in mixed soils, followed by the SA, Blue Book, and Driven methods, in that order, with ϕ values of 0.82, 0.79, 0.78, 0.77, and 0.72, respectively. However, in clay and mixed soils, the differences in the values of the resistance factors for different WEAP methods are not significant. A summary of the preliminary LRFD resistance factors and the corresponding efficiency factors based on a target reliability of 2.33 for sand, clay, and mixed soils are provided in Figures 6.41, 6.42, and 6.43, respectively. On the other hand, it was observed that the resistance factors were reduced by an average of 20% for non-redundant pile groups when compared to those of redundant piles.

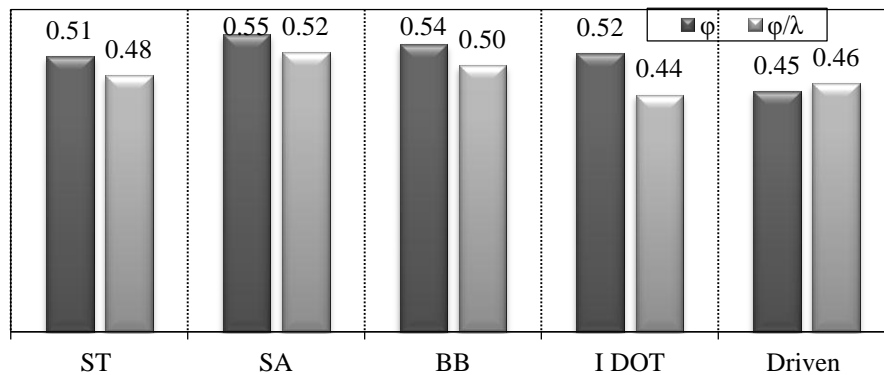


Figure 6.41: Summary of the preliminary LRFD resistance factors of WEAP and the corresponding efficiency factors based on a target reliability of 2.33 for sand soil

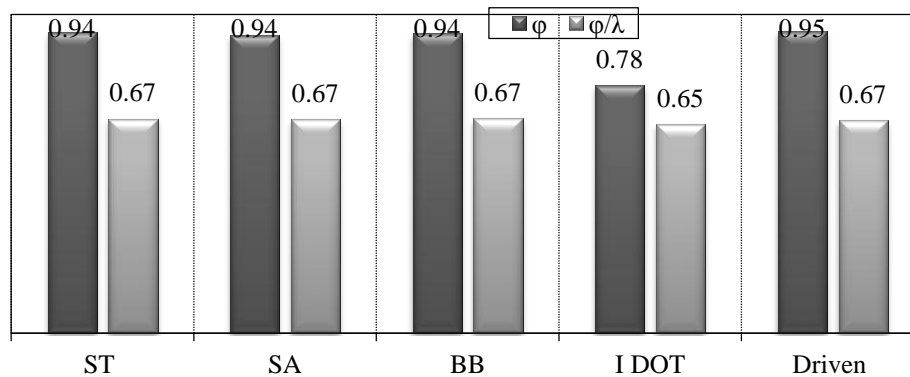


Figure 6.42: Summary of the preliminary LRFD resistance factors for WEAP and the corresponding efficiency factors based on a target reliability of 2.33 for clay soil

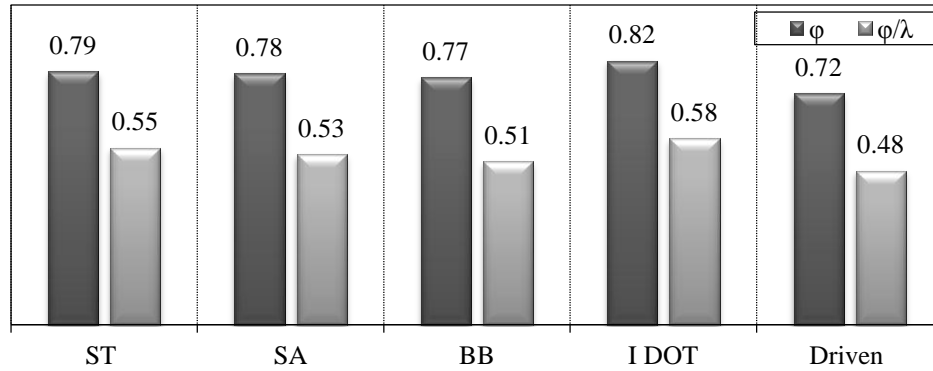


Figure 6.43: Summary of the preliminary LRFD resistance factors for WEAP and the corresponding efficiency factors based on a target reliability of 2.33 for mixed soil

6.2.5. Sensitivity to Reliability Index

A sensitivity analysis was conducted to determine the effect of changing the target reliability index (β) on the preliminary LRFD resistance factors. As shown in Figure 6.44 for sand soils, the resistance factors are found to be very sensitive to any slight change in the reliability index. The analysis was designed to cover a wide range of β starting from 1.5 to 4.0 in order to include all possible variations in the target reliability of bridge foundations. The same analysis was conducted for clay and mixed soils as shown in Figures 6.45 and 6.46, respectively. The design engineer can select the appropriate LRFD resistance factors corresponding to any target reliability index by using Figures 6.44, 6.45, and 6.46. As previously mentioned, however, a β of 2.33 for redundant pile groups (five piles or more for each pile cap) is recommended by the NCHRP-507 for the design of bridge pile foundations.

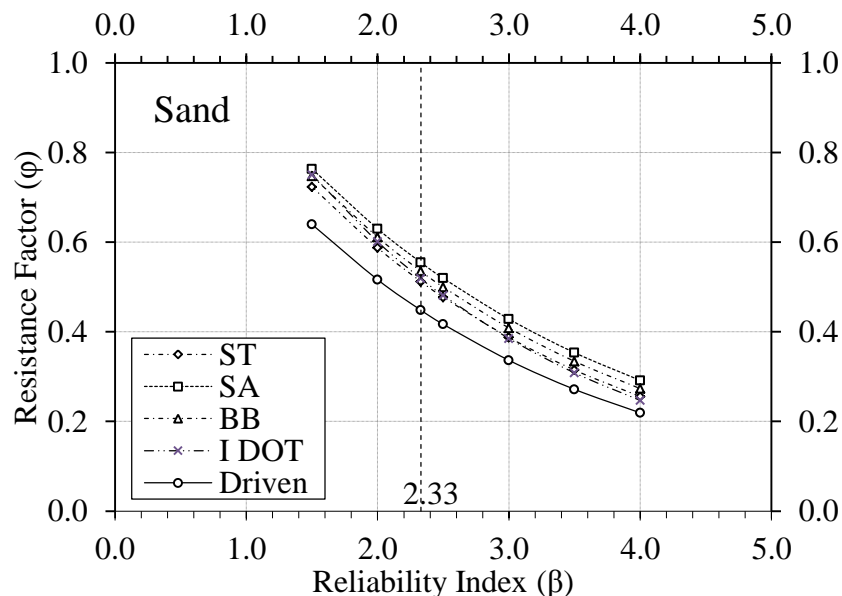


Figure 6.44: Preliminary LRFD resistance factors for WEAP corresponding to a wide range of reliability indices in sand soils

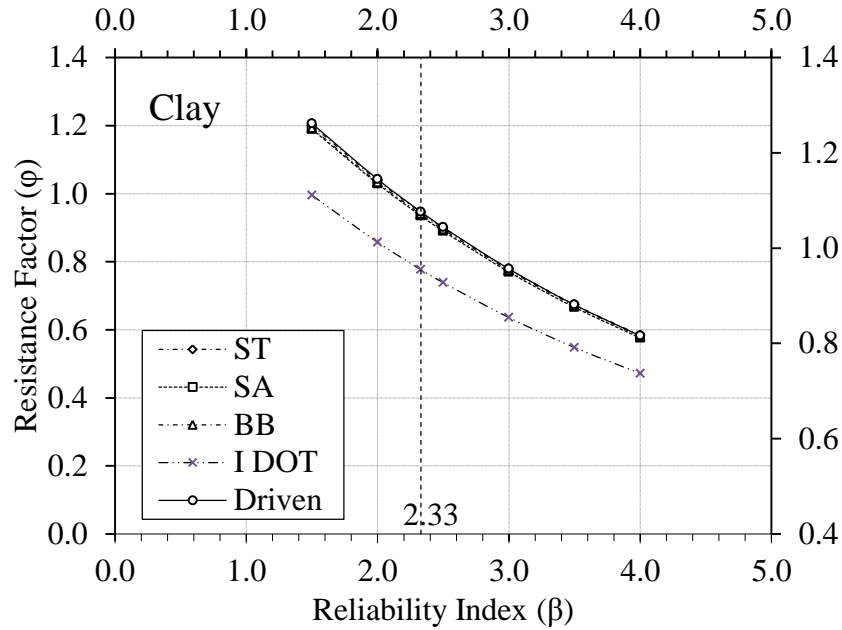


Figure 6.45: Preliminary LRFD resistance factors for WEAP corresponding to a wide range of reliability indices in clay soils

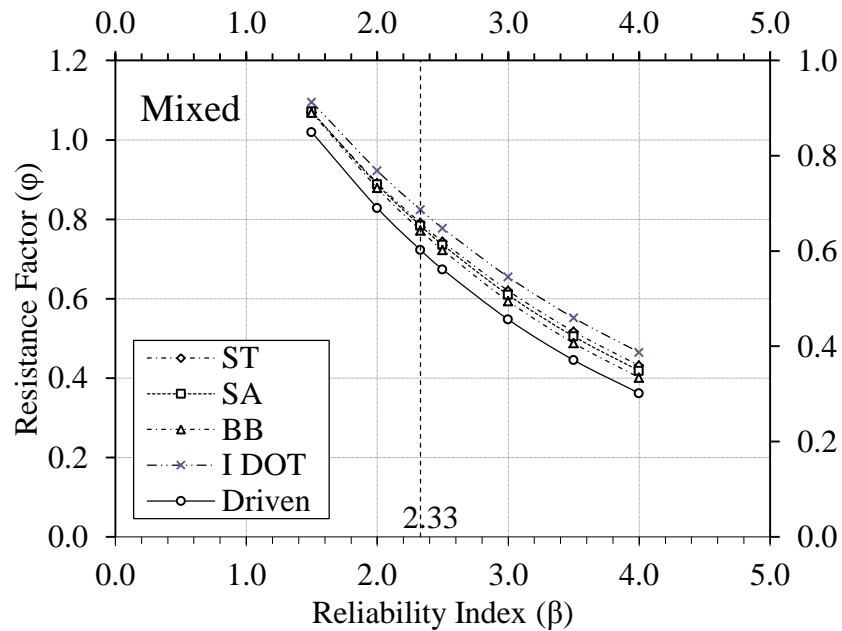


Figure 6.46: Preliminary LRFD resistance factors for WEAP corresponding to a wide range of reliability indices in mixed soils

6.2.6. Efficiency of Different Methods

The efficiency factor was calculated in order to determine the efficiency of different WEAP methods relative to the actual pile behavior under SLT, as well as to appropriately compare different WEAP input methods. This efficiency factor (ϕ/λ) is equal to the ratio of the LRFD

resistance factor to the mean bias of the method. The efficiency factor represents an indication of the bias of the WEAP capacity to the actual pile behavior, hence the economy of the WEAP method. In Table 6.11, the ϕ/λ factor was calculated for all groups and it was found that the differences among the WEAP soil input methods are not significant. However, the WEAP based on the Iowa DOT ENR soil input method is used most commonly in current practice by Iowa DOT. Figures 6.47, 6.48, and 6.49 provide the rate of change in the efficiency factors of different WEAP methods corresponding to changing the target reliability index. Therefore, the design engineer not only selects the target β based on the resistance factors, but also determines the required efficiency and economy in the design.

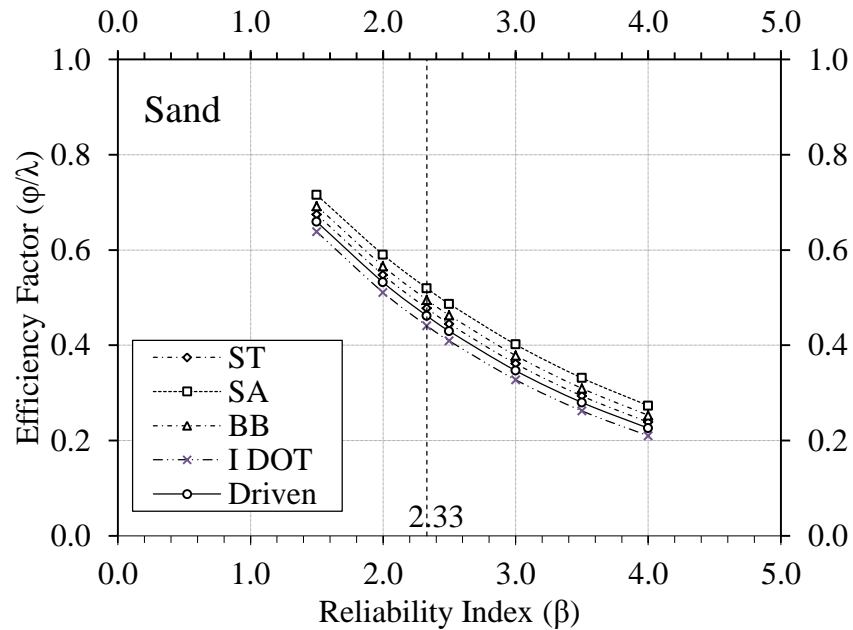


Figure 6.47: Efficiency factors for WEAP corresponding to different β in sand

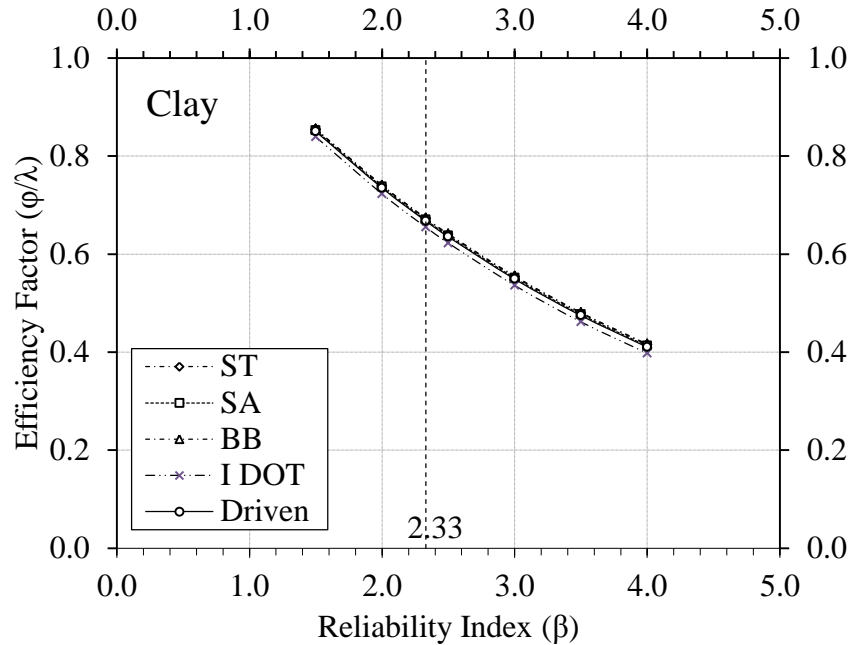


Figure 6.48: Efficiency factors for WEAP corresponding to different β in clay

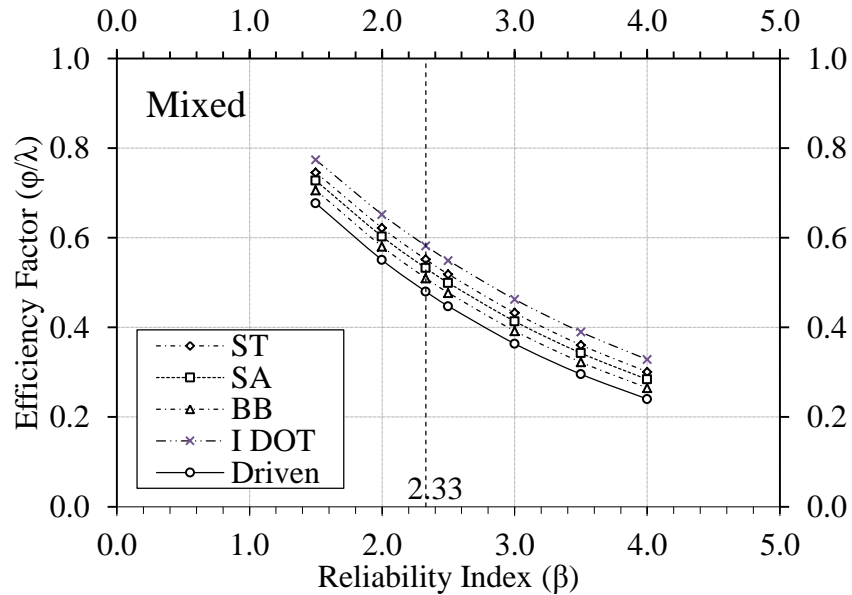


Figure 6.49: Efficiency factors for WEAP corresponding to different β in mixed soil

6.2.7. Equivalent Factor of Safety

The economy of the LRFD resistance factors can also be measured by means of the equivalent factor of safety (FS) to the ASD. This equivalent FS is calculated based on the simplified relation provided by Barker et al. (1991) as was discussed in Chapter 2. As shown in Table 6.11, the equivalent FS is presented for each subset based on a $DL/LL = 2$, $\gamma_L = 1.75$, and $\gamma_D = 1.25$, the $FS = 1.4167/\phi$. The equivalent FS should be considered while comparing the economy of a design method based on the LRFD approach relative to that based on the ASD approach. Table 6.11 shows that the equivalent FS for different WEAP methods ranges from 1.5 to 3.1 with an average

of 2.0. On the other hand, the actual FS is calculated by multiplying the mean bias by the equivalent FS. The actual FS represents the overall economy of the method, thus whenever the actual FS is lower, the foundation cost is reduced and vice versa. The back-calculated equivalent FS to the LRFD approach is less than that assumed in the ASD specifications, ranging between 2.1 to 3.2. Moreover, the equivalent FS is corresponding to a fixed and assured degree of reliability. Hence, when using the WEAP methods for the design and/or construction of bridge pile foundations in different soil types, the LRFD approach will be consistently more reliable than the ASD approach.

6.2.8. Regional Factors vs. Design Specifications

In this study, the 2008 AASHTO-LRFD specifications and the NCHRP-507 (after Paikowsky et al., 2004) were selected to be compared with the preliminary LRFD resistance factors for WEAP. Table 6.12 presents the different values of the LRFD resistance factors provided in design specifications for WEAP in comparison to the Iowa preliminary regionally calibrated factors. From Table 6.12, it can be seen that the resistance factor for the WEAP-ST based method in sand soil is approximately 28% greater than the factor provided in the 2007 AASHTO specifications. Similarly, the preliminary resistance factors in clay and mixed soils, are greater by 60% and 100%, respectively (see Table 6.12).

Table 6.12: Different values of the LRFD resistance factors provided for WEAP in design specifications versus the Iowa preliminary regionally calibrated factors

Soil Type	WEAP Soil Input Method	Iowa Preliminary Resistance Factor	AASHTO 2008 Interim	NCHRP 507 Resistance Factors
Sand	ST	0.51	0.40	0.39
	SA	0.55	N/A	N/A
	BB	0.54	N/A	N/A
	I DOT	0.52	N/A	N/A
	Driven	0.45	N/A	N/A
Clay	ST	0.94	0.40	0.39
	SA	0.94	N/A	N/A
	BB	0.94	N/A	N/A
	I DOT	0.78	N/A	N/A
	Driven	0.95	N/A	N/A
Mixed	ST	0.79	0.40	0.39
	SA	0.78	N/A	N/A
	BB	0.77	N/A	N/A
	I DOT	0.82	N/A	N/A
	Driven	0.72	N/A	N/A

6.2.9. Examination of the Resistance Factors

For the 10 piles tested in the field, the nominal design capacities were back-calculated using WEAP, and the recently developed preliminary LRFD resistance factors were applied to these values to determine the factored design capacities. The nominal and the factored design capacities calculated using WEAP analysis were then compared to the actual capacity of the piles measured in the field during the SLT. This was done in order to monitor the performance as well as validate the usage of preliminary resistance factors and assist in developing the final recommendations.

Figure 6.50 presents the calculated nominal and factored capacities of the test pile at Clarke County (clay site) using five different WEAP soil data input methods and SLT using Davisson's criterion. For WEAP, the factored capacities were calculated based on the regionally calibrated resistance factors. On the other hand, the 2007 AASHTO recommended resistance factor of 0.8 was used for calculating the actual factored capacity measured from the SLT, as the variability of the test site was assumed to be low.

Figure 6.50 shows the WEAP based on Iowa DOT ENR provided the highest nominal capacity of 166 kips, and vice versa for WEAP based on Driven. However, all methods were conservative and did not exceed the actual nominal capacity attained from the SLT. After multiplying the WEAP nominal capacities by the LRFD resistance factors, the WEAP-ST based method provided the highest and most efficient capacity of 136 kips in comparison to the SLT capacity of 194 kips, along with other WEAP methods. As a preliminary conclusion, the developed LRFD resistance factors increased the degree of reliability and economy of WEAP, providing a consistent range of pile design capacities in clay soils, with no large variation from one method to another.

Figures 6.51 and 6.52 represent the same comparison between the predicted nominal and factored pile capacities using different WEAP methods versus the measured pile capacities from SLT, and that for Cedar and Poweshiek Counties (Sand and Mixed soils), respectively. It is clear from the figure that the same previously mentioned behavior was almost observed, indicating that the regionally developed LRFD resistance factors for Iowa soils seemed appropriate for sand and mixed soils. Table 6.13 summarizes the 10 field tests' ID numbers, location, average soil formation, measured nominal capacities from SLT using Davisson's criterion, as well as the predicted nominal capacities using different WEAP analysis soil data input methods.

After comparing the capacity from WEAP to that of the field measured, and after applying the recently developed resistance factors, it was found that WEAP was relatively conservative compared to SLT based on Davisson's criterion. However, it was found that the WEAP based on Iowa DOT, SA, and ST methods seemed to be, overall, less conservative compared to Driven methods. Overall, this degree of conservatism associated with the LRFD was relatively low compared to the conventional ASD approach and its factor of safety. Consequently, the preliminary regionally calibrated LRFD resistance factors for Iowa were found to provide a reliable and economic design and can be used in developing final recommendations.

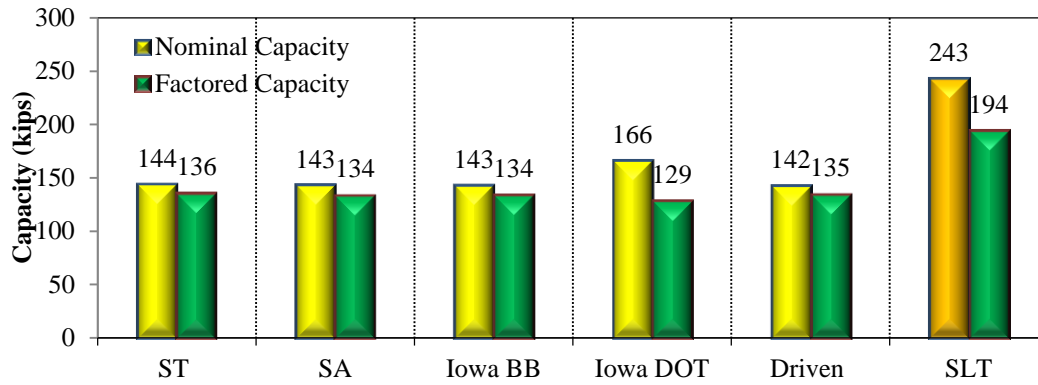


Figure 6.50: Nominal and Factored pile design capacities using WEAP different soil input methods and compared to SLT results for Clarke – Clay soil

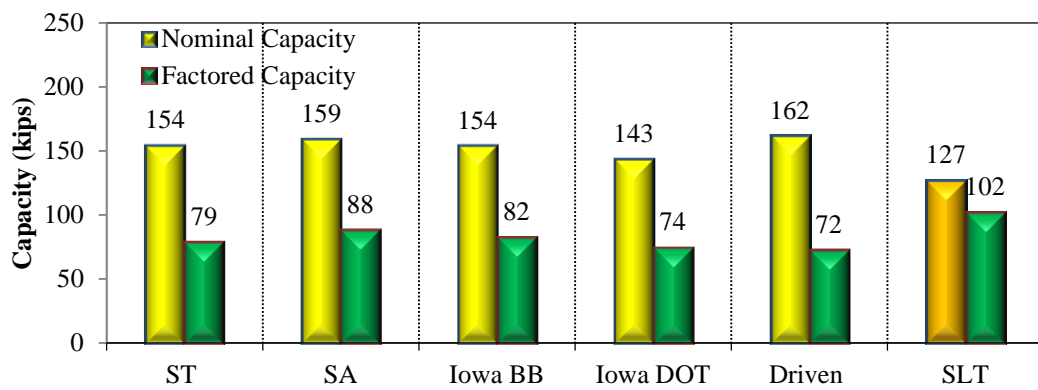


Figure 6.51: Nominal and Factored pile design capacities using WEAP different soil input methods and compared to SLT results for Cedar – Sand soil

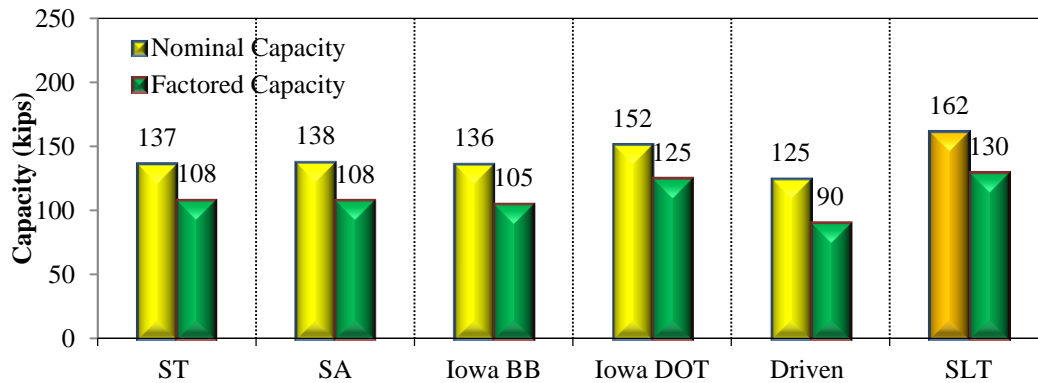


Figure 6.52: Nominal and Factored pile design capacities using WEAP different soil input methods and compared to SLT results for Poweshiek – Mixed soil

Table 6.13: Summary of the 10 field tests' ID, location, average soil formation, measured nominal capacities, and predicted nominal capacities using WEAP

County	ID	Soil Type	Pile Capacity (kips)	Nominal WEAP Capacity (kips)				
				ST	SA	BB	I DOT	Driven
Mahaska	ISU-1	Mix	212	107	102	106	117	131
Mills	ISU-2	Clay	125	77	77	77	95	78
Polk	ISU-3	Clay	150	82	82	82	92	82
Jasper	ISU-4	Clay	154	98	95	95	115	95
Clarke	ISU-5	Clay	243	144	143	143	166	142
Buchanan	ISU-6	Clay	212.6	135	138	140	164	135
Buchanan	ISU-7	Mix	53	8	9	9	10	13
Poweshiek	ISU-8	Mix	162	137	138	136	152	125
Des Moines	ISU-9	Sand	158	178	160	166	155	184
Cedar	ISU-10	Sand	127	154	159	154	143	162

Figures 6.53 and 6.54 provide a better illustration of the LRFD resistance factors' performance and summarize the previous observations. As shown in Figure 6.53, the x-axis represents the measured pile nominal capacity for the 10 field tests using Davisson's criterion, while the y-axis represents the nominal capacity calculated for the same 10 piles using WEAP methods. As can be observed from the figure, the points are mainly scattered below the neutral line, meaning that WEAP under-estimates the capacity of the piles, which is conservative. On the other hand, Figure 6.54 represents the same data only after multiplying the nominal capacities by the corresponding LRFD resistance factors. Figure 6.54 shows the factored design capacities calculated using WEAP did not exceed the actual factored capacities for any case. This indicates that the LRFD resistance factors succeeded to retain the factored capacities below the neutral line and ensured reliable designs for the 10 piles. Another observation from Figure 6.54 was that the WEAP based on Iowa DOT, SA, and ST methods provided the most economic capacities, as the points were relatively closer to the neutral line.

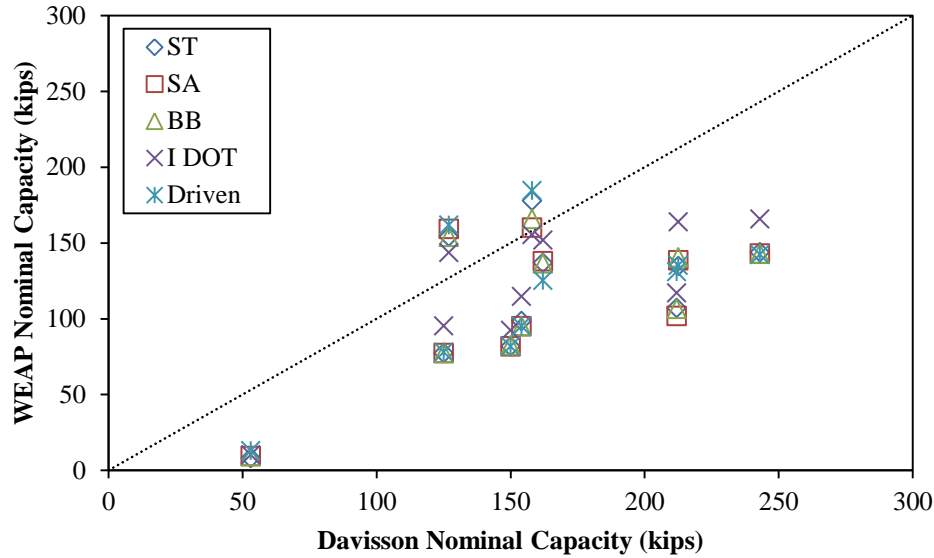


Figure 6.53: Nominal measured and calculated capacities for the 10 field tested piles using Davisson's criterion versus WEAP

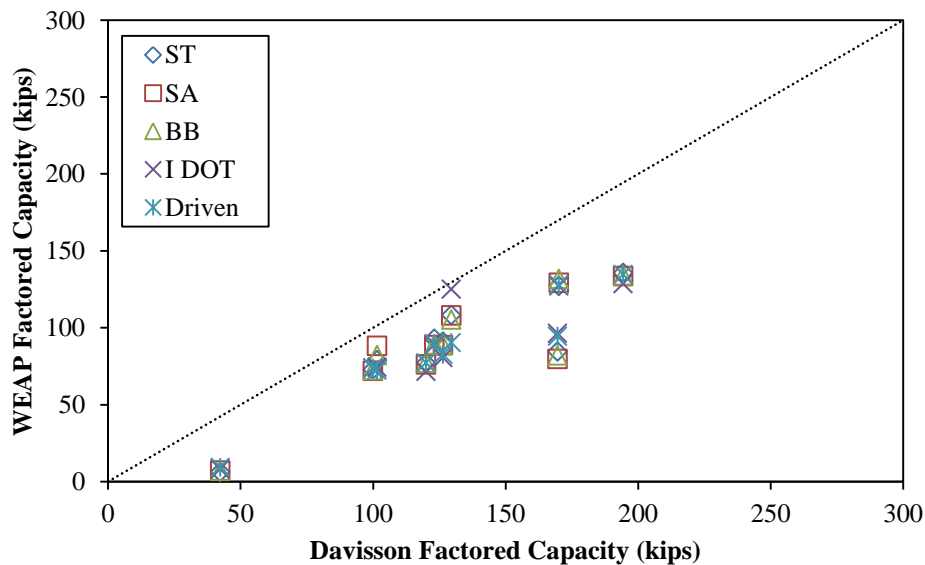


Figure 6.54: Factored measured and calculated capacities for the 10 field tested piles using Davisson's criterion versus WEAP

6.2.10. Soil Setup

Soil setup is typically investigated using dynamic analysis methods, which require field re-striking of piles several times after the end of driving (EOD). Although some engineers have considered pile re-strikes as the routine construction practice, restrikes might not be practical or economical. Due to limited database available for accurate soil setup estimations, a full-scale steel H-pile test program was conducted by Iowa State University that performed pile re-strikes shortly after EOD and pile responses were recorded using the Pile Driving Analyzer before executing static load tests. From the test program, we developed a new and practical soil setup equation in terms of the commonly used Standard Penetration Test N-value, initial pile capacity estimated at EOD (R_{EOD}) using either Wave Equation Analysis Program (WEAP) or CAsE Pile

Wave Analysis Program (CAPWAP), and an initial time of 1 minute at EOD (t_{EOD}). This soil setup equation integrates the stratigraphy of different clay layers along a pile by weighting the SPT N-value (N_i) at each clay layer (i) by its thickness (ℓ_i) for a total of n clay layers, which defines the average SPT N-value (N_a) given by Eq. [6.1]. Three soil input procedures used in WEAP analysis: SA, IA Blue Book and Iowa DOT, were selected for soil setup evaluations. Ng et al. (2012a) has explicitly described the development and verification of the soil setup method given by Eq. [6.2]. The amount of pile setup (R_{setup}) at any time (t) is the difference between the final pile capacity (R_t) and the pile capacity at EOD (R_{EOD}) given by Eq. [6.3].

$$N_a = \frac{\sum_{i=1}^n N_i \ell_i}{\sum_{i=1}^n \ell_i} \quad [6.1]$$

$$\frac{R_t}{R_{EOD}} = \left[\frac{a \log_{10}\left(\frac{t}{t_{EOD}}\right)}{(N_a)^b} + 1 \right] \left(\frac{L}{L_{EOD}} \right) \quad [6.2]$$

$$R_{setup} = R_t - R_{EOD} \quad [6.3]$$

where

- R_t = estimated pile capacity at time t , kip;
- R_{EOD} = estimated pile capacity at EOD, kip;
- t_{EOD} = time at EOD (assumed 1 second), sec;
- N_a = Average SPT N-value;
- N_i = SPT N-value at clay layer i ;
- ℓ_i = thickness of clayey soil layer i where the SPT N-value is taken;
- L = pile penetration at time t , ft;
- L_{EOD} = pile penetration at EOD, ft;
- a = method dependent scale factor (see Table 6.14); and
- b = method dependent concave factor (see Table 6.14).

Table 6.14: Method dependent scale factors and concave factors for Eq. 6.2

Methods	Scale Factor, a	Concave Factor, b	Coefficient of Determination, R^2
WEAP-SA	0.217	0.141	0.472
WEAP-Iowa Blue Book	0.215	0.144	0.523
WEAP-Iowa DOT	0.246	0.192	0.264
CAPWAP	0.432	0.606	0.968

If the pile is not re-tapped or there is no additional penetration that occurs after EOD, the ratio of L and L_{EOD} shall be reasonably assumed as unity. Eq. [6.2] shows that an increase in pile capacity is inversely proportional to SPT N-values. In other words, a pile embedded in a denser, clayey soil with a higher average SPT N-value will experience a smaller gain in capacity. The constant scale factor (a) and concave factor (b) are the empirical coefficients of a power regression line established from the correlation study in pile setup factor and N_a . Among the three soil input procedures for WEAP, the IA Blue Book procedure with the highest coefficient of determination (R^2) of 0.523 is recommended for the pile setup estimation using Eq. [6.3]. Comparing with WEAP, CAPWAP provides the best method for estimating a pile setup using Eq. [6.3].

In addition, the method was expanded by developing soil setup design charts in terms of corrected normalized pile capacity $((R_t/R_{EOD}) \times (L_{EOD}/L))$ based on a range of average SPT N-value (N_a) ranging from 1 to 50 and a time lapsed (t) of 1 day, 3 days, 5 days, 7 days, 14 days, 21 days, and 30 days after EOD, as shown in Figure 6.55. The purpose of these setup design charts is to provide pile designers a quick and convenient approach to realistically estimating the increase in pile capacity using WEAP and CAPWAP.

6.2.11. LRFD Considering Soil Setup

Incorporating soil setup improves pile capacity estimation and achieves an economical pile design. Thus, it is indispensable to consider soil setup in the context of the LRFD. Using all usable data points from the PILOT and/or from the ISU field tests, we determined the LRFD parameters, as given in Table 6.15 for WEAP based on the three soil input procedures, at four conditions: (1) end of driving (EOD); (2) normal (see definition below); (3) beginning of re-strike (BOR) on the last dynamic test; and (4) pile setup capacity estimated using Eq. [6.2]. The LRFD parameters at the first condition (EOD) were determined by comparing the estimated pile capacity at EOD using WEAP ($R_{EOD/WEAP}$) or CAPWAP ($R_{EOD/CAPWAP}$), with the measured pile capacity using SLT at EOD ($R_{EOD/SLT}$). The measured pile capacity at EOD was estimated from the measured capacity at time t ($R_{t/SLT}$) using Eq. [6.2]. This approach eliminates the effect of pile setup and provides the best estimates of LRFD parameters at EOD. The second condition is a normal approach that was implemented by Paikowsky et al. (2004) and adopted by AASHTO (2007) based on the measured pile capacity at any time t . This approach was initially used in Section 6.2.4 for the LRFD calibrations. Because clay soil exhibits pile setup and increases pile capacity with time, the LRFD calibration procedure generates unreasonably high resistance factors (possibly greater than one) that indirectly incorporates the setup as illustrated in Table 6.15. For example, the resistance factor for IA Blue Book procedure increased from 0.65 at EOD to 1.01 at normal condition for β_T of 2.33. This increase is mainly due to the effect of pile setup. For the third condition, LRFD calibrations were also performed based on field re-strike test results, specifically at the beginning of re-strike (BOR) of the last dynamic test. This condition is applicable when the last re-strike is conducted at a time closer to a static load test. To avoid physical and uneconomical pile re-strikes, pile setup can be estimated using Eq. [6.3] and incorporated into LRFD (refer to Section 5.6 in Vol. II). Recognizing different uncertainties associated with the EOD and the setup components, different resistance factors (ϕ_{EOD} and ϕ_{setup}) were established and incorporated in the LRFD framework as given by Eq. [6.4] rather than using a single resistance factor for both components based on the second condition.

$$\gamma Q \leq \phi_{EOD} R_{EOD} + \phi_{setup} R_{setup} \quad [6.4]$$

where

γ = load factor;

Q = applied load, kips;

R_{EOD} = estimated pile capacity at EOD, kips;

R_{setup} = estimated pile setup capacity, kips;

ϕ_{EOD} = resistance factor for the EOD condition (i.e., first condition); and

ϕ_{setup} = resistance factor for the setup condition (i.e., fourth condition);

Table 6.15: LRFD parameters for WEAP and CAPWAP at EOD, normal, BOR, and EOD plus setup

Method	Source	Condition	N	Soil	Soil Input Procedure	λ_R	COV _R	$\beta_T = 2.33$			$\beta_T = 3.00$			Nominal Capacity, R
								ϕ	ϕ/λ	FS	ϕ	ϕ/λ	FS	
WEAP	Iowa	1 st (EOD)	17	Clay	SA	0.922	0.157	0.65	0.71	2.18	0.54	0.59	2.61	R = R _{EOD}
					Blue Book	0.926	0.155	0.65	0.71	2.16	0.55	0.59	2.59	
					Iowa DOT	0.786	0.173	0.54	0.69	2.62	0.45	0.57	3.16	
		2 nd (Normal)	17	Clay	SA	1.475	0.176	1.01	0.69	1.40	0.84	0.57	1.69	R = R _{EOD}
					Blue Book	1.472	0.173	1.01	0.69	1.40	0.84	0.57	1.69	
					Iowa DOT	1.252	0.188	0.84	0.67	1.69	0.69	0.55	2.05	
		3 rd (BOR on Last Dynamic Test)	5	Clay	SA	0.966	0.116	0.72	0.74	1.97	0.61	0.63	2.32	R = R _{BOR}
					Blue Book	0.967	0.117	0.72	0.74	1.97	0.61	0.63	2.32	
					Iowa DOT	0.815	0.103	0.62	0.76	2.29	0.52	0.64	2.72	
		4 th (Setup using Eq. [6.2])	17	Clay	SA	0.863	0.335	0.21	0.24	-	0.19	0.21	-	R = R _{setup}
					Blue Book	0.862	0.330	0.21	0.24	-	0.19	0.22	-	
					Iowa DOT	0.615	0.235	0.26	0.43	-	0.22	0.35	-	
CAP-WAP	NCHRP	2 nd (Normal)	99	All Soils	-	1.656	0.724	0.39	0.24	3.63	0.25	0.24	5.67	R = R _{EOD}
	AASHTO	2 nd (Normal)	-	All Soils	-	-	-	0.40	-	3.54	0.32	-	4.43	R = R _{EOD}
	Iowa	1 st (EOD)	5	Clay	-	0.958	0.063	0.75	0.51	1.89	0.64	0.43	2.21	R = R _{EOD}
		2 nd (Normal)	5	Clay	-	1.328	0.169	0.92	0.69	1.54	0.76	0.58	1.86	R = R _{EOD}
		3 rd (BOR on Last Dynamic Test)	5	Clay	-	0.996	0.02	0.80	0.80	1.77	0.69	0.69	2.05	R = R _{BOR}
		4 th (Setup using Eq. [6.2])	5	Clay	-	1.006	0.179	0.37	0.37	-	0.38	0.38	-	R = R _{setup}
	NCHRP	2 nd (Normal)	37 7	All Soils	-	1.368	0.453	0.59	0.43	2.40	0.43	0.31	3.29	R = R _{EOD}
	NCHRP	3 rd (BOR) and At Least One Production Pile Per Pier	16 2	All Soils	-	1.158	0.339	0.65	0.56	2.18	0.51	0.44	2.78	R = R _{BOR}
	AASHTO	3 rd (BOR) and At Least One Production Pile Per Pier	-	All Soils	-	-	-	0.65	-	2.18	0.51	-	2.78	R = R _{BOR}

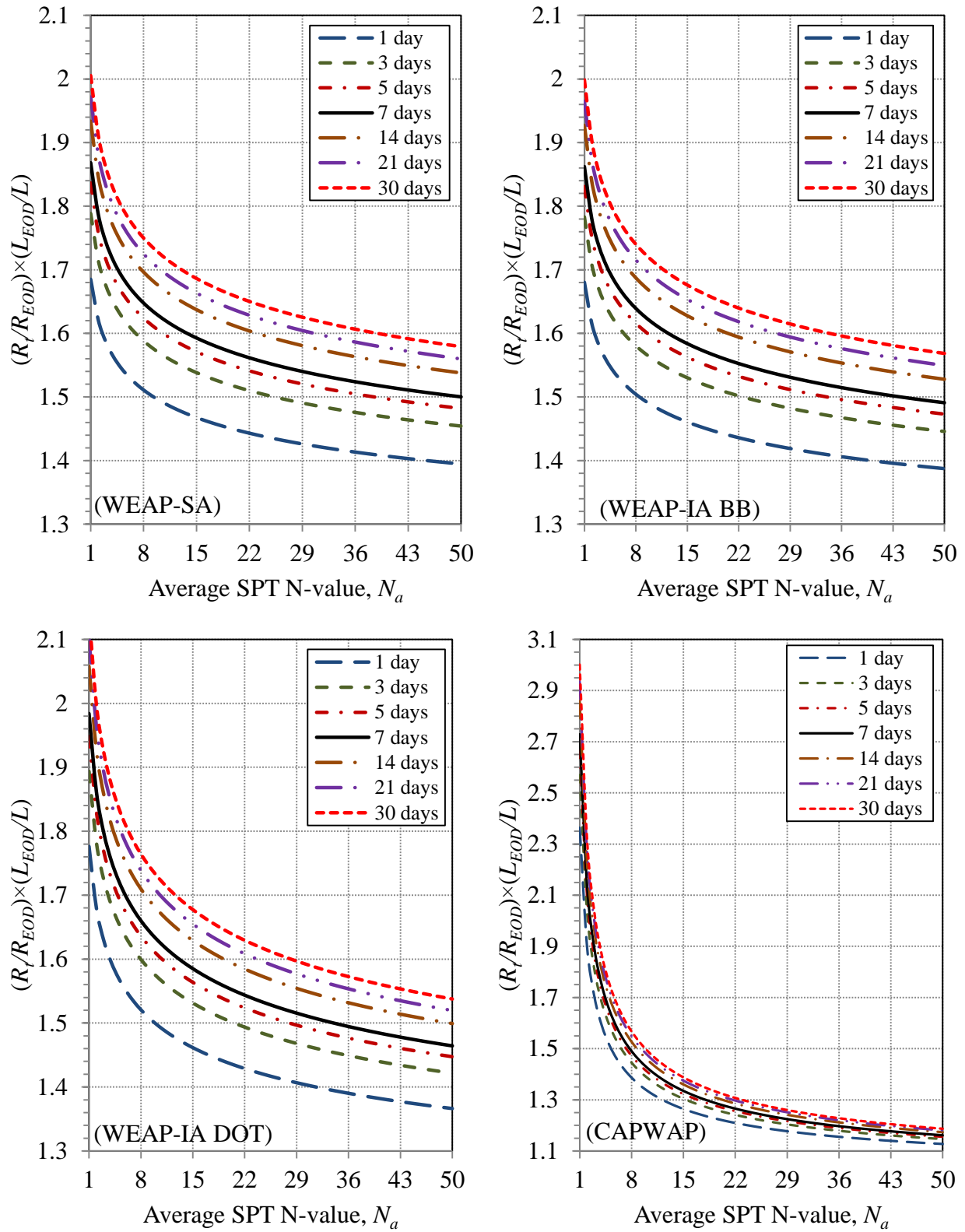


Figure 6.55: Soil setup design charts for WEAP and CAPWAP

When compared with the recommendation proposed by Paikowsky et al. (2004), which was adopted in the AASHTO (2007) LRFD specifications, the proposed combination using Eq. [6.4] improves the ϕ/λ of the steel H-pile foundation design in Iowa clay soil by about 200% and 150% for β_T of 2.33 and β_T of 3.0, respectively.

Since the historical data in PILOT database contains no PDA record for CAPWAP analysis, only five data points from the recent field tests were used in the LRFD calibrations for CAPWAP with consideration to pile setup in clay. Referring to Table 6.15, similar observations as those described above for WEAP are observed for CAPWAP. When compared with the recommendation given by Paikowsky et al. (2004), the consideration of pile setup using Eq. [6.4] improves the efficiency factors of the steel H-pile foundation design in clay soil. When comparing the corresponding resistance and efficiency factors for setup with those of WEAP, CAPWAP is found to be a better method for accounting pile setup.

6.2.12. Construction Control

6.2.12.1. Introduction and Framework

Construction control involves procedures and methods for nondestructive verification of designed pile capacity during construction. As noted, the Iowa DOT currently uses the Iowa in-house method based on the Blue Book (originally written by Dirks and Patrick Kam, 1989) to design piles, and uses WEAP as a construction control method to verify the designed pile capacity during construction. If the desired pile capacity is not attained at the end of driving and during retap, pile extensions will be needed to increase the pile lengths. This adjustment will result both cost increment and significant delays in construction. Besides ascertaining that the pile achieves its designed capacity, the construction control method is used to detect the pile integrity and any possible pile damage. To improve the accuracy of pile capacity and cost estimations during the design stage as well as to ensure an adequate pile performance, the construction control method using WEAP is desired to be integrated as a part of the design procedures. For a practical purpose, the Iowa DOT soil profile input procedure used in WEAP, as explicitly described in Volume II by Ng et al. (2011), is selected for the following construction control evaluation and analysis. Data from both PILOT and field tests were combined and used in the analysis. The total available data points for clay, mixed, and sand profiles were 13, 14 and 15, respectively. The construction control evaluation at the end of driving (EOD) condition was considered for clay, mixed, and sand soil profiles, where the construction control evaluation, including setup consideration, was accounted only for clay. As similarly suggested by Paikowsky et al. (2004), a framework was developed to account for the two construction control conditions by determining a construction control factor (ξ_{EOD}) at EOD and a construction control factor for considering soil setup (ξ_s). The factors were multiplied to the resistance factors (ϕ) originally developed for the Iowa Blue Book and the nominal capacity (R) estimated using Blue Book as given by Equation [6.5] to adjust the designed pile capacity for the construction control considerations.

$$\gamma Q < \xi_s \xi_{EOD} \phi R, \text{ or } \Pi \xi \phi R \quad [6.5]$$

where

- ξ_s = Construction control factor for considering soil setup;
 ξ_{EOD} = Construction control factor at the end of driving condition;
 $\Pi\xi$ = Product of all construction control factors;
 ϕ = Originally developed resistance factor for Iowa Blue Book; and
 R = Nominal pile capacity estimated using Iowa Blue Book.

6.2.12.2. Determination of Construction Control Factors at EOD Condition

Figure 6.56 shows the cumulative probability distribution curves of the ratio of the factored pile capacity predicted using WEAP to that predicted by the Iowa Blue Book method for clay, mixed, and sand soils at the EOD condition, respectively. The originally developed resistance factors used in calculating the factored capacities for WEAP and Blue Book are listed in Table 6.16. The cumulative probability at the y-axis indicates the chance that the factored pile capacity predicted by WEAP will be less than that predicted by the Iowa Blue Book. The straight line is the theoretical, cumulative, normal distribution of the data and the variation in the data points reflected that it is not a perfect normal distribution. The two curved lines in between the straight lines represent the 95% confidence interval of the theoretical normal distribution. Figure 6.56 shows that all the data points fall within the 95% confidence interval. Thus, the theoretical normal distribution lines can be confidently used to determine the WEAP/Blue Book ratio at the corresponding desired cumulative percentage. To minimize the average discrepancy in the factored pile capacities of WEAP and Iowa Blue Book methods, a cumulative value of 50% was chosen.

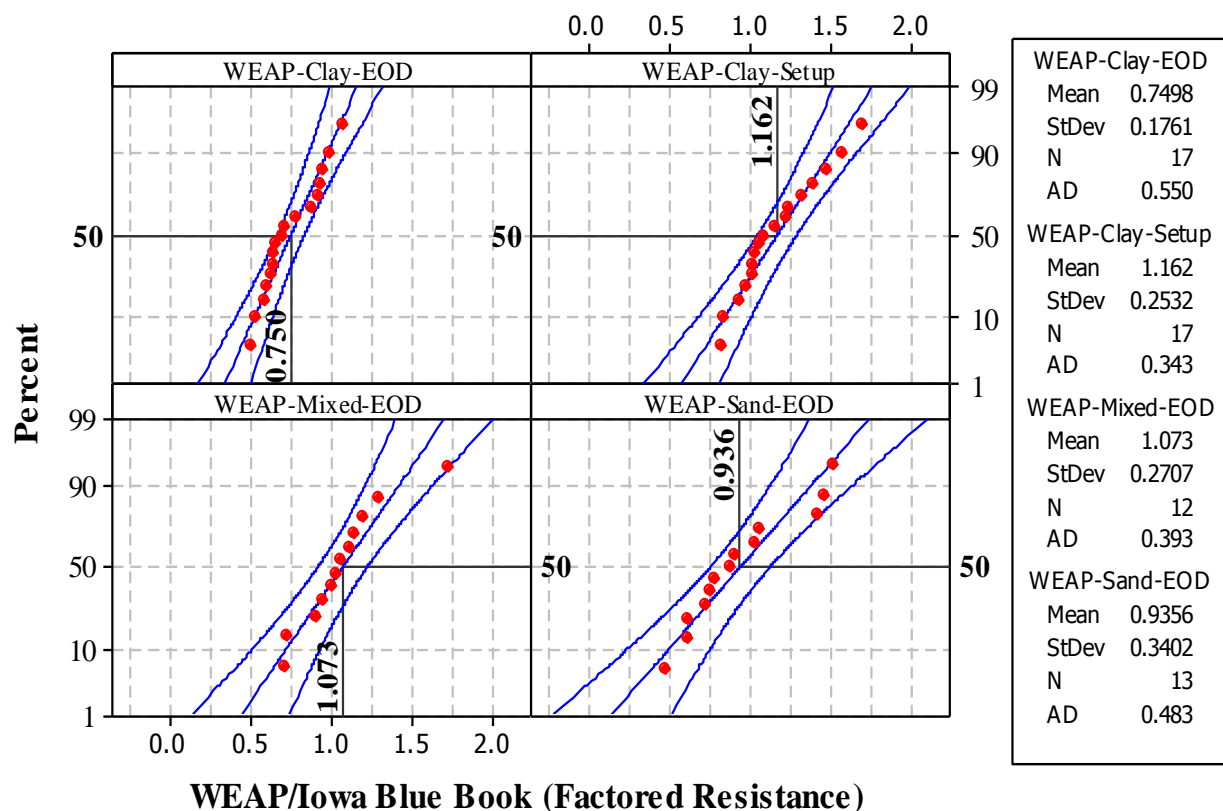


Figure 6.56: Cumulative distribution of the ratio of WEAP to Iowa Blue Book

Based on the theoretical normal distributions as shown in Figure 6.56, the ratios of the WEAP and the Blue Book for clay, mixed, and sand soils at EOD are determined as 0.75, 1.073, and 0.936, respectively, at the desired cumulative value of 50%. The estimated ratio is defined as the construction control factor at EOD condition (ξ_{EOD}). Applying the construction control factor (ξ_{EOD}) to the factored capacity (ϕR), estimated using Iowa Blue Book, reduces the mean ratio of WEAP and Iowa Blue Book to unity as illustrated in Figures 6.57, 6.58, and 6.59.

Table 6.16: The original resistance factors used in calculating the designed pile capacities

Soil Profiles	Methods	Original Resistance Factor, ϕ
Clay	Iowa Blue Book	0.63
	WEAP for EOD	0.65
	WEAP for Setup	0.21
Mixed	Iowa Blue Book	0.60
	WEAP at EOD	0.80
Sand	Iowa Blue Book	0.55
	WEAP at EOD	0.54

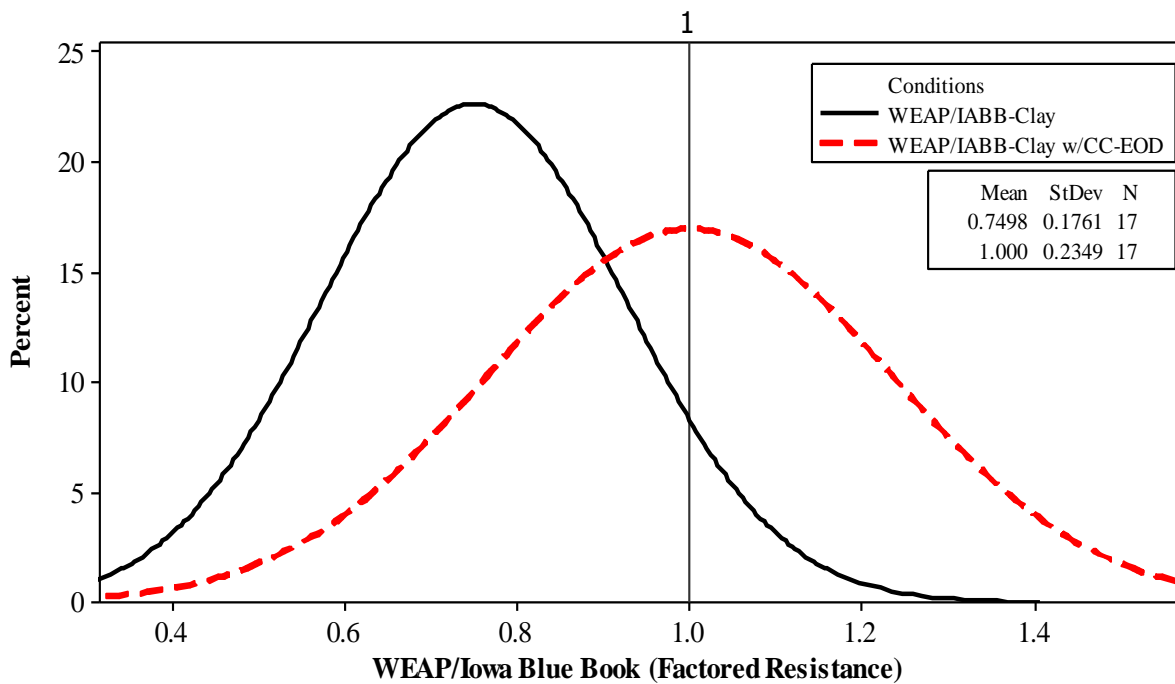


Figure 6.57: Normal distribution comparison for clay before and after considering construction control at EOD condition

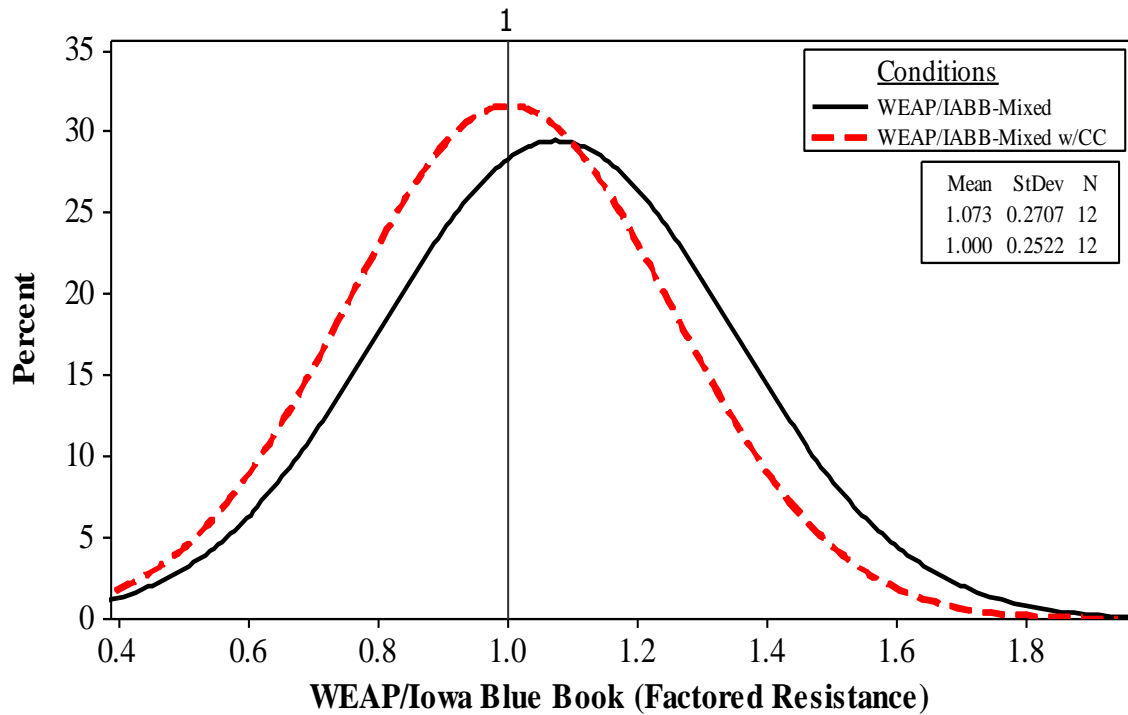


Figure 6.58: Normal distribution comparison for mixed soil before and after considering construction control at EOD condition

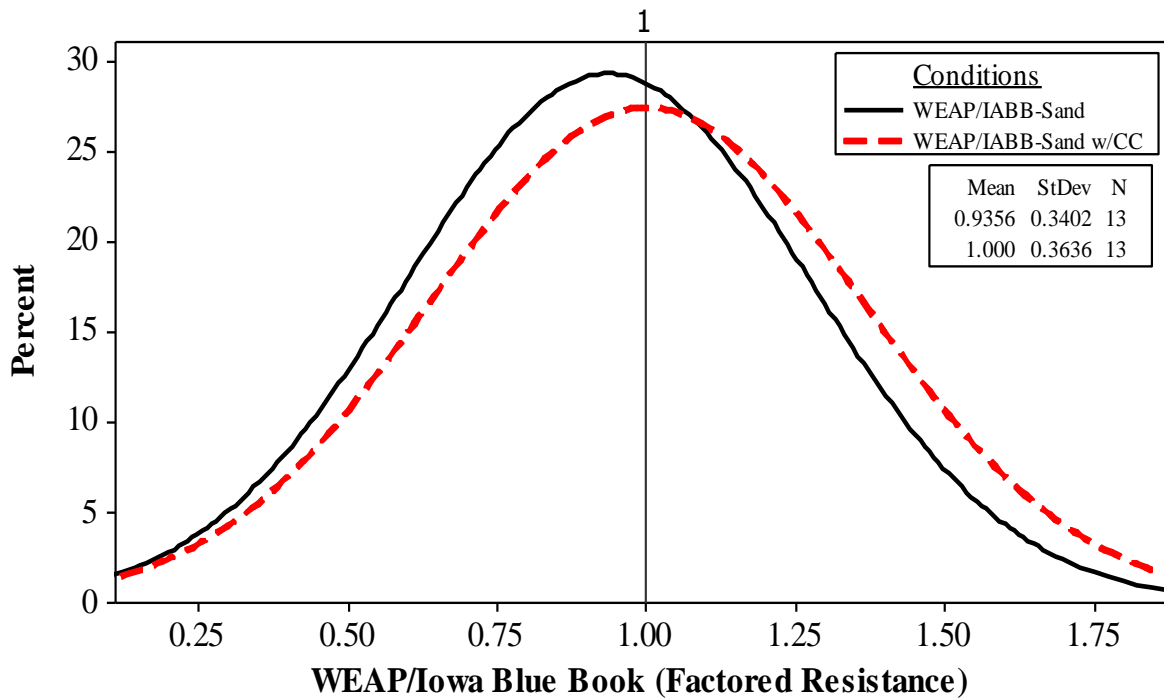


Figure 6.59: Normal distribution comparison for sand soil before and after considering construction control at EOD condition

6.2.12.3. Additional Construction Control Factors for Soil Setup in Clay

To account for soil setup in clay during design, a cumulative probability distribution for the ratio of design capacities estimated using WEAP with setup consideration, to that estimated using Iowa Blue Book as shown in Figure 6.56 was used to estimate the additional construction control factor for soil setup (ξ_s). Note that the estimated pile resistance from Iowa Blue Book has been corrected by accounting for the construction control correction at EOD. Similar to the EOD condition, the cumulative value of 50% is chosen to minimize the difference in design capacities with setup consideration between WEAP and Iowa Blue Book. The corresponding ratio is defined as the additional construction control factor for soil setup (ξ_s) and is determined to be 1.162. After applying the ξ_s , the normal distribution improves, the mean ratio reduces towards unity, and the standard deviation reduces from 0.242 to 0.235 as illustrated in Figure 6.60.

6.2.12.4. Maximum Limits for Construction Control Factors

After applying the desired construction control factors to the originally calculated factored capacity (ϕR) using Iowa Blue Book method, it is intuitively believed that the revised factored capacity ($\Pi \xi \phi R$) remains adequately smaller than the measured capacity determined from a static load test. The reason for this belief is that the resistance factors for WEAP were calibrated from the same measured pile capacity used in the resistance factor calibrations for Iowa Blue Book. Another reason being the fact that WEAP will be specified during construction to verify the pile capacity estimated using Iowa Blue Book during design stage and to ensure the design pile capacity does not exceed the measured pile capacity. The original target reliability index (β_T) of 2.33 reduces with increasing effective resistance factors ($\Pi \xi \phi$) while maintaining the same values for the other parameters as illustrated using the First Order, Second Moment (FOSM) relationship given in Eq. 6.6. The reduction in the β_T increases the probability of failure, and therefore, it is desired to set a maximum limit to the recommended construction control factors ($\Pi \xi$).

$$\beta_T = \frac{\ln \left[\lambda_R \left(\frac{\gamma_D Q_D}{Q_L} + \gamma_L \right) \sqrt{\frac{(1 + \text{COV}_D^2 + \text{COV}_L^2)}{(1 + \text{COV}_R^2)}} \right] - \ln \left[\frac{\lambda_D Q_D}{Q_L} + \lambda_L \right] - \ln [\Pi \xi_I \phi]}{\sqrt{\ln[(1 + \text{COV}_R^2)(1 + \text{COV}_D^2 + \text{COV}_L^2)]}} \quad [6.6]$$

The maximum factor limit is determined after considering the desired construction control factors to ensure that the design capacity estimated using the Blue Book does not exceed that estimated based on the static load test. The resistance factor used in the following analysis for the static load test method is 0.80, which was selected from the AASHTO (2010) LRFD Bridge Design Specifications.

Figure 6.61 shows the primary relationship between the factored pile capacity ratio of WEAP and Blue Book after considering the construction control correction at the EOD condition (at left y-axis) and a range of possible construction control factors (ξ_{EOD}) for clay. As similarly indicated in Figure 6.56, the desired construction control factor of 0.75 or the effective resistance factor ($\xi_{\text{EOD}} \phi$) of 0.47 is determined when the primary factored capacity ratio is equal to one. Figure 6.61 also shows the secondary relationship between the factored pile capacity ratio of

static load test and Blue Book after considering the construction control correction at EOD condition (at right y-axis) and a range of possible construction control factors (ξ_{EOD}). From this secondary relationship, the maximum limit for ξ_{EOD} of 0.79 or an effective resistance factor ($\xi_{EOD} \phi$) of 0.50 is determined when the secondary factored capacity ratio is equal to one. The application of the recommended construction control correction for clay at the EOD condition is adequate since the recommended ξ_{EOD} of 0.75 is smaller than the maximum limit of 0.79 or the recommended $\xi_{EOD} \phi$ of 0.47 is smaller than the maximum limit of 0.50.

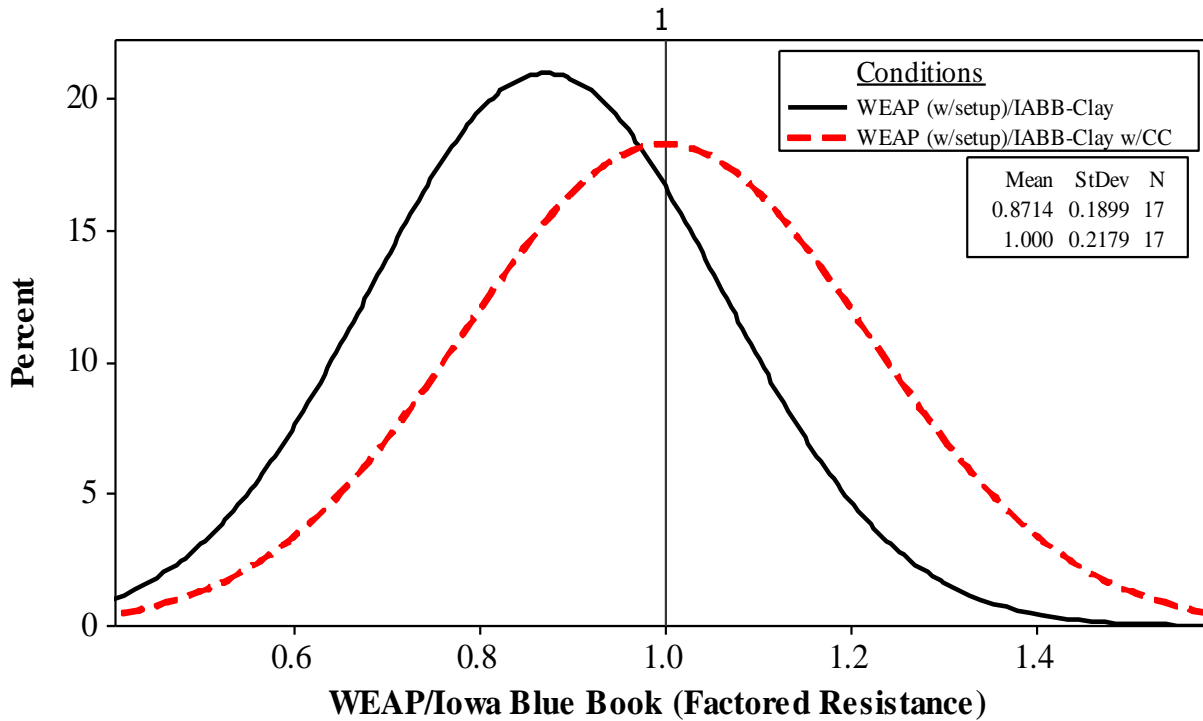


Figure 6.60: Normal distribution comparison for clay soil before and after considering additional construction control factor for soil setup

Similar to the EOD condition, Figure 6.62 shows the determination of the maximum limit for the construction control factor including soil setup ($\xi_s \xi_{EOD}$) for clay. Since the product of the recommended ξ_s and ξ_{EOD} of 0.87 is smaller than the maximum limit of 1.37 or the recommended $\xi_s \xi_{EOD} \phi$ of 0.55 is smaller than the maximum limit of 0.83, the application of the recommended construction control correction for clay at the EOD, plus setup condition is adequate. In order to determine the maximum limits of the construction control factors, similar analyses were performed for mixed soil and sand as shown in Figures 6.63 and 6.64. Figure 6.63 shows that the maximum construction control of 1.90 is greater than the recommended ξ_{EOD} of 1.07 or the maximum effective resistance factor of 1.14 is greater than the recommended $\xi_{EOD} \phi$ of 0.64. Thus, the recommended construction control correction for mixed soil at EOD condition is adequate. Likewise, the maximum limit of the construction control factor for sand is 1.34, which is greater than the recommended ξ_{EOD} of 0.94 and the recommended construction control correction for sand at EOD condition is adequate as well.

6.2.12.5. Summary and Recommendations

The purpose of performing the above mentioned construction control analyses is (1) to minimize the difference in the factored capacities estimated using the Iowa Blue Book method and WEAP as the construction control method; and (2) to account for pile performance verification using WEAP during pile design. The Iowa DOT soil profile input procedure used in WEAP is selected for the construction control evaluations and analyses. The end of driving (EOD) condition is considered for clay, mixed soil, and sand profiles, and the second condition with setup consideration is only accounted for piles in clay. A framework, given by Eq. [6.5] was developed to account for the two construction control conditions. The recommended construction control factors (ξ_s , ξ_{EOD}), the effective resistance factors ($\Pi\xi\phi$), and their maximum limits are summarized in Table 6.17 for both construction control methods, WEAP and CAPWAP.

Table 6.17: Summary of recommended parameters for considering construction control

Construction Control Method	Soil Type	Condition	Original ϕ	ξ_{EOD}	ξ_s	ξ_{BOR}	$\Pi\xi < \text{Limit}$	Revised ϕ	%Gain
WEAP	Clay	EOD+ setup	0.63	0.75	1.16		$0.87^a < 1.32$	0.63	0%
	Mixed	EOD	0.60	1.07	1.00		$1.07 < 1.90$	0.64	7%
	Sand	EOD	0.55	0.94	1.00		$0.94^a < 1.34$	0.55	0%
CAPWAP	Clay	EOD+ setup	0.63	0.87	1.25		$1.08 < 1.37$	0.68	8%
		BOR	0.63	-	-	1.38	$1.38 > 1.27^b$	0.80	27%
	Mixed	EOD	0.60	1.40	1.00	1.40	$1.40 < 1.63$	0.80	33%
		BOR	0.60	-	-	1.18	$1.18 < 1.63$	0.71	18%
	Sand	EOD	0.55	1.46	1.00	1.46	$1.46 < 1.25$	0.69	25%
		BOR	0.55	-	-	1.06	$1.06 < 1.25$	0.58	6%

^a the minimum value of 1.00 was suggested (i.e., construction control consideration is not considered); and ^b this value was suggested so that the modified ϕ for the Iowa Blue Book does not exceed 0.80.

When considering the above-mentioned construction control in a practical application, the effective resistance factors ($\Pi\xi\phi$) will be directly applied and multiplied to the nominal pile capacity (R) estimated using the Iowa Blue Book to yield the revised factored pile capacity. When comparing the revised ϕ values with the original ϕ values for designs using Iowa Blue Book method and construction control using CAPWAP, the corresponding gains for clay, mixed soil and sand are estimated to be 8%, 18% and 6%, respectively. It is important to note that when using the revised ϕ value in pile designs, the corresponding construction control method and condition must be applied during pile installation and field verification.

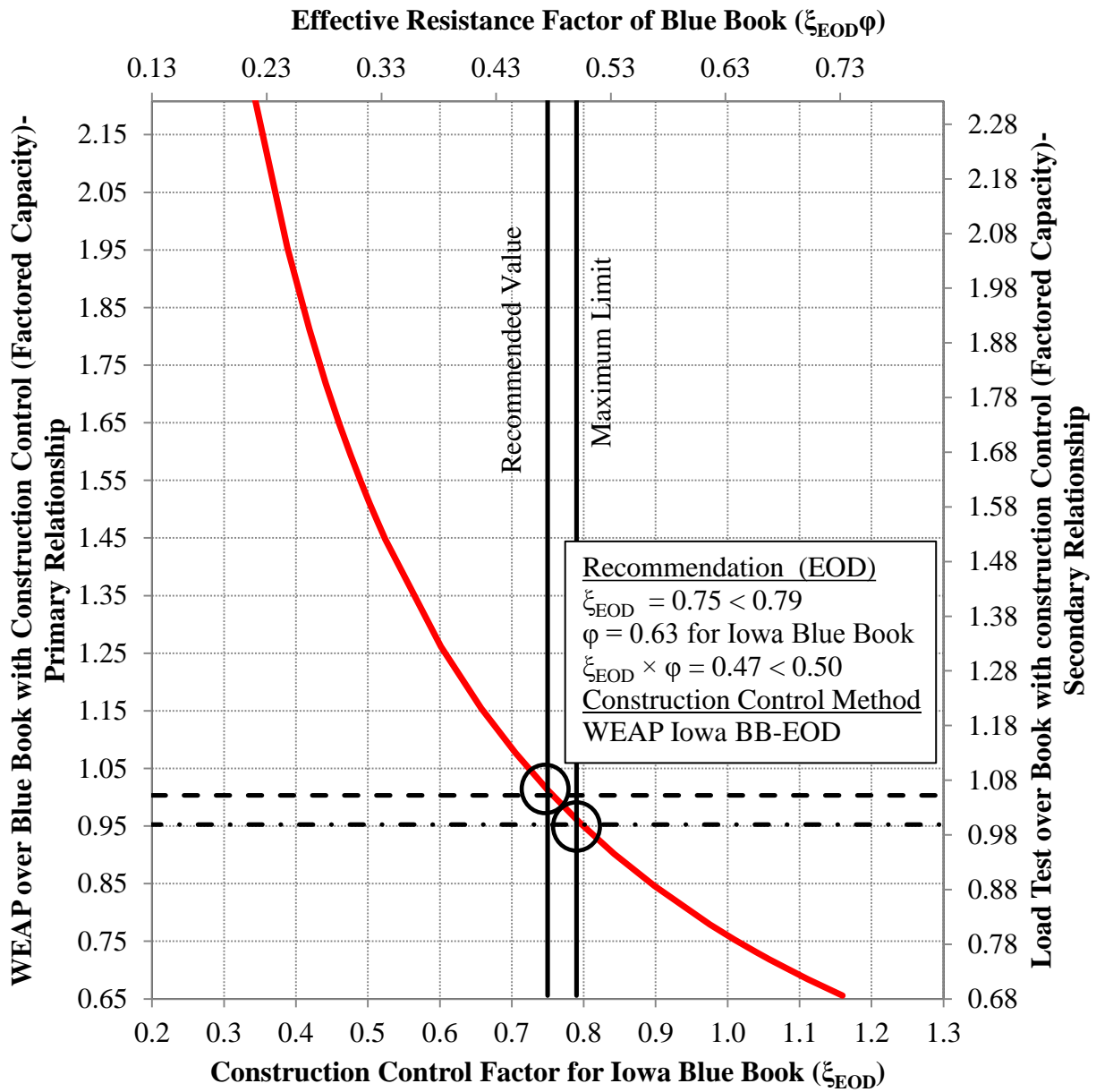


Figure 6.61: The maximum limit of the construction control factor at EOD for clay

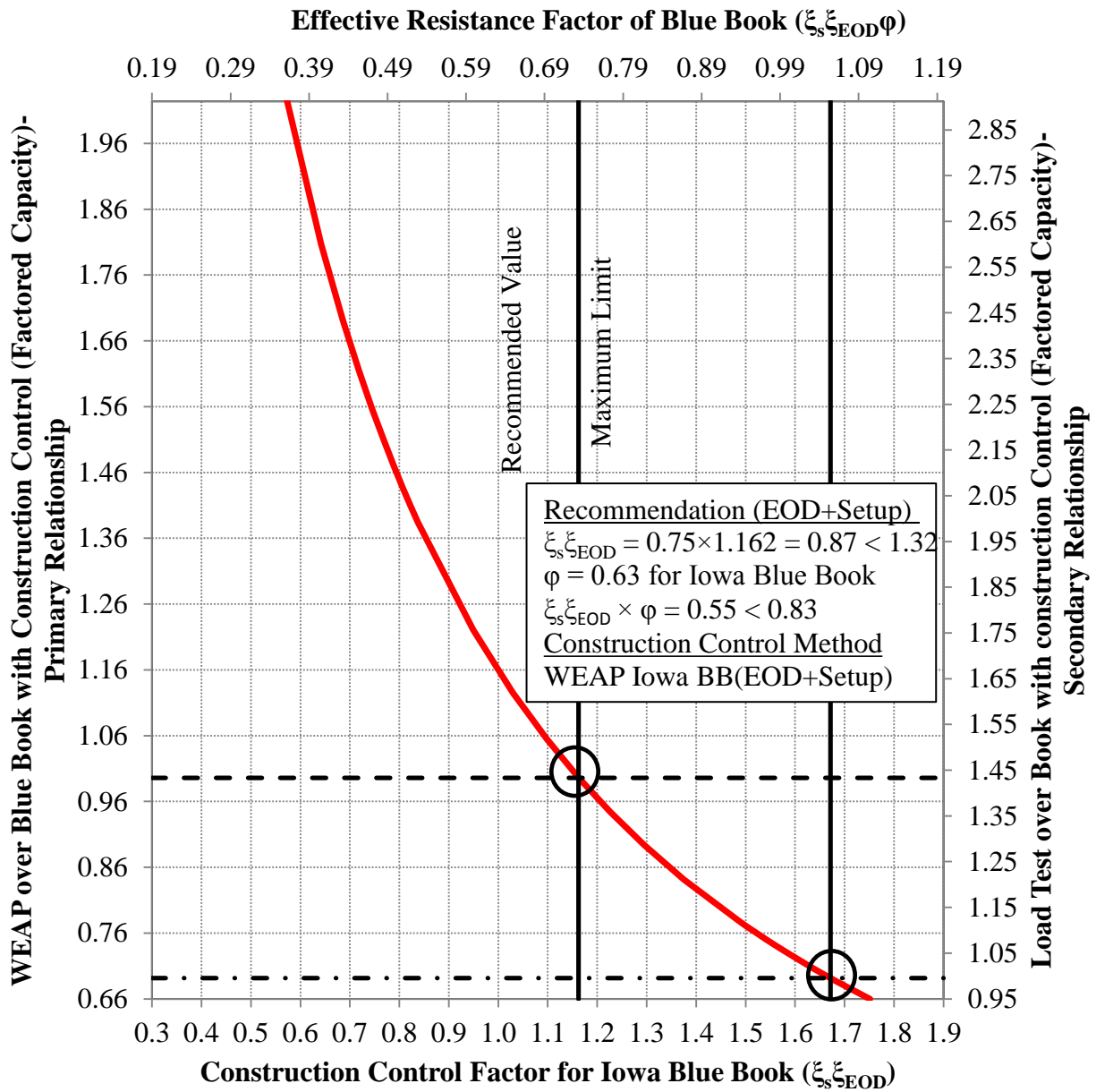


Figure 6.62: The maximum limit of the construction control factor for the EOD plus setup condition for clay

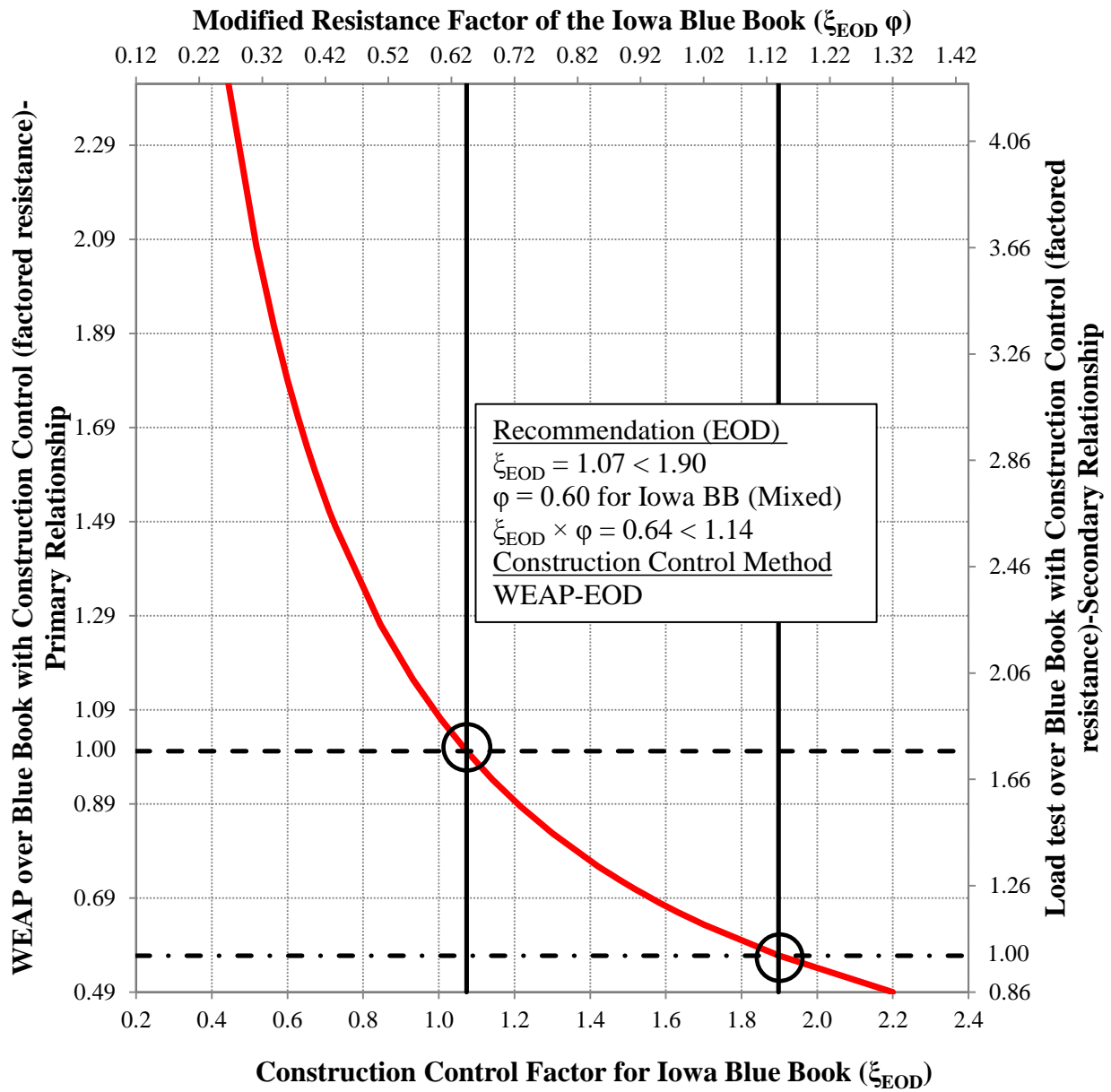


Figure 6.63: The maximum limit of the construction control factor for the EOD condition for mixed soil

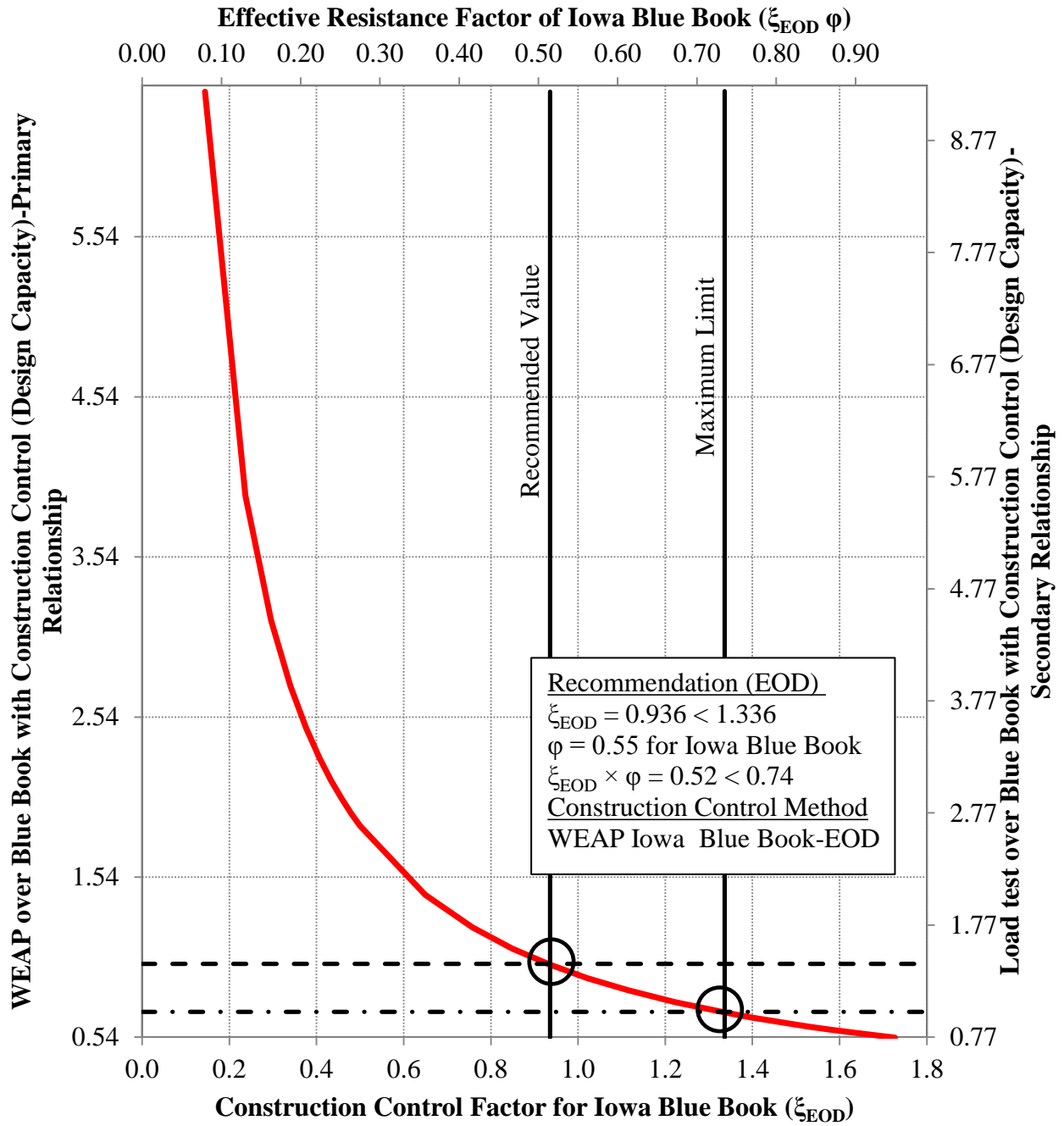


Figure 6.64: The maximum limit of the construction control factor for the EOD condition for sand soil

6.3. Dynamic Formulas

As previously introduced, seven dynamic formulas were used in this study: the Gates formula, FHWA modified Gates, ENR, Iowa DOT ENR, Janbu, PCUBC, and Washington DOT formula. All the dynamic formulas were presented in Chapter 3. The capacity of the piles from PILOT database was calculated using these dynamic formulas for all data points that had hammer and driving information necessary for analysis (i.e., 32 piles). The Davisson's criterion method was used for determining the actual nominal pile capacity from the load test results.

6.3.1. Pile Capacity

Tables 6.18, 6.19, and 6.20 represent the nominal capacity of the piles from PILOT database calculated using Davisson's criterion as well as the dynamic formulas in clay, sand, and mixed soils, respectively. As can be seen in the tables, the identification number and the representative Iowa county for each site from the database are presented and sorted according to different soil types. The tables also show the different steel H-piles sizes, as well as the time between EOD and conducting of the SLT. The number of tests available in clay, sand, and mixed soils were 12, 11, and 9, respectively. It is also important to note that the average time of performing the SLT after EOD was about five (5) days. In order to roughly compare the actual and predicted capacities for the available piles from the database PILOT, an accumulative summation of all capacities calculated using dynamic formulas was presented and compared to the actual capacities established from the SLT results (see Figure 6.65). According to Figure 6.65, it is clear that dynamic formulas tend to overestimate the pile capacity at the EOD when compared to the actual SLT results, especially the ENR formula.

Table 6.18: Nominal Davisson's capacity of the piles from PILOT as well as using different dynamic formulas in clay

ID #	County	Pile Type	L (ft)	D (kips)	Dynamic Formula Capacities (kips)						
					G ¹	F-G ²	ENR ³	IA ⁴	Janbu ⁵	PC ⁶	WS ⁷
6	Decatur	10x42	53	118	112	165	165	141	113	129	121
12	Linn	10x42	23.78	204	163	263	570	243	241	211	194
42	Linn	10x42	23.5	82	124	177	285	125	136	137	148
44	Linn	10x42	36.5	136	151	236	437	202	187	173	203
51	Johnson	10x42	29.5	190	166	268	578	213	218	187	205
57	Hamilton	10x42	57	168	137	225	211	168	150	154	150
62	Kossuth	10x42	45	100	116	157	249	107	113	109	124
63	Jasper	10x42	63	66	131	211	182	155	140	144	128
64	Jasper	10x42	71	122	138	226	192	161	146	145	135
67	Audubon	10x42	32	140	144	221	395	155	171	160	185
102	Poweshiek	10x42	43	130	120	184	152	143	128	140	107
109	Poweshiek	12x53	51	176	140	212	424	158	168	145	142

¹ Gates Formula; ² FHWA Modified Gates Formula; ³ ENR Formula; ⁴ Iowa DOT Modified ENR Formula; ⁵ Janbu Formula; ⁶ PCUBC Formula; ⁷ Washington DOT Modified Gates Formula

Table 6.19: Nominal Davisson's capacity of the piles from PILOT as well as using different dynamic formulas in mixed soil

ID #	County	Pile Type	L (ft)	D (kips)	Dynamic Formula Capacities (kips)						
					G	F-G	ENR	IA	Janbu	PC	WS
7	Cherokee	10x42	39	176	134	218	206	169	149	157	147
8	Linn	10x42	54	170	162	261	536	222	195	168	209
25	Harrison	10x42	58	224	164	264	549	209	193	164	210
43	Linn	10x42	36	142	146	226	403	186	176	165	196
46	Iowa	10x42	48	164	141	233	225	203	167	181	160
66	Black Hawk	10x42	42.5	180	156	247	488	189	192	169	197
73	Johnson	10x42	46.7	232	156	247	482	166	173	149	201
90	Black Hawk	12x53	64.7	190	197	367	328	263	255	228	227
106	Pottawattamie	10x42	36	148	108	155	165	128	107	121	122

Table 6.20: Nominal Davisson's capacity of the piles from PILOT as well as using different dynamic formulas in sand soil

ID #	County	Pile Type	L (ft)	D (kips)	Dynamic Formula Capacities (kips)						
					G	F-G	ENR	IA	Janbu	PC	WS
10	Ida	10x42	52.3	116	82	94	116	84	69	79	87
17	Fremont	10x42	58	132	152	259	243	230	182	187	171
20	Muscatine	10x42	59	120	136	203	387	153	146	126	140
24	Harrison	10x42	78	184	188	346	312	218	209	184	216
34	Dubuque	10x42	57	224	137	205	388	150	149	129	146
48	Black Hawk	10x42	42	144	126	197	189	159	137	151	136
70	Mills	10x42	78	128	156	246	480	160	159	135	200
74	Benton	10x42	55	150	157	248	497	205	185	159	194
99	Wright	10x42	31	104	107	154	156	137	106	123	115
151	Pottawattamie	10x42	77.5	200	145	222	369	155	146	136	247
158	Dubuque	14x89	73.6	582	315	601	2222	818	465	360	674

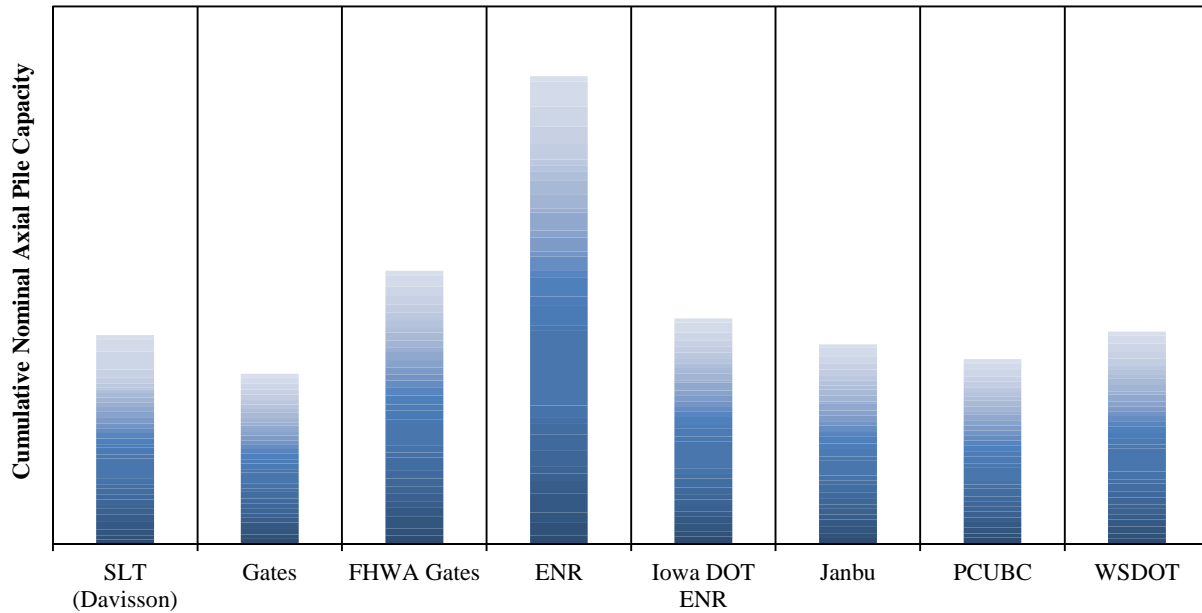


Figure 6.65: Accumulative actual PILOT pile capacities using Davisson and the predicted pile capacities using different dynamic formulas

6.3.2. Goodness of Fit Test

For subsets in different soil types, the K_{sx} (i.e., mean bias that represents the actual nominal pile capacity to the predicted pile capacity) was calculated by dividing the Davisson capacity by the predicted pile capacity using each of the seven dynamic formulas.

Figures 6.69 to 6.71 represent normal distribution plots of the 95% CI for the PDFs of the K_{sx} ratio between pile capacities using Davisson and the capacity using the Iowa DOT ENR dynamic formula in sand, clay, and mixed soils, respectively, while Figures 6.72 to 6.74 represent the corresponding lognormal distribution plots. The figures also present the AD value (or the Anderson Darling coefficient value). In order to determine which distribution is best-fitting to the PDFs, the 95% CI probability of the best-fit should be greater than 0.05, while the AD value should be less than that of the least-fit distribution. As can be noticed from the figures, the AD value for all subsets is lower in the case of lognormal, and the probability of 95% CI is greater in the case of lognormal and is still greater than 0.05. Therefore, all groups are following the lognormal distribution. Hence, the FOSM equation presented in Chapters 2 and 5 is valid for the calculations of the LRFD resistance factors. Additional figures representing the 95% CI for the remaining dynamic formulas in different soil types are presented in Appendix-B.

6.3.3. Histograms and Frequency Distribution

As shown in Figures 6.69 to 6.74, the normal and the lognormal distributions for different dynamic formulas in different soil types were plotted together in order to compare different distribution types, as well as to determine the differences and scatter among different formulas. The figures represent the normal and lognormal distributions of PDFs in sand, clay, and mixed soils, respectively, using same plotting scale for comparison purposes. As before, an obvious

observation from the figures was noticed, as the K_{sx} ratios were extending into the negative region beyond the y axis for normal distribution of all soil types, which is meaningless. This strengthens and validates the use of the lognormal distribution, which was previously discussed in the preceding sections.

A comprehensive illustration of the different dynamic formulas' performance can be achieved by presenting the histogram of the K_{sx} ratio, and by overlaying the best-fit distribution (lognormal) on the histogram. Figure 6.75 presents the histogram and frequency distribution of the K_{sx} ratio between the capacity from Davisson's and the Iowa DOT ENR dynamic formula for 13 cases of driven steel H-piles in sand soils. The parameters of lognormal distributed PDFs such as N (sample size), Loc (location), and the Scale are presented. Figures 6.76 and 6.77 represent the histograms and frequency distributions of the same K_{sx} in clay and mixed soils, respectively. The histograms and frequency distributions for other dynamic formulas in different soil types are provided in the Appendix-B.

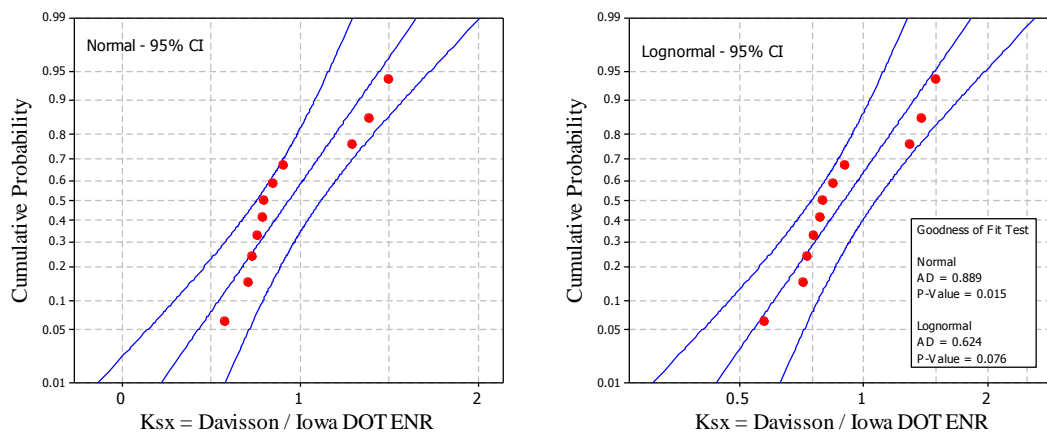


Figure 6.66: Goodness of fit test for the Iowa DOT ENR formula in sand

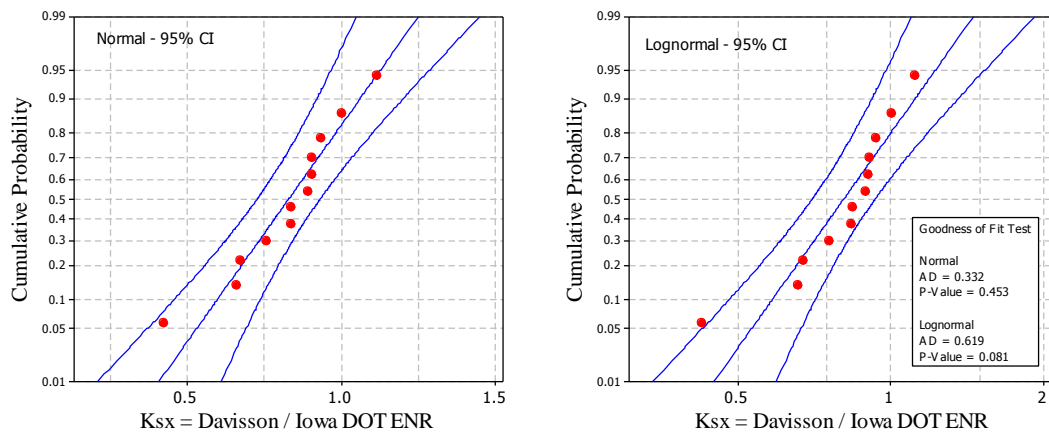


Figure 6.67: Goodness of fit test for the Iowa DOT ENR formula in clay

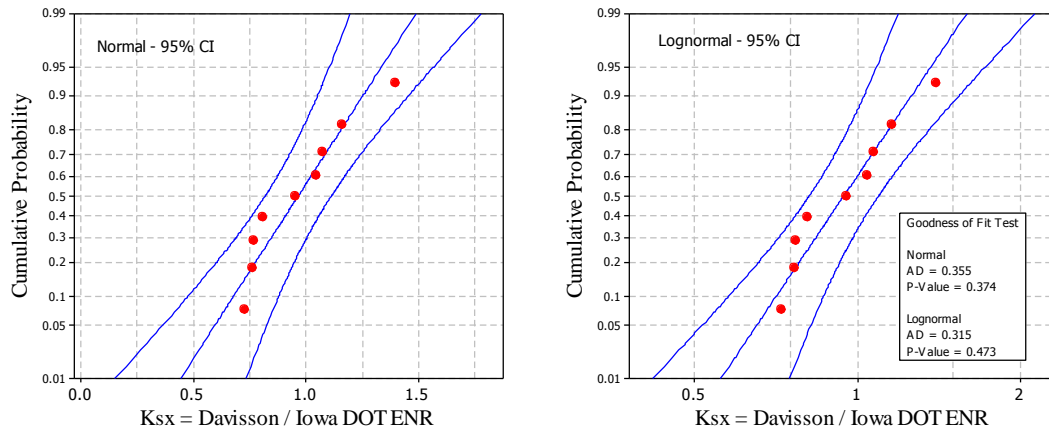


Figure 6.68: Goodness of fit test for the Iowa DOT ENR formula in mixed soils

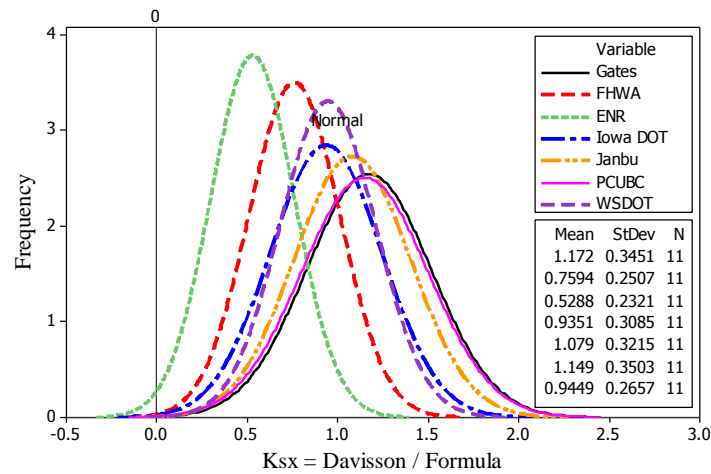


Figure 6.69: Summary of the normal distributed PDFs of the K_{sx} for the 13 cases of steel H-piles designed using different dynamic formulas in sand

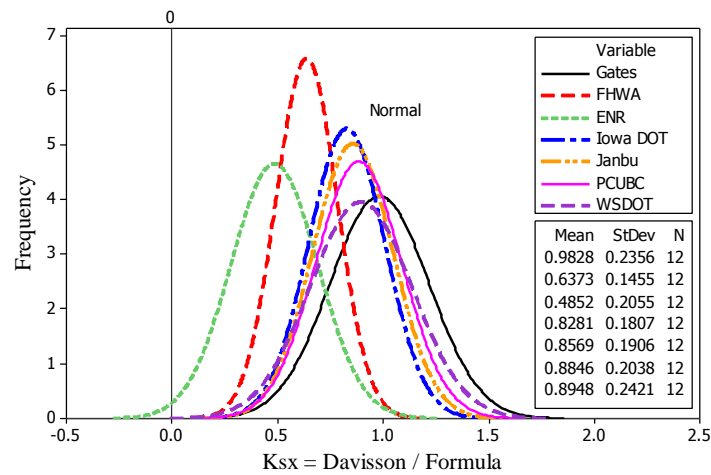


Figure 6.70: Summary of the normal distributed PDFs of the K_{sx} for the eight cases of steel H-piles designed using different dynamic formulas in clay

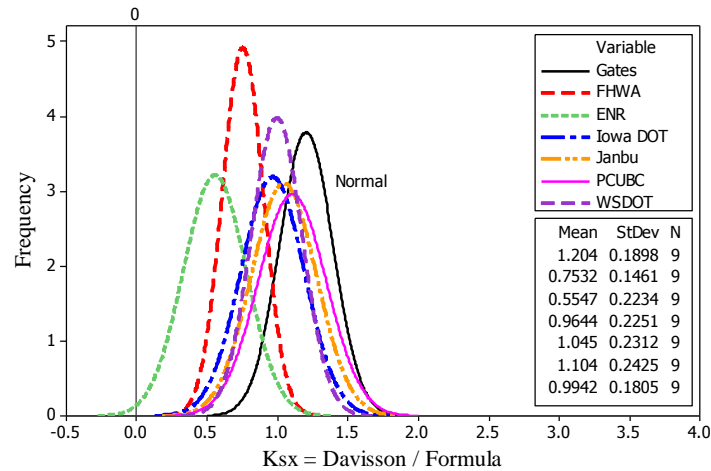


Figure 6.71: Summary of the normal distributed PDFs of the K_{sx} for the 13 cases of steel H-piles designed using different dynamic formulas in mixed soils

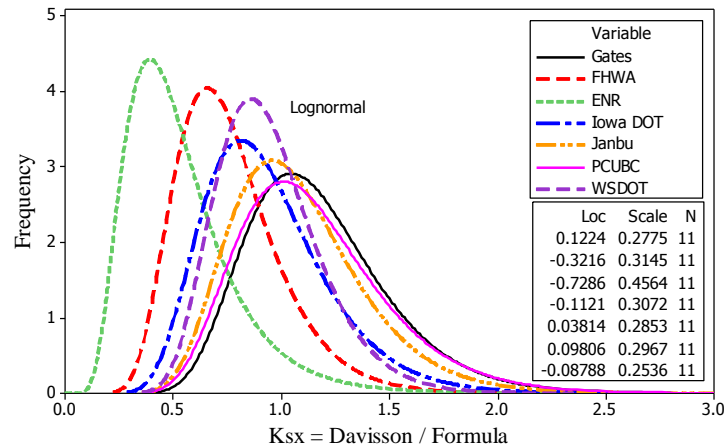


Figure 6.72: Summary of the lognormal distributed PDFs of the K_{sx} for the 13 cases of steel H-piles designed using different dynamic formulas in sand

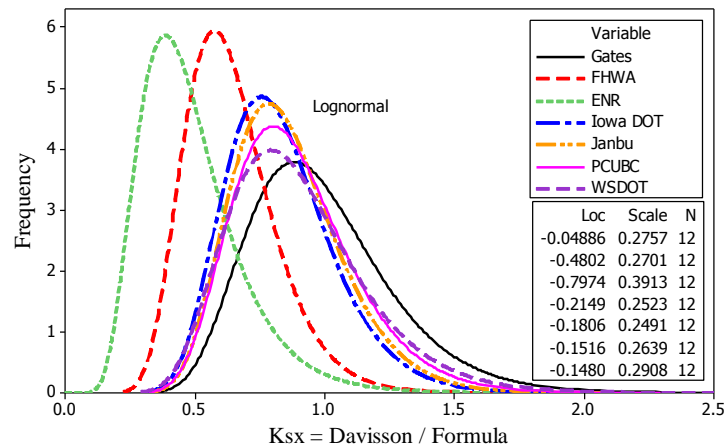


Figure 6.73: Summary of the lognormal distributed PDFs of the K_{sx} for the eight cases of steel H-piles designed using different dynamic formulas in clay

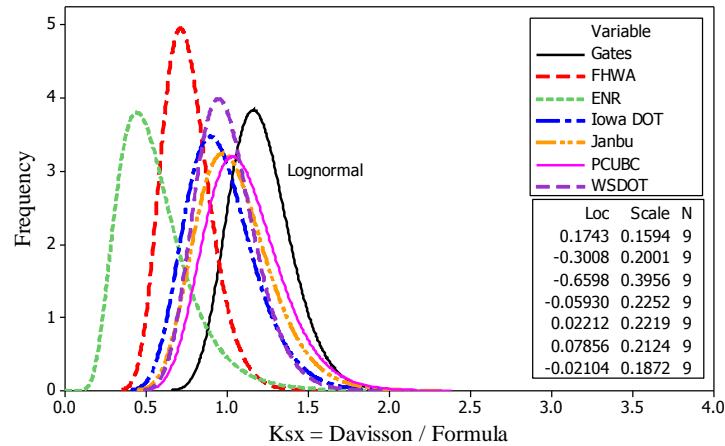


Figure 6.74: Summary of the lognormal distributed PDFs of the K_{sx} for the 13 cases of steel H-piles designed using different dynamic formulas in mixed soils

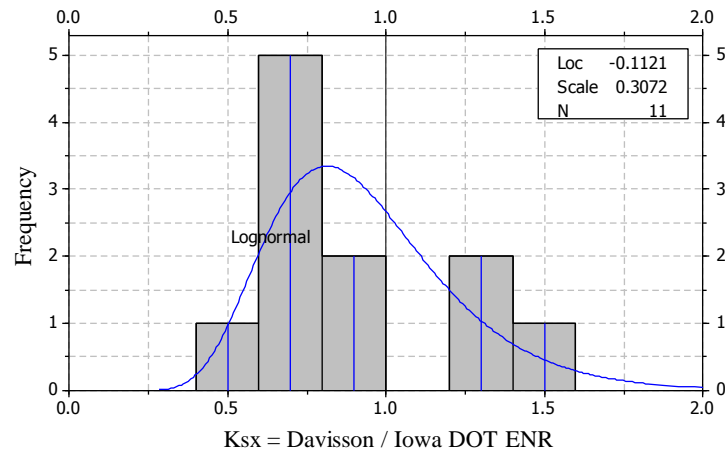


Figure 6.75: Histogram and frequency distribution of K_{sx} for 11 cases of steel H-piles designed using Iowa DOT ENR formula in sand

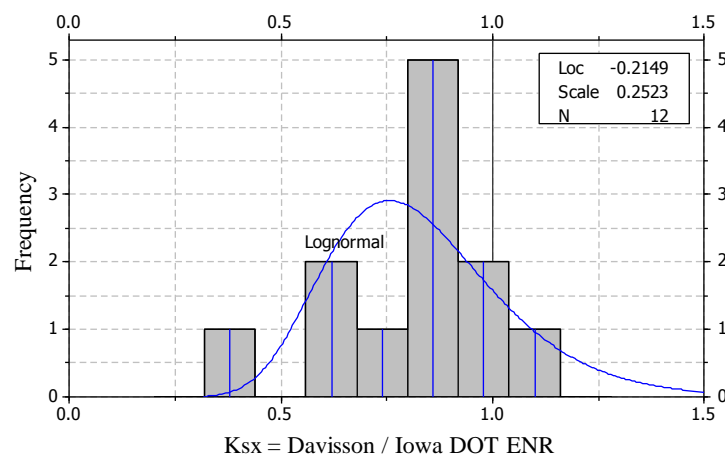


Figure 6.76: Histogram and frequency distribution of K_{sx} for 12 cases of steel H-piles designed using Iowa DOT ENR formula in clay

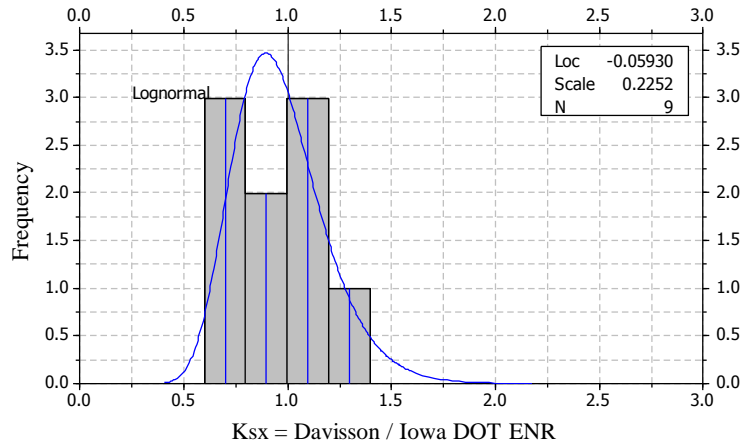


Figure 6.77: Histogram and frequency distribution of K_{sx} for nine cases of steel H-piles designed using Iowa DOT ENR formula in mixed soils

6.3.4. LRFD Resistance Factors

Table 6.21 presents a summary of the preliminary regionally calibrated LRFD resistance factors for seven different dynamic formulas, as well as for driven steel H-piles in sand, clay, and mixed soils. The table includes the required statistical parameters that were used in the FOSM analysis for each group: the sample size (N), mean bias (λ), standard deviation (σ), and the Coefficient of Variation (COV). The LRFD resistance factors were calculated for redundant and non-redundant pile groups assuming $\beta=2.33$, and 3.00, respectively. Table 6.21 also includes some additional essential factors that provide an indication of the accuracy/economy of each dynamic formula.

For redundant pile groups, the results presented in Table 6.21 indicate that the highest resistance factor (ϕ) in sand soils is that of the Gates formula, followed by PCUBC, Janbu, WSDOT, Iowa DOT ENR, FHWA modified Gates, and ENR formulas, in that order, as ϕ values were equal to 0.65, 0.62, 0.59, 0.54, 0.48, 0.39, and 0.21, respectively. The table also shows that the highest ϕ in clay soils is still the Gates formula, followed by PCUBC, Janbu, Iowa DOT ENR, WSDOT, FHWA Gates, and the ENR formula, in that order, as ϕ values were equal to 0.60, 0.55, 0.54, 0.53, 0.52, 0.40, and 0.20, respectively. Table 6.21 also indicates that the Gates, PCUBC, WSDOT, and Janbu formulas provide the highest ϕ in mixed soils, followed by the Iowa DOT ENR, FHWA modified Gates, and the ENR formula, in that order, with ϕ values of 0.85, 0.70, 0.67, 0.66, 0.60, 0.50, and 0.24, respectively. However, the differences in the values of the resistance factors for different dynamic formulas are not large for different soil types. A summary of the LRFD resistance factors and the corresponding efficiency factors based on a target reliability of 2.33 for sand, clay, and mixed soils are provided in Figures 6.78, 6.79, and 6.80, respectively. On the other hand, it was observed that the resistance factors were reduced by an average of 20% for non-redundant pile groups compared to those of redundant piles.

Table 6.21: Summary of the preliminary regionally calibrated LRFD resistance factors for dynamic formulas in different soil types

Soil Type	N	Dynamic Formula	Mean (λ)	St. Dev. (σ)	COV	$\beta=2.33$ (redundant)				$\beta=3.00$ (non-redundant)			
						ϕ^1	ϕ/λ^2	F.S. ³	F.S. _{xλ} ⁴	ϕ	ϕ/λ	F.S.	F.S. _{xλ}
Sand	11	Gates	1.17	0.35	0.29	0.65	0.55	2.19	2.57	0.51	0.43	2.80	3.28
	11	FHWA-G	0.76	0.25	0.33	0.39	0.51	3.64	2.76	0.30	0.39	4.73	3.59
	11	ENR	0.53	0.23	0.44	0.21	0.41	6.59	3.49	0.16	0.30	9.06	4.79
	11	IA-ENR	0.94	0.31	0.33	0.48	0.51	2.95	2.76	0.37	0.39	3.84	3.59
	11	Janbu	1.08	0.32	0.30	0.59	0.55	2.40	2.59	0.46	0.43	3.06	3.31
	11	PCUBC	1.15	0.35	0.30	0.62	0.54	2.28	2.62	0.48	0.42	2.93	3.36
	11	WSDOT	0.94	0.27	0.28	0.54	0.57	2.65	2.50	0.42	0.45	3.36	3.17
Clay	12	Gates	0.98	0.24	0.24	0.60	0.61	2.35	2.31	0.49	0.49	2.92	2.87
	12	FHWA-G	0.64	0.15	0.23	0.40	0.63	3.55	2.26	0.32	0.51	4.39	2.79
	12	ENR	0.49	0.21	0.42	0.20	0.42	6.95	3.37	0.15	0.31	9.47	4.60
	12	IA-ENR	0.83	0.18	0.22	0.53	0.64	2.68	2.22	0.43	0.52	3.30	2.73
	12	Janbu	0.86	0.19	0.22	0.54	0.63	2.61	2.24	0.44	0.51	3.22	2.76
	12	PCUBC	0.88	0.20	0.23	0.55	0.62	2.57	2.27	0.45	0.50	3.17	2.81
	12	WSDOT	0.89	0.24	0.27	0.52	0.58	2.74	2.45	0.41	0.46	3.45	3.09
Mixed	9	Gates	1.20	0.19	0.16	0.85	0.70	1.67	2.01	0.71	0.59	2.00	2.41
	9	FHWA-G	0.75	0.15	0.19	0.50	0.66	2.83	2.13	0.41	0.55	3.44	2.59
	9	ENR	0.55	0.22	0.40	0.24	0.44	5.81	3.22	0.18	0.33	7.84	4.35
	9	IA-ENR	0.96	0.23	0.23	0.60	0.62	2.37	2.28	0.48	0.50	2.93	2.83
	9	Janbu	1.04	0.23	0.22	0.66	0.63	2.14	2.23	0.54	0.51	2.63	2.75
	9	PCUBC	1.10	0.24	0.22	0.70	0.64	2.02	2.23	0.57	0.52	2.48	2.74
	9	WSDOT	0.99	0.18	0.18	0.67	0.68	2.10	2.09	0.56	0.56	2.54	2.53

¹ LRFD geotechnical resistance factor for PILOT

² Efficiency factor

³ Equivalent factor of safety to ASD

⁴ Actual mean factor of safety

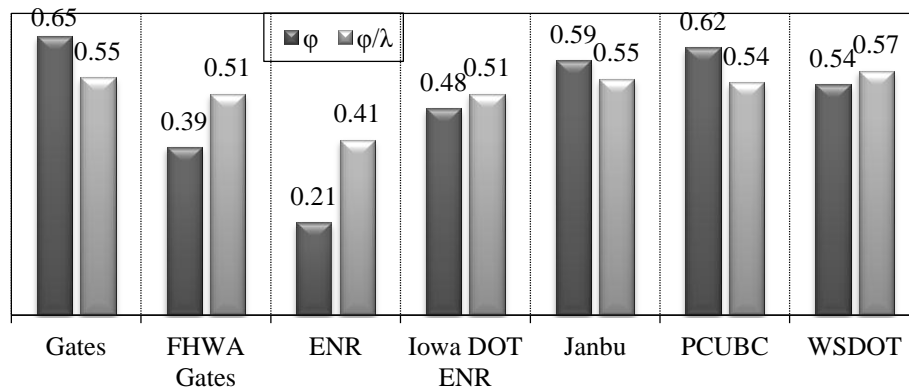


Figure 6.78: Summary of the preliminary LRFD resistance factors of dynamic formulas and the corresponding efficiency factors based on a target reliability of 2.33 for sand soil

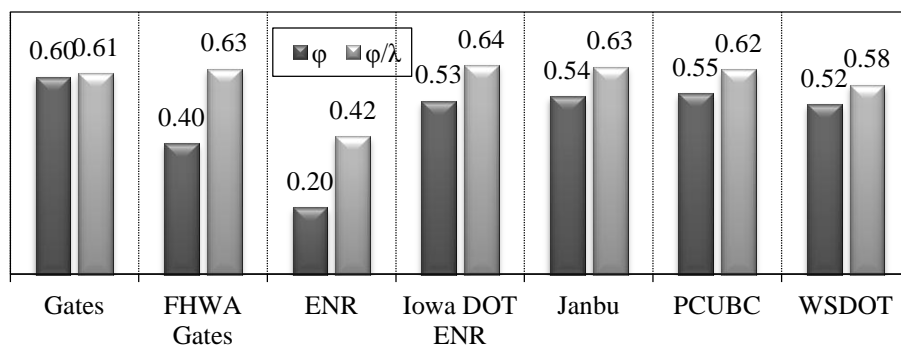


Figure 6.79: Summary of the preliminary LRFD resistance factors for dynamic formulas and the corresponding efficiency factors based on a target reliability of 2.33 for clay soil

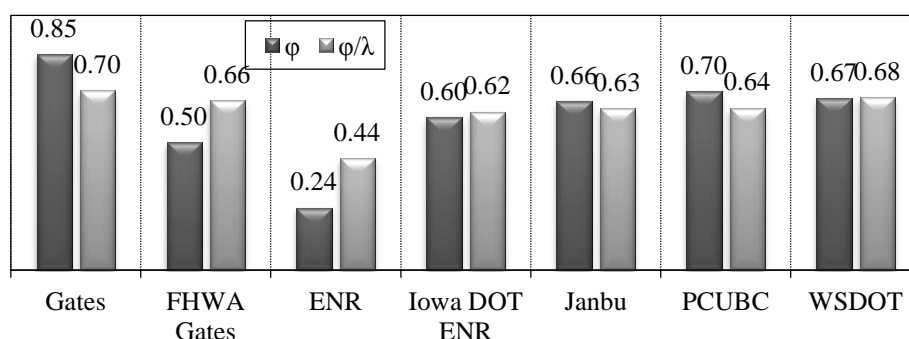


Figure 6.80: Summary of the preliminary LRFD resistance factors for dynamic formulas and the corresponding efficiency factors based on a target reliability of 2.33 for mixed soil

6.3.5. Sensitivity to Reliability Index

A sensitivity analysis was conducted to determine the effect of changing the target reliability index (β) on the LRFD resistance factors. As shown in Figure 6.81 for sand soils, the resistance factors are found to be very sensitive to any slight change in the reliability index. The analysis was designed to cover a wide range of β starting from 1.5 to 4.0 in order to include all possible variations in the target reliability of bridge foundations. The same analysis was conducted for clay and mixed soils as shown on Figures 6.82 and 6.83, respectively. Using Figures 6.81, 6.82, and 6.83, the design engineer can select the appropriate LRFD resistance factors corresponding to any target reliability index, according to the redundancy of the pile groups, importance and life time of the bridge structure, degree of construction control, extent of conservatism in the design, and engineering judgment. As previously mentioned, a β of 2.33 for redundant pile groups (five piles or more for each pile cap) is recommended by the NCHRP-507 for the design of bridge pile foundations, corresponding to a probability of failure of 1/100.

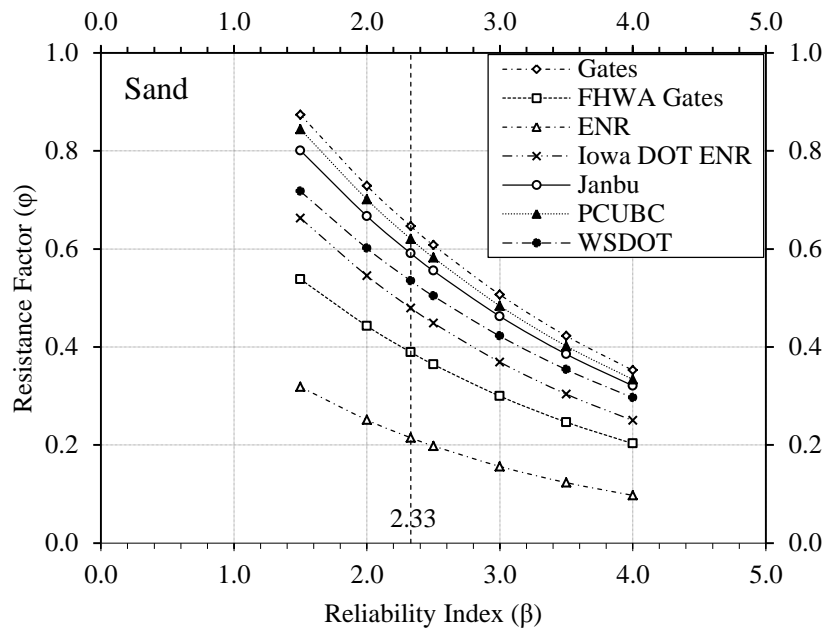


Figure 6.81: Preliminary LRFD resistance factors for different dynamic formulas corresponding to a wide range of reliability indices in sand soils

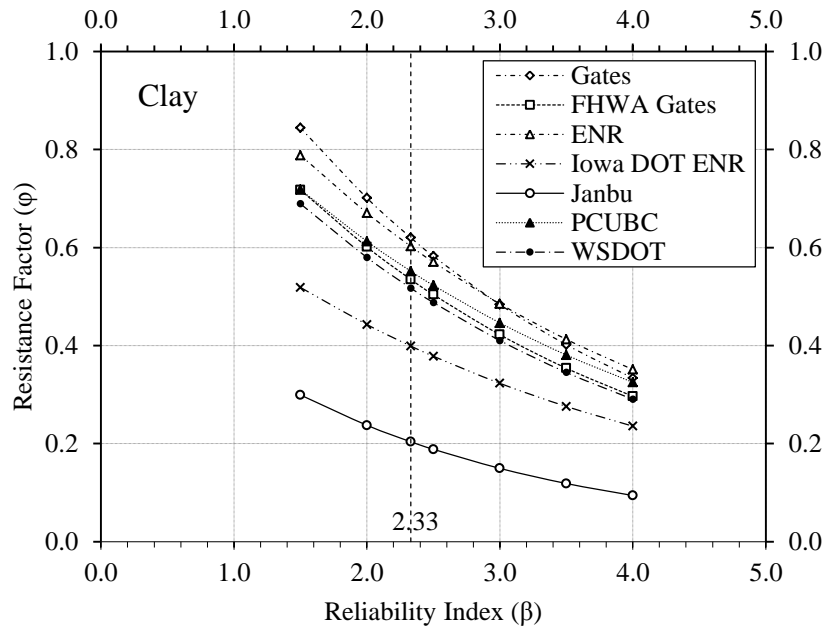


Figure 6.82: Preliminary LRFD resistance factors for different dynamic formulas corresponding to a wide range of reliability indices in clay soils

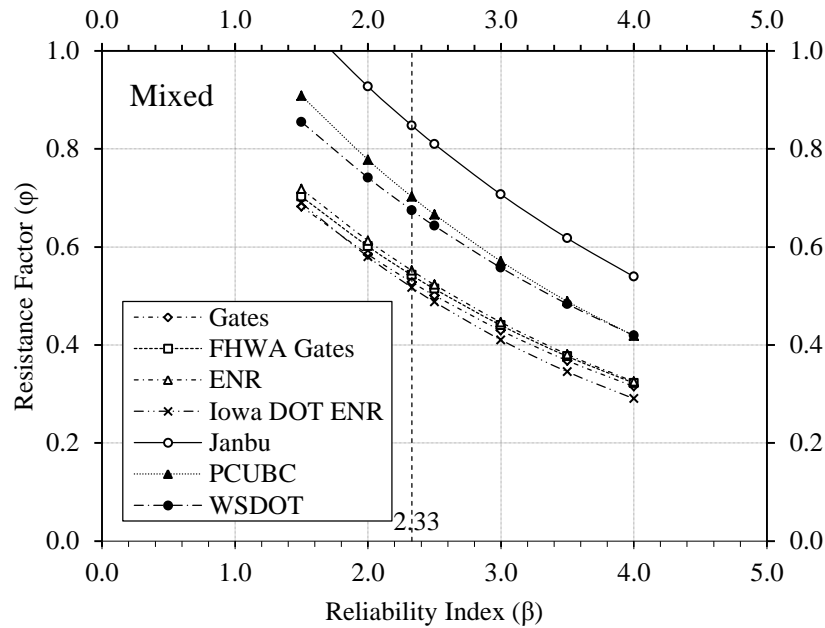


Figure 6.83: Preliminary LRFD resistance factors for different dynamic formulas corresponding to a wide range of reliability indices in mixed soils

6.3.6. Efficiency of Different Methods

The efficiency factor was calculated in order to determine the efficiency of different dynamic formulas relative to the actual pile behavior under SLT, as well as appropriately compare among the different formulas. This efficiency factor (ϕ/λ) is equal to the ratio of the LRFD resistance factor to the mean bias of the method. The efficiency factor represents an indication of the bias of the formula to the actual pile behavior, hence the economy of the dynamic formula. In Table 6.21, the ϕ/λ factor was calculated for all groups, and it was found that differences among dynamic formulas are not great. However, the Iowa DOT ENR formula provided the highest efficiency in clay and mixed soils. Figures 6.84, 6.85, and 6.86 provide the rate of change in the efficiency factor of different dynamic formulas corresponding to the changing of the target reliability index. Hence, the design engineer can select the target β not only based on the resistance factors but by the required efficiency and economy in the design as well.

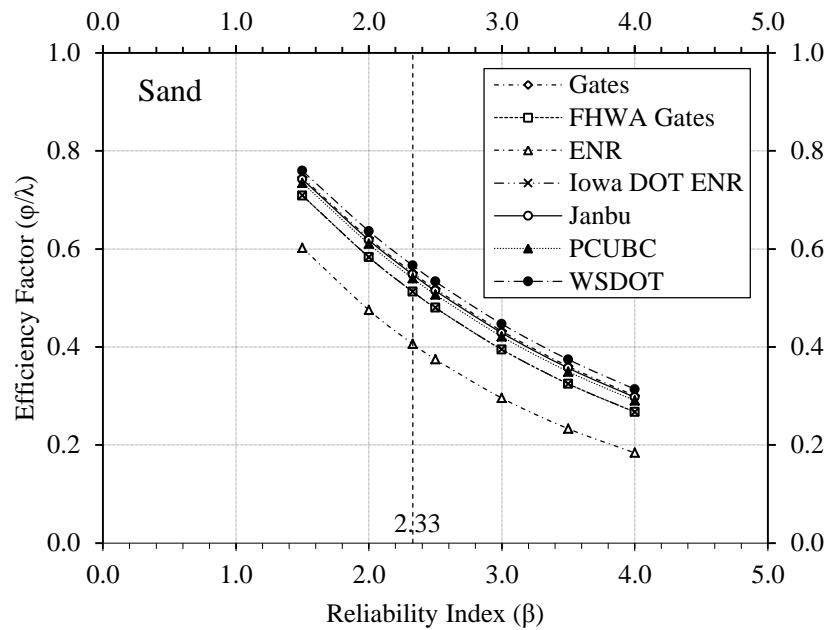


Figure 6.84: Efficiency factors for dynamic formulas corresponding to different β in sand

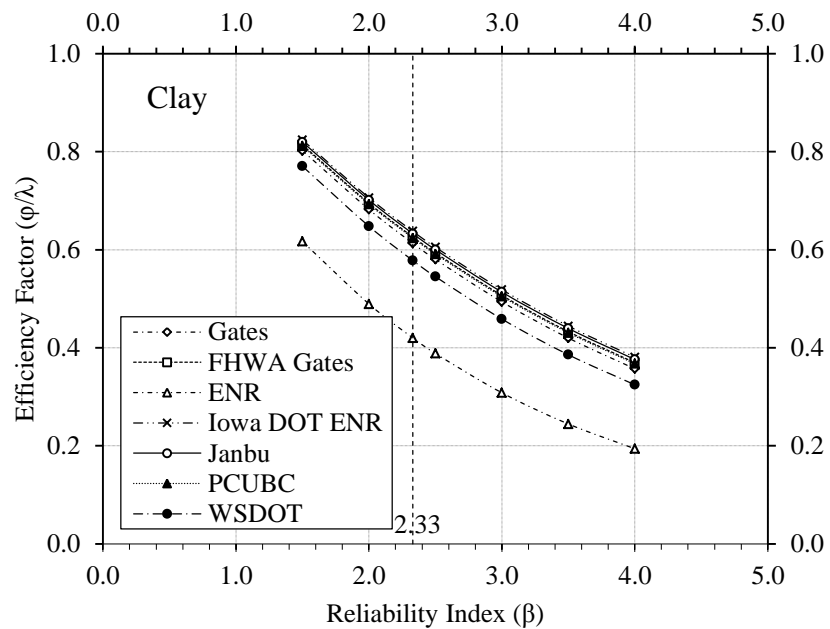


Figure 6.85: Efficiency factors for dynamic formulas corresponding to different β in clay

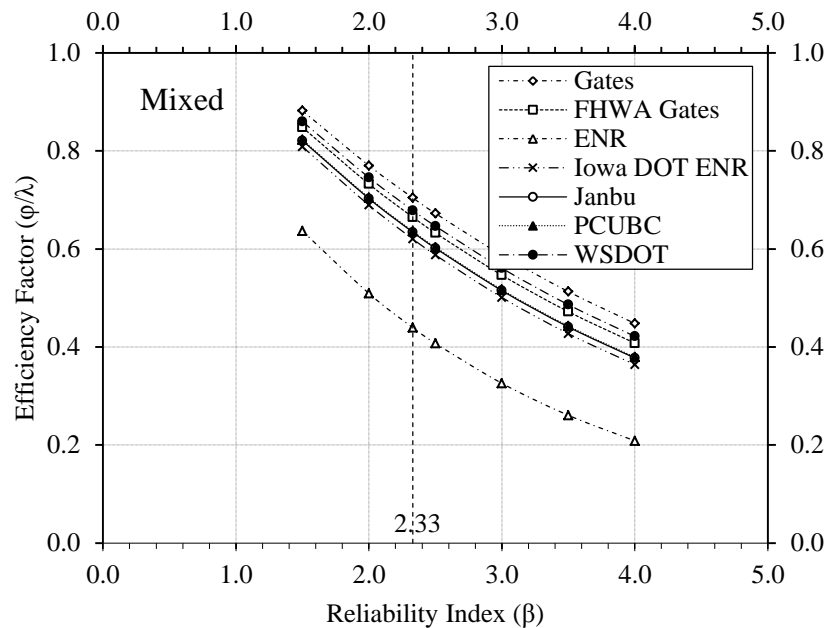


Figure 6.86: Efficiency factors for dynamic formulas corresponding to different β in mixed soil

6.3.7. Equivalent Factor of Safety

The economy of the LRFD resistance factors can also be measured by means of the equivalent factor of safety (FS) to the ASD. This equivalent FS is calculated based on the simplified relation provided by Barker et al. (1991) and is discussed in Chapter 2. As shown in Table 6.21, the equivalent FS is presented for each subset based on a $DL/LL = 2$, $\gamma_L = 1.75$, and $\gamma_D = 1.25$, the $FS = 1.4167/\phi$. The equivalent FS should be considered while comparing the economy of a design method based on the LRFD approach relative to that based on the ASD approach. As can be observed from Table 6.21, the equivalent FS for different dynamic formulas, ranges from 1.6 to 6.5 with an average of 3.1 without using any construction control methods. On the other hand, the actual FS is calculated by multiplying the mean bias by the equivalent FS. The actual FS represents the overall economy of the method, meaning that whenever the actual FS is lower, the foundation cost is reduced, and vice versa. The back-calculated equivalent FS to the LRFD approach is less than that assumed in the ASD specifications that ranged between 2.0 to 3.4. Moreover, the equivalent FS is corresponding to a fixed and assured degree of reliability. Hence, when using dynamic formulas for the design and/or construction of bridge pile foundations in different soil types, the LRFD approach will be consistently reliable than the ASD approach.

6.3.8. Regional Factors vs. Design Specifications

In this study, the 2008 AASHTO-LRFD specifications, as well as the NCHRP-507 (after Paikowsky et al., 2004) were selected to be compared with the preliminary LRFD resistance factors for dynamic formulas. Table 6.22 presents the different values of the LRFD resistance factors provided in design specifications for dynamic formulas versus the Iowa preliminary regionally calibrated factors. From Table 6.22 it can be observed that the resistance factor for the ENR dynamic formula in sand soils is greater than the factor provided in AASHTO

specifications by around 115%. Similarly, the preliminary resistance factors of the ENR formula in clay and mixed soils increase by 100% and 140%, respectively (see Table 6.22). Overall, the preliminary regionally calibrated resistance factors for dynamic formulas show a high tendency of cost reduction, compared to the design specifications adapted for the design/construction of deep bridge foundations in the State of Iowa.

Table 6.22: Different values of the LRFD resistance factors provided for dynamic formulas in design specifications versus the Iowa preliminary regionally calibrated factors

Soil Type	Dynamic Formula	Iowa Preliminary Resistance Factor	AASHTO 2008 Interim	NCHRP 507 Resistance Factors
Sand	Gates	0.65	N/A	0.75
	FHWA Gates	0.39	0.40	0.40
	ENR	0.21	0.10	0.25
	Iowa DOT ENR	0.48	N/A	N/A
	Janbu	0.59	N/A	N/A
	PCUBC	0.62	N/A	N/A
	WSDOT	0.54	N/A	N/A
Clay	Gates	0.60	N/A	0.75
	FHWA Gates	0.40	0.40	0.40
	ENR	0.20	0.10	0.25
	Iowa DOT ENR	0.53	N/A	N/A
	Janbu	0.54	N/A	N/A
	PCUBC	0.55	N/A	N/A
	WSDOT	0.52	N/A	N/A
Mixed	Gates	0.85	N/A	0.75
	FHWA Gates	0.50	0.40	0.40
	ENR	0.24	0.10	0.25
	Iowa DOT ENR	0.60	N/A	N/A
	Janbu	0.66	N/A	N/A
	PCUBC	0.70	N/A	N/A
	WSDOT	0.67	N/A	N/A

6.3.9. Examination of the Resistance Factors

The 10 full-scale pile load test data from different locations in the State of Iowa were again used to examine the preliminary LRFD resistance factors. The nominal as well as the factored design capacities that were calculated using the dynamic formulas were then compared to the actual capacity of the piles measured in the field as part of this exercise.

Figure 6.87 presents the calculated nominal and factored capacities of the test pile at Clarke County (clay site) using seven different dynamic formulas, and compares them to the actual nominal and factored capacities from the SLT using Davisson's criterion. For the formulas, the factored capacities were calculated based on the regionally calibrated resistance factors. On the other hand, the 2007 AASHTO recommended resistance factor of 0.8 was used for calculating

the actual factored capacity measured from the SLT, as the test site variability was assumed to be low.

Compared to the SLT measured nominal capacity of 243 kips, Figure 6.87 shows that the ENR formula provided the highest nominal capacity of 775 kips, while Gates formulas provided the lowest nominal capacity of 191 kips. It was also observed that at least four dynamic formulas were overestimating the nominal capacity, which is unsafe. After multiplying the nominal capacities calculated using the dynamic formulas by the LRFD resistance factors, the Iowa DOT ENR formulas were still providing the highest and most efficient capacity of 155 kips compared to the SLT capacity of 194 kips and other formulas. As a preliminary conclusion, the developed LRFD resistance factors increased the degree of reliability of the dynamic formulas, providing a consistent range of pile design capacities with no large variation from one method to another.

Figures 6.88 and 6.89 represent the same comparison between the predicted nominal and factored pile capacities using different dynamic formulas versus the measured pile capacities from SLT for Cedar and Poweshiek Counties (sand and mixed soils), respectively. It is clear from the figure that almost the same behavior mentioned above was observed, indicating that the regionally developed LRFD resistance factors for Iowa soils are functioning properly overall. However, the Iowa DOT method exceeded the actual capacity in the case of sand soil. Janbu and WSDOT formulas were also performing better in sand and mixed soils, respectively.

Table 6.23 summarizes the 10 field tests ID numbers, location, average soil formation, measured nominal capacities from SLT using Davisson's criterion, as well as the predicted nominal capacities using different dynamic formulas.

Generally, after comparing the capacity from dynamic formulas to that of the field measured, and after applying the recently developed resistance factors, it was found that the factored capacity from dynamic formulas is slightly conservative compared to SLT based on Davisson's criterion. However, it was found that the Iowa DOT ENR, WSDOT, and Janbu formulas seemed to be, overall, less conservative compared to other formulas, which agrees with what was mentioned in the previous section about the efficiency of each method. Overall, this degree of conservatism associated with the LRFD is relatively low compared to the conventional ASD approach and its factor of safety. Consequently, the preliminary regionally calibrated LRFD resistance factors for Iowa provide a reliable design and can be certainly used in developing final recommendations.

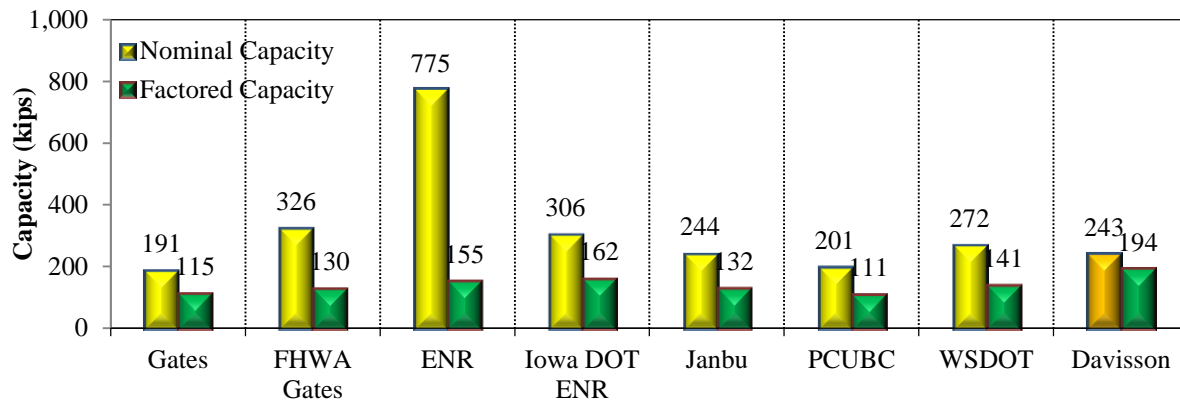


Figure 6.87: Nominal and Factored pile design capacities using different dynamic formulas and compared to SLT results for Clarke – Clay soil

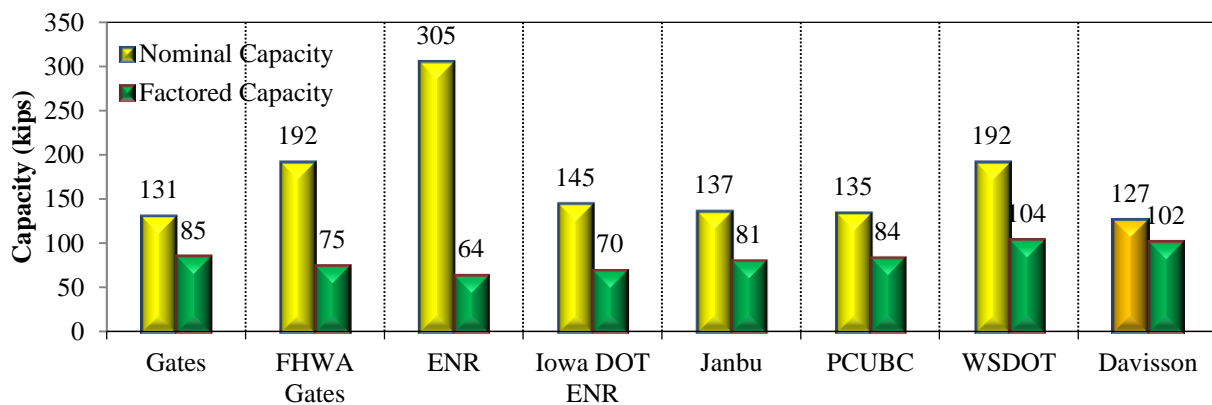


Figure 6.88: Nominal and Factored pile design capacities using different dynamic formulas and compared to SLT results for Cedar – Sand soil

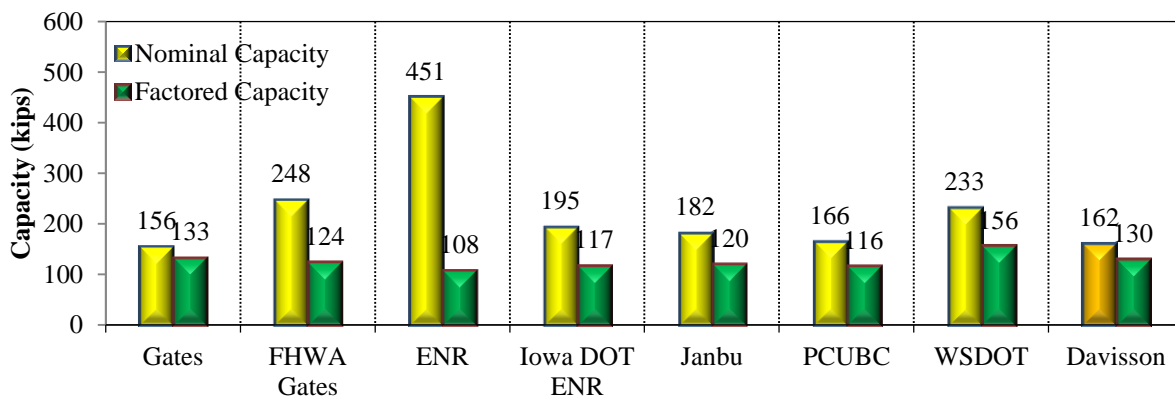


Figure 6.89: Nominal and Factored pile design capacities using different dynamic formulas and compared to SLT results for Poweshiek – Mixed soil

Table 6.23: Summary of the 10 field tests ID, location, average soil formation, measured nominal capacities, and the predicted nominal capacities using different dynamic formulas

County	ID	Soil Type	Measured Capacity (kips)	Predicted Nominal Pile Capacity (kips)						
				G	F-G	ENR	Iowa ENR	Janbu	PCU BC	WS DOT
Mahaska	ISU-1	Mixed	212	128	184	288	132	137	142	186
Mills	ISU-2	Clay	125	123	173	266	116	118	116	170
Polk	ISU-3	Clay	150	117	161	242	104	108	107	160
Jasper	ISU-4	Clay	154	150	235	418	181	171	157	216
Clarke	ISU-5	Clay	243	191	326	775	306	244	201	272
Buchanan	ISU-6	Clay	212.6	161	259	491	217	194	175	237
Buchanan	ISU-7	Mixed	53	24	0	71	36	34	38	46
Poweshiek	ISU-8	Mixed	162	156	248	451	195	182	166	233
Des Moines	ISU-9	Sand	158	162	260	473	233	203	194	269
Cedar	ISU-10	Sand	127	131	192	305	145	137	135	192

Figures 6.90 and 6.91 provide a better way to illustrate the performance of the LRFD resistance factors and summarize the previous observations. As shown in Figure 6.90, the x-axis represents the measured pile nominal capacity for the 10 field tests using Davisson's criterion, while the y-axis represents the nominal capacity calculated for the same 10 piles using seven different dynamic formulas. As can be observed from the figure, the points are scattered above and below the neutral line, meaning that dynamic formulas tend to overestimate the capacity of the piles, which is unsafe. On the other hand, Figure 6.91 represents the same data after multiplying the nominal capacities by the corresponding LRFD resistance factors. As can be seen from Figure 6.91, the factored design capacities calculated using dynamic formulas were adjusted to avoid the exceeding of actual factored capacities for the load tested piles, except for the Iowa DOT ENR formula, which exceeded the measured capacity in some cases. This indicates that the LRFD resistance factors, overall, succeeded to lower the capacities below the neutral line and ensured reliable designs for the 10 piles. Another observation that can be made from Figure 6.91 is that the Iowa DOT ENR, WSDOT, and Janbu formulas were the most economic, as the points were relatively closer to the neutral line than other formulas.

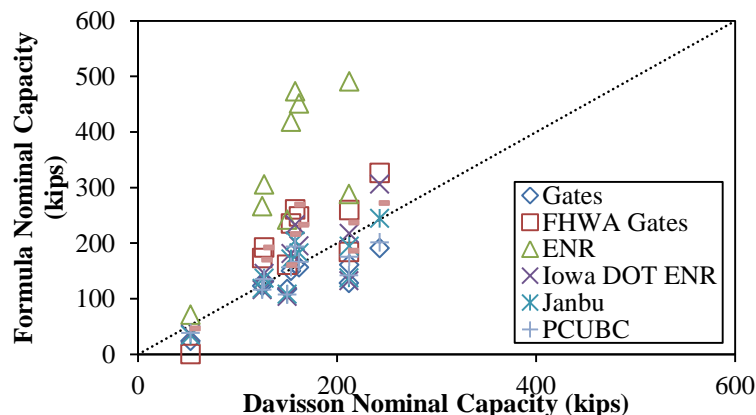


Figure 6.90: Nominal measured and calculated capacities for the 10 field tested piles using Davisson's criterion versus dynamic formulas

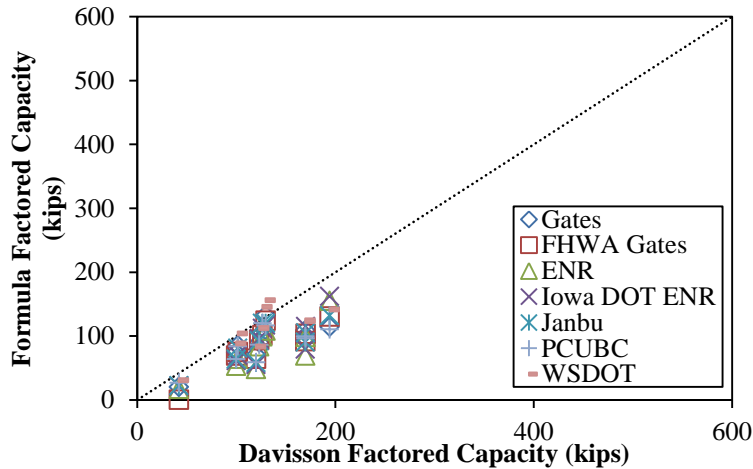


Figure 6.91: Factored measured and calculated capacities for the 10 field tested piles using Davisson’s criterion versus dynamic formulas

6.3.10. Construction Control

As indicated earlier and in AbdelSalam et al. (2010), the Iowa DOT currently uses an in-house static analysis method, known as the Iowa Blue Book method (Dirks and Kam 1989), to predict the required length of piles that are to be driven in the field. Moreover, during actual pile driving, the Iowa DOT Modified ENR formula is the dynamic pile driving formula that is preferred by the Iowa DOT and some counties for determining when a pile has developed adequate axial capacity. The results of the LRFD resistance factor calibration process presented in this report indicate that the current design and construction control procedures for driven pile foundations in the State of Iowa are some of the most efficient design methods, and the other alternative methods are not recommended. Provided this information, an attempt to further enhance the LRFD resistance factors recommended earlier for the Iowa Blue Book method can be made so that the recognized use of the Iowa DOT Modified ENR formula for pile driving termination is taken into account.

In an ideal situation, the length of piling predicted by the Iowa Blue Book method would agree with the actual pile length driven in the field, where the Iowa DOT Modified ENR formula is used to terminate driving. Due to uncertainties involved with the pile driving process, this ideal situation is rarely achieved. However, the probability that the length of piling driven will be greater or less than that predicted by the Iowa Blue Book method can be quantified by looking at the cumulative probability distribution for the ratio of the design pile capacity predicted by the Iowa DOT ENR formula to that predicted by the Iowa Blue Book method.

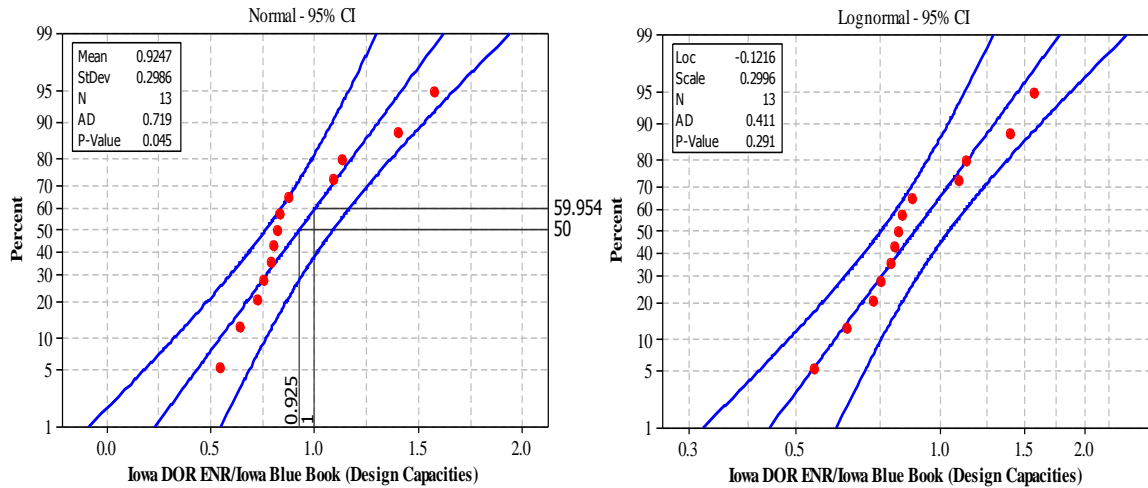


Figure 6.92: AD test for the Iowa DOT Modified ENR to Iowa Blue Book ratio in sand soil for the usable steel piles for dynamic formulas

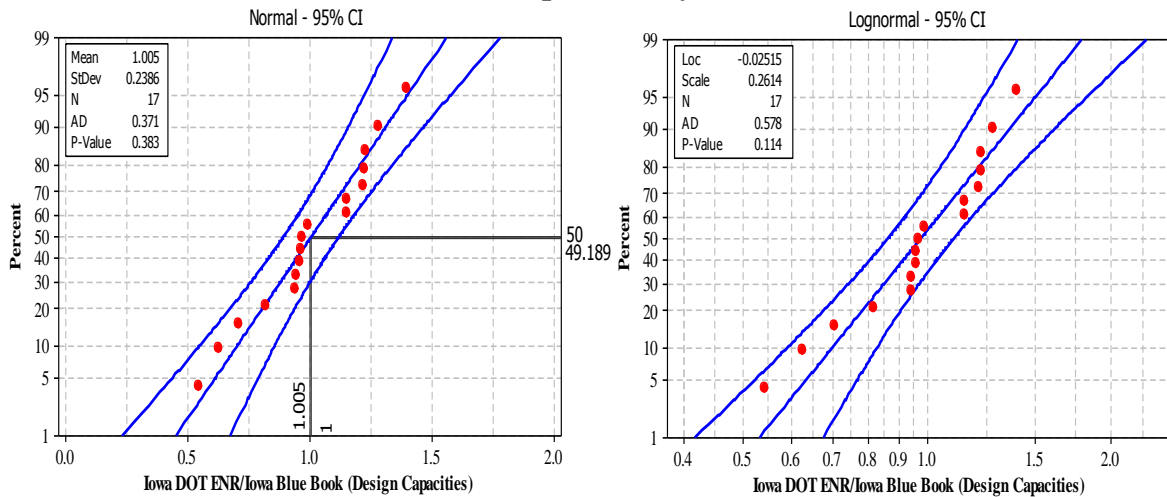


Figure 6.93: AD test for the Iowa DOT Modified ENR to Iowa Blue Book ratio in clay soil for the usable steel piles for dynamic formulas

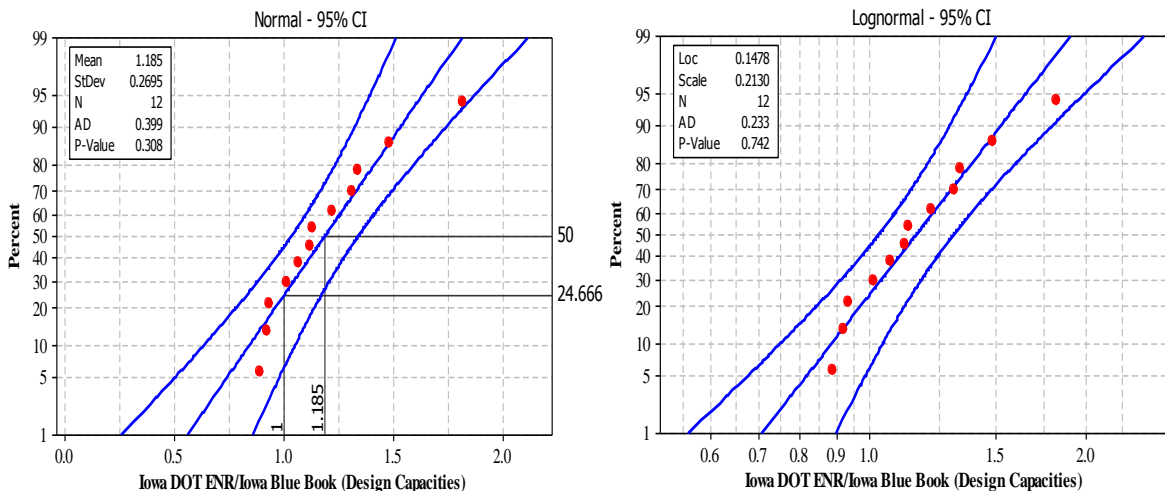


Figure 6.94: AD test for the Iowa DOT Modified ENR to Iowa Blue Book ratio in mixed soil for the usable steel piles for dynamic formulas

Provided in Figures 6.92, 6.93, and 6.94 are the Minitab[®] probability distribution identification results for the Iowa DOT Modified ENR to Iowa Blue Book design capacity ratio that was used in combination with the sand, clay, and mixed soil subsets of the amassed PILOT usable-dynamic, steel H-pile dataset, respectively. This amassed PILOT usable-dynamic, steel H-pile dataset simply combines the original PILOT usable-dynamic, steel H-pile dataset with the information acquired from the 10 full-scale field load tests that were conducted as a part of this research. Furthermore, the design capacities established by the Iowa DOT Modified ENR formula were achieved through the application of the appropriate LRFD resistance factors that were recommended, while for the Iowa Blue Book method, the appropriate LRFD resistance factors recommended earlier were used; namely, resistance factors of 0.55, 0.63, and 0.60 were used for piles embedded in sand, clay, and mixed soil profiles, respectively.

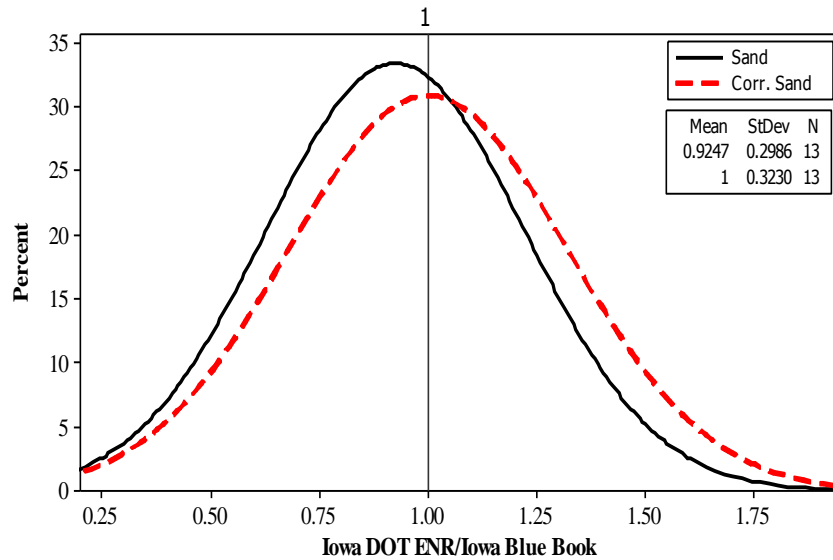


Figure 6.95: Original and corrected lognormal probability distributions in sand soil

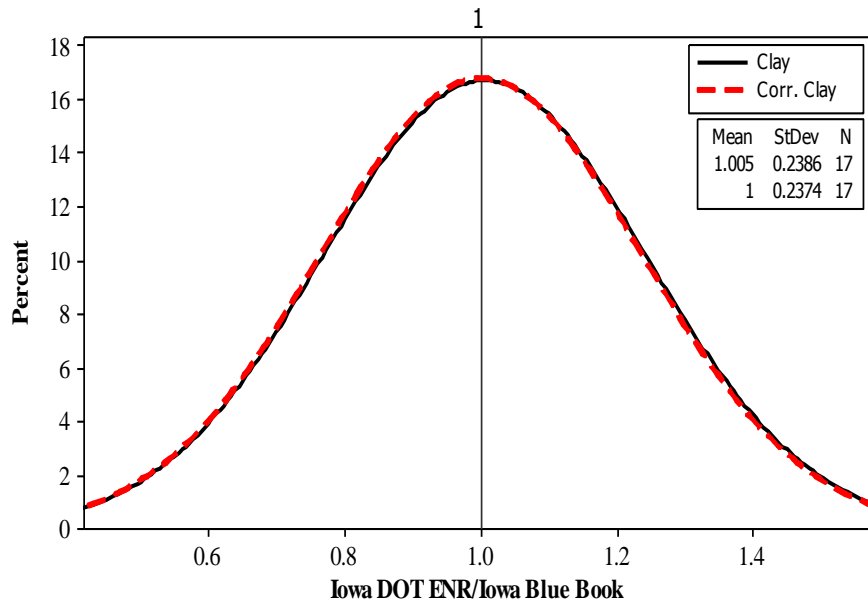


Figure 6.96: Original and corrected lognormal probability distributions in clay soil

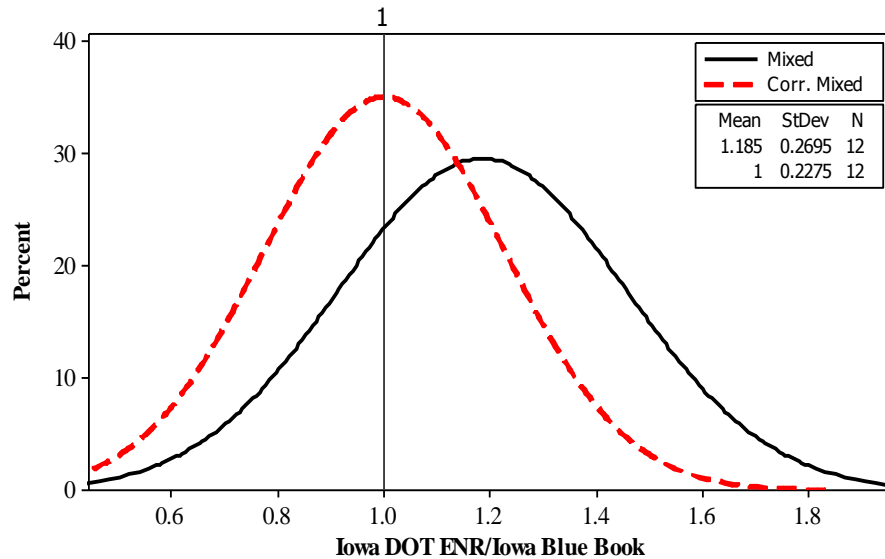


Figure 6.97: Original and corrected lognormal probability distributions in mixed soil

As indicated in the above figures, the assumption of a normal probability distribution for the three sample sets of Iowa DOT Modified ENR to Iowa Blue Book design capacity ratios was accepted at the 5% significance level in all cases. Therefore, the best-fit, normal, and cumulative probability distributions depicted in the leftmost plot of Figures 6.92, 6.93, and 6.94 will be used for the development of enhanced LRFD resistance factors for the Iowa Blue Book method. However, before such enhanced resistance factors are developed, an explanation of what these cumulative probability distributions actually indicate must be given. First, the y-axis of these plots designate the probability that the Iowa DOT Modified ENR to Iowa Blue Book design capacity ratio will be less than or equal to the specified design capacity ratio found on the x-axis. In other words, for piles driven in sand soil profiles, a value of unity for the design capacity ratio corresponds to a cumulative probability of about 60%, whereas for piles driven in clay and mixed soil profiles a value of unity for the design capacity ratio corresponds to cumulative probabilities of about 49.2% and 24.7%, respectively. This indicates that there is a 60% probability that the Iowa DOT Modified ENR to Iowa Blue Book design capacity ratio will be less than one for any given pile driven in a sand soil profile, while the probability that this design capacity ratio will be less than one for any given pile driven in a clay or mixed soil profile is 49.2% and 24.7%, respectively. Thus, for piles driven in a sand soil profile in particular, 60% of the time it can be expected that the length of piling driven in the field will be greater than that predicted by the Iowa Blue Book method. Conversely, the length of piling driven will be less than that predicted by the Iowa Blue Book method 40% of the time.

Hence, the design pile capacity established by either the Iowa Blue Book method or the Iowa DOT Modified ENR formula can be corrected to change this probability. For instance, the majority of the time it may be desired that the length of piling driven in the field be less than that predicted by the Iowa Blue Book method in the design stages of the project. Driving piles longer than predicted may require splicing or even the acquisition of additional piling from off-site. On the other hand, it may also be desirable to correct one of the formulas so that half of the time the length of piling driven is shorter than that predicted and half of the time it is longer than predicted as it has been handled earlier for WEAP. Based on the available data, this would

represent a best guess for making the actual and predicted pile lengths agree. Thus, at a cumulative probability of 50%, the Iowa DOT Modified ENR to Iowa Blue Book design capacity ratio takes on values of 0.93, 1.00, and 1.17 when considering sand, clay, and mixed soil profiles, respectively. In other words, if a 50% probability associated with the event in which the driven pile lengths are longer than those predicted by the Iowa Blue Book method is desired, it would be necessary to multiply the design pile capacity established by the Iowa Blue Book method by a factor of 0.93, 1.00, or 1.17 depending on whether the embedded length of the pile was characterized by a sand, clay, or mixed soil profile. By incorporating these correction factors into the original LRFD resistance factors established for the Iowa Blue Book method, one arrives at the following enhanced LRFD resistance factors: 0.51, 0.63, and 0.70, which are to be used in conjunction with piles embedded in sand, clay, and mixed soil profiles, respectively.

As demonstrated in Figures 6.95, 6.96, and 6.97, the enhanced LRFD resistance factors for the Iowa Blue Book method, which account for the use of the Iowa DOT Modified ENR formula for pile design verification, successfully shift the normal probability distributions for the Iowa DOT Modified ENR to Iowa Blue Book design capacity ratios achieved in sand, clay and mixed soil profiles so that their expected value is equal to one. Although the reliability assured by these enhanced LRFD resistance factors is no longer equal to 2.33, it is important to reiterate that these factors are only to be used in situations where it is known that the Iowa DOT Modified ENR formula will be used in the field as a construction control measure. In other words, since embedded pile lengths will ultimately be determined via the Iowa DOT Modified ENR formula, regardless of what was established by the Iowa Blue Book method in the design stages of the project, a reliability of 2.33 is ensured by means of the LRFD resistance factors calibrated for the Iowa DOT Modified ENR formula. Once more, it is the sole function of these enhanced resistance factors to minimize the discrepancy between the design and production pile lengths.

CHAPTER 7: RECOMMENDATIONS FOR DESIGN AND CONSTRUCTION

In Chapter 6, the preliminary LRFD resistance factors were developed using the PILOT database and were verified based on the 10 new pile load tests completed as a part of this study. The preliminary resistance factors have proven to satisfy the LRFD framework and economic for all methods of analysis including static and dynamic analysis methods as well as dynamic formulas. To develop the final recommended LRFD resistance factors for design and construction, the 10 new pile load tests were added to the PILOT database, and the resistance factors were re-calibrated using the expanded database. Therefore, the sample size used for the calibration was increased, providing the final recommendations with even more confidence and efficiency. Among the 10 new load tests added to the database, five were in clay soils, two were in sand soils, and the remaining three were mixed soil sites. The analysis was conducted for all the previously selected static/dynamic methods and formulas. In this chapter, comprehensive design tables and charts are provided for each individual analysis method. A final table was presented including the recommended resistance factors for all methods, along with explanations for the modified recommended values.

7.1. Static Methods

The same five static analysis methods were used for predicting the design nominal capacity of steel H-piles: the Nordlund method, α -API method, β -method, SPT-Meyerhof method, and the Iowa DOT design charts (Blue Book method, or BB). The number of data points (load tests) used for developing the final LRFD recommendations increased from 20 to 25 in clay soils, 26 to 29 in mixed soils, and 34 to 36 in sand soils.

7.1.1. Design Tables

Table 7.1 summarizes the final LRFD resistance factors obtained for the different static analysis methods used to predict the capacity of driven steel H-piles in sand, clay, and mixed soils. The LRFD resistance factors were calculated for redundant and non-redundant pile groups for β values equal to 2.33 and 3.00, respectively. For redundant pile groups, the final recommendations are summarized in Table 7.1, which indicates that the highest resistance factor for sand soils was produced by the Blue Book method, followed by SPT-Meyerhof, β -method, α -API, Nordlund method, in that order, as ϕ values were equal to 0.55, 0.42, 0.32, 0.31, and 0.31, respectively. The table also shows that the highest ϕ in clay soils was also obtained for the Blue Book method, followed by SPT-Meyerhof method, Nordlund method, α -API method, and β -method, in that order, as the ϕ values were equal to 0.63, 0.51, 0.41, 0.34, and 0.31, respectively. Table 6.5 also indicates that the highest ϕ in mixed soils corresponded to the SPT-Meyerhof method, followed by the Blue Book method, α -API method, Nordlund method, and the β -method, in that order, as the ϕ values were equal to 0.67, 0.60, 0.44, 0.42, and 0.41, respectively. For non-redundant pile groups, it was observed that the resistance factors were reduced from those of redundant piles by an average of 30%. Nevertheless, it is important to highlight the fact that the efficiency of different methods is better indicated by the efficiency factors (ϕ/λ) provided in Table 7.1. For all soil types, the Blue Book method has found to be the most efficient method. Table 7.2 provides the two static analysis methods that are recommended to be used for design of driven piles in Iowa, along with the corresponding final LRFD resistance and efficiency factors

based on a target reliability index of 2.33 for sand, clay, and mixed soils. These two methods were chosen based on the efficiency factor and following typical practices as recommended in AASHTO (2010).

Table 7.1: Recommended LRFD resistance factors for static methods

Soil Type	Static Analysis Method	$\beta=2.33$		$\beta=3.00$	
		ϕ^1	ϕ/λ^2	ϕ	ϕ/λ
Sand	SPT-Meyerhof	0.42	0.25	0.27	0.16
	α -API Method	0.31	0.26	0.21	0.17
	β -Method	0.32	0.37	0.23	0.27
	Nordlund	0.31	0.34	0.21	0.23
	Blue Book	0.55	0.47	0.41	0.36
Clay	SPT-Meyerhof	0.51	0.27	0.34	0.18
	α -API Method	0.34	0.33	0.24	0.22
	β -Method	0.31	0.31	0.21	0.21
	Nordlund	0.41	0.34	0.28	0.23
	Blue Book	0.63	0.43	0.46	0.32
Mixed	SPT-Meyerhof	0.67	0.46	0.51	0.35
	α -API Method	0.44	0.42	0.32	0.31
	β -Method	0.41	0.44	0.30	0.33
	Nordlund	0.42	0.37	0.30	0.26
	Blue Book	0.60	0.50	0.46	0.38

¹ LRFD resistance factor

² Efficiency factor

Table 7.2: Highest efficiency static methods and corresponding resistance factors

Soil Type	Resistance Factor and Efficiency	First Recommended Method		Second Recommended Method	
Sand	ϕ	Blue Book	0.55	β -Method	0.32
	ϕ/λ		0.47		0.37
Clay	ϕ	Blue Book	0.63	α -API	0.34
	ϕ/λ		0.43		0.33
Mixed	ϕ	Blue Book	0.60	β -Method	0.41
	ϕ/λ		0.50		0.44

7.1.2. Design Charts

A sensitivity analysis was conducted in order to determine how changing the target reliability index (β) would affect the LRFD resistance factors. As shown in Figure 7.1 for sand soils, the resistance factors are found to be very sensitive to any slight change in the reliability index. The analysis covered a wide range of β starting from 1.5 to 4.0, in order to include all possible

variations in the target reliability of bridge foundations. The same analysis was conducted for clay and mixed soils as shown in Figures 7.2 and 7.3, respectively. The design engineer can select the appropriate LRFD resistance factors corresponding to any target reliability index using Figures 7.1, 7.2, and 7.3 according to the redundancy of the pile groups, importance and life time of the bridge structure, degree of construction control, extent of conservatism in the design, and engineering judgment. As previously mentioned, however, in correspondence to a probability of failure of 1/100, a β of 2.33 for redundant pile groups (five piles or more for each pile cap) is recommended by the design codes.

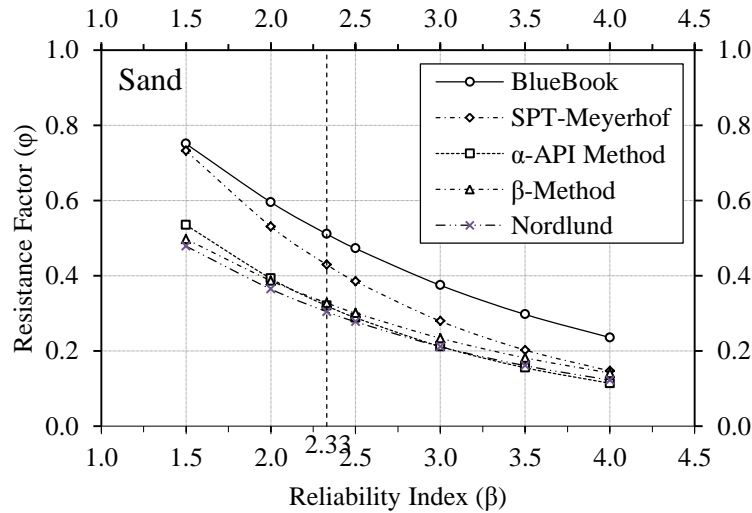


Figure 7.1: Resistance factors for static methods corresponding to different β in sand soil

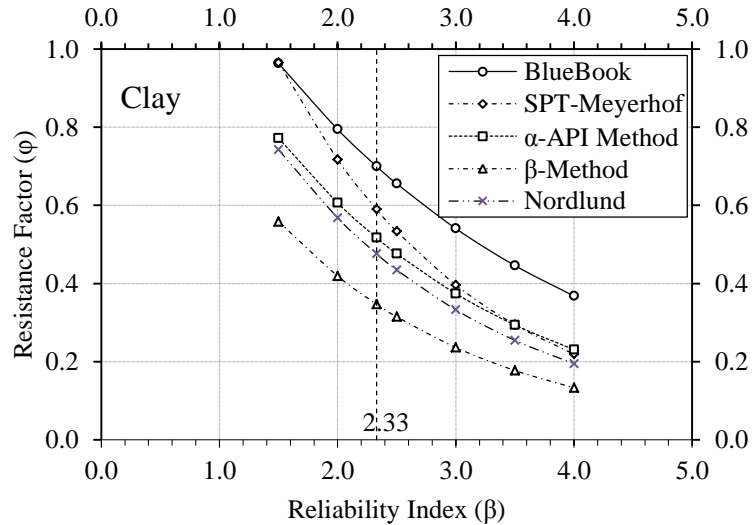


Figure 7.2: Resistance factors for static methods corresponding to different β in clay soil

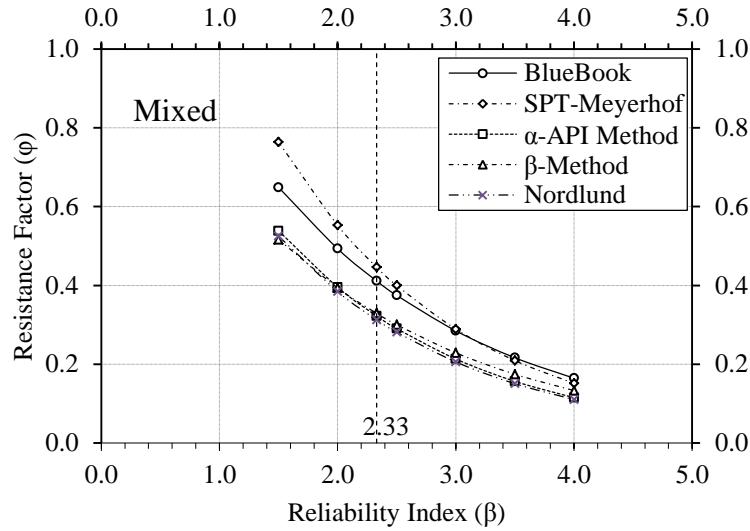


Figure 7.3: Resistance factors for static methods corresponding to different β in mixed soil

7.1.3. Improved Resistance Factors for Iowa Blue Book Method

Table 7.2 shows that the Iowa Blue Book method provides the highest efficiency for pile designs in Iowa. However, the calibrated resistance factors for $\beta=2.33$ (i.e., 0.5, 0.63 and 0.60 for piles installed in sands, clay and mixed soils, respectively) are relatively lower than the single resistance factor of 0.725 currently used by the Iowa DOT in an interim LRFD design procedure for bridge pile foundations. The interim procedure is being used as a short-term adaptation to LRFD while the resistance factor of 0.725 was established for the Iowa Blue Book method by fitting to an ASD safety factor of 2.0 for all soil types. Despite the differences, a verification study conducted by Ng et al. (2012b) on 604 production steel H-piles installed in clay at 17 bridge project sites in Iowa revealed that the factored geotechnical resistance was about 4% less when using the proposed LRFD procedure, as opposed to the interim procedure. In terms of the total plan pile length estimated for all 604 piles in clay soil, the LRFD procedure only increased it by about 3.3%. This insignificant difference concluded that using the Iowa Blue Book method based on the proposed LRFD procedure for pile design, is economically comparable to the current interim procedure for clay soil. While a similar investigation is currently underway for sand and mixed soils, it is most likely that the proposed LRFD resistance factors for these soils producing longer pile lengths than that may be used using $\phi = 0.725$ as per the interim procedure. In other words, the proposed LRFD procedure may increase the driven pile foundation costs in sand and mixed soils. To improve the resistance factors calibrated using the FOSM method described in Section 2.2.4.1, a modified FOSM method proposed by Bloomquist et al. (2007) as described in Section 2.2.4.2 was used. Table 7.3 summarizes and compares the resistance factors calibrated using both FOSM and modified FOSM methods. On average, the resistance factors improve 10% and 14% for $\beta=2.33$ and $\beta=3.00$, respectively. These improvements increase the resistance factors closer to 0.725 and will minimize additional design and construction costs incurred with switching the pile design method based on the interim procedure to the proposed LRFD procedure. Most importantly, it must be realized that the higher resistance factor obtained for the interim procedure, therefore, corresponds to a β less than 2.33 and that it increases the

likelihood of pile failure, both of which will not satisfy the LRFD expectation of ensuring uniform reliability in bridge design.

Table 7.3: Improved resistance factors for Iowa Blue Book method

Method	Soil Type	ϕ ($\beta=2.33$)			ϕ ($\beta=3.00$)		
		FOSM	Modified FOSM	Improved	FOSM	Modified FOSM	Improved
Iowa Blue Book	Sand	0.55	0.61	10.3%	0.41	0.47	14.0%
	Clay	0.63	0.69	9.2%	0.46	0.52	12.7%
	Mixed	0.60	0.67	11.0%	0.46	0.53	15.1%

7.2. Dynamic Analysis

Five soil input methods for the WEAP analysis were used for predicting the nominal capacity of steel H-piles. These methods are: the ST, SA, Iowa Blue Book, Iowa DOT method, and Driven methods. The number of data points used for developing the final LRFD recommendations increased from 12 to 17 in clay soils, from 9 to 11 in mixed soils, and from 11 to 13 in sand soils.

7.2.1. Design Tables

Table 7.4 summarizes the final LRFD resistance factors for WEAP dynamic analysis based on five different soil data input methods for driven steel H-piles in sand, clay, and mixed soils. The LRFD resistance factors were calculated for redundant and non-redundant pile groups by adapting β values equal to 2.33 and 3.00, respectively.

For redundant pile groups, the final recommendations are summarized in Table 7.4, which indicates that the WEAP based on the SA method has the highest resistance factor (ϕ) in sand soils, followed by Blue Book, Iowa DOT, ST, and Driven based methods, in that order, as ϕ values were equal to 0.55, 0.54, 0.52, 0.51, and 0.46, respectively. Table 7.4 also indicates that the Iowa DOT, ST and SA WEAP-based methods provide the highest ϕ in mixed soils, followed by the Blue Book and Driven methods, in that order, with ϕ values of 0.83, 0.81, 0.81, 0.80, and 0.77, respectively. On the other hand, for non-redundant pile groups, it was observed that the resistance factors were reduced more than those of redundant piles by an average of 20%. The effect of soil setup was examined for clay, and the corresponding final resistance factors were summarized in Table 6.15 in Section 6.2.11. Table 7.5 summarizes the selected LRFD resistance and efficiency factors for the construction control of pile foundations in Iowa based on a target reliability of 2.33 for sand, clay, and mixed soils.

Table 7.4: Recommended LRFD resistance factors for WEAP

Soil Type	WEAP Input Method	Condition	$\beta=2.33$		$\beta=3.00$	
			ϕ^1	ϕ/λ^2	ϕ	ϕ/λ
Sand	ST	EOD	0.51	0.49	0.39	0.37
	SA		0.55	0.53	0.43	0.41
	BB		0.54	0.51	0.41	0.39
	I DOT		0.52	0.46	0.39	0.34
	Driven		0.46	0.48	0.35	0.37
Clay ³	SA	EOD	0.65	0.71	0.54	0.59
		Setup	0.21	0.24	0.19	0.21
		BOR	0.72	0.74	0.61	0.63
	BB	EOD	0.65	0.71	0.55	0.59
		Setup	0.21	0.24	0.19	0.22
		BOR	0.72	0.74	0.61	0.63
	I DOT	EOD	0.54	0.69	0.45	0.57
		Setup	0.26	0.43	0.22	0.35
		BOR	0.62	0.76	0.52	0.64
Mixed	ST	EOD	0.81	0.56	0.64	0.44
	SA		0.81	0.54	0.63	0.42
	BB		0.80	0.53	0.62	0.41
	I DOT		0.83	0.58	0.66	0.46
	Driven		0.77	0.51	0.59	0.40

¹ LRFD resistance factor, ² Efficiency factor, ³For more discussion see Table 6.15 in Section 6.2.11.

Table 7.5: Highest efficiency WEAP methods and corresponding resistance factors

Soil Type	Resistance Factor and Efficiency	First Recommended Method		Second Recommended Method	
Sand	ϕ	SA	0.55	Blue Book	0.54
	ϕ/λ		0.53		0.51
Clay [BOR on last dynamic test]*	ϕ	I DOT	0.62	Blue Book	0.72
	ϕ/λ		0.76		0.74
Clay [EOD + setup]*	ϕ	Blue Book	0.65; 0.21	I DOT	0.54; 0.26
	ϕ/λ		0.71; 0.24		0.69; 0.43
Mixed	ϕ	I DOT	0.83	ST	0.81
	ϕ/λ		0.58		0.56

*For more discussion see Table 6.15 in Section 6.2.11

7.2.2. Design Charts

A sensitivity analysis was conducted to determine the effect that changing the target reliability index (β) would have on the LRFD resistance factors. For sand soils, the resistance factors were found to be very sensitive to any slight change in the reliability index, as shown in Figure 7.4. The analysis was designed to cover a wide range of β starting from 1.5 to 4.0 in order to include all possible variations in the target reliability of bridge foundations. The same analysis was conducted for clay at the EOD, setup, and BOR conditions as shown in Figures 7.5, 7.6, and 7.7, while the analysis for mixed soils is shown in Figure 7.8. By using Figures 7.4, 7.5, 7.6, 7.7, and 7.8, a design engineer can select the appropriate LRFD resistance factors corresponding to any target reliability index using Figures 7.4, 7.5, 7.6, 7.7, and 7.8 according to the redundancy of the pile groups, importance and life time of the bridge structure, degree of construction control, extent of conservatism in the design, and engineering judgment. However, a minimum β value of 2.33 for redundant pile groups is recommended by various design codes.

Enhancements on the LRFD resistance factors for Iowa Blue Book method were executed to include several aspects such as the increase in pile design capacity when using WEAP as the construction control method, as well as the probable gain in the capacity when considering the effect of soil setup with respect to time. For recommendations concerning the effects that construction control aspects and soil setup have on the resistance factors using dynamic analysis methods, see Sections 6.2.10 to 6.2.12 of this report. Noted that the enhancement by considering construction control aspects and soil setup, described in Sections 6.2.10 to 6.2.12, were evaluated using the resistance factors given in Table 7.4. The modified FOSM method, described in Section 2.2.4.2 and used to improve the resistance factors for Iowa Blue Book method in Section 7.1.3, was not used in this section, because 1) relatively high resistance factors have been obtained for dynamic analysis methods; and 2) the enhancement of resistance factors for Iowa Blue Book Method using improved resistance factors for dynamic analysis methods will not be as effective as observed in Section 7.1.3 and summarized in Table 7.3.

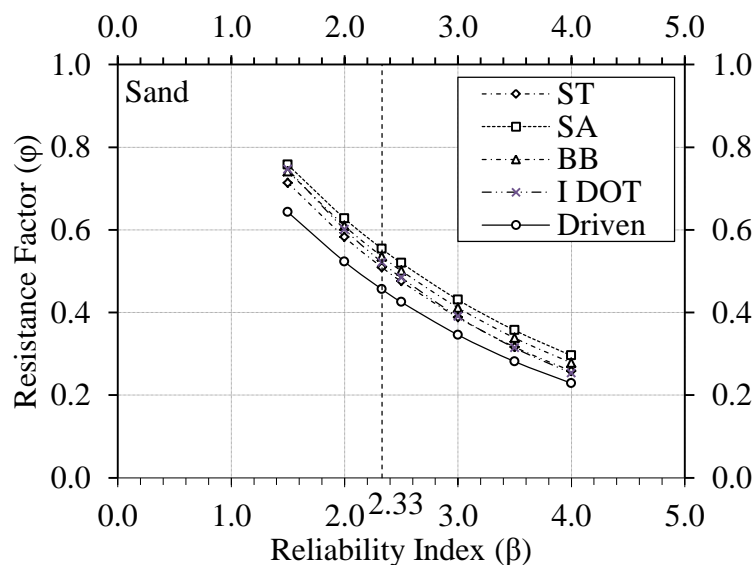


Figure 7.4: Resistance factors for WEAP corresponding to different β in sand

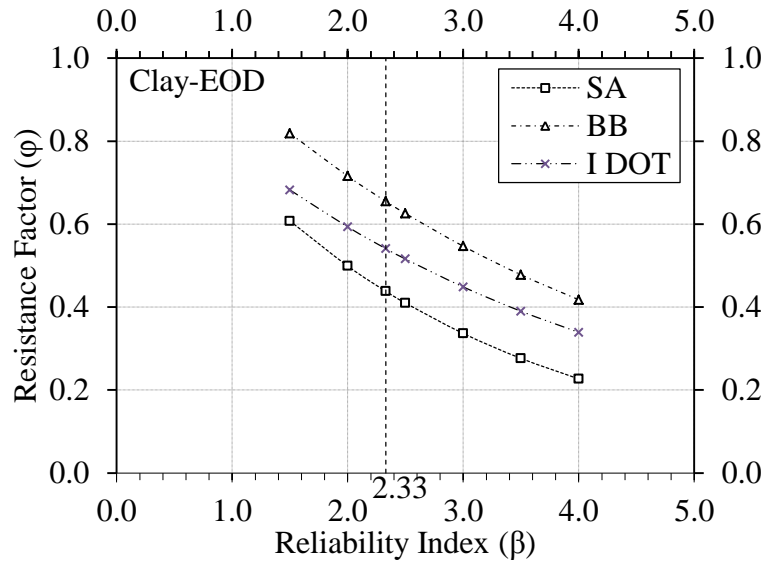


Figure 7.5: Resistance factors for WEAP corresponding to different β in clay for EOD

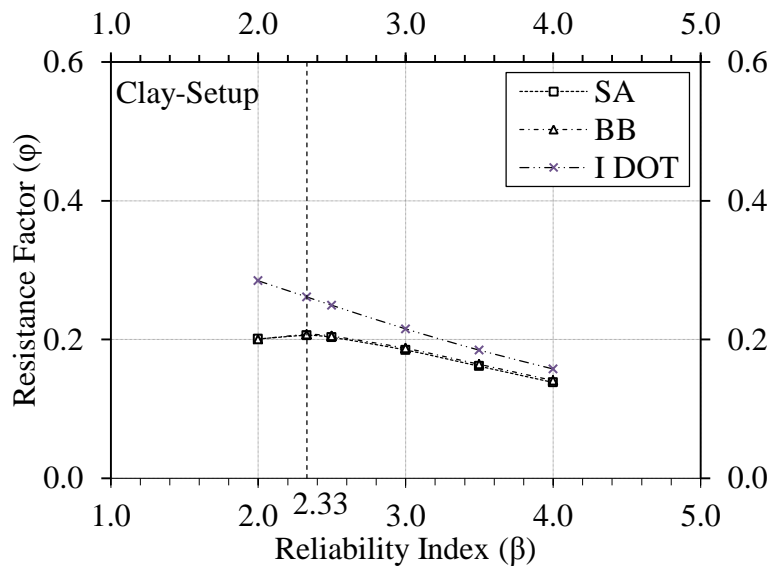


Figure 7.6: Resistance factors for WEAP corresponding to different β in clay for setup

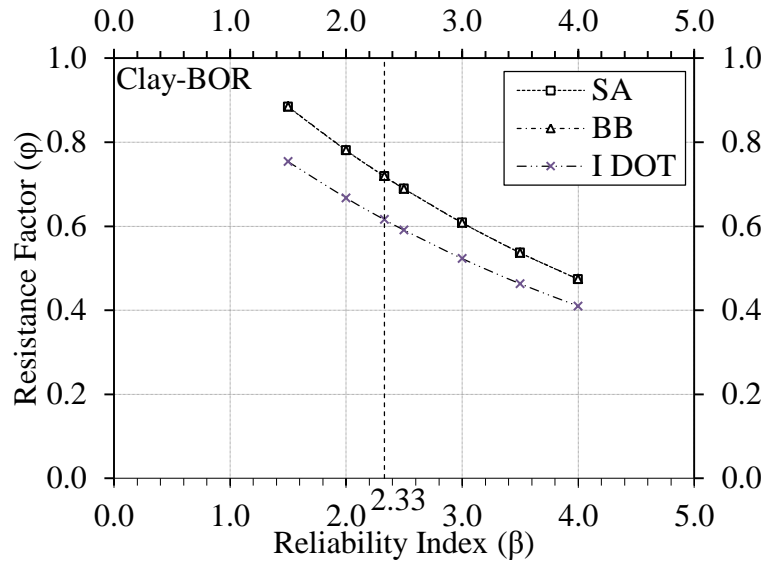


Figure 7.7: Resistance factors for WEAP corresponding to different β in clay for BOR

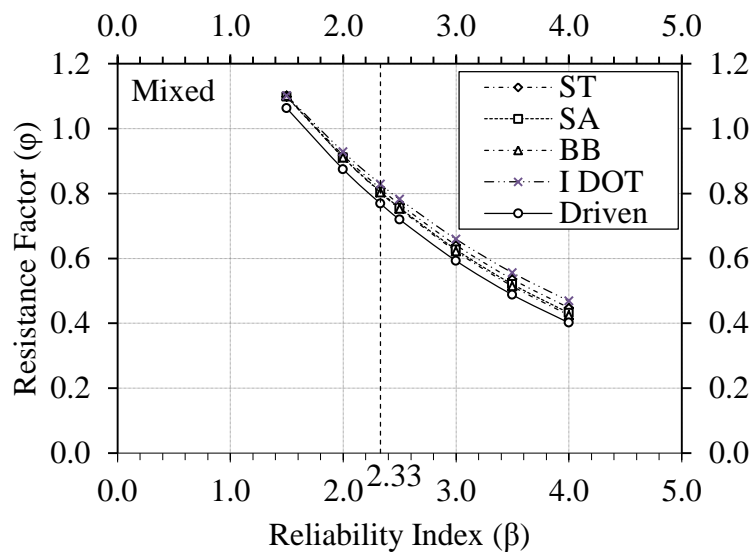


Figure 7.8: Resistance factors for WEAP corresponding to different β in mixed soil

7.3. Dynamic Formulas for Steel H-Piles

The following seven dynamic formulas examined in Chapter 6 were re-calibrated: the Gates formula, FHWA modified Gates, ENR, Iowa DOT ENR, Janbu, PCUBC, and Washington DOT formula. The number of data points used for developing the final LRFD recommendations for steel H-piles increased from 12 to 17 in clay soils, from 9 to 12 in mixed soils, and from 11 to 13 in sand soils.

7.3.1. Design Tables

Table 7.6 summarizes the final LRFD resistance factors of the seven different dynamic formulas

for driven steel H-piles in sand, clay, and mixed soils. The LRFD resistance factors were calculated for redundant and non-redundant pile groups assuming $\beta=2.33$ and 3.00, respectively.

For redundant pile groups, the results presented in Table 7.6 indicate that the highest resistance factor (ϕ) in sand soils is that of the Gates formula, followed by PCUBC, Janbu, WSDOT, Iowa DOT ENR, FHWA modified Gates, and ENR formulas, in that order, as ϕ values are equal to 0.64, 0.60, 0.58, 0.49, 0.48, 0.39, and 0.21, respectively. The table also shows that the Gates formula has the highest ϕ in clay soils, followed by PCUBC, Janbu, Iowa DOT ENR, WSDOT, FHWA Gates, and the ENR formula, in that order, as ϕ values are equal to 0.66, 0.60, 0.58, 0.54, 0.54, 0.43, and 0.22, respectively. Table 7.6 and Table 7.7 also indicate that the Gates and the PCUBC formulas provide the highest ϕ in mixed soils followed by the Janbu, WSDOT, Iowa DOT ENR, the FHWA modified Gates, and ENR, in that order, with ϕ values of 0.76, 0.74, 0.67, 0.66, 0.60, 0.49, and 0.26, respectively. In addition, it was observed that the resistance factors were reduced for non-redundant pile groups by an average of 20% compared to those of redundant piles. The two most efficient LRFD resistance and efficiency factors based on a target reliability of 2.33 for sand, clay, and mixed soils are summarized in Table 7.7.

Table 7.6: Recommended LRFD resistance factors for dynamic formulas and steel H-piles

Soil Type	Dynamic Formula	$\beta=2.33$		$\beta=3.00$	
		ϕ	ϕ/λ	ϕ	ϕ/λ
Sand	Gates	0.64	0.56	0.51	0.44
	FHWA Gates	0.39	0.53	0.30	0.41
	ENR	0.21	0.41	0.15	0.30
	Iowa DOT ENR	0.48	0.53	0.37	0.41
	Janbu	0.58	0.55	0.45	0.43
	PCUBC	0.60	0.54	0.47	0.42
	WSDOT	0.49	0.54	0.38	0.42
Clay	Gates	0.66	0.64	0.54	0.52
	FHWA Gates	0.43	0.64	0.35	0.52
	ENR	0.22	0.46	0.16	0.34
	Iowa DOT ENR	0.54	0.61	0.43	0.49
	Janbu	0.58	0.62	0.47	0.51
	PCUBC	0.60	0.61	0.48	0.49
	WSDOT	0.54	0.62	0.43	0.50
Mixed	Gates	0.76	0.58	0.60	0.46
	FHWA Gates	0.49	0.64	0.40	0.52
	ENR	0.26	0.47	0.20	0.35
	Iowa DOT ENR	0.60	0.57	0.47	0.45
	Janbu	0.67	0.60	0.54	0.49
	PCUBC	0.74	0.65	0.60	0.53
	WSDOT	0.66	0.67	0.55	0.55

Table 7.7: Highest efficiency dynamic formulas and corresponding resistance factors for steel H-piles

Soil Type	Resistance Factor and Efficiency	First Recommended Formula		Second Recommended Formula	
Sand	ϕ	Gates	0.64	Janbu	0.58
	ϕ/λ		0.56		0.55
Clay	ϕ	Gates	0.66	FHWA Gates	0.43
	ϕ/λ		0.64		0.64
Mixed	ϕ	WSDOT	0.66	PCUBC	0.74
	ϕ/λ		0.67		0.65

7.3.2. Design Charts

A sensitivity analysis was conducted to determine what effect changing the target reliability index (β) would have on the LRFD resistance factors. As shown in Figure 7.9, the resistance factors for sand soils are found to be very sensitive to any change in the reliability index. The analysis was designed to cover a wide range of β starting from 1.5 to 4.0. The same analysis was conducted for clay and mixed soils as shown in Figures 7.10 and 7.11, respectively. Using Figures 7.9, 7.10, and 7.11, a design engineer can select the appropriate LRFD resistance factors corresponding to any target reliability index according to the redundancy of the pile groups, importance and lifetime of the bridge structure, degree of construction control, extent of conservatism in the design, and engineering judgment. However, as previously noted, a β of 2.33 has been recommended for redundant pile groups. In addition, optional enhancements were executed on the LRFD resistance factors to include the increase in the pile design capacity when using construction control methods based on dynamic formulas. For recommendations concerning the effect of utilizing the dynamic formulas for construction control, see Section 6.3.10 of this report.

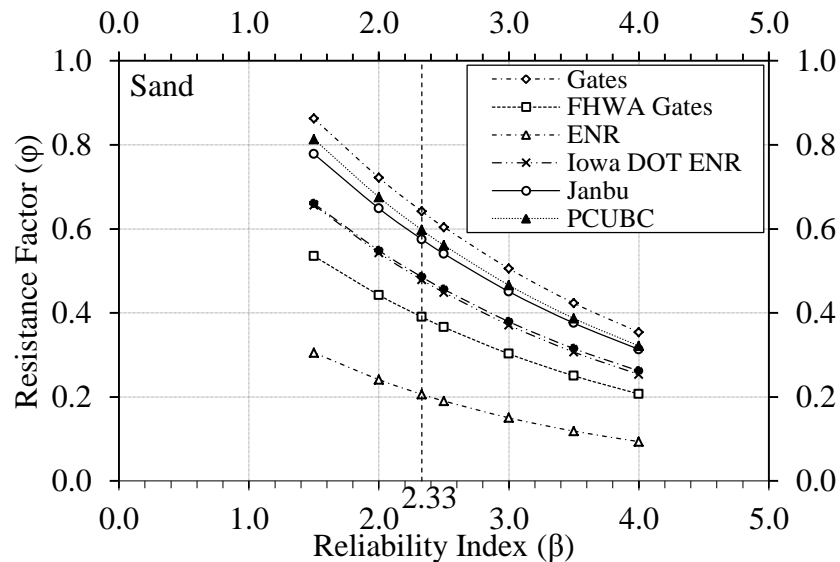


Figure 7.9: Resistance factors for dynamic formulas and steel H-piles corresponding to different β in sand

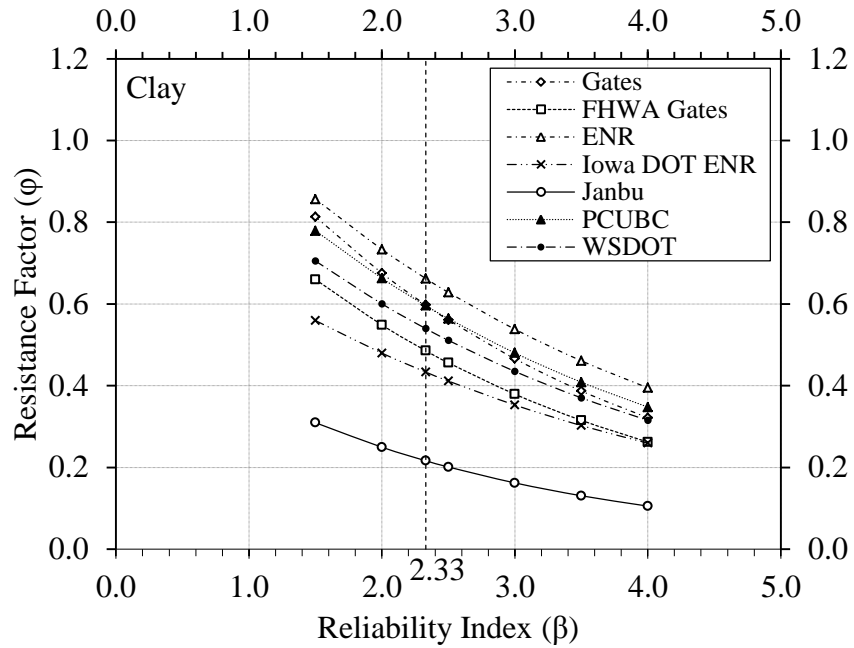


Figure 7.10: Resistance factors for dynamic formulas and steel H-piles corresponding to different β in clay

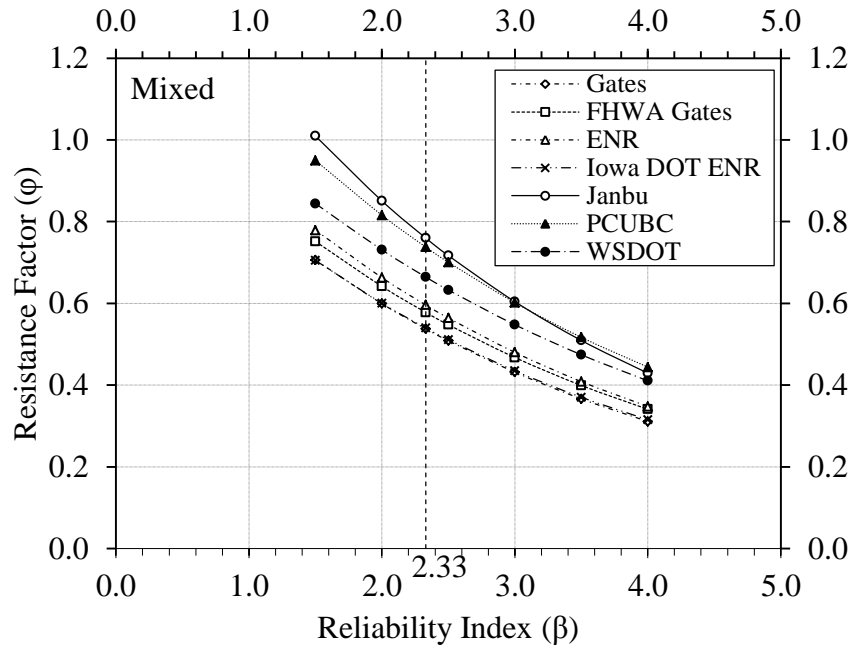


Figure 7.11: Resistance factors for dynamic formulas and steel H-piles correspond to different β in mixed soil

7.4. Dynamic Formulas for Timber Piles

According to the survey conducted as part of this research, 72.2% of Iowa County engineers have used a deep foundation system comprised of timber piles to support low-volume bridges and 55.6% of them use timber piles for short span bridges as described in Section 4.2.2 and Figure 4.16. In regards to the method of analysis most commonly used for the design of driven pile foundations, 86% of respondents cited the use of dynamic pile driving formulas (i.e., ENR, Gates, etc. with appropriate assumptions) for this particular task, while the remaining 14% reported the use of static analysis methods (i.e., SPT-Meyerhof, Blue Book methods, etc.) as presented in Figure 4.21. In particular, the Iowa DOT ENR formula was the unanimous dynamic pile driving formula of choice for the design of driven pile foundations by Iowa County engineers. In response to those needs, LRFD recommendations were formulated for dynamic formulas and timber piles. Unlike steel H-piles, only nine usable data points on timber piles compiled in the PILOT database are available for resistance factors calibration, in which two timber piles were embedded in sand, four in clay and three in mixed soils.

7.4.1. Design Tables

Table 7.8 summarizes the final LRFD resistance factors of the seven dynamic formulas for timber piles. The LRFD resistance factors were calculated for redundant and non-redundant pile groups corresponding to $\beta=2.33$ and 3.00 , respectively. For redundant pile groups, the results presented in Table 7.8 indicate that the Gates formula has the highest resistance factor (ϕ) followed by WSDOT, Janbu, PCUBC, Iowa DOT ENR, ENR, and FHWA modified Gates formulas. It was expected that the resistance factors would be reduced by an average of 20% for non-redundant pile groups compared to those of redundant piles. Among the seven different dynamic formulas, the Gates formula has the highest resistance factor of 0.64 and efficiency factor (ϕ/λ) of 0.56, followed by the WSDOT formula with a resistance factor of 0.60 and efficiency factor of 0.50. Both the Gates formula and the WSDOT formula were recommended in Table 7.9. Regarding the Iowa County engineers' choice for the design of timber piles, the resistance factors calibrated for the Iowa DOT ENR formula are 0.35 and 0.24 for redundant and non-redundant pile groups corresponding to $\beta=2.33$ and 3.00 , respectively.

Table 7.8: Recommended LRFD resistance factors for dynamic formulas and timber piles

Soil Type	Dynamic Formula	$\beta=2.33$		$\beta=3.00$	
		ϕ	ϕ/λ	ϕ	ϕ/λ
All	Gates	0.64	0.56	0.50	0.44
	FHWA Gates	0.23	0.20	0.14	0.13
	ENR	0.26	0.42	0.19	0.30
	Iowa DOT ENR	0.35	0.36	0.24	0.26
	Janbu	0.57	0.47	0.43	0.36
	PCUBC	0.55	0.49	0.42	0.38
	WSDOT	0.60	0.50	0.46	0.39

Table 7.9: Highest efficiency dynamic formulas and corresponding resistance factors for timber piles

Soil Type	Resistance Factor and Efficiency	First Recommended Formula		Second Recommended Formula	
All	ϕ	Gates	0.64	WSDOT	0.60
	ϕ/λ		0.56		0.50

7.4.2. Design Charts

A sensitivity analysis was conducted to determine what effect changing the target reliability index (β) would have on the LRFD resistance factors. As shown in Figure 7.11, the resistance factors are found to reduce with increase in the reliability index for timber piles for the combined soil group. The analysis covered a wide range of β starting from 1.5 to 4.0, in order to include all possible variations in the target reliability of bridge foundations. Using Figure 7.11, a design engineer can select the appropriate LRFD resistance factors corresponding to any target reliability index according to the redundancy of the pile groups, importance and lifetime of the bridge structure, degree of construction control, extent of conservatism in the design, and engineering judgment, although a minimum β of 2.33 for redundant pile groups is recommended. As previously noted, optional enhancements were executed on the LRFD resistance factors to include the increase in the pile design capacity when using construction control methods based on dynamic formulas. For recommendations concerning the effect of utilizing the dynamic formulas for construction control, see Section 6.3.10 of this report.

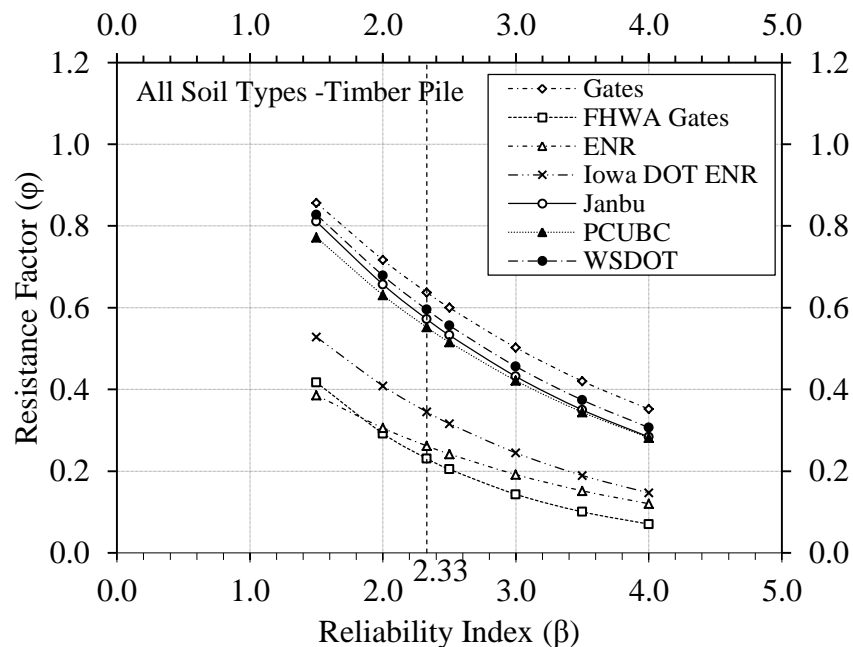


Figure 7.12: Resistance factors for dynamic formulas and timber piles correspond to different β

7.5. Summary of Resistance Factors

With a reliability index of 2.33 for a redundant pile group, Table 7.10 summarizes the resistance factors for the Iowa Blue Book as a design method, while Table 7.11 summarizes the resistance factors of the WEAP, CAPWAP, Iowa DOT ENR formula, and pile load test as construction control methods. As can be seen in Table 7.2, with input from the Iowa DOT and representative county engineering offices, the Iowa Blue Book method was recommended for pile design because it provides the most efficient design and also reflects regional design practices in Iowa. Among the different dynamic formulas, Iowa DOT ENR formula was recommended in order to reflect the current regional construction practices in Iowa. To maintain a consistency between pile designs and construction, the Iowa Blue Book soil input procedure was selected among the other procedures for WEAP. To report the originality of the calibrated resistance factors, these factors summarized in Table 7.10 and Table 7.11 are not rounded to the nearest 0.05. However, resistance factors are rounded to the nearest 0.05 when summarized in Table 7.12 for the design stage and in Table 7.13 for the construction stage. Some of the resistance factors were adjusted to maintain consistency and resolve any anomalies observed among the factors. The rational decision of each adjustment is described under each table. It is important to note that the resistance factors presented in this section were obtained mainly for steel H-piles, and therefore these resistance factors shall be thoughtfully used for other driven pile types. This topic is further discussed in Volume IV, the final report of this project (Green et al., 2012).

During the design stage, an appropriate resistance factor will be selected depending on the type of soil profile that production steel H-piles will be installed in and the construction control method that will be employed during construction to verify the target pile performance. During the construction stage, either Iowa DOT ENR formula or WEAP with the option of restrikes are recommended as a construction control method to establish production pile driving criteria. In addition, static pile load test or PDA with subsequent CAPWAP analysis and the option of restrike can be included to enhance the construction control procedure. Appropriate resistance factors shall be selected depending on the soil profile and the construction control procedure.

Based on the outcome of the research, pile setup resistance (R_{setup}) in clay soil profiles will be quantified based on the method described in Section 6.2.10 of this report and Section 5 of LRFD Report Vol. II (Ng et al., 2011b) while the pile resistance at EOD (R_{EOD}) will be determined using either WEAP or CAPWAP. The total factored pile resistance shall be determined using Eq. [6.4]. Pile setup is not accounted for piles driven in sand and mixed soil profiles. As noted in each table, some of the calibrated resistance factors were again adjusted to resolve the anomalies among different soil profiles and construction control methods. The rationale behind the adjustment of the resistance factors is described below with respect to the superscripted notes included in each table:

- 1) Note 'g': The originally calibrated resistance factor of 0.63 for Iowa Blue Book design method, summarized in Table 7.3 for clay sites, was improved to 0.68 (see Table 6.17) by considering the construction control procedure as described in Section 6.2.12. This improvement is allowed during design if the pile setup effect is considered, WEAP is specified to establish driving criteria, and CAPWAP is included as a construction control method.
- 2) Note 'h': Although the construction control procedure described in Section 6.2.12

increased the resistance factor of 0.60 to 0.80 for Iowa Blue Book design method as summarized in Table 7.3 for mixed site (see Table 6.17), a smaller factor of 0.68 for clay was recommended to eliminate any bias towards designing piles in mixed soils as well as to avoid the perception that the accuracy of this procedure matches the pile load test method without considering pile restrikes during construction.

- 3) Note 'i': By considering the construction control procedure described in Section 6.2.12, the improved resistance factor of 0.58 (see Table 6.17) was assumed for both construction control options, with and without 7-day restrrike, because no pile setup was assumed in sand. Because a smaller sample size was used in the LRFD calibration for CAPWAP, the smaller of the two resistance factors (i.e., 0.58) was preferred over 0.69.
- 4) Note 'j': In order to maintain consistency among resistance factors as observed in Table 7.3 (i.e., a relative higher resistance factor for clay, a lower resistance factor for sand, and a median resistance factor for mixed site) and to minimize discrepancy in design and construction control for piles in clay and mixed soils, the modified resistance factor of 0.64 (see Table 6.17) for the mixed site was reduced to 0.63 at the design stage. This reduction was permitted when Iowa Blue Book method is used for design and WEAP is specified as the construction control method. Similarly, when Iowa DOT ENR formula was employed to verify pile performance during construction, the resistance factor of 0.59 was reduced to 0.54 as of clay site with an intention to resolve the possible change in site soil classification when and if pile extensions are required.
- 5) Note 'k': To enhance the economic advantages of the proposed LRFD procedure, improved resistance factors calibrated based on modified FOSM method as summarized in Table 7.3 can be used during pile design (i.e., 0.69 for clay, 0.67 for mixed soil, and 0.61 for sand before rounding them to the nearest 0.05)
- 6) Note 'l': In order to demote the application of the relatively less accurate Iowa DOT ENR formula in respect to the more reliable WEAP method, the originally calibrated resistance factors of 0.63 for clay and 0.55 for sand (see Table 7.3) were reduced to 0.60 and 0.50, respectively, so that the recommended resistance factors are smaller than those used WEAP as a construction control method.
- 7) Note 'm': To eliminate the potential influence of some pile setup in mixed soil profile, the originally calibrated resistance factor of 0.80 (see Table 7.4) was reduced to 0.65 to match the resistance factor calibrated for clay at the EOD condition.
- 8) Note 'n': A maximum resistance factor of 0.80 was adopted from the AASHTO LRFD Bridge Specifications (2010).
- 9) Note 'o': Due to pile setup effect in mixed soil, an unusually high resistance factor of 0.80 for WEAP was obtained (see Table 7.4). Additionally, a relatively smaller resistance factor of 0.74 was calibrated based on all soil types (i.e., combining clay, sand and mixed). However, this factor of 0.74 remained higher than those obtained for clay (0.72) and sand (0.54), and a resistance factor of 0.65 was assumed for WEAP with 7-days restrrike in order to maintain the consistent trend of resistance factors observed (i.e., smaller than the calibrated resistance factor of 0.71 for CAPWAP and a factor between 0.72 for clay and 0.54 for

sand). For CAPWAP analysis, a resistance factor of 0.71 calibrated based on all soil types was assumed for mixed as well as sand instead of relatively high factors for mixed soil (0.93) and sand (0.77).

- 10) Note 'p': If timber piles are used instead of steel H-piles, the resistance factor for Iowa DOT ENR formula that is used as a construction control method shall be reduced to 0.35 for all soil types as described in Section 7.4.
- 11) Note 'q': If timber piles instead of steel H-piles are used, the resistance factor for WEAP used as a construction control method shall be reduced to 0.40 for all soil types in accordance with the AASHTO LRFD Bridge Specifications (2010).

Table 7.10: Summary of recommended resistance factors for design

Theoretical Analysis ^b	Stage	Construction control (field verification)					Resistance factor (ϕ) ^a				
		Driving Criteria Basis		PDA/ CAPWAP	Restrike Test after EOD	Static Pile Load Test	Clay			Mixed	Sand
		Iowa DOT ENR	WEAP				ϕ	ϕ_{EOD}	ϕ_{setup}	ϕ	ϕ
Iowa Blue Book	Design ^c	Yes	-	-	-	-	0.60 ^l	-	-	0.60	0.50 ^l
		No	Yes ^e	-	-	-	0.63 ^k	-	-	0.63 ^{j k}	0.55 ^k
				Yes	-	-	0.68 ^{g k}	-	-	0.68 ^h	0.58 ^{i k}
					Yes	-	0.80	-	-	0.71	

Note:

^a provide a minimum of five piles per redundant pile group

^b use the Iowa Blue Book to estimate the theoretical nominal pile resistance

^c use the applicable resistance factor to estimate factored resistance using Iowa Blue Book method during design

^d use the applicable resistance factor to determine the driving criteria required to achieve the target nominal driving resistance

^e use the Iowa Blue Book soil input procedure in WEAP analysis

^g setup effect has been included when WEAP is used to establish driving criteria and CAPWAP is used as a construction control (see more details in Section 7.5)

^h similar value of 0.68 for clay was recommended for mixed soil rather than 0.80 (see Table 6.17)

ⁱ assumed for both conditions due to the fact that pile setup does not occur in sand

^j 0.63 was adjusted from 0.64 to minimize discrepancies in design and construction control for piles in clay and mixed soils.

^k improved resistance factors calibrated based on modified FOSM as summarized in Table 7.3 can be used (i.e., 0.69 for clay, 0.67 for mixed soil, and 0.61 for sand)

^l 0.60 was adjusted from 0.63 for clay and 0.50 was adjusted from 0.55 for sand so that the recommended resistance factors are smaller than those used either WEAP or CAPWAP as a construction control method

Table 7.11: Summary of recommended resistance factors for construction control

Theoretical Analysis ^b	Stage	Construction control (field verification)					Resistance factor (ϕ) ^a				
		Driving Criteria Basis		PDA/ CAPWAP	Restrike Test after EOD	Static Pile Load Test	Clay			Mixed	Sand
		Iowa DOT ENR	WEAP				ϕ	ϕ_{EOD}	ϕ_{setup}	ϕ	ϕ
Iowa Blue Book	Construction ^d	Yes	-	-	-	-	0.54 ^p	-	-	0.54 ^{j p}	0.48 ^p
		No	Yes ^{e q}	-	-	-	-	0.65	0.21	0.65 ^{m o}	0.54 ⁱ
				-	Yes	-	0.72	-	-		
				Yes ^f	-	-	-	0.75	0.37	0.71 ^o	0.71 ^{i o}
					Yes	-	0.80	-	-		
				-	-	Yes	0.80 ⁿ	-	-	0.80 ⁿ	0.80 ⁿ

Note:

^a provide a minimum of five piles per redundant pile group

^b use the Iowa Blue Book to estimate the theoretical nominal pile resistance

^d use the applicable resistance factor to determine the driving criteria required to achieve the target nominal driving resistance

^e use the Iowa Blue Book soil input procedure in WEAP analysis

^f use signal matching to estimate total resistance

ⁱ assumed for both conditions due to the fact that pile setup does not occur in sand

^j 0.59 was reduced to 0.54 to minimize discrepancies in design and construction control for piles in clay and mixed soils.

^m 0.65 was adjusted from 0.80 (see Table 7.4) to eliminate the effect of some pile setup in mixed site

ⁿ 0.80 was adopted from AASHTO Specifications (2010)

^o 0.65 for WEAP and 0.71 for CAPWAP (see Table 6.15) were assumed as limited samples were available for resistance factors calibration

^p resistance factor shall be reduced to 0.35 for redundant pile groups if Iowa DOT ENR formula is used in construction control of timber piles

^q resistance factor shall be reduced to 0.40 for redundant pile groups if WEAP is used in construction control of timber piles

Table 7.12: Recommended resistance factors for design rounded to nearest 0.05

Theoretical Analysis ^b	Stage	Construction control (field verification)					Resistance factor (ϕ) ^a				
		Driving Criteria Basis		PDA/ CAPWAP	Restrike Test after EOD	Static Pile Load Test	Cohesive			Mixed	Non-cohesive
		Iowa DOT ENR	WEAP				ϕ	ϕ_{EOD}	ϕ_{setup}	ϕ	ϕ
Iowa Blue Book	Design ^c	Yes	-	-	-	-	0.60 ^l	-	-	0.60	0.50 ^l
		No	Yes ^e	-	-	-	0.65 ^k	-	-	0.65 ^{j k}	0.55 ^k
				Yes	-	-	0.70 ^g	-	-	0.70 ^h	0.60 ⁱ
					Yes	-	0.80	-	-	0.70	

Note:

^a provide a minimum of five piles per redundant pile group

^b use the Iowa Blue Book to estimate the theoretical nominal pile resistance

^c use the applicable resistance factor to estimate factored resistance using Iowa Blue Book method during design

^e use the Iowa Blue Book soil input procedure in WEAP analysis

^g setup effect has been included when WEAP is used to establish driving criteria and CAPWAP is used as a construction control (see more details in Section 7.5)

^h similar value of 0.70 for clay was recommended for mixed soil rather than 0.80 (see Table 6.17)

ⁱ assumed for both conditions due to the fact that pile setup does not occur in sand

^j 0.65 was adjusted from 0.64 to minimize design discrepancy for piles in clay and mixed soils

^k improved resistance factors calibrated based on modified FOSM and rounded to nearest 0.05 can be used (i.e., 0.70 for clay, 0.65 for mixed soil, and 0.60 for sand)

^l 0.60 was adjusted from 0.63 for clay and 0.50 was adjusted from 0.55 for sand so that the recommended resistance factors are smaller than those considering either WEAP or CAPWAP as a construction control method

Table 7.13: Recommended resistance factors for construction control rounded to nearest 0.05

Theoretical Analysis ^b	Stage	Construction control (field verification)					Resistance factor (ϕ) ^a				
		Driving Criteria Basis		PDA/ CAPWAP	Restrike Test after EOD	Static Pile Load Test	Cohesive			Mixed ϕ	Non- cohesive ϕ
		Iowa DOT ENR	WEAP				ϕ	ϕ_{EOD}	ϕ_{setup}		
Iowa Blue Book	Construction ^d	Yes	-	-	-	-	0.55 ^p	-	-	0.55 ^p	0.50 ^p
		No	Yes ^{e,q}	-	-	-	-	0.65	0.20	0.65 ^{m,o}	0.55
				-	Yes	-	0.70	-	-		
				Yes ^f	-	-	-	0.75	0.40	0.70 ^o	0.70 ⁱ
					Yes	-	0.80	-	-		
				-	-	Yes	0.80 ⁿ	-	-	0.80 ⁿ	0.80 ⁿ

Note:

^a provide a minimum of five piles per redundant pile group

^b use the Iowa Blue Book to estimate the theoretical nominal pile resistance

^d use the applicable resistance factor to determine the driving criteria required to achieve the target nominal driving resistance

^e use the Iowa Blue Book soil input procedure in WEAP analysis

^f use signal matching to estimate total resistance

ⁱ assumed for both conditions due to the fact that pile setup does not occur in sand

^m0.65 was adjusted from 0.80 (see Table 7.4) to eliminate the effect of some pile setup in mixed site

ⁿ0.80 was adopted from AASHTO Specifications (2010)

^o 0.65 for WEAP and 0.70 for CAPWAP were assumed as limited samples were available for resistance factors calibration

^p resistance factor shall be reduced to 0.35 for redundant pile groups if Iowa DOT ENR formula is used in construction control of timber piles

^q resistance factor shall be reduced to 0.40 for redundant pile groups if WEAP is used in construction control of timber piles

7.6. Pile Resistance and Target Driving Resistance

Following the Iowa DOT current practice and the established recommendations in Section 7.5, this section discusses how production piles can be designed using the Iowa Blue Book method to determine a nominal pile resistance (R_{IABB}) using Eq. [7.1] as well as a contract pile length using the Iowa DOT Bridge Design Manual geotechnical resistance chart. That is,

$$R_{IABB} = \frac{\Sigma \gamma Q}{\phi_{IABB}} \quad [7.1]$$

where

- γ = Load Factor based on AASHTO Strength I load combination;
- Q = Load applied to an individual pile, kips; and
- ϕ_{IABB} = Resistance factor for the Iowa Blue Book method from Table 7.12 based on embedded soil type and the construction control method to be engaged during construction.

In terms of achieving the target resistance, pile performance should be verified using either the Iowa DOT ENR formula, WEAP, PDA/CAPWAP and/or static load test. However, based on the Iowa DOT current construction practice, pile driving criteria in terms of hammer blow count (i.e., number of hammer blows per unit pile penetration) should be established using either the Iowa ENR formula or WEAP. For piles embedded in non-cohesive or mixed soil profiles or if the effect of pile setup in cohesive soil should not be considered using the semi-empirical method proposed in Section 6.2.10, the pile performance should be satisfied during driving when the recorded pile resistance estimated using the Iowa DOT ENR formula, WEAP, and/or PDA/CAPWAP exceeds the target nominal pile driving resistance (R_{target}) calculated as

$$R_{target} = \frac{\Sigma \gamma Q}{\phi} \quad [7.2]$$

where

- γ = Load Factor based on AASHTO Strength I load combination;
- Q = Load applied to an individual pile, kips; and
- ϕ = Resistance factor from Table 7.13 based on the construction control procedure engaged during construction.

For piles embedded in a cohesive soil profile, the effect of pile setup described in Section 6.2.10 should be considered during design and verified at the end of driving (EOD) during construction, and the corresponding LRFD limit state equation can be written as

$$\Sigma \gamma Q \leq \phi_{EOD} R_{EOD} + \phi_{setup} R_{Setup} \quad [7.3]$$

where

- γ = Load Factor based on AASHTO Strength I load combination;
- Q = Load applied to an individual pile;
- R_{EOD} = Pile resistance at EOD determined from a bearing graph generated using WEAP, kips;
- R_{setup} = Pile setup resistance estimated using Eq. [6.3], kips;
- ϕ_{EOD} = Resistance factor for R_{EOD} ; and
- ϕ_{setup} = Resistance factor for R_{setup} .

Considering the effect of pile setup and rearranging Eq. [7.3], the target nominal pile driving resistance at EOD ($R_{\text{Target,EOD}}$), which will be verified using either WEAP and/or PDA/CAPWAP during construction, can be computed via

$$R_{\text{target,EOD}} = \frac{\Sigma \gamma Q}{\varphi_{\text{EOD}} + \varphi_{\text{setup}} \left[\frac{a \log\left(\frac{t}{t_{\text{EOD}}}\right)}{(N_a)^b} \right]} \quad [7.4]$$

where

- t_{EOD} = Time at EOD (assumed 1 second), sec;
- N_a = Weighted average SPT N-value (see Eq. [6.1]);
- a = Method dependent scale factor (see Table 6.14); and
- b = Method dependent concave factor (see Table 6.14).

If the recorded pile driving resistance at EOD (estimated from WEAP or PDA/CAPWAP) is less than the $R_{\text{Target,EOD}}$, then the pile will be retapped about 24 hours after EOD. Since pile setup would have occurred immediately after the EOD (i.e., pile resistance would have increased), the recorded pile driving resistance obtained at the 24-hour retap should be verified against a higher target driving resistance, in which the increased pile resistance due to the 24-hour setup will be considered. Based on independent data sets obtained from recorded production steel H-piles installed throughout Iowa during bridge construction in 2009 and 2010 (Ng et al., 2012a), 26 production piles installed in five different Iowa Counties as summarized in Table 7.14 were retapped at about 24 hours after EOD. Because there were no PDA records collected for CAPWAP analysis, the recorded pile driving resistances were obtained from WEAP at the retap ($R_{t=24 \text{ hours}}$). Based on the average SPT N-value (N_a) given in Table 7.14 and the appropriate factors for WEAP (i.e., $\varphi_{\text{EOD}} = 0.65$, $\varphi_{\text{setup}} = 0.20$, $a = 0.215$, and $b = 0.144$), the $R_{\text{Target,EOD}}$ of each production pile was calculated using Eq. [7.4]. Figure 7.13 shows all 26 ratios of $R_{t=24 \text{ hours}}$ to $R_{\text{Target,EOD}}$, which are plotted in respect to the corresponding N_a values. These ratios indicate the amount of pile resistance increases in reference to the estimated $R_{\text{Target,EOD}}$ value. The mean ratio was determined to be 1.33, concluding that the average pile resistance increases by about 33% from the $R_{\text{Target,EOD}}$ value, while the standard deviation was determined as 0.147. As documented in the pile driving records obtained from the Iowa DOT, 21 production piles satisfied target driving resistances at the 24-hour retap, which were represented by filled markers in Figure 7.13. The remaining five production piles that did not achieve the target driving resistance during the 24-hour retap were extended 10 ft in the pile length, and were represented by five opened markers. Comparing these five opened markers to the ratio of $R_{t=24 \text{ hours}}$ to $R_{\text{Target,EOD}}$, Figure 7.13 suggests that a production pile with a ratio greater than about 1.20 will satisfy the target driving resistance and vice-versa. Based on the above observation, the target driving resistance for a 24-hour retap and the proposed LRFD procedure can be approximated as:

$$R_{\text{target,24-hour}} \cong 1.2 \times R_{\text{target,EOD}} = \frac{1.2 \times \Sigma \gamma Q}{\varphi_{\text{EOD}} + \varphi_{\text{setup}} \left[\frac{a \log\left(\frac{t}{t_{\text{EOD}}}\right)}{(N_a)^b} \right]} \quad [7.5]$$

Table 7.14: Summary of 26 production steel H-piles that were retapped at 24 hours

Iowa County	Pier/ Abutment	Pile No.	Pile Size	Hammer	Brief Soil Description	Average SPT N-value, N _a	Plan Pile Length (ft)
Lee-138	West Abutment	1	HP 10×57	Delmag D19-32	Stiff silty clay to firm glacial clay	15	70
		3					70
		4					70
		5					70
		6					70
	Pier 1	5	HP 12×53			17	45
		19					45
		21					45
Jasper-44	West Abutment	1	HP 10×57	Delmag D19-42	Silty clay	14	70
		2					70
		3					70
		4					70
		5					80
		6					70
		7					70
	Lee-148	Pier	9	HP 10×57	Kobe K-25	Very firm glacial clay	40
Tama-114	Pier	24	HP 10×57	APE D19-42	Silty clay to firm glacial clay	51	44
		25					44
	North Abutment	4				47	64
		8					64
		11					64
		12					64
	South Abutment	8				38	70
		11					70
Tama-119	Pier	7	HP 10×57	Delmag D19-42	Very firm glacial clay	28	45
		14					45

If the 24-hour retap does not indicate enough driven resistance or the recorded driving resistance is less than the $R_{\text{target},24\text{-hour}}$, additional restrikes can be performed at later days to verify the pile performance. Otherwise, a pile extension will be added immediately after the 24-hour retap until the recorded driving resistance is equal to or exceeds the $R_{\text{Target,EOD}}$. The details of the pile construction control procedure will be discussed in the Volume IV and final report of this project (Green et al, 2012). Additionally, based on the completed effort of the project, a design guide and track examples, accounting for further input from designers and demonstrating the application of the design and construction control methods, are currently underway. This information will be published in the Volume IV.

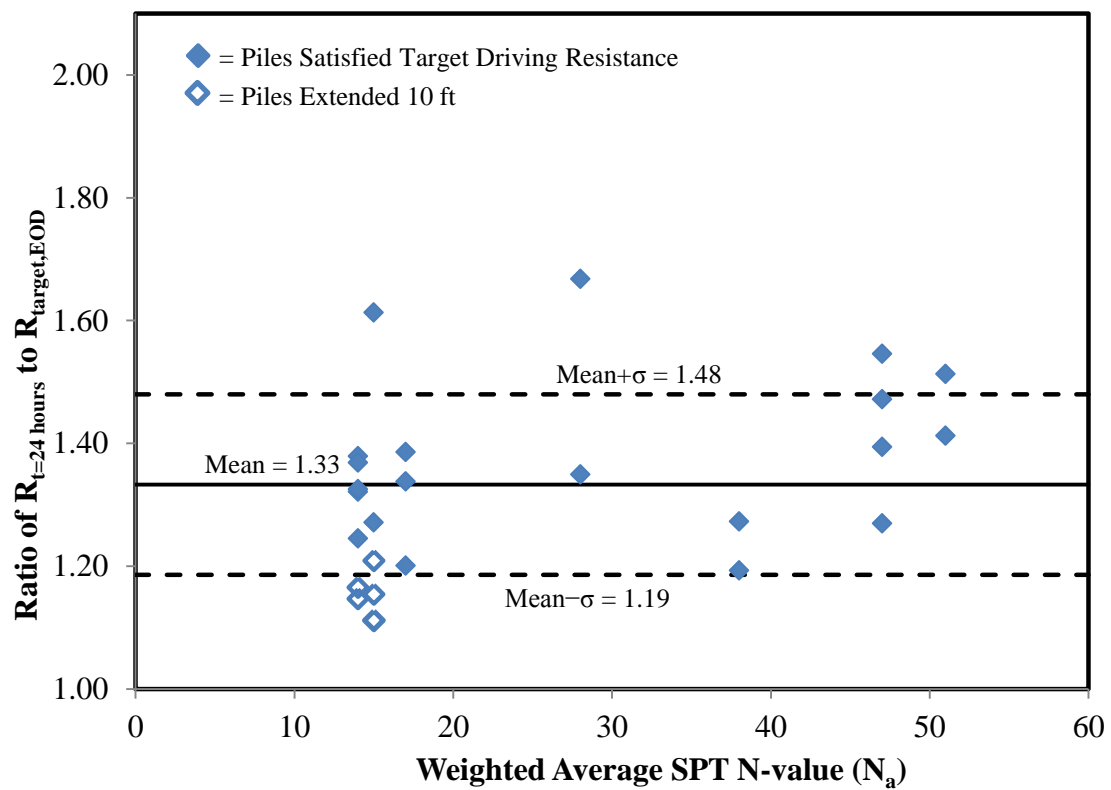


Figure 7.13: Ratio of pile driving resistance at 24-hour retap to target driving resistance at EOD plotted in respect to N_a

CHAPTER 8: SUMMARY AND CONCLUSIONS

8.1. Summary of Research

The overall scope of the research project described in this report was to develop LRFD resistance factors for bridge pile foundations in Iowa with due consideration to reliability theory, focusing on the strength limit state. The analysis was extended to incorporate the construction control aspects and soil setup into the design process. In Chapter 1 of this report, the challenges associated with design and construction of bridge pile foundations have been briefly discussed, emphasizing on the advantages and benefits of LRFD compared to the ASD method. A review on the published literature has been presented in Chapter 2, which includes the basic principles of the LRFD approach and the typical calibration framework. The most popular and local pile design and construction methods including static and dynamic analysis methods, as well as dynamic formulas have been presented in Chapter 3, which provides the necessary background information required to use any of these methods. To have a better understanding of the current bridge foundation design and construction practices, nationwide and local surveys to State DOTs and County engineers were conducted, and the results have been summarized in Chapter 4. Chapter 4 also included a brief overview of the pile load test database (PILOT) that was mainly used for developing the LRFD resistance factors as well as an overview of the new 10 full-scale instrumented pile load tests that were conducted as part of this project, covering all possible soil types and geological formations in the State of Iowa. The selected calibration framework in this research has been summarized and presented in Chapter 5, providing a better understanding of the most suitable calibration approach for Iowa DOT and allowing for future revisions. The preliminary LRFD regionally calibrated resistance factors for static methods, dynamic methods and dynamic formulas were calculated and presented in Chapter 6. The performance of the preliminarily developed resistance factors was evaluated by means of the full-scale instrumented pile load test data, and the verification results were presented in Chapter 6. Following the LRFD framework, Chapter 6 also included the incorporation of the construction control aspects and pile setup. Chapter 7 provides the final recommendations in the form of design/construction tables and charts, which involved re-calibration of the resistance factors after incorporating the 10 load test data into PILOT.

8.2. Major Outcomes and Conclusions

In this research, the LRFD resistance factors calibration framework was selected to follow the 2008 AASHTO and the NCHRP-507 guidelines, taking into consideration the local practices in the State of Iowa. The resistance factors were developed for general and in-house design and construction methods. Compared with the current AASHTO LRFD specifications and the NCHRP-507 guidelines, a substantial increase in the regionally calibrated resistance factors was observed. Comprehensive tables and figures are provided in Chapter 7, summarizing the recommended LRFD resistance factors and the reasons were making further adjustments to these factors. The following sections briefly summarize the major outcomes of the research that has focused on static analysis methods, dynamic analysis methods, and dynamic formulas, as well as associated recommendations.

8.2.1. Static Analysis Methods

Five different static analysis methods were used for calculating the design nominal capacity of steel H-piles in this study. These methods were Nordlund method, α -API method, β -method, SPT-Meyerhof method, and the Iowa DOT design charts (Blue Book method). The LRFD calibration was conducted based on the PILOT database for driven steel H-piles in different soil types. The number of tests available for LRFD calibration in clay, sand, and mixed soils were 25, 36, and 29, respectively. All probability density functions were confirmed to follow the lognormal distribution and the FOSM reliability approach was used for the LRFD calibration.

For redundant pile groups, the results indicated that the Blue Book method has the highest resistance factor (ϕ) in sand soils, followed by SPT-Meyerhof, β -method, α -API, Nordlund method, in that order, with ϕ values ranging between 0.55 and 0.31. For clay soils, the Blue Book method has the highest ϕ , followed by SPT-Meyerhof method, Nordlund method, α -API method, and β -method, in that order, with ϕ in the range between 0.63 and 0.34. For mixed soils, the SPT-Meyerhof has the highest ϕ , followed by the Blue Book method yielded, α -API method, Nordlund method, and β -method, in that order, with ϕ values ranging between 0.67 and 0.41. For non-redundant pile groups, it was observed that the resistance factors were reduced by an average of 30%. Compared to other static analysis methods, it was found that the Iowa Blue Book method was the most efficient static analysis method in sand, clay, and mixed soils, and the corresponding efficiency factors (ϕ/λ) were equal to 0.47, 0.43, and 0.50, respectively. Furthermore, using the improved FOSM method for LRFD calibration, the resistance factors for the Iowa Blue Book method were improved to 0.61, 0.69 and 0.67 for piles in sand, clay, and mixed soil, respectively.

The regionally developed resistance factors were also compared to those provided in the design specifications to determine the percent increase in the factored capacity. The developed resistance factor of the SPT-Meyerhof method in sand soil was about 40% greater than the factor provided in 2010 AASHTO specifications. For β -method in sand, the developed resistance factor was about 3% greater than that recommended by the NCHRP. For clay soils, the developed resistance factor for β -method was found to be around 25% and 55% greater than those recommended by NCHRP and AASHTO, respectively. For mixed soils, a significant increase of about 60% in the resistance factors was observed for β -method compared to AASHTO. Moreover, an increase in the resistance factors of about 25% and 20% was obtained for the α -API and Nordlund methods, respectively, compared to the NCHRP values in mixed soils.

When verified using the recently conducted pile load tests, it was generally found that the nominal (un-factored) capacity of the piles calculated using many of the static analysis methods was higher than measured values. However, after multiplying the nominal static capacity by the corresponding resistance factors, the factored design capacities did not exceed the actual measurements for any of the selected method. A large variation between the calculated nominal capacities using different static methods was observed, but this variation was also significantly reduced after applying the LRFD resistance factors. Moreover, the Blue Book design method was found to be the most efficient static analysis method for all soil types. This indicates that the selected method and corresponding LRFD resistance factors succeeded in limiting the design-factored capacity from exceeding the actual measurements and do so without large variation between different static methods. In conclusion, the recently developed LRFD resistance factors

for the Blue Book ensure reliable, consistent and economic designs for driven bridge pile foundations in Iowa.

8.2.2. Dynamic Analysis Methods

Five different methods for inputting the soil parameters during the WEAP dynamic analysis were used for predicting the nominal capacity of steel H-piles. These methods were the ST, SA, Iowa Blue Book, Iowa DOT, and Driven procedures. The LRFD calibration was conducted for WEAP based on PILOT database for driven steel H-piles in different soil types. The number of tests available in clay, sand, and mixed soils were 17, 13, and 11, respectively. All probability density functions (based on different soils and WEAP input methods) were confirmed to follow the lognormal distribution and the FOSM reliability approach was again used for the LRFD calibration.

For redundant pile groups, the results indicated that the highest resistance factor (ϕ) in sand soils based on the SA method for inputting soil data followed by Blue Book, Iowa DOT, ST, and Driven procedures, in that order. The corresponding ϕ values ranged between 0.55 and 0.46. For mixed soils, the Iowa DOT, ST, and SA procedures provided the highest ϕ in mixed soils, followed by the Blue Book and Driven procedures, in that order, with ϕ values ranging between 0.83 and 0.77. For non-redundant pile groups, it was observed that the resistance factors were reduced by an average of 20%. On the other hand, the ϕ/λ factor was calculated for all groups and it was found that the most efficient WEAP input methods in sand and mixed soils were the SA and Iowa DOT methods, with values equal to 0.53 and 0.58, respectively. For clay soils, the highest ϕ for WEAP at the beginning of restrike (BOR) was based on the Blue Book followed by SA, and Iowa DOT procedures, in that order, and the ϕ values ranged between 0.72 and 0.62. For the EOD component, the SA and Blue Book procedures provided the highest efficiency, followed by Iowa DOT procedure. For the setup component, the Iowa DOT procedure gave the highest efficiency, followed by the SA and Blue Book procedures. Nevertheless, the efficiency differences among the different WEAP procedures was not significant for any given soil type.

The regionally developed resistance factors were also compared to those provided in the design specifications to determine the percentage of increase in the factored capacity of the piles. The developed resistance factor for the WEAP-SA based method in sand soils was greater than the factor provided in AASHTO Specifications (2010) by around 10%. Moreover, a greater potential for cost reduction can be attained by using the developed resistance factors in clay and mixed soils, as the resistance factors increased by at least 30%. Overall, the regionally calibrated LRFD resistance factors for WEAP have shown a high potential for reducing foundation costs in Iowa when compared to AASHTO recommended design specifications which is intended for broad use across the nation.

When compared to the measured data from the recently tested 10 piles, the nominal WEAP capacity was already lower than the measured capacity of the piles. After multiplying by the LRFD resistance factors, it was found that the WEAP-Iowa DOT based method seemed to be, overall, less conservative compared to other WEAP input methods. The degree of conservatism associated with the LRFD is also relatively low compared to the ASD approach. Consequently, the regionally calibrated factors for WEAP are regarded as a reliable and economic, and it can be used for the construction of pile foundations in Iowa in order to satisfy the LRFD approach

without significantly increasing the foundation costs.

8.2.3. Dynamic Formulas

The seven different dynamic formulas used in this study are as follows: the Gates formula, FHWA modified Gates, ENR, Iowa DOT ENR, Janbu, PCUBC, and Washington DOT formula. For dynamic formulas also, the LRFD calibration was first conducted based on PILOT database for driven steel H-piles in different soil types. The number of tests available in clay, sand, and mixed soils were 17, 13, and 12, respectively. All probability density functions were ensured to follow the lognormal distribution and the FOSM reliability approach was used for the LRFD calibration.

For redundant pile groups, the results indicated that the highest resistance factor in sand soils was obtained for the Gates formula followed by PCUBC, Janbu, WSDOT, Iowa DOT ENR, FHWA modified Gates, and ENR formulas, in that order, with ϕ values ranging from 0.64 to 0.24. For clay soils, the highest ϕ was still for the Gates formula followed by PCUBC, Janbu, Iowa DOT ENR, WSDOT, FHWA Gates, and the ENR formula, in that order, and the ϕ values ranged between 0.67 and 0.22. For mixed soils, the Gates formula provided the highest ϕ , followed by the PCUBC, Janbu, WSDOT, Iowa DOT ENR, FHWA modified Gates, and ENR formulas, in that order, and the ϕ values were between 0.83 and 0.11. For non-redundant pile groups, as with the dynamic analysis methods, it was observed that the resistance factors were reduced by an average of 20% compared to those of redundant piles.

The regionally developed resistance factors were also compared to those provided in the AASHTO design specifications to determine the percentage of increase in the factored capacity of the piles. For example, the resistance factor developed for the ENR dynamic formula in sand soil is greater than that provided in 2008 AASHTO specifications by around 114%, which corresponds to a considerable reduction in the cost of bridge pile foundations. Similar cost reductions can be attained by using the developed resistance factors for ENR in clay and mixed soils, and the corresponding increase in ϕ value were about 100% and 140%, respectively.

When the preliminary LRFD resistance factors were tested against recently measured field data, it was found that estimated capacities sometimes exceeded the nominal measured values. When the factored capacities were compared, all dynamic formulas produce values below the measured values except for WSDOT and Janbu at selected sites. Overall, Iowa DOT consistently gave factored capacity less than the factored measured values. This method was also found to be sufficiently efficient, and thus it was selected for regional use to stay consistent with the current foundation practice in Iowa.

In addition, the LRFD recommendations were also provided for timber piles using the same seven different dynamic analysis methods. Unfortunately, only nine usable data sets of timber piles were available from PILOT for resistance factor calibration, and thus the soil classification was not considered here. For redundant pile groups, the Gates formula produced the highest resistance factor followed by WSDOT, Janbu, PCUBC, Iowa DOT ENR, ENR, and FHWA modified Gates formulas. It was observed that the resistance factors were reduced by an average of 20% for non-redundant pile groups compared to those of redundant piles. While the Gates formula gave the highest resistance factor of 0.64 and efficiency factor (ϕ/λ) of 0.56, the

WSDOT formula led to a resistance factor of 0.60 and efficiency factor of 0.50. As for the Iowa County engineers' choice for design of timber piles, the resistance factors calibrated for the Iowa DOT ENR formula were 0.35 and 0.24 for redundant and non-redundant pile groups corresponding to $\beta=2.33$ and 3.00, respectively.

8.2.4. Recommendations

Based on the completed study, the Iowa Blue Book method is recommended for all pile design, because it provided the most efficient design and endorses the most frequently used adopted regional design practice in Iowa. Among the different dynamic formulas, Iowa DOT ENR formula is recommended to reflect regional construction practices in Iowa. To maintain a consistency between pile design and construction, the Iowa Blue Book soil input procedure is selected among the other procedures (i.e., ST, SA, DRIVEN and Iowa DOT procedures) for WEAP analysis. Additionally, other pile construction control methods: PDA with CAPWAP and static load test are included and could be used where possible. It is important to note that the recommended resistance factors were developed for steel H-piles and to some extent for timber piles. Hence, these resistance factors shall be thoughtfully used for other driven pile types. At the design stage, an appropriate resistance factor will be selected depending on the type of soil profile in which production steel H-piles will be installed and the construction control method that will be employed during construction of these piles to verify the target pile performance. During the construction stage, either Iowa DOT ENR formula or WEAP, whichever was selected using design, with an option of restrikes is recommended as a construction control method to establish production pile driving criteria. In addition, static pile load test or PDA with subsequent CAPWAP analysis with an option of restrike can be included to enhance the construction control procedure. Appropriate resistance factors shall be selected, depending on the soil profile and the construction control procedure. The recommended resistance factors were summarized in Section 7.5. The complete design guide and track examples to demonstrate the application of the proposed LRFD procedure are discussed in LRFD Report Volume IV by Green et al. (2012).

8.3. Future Research

Although a significant progress was made in the implementation of LRFD procedure for driven piles in Iowa with the research presented in this report, further advancements can be made for continuous improvements of pile foundations. Some of them are noted below:

- 1) LRFD calibration for serviceability limit state, including vertical and horizontal displacements.
- 2) Integrating serviceability limit states into the LRFD procedure.
- 3) Integrating extreme loads into design.
- 4) Accounting for soil relaxation aspects in LRFD practice.
- 5) Increasing the database to include more drivability information, especially in clay soils.
- 6) Verifying the resistance factors of timber piles and making appropriate revisions.

REFERENCES

- AASHTO-LRFD Bridge and Construction Specifications (1994). AASHTO, Washington, D.C.
- AASHTO-LRFD Bridge Design Specifications (2004). AASHTO, Washington, D.C.
- AASHTO-LRFD Bridge Design Specifications (2006). AASHTO, Washington, D.C.
- AASHTO-LRFD Bridge Design Specifications (2007). Customary U.S. Units, 4th edition (2008 Interim), American Association of State Highway and Transportation Officials, Washington, D.C.
- AASHTO-LRFD Bridge Design Specifications (2010). Interim Revision. 5th Edition, American Association of State Highway and Transportation Officials, Washington, D.C.
- AbdelSalam S. S., Sritharan S., and Suleiman M. T. (2008). "Current design and construction practices of bridge pile foundations". Proceedings of the International Foundations Congress and Equipment Expo, March 2009, Orlando, FL.
- AbdelSalam S. S. (2010). Behavior characterization and Development of LRFD Resistance Factors for Axially-loaded Steel Piles in Bridge Foundations. Ph.D. Thesis. Iowa State University of Science and Technology, Ames, IA.
- Abu-Hejleh, N., Dimaggio, J, and Kramer, W. (2009) "AASHTO Load and Resistance Factor Design Axial Design of Driven Pile at Strength Limit State". Transportation Research Board 88th Annual Meeting, 2009, Paper #09-1034, Washington D.C.
- Allen, T. M., Nowak, A. S., and Bathurst, R. J. (2005). Calibration to determine load and resistance factors for geotechnical and structural design. Transportation Research Circular Number E-C079, TRB, Washington, D.C., 83 p.
- Allen, T. M. (2005). Development of the WSDOT Pile Driving Formula and Its Calibration and Resistance Factor Design (LRFD), FHWA Report, WA-RD 610.1, Washington State Department of Transportation.
- American Concrete Institute. (1974). "Recommendations for Timber Piles Design, Manufacture and Installation of Concrete Piles," ACI Report No. 543R-74.
- Argo, D. E. (1987). Dynamic Formulas to Predict Driven Pile Capacity, Department of Civil and Environmental Engineering, Washington State University, Pullman, WA.
- ASTM D1143/D1143M (2007). Standard Test Methods for Deep Foundations under Static Axial Compressive Load. American Society for Testing and Materials, Philadelphia, PA.
- ASTM D-2487 (2006). Annual Book of ASTM Standards, Soil and Rock (I), Vol. 4.08, American Society for Testing and Materials, Philadelphia, PA.
- Barker, R., Duncan, J., Rojiani, K., Ooi, P., Tan, C., and Kim, S. (1991). NCHRP Report 343: Manuals for the Design of Bridge Foundations, Transportation Research Board, National Research Council, Washington, D.C.
- Becker D. E. and Devata M.(2005). Implementation and Application Issues of Load and Resistance Factor Design (LRFD) for Deep Foundations, ASCE Conference Proceedings, 156, 1, DOI:10.1061/40777(156)1.
- Becker, D. (1996). Eighteenth Canadian Geotechnical Colloquium: Limit States Design for Foundations. Part I. An overview of the foundation design process. Canadian Geotechnical Journal, Vol. 33, No. 6, December, pp. 956–983.
- Belcher, D. J., and Flint, R. F. (1946). Soil Deposits Map of United States and Canada. Geological Society of America, Washington, D.C.
- Bloomquist, D., McVay, M., and Hu, Z. (2007). Updating Florida Department of Transportation's (FDOT) Pile/Shaft Design Procedures Based on CPT & DTP Data.

- Department of Civil and Coastal Engineering, University of Florida, Gainesville, FL.
- Bowles, J. (1977/1996). *Foundation Analysis and Design*. McGraw-Hill, NY.
- Broms, B. (1964). "Lateral Resistance of Piles in Cohesive Soils." *Journal of the Soil Mechanics and Foundations Division, ASCE*, Vol. SM2, March, pp. 27–63.
- Burland, J.B., (1973). *Shaft Friction of Piles in Clay*. *Ground Engineering*, London, Vol. 6, No.3, 3042 p.
- Butler, H.D., and Hoy, H.E. (1977). *User's Manual for the Texas Quick-Load Method for Foundation Load Testing*. FHWA-IP- 77-8. FHWA, Office of Development, Washington, D.C.
- Canadian Foundation Engineering Manual, (1985). Second Edition, Part 3: Deep Foundations;. Canadian Geotechnical Society, BiTech Publishers, Vancouver, 456 p.
- Chang, N.Y. (2006). *CDOT Foundation Design Practice and LRFD Strategic Plan*, Colorado DOT Research Branch, Report No. CDOT-DTD-R-2006-7
- Chellis, R. D. (1949). *The Relationship Between Pile Formulas and Load Tests*. *American Society of Civil Engineers Transactions* 114, pp. 290–320.
- Cheney, R. S. and Chassie, R. G. (1993), *Soils and Foundations Workshop Manual*, Report No. FHWA-HI-88-009.
- Chin, F. V. (1970). "Estimation of the Ultimate Load of Piles Not Carried to Failure." *Proceedings of the 2nd Southeast Asian Conference on Soil Engineering*, pp. 81–90.
- Coduto, D.P. (2001). *Foundation design: principles and practices*. Prentice-Hall Inc., Englewood Cliffs, NJ.
- Cummings, A. E. 1940. *Dynamic Pile Driving Formulas*. *Journal of the Boston Society of Civil Engineers* 27, pp. 6–27.
- Davissom, M. (1972). *High Capacity Piles*. In *Proceedings, Soil Mechanics Lecture Series on Innovations in Foundation Construction*, ASCE, IL Section, Chicago, IL, pp. 81–112.
- DiMaggio, J., Saad, T., Allen, T., Barry, R., Al Dimillio, Goble, G., Passe, P., Shike, T., and Person, G. (1999). *FHWA International Technology Exchange Program*, report number FHWA-PL-99-013.
- Dirks, K. and Kam P. (2003). *Foundation Soils Information Chart – Pile Foundation*. Iowa Department of Transportation, Office of Road Design, Ames, IA.
- Ellingwood, B., Galambos, T. V., MacGregor, J. G., and Cornell, C. A. (1980). "Development of a probability based load criterion for American National Standard A58—Building code requirements for minimum design loads in buildings and other structures." *National Bureau of Standards*, Washington, D.C.
- Esrig, M. I., and Kirby, R. C. (1979). *Soil Capacity for Supporting Deep Foundation Members in Clay*. ASTM STP. No. 670, pp. 27–63.
- Fellenius, B. H., (1991). *Summary of pile capacity predictions and comparison with observed behavior*. *American Society of Civil Engineers, ASCE, Journal of Geotechnical Engineering*, Vol. 117, No. 1, pp. 192–195.
- FHWA (1997). *Design and Construction of Driven Pile Foundations*, Workshop manual, Volumes I, publication FHWA-HI-97-013
- FHWA (2007). *Load and Resistance Factor Design (LRFD) for Highway Bridge Superstructures*, April 2007. Publication number FHWA-NHI-07-034.
- Foye, K. C., Abou-Jaoude, G., Prezzi, M., and Salgado, R. (2009). "Resistance factors in load and resistance factor design of driven pipe piles in sand". *Journal of Geotechnical and Geoenvironmental Engineering*, ASCE, v 135, n 1, 2009, pp. 1–13.

- Fragaszy, Richard J., Douglas E. Argo, and Jerry D. Higgins. 1989. "Comparison of Formula Predictions with Pile Load Tests." *Transportation Research Record*, Journal of the Transportation Research Board No. 1219, pp. 1–12.
- Gates, Marvin. 1957. Empirical Formula for Predicting Pile Bearing Capacity. *Civil Eng.*, 65-66.
- Gibbs, H. J. & Holtz, W. G. (1957). Research on Determining the Density of Sands by Spoon Penetration Testing. *Proceedings of 4th International Soil Mechanics and Foundation Engineering*, London 1, pp. 35–39.
- Green, R. (1994). "LRFD Code for Ontario Bridge Substructures". *Transportation Research Record*, No. 1447, pp. 73–79.
- Green, D., Ng, K.W., Dunker, K., and Sritharan, S. (2012). "Development of LRFD Design Procedures for Bridge Pile Foundations in Iowa – Design Guide and Track Examples." *Final Report Vol. IV. Institute for Transportation*, Iowa State University, Ames, IA.
- GRL, Inc. (1999). *Pile-Driving Analyzer, PAK User's Manual*. Goble, Rausche, Likins and Associates.
- Gulhati, Sahashi K., and Manoj Datta. 2005. *Geotechnical Engineering*. New Delhi, Haryana India: Tata McGraw-Hill Publishing Company Limited.
- Hamilton, J., and Murff, J. (1992). *Selection of LRFD Resistance Factors for Pile Foundation Design*. ASCE.
- Hannigan, P.J., G.G.Goble, G. Thendean, G.E. Likins and F. Rausche (2005). "Design and Construction of Driven Pile Foundations"—Volume I and II, Federal Highway Administration Report No. FHWA-HI-05, Washington, D.C.
- Hannigan, P.J., Goble, G.G., Thendean, G., Likins, G.E. and Rausche, F. (1998). *Design and Construction of Driven Pile Foundations – Volume I and II*, FHWA-HI-97-013. National Highway Institute, Federal Highway Administration, U.S. Department of Transportation, Washington, D.C.
- Hansen, J. B. (1963). "Hyperbolic Stress-strain Response: Cohesive Soils" *Journal of the Soil Mechanics and Foundations Division, American Society of Civil Engineers*, Vol. 89, No. SM4, NY.
- Hara, A., Ohta, T., Niwa, M., Tanaka, S., and Banno, T. (1974). "Shear Modulus and Shear Strength of Cohesive Soils". *Soils and Foundations*, Vol. 14, No. 3, September, pp. 1–12.
- Iowa DOT (2008). *Standard Specifications with GS-01014 Revisions. Iowa DOT Electronic Reference Library*. (http://www.erl.dot.state.ia.us/Apr_2008/GS/frames.htm).
- Iowa DOT LRFD Design Manual (2009). *Office Policies and Procedures, Office of Bridges and Structures*. (<http://165.206.203.34/dotmain/bridges/policy/62PileLRFDJa09.pdf>).
- Jardine R.J, Chow, F.C, Overy, R and Standing, J (2005) *ICP Design Methods for Driven Piles in Sands and Clays*, Publishers Thomas Telford.
- Jumikis, Alfreds R. 1971. *Foundation Engineering*, NY: Intext Educational Publishers.
- Kerkhoff, G. O., L. T. Oehler, and W. S. Housel. 1965. *A Performance Investigation of Pile Driving Hammers and Piles*. Lansing, Michigan State Highway Commission, MI.
- Kulhawy, F., and Phoon, K. (1996). Engineering Judgment in the evolution from Deterministic to Reliability-Based Foundation Design. *Proceedings of the 1996 Conference on Uncertainty in the Geologic Environment, UNCERTAINTY'96*. Part 1 (of 2), July 31–Aug. 31, Madison, WI, pp. 29–48.
- Kulhawy, F.H. and Mayne, P.W., (1990). "Manual on Estimating Soil Properties for Foundation Design", Rpt. EL-6800, Electric Power Research Inst., Palo Alto, 306 p.
- Kuo, C. L., McVay, M. C., and M., Birgisson, B. (2002). "Calibration of Load and Resistance

- Factor Design: Resistance factors for drilled shaft design". Transportation Research Record, No. 1808, pp. 108–111.
- Kyung, K. J. (2002). "Development of Resistance Factors for Axial Capacity of Driven Piles in North Carolina". Dissertation for a PhD degree, North Carolina State University, Raleigh, NC.
- Lai, P., and Graham, K. (1995). Static Pile Bearing Analysis Program. SPT94. (<http://www.dot.state.fl.us/structures/manuals/spt94.zip>).
- Lai, P., McVay, M.; Bloomquist, D., and Badri, D. (2008). "Axial Pile Capacity of Large Diameter Cylinder Piles". Proceedings of From Research to Practice in Geotechnical Engineering Congress 2008.
- Liang, R., and Nawari, N. O. (2000). "Evaluation of Resistance Factors for Driven Piles". New Technological and Design Developments in Deep Foundations (GSP 100), Proceedings of Sessions of Geo-Denver 2000, pp. 178–191.
- Mathias D., and M. Cribbs (1998). "DRIVEN 1.0: A Microsoft Windows Based Program for Determining Ultimate Static Pile Capacity." Federal Highway Administration.
- McVay, M., Birgisson, B., Zhang, L., Perez., A, and Putcha, S. (2000). Load and Resistance Factor Design (LRFD) for Driven Piles Using Dynamic Methods—A Florida Perspective. Geotechnical Testing Journal, Vol. 23, No. 1, pp. 55–66.
- McVay, M.; Klammler, H., Bloomquist, D., Otero, J., and Farone, M. (2010). "Modification of LRFD Resistance Factors Based on Site Variability". NTIS website accessed March 2010.
- Meyerhof, G. (1970). Safety Factors in Soil Mechanics, Canadian Geotechnical Journal, Vol. 7, No. 4, pp. 349–355.
- Meyerhof, G. (1976). Bearing Capacity and Settlement Of Pile Foundations. American Society of Civil Engineers, Journal of the Geotechnical Engineering Division, Vol. 102, No. 3, March, pp. 195–228.
- Misra, A. and Roberts, L.A. (2006). "Probabilistic Analysis of Drilled Shaft Service Limit State Using the "t-z" Method". Canadian Geotechnical Journal, pp. 1324–1332.
- Misra, A., Roberts, L. A. and Levorson, S. M. (2007). "Reliability of Drilled Shaft Behavior Using Finite Difference Method and Monte Carlo Simulation." Journal of Geotechnical and Geoenvironmental Engineering, ASCE, pp. 65–77.
- Moore, J. (2004/2005). AASHTO-LRFD Oversight Committee (OC) survey 2004 and the Update 2005, New Hampshire DOT, AASHTO Load and Resistance Factor Design (LRFD) Bridge Specifications information website: (<http://www.ridot.us/aashto/agenda.htm>), accessed May, 2008.
- Moore, J. (2007). AASHTO-LRFD Oversight Committee (OC) Update 2007, New Hampshire DOT, AASHTO Load and Resistance Factor Design (LRFD) Bridge Specifications information website. (<http://www.transportation.org/sites/bridges>), accessed May, 2008.
- Ng, K.W., Suleiman, M.T., and Sritharan, S. (2010). "LRFD Resistance Factors Including the Influence of Pile Setup for Design of Steel H-Pile Using WEAP." Geotechnical Special Publication No. 199, Advances in Analysis, Modeling & Design, Proc. of the Annual Geo-Congress of the Geo-Institute, ASCE, Feb 20-24, Fratta, D., Puppala, A.J., and Muhunthan, B., ed., West Palm Beach, FL, pp. 2153–2161.
- Ng, K. W. (2011). Pile Setup, Dynamic Construction control and Load and Resistance Factor Design of Vertically Loaded Steel H-Piles. Ph.D. Thesis. Iowa State University of Science and Technology, Ames, IA.

- Ng, K.W., Suleiman, M.T., Sritharan, S., Roling, M., and AbdelSalam, S.S. (2011a). "Development of LRFD Design Procedures for Bridge Piles in Iowa – Soil Investigation and Full-Scaled Pile Tests." Final Report Vol. II. IHRB Project No. TR-583. Institute for Transportation, Iowa State University, Ames, IA.
- Ng, K.W., Suleiman, M.T., and Sritharan, S. (2012a) "Pile Setup in Cohesive Soil with Emphasis on LRFD: Analytical Quantifications and Design Recommendations." *Journal of Geotechnical and Geoenvironmental Engineering*, ASCE. (Accepted for publication)
- Ng, K.W., Sritharan, S., and Dunker, K.F. (2012b) "Verification of Recommended Load and Resistance Factor Design Approach to Pile Design and Construction in Cohesive Soils." Transportation Research Board, 91st annual meeting, Washington, D.C.
- Nordlund, R. L. (1963/1979). "Bearing capacity of piles in cohesionless soils." *Journal of Soil Mechanics and Foundation Engineering*, *Journal of Soil Mechanics and Foundation Division*, ASCE, Vol. 89, SM 3, pp. 1–36.
- Nottingham, L., and Schmertmann, J. (1975). An Investigation of Pile Capacity Design Procedures. Final Report D629 to Florida Department of Transportation, Department of Civil Engineering, University of Florida, 159 p.
- Nowak A. S. and Collins K. R. (2000). "Reliability Of Structures". Publisher: McGraw-Hill Inc.
- Nowak, A. (1999). NCHRP Report 368: Calibration of LRFD Bridge Design Code. Transportation Research Board, Washington, D.C.
- Olson, Roy E., and Kaare S. Flaate. 1967. Pile-Driving Formulas for Friction Piles in Sand. *Journal of Soil Mechanics and Foundation Division*, ASCE, No. SM 6, pp. 279–296.
- O'Neill, M.W. and Reese, L.C. (1999). "Drilled Shafts: Construction Procedures and Design Methods," FHWA Report No. IF-99-025, Federal Highway Administration, Washington, D.C.
- Paikowsky, S. G. with contributions from Birgisson, B., McVay, M., Nguyen, T., Kuo, C., Baecher, G., Ayyab, B., Stenersen, K., O'Malley, K., Chernauskas, L., and O'Neill, M. (2004). Load and Resistance Factor Design (LRFD) for Deep Foundations, NCHRP Report 507, Transportation Research Board, Washington D.C.
- Passe, P. (1997). Florida's Move to the AASHTO-LRFD Code, STGEC 97, Chattanooga. TN.
- Peck, R. B., W. E. Hanson, and T. H. Thornburn (1974) "Foundation Engineering," John Wiley & Sons, 514 p.
- Pile Dynamics, Inc. (2000). CAPWAP for Windows Manual. Pile Dynamics, Inc., Cleveland, OH.
- Prakash, S., and Sharma, H. D. (1990). *Pile Foundations in Engineering Practice*, Wiley, NY.
- Ramey, G. E., and A. P. Hudgins. 1975. Modification of Pile Capacity and Length Prediction Equations Based on Historical Alabama Pile Test Data. State of Alabama Highway Department - Bureau of Research and Development. Montgomery, AL.
- Rausche, F., & Goble, G. (1979). Determination of Pile Damage by Top Measurements. American Society for Testing and Materials. Philadelphia, PA.
- Roberts, L. A., Gardner, B.S., and Misra, A. (2008). "Multiple Resistance Factor Methodology for Service Limit State Design of Deep Foundations using a 't-z' Model Approach", *Proceedings of the GeoCongress 2008*, New Orleans, LA.
- Robertson, P. K., and Campanella, R. G. (1983). "Interpretation of Cone Penetration Tests". *Canadian Geotechnical Journal*, Vol. 20, No. 4.
- Roling, M J., Sritharan, S., and Suleiman, M. T. (2010). Development of LRFD design Procedures for Bridge Piles in Iowa – An Electronic Database for Pile LOad Tests in

- Iowa (PILOT-Iowa). Final Report Vol. I. IHRB Project No. TR-573, TR-583 and TR-584. Institute for Transportation, Iowa State University, Ames, IA.
- Roling, M. J. (2010). Establishment of a Suitable Dynamic Pile Driving Formula for the Construction Control of Iowa Driven Pile Foundations and its Calibration for Load and Resistance Factor Design. Master These submitted to the Department of Civil, Construction, and Environmental Engineering, Iowa State University, Ames, IA.
- Rosenblueth, E., and Esteva, L. (1972). Reliability Basis for Some Mexican Codes. ACI Publication SP-31. American Concrete Institute, Detroit, MI.
- Schmertmann, J. H. (1975). Measurement of in situ shear strength, state-of-the-art report. Proceedings of the American Society of Civil Engineers Conference on In Situ Measurements of Soil Properties, Raleigh, NC, pp. 57–138.
- Schmertmann, J.H. (1978). "Guidelines for Cone Penetration Test, Performance and Design". Report No. FHWA-TS-78-209, U.S. Department of Transportation, Washington, D.C., 145 p.
- Scott, B., Kim, B. and Salgado, R. (2003). "Evaluation of Load Factors for Use in Geotechnical Design." Journal of Geotechnical and Geoenvironmental Engineering, ASCE, 129(4), pp. 287–295.
- Skempton, A.W. (1951), "The Bearing Capacity of Clays," Proceedings of Building Research Congress, Vol. 1, pp. 180–189.
- Smith, E. (1962). Pile-Driving Analysis by the Wave Equation. Journal of the Soil Mechanics and Foundation Division, ASCE, paper No. 3306, Vol. 127, Part 1, pp. 1145–1193.
- Smith, E. A. L. 1962. Pile-Driving Analysis by the Wave Equation. American Society of Civil Engineers Transactions 127, pp. 1145–1193.
- Spangler, M. G., and H. F. Mumma. 1958. Pile Test Loads Compared with Bearing Capacity Calculated by Formulas. Paper read at Thirty-Seventh Annual Meeting of the Highway Research Board, at Washington, D.C.
- Tang, W. (1993). Recent Developments in Geotechnical Reliability. Proceedings of the Conference on Probabilistic Methods in Geotechnical Engineering Li, K., and Lo, S-C. eds., Canberra, Australia, February 10–12, Balkema, Rotterdam, Netherlands, pp. 3–28.
- Terzaghi, K., and Peck, R.B. (1967). Soil Mechanics in Engineering Practice. Wiley.
- Thibodeau, E., and Paikowsky, S. (2005). "Performance Evaluation of a Large Scale Pile Load Testing Program in Light of Newly Developed LRFD Parameters". Proceeding Session of the Geo-Frontiers 2005 Congress, January 24-26, 2005, Austin, TX.
- Tomlinson, M. J. (1957). "The Adhesion of Piles Driven in Clay Soils," in Proceedings of the 4th International Conference on Soil Mechanics and Foundation Engineering, Vol. 2, 1957, pp. 66-71, Butterworths Scientific Publications, Ltd., London, England.
- Tomlinson, M.J. (1980/1995). Foundation Design and Construction, 6th Edition. Longman Scientific & Technical, Essex, England
- U.S. Army Corps of Engineers, (1992), "Pile Layout to Minimize Interference," Engineer Technical Letter ETL 1110-8-17(FR), Department of the Army, US Army Corps of Engineers, Washington, D.C.
- Van der Veen, C. (1953). "The Bearing Capacity of a Pile." Proceedings of the 3rd International Conference on Soil Mechanics and Foundation Engineering, Vol. 2, pp. 84–90.
- Vesic, A.S. (1977). Design of pile foundations. National Cooperative Highway Research Program Synthesis of Highway Practice No. 42, Transportation Research Board, Washington, D.C.

- Vijayvergiya, V.N., and Focht Jr., J.A. 1972. A New Way to Predict Capacity of Piles In Clay.
Proceedings of the 4th Annual Offshore Technology Conference, Houston, TX.
- Withiam, J. L., Voytko, E. P., Barker, R. M., Duncan, J. M., Kelly, B. C., Musser, S. C., and
Elias, V. (1998). "Load and resistance design LRFD for highway bridge substructures."
Federal Highway Administration, Washington, D.C.

APPENDIX A: FLOWCHARTS SUMMARIZING TWO LRFD SURVEYS

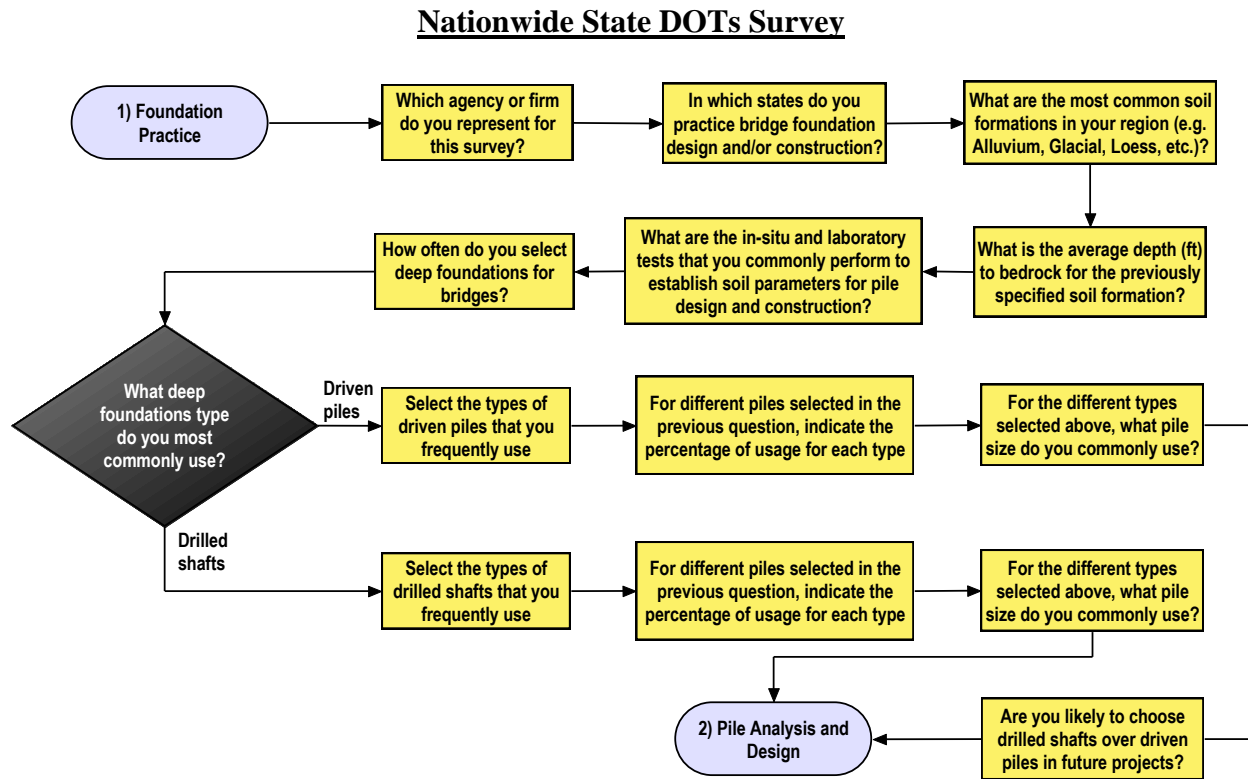


Figure A.1. Flowchart representing questions of the first section of the nationwide survey

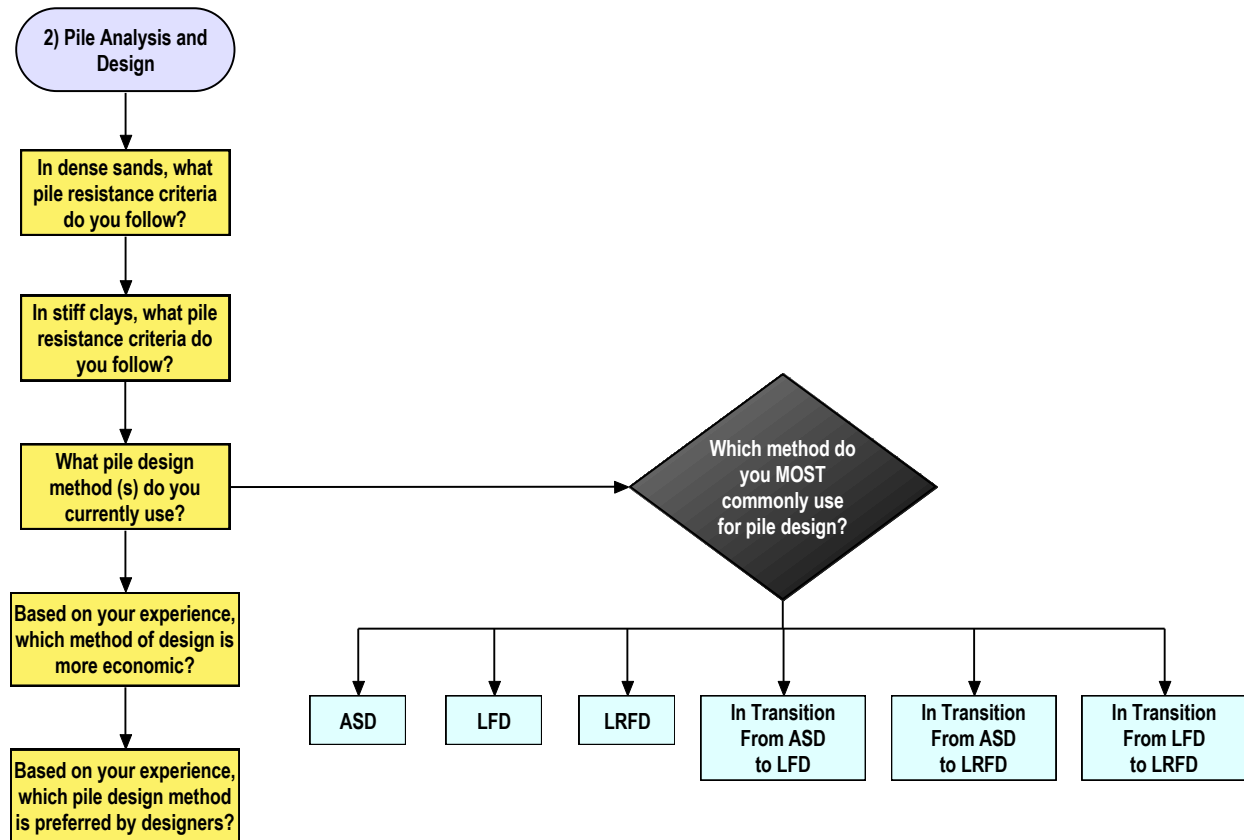


Figure A.2. Flowchart representing questions of the second section of the nationwide survey

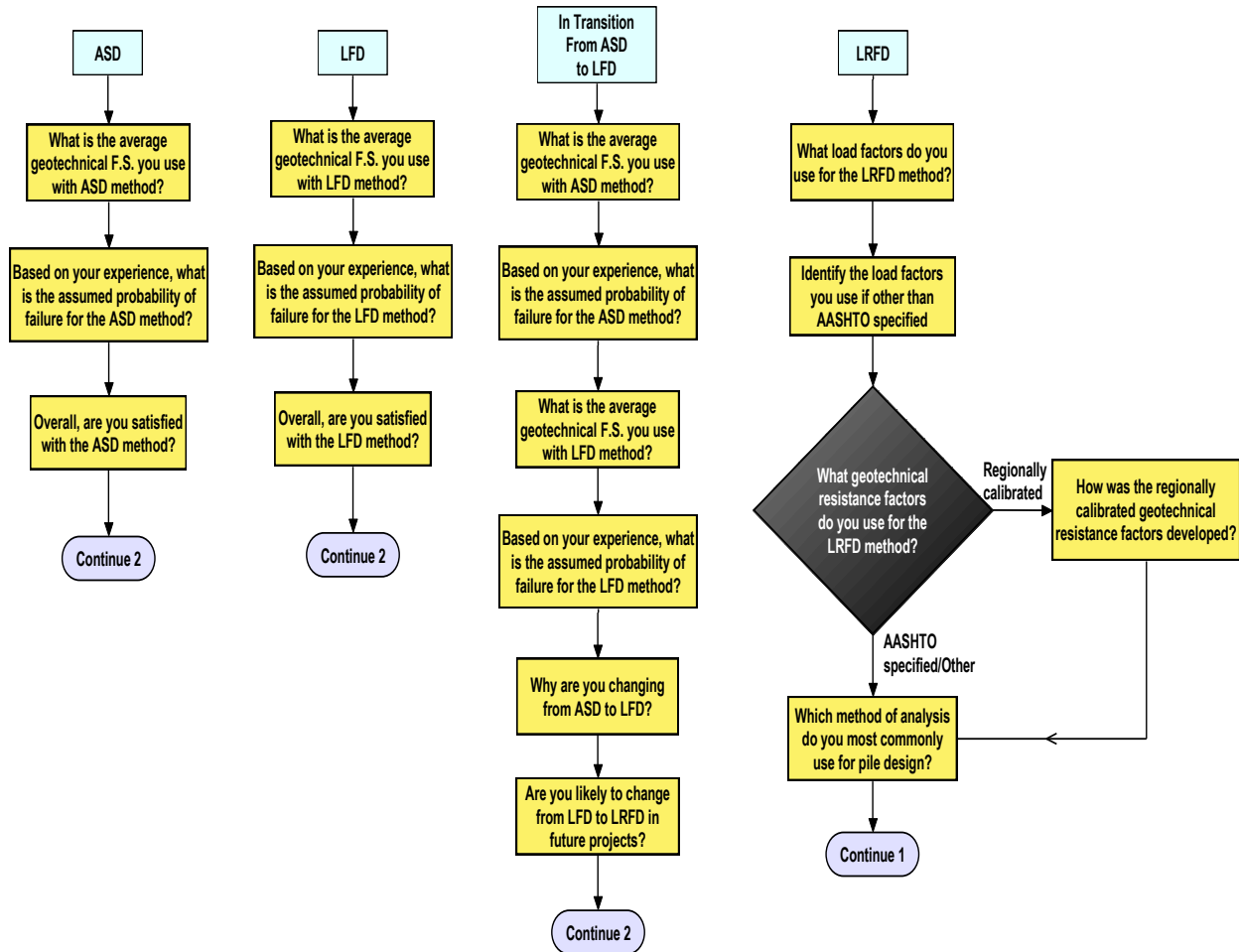


Figure A.3. Continue questions of the second section of the nationwide survey

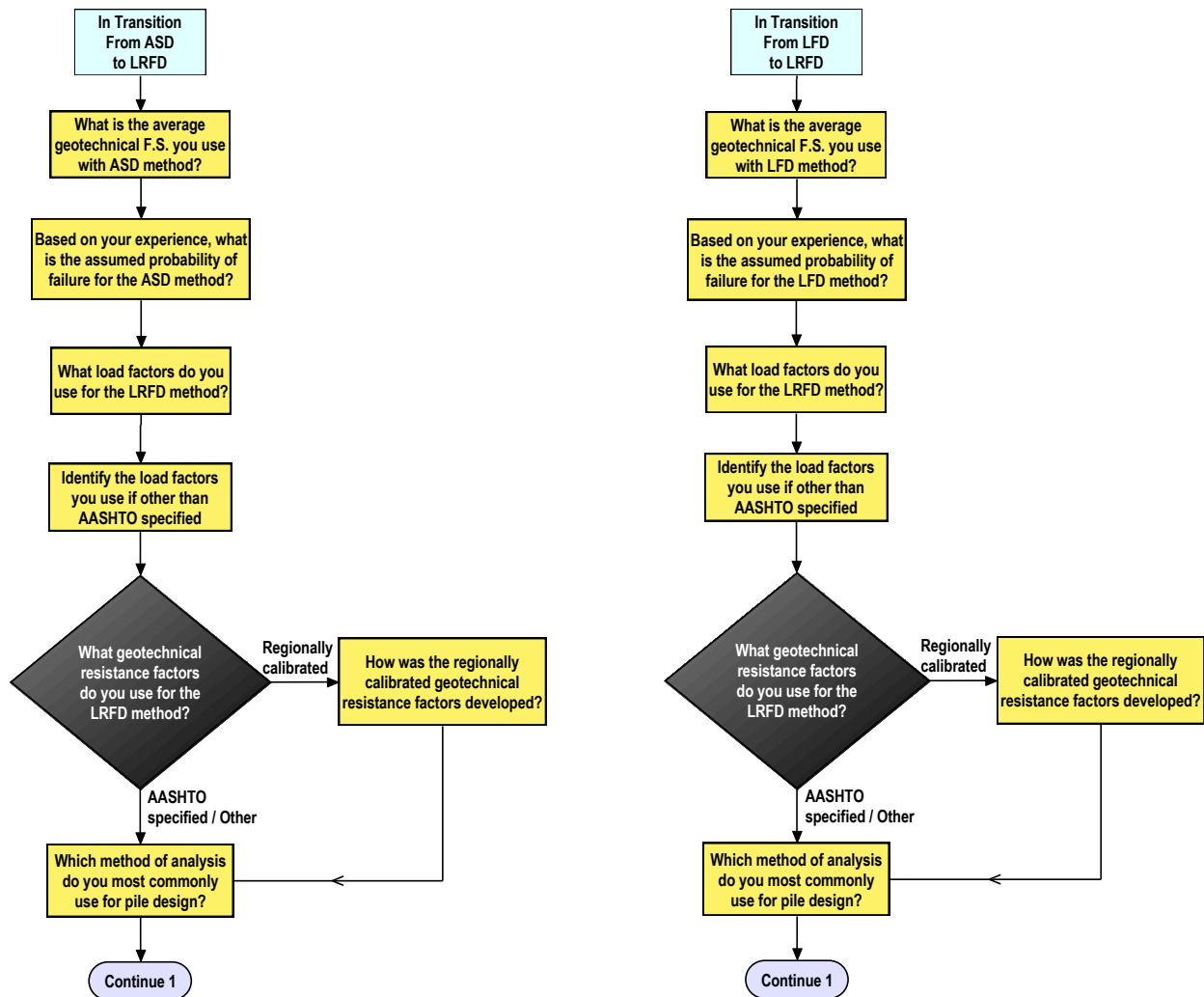


Figure A.4. Continue questions of the second section of the nationwide survey

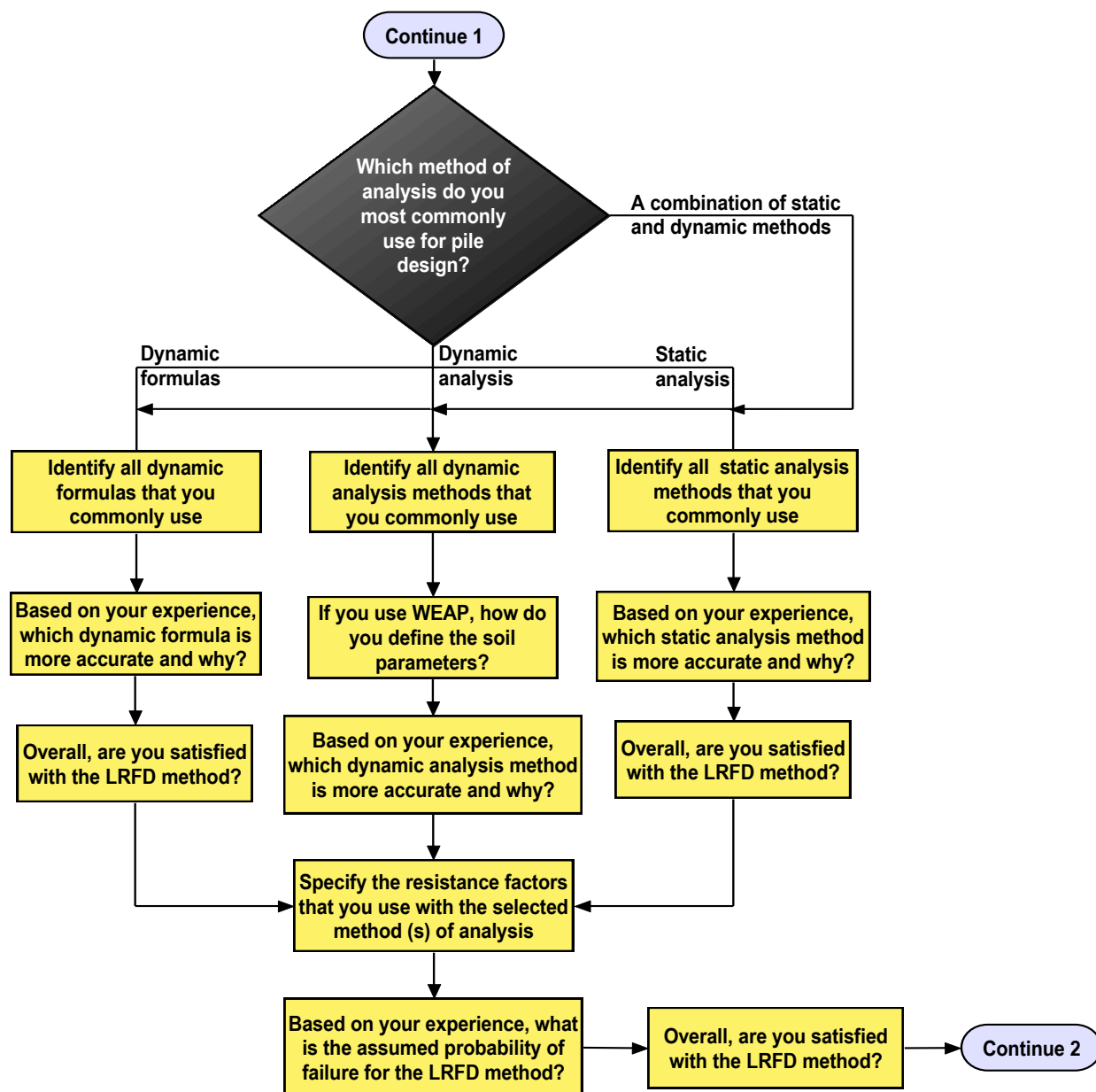


Figure A.5. Continue questions of the second section of the nationwide survey

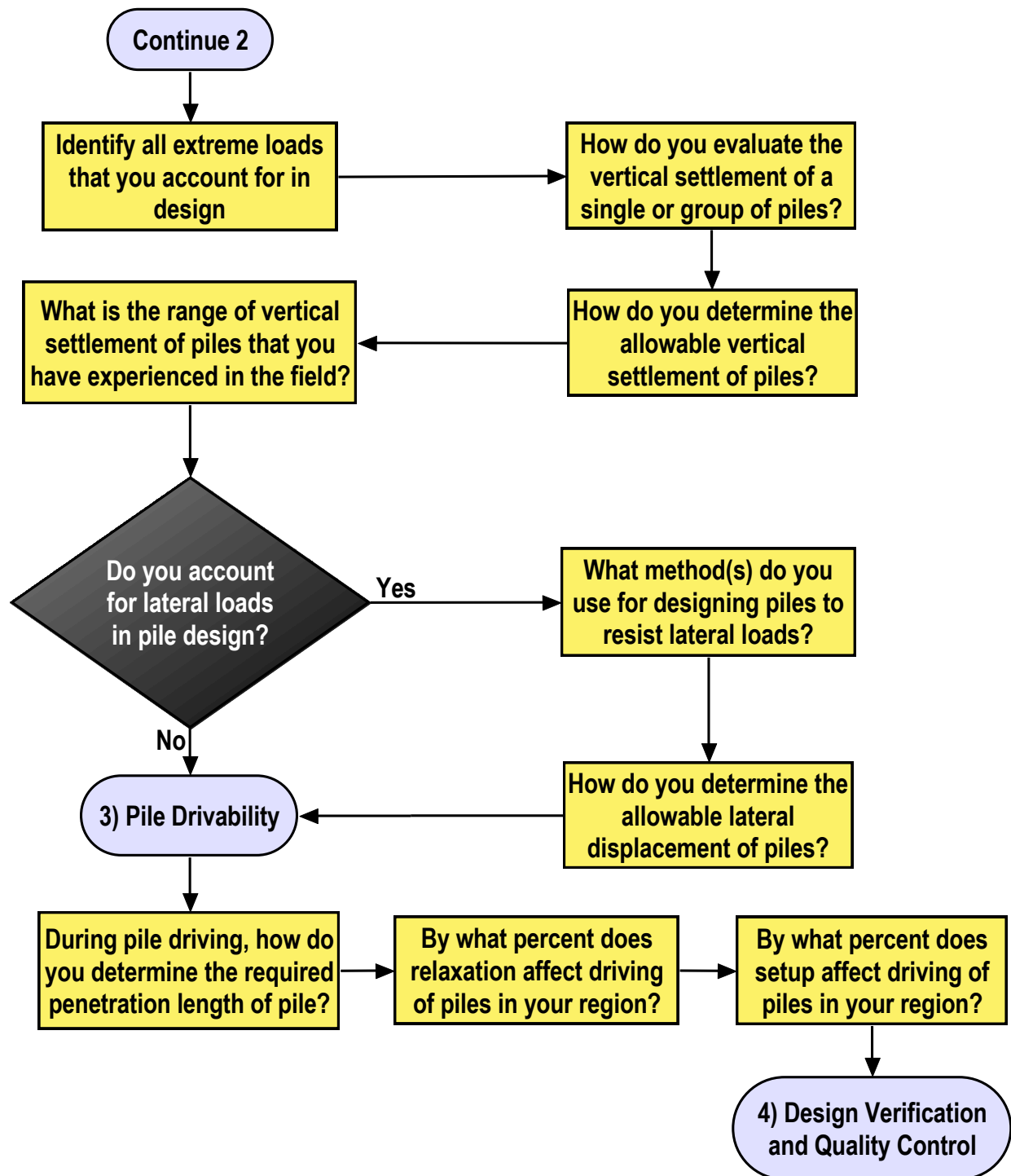


Figure A.6. Flowchart representing questions of the third section of the nationwide survey

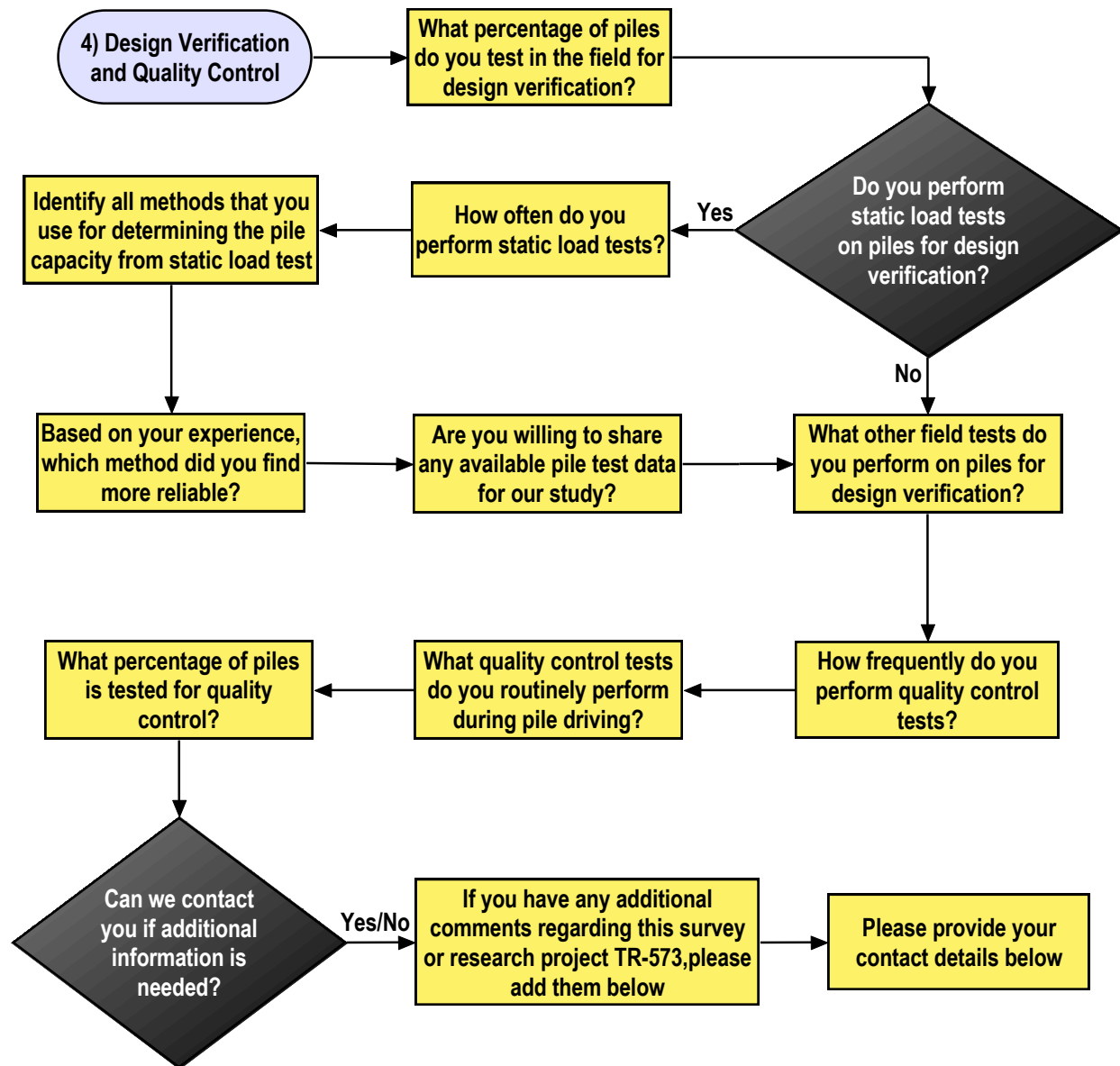


Figure A.7. Flowchart representing questions of the fourth section of the nationwide survey

Local Iowa Counties Survey

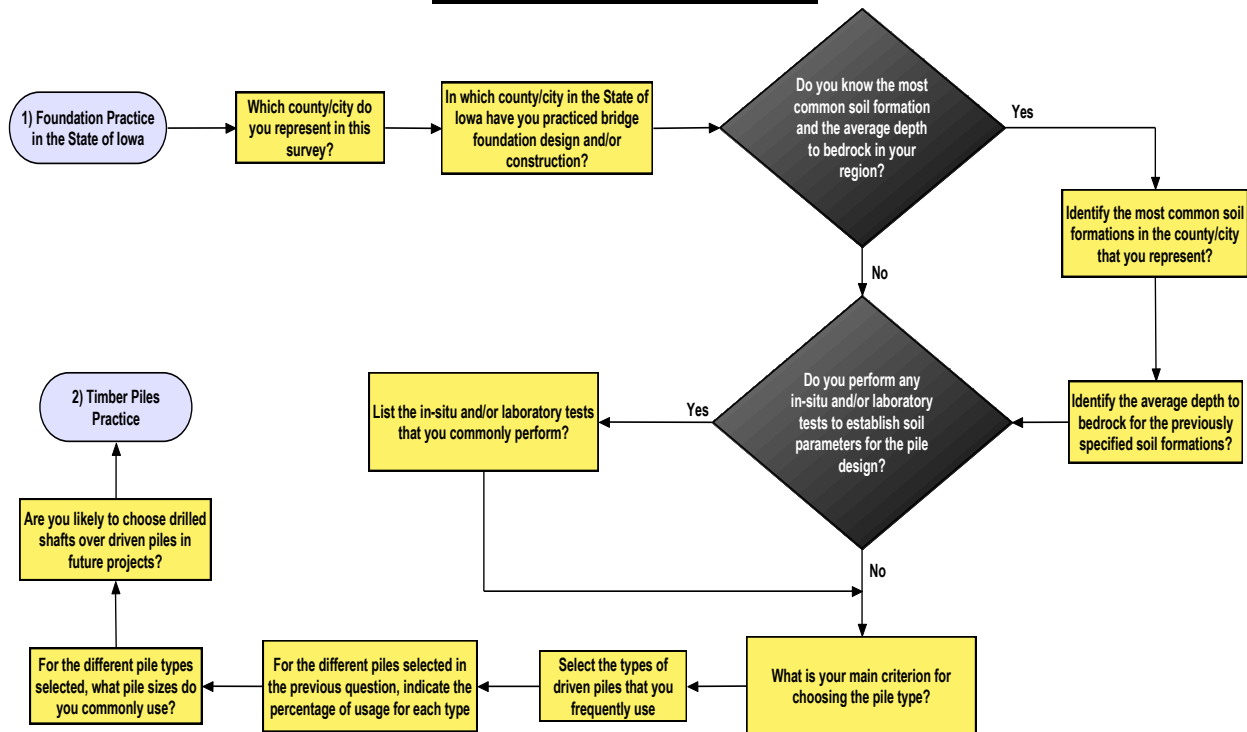


Figure A.8. Flowchart representing questions of the first section of the local survey

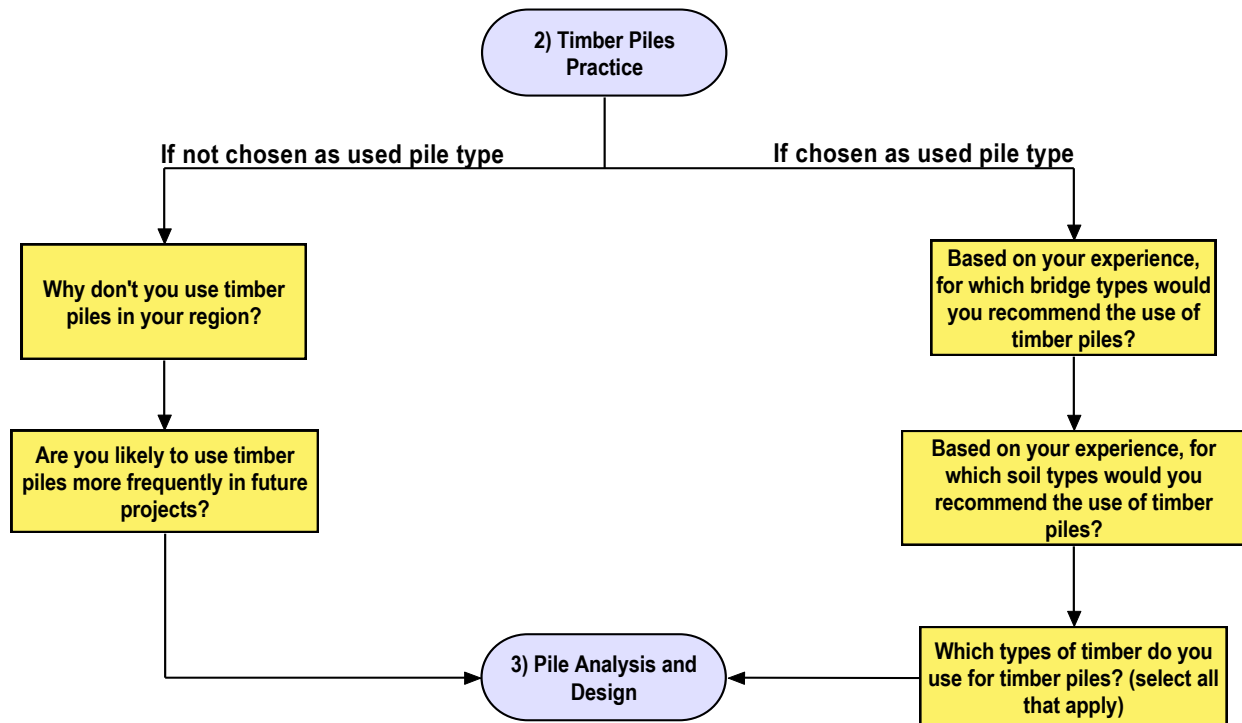


Figure A.9. Flowchart representing questions of the second section of the local survey

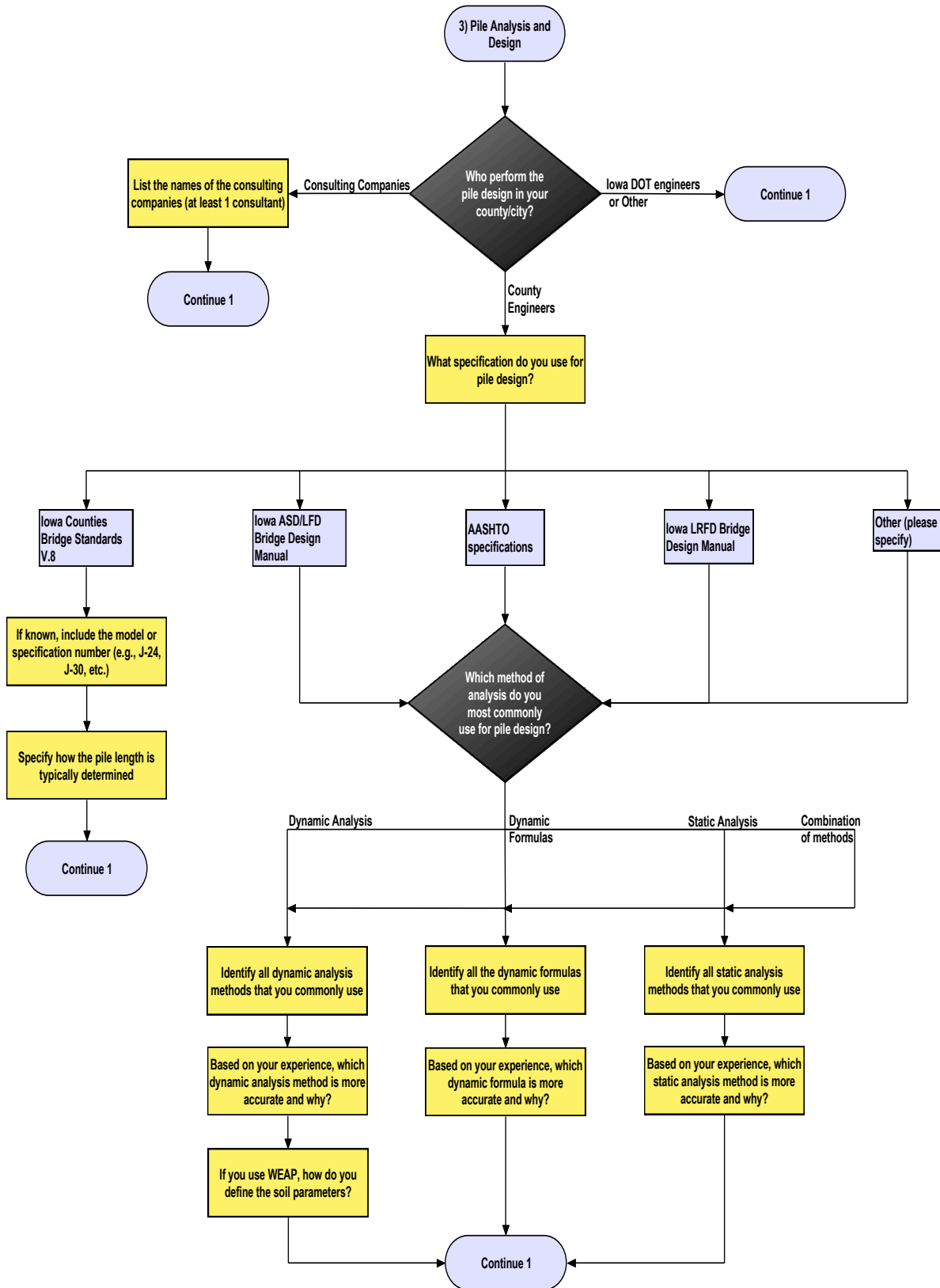


Figure A.10. Flowchart representing questions of the third section of the local survey

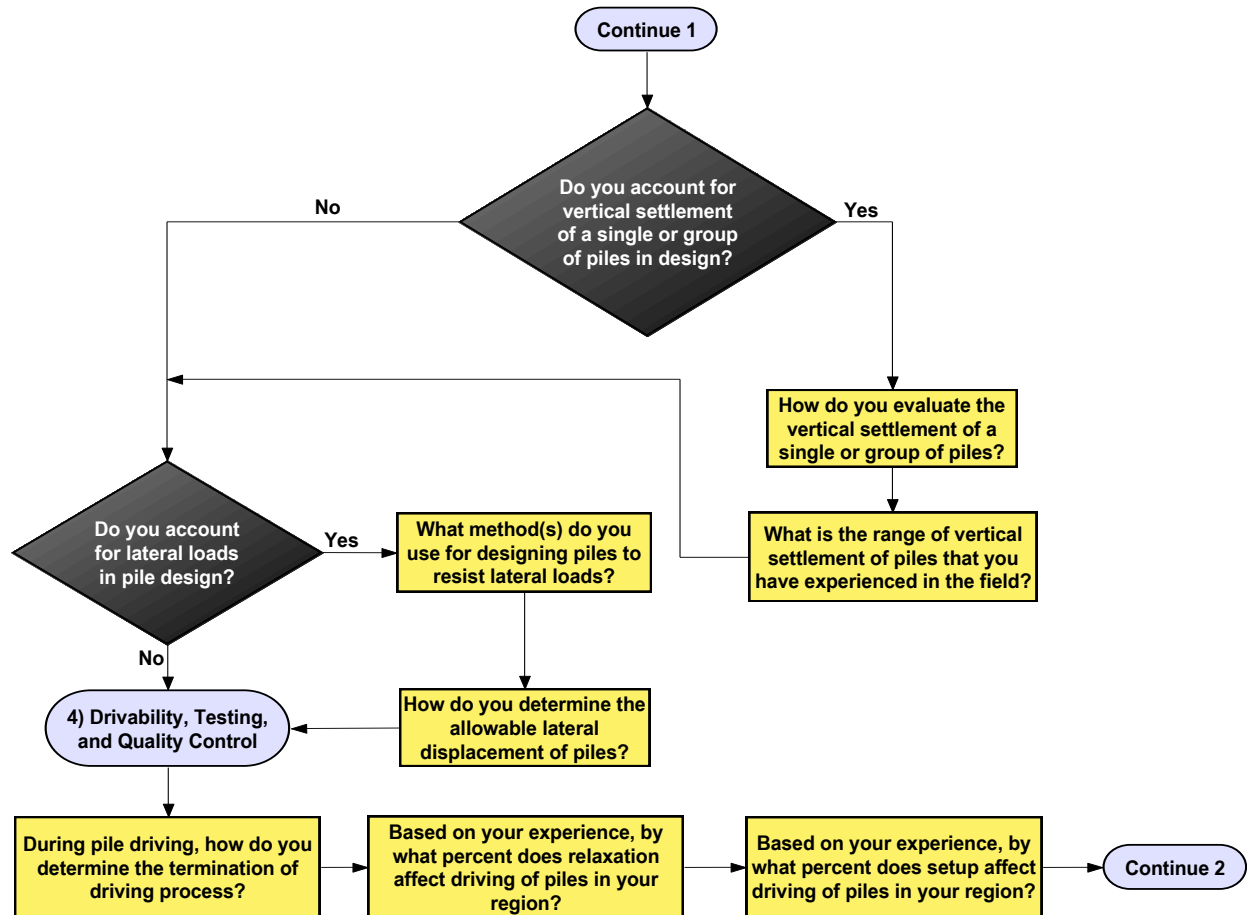


Figure A.11. Flowchart representing questions of the third/fourth sections of the local survey

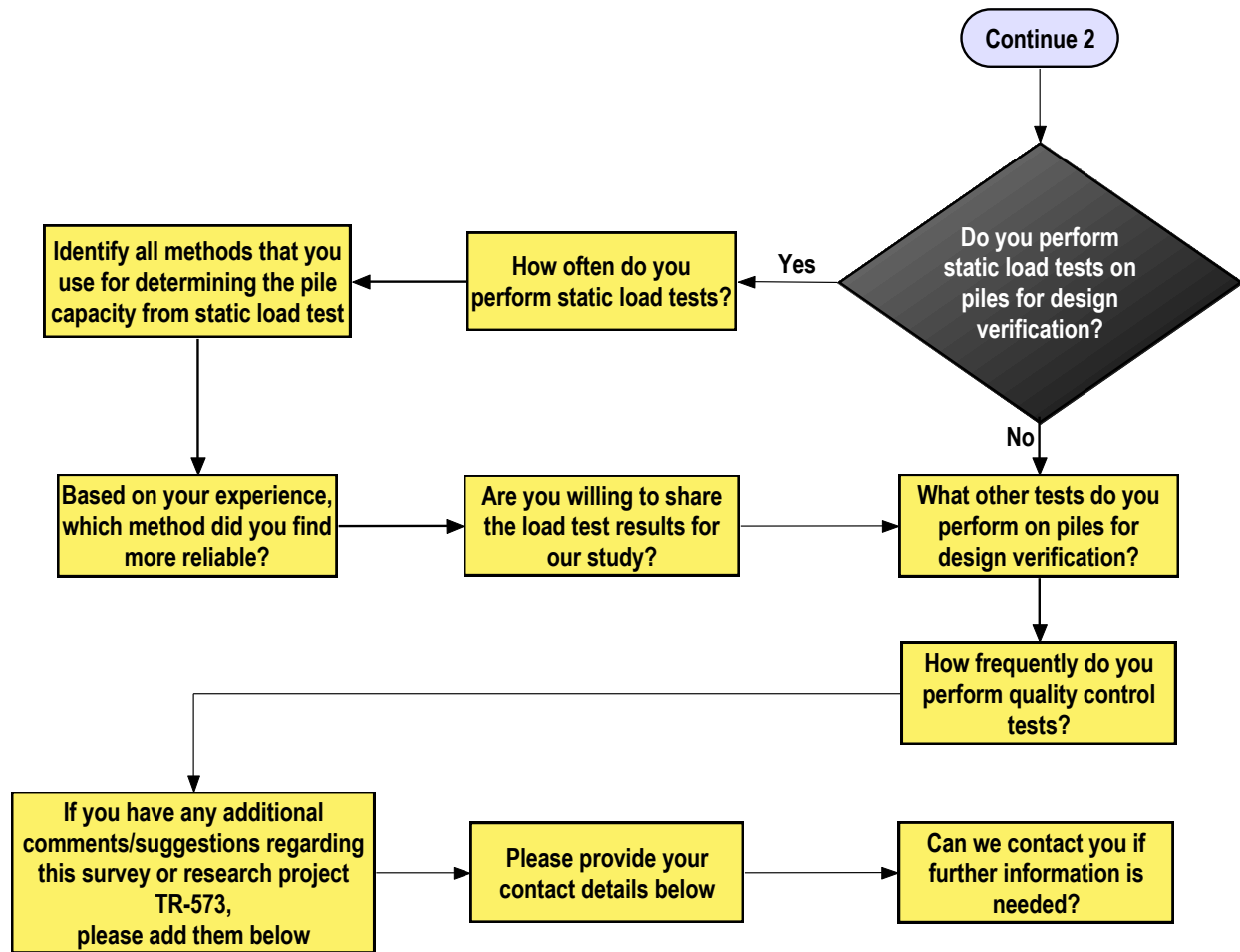


Figure A.12. Flowchart representing questions of the fourth section of the local survey

APPENDIX B: SUPPLEMENTAL GRAPHS SUMMARIZING ADDITIONAL LRFD CALIBRATION

Static Analysis Methods

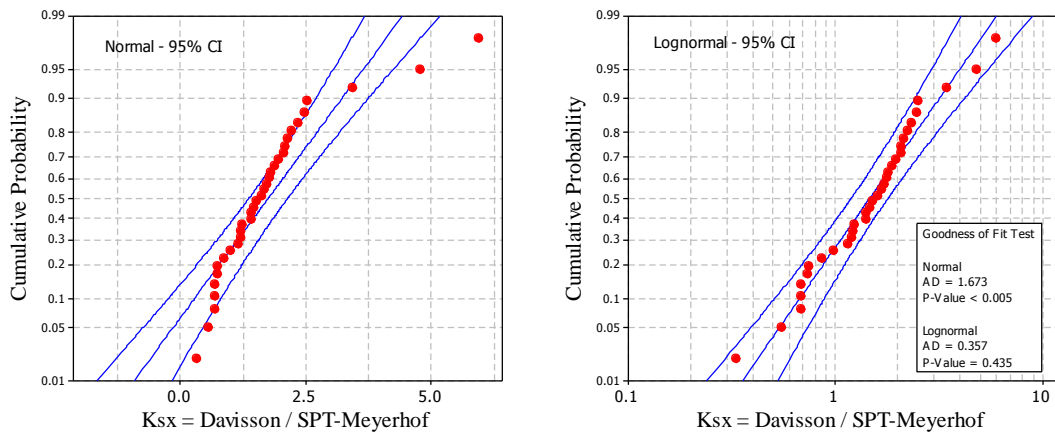


Figure B.1. Goodness of fit test for the SPT-Meyerhof method in sand

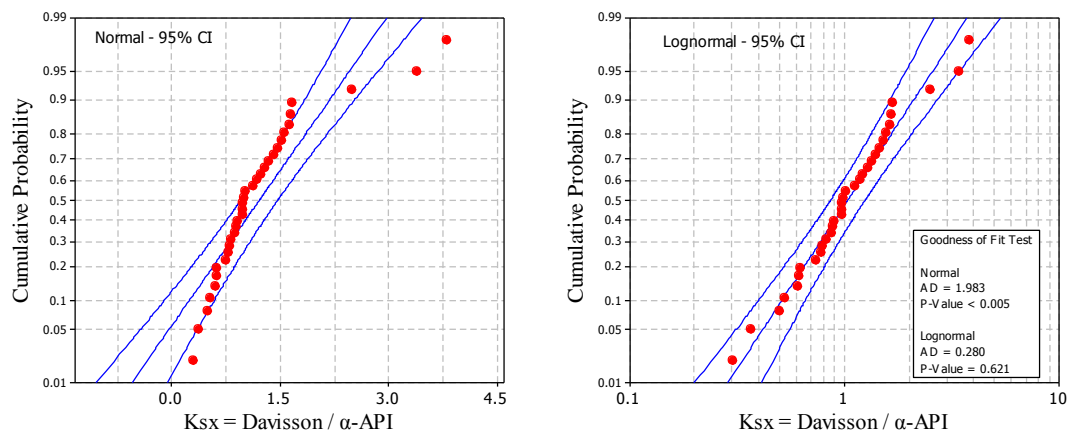


Figure B.2. Goodness of fit test for the α -API method in sand

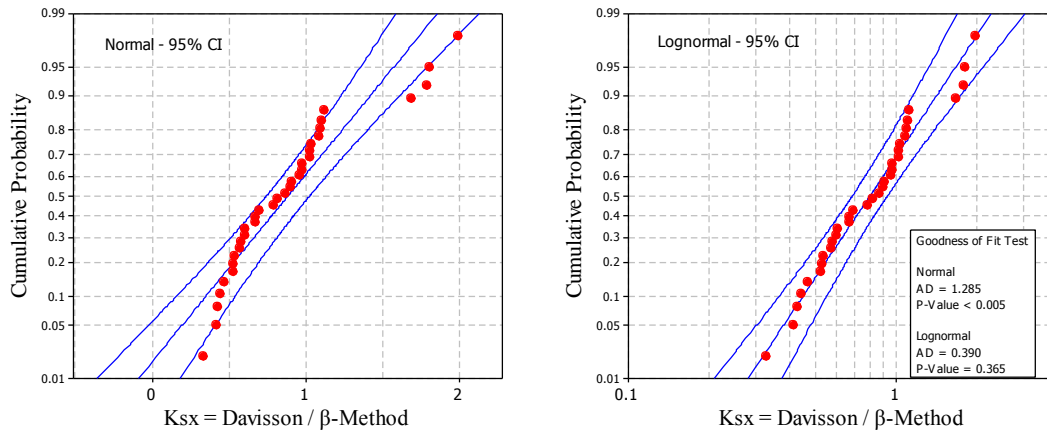


Figure B.3. Goodness of fit test for the β -Method in sand

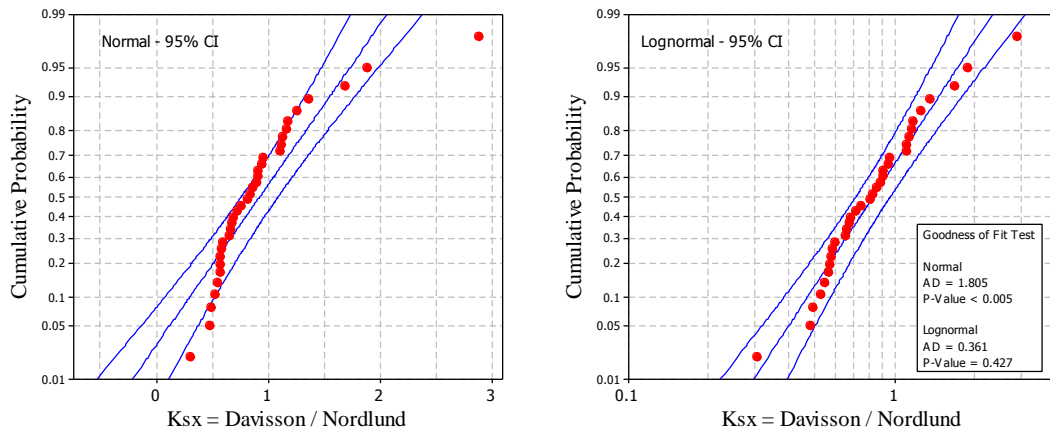


Figure B.4. Goodness of fit test for the Nordlund method in sand

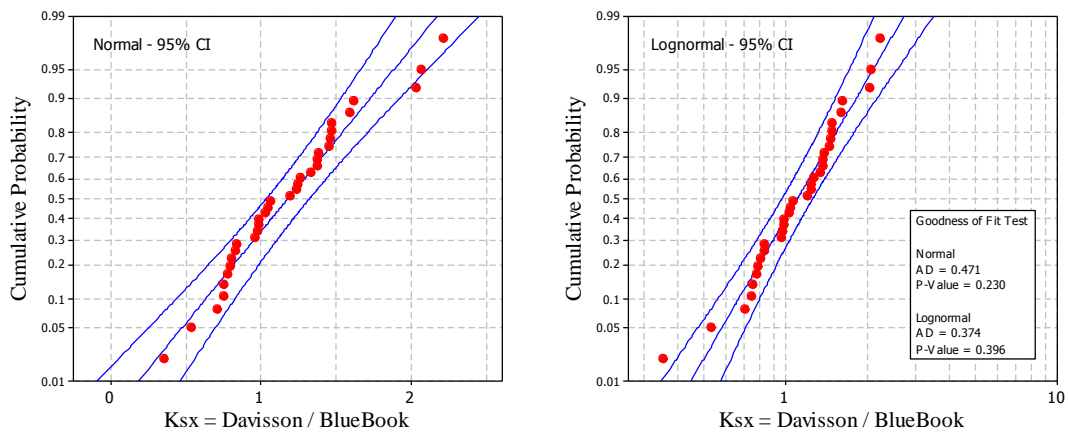


Figure B.5. Goodness of fit test for the Blue Book method in sand

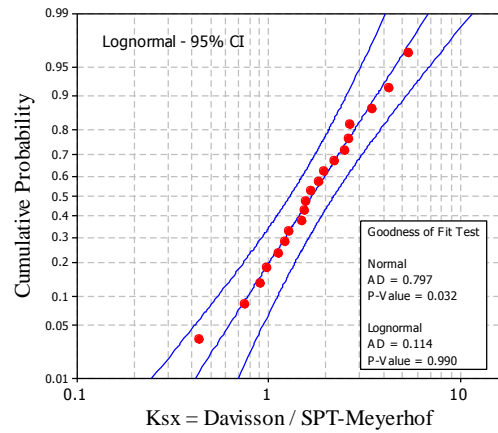
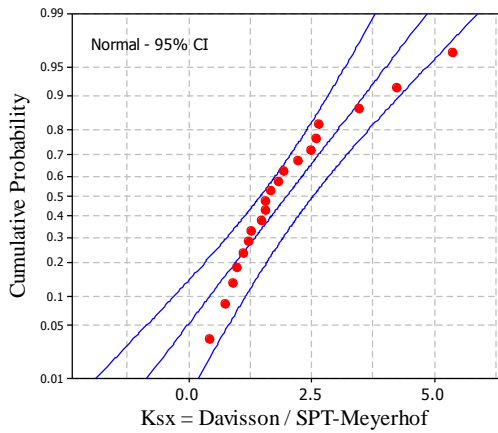


Figure B.6. Goodness of fit test for the SPT-Meyerhof method in clay

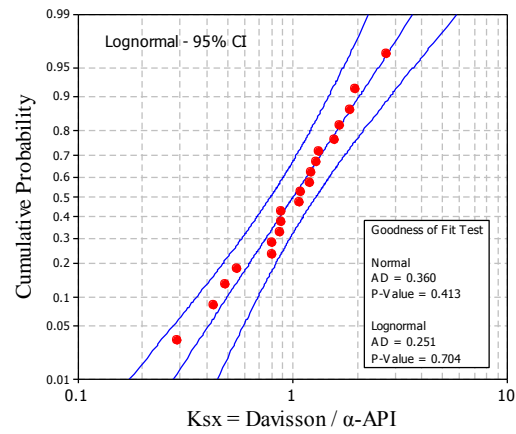
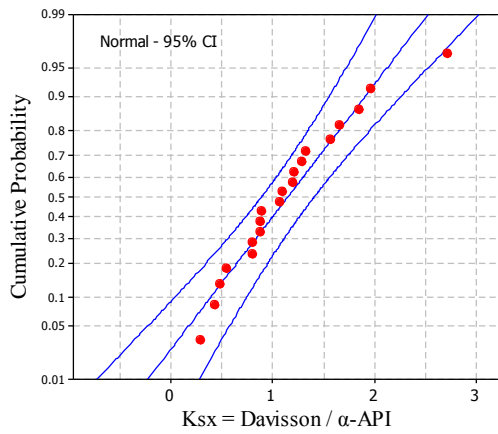


Figure B.7. Goodness of fit test for the α -API method in clay

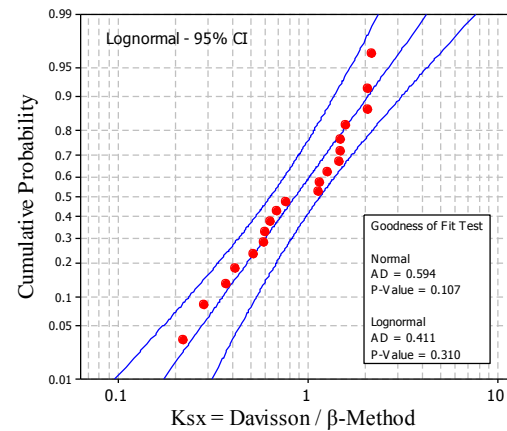
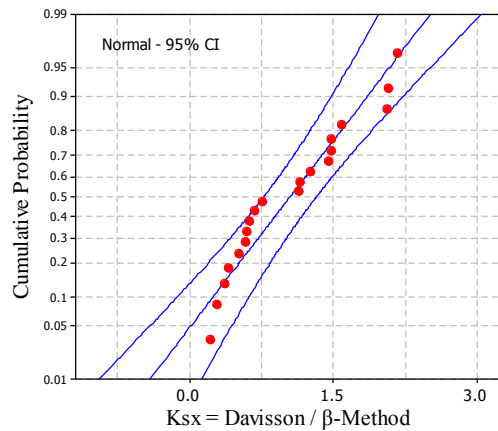


Figure B.8. Goodness of fit test for the β -Method in clay

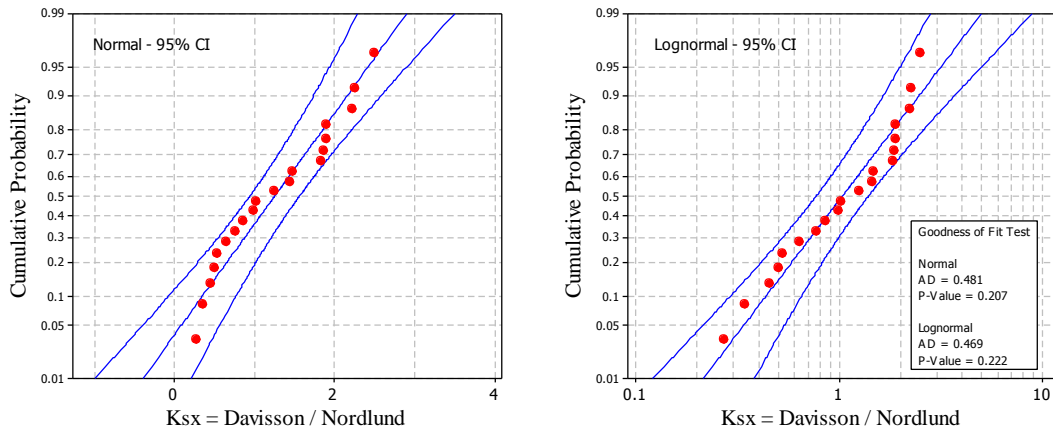


Figure B.9. Goodness of fit test for the Nordlund method in clay

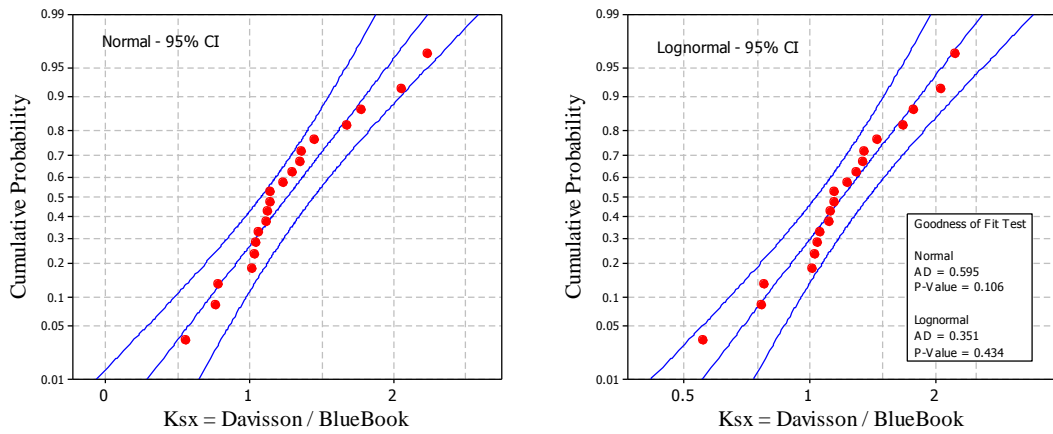


Figure B.10. Goodness of fit test for the Blue Book method in clay

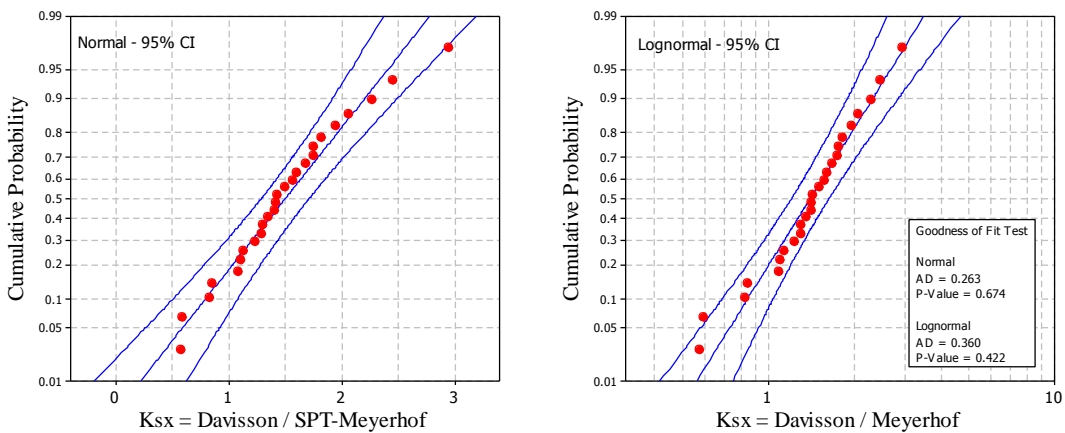


Figure B.11. Goodness of fit test for the SPT-Meyerhof method in mixed soil

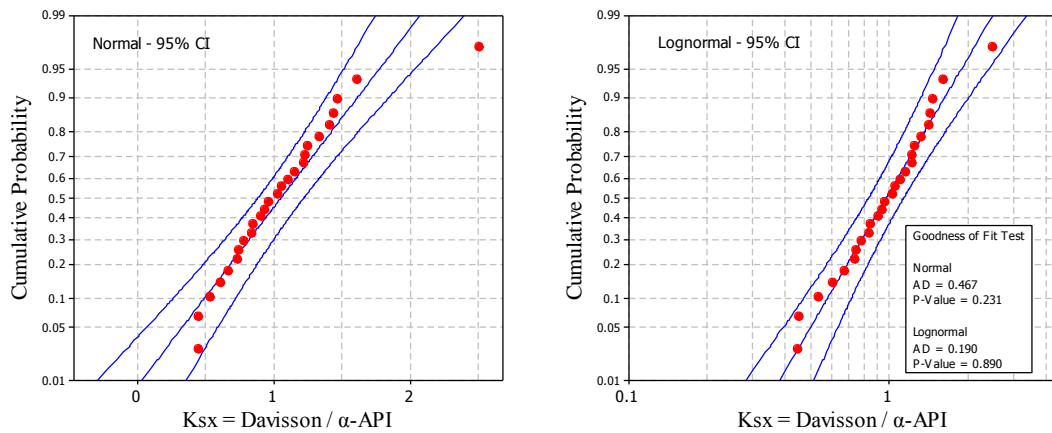


Figure B.12. Goodness of fit test for the α -API method in mixed soil

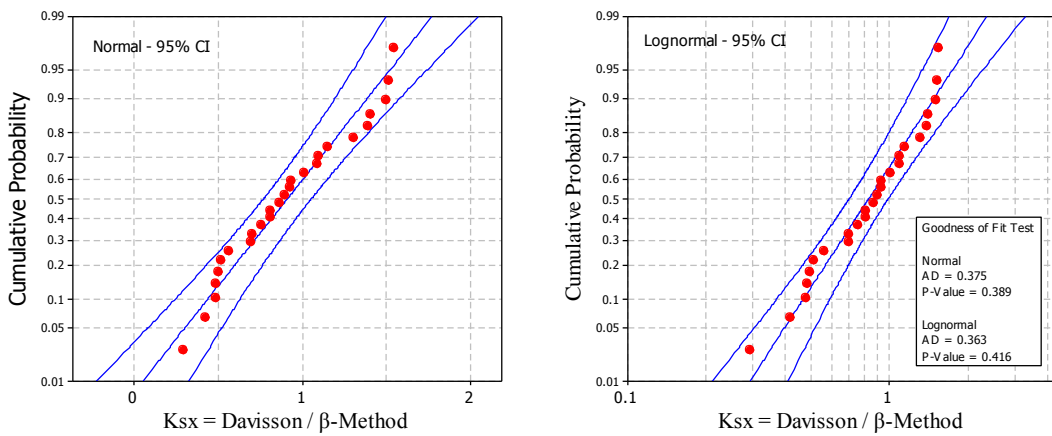


Figure B.13. Goodness of fit test for the β -Method in mixed soil

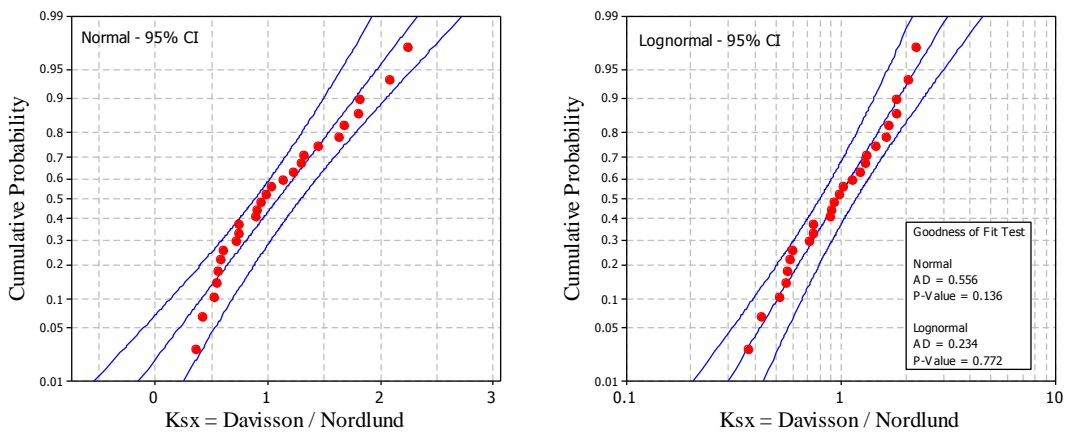


Figure B.14. Goodness of fit test for the Nordlund method in mixed soil

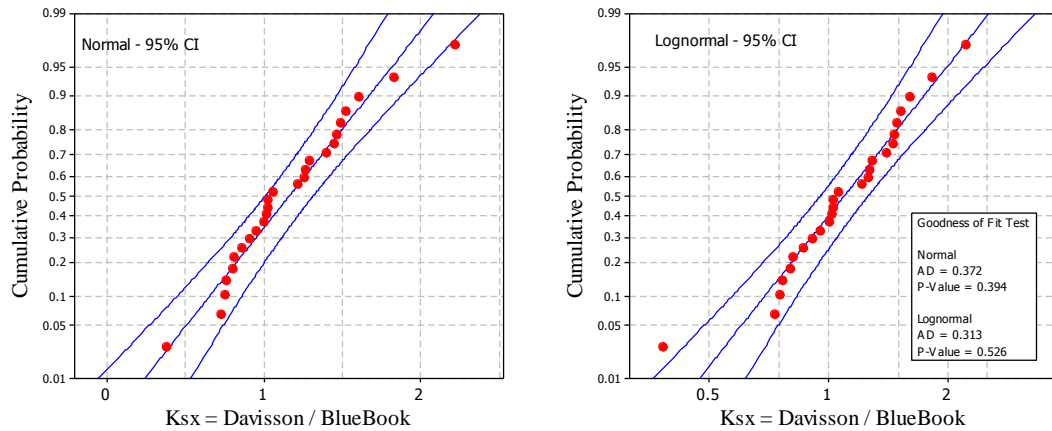


Figure B.15. Goodness of fit test for the Blue Book method in mixed soil

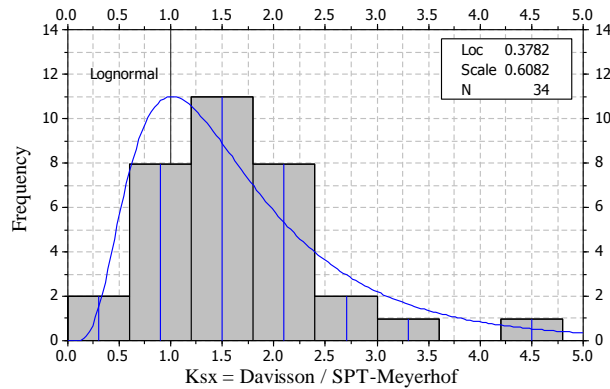


Figure B.16. Histogram and frequency distribution of K_{sx} for 35 cases of steel H-piles designed in sand using the SPT-Meyerhof method

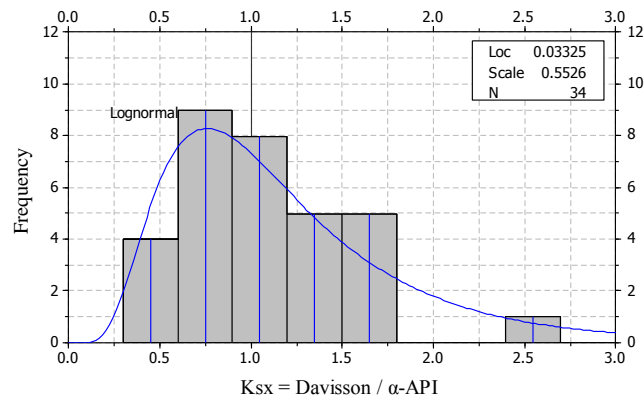


Figure B.17. Histogram and frequency distribution of K_{sx} for 35 cases of steel H-piles designed in sand using the α -API method

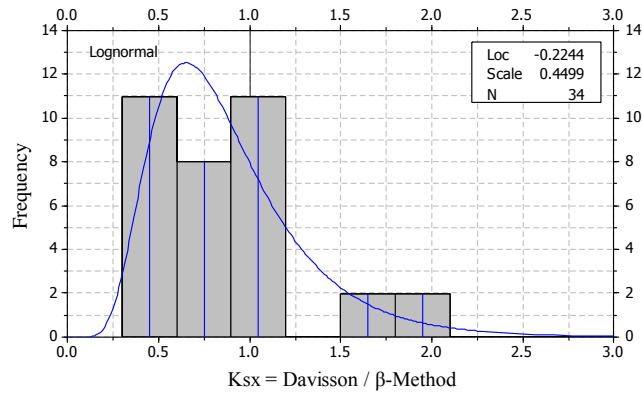


Figure B.18. Histogram and frequency distribution of K_{sx} for 35 cases of steel H-piles designed in sand using the β -method

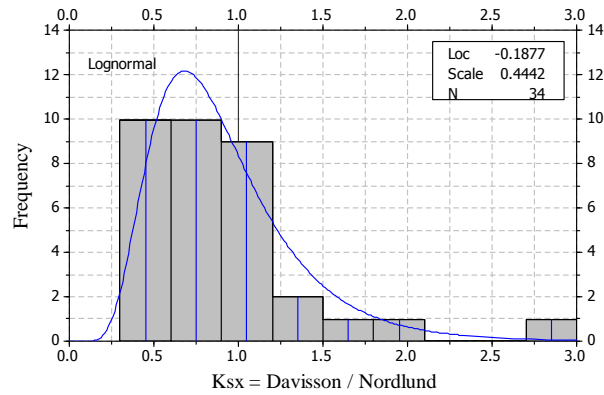


Figure B.19. Histogram and frequency distribution of K_{sx} for 35 cases of steel H-piles designed in sand using the Nordlund method

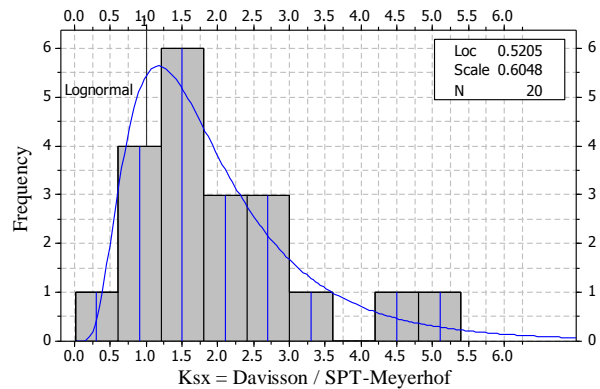


Figure B.20. Histogram and frequency distribution of K_{sx} for 15 cases of steel H-piles designed in clay using the SPT-Meyerhof method

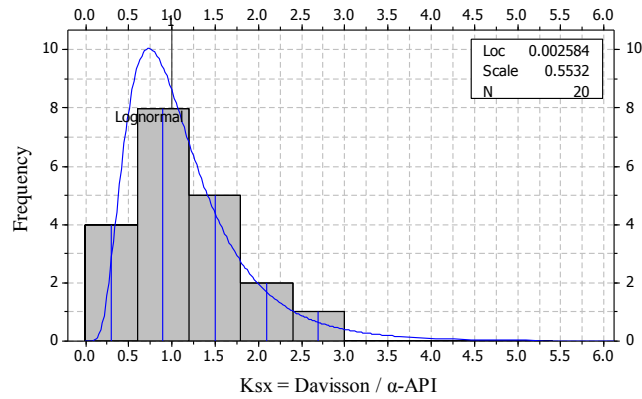


Figure B.21. Histogram and frequency distribution of K_{sx} for 15 cases of steel H-piles designed in clay using the α -API method

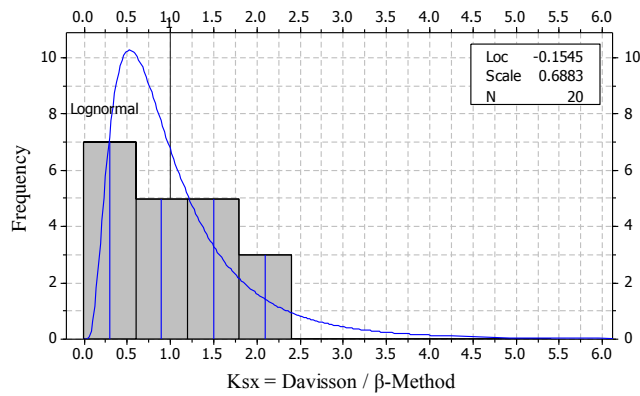


Figure B.22. Histogram and frequency distribution of K_{sx} for 15 cases of steel H-piles designed in clay using the β -method

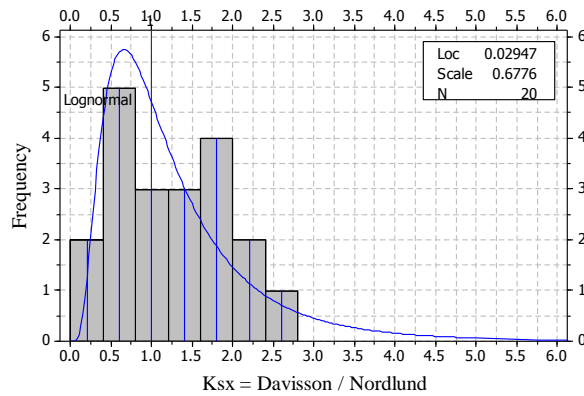


Figure B.23. Histogram and frequency distribution of K_{sx} for 15 cases of steel H-piles designed in clay using the Nordlund method

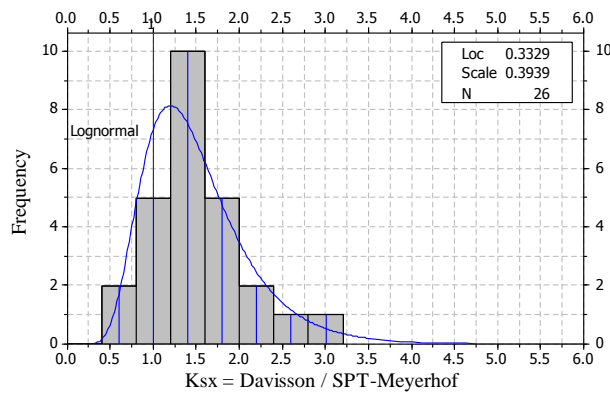


Figure B.24. Histogram and frequency distribution of K_{sx} for 32 cases of steel H-piles designed in mixed soil using the SPT-Meyerhof method

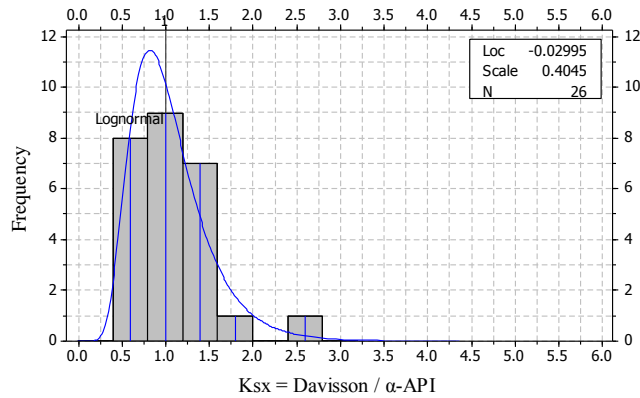


Figure B.25. Histogram and frequency distribution of K_{sx} for 32 cases of steel H-piles designed in mixed soil using the α -API method

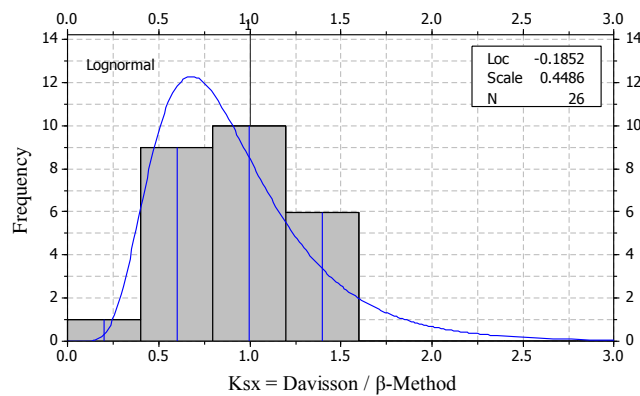


Figure B.26. Histogram and frequency distribution of K_{sx} for 32 cases of steel H-piles designed in mixed soil using the β -method

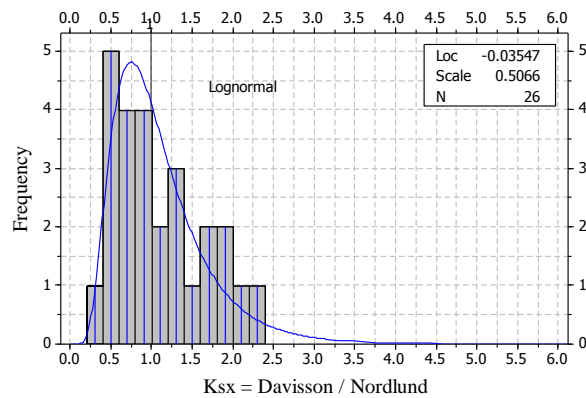


Figure B.27. Histogram and frequency distribution of K_{sx} for 32 cases of steel H-piles designed in mixed soil using the Nordlund method

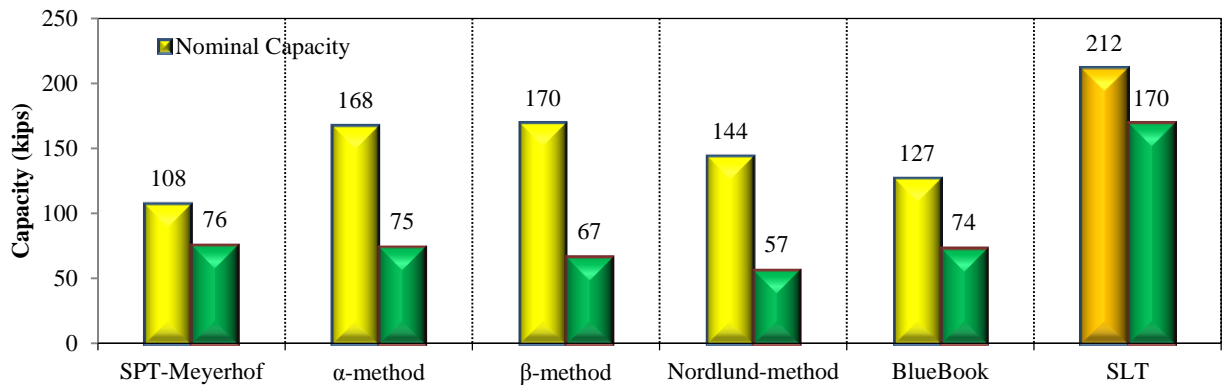


Figure B.28. Nominal and Factored pile design capacities using different static methods and compared to SLT results for Mahaska – Mixed soil

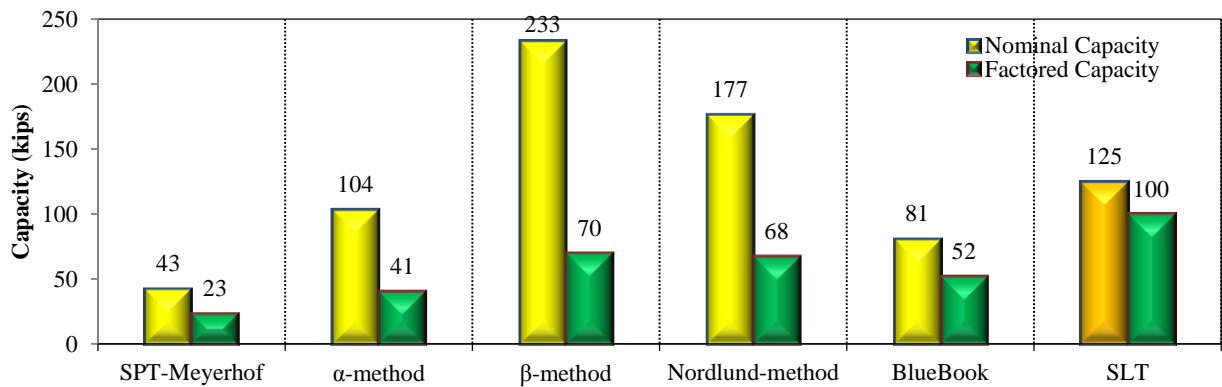


Figure B.29. Nominal and Factored pile design capacities using different static methods and compared to SLT results for Mills – Clay soil

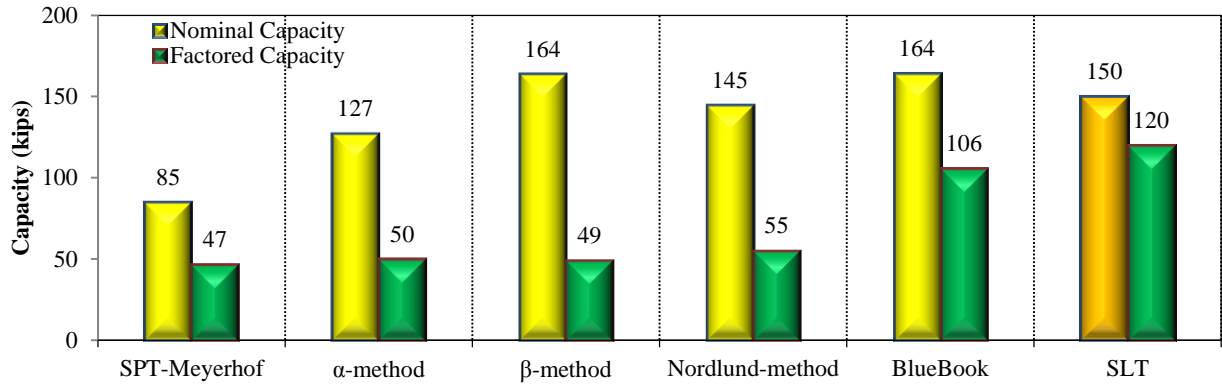


Figure B.30. Nominal and Factored pile design capacities using different static methods and compared to SLT results for Polk – Clay soil

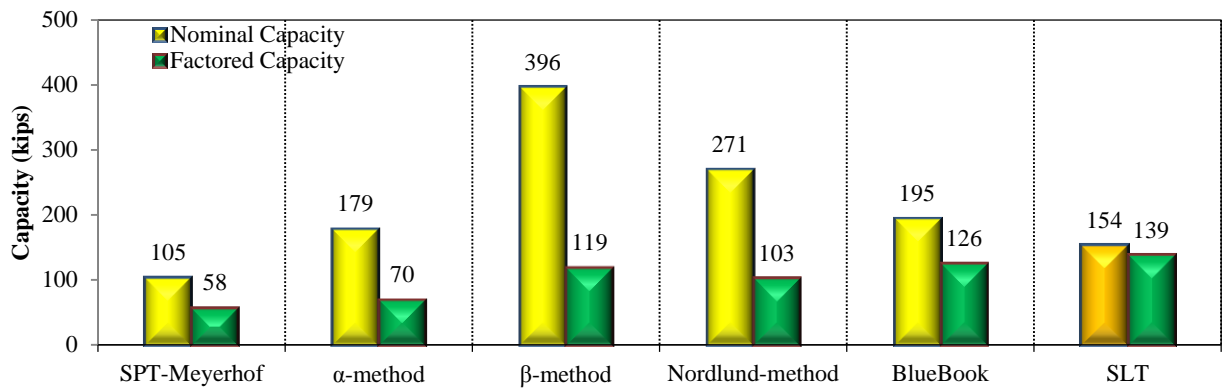


Figure B.31. Nominal and Factored pile design capacities using different static methods and compared to SLT results for Jasper – Clay soil

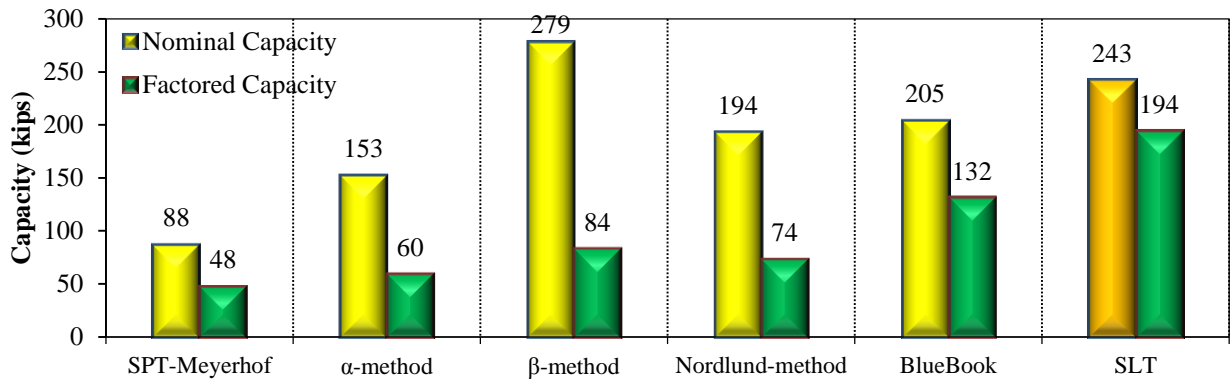


Figure B.32. Nominal and Factored pile design capacities using different static methods and compared to SLT results for Clarke – Clay soil

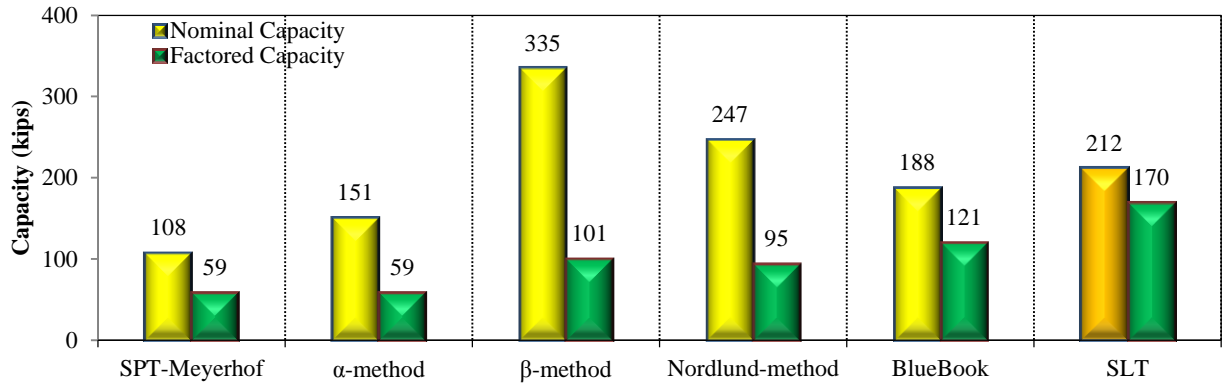


Figure B.33. Nominal and Factored pile design capacities using different static methods and compared to SLT results for Buchanan (long) – Clay soil

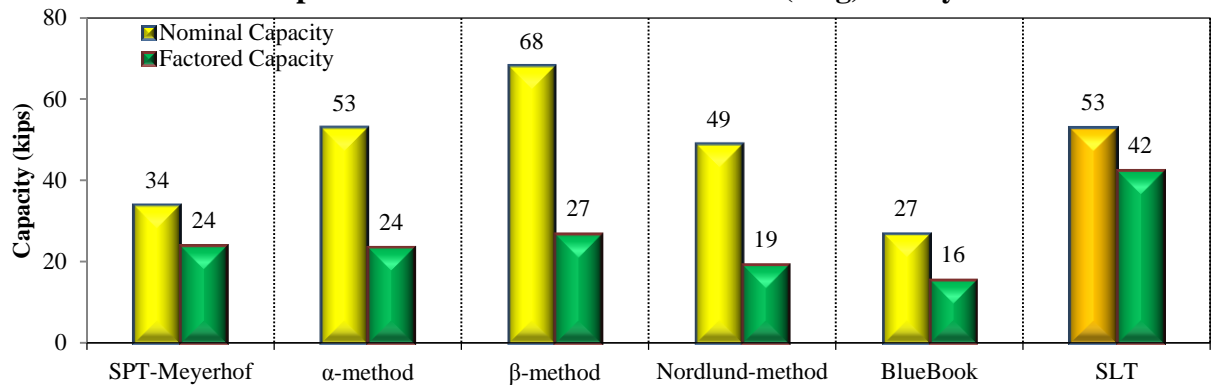


Figure B.34. Nominal and Factored pile design capacities using different static methods and compared to SLT results for Buchanan (short) – Mixed soil

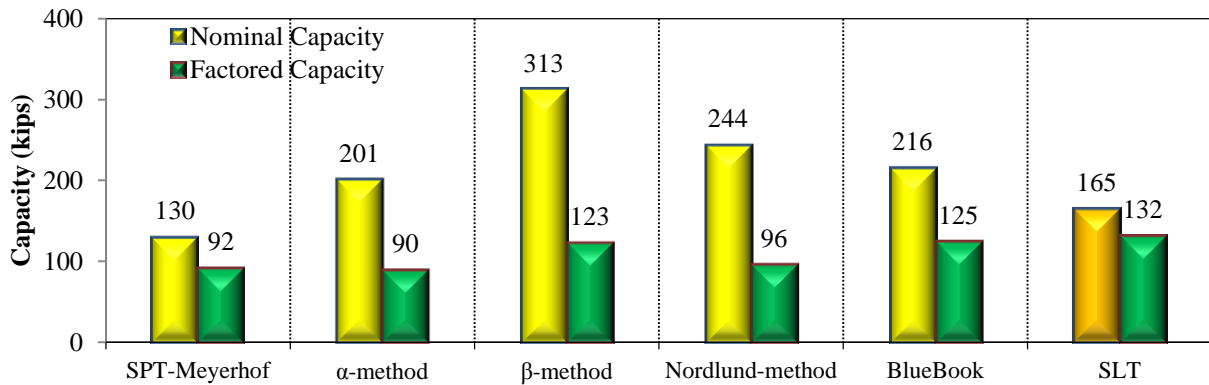


Figure B.35. Nominal and Factored pile design capacities using different static methods and compared to SLT results for Poweshiek – Mixed soil

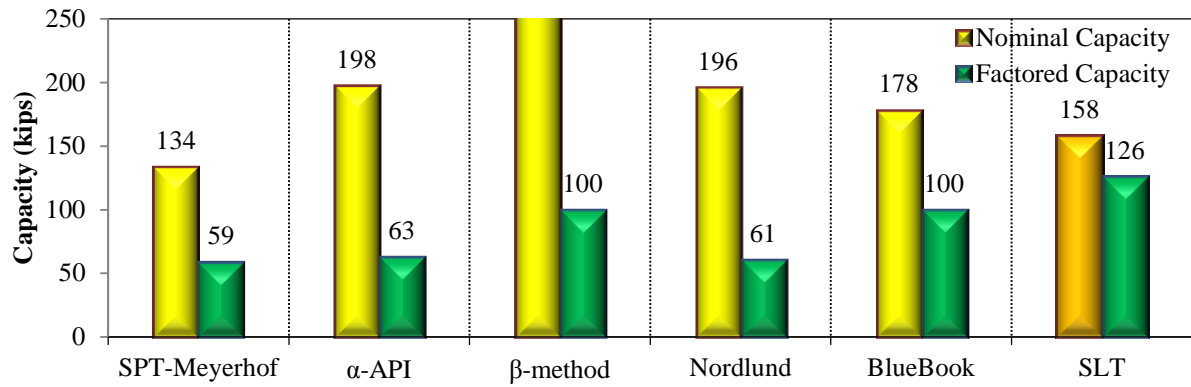


Figure B.36. Nominal and Factored pile design capacities using different static methods and compared to SLT results for Des Moines – Sand soil

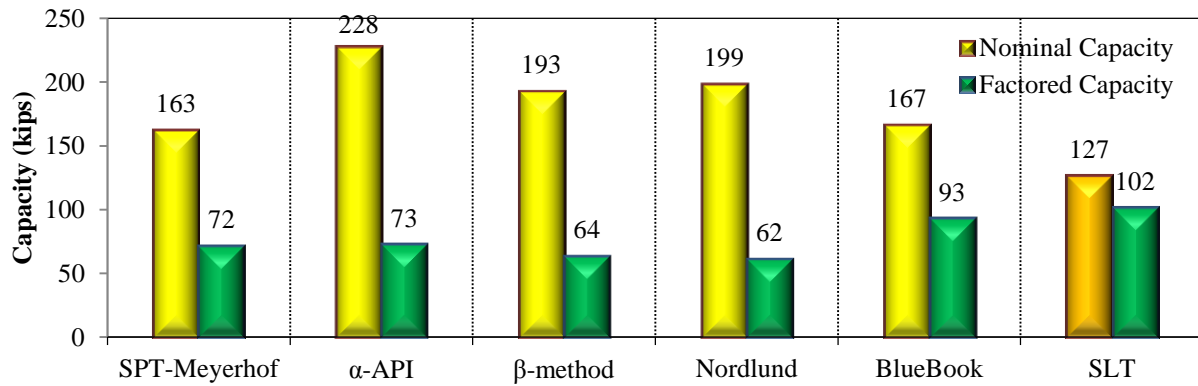


Figure B.37. Nominal and Factored pile design capacities using different static methods and compared to SLT results for Cedar – Sand soil

Dynamic Analysis (WEAP)

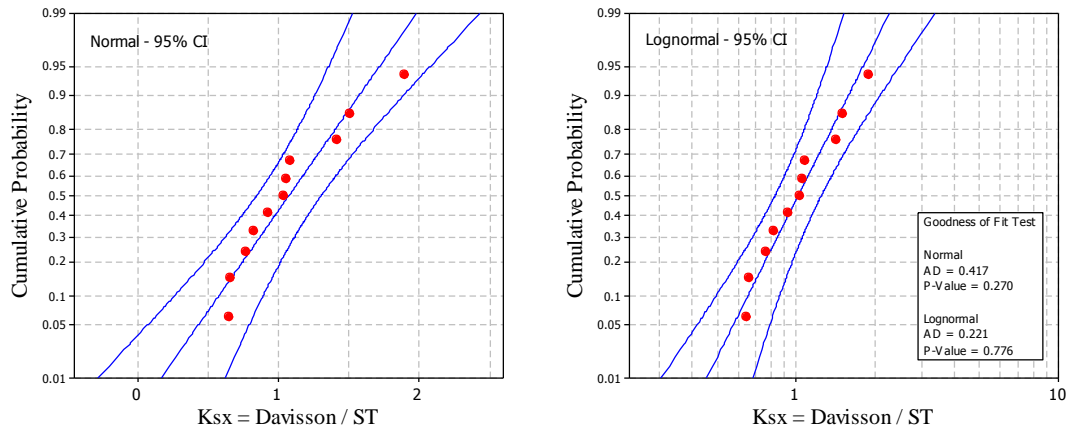


Figure B.38. Goodness of fit test for the WEAP based on ST method in sand

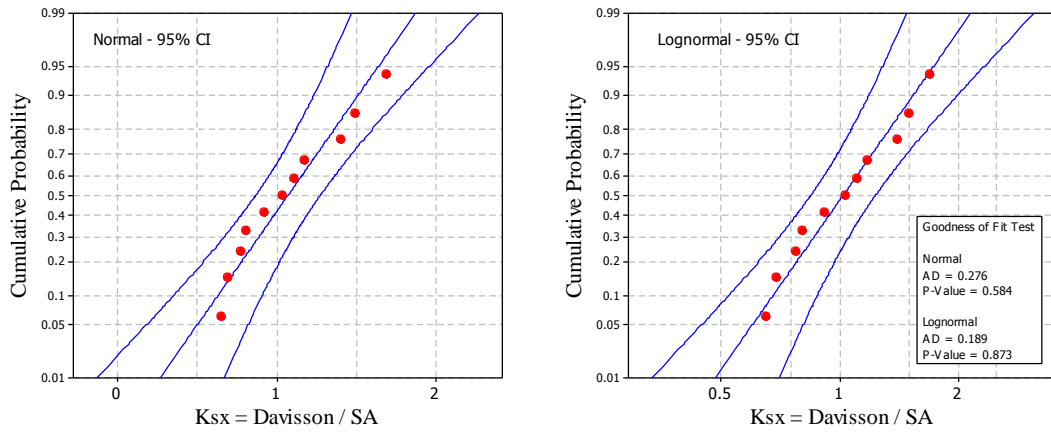


Figure B.39. Goodness of fit test for the WEAP based on SA method in sand

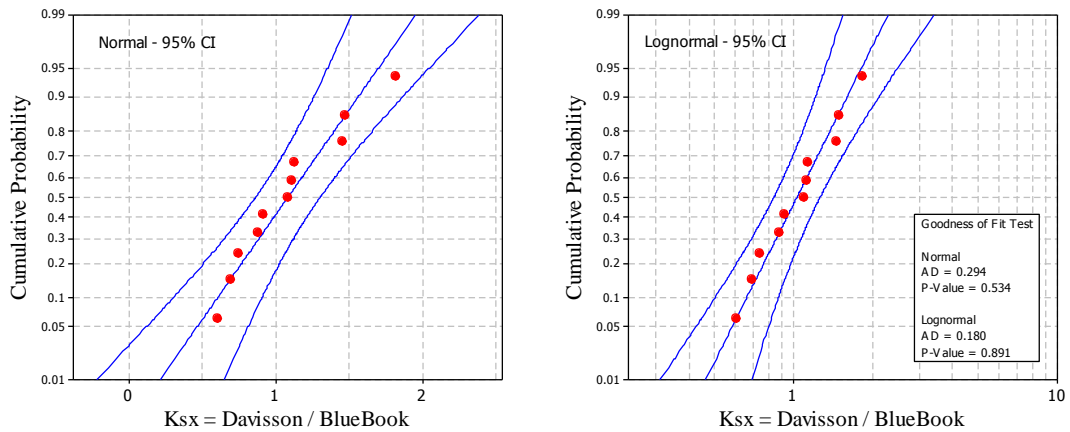


Figure B.40. Goodness of fit test for the WEAP based on Blue Book method in sand

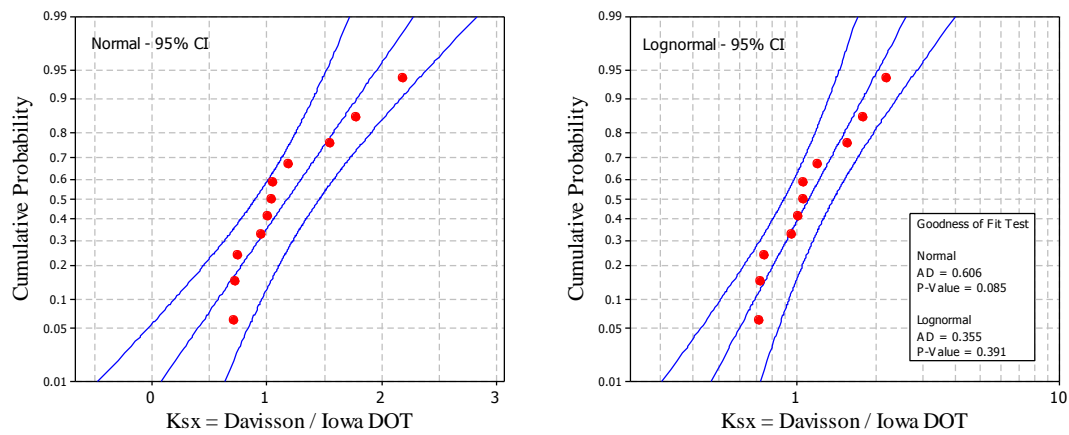


Figure B.41. Goodness of fit test for the WEAP based on Iowa DOT in sand

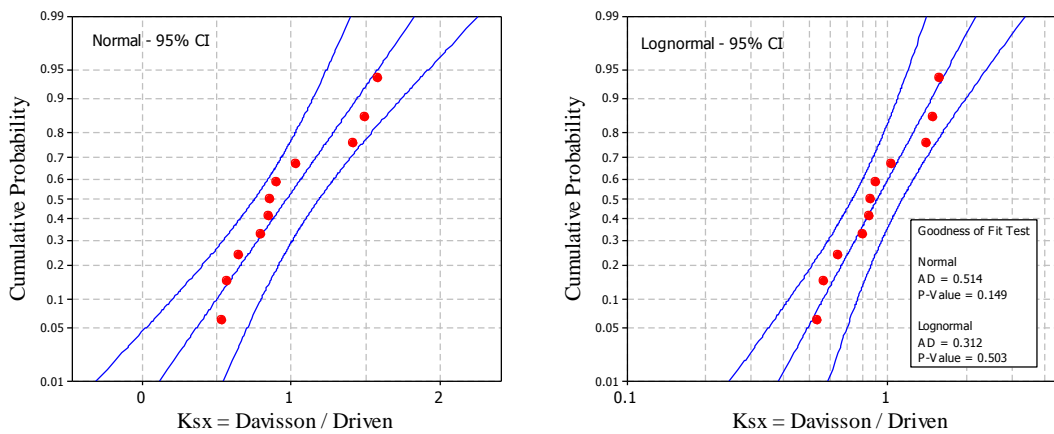


Figure B.42. Goodness of fit test for the WEAP based on Driven method in sand

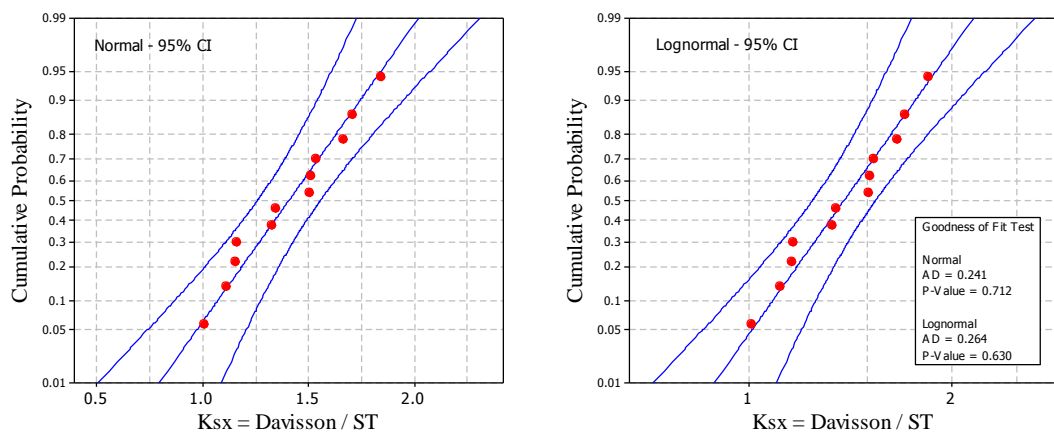


Figure B.43. Goodness of fit test for the WEAP based on ST method in clay

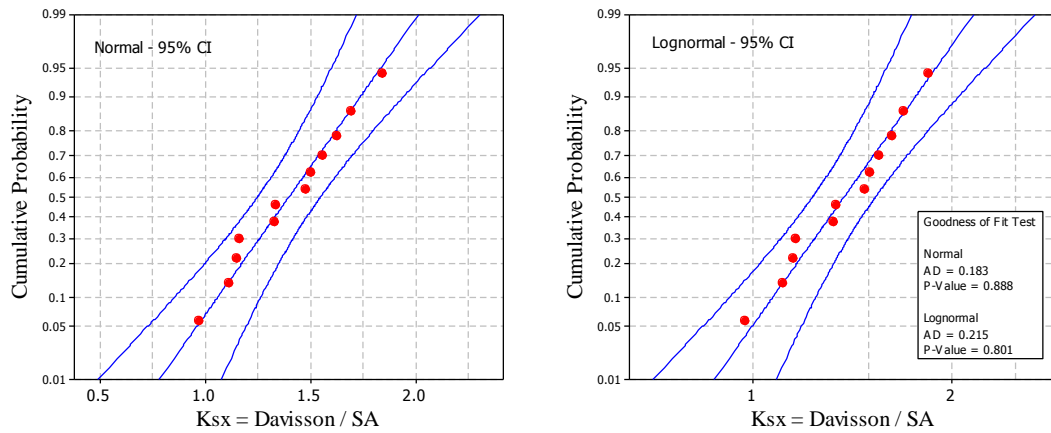


Figure B.44. Goodness of fit test for the WEAP based on SA method in clay

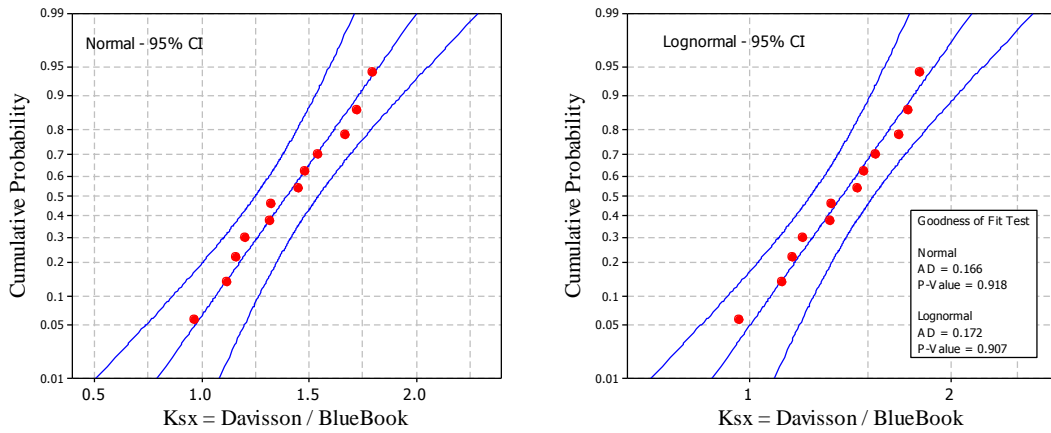


Figure B.45. Goodness of fit test for the WEAP based on Blue Book method in clay

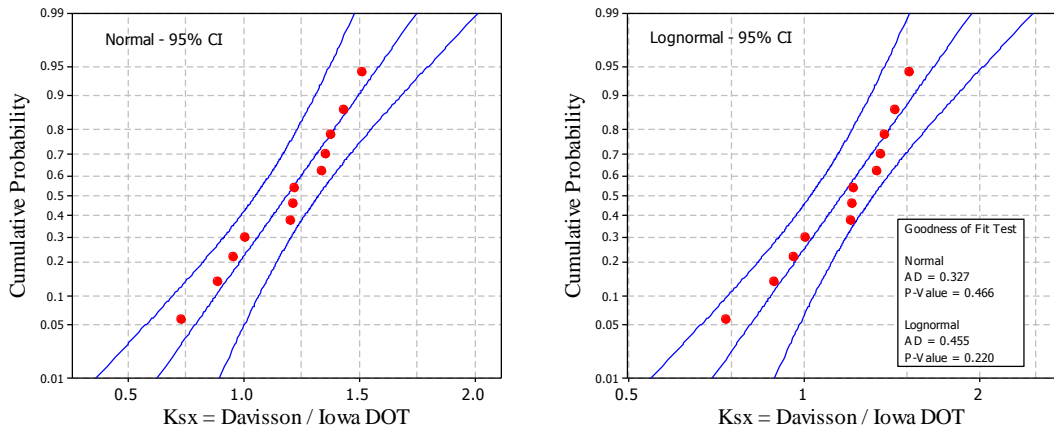


Figure B.46. Goodness of fit test for the WEAP based on Iowa DOT in clay

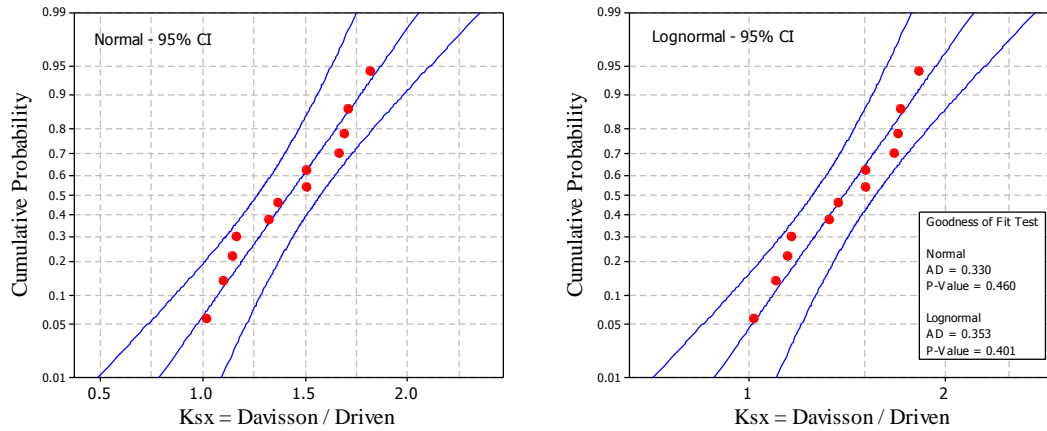


Figure B.47. Goodness of fit test for the WEAP based on Driven method in clay

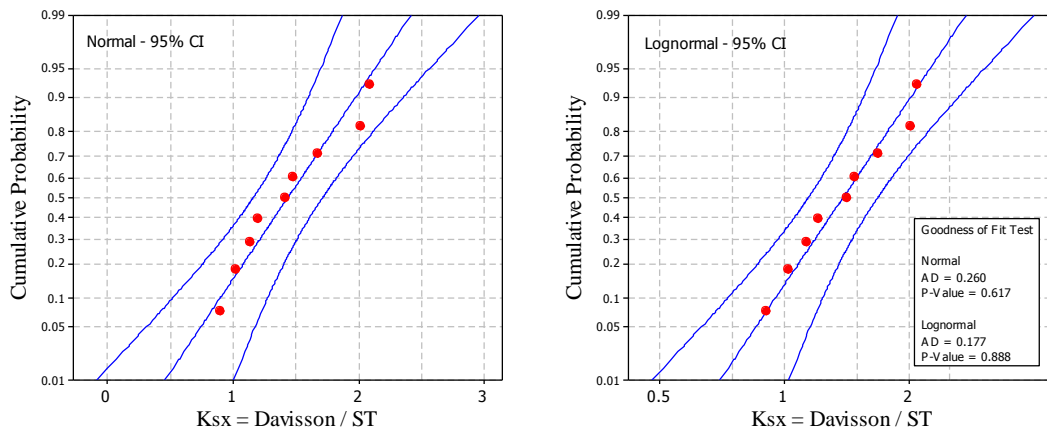


Figure B.48. Goodness of fit test for the WEAP based on ST method in mixed soil

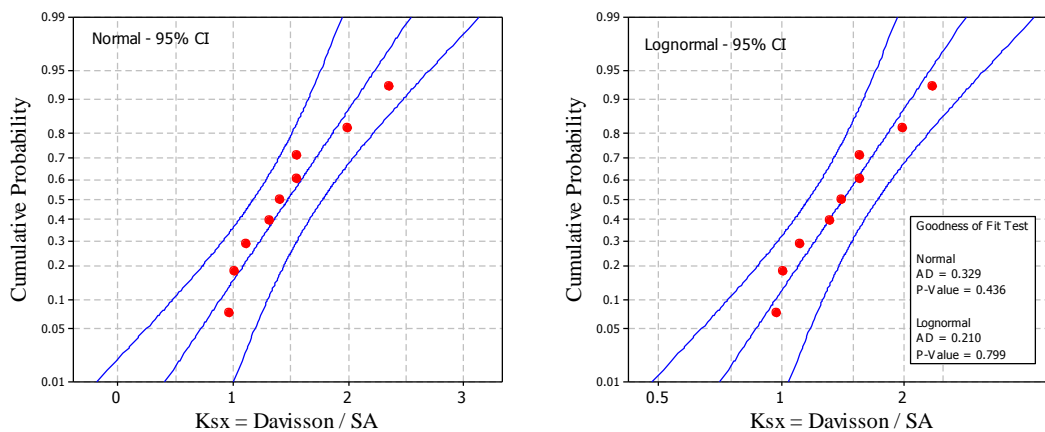


Figure B.49. Goodness of fit test for the WEAP based on SA method in mixed soil

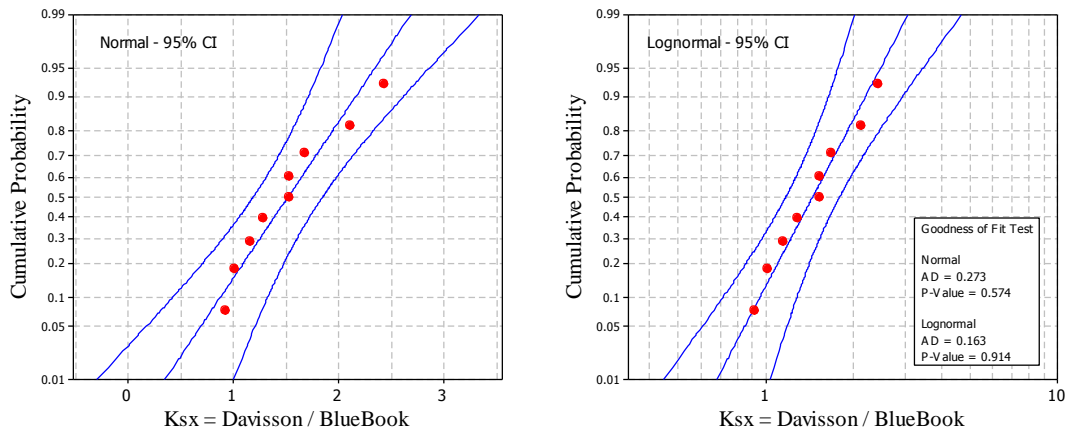


Figure B.50. Goodness of fit test for the WEAP based on Blue Book method in mixed soil

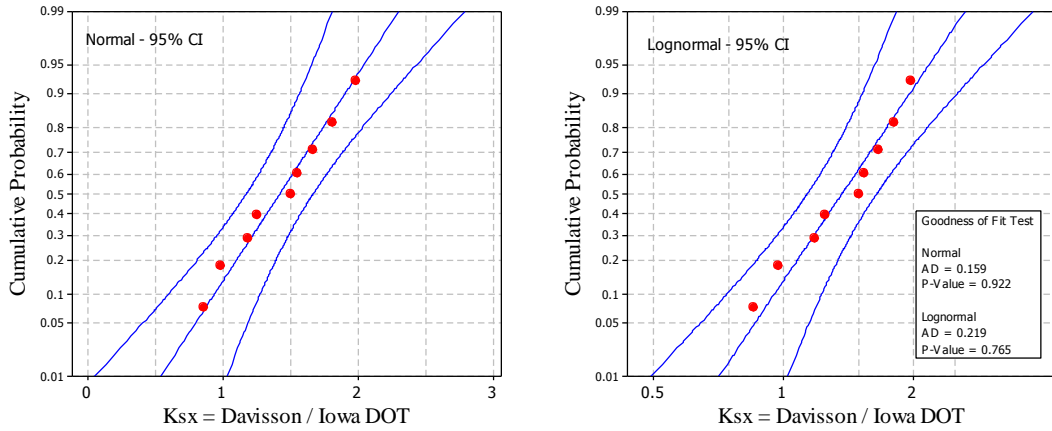


Figure B.51. Goodness of fit test for the WEAP based on Iowa DOT in mixed soil

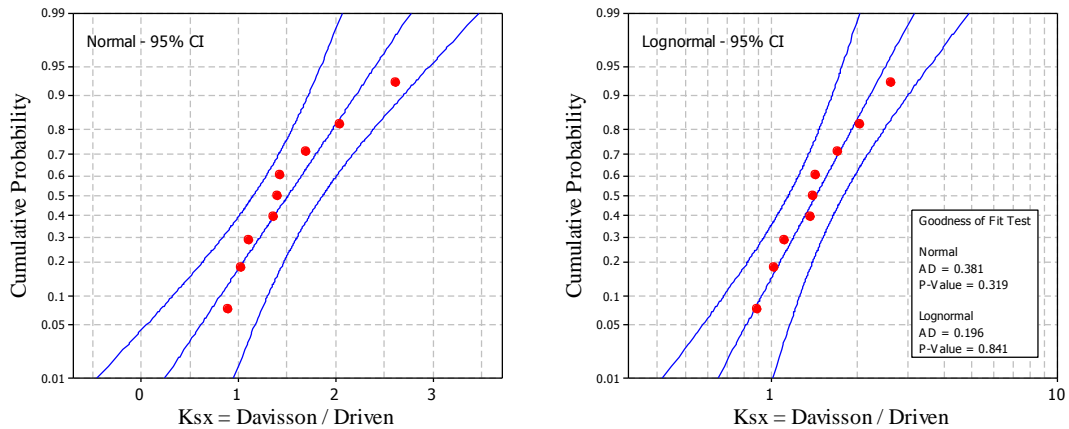


Figure B.52. Goodness of fit test for the WEAP based on Driven method in mixed soil

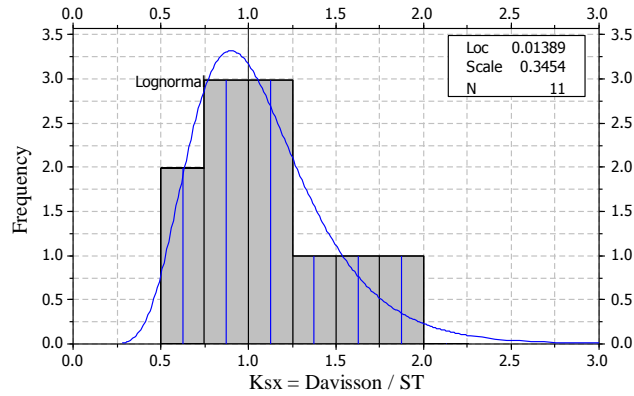


Figure B.53. Histogram and frequency distribution of K_{sx} for 13 cases of steel H-piles designed using WEAP in sand based on the ST method

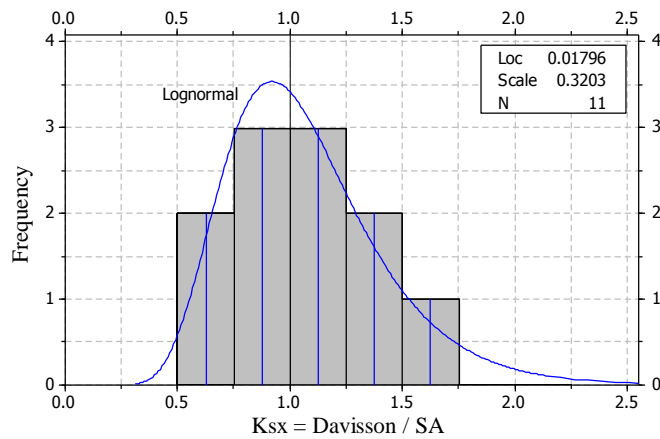


Figure B.54. Histogram and frequency distribution of K_{sx} for 13 cases of steel H-piles designed using WEAP in sand based on the SA method

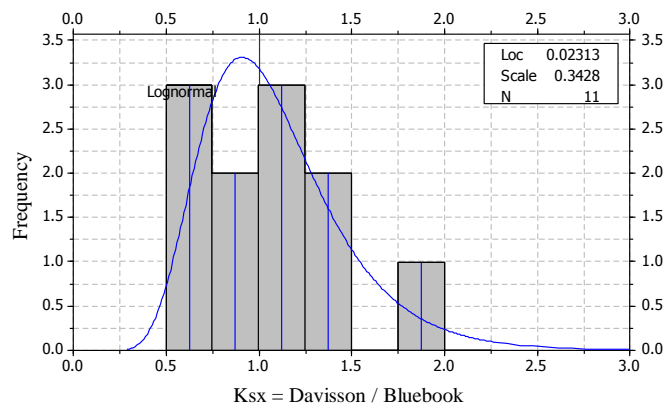


Figure B.55. Histogram and frequency distribution of K_{sx} for 13 cases of steel H-piles designed using WEAP in sand based on the Blue Book method

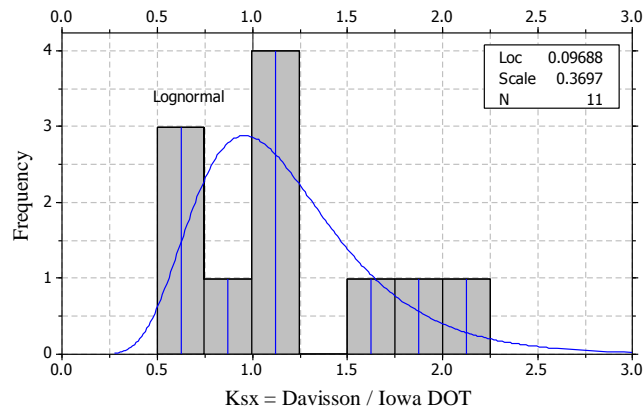


Figure B.56. Histogram and frequency distribution of K_{sx} for 13 cases of steel H-piles designed using WEAP in sand based on the Iowa DOT method

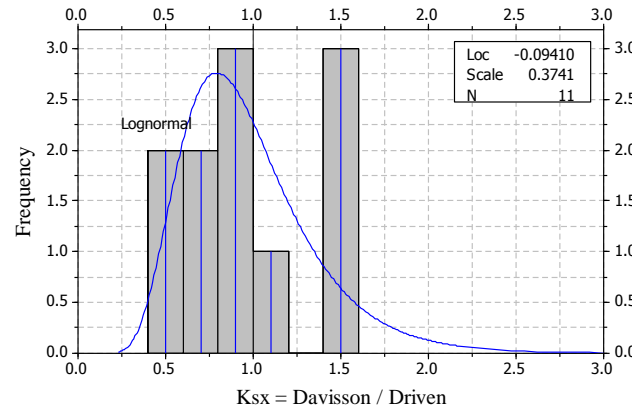


Figure B.57. Histogram and frequency distribution of K_{sx} for 13 cases of steel H-piles designed using WEAP in sand based on the Driven method

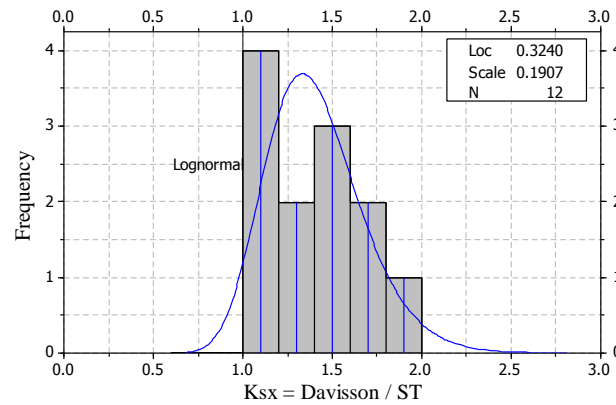


Figure B.58. Histogram and frequency distribution of K_{sx} for 8 cases of steel H-piles designed using WEAP in clay based on the ST method

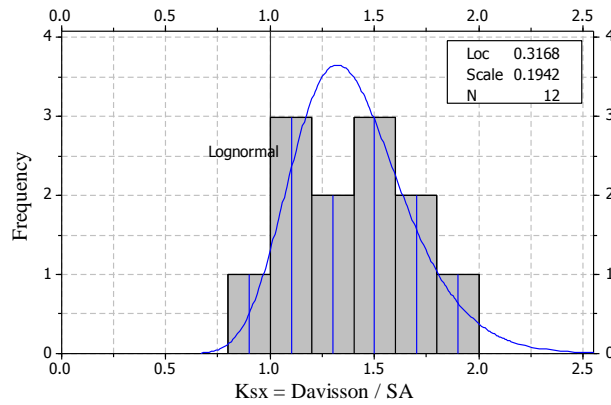


Figure B.59. Histogram and frequency distribution of K_{sx} for 8 cases of steel H-piles designed using WEAP in clay based on the SA method

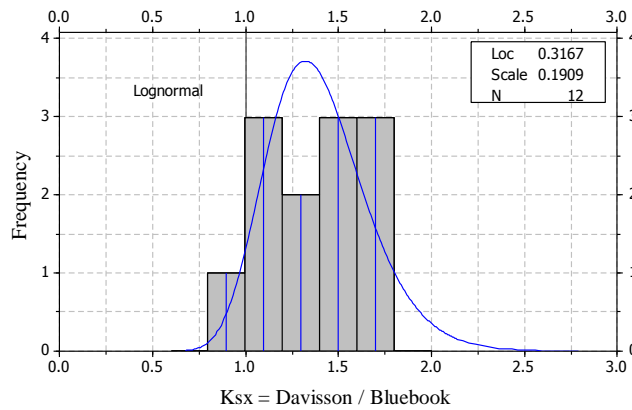


Figure B.60. Histogram and frequency distribution of K_{sx} for 8 cases of steel H-piles designed using WEAP in clay based on the Blue Book method

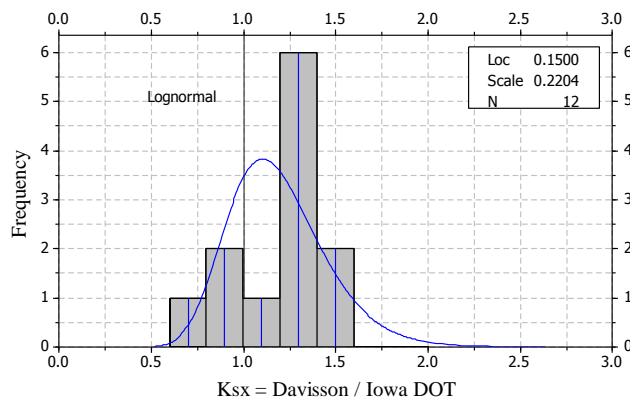


Figure B.61. Histogram and frequency distribution of K_{sx} for 8 cases of steel H-piles designed using WEAP in clay based on the Iowa DOT method

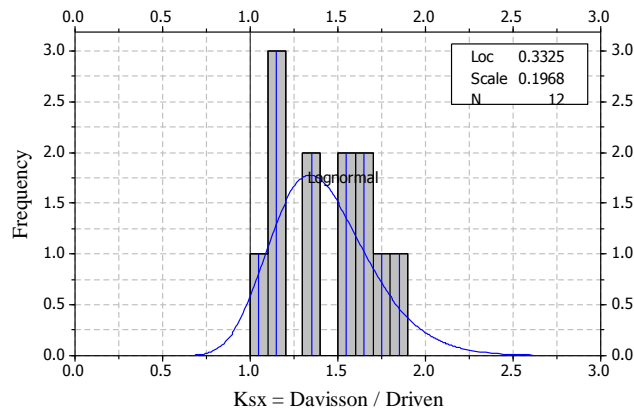


Figure B.62. Histogram and frequency distribution of K_{sx} for 8 cases of steel H-piles designed using WEAP in clay based on the Driven method

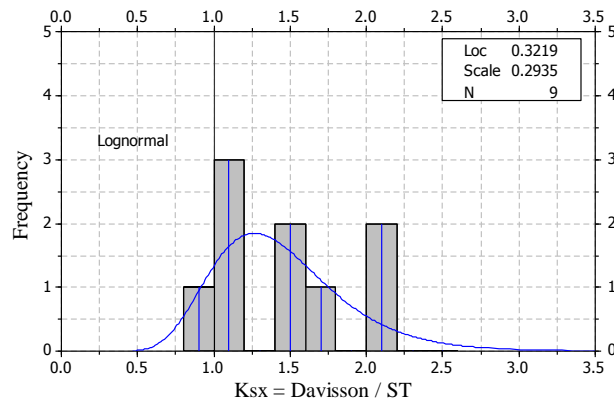


Figure B.63. Histogram and frequency distribution of K_{sx} for 12 cases of steel H-piles designed using WEAP in mixed soil based on the ST method

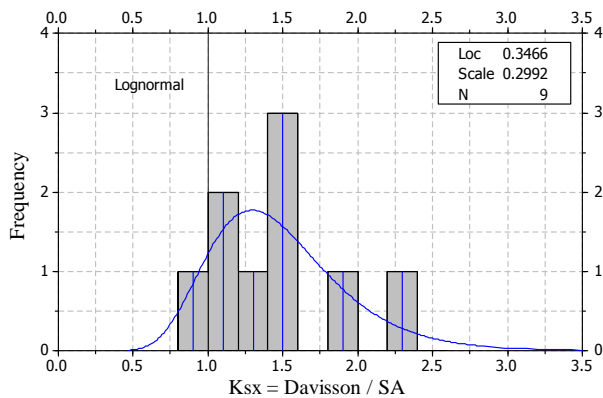


Figure B.64. Histogram and frequency distribution of K_{sx} for 12 cases of steel H-piles designed using WEAP in mixed soil based on the SA method

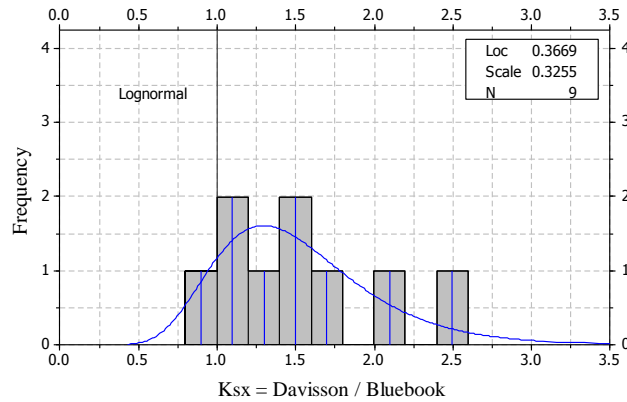


Figure B.65. Histogram and frequency distribution of K_{sx} for 12 cases of steel H-piles designed using WEAP in mixed soil based on the Blue Book method

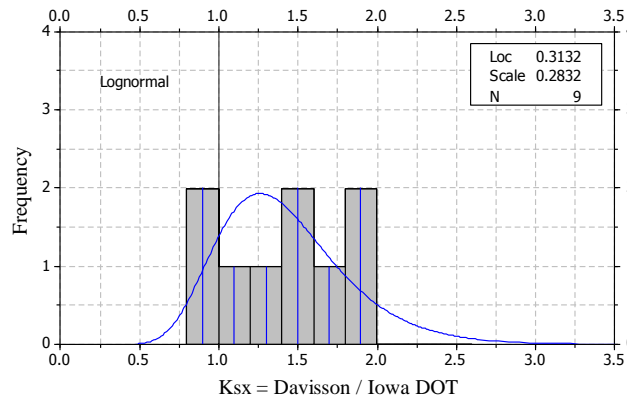


Figure B.66. Histogram and frequency distribution of K_{sx} for 12 cases of steel H-piles designed using WEAP in mixed soil based on the Iowa DOT method

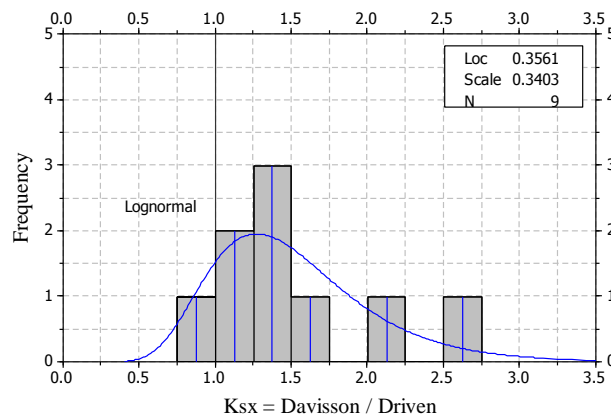


Figure B.67. Histogram and frequency distribution of K_{sx} for 12 cases of steel H-piles designed using WEAP in mixed soil based on the Driven method

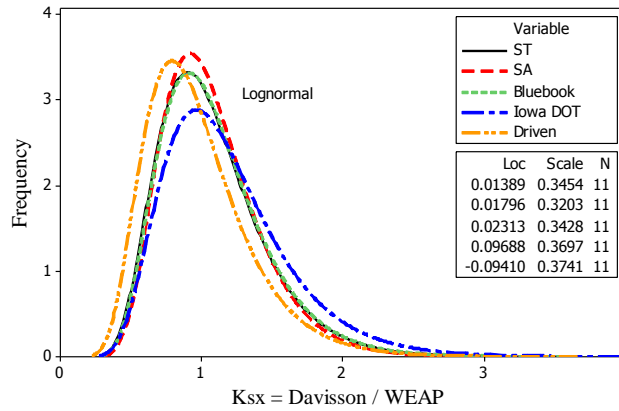


Figure B.68. Summary of the lognormal distributed PDFs of the K_{sx} for the 13 cases of steel H-piles designed using WEAP in sand based on different input approaches

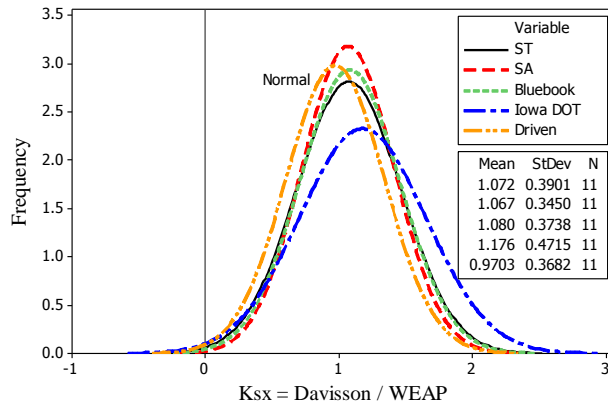


Figure B.69. Summary of the normal distributed PDFs of the K_{sx} for the 13 cases of steel H-piles designed using WEAP in sand using different input approaches

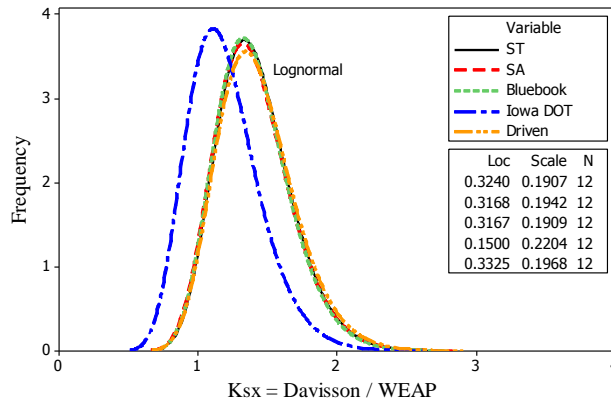


Figure B.70. Summary of the lognormal distributed PDFs of the K_{sx} for the 8 cases of steel H-piles designed using WEAP in clay based on different input approaches

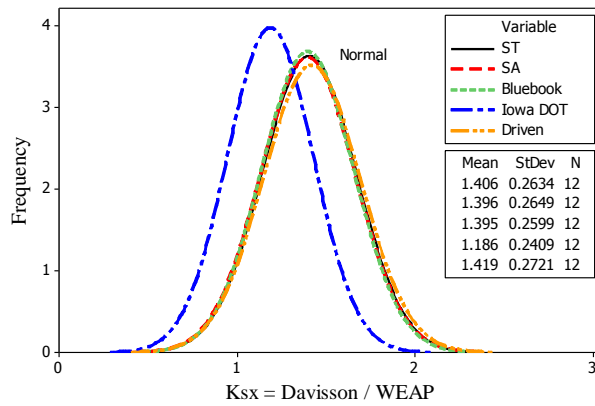


Figure B.71. Summary of the normal distributed PDFs of the K_{sx} for the 8 cases of steel H-piles designed using WEAP in clay using different input approaches

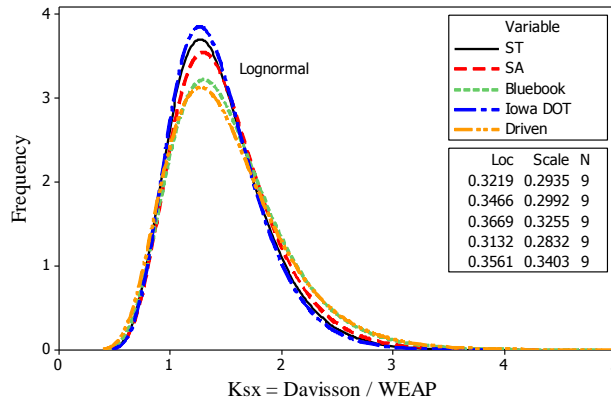


Figure B.72. Summary of the lognormal distributed PDFs of the K_{sx} for the 12 cases of steel H-piles designed using WEAP in mixed soil based on different input approaches

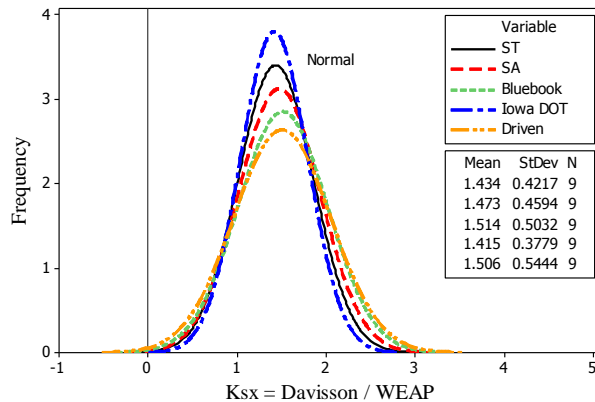


Figure B.73. Summary of the normal distributed PDFs of the K_{sx} for the 12 cases of steel H-piles designed using WEAP in mixed soil using different input approaches

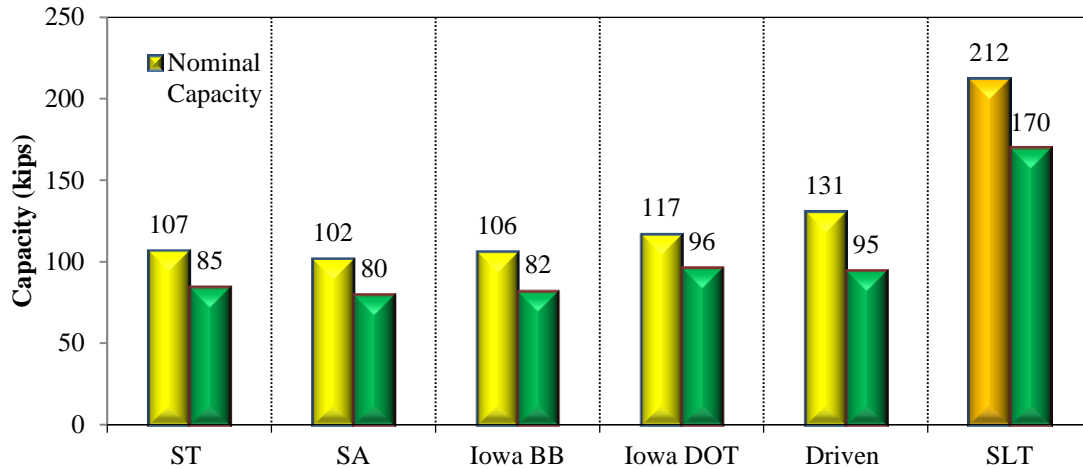


Figure B.74. Nominal and Factored pile design capacities using WEAP different soil input methods and compared to SLT results for Mahaska – Mixed soil

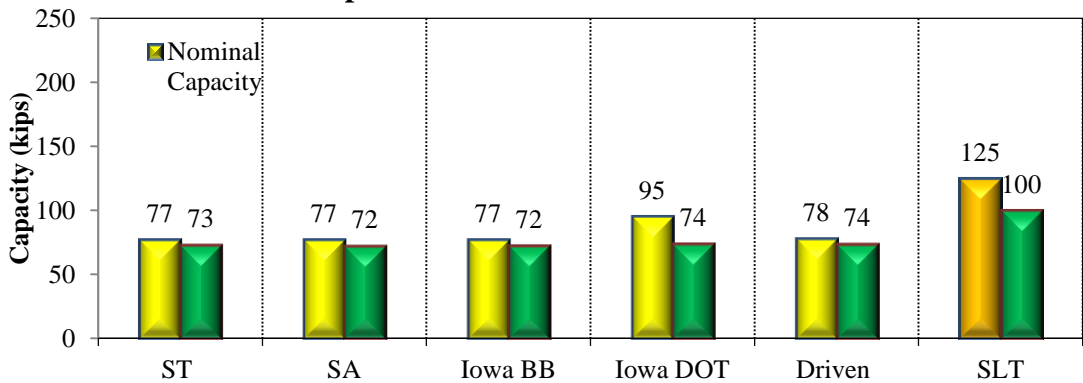


Figure B.75. Nominal and Factored pile design capacities using WEAP different soil input methods and compared to SLT results for Mills – Clay soil

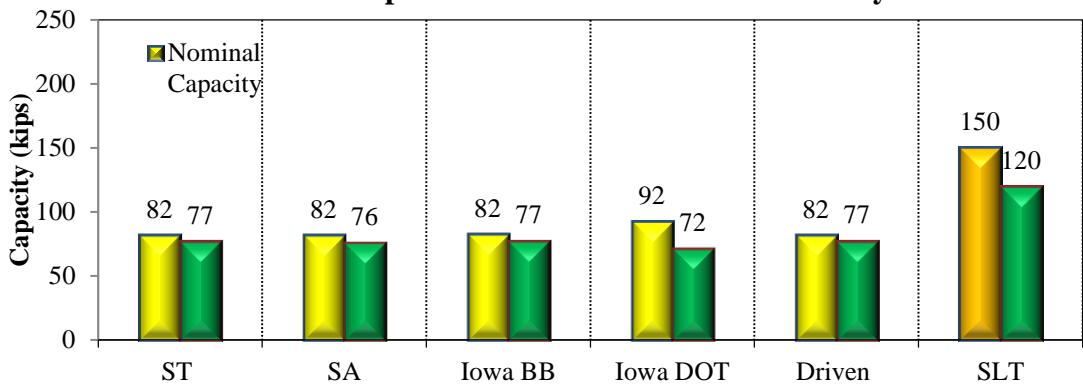


Figure B.76. Nominal and Factored pile design capacities using WEAP different soil input methods and compared to SLT results for Polk – Clay soil

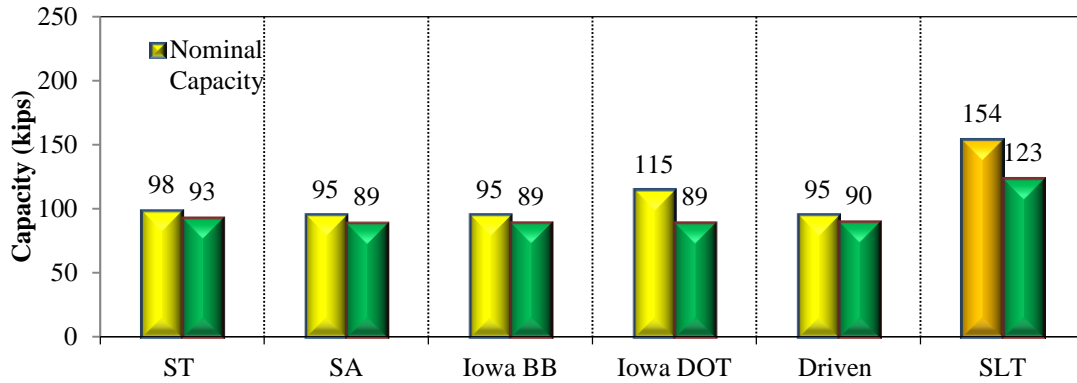


Figure B.77. Nominal and Factored pile design capacities using WEAP different soil input methods and compared to SLT results for Jasper – Clay soil

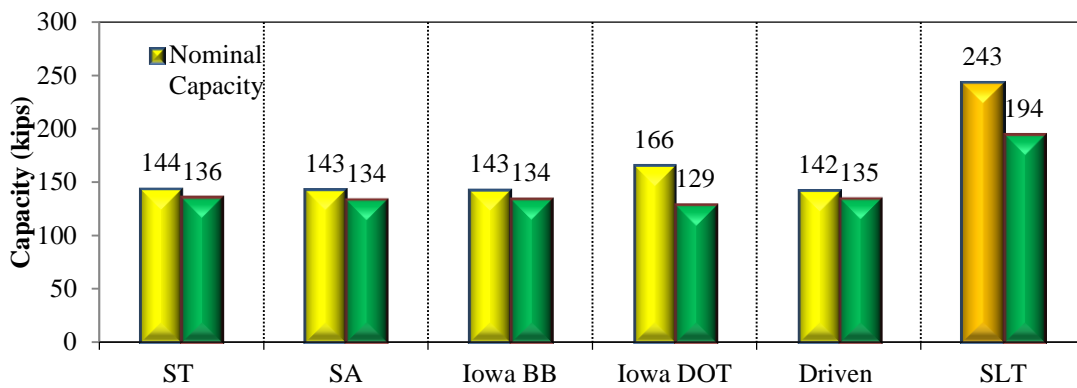


Figure B.78. Nominal and Factored pile design capacities using WEAP different soil input methods and compared to SLT results for Clarke – Clay soil

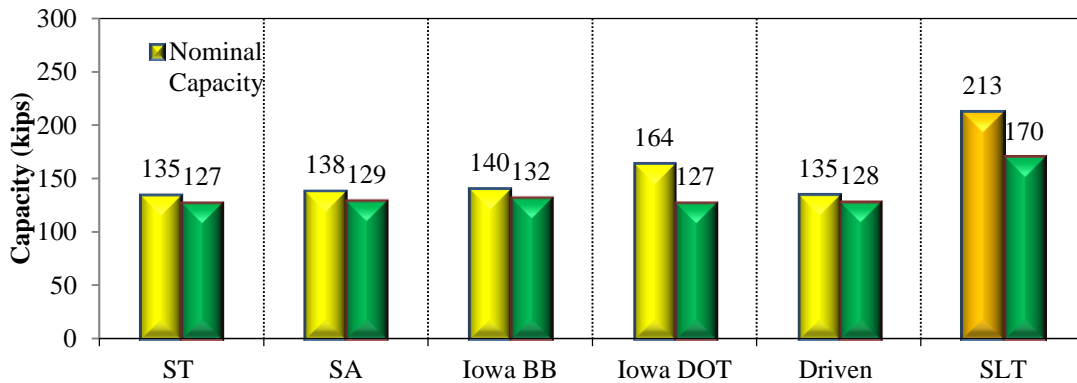


Figure B.79. Nominal and Factored pile design capacities using WEAP different soil input methods and compared to SLT results for Buchanan (long) – Mixed soil

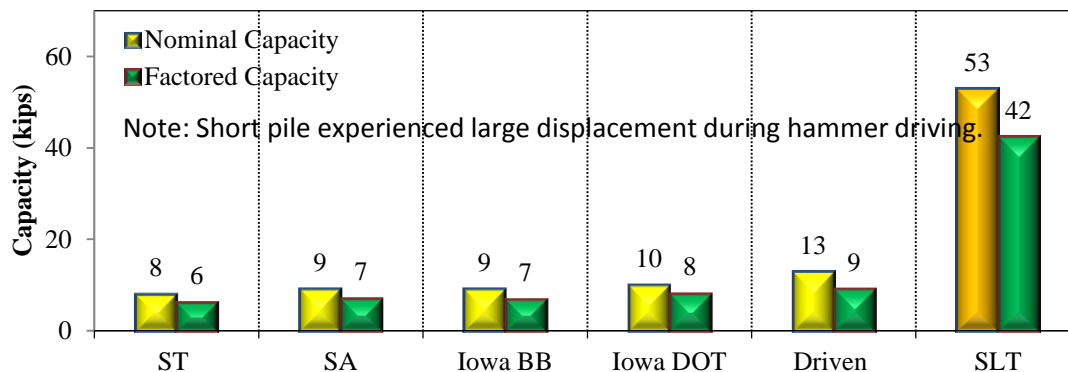


Figure B.80. Nominal and Factored pile design capacities using WEAP different soil input methods and compared to SLT results for Buchanan (short) – Mixed soil

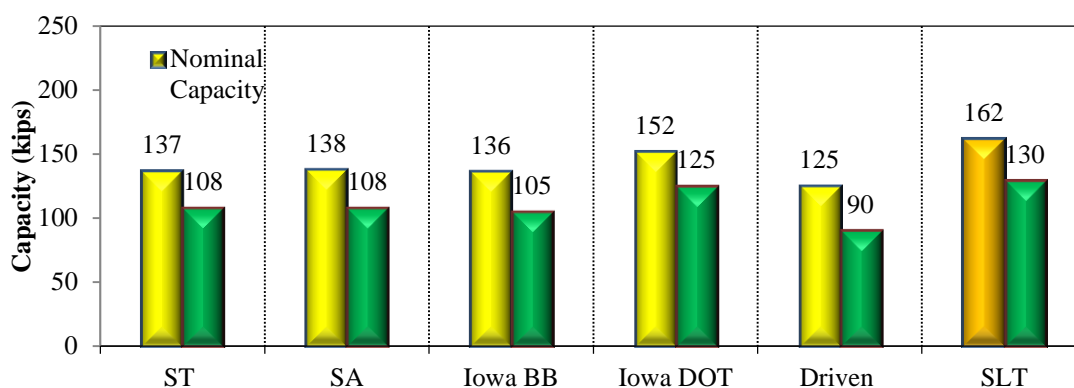


Figure B.81. Nominal and Factored pile design capacities using WEAP different soil input methods and compared to SLT results for Poweshiek – Mixed soil

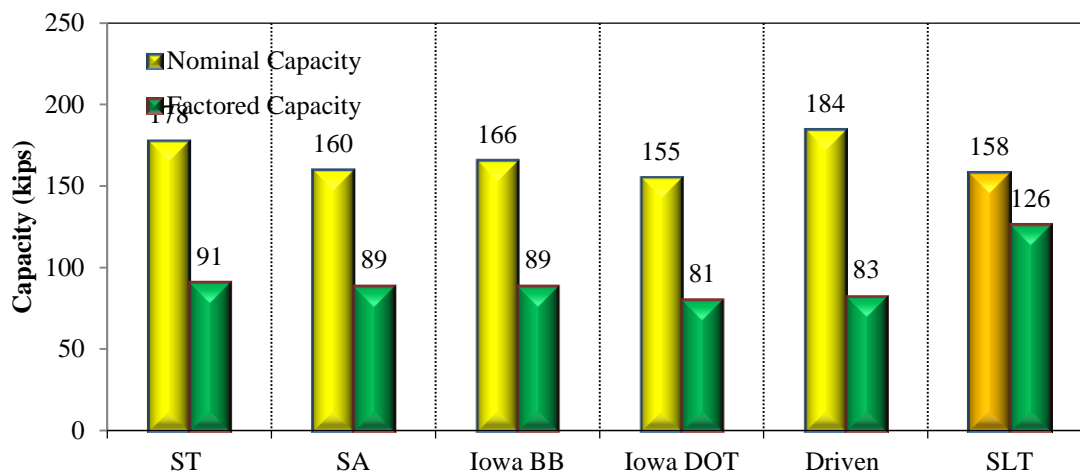


Figure B.82. Nominal and Factored pile design capacities using WEAP different soil input methods and compared to SLT results for Des Moines – Sand soil

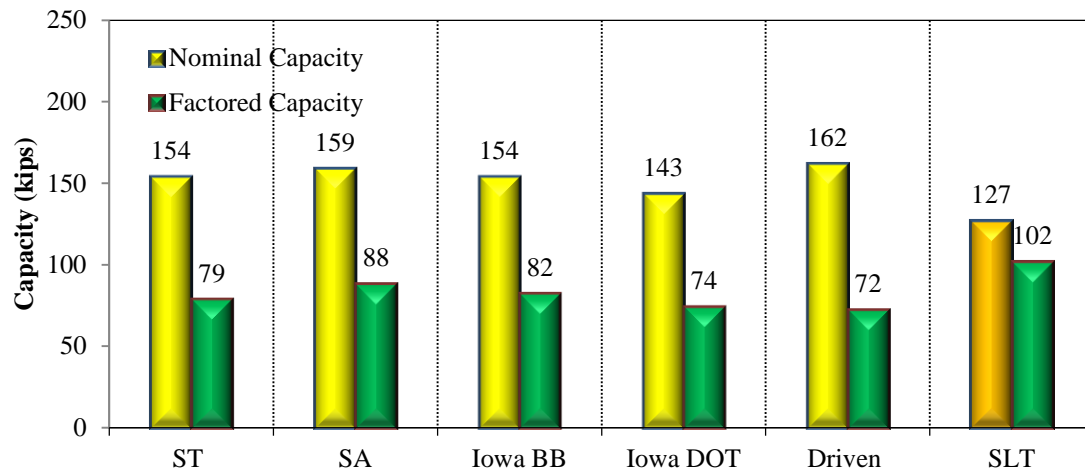


Figure B.83. Nominal and Factored pile design capacities using WEAP different soil input methods and compared to SLT results for Cedar– Sand soil

Dynamic Formulas

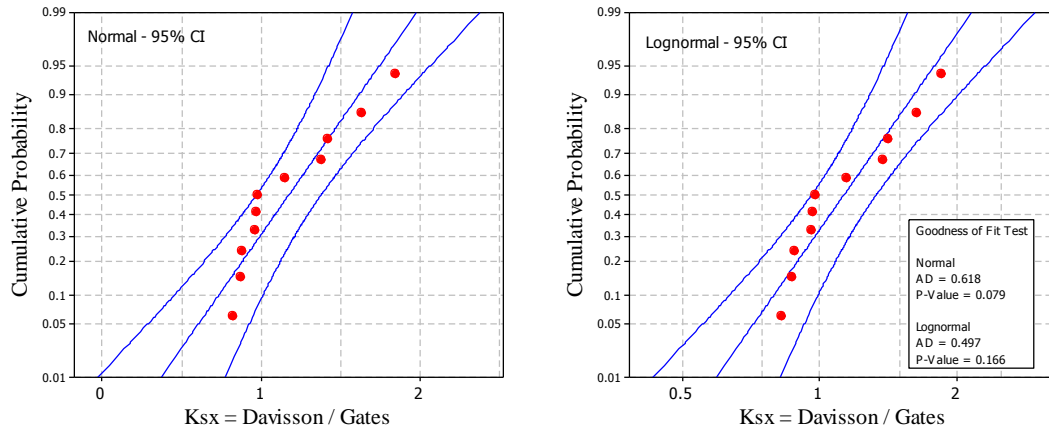


Figure B.84. Goodness of fit test for the Gates formula in sand

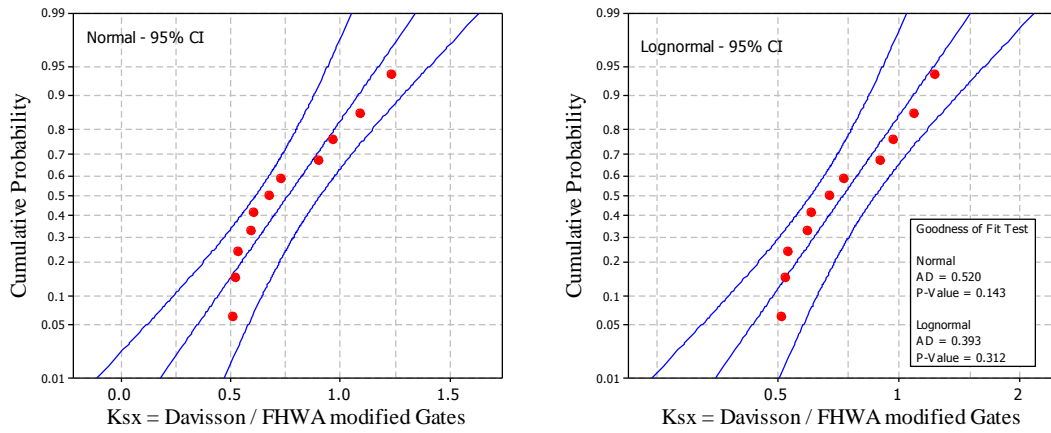


Figure B.85. Goodness of fit test for the FHWA formula in sand

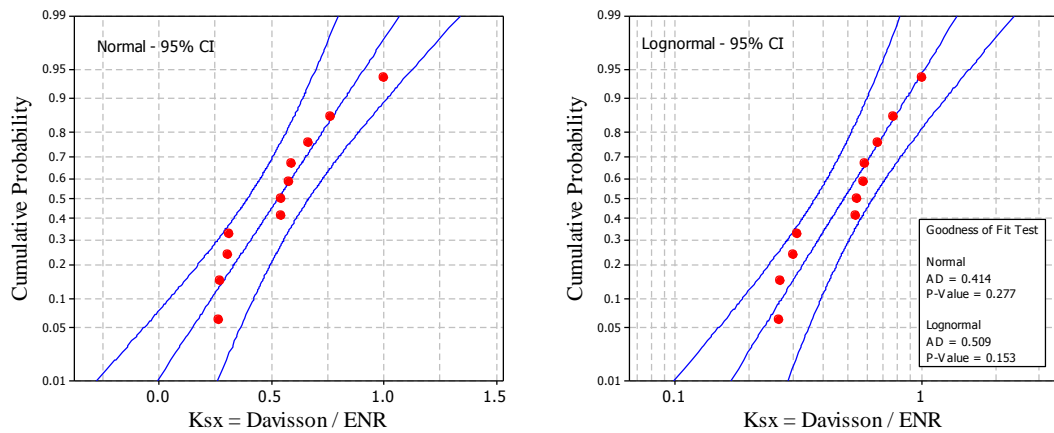


Figure B.86. Goodness of fit test for the ENR formula in sand

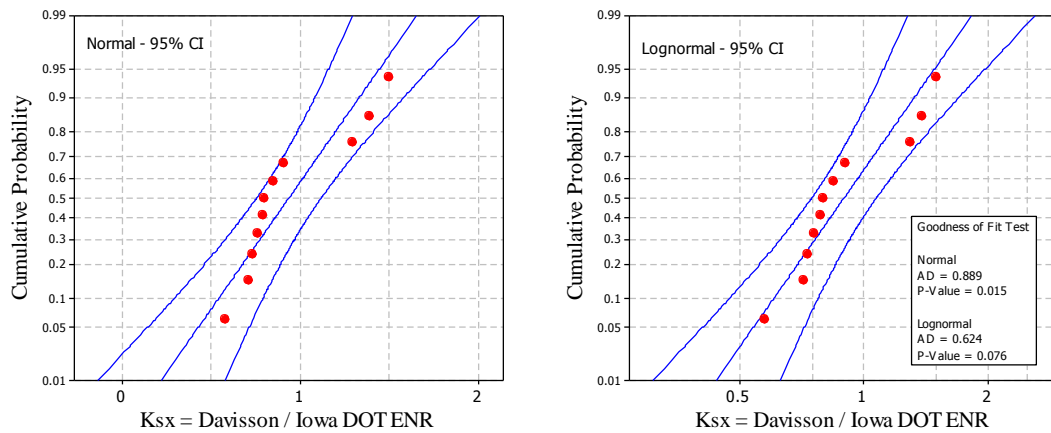


Figure B.87. Goodness of fit test for the Iowa DOT ENR formula in sand

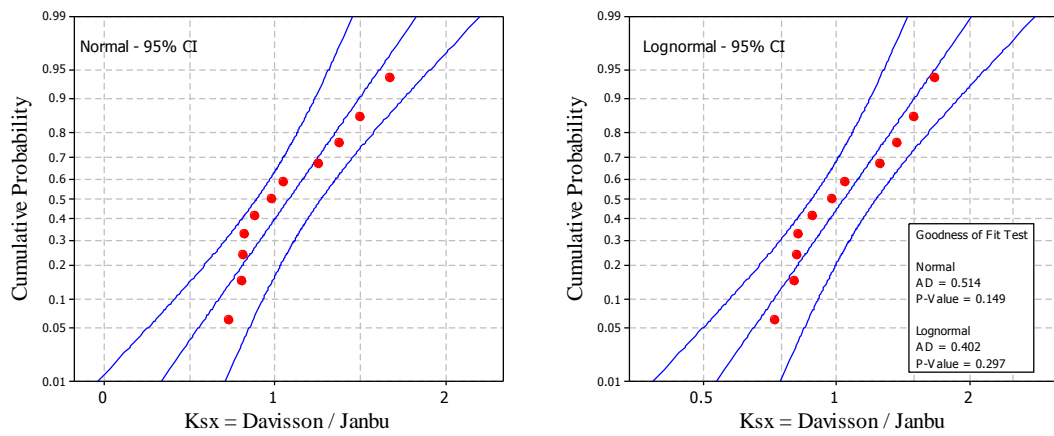


Figure B.88. Goodness of fit test for the Janbu formula in sand

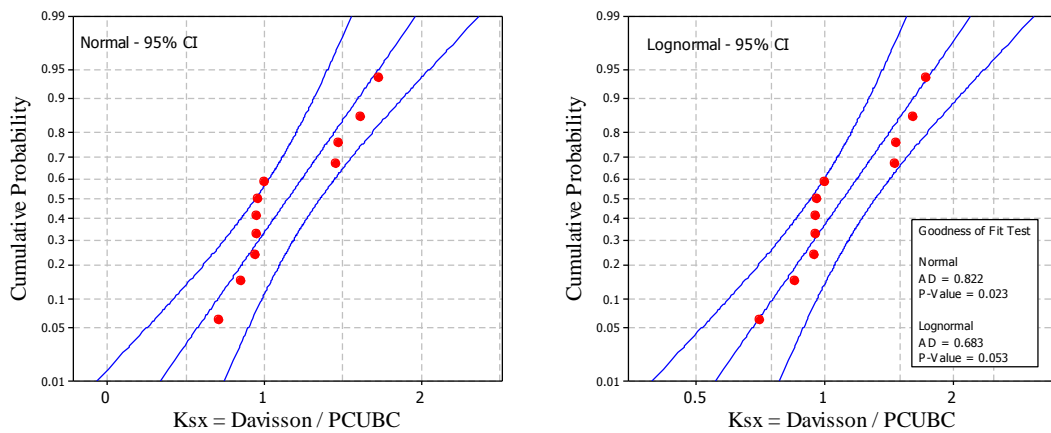


Figure B.89. Goodness of fit test for the PCUBC formula in sand

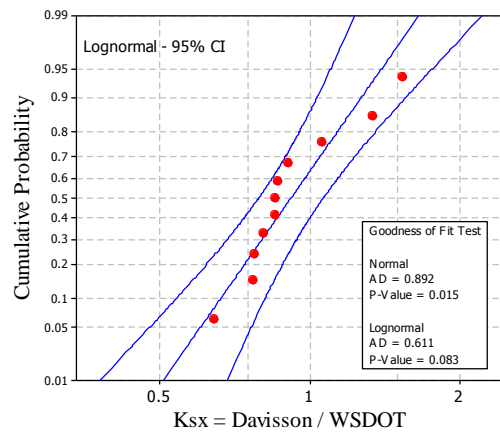
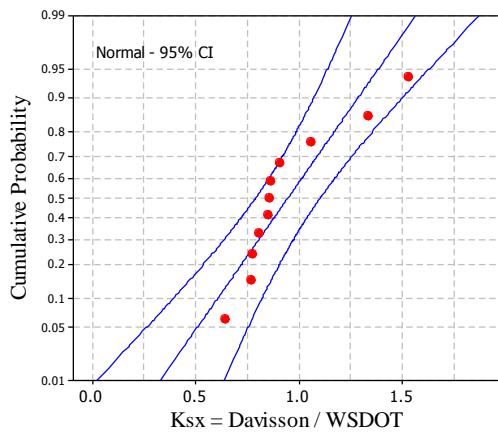


Figure B.90. Goodness of fit test for the WSDOT formula in sand

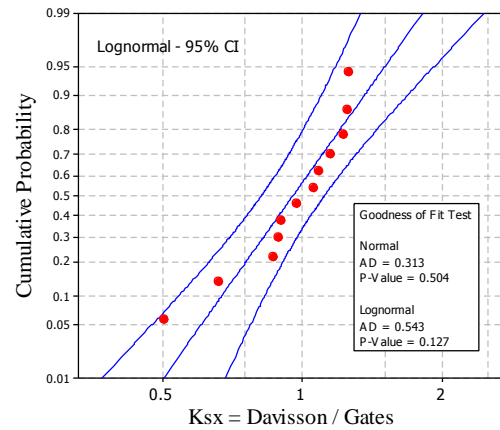
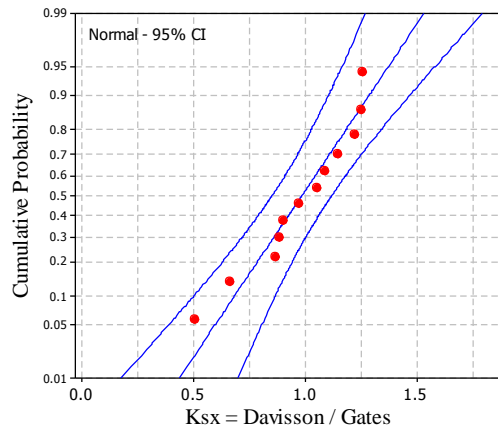


Figure B.91. Goodness of fit test for the Gates formula in clay

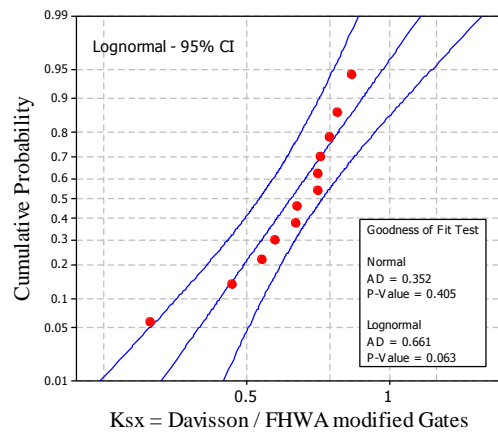
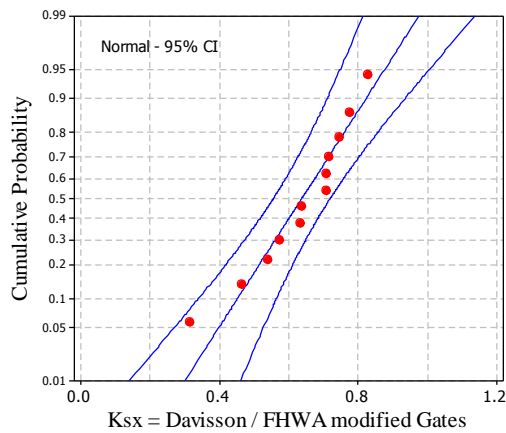


Figure B.92. Goodness of fit test for the FHWA formula in clay

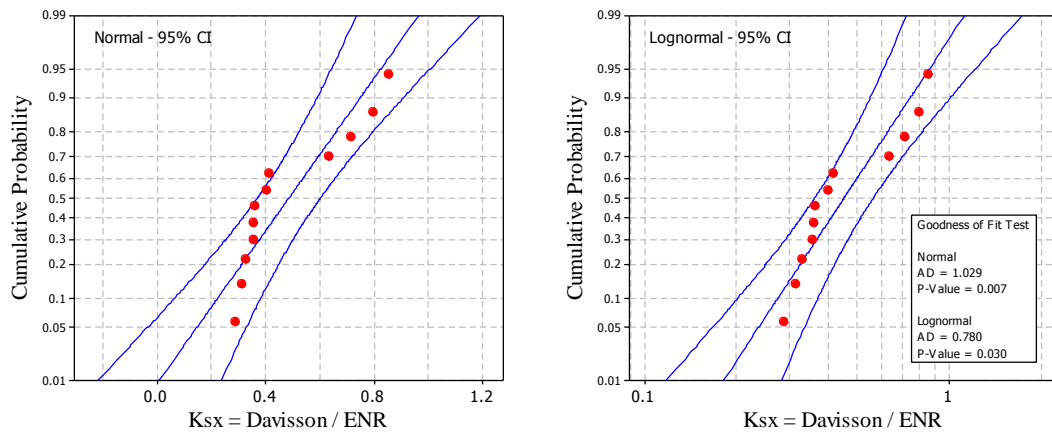


Figure B.93. Goodness of fit test for the ENR formula in clay

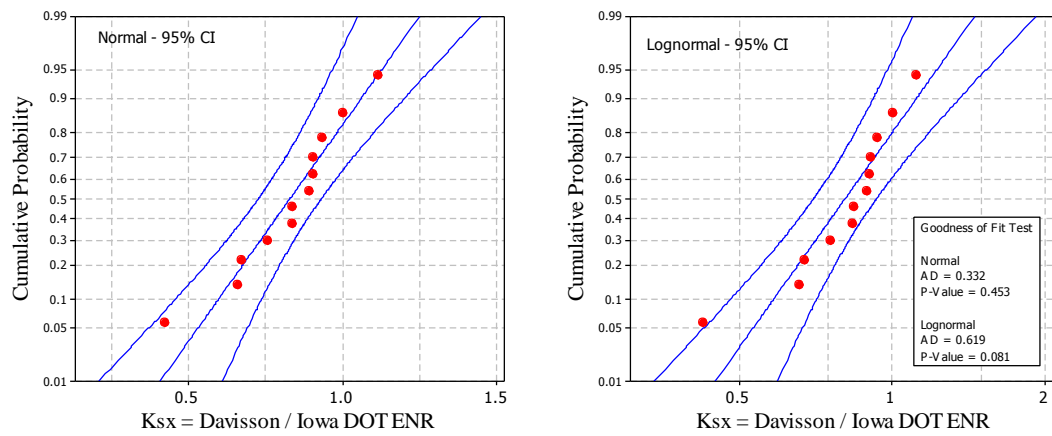


Figure B.94. Goodness of fit test for the Iowa DOT ENR formula in clay

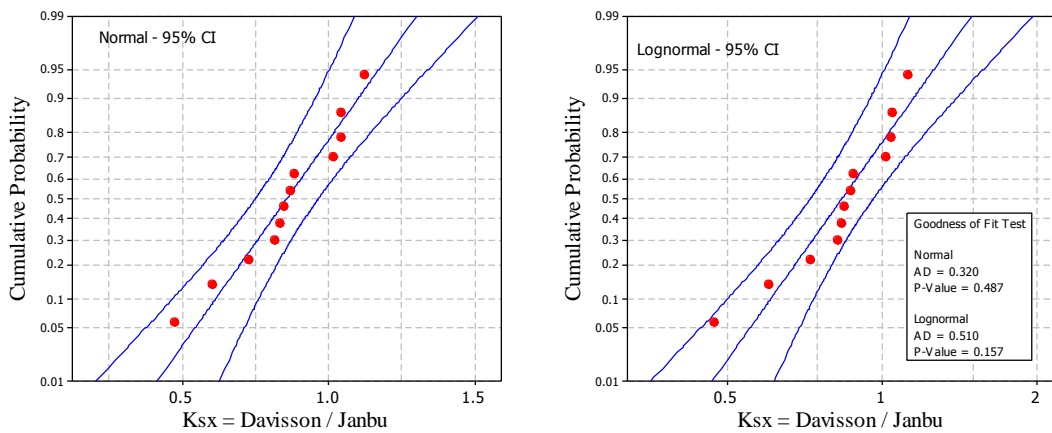


Figure B.95. Goodness of fit test for the Janbu formula in clay

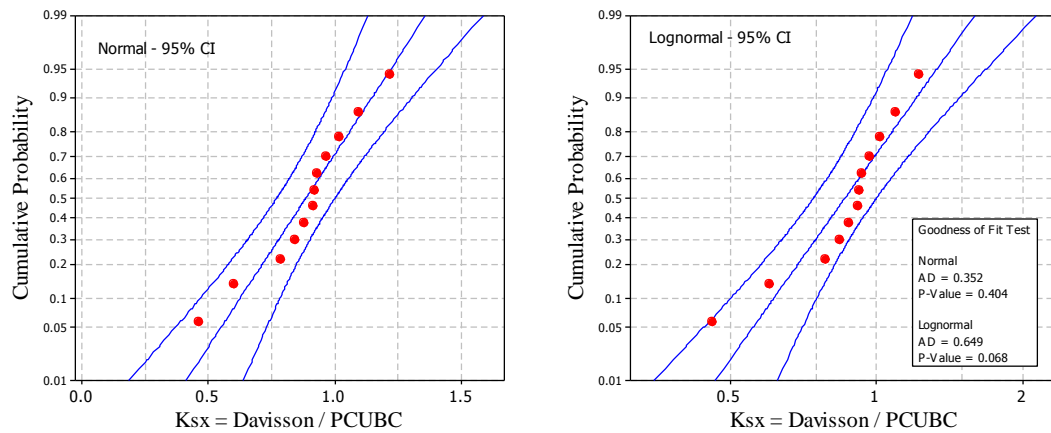


Figure B.96. Goodness of fit test for the PCUBC formula in clay

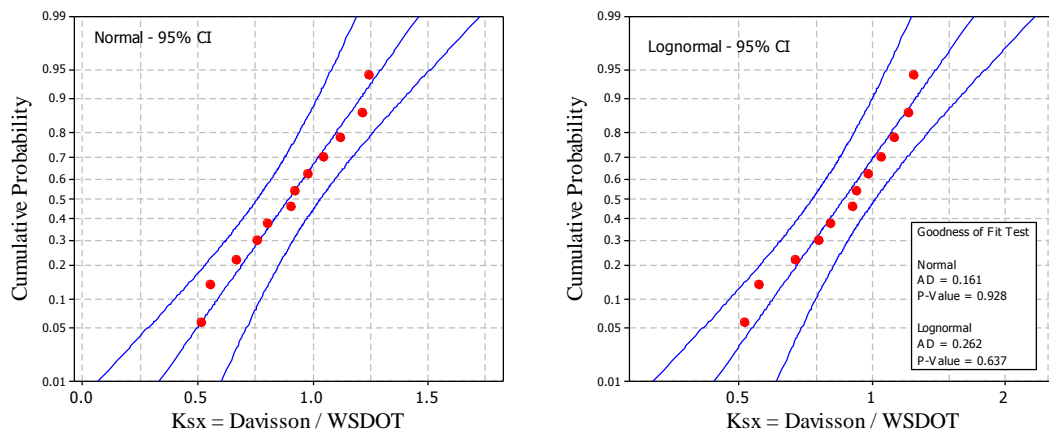


Figure B.97. Goodness of fit test for the WSDOT formula in clay

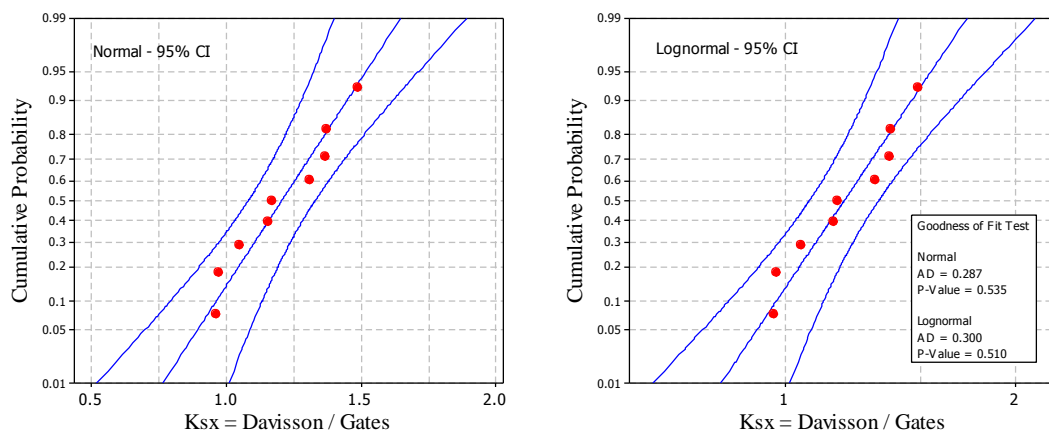


Figure B.98. Goodness of fit test for the Gates formula in mixed soils

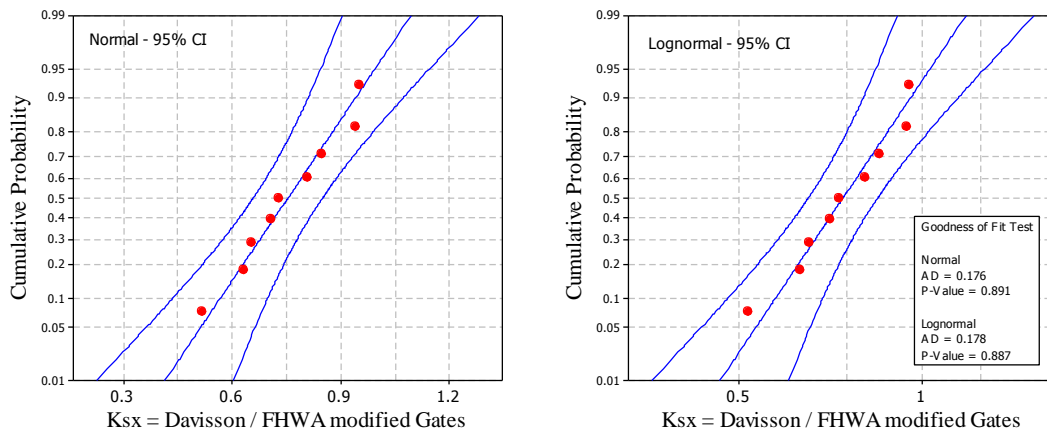


Figure B.99. Goodness of fit test for the FHWA formula in mixed soils

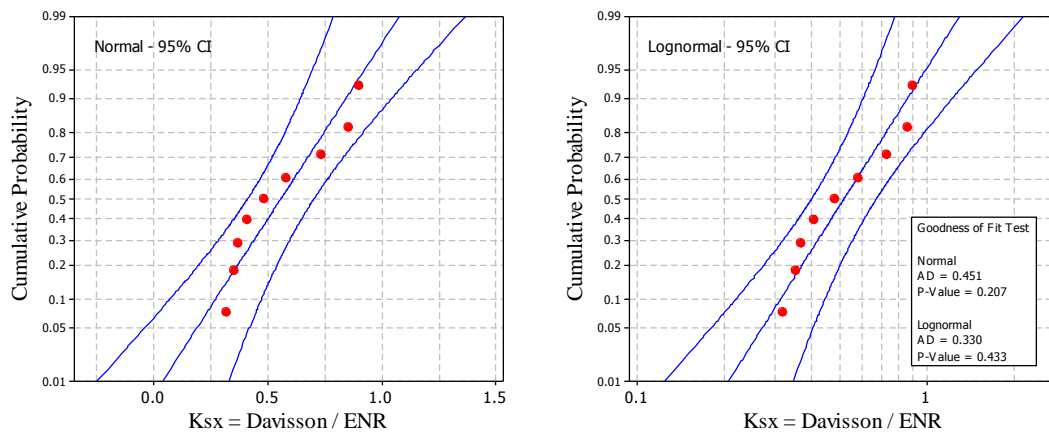


Figure B.100. Goodness of fit test for the ENR formula in mixed soils

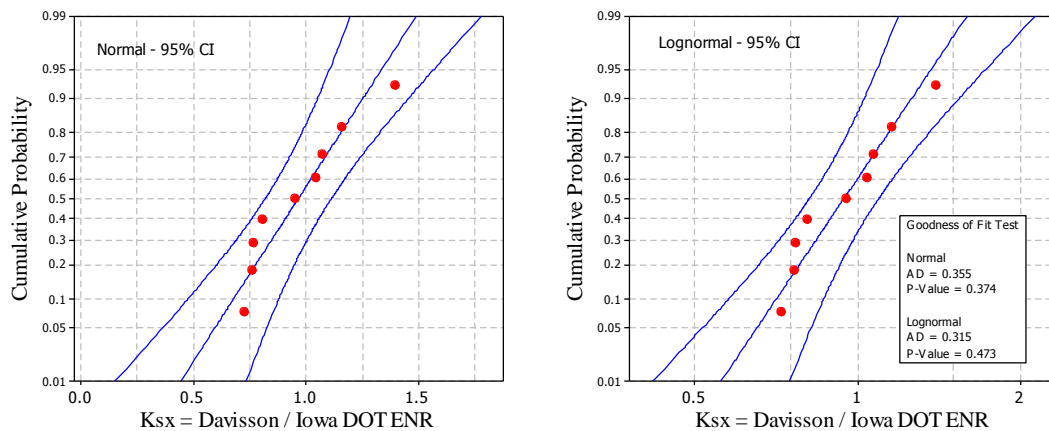


Figure B.101. Goodness of fit test for the Iowa DOT ENR formula in mixed soils

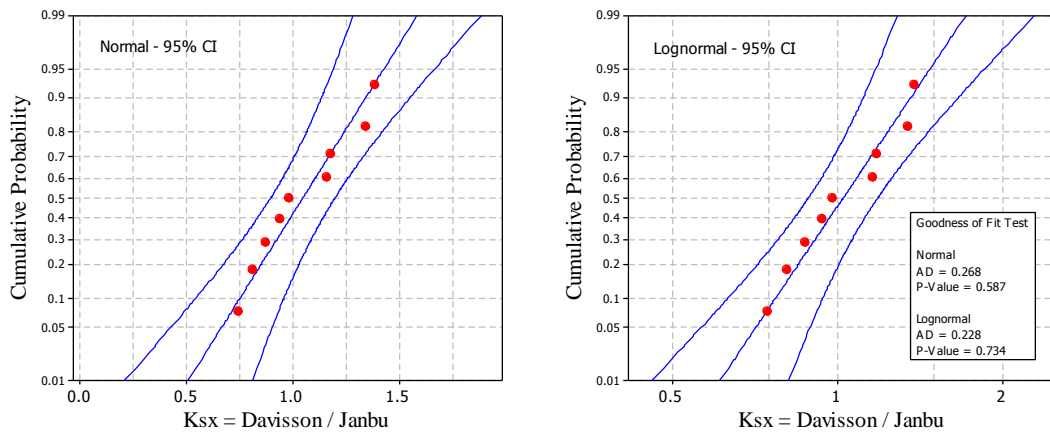


Figure B.102. Goodness of fit test for the Janbu formula in mixed soils

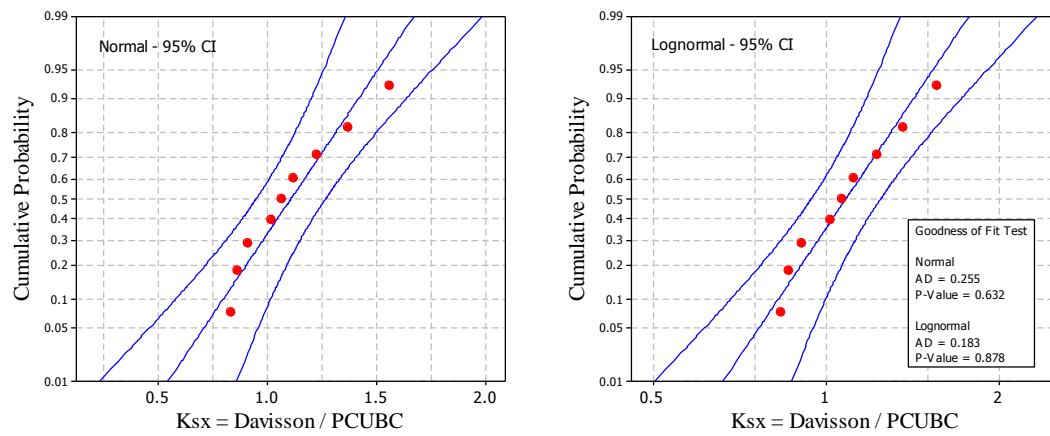


Figure B.103. Goodness of fit test for the PCUBC formula in mixed soils

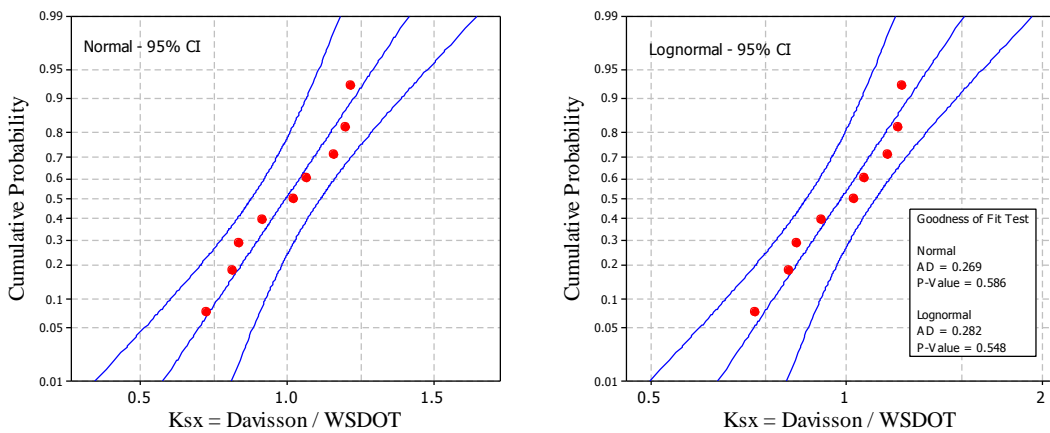


Figure B.104. Goodness of fit test for the WSDOT formula in mixed soils

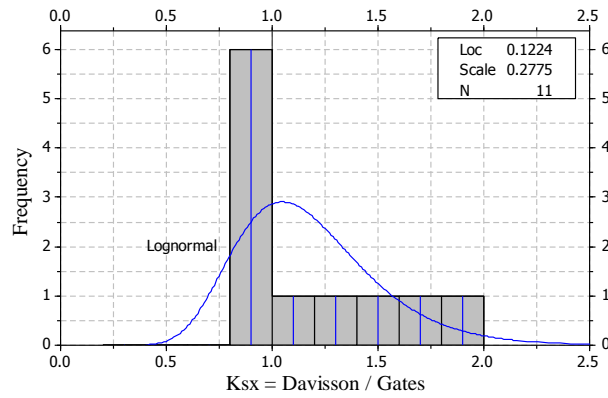


Figure B.105. Histogram and frequency distribution of K_{sx} for 11 cases of steel H-piles designed using Gates formula in sand

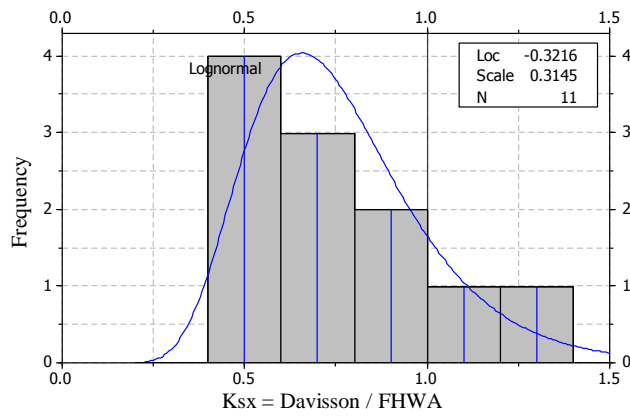


Figure B.106. Histogram and frequency distribution of K_{sx} for 11 cases of steel H-piles designed using FHWA formula in sand

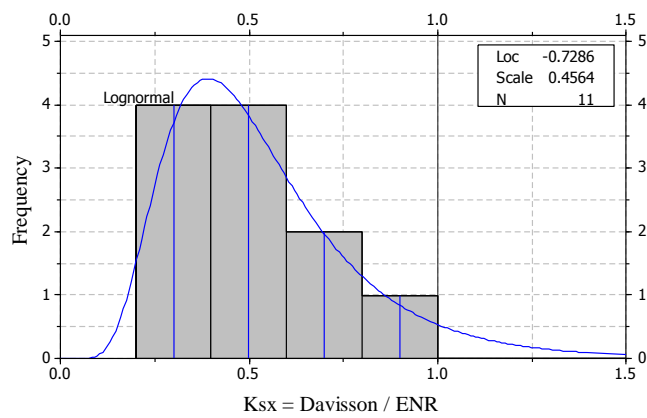


Figure B.107. Histogram and frequency distribution of K_{sx} for 11 cases of steel H-piles designed using ENR formula in sand

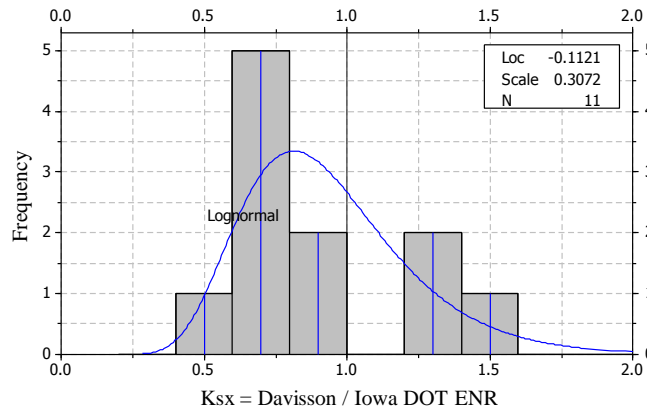


Figure B.108. Histogram and frequency distribution of K_{sx} for 11 cases of steel H-piles designed using Iowa DOT ENR formula in sand

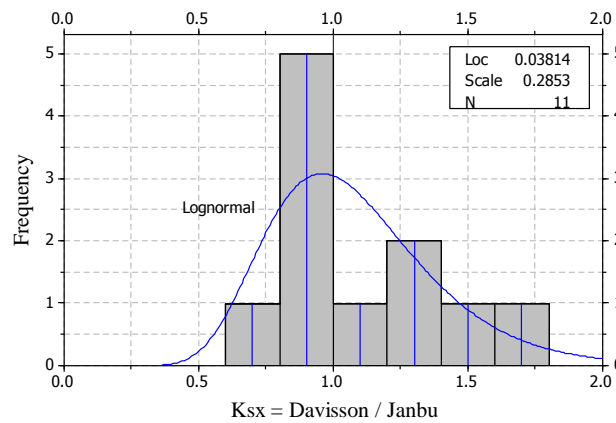


Figure B.109. Histogram and frequency distribution of K_{sx} for 11 cases of steel H-piles designed using Janbu formula in sand

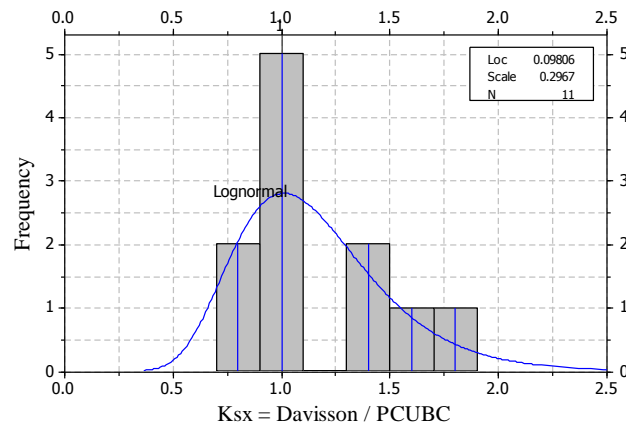


Figure B.110. Histogram and frequency distribution of K_{sx} for 11 cases of steel H-piles designed using PCUBC formula in sand

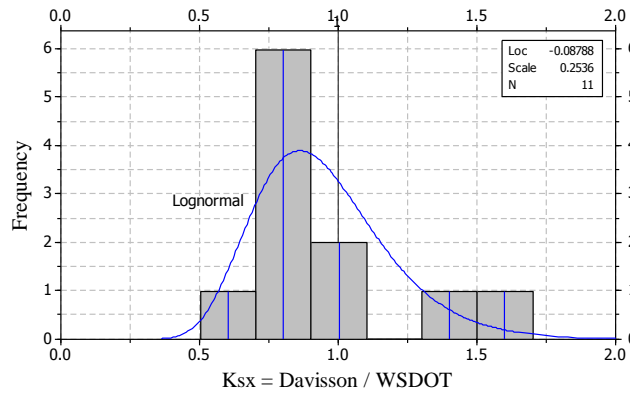


Figure B.111. Histogram and frequency distribution of K_{sx} for 11 cases of steel H-piles designed using WSDOT formula in sand

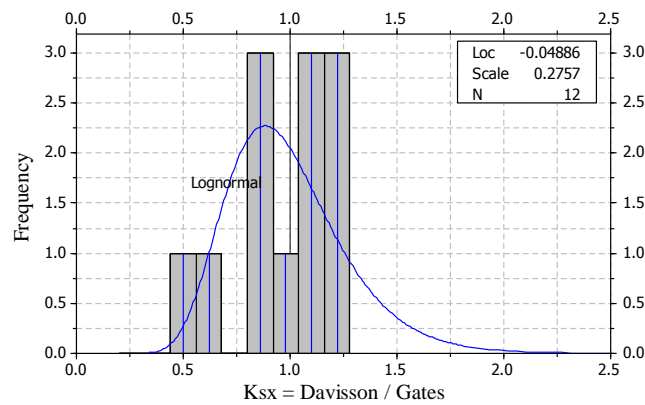


Figure B.112. Histogram and frequency distribution of K_{sx} for 12 cases of steel H-piles designed using Gates formula in clay

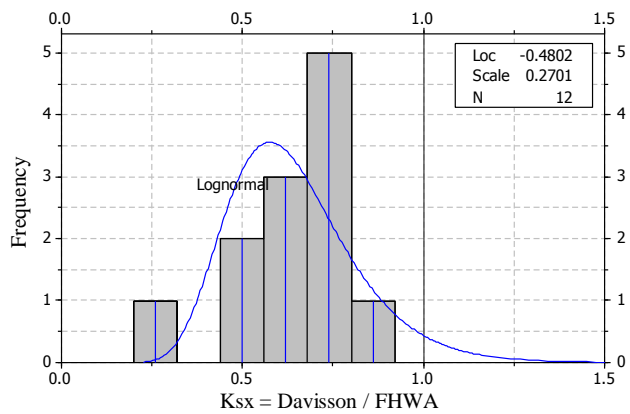


Figure B.113. Histogram and frequency distribution of K_{sx} for 12 cases of steel H-piles designed using FHWA formula in clay

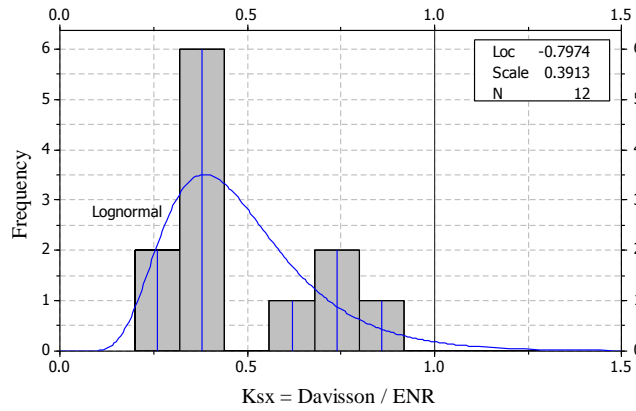


Figure B.114. Histogram and frequency distribution of K_{sx} for 12 cases of steel H-piles designed using ENR formula in clay

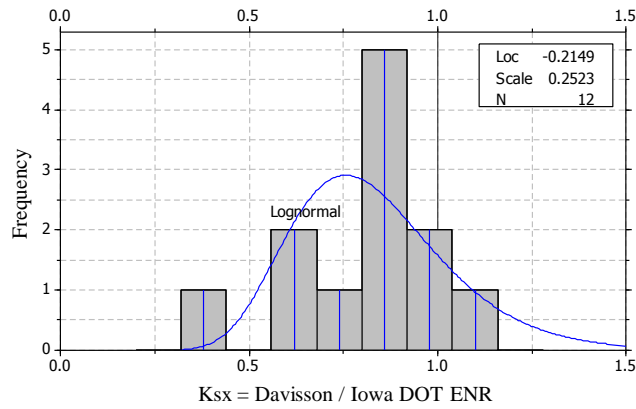


Figure B.115. Histogram and frequency distribution of K_{sx} for 12 cases of steel H-piles designed using Iowa DOT ENR formula in clay

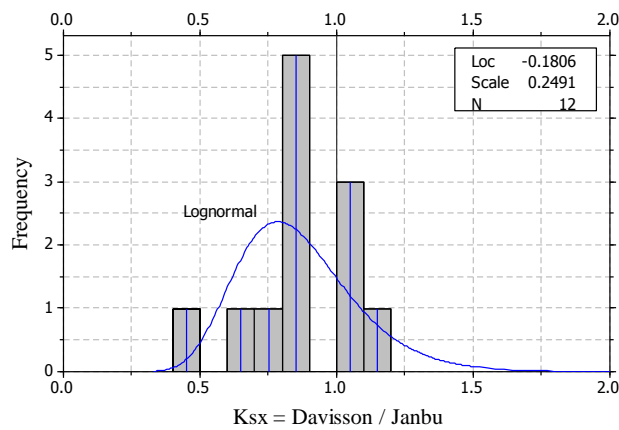


Figure B.116. Histogram and frequency distribution of K_{sx} for 12 cases of steel H-piles designed using Janbu formula in clay

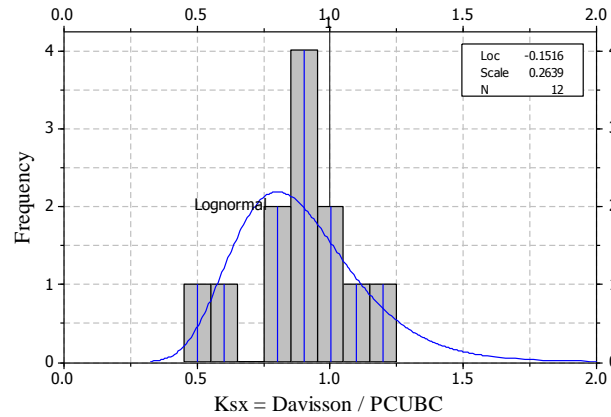


Figure B.117. Histogram and frequency distribution of K_{sx} for 12 cases of steel H-piles designed using PCUBC formula in clay

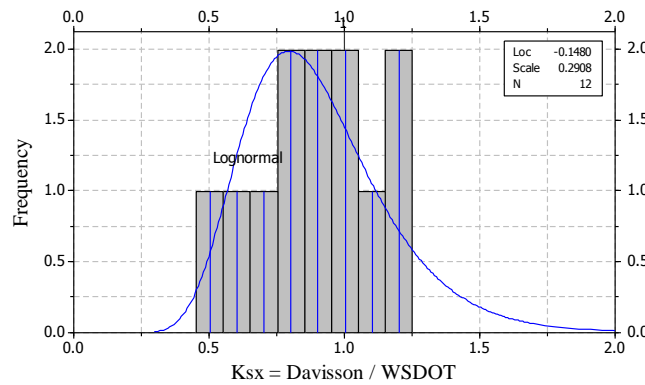


Figure B.118. Histogram and frequency distribution of K_{sx} for 12 cases of steel H-piles designed using WSDOT formula in clay

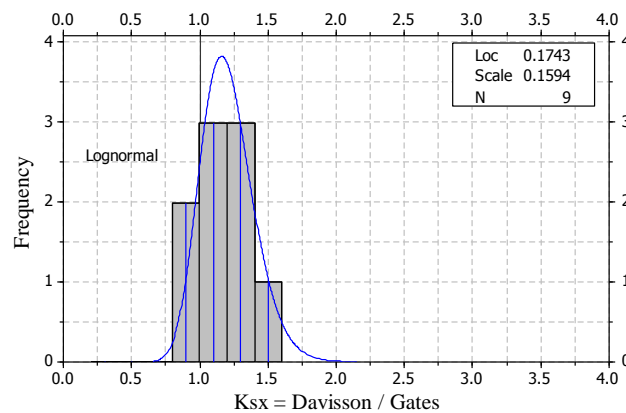


Figure B.119. Histogram and frequency distribution of K_{sx} for 9 cases of steel H-piles designed using Gates formula in mixed soils

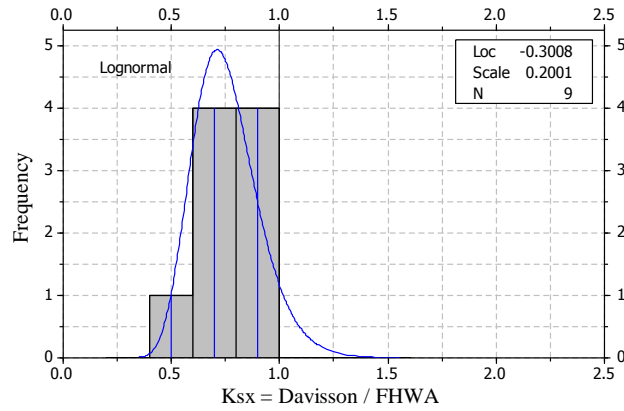


Figure B.120. Histogram and frequency distribution of K_{sx} for 9 cases of steel H-piles designed using FHWA formula in mixed soils

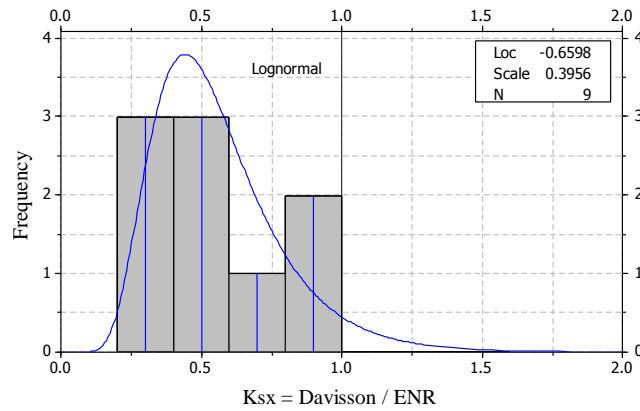


Figure B.121. Histogram and frequency distribution of K_{sx} for 9 cases of steel H-piles designed using ENR formula in mixed soils

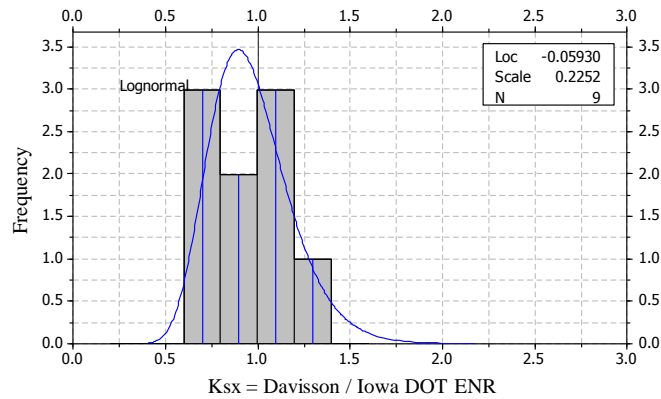


Figure B.122. Histogram and frequency distribution of K_{sx} for 9 cases of steel H-piles designed using Iowa DOT ENR formula in mixed soils

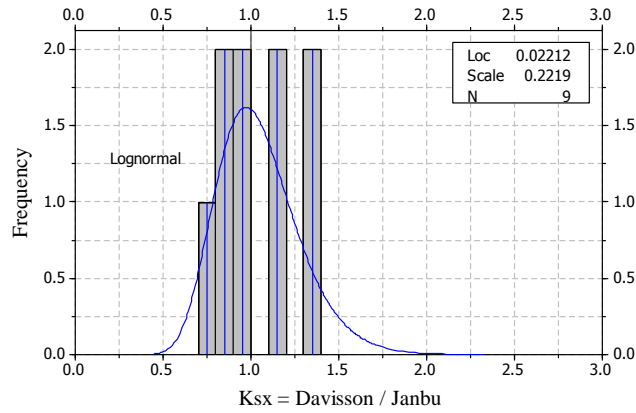


Figure B.123. Histogram and frequency distribution of K_{sx} for 9 cases of steel H-piles designed using Janbu formula in mixed soils

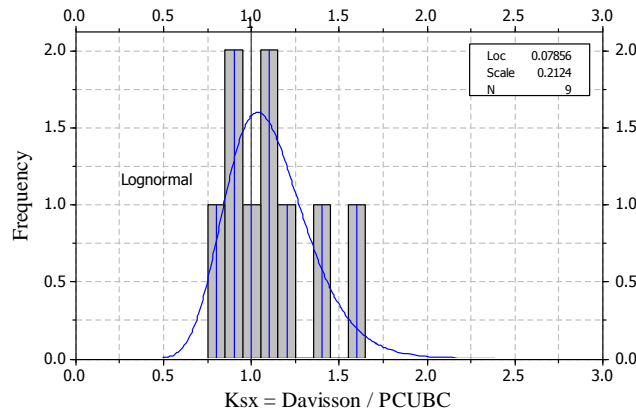


Figure B.124. Histogram and frequency distribution of K_{sx} for 9 cases of steel H-piles designed using PCUBC formula in mixed soils

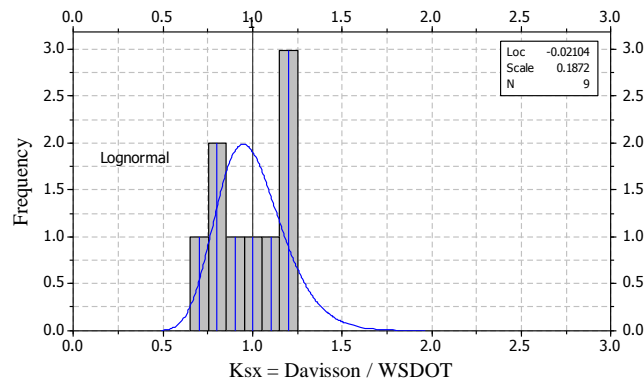


Figure B.125. Histogram and frequency distribution of K_{sx} for 9 cases of steel H-piles designed using WSDOT formula in mixed soils

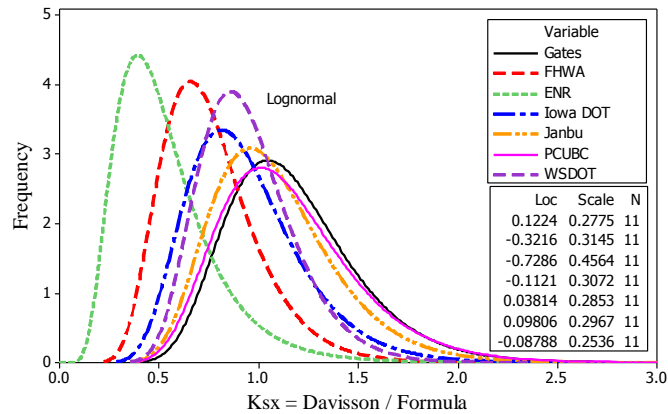


Figure B.126. Summary of the lognormal distributed PDFs of the K_{sx} for the 11 cases of steel H-piles designed using different dynamic formulas in sand

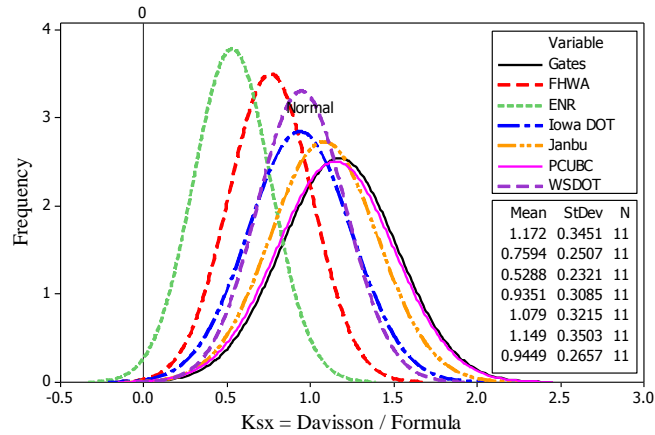


Figure B.127. Summary of the normal distributed PDFs of the K_{sx} for the 11 cases of steel H-piles designed using different dynamic formulas in sand

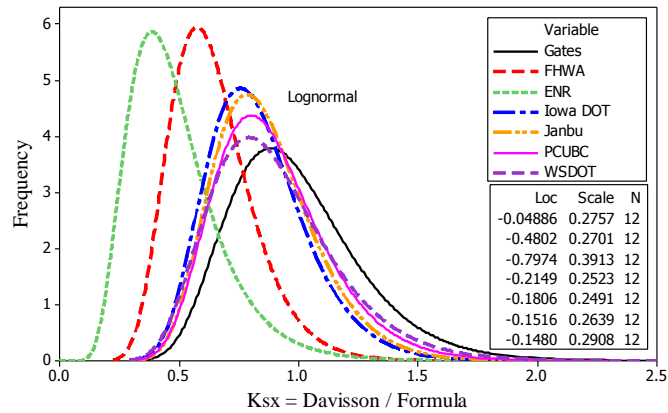


Figure B.128. Summary of the lognormal distributed PDFs of the K_{sx} for the 12 cases of steel H-piles designed using different dynamic formulas in clay

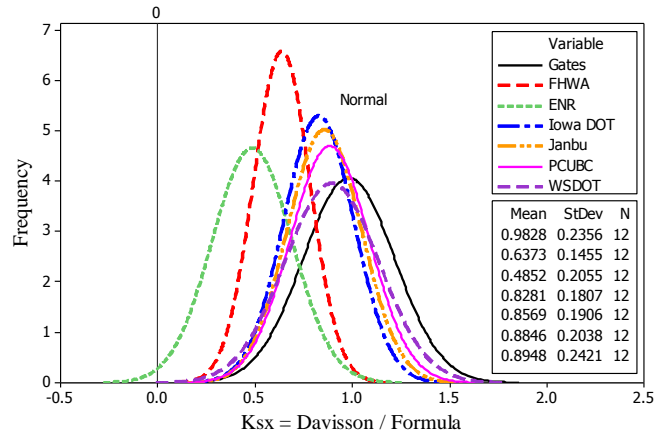


Figure B.129. Summary of the normal distributed PDFs of the K_{sx} for the 12 cases of steel H-piles designed using different dynamic formulas in clay

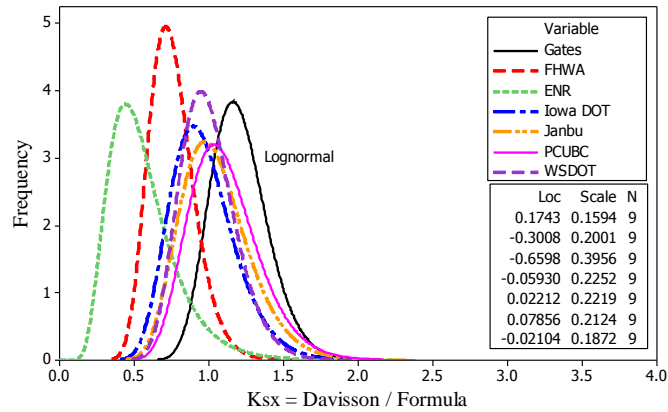


Figure B.130. Summary of the lognormal distributed PDFs of the K_{sx} for the 9 cases of steel H-piles designed using different dynamic formulas in mixed soils

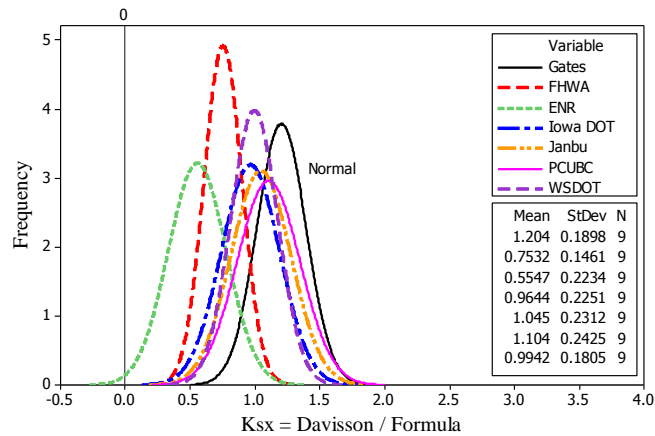


Figure B.131. Summary of the normal distributed PDFs of the K_{sx} for the 9 cases of steel H-piles designed using different dynamic formulas in mixed soils

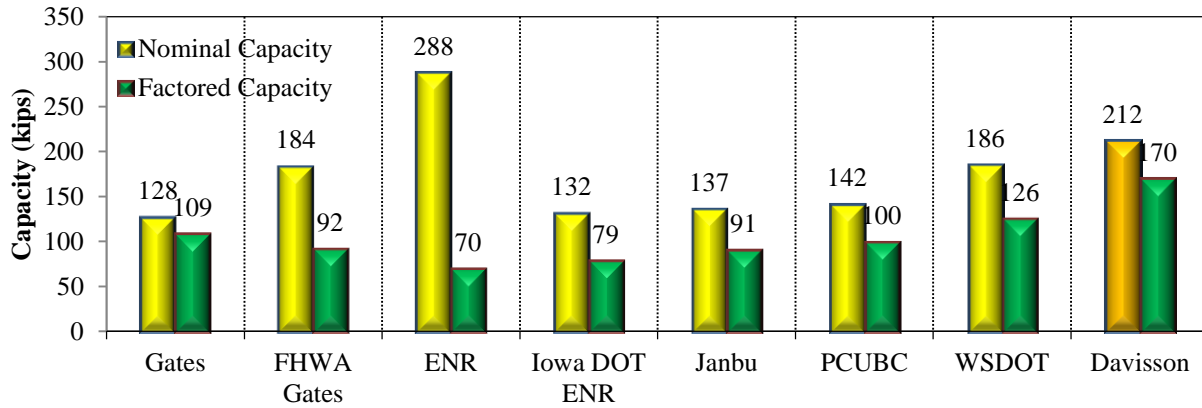


Figure B.132. Nominal and Factored pile design capacities using dynamic formulas and compared to SLT results for Mahaska – Mixed soil

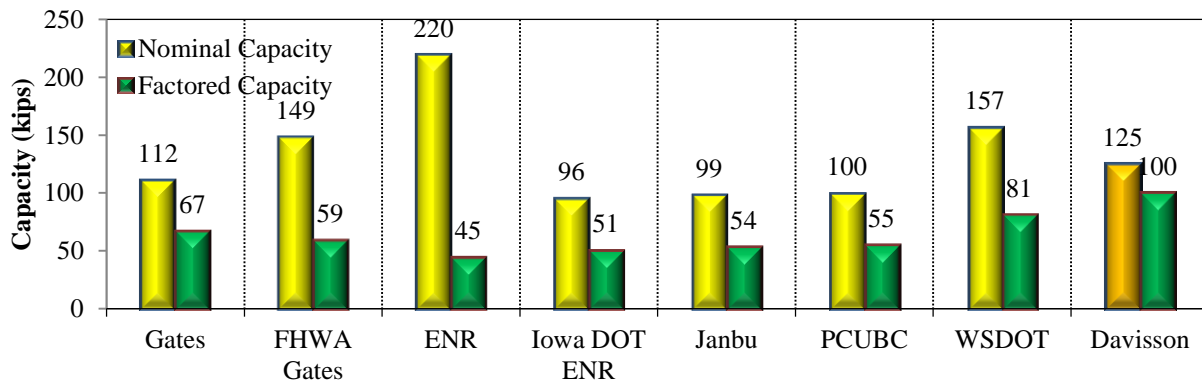


Figure B.133. Nominal and Factored pile design capacities using dynamic formulas and compared to SLT results for Mills – Clay soil

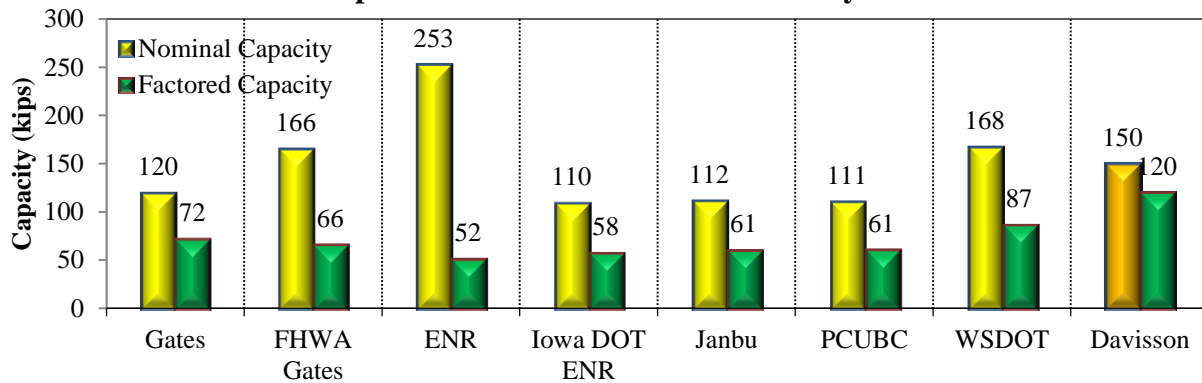


Figure B.134. Nominal and Factored pile design capacities using dynamic formulas and compared to SLT results for Polk – Clay soil

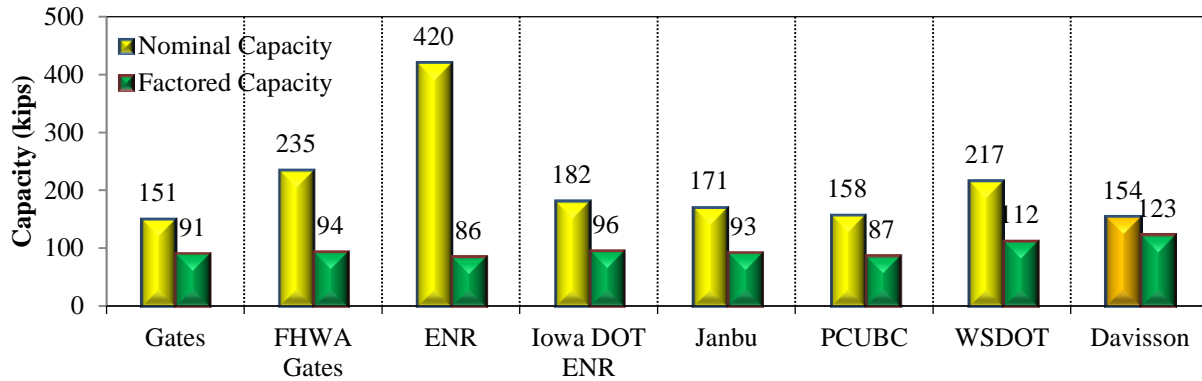


Figure B.135. Nominal and Factored pile design capacities using dynamic formulas and compared to SLT results for Jasper – Clay soil

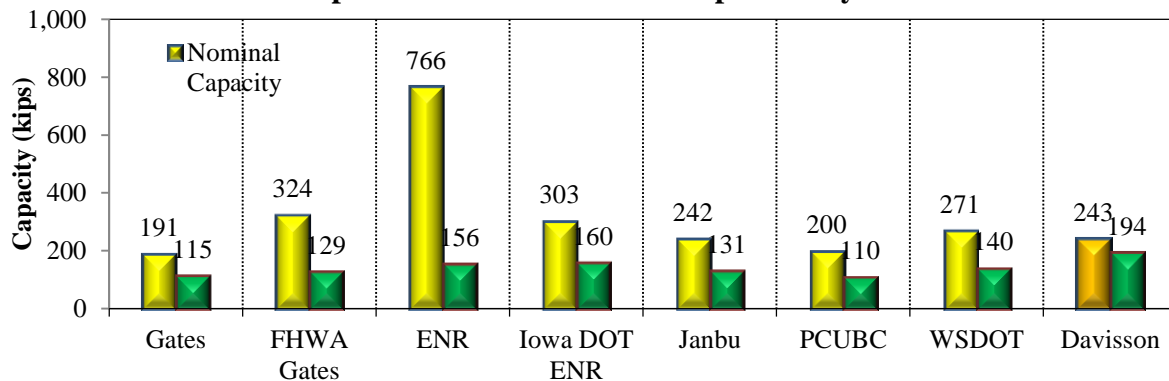


Figure B.136. Nominal and Factored pile design capacities using dynamic formulas and compared to SLT results for Clarke – Clay soil

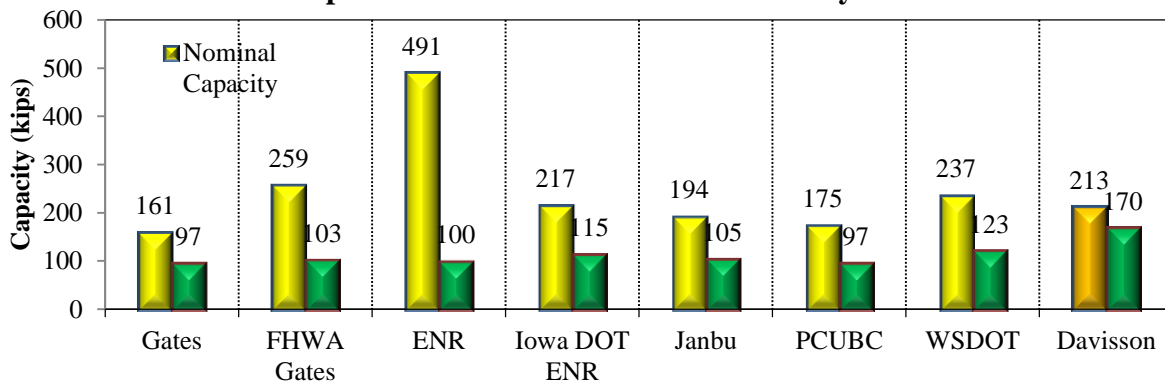


Figure B.137. Nominal and Factored pile design capacities using dynamic formulas and compared to SLT results for Buchanan (long) – Clay soil

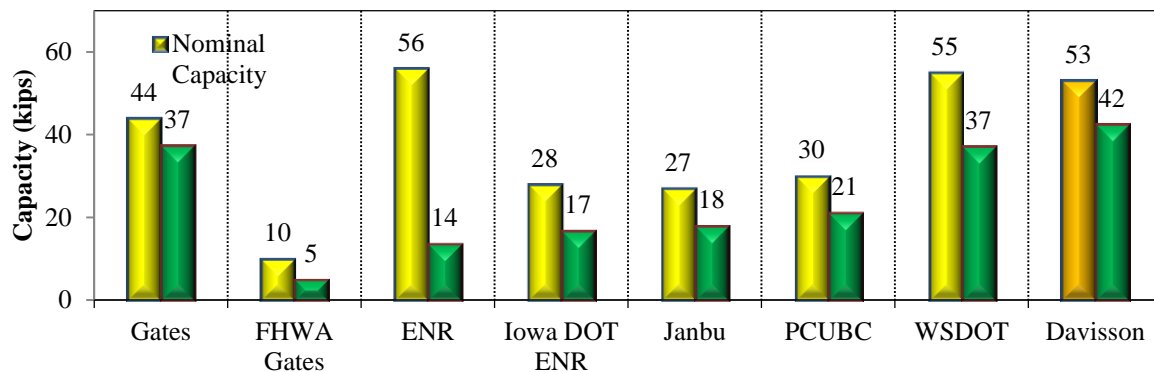


Figure B.138. Nominal and Factored pile design capacities using dynamic formulas and compared to SLT results for Buchanan (short) – Mixed soil

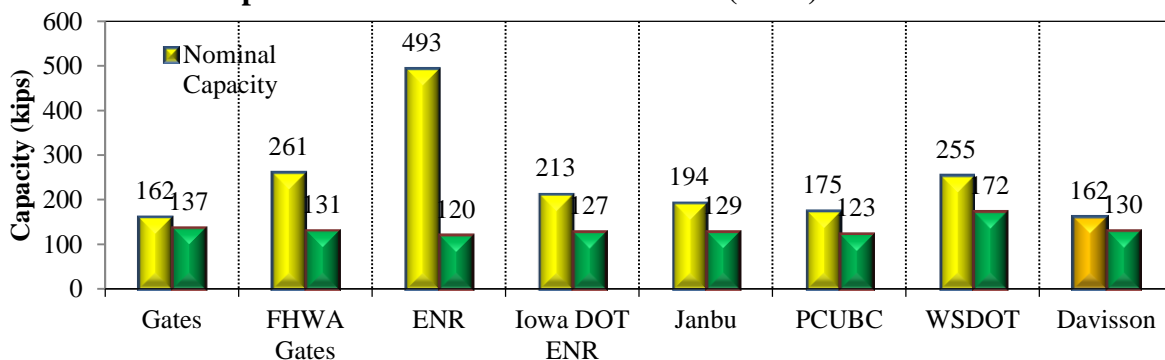


Figure B.139. Nominal and Factored pile design capacities using dynamic formulas and compared to SLT results for Poweshiek – Mixed soil

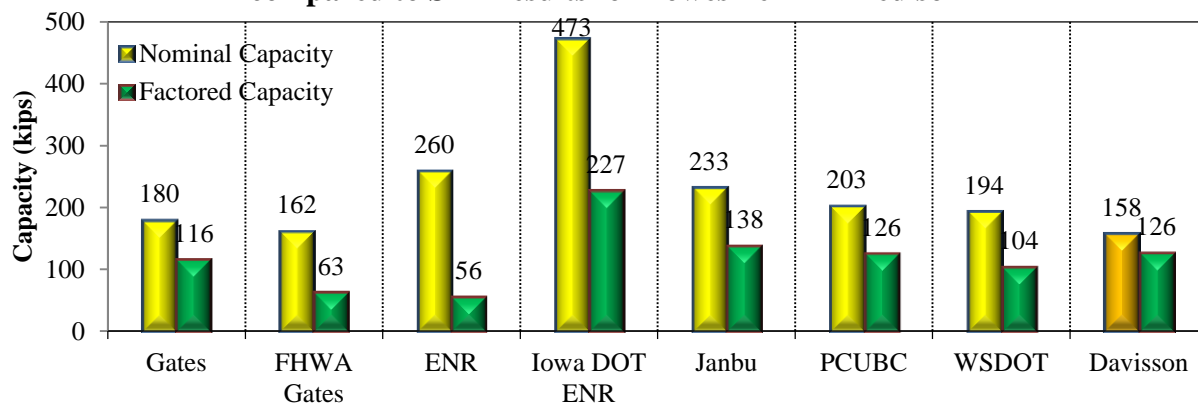


Figure B.140. Nominal and Factored pile design capacities using dynamic formulas and compared to SLT results for Des Moines – Sand soil

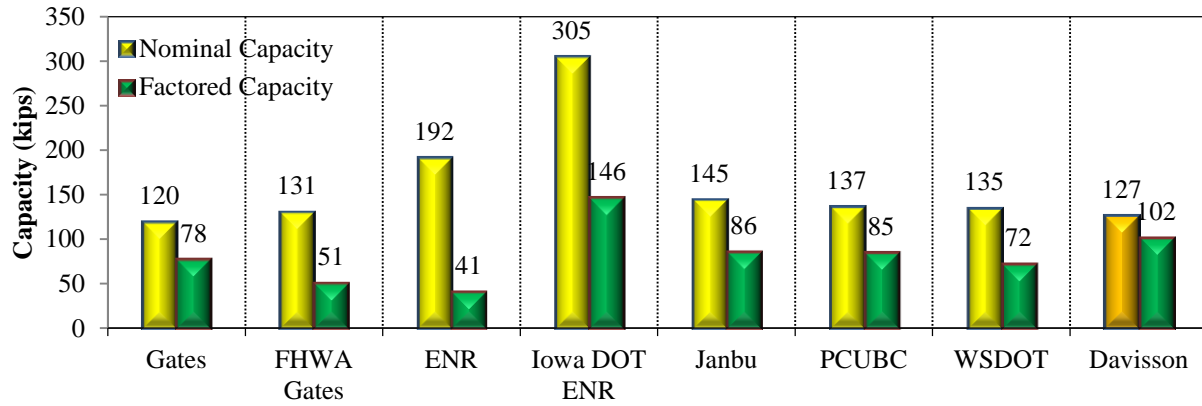


Figure B.141. Nominal and Factored pile design capacities using dynamic formulas and compared to SLT results for Cedar – Sand soil